NUREG/CP-0041
Vol. 4

Proceedings of the U.S. Nuclear Regulatory Commission

Tenth Water Reactor Safety Research Information Meeting

Volume 4
- Materials Engineering Research

Held at
National Bureau of Standards
Gaithersburg, Maryland
October 12-15, 1982

U.S. Nuclear Regulatory Commission

Office of Nuclear Regulatory Research

Available from

GPO Sales Program
Division of Technical Information and Document Control
U.S. Nuclear Regulatory Commission
Washington, DC 20555

Printed copy price: $9.00

and

National Technical Information Service
Springfield, VA 22161

NUREG/CP-0041
Vol. 4
RF and R5

Proceedings of the U.S. Nuclear Regulatory Commission

Tenth Water Reactor Safety Research Information Meeting

Volume 4
- Materials Engineering Research

Held at
National Bureau of Standards
Gaithersburg, Maryland
October 12-15, 1982

Date Published: January 1983

Compiled by: Stanley A. Szawlewicz, Consultant

Office of Nuclear Regulatory Research
U.S. Nuclear Regulatory Commission
Washington, D.C. 20555

ABSTRACT

This report is a compilation of papers which were presented at the Tenth Water Reactor Safety Research Information Meeting held at the National Bureau of Standards, Gaithersburg, Maryland, October 12-15, 1982. It consists of six volumes. The papers describe recent results and planning of safety research work sponsored by the Office of Nuclear Regulatory Research, NRC. It also includes a number of invited papers on water reactor safety research prepared by the Electric Power Research Institute and various government and industry organizations from Europe and Japan.

PROCEEDINGS OF THE
TENTH WATER REACTOR SAFETY RESEARCH
INFORMATION MEETING

October 12-15, 1982

PUBLISHED IN SIX VOLUMES

GENERAL INDEX

VOLUME 1
- PLENARY SESSION
- INTEGRAL SYSTEMS EXPERIMENTS
- SEPARATE EFFECTS EXPERIMENTAL PROGRAMS
- MODEL DEVELOPMENT EXPERIMENTAL PROGRAMS
- 2D/3D RESEARCH PROGRAM
- FOREIGN PROGRAMS IN THERMAL HYDRAULICS

VOLUME 2
- ANALYSIS OF TRANSIENTS IN LIGHT WATER REACTORS
- FUEL BEHAVIOR AND FISSION PRODUCT RELEASE
- SEVERE ACCIDENT ASSESSMENT
- SEVERE ACCIDENT SEQUENCE ANALYSIS

VOLUME 3
- HUMAN FACTORS RESEARCH
- INSTRUMENTATION AND CONTROL RESEARCH
- OCCUPATIONAL RADIATION PROTECTION
- SAFETY/SAFEGUARDS INTERACTION

VOLUME 4
- MATERIALS ENGINEERING RESEARCH

VOLUME 5
- MECHANICAL/STRUCTURAL ENGINEERING
- LOAD COMBINATIONS
- SEISMIC SAFETY MARGINS
- STRUCTURAL ENGINEERING
- ELECTRICAL EQUIPMENT QUALIFICATION
- PROCESS CONTROL AND ACCIDENT MITIGATION

VOLUME 6
- RISK ANALYSIS
- EPRI SAFETY RESEARCH PROGRAM

PROCEEDINGS OF THE
TENTH WATER REACTOR SAFETY RESEARCH
INFORMATION MEETING

held at the

NATIONAL BUREAU OF STANDARDS
GAITHERSBURG, MARYLAND

October 12-15, 1982

TABLE OF CONTENTS - VOLUME 4

PR_FACE xi

MATERIALS ENGINEERING RESEARCH
Steam Generators and Environmentally Assisted Pipe Cracking
Chairman: J. Muscara, NRC

Environmentally Assisted Cracking in Light Water Reactors
William J. Shack, ANL 1

Work of the ICCGR on Environmentally Affected Crack Growth
W. H. Cullen, Materials Engineering Associates, Inc. . 9

Steam Generator Integrity Program - Steam Generator Group Project
R. A. Clark and M. Lewis, PNL 23

Tests with Inconel 600 to Obtain Quantitative Stress Corrosion Cracking Data for Evaluating Service Performance
R. Bandy and D. van Rooyen, BNL 36

Improved Eddy-Current Testing for Longitudinal and Circumferential Flaws in Steam Generator Tubing
C. V. Dodd, ORNL 47

Piping Integrity Programs
Chairman: Jack Strosnider, NRC

The Development of a Plan for the Assessment of Degraded Nuclear Piping by Experimentation and Tearing Instability Fracture Mechanics Analysis
M. F. Kanninen, et al., BCL 61

Compact Specimen Geometry and Elastic Compliance Test Method Effects on the J-Integral R-Curve
J. P. Gudas, et al., David Taylor Naval Ship R&D Center . 94

Degraded Pipe Experimental Program
J. P. Gudas and M. G. Vassilaros, David Taylor Naval Ship R&D Center 119

MATERIALS ENGINEERING RESEARCH
Piping Integrity Programs (Cont'd)

Piping Reliability Model Development, Validation, and Its Applications to Light Water Reactor Piping
H. H. Woo, LLNL 147

Irradiation Effects
Chairman: C. Z. Serpan, Jr., NRC

Irradiation and Annealing Sensitivity Studies
J. R. Hawthorne, Materials Engineering Associates, Inc. . 157

Fracture Toughness Characterization of Irradiated, Low-Upper Shelf Welds
F. J. Loss, B. H. Menke, and A. L. Hiser, Materials Engineering Associates, Inc.. 168

Verification of Effects of Fuel Management Schemes on the Condition of Pressure Vessels and Their Support Structures
W. N. McElroy, et al., PNL 184

Description and Status of the NESTOR Dosimetry Improvement Programme (NESDIP)
M. Austin, Rolls-Royce & Associates Ltd.. 228

Fracture Mechanics and Thermal Shock
Chairman: Milton Vagins, NRC

The Integrity of PWR Pressure Vessels During Overcooling Accidents
R. D. Cheverton, S. K. Iskander, and G. D. Whitman, ORNL. 232

Failure Probability of a PWR Pressure Vessel Subjected to Pressurized Thermal Shock
Jack Strosnider, NRC 242

Pressurized-Thermal-Shock Experiments
G. D. Whitman and R. W. McCulloch, ORNL 262

Small-Scale Clad Effects Study
G. C. Robinson, ORNL 272

Results of Thermal-Shock Experiment TSE-6 and Proposal for TSE-7, 8, and 9
R. D. Cheverton, ORNL 282

Results of Low Ductile Shelf Intermediate Vessel Test V-8A
R. H. Bryan, ORNL 289

MATERIALS ENGINEERING RESEARCH
Fracture Mechanics and Thermal Shock (Cont'd)

Preliminary Results of International Round Robin on ITV-8A
J. G. Merkle, ORNL 301

New Method for Analyzing Small Scale Fracture Specimen Data in the Transition Zone
J. G. Merkle, ORNL 307

PREFACE

This report, published in six volumes, includes 160 papers which were presented at the Tenth Water Reactor Safety Research Information Meeting. The papers are printed in the order of their presentation in each session. The titles of the papers and the names of the authors have been updated and may differ from those which appeared in the Final Agenda for this meeting.

Five papers, which were submitted for presentation at the meeting but could not be scheduled, are also included in this report. They are the following:

Calculations of Pressurized Thermal Shock Problems with the SOLA-PTS Method, B. J. Daly, B. A. Kashiwa, and M. D. Torrey, LANL, (Pages 113-130, Volume 2)

Hydrogen Migration Modeling for the EPRI/HEDL Standard Problems, J. R. Travis, LANL, (Pages 131-144, Volume 2)

Independent Code Assessment at BNL in FY 1982, P. Saha, U. S. Rohatgi, J. H. Jo, L. Neymotin, G. Slivik, and C. Yuelys-Miksis, BNL, (Pages 145-168, Volume 2)

Experimental Evidence for the Depencence of Fuel Relocation upon the Maximum Local Power Attained, D. D. Lanning, PNL, (Pages 285-296, Volume 2)

PRA Has Many Faces - Can the Safety Goal Be Well-Posed? H. Bargmann, Swiss Federal Institute for Reactor Research, (Pages 105-114, Volume 6).

Environmentally Assisted Cracking
in Light Water Reactors
(A2212)

Dr. William J. Shack

Materials Science and Technology Division
Argonne National Laboratory
9700 South Cass Avenue
Argonne, Illinois 60439

Introduction

The objective of this program are to develop an independent capability for the detection and control of stress-corrosion cracking (SCC) in light-water reactor (LWR) systems and to evaluate of the technical merits of proposed remedies for the problem. Because the EPRI/BWR Owners Group Program is approaching completion and the NRC is being faced with decisions on the remedies developed by the Owners Group, and because cracking due to SCC continues to occur in boiling water reactors (BWRs), the experimental work is initially concentrated on problems related to intergranular SCC (IGSCC) in BWR piping systems.

The BWR utilities, the reactor vendors, and related research organizations both here and abroad have developed remedies for the pipe cracking problems and have begun to develop the crack-growth-rate data base which is needed to assure the integrity of degraded piping and to develop an adequate plan for the inspection and monitoring of such piping. The performance of the remedies in laboratory tests is quite encouraging, but there are still technical questions which must be addressed to ensure that the laboratory results will accurately reflect performance in-reactor. First, most of the previous studies have been carried out in high purity water, and the effects of the impurities present in an actual reactor coolant system on the proposed remedies and on the crack growth rates must be assessed. Second, the strain rates associated with the loading histories used in most laboratory testing are in some cases several orders of magnitude higher than those associated with actual reactor loading history. Since strain rate appears to be the critical mechanical variable influencing SCC, the adequacy of extrapolations from laboratory data to predict field performance must be demonstrated. Third, there is evidence to suggest that the particular thermomechanical history used to produce a given laboratory measure of sensitization may have an important effect on SCC initiation and propagation. Additional understanding of these effects is needed to ensure that the susceptibility of actual reactor materials can be assessed and that the heat treatments used in laboratory testing adequately simulate the IGSCC susceptibility produced by welding and subsequent long-term aging at reactor operating temperatures.

For existing plants even with the assurance of leak-before-break it is important to upgrade the capability to detect leaks rather than completely relying on periodic in-service inspection. Although other leak detection systems (e.g., moisture-sensitive tapes) will be considered, acoustic leak detection systems seem to offer the best combination of sensitivity, ability to locate a leak, and leak-rate measurement, and the assessment and development of a practical leak detection system is another important objective of this program.

Technical Progress

Important technical results have been obtained in both the work on leak detection and the work on the effects of water chemistry and loading history on SCC susceptibility. The leak test facility is now complete. It can supply water at temperatures up to 600°F and pressures up to 2500 psi. Actual field cracks and laboratory grown cracks as well as other types of artificial defects can be introduced into the simulated 30-ft. piping run. Three large autoclave and load frame systems for multi-specimen crack-growth tests are operational and a fourth is near completion. Nine small autoclave systems for slow strain rate tests ranging from $\dot{\epsilon} = 10^{-8}$ to 10^{-5} s^{-1} have been constructed. Four pipe test stands are under construction at Battelle-Pacific Northwest National Laboratories, and additional water loops and autoclave systems for studies of crack tip chemistry and mechanistic studies of the crack growth rate dependence on loading mode are near completion.

In the leak detection studies acoustic emission (A.E.) from IGSCC, EDM slits, and drilled holes has been investigated. The frequency spectrum for A.E. from leaks ranges from 0-400 kHz with the greatest signal content at frequencies less than 200 kHz (Fig. 2). However, consideration of the frequency spectrum of background noise in operating reactors suggests that to obtain satisfactory signal to noise ratios the practical window for leak detection is 300-400 kHz. The current (limited) data suggest that with a transducer spacing of 2m leaks of ~0.01 g/min from IGSCC can be detected in reactor. This corresponds to an IGSCC crack with an exit length on the outer surface of ~3 mm. A major problem in developing a sensitive leak detection system is discrimination between leakage from cracks and essentially benign leakage from valve packing, seal leakage, etc. Two approaches to the discrimination problem seem promising. One is to use cross-correlation techniques to locate leaks. This has been done successfully at low frequencies (30 kHz) for flow through an artificial flaw (Fig. 1), and currently software is being developed to carry out the cross-correlation at higher frequencies. The other approach is to use signal processing techniques to characterize the signal from a source. Auto-correlation techniques have been applied to signals from EDM slits, drilled holes, and IGSCC and significant differences can be seen in the signals from the different leak sources. Pattern recognition techniques developed in other NRC sponsored work will also be used to try to characterize the leak source in terms of its A.E. signal.

Work thus far on the effect of water chemistry indicates that impurity levels within the Reg. Guide 1.56 limits have a significant effect on the IGSCC behavior of sensitized austenitic stainless steels. Results for additions of H_2SO_4 (a product of cation resin decomposition) are shown in Figs. 3 and 4 and some additional results for additions of HCl are shown in Table II. As Fig. 3 shows, impurity additions have a larger effect on lightly sensitized materials. In fact, with the sulfate additions the lightly sensitized material becomes more susceptible to IGSCC than the more heavily sensitized material. Figure 4 also shows that some care must be exercised in choosing a test environment to assess the effects of impurities. For the material with an EPR of 20 C/cm^2 there is almost no effect of sulfuric acid in water with 8 ppm oxygen. However, in water with 0.2 ppm oxygen there is a strong effect of the sulfuric acid additions.

Under the conditions examined thus far ($\dot{\epsilon} = 2 \times 10^{-6}$ s^{-1}, 8 ppm oxygen) there is a much smaller effect of impurity additions for Type 316NG SS. Sulfuric acid seems to have very little effect, but chloride additions produce some transgranular SCC (TGSCC). Results from a few of the tests which have been carried out to compare the behavior of a conventional Type 316 SS (.05 C) with Type 316NG SS are given in Table II. Neither material is susceptible to cracking in the solution annealed condition in either high purity water or a 0.5 ppm Cl^- environment. After heat treatment the conventional SS is susceptible to IGSCC in both environments, although the addition of HCl substantially increases the susceptibility. After heat treatment the Type 316NG SS shows no susceptibility to cracking in the high purity water, but cracks transgranularly in the Cl^- environment. However, the TGSCC crack growth rate is much less than the IGSCC crack growth rate observed in the conventional material.

Baseline fracture mechanics crack growth rate tests have been completed and are summarized in Table I. For the tests under cyclic loading where the strain rate due to the variations in the external load is much larger than that due to creep at the crack tip the crack tip strain rate $\dot{\varepsilon}_T$ can be estimated from LEFM. With this estimate of $\dot{\varepsilon}_T$ the dependence on R ratio and frequency in these tests is consistent with the $\dot{a} \sim \dot{\varepsilon}^{\frac{1}{2}}$ relationship proposed by F. P. Ford. This type of correlation is important in developing confidence in extrapolations of data obtained under laboratory loading histories to more realistic histories. A number of different degrees of sensitization (DOS) have been considered in these tests. The results suggest that although the crack growth rate is very strongly dependent on DOS at very low levels, it is only weakly dependent on DOS at the somewhat higher levels most characteristic of weld and furnace sensitization in high carbon materials.

Finite element calculations of the influence of applied load on the residual stresses associated with Induction Heating Stress Improvement (IHSI) have been carried out. The results (see Figs. 5, 6 and Table III) indicate that although under loads corresponding to the design allowable S_m (roughly internal pressure plus 0.5 σ_y in Table III) the total axial stresses on the inner surface of 4-in. and 24-in. piping are tensile, the stresses in the IHSI treated pipes are substantially lower than in as-welded pipes. This benefit persists even with total axial stresses somewhat greater than yield. The results also indicate that after IHSI the stress distributions in small and large diameter weldments are similar and in that sense the 4-in. pipe is a good model for the larger diameter weldments.

During FY 83 the study of the effect of water chemistry will continue. Tests will be carried out to assess the effect of specific anions and pH as independent variables as well as the effectiveness of H_2 additions. Increased emphasis will be placed on low strain rate tests (10^{-7} – 10^{-8} s^{-1}) more nearly characteristic of realistic loading histories. Crack growth rate data will be obtained for Type 304 SS in BWR environments with impurity additions. Pipe tests on Type 316NG SS and IHSI treated weldments under alternate loading conditions and alternate water chemistries will be initiated. The studies of the effect of plastic strain and thermomechanical history on susceptibility to IGSCC will be continued, and Mode I/Mode III comparative tests will be carried out to determine the actual mechanism of crack advance.

Publications

1. W. J. Shack et al., Environmentally Assisted Cracking in Light Water Reactors: Critical Issues and Recommended Research, NUREG/CR-2541, ANL-82-2, (February 1982).

2. Light-Water-Reactor Safety Research Program: Quarterly Progress Report, April-June 1981, NUREG/CR-2437 Vol. II, ANL-81-77 Vol. II (April-June 1981).

3. Light-Water-Reactor Safety Research Program: Quarterly Progress Report, NUREG/CR-2437 Vol. III, ANL-81-77 Vol. III (July-September 1981).

4. Light-Water-Reactor Safety Research Program: Quarterly Progress Report, NUREG/CR-2437 Vol. IV, ANL-81-77 Vol. IV (October-December 1981).

5. Light-Water-Reactor Safety Research Program: Quarterly Progress Report, January-March 1982, NUREG/CR-   Vol. I, ANL-82-41 Vol. I (January-March 1982).

ENVIRONMENTALLY ASSISTED
CRACKING IN LWR SYSTEMS

ARGONNE NATIONAL LABORATORY
GARD INC.
BATTELLE-PACIFIC NORTHWEST NATIONAL LABORATORY
UNIVERSITY OF TULSA

OBJECTIVE:

DEVELOP AN INDEPENDENT CAPABILITY FOR PREDICTION, DETECTION, AND CONTROL OF SCC IN LWR SYSTEMS AND FOR THE EVALUATION OF THE TECHNICAL MERITS OF PROPOSED SOLUTIONS.

ENVIRONMENTALLY ASSISTED CRACKING IN BWRs

OBJECTIVES

- INVESTIGATE THE ROLE OF WATER CHEMISTRY ON SUSCEPTIBILITY TO CRACKING OF BWR PIPING MATERIALS
  - TYPE 316NG ( ) AND IHSI REMEDIES
  - DEAERATION AND HYDROGEN ADDITIONS
  - CRACK PROPAGATION RATES FOR SUSCEPTIBLE MATERIALS
  - EFFECT OF TRANSIENT WATER CHEMISTRIES
- INVESTIGATE THE ROLE OF LOADING HISTORY ON SUSCEPTIBILITY TO SCC AND ON THE INTERPRETATION AND EXTRAPOLATION OF LABORATORY TEST RESULTS
  - STRAIN RATE EFFECTS ON SUSCEPTIBILITY
  - LOAD RATIO AND FREQUENCY EFFECTS ON CRACK PROPAGATION RATES; SPECIMEN GEOMETRY EFFECTS
  - REDISTRIBUTION OF RESIDUAL STRESS UNDER IN-SERVICE LOADS
  - EVALUATION OF THE MARGIN OF IMPROVEMENT FOR REMEDIES
- INVESTIGATE LTS POTENTIAL IN REMEDY PROCEDURES AND EFFECT OF THERMOMECHANICAL HISTORY ON IGSCC INITIATION AND PROPAGATION
- DEVELOP ACOUSTIC LEAK DETECTION SYSTEMS TO DETECT LEAKAGE FROM CRACKED PIPING
  - SENSITIVITY FOR LOW LEAKAGE LEVELS
  - LOCATION ABILITY
  - CHARACTERIZE LEAKS FROM REAL SOURCES (IGSCC AND FATIGUE) AND EXAMINE EFFECT OF LEAK GEOMETRY AND FLOW VARIABLES ON A.E. CHARACTERISTICS
- INVESTIGATE ULTRASONIC METHODS FOR THROUGH-WELD INSPECTION OF IGSCC AND ALTERNATIVE APPROACHES FOR DISTINGUISHING IGSCC FROM GEOMETRICAL REFLECTORS

PROGRESS

FACILITIES

- LEAK TEST FACILITY COMPLETE
- 3 LARGE AUTOCLAVE AND LOAD FRAME SYSTEMS OPERATIONAL AND A FOURTH NEAR COMPLETION (MULTI-SPECIMEN CRACK GROWTH TESTS)
- 9 SLOW STRAIN RATE AND CYCLIC LOAD SMALL AUTOCLAVE SYSTEMS ($\dot{\varepsilon} = 10^{-8} - 10^{-5}\ s^{-1}$)
- 4 PIPE TEST STANDS UNDER CONSTRUCTION AT PNL
- ADDITIONAL WATER LOOPS AND AUTOCLAVE SYSTEM FOR CRACK TIP CHEMISTRY AND MECHANISTIC STUDIES OF CRACK GROWTH RATE DEPENDENCE ON LOADING MODE NEAR COMPLETION

LEAK DETECTION

HIGHLIGHTS

- A.E. FROM IGSCC, EDM SLITS, AND DRILLED HOLES INVESTIGATED
- FREQUENCY SPECTRUM FOR A.E. FROM LEAKS 0-400 KHZ; FREQUENCY WINDOW FOR APPLICATIONS 300-400 KHZ
- CURRENT (LIMITED) DATA ON A.E. FROM IGSCC AND REACTOR BACKGROUND NOISE INDICATES LEAKS OF ~0.01 GAL/MIN SHOULD BE DETECTABLE AT A 2M SPACING
- CROSS-CORRELATION TECHNIQUE FOR LEAK LOCATION APPEARS PROMISING
- LEAK CHARACTERIZATION BY AUTO-CORRELATION HAS BEEN CARRIED OUT AND CHARACTERIZATION USING PATTERN RECOGNITION TECHNIQUES WILL BE INVESTIGATED

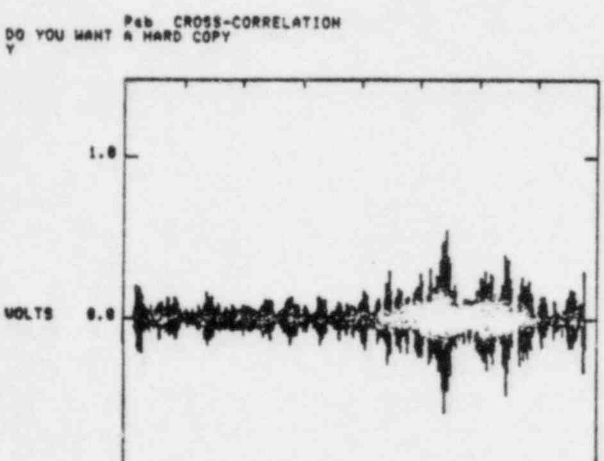

Fig. 1

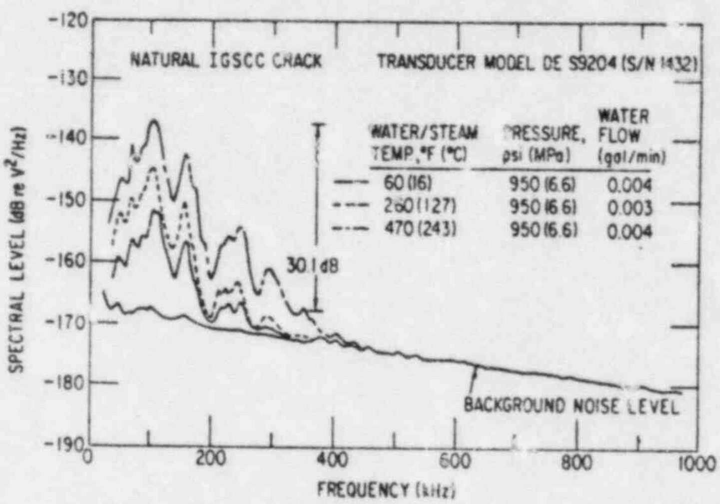

Fig. 2

EFFECT OF WATER CHEMISTRY AND LOADING HISTORY

HIGHLIGHTS

- IMPURITY LEVELS WITHIN REG. GUIDE 1.56 LIMITS HAVE A SIGNIFICANT EFFECT ON THE IGSCC BEHAVIOR OF SENSITIZED AUSTENITIC SS
  1) FIXED SENSITIZATION LEVEL IMPURITIES INCREASE SUSCEPTIBILITY IN TERMS OF TIME TO FAILURE, CRACK-GROWTH RATE, ETC.
  2) LOWER SENSITIZATION LEVEL REQUIRED FOR CRACKING
- IMPURITY LEVELS WITHIN REG. GUIDE 1.56 LIMITS HAVE RELATIVELY LITTLE EFFECT ON CRACKING OF TYPE 316NG SS UNDER TEST CONDITIONS STUDIED THUS FAR
- BASELINE CRACK GROWTH TESTS ON TWO HEATS OF TYPE 304 SS IN HIGH PURITY WATER COMPLETED
- FE CALCULATIONS OF RESIDUAL STRESS IN 4-IN. AND 24-IN. WELDMENTS INDICATE SIGNIFICANT BENEFIT OF IHSI TREATMENT UNDER APPLIED STRESSES UP TO S_M

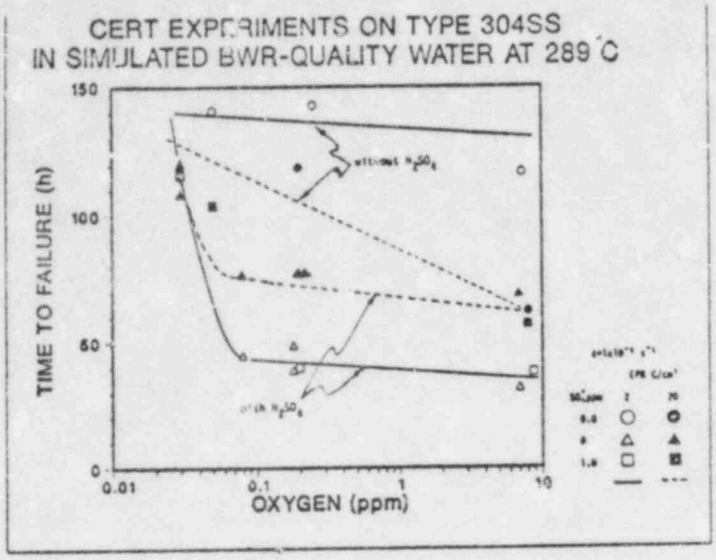

Fig. 3

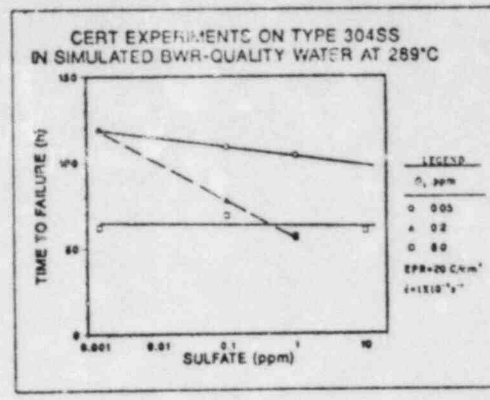

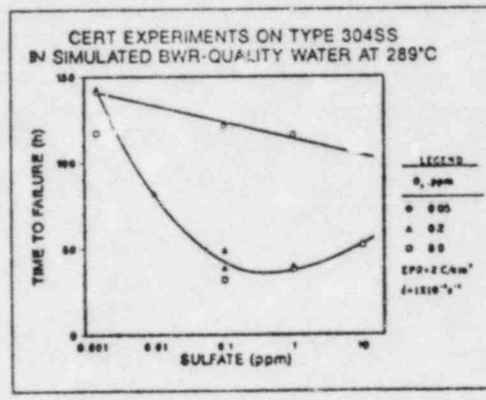

Fig. 4

Table I

CRACK GROWTH RATE TESTS

MATERIAL	HT	EPR (C/cm^2)	ENVIRONMENT	K_{MAX} ($MPa \cdot m^{½}$)	R	ν(HZ)	$\dot{a}$ (10^{-10} m/s)
304	10285	15	8 ppm O_2	32	0.5	2×10^{-3}	30
		15		33	1	-	2
		15		31	0.94	2×10^{-3}	2
		4		33	0.5	2×10^{-3}	40
		4		34	1	-	1
		4		31	0.94	2×10^{-3}	3
	30956	20		28	0.95	8×10^{-2}	8
		2		28	0.95	8×10^{-2}	~0.1
		SA		28	0.95	8×10^{-2}	~0
		20		28	0.95	8×10^{-4}	1
		2		28	0.95	8×10^{-4}	~0
		SA		28	0.95	8×10^{-4}	~0

- FOR CYCLE CONTROLLED STRAIN RATES ($\dot{\varepsilon} = -\nu \ln[1 - (1 - R)^2/2]$) DEPENDENCE ON R AND ν ROUGHLY CONSISTENT WITH $\dot{a} \sim \dot{\varepsilon}^{½}$ BEHAVIOR.
- CRACK GROWTH RATE VERY STRONGLY DEPENDENT ON SENSITIZATION AT VERY LOW LEVELS; ONLY WEAKLY DEPENDENT AT SOMEWHAT HIGHER LEVELS.

Table II

CERT TESTS ON TYPE 316 AND TYPE 316NG SS

MATERIAL	HT TREATMENT	CL^- (PPM)	T_F (H)	MAXIMUM STRESS (MPA)	UNIFORM ELONGATION %	$\dot{a}$ (10^{-10} m/s)
TYPE 316 HT 0590019	SA	0	55	493	35	0
	SA	0.5	57	497	35	0
	650°C/24H	0	42	482	29	70
	650°C/24H	0.5	28	-	15	180
TYPE 316NG HT P91576	SA	0	44	449	29	0
	SA	0.5	56	439	34	~0
	700°C/4H	0	49	440	30	0
	700°C/4H	0.5	57	440	30	27*

*TGSCC

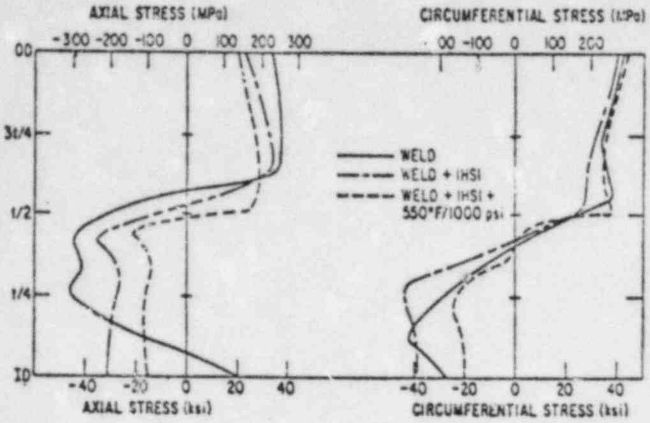

Fig. 5

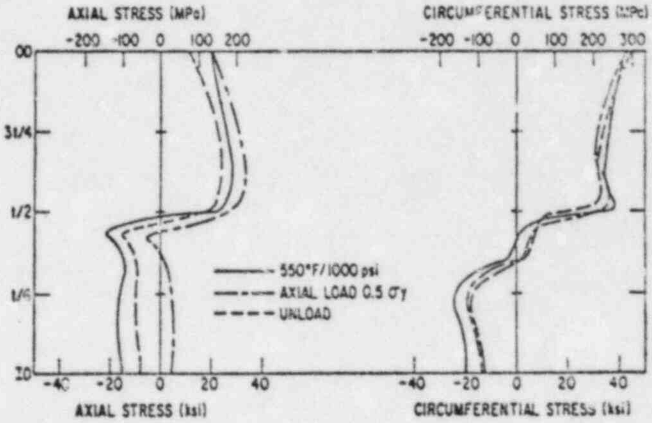

Fig. 6

Table III

Total Stresses on the Inner Surface in the HAZ

External Loading	With IHSI				Without IHSI			
	4-in.		24-in.		4-in.		24-in.	
	Ax	Circ	Ax	Circ	Ax	Circ	Ax	Circ
0	-36	-40	-32	-39	22	44	24	-21
Internal Pressure	-20	-26	-15	-20	19	41	27	-8
+0.5 σ_y	8	-16	5	-13	31	32	34	8
+0.8 σ_y	21	-5	22	-4	33	23	30	12
+1.0 σ_y	28	5	27	1	31	7	30	9

Planned Near Term Activities:

- Obtain crack growth rate data for Type 304 SS in BWR environments with impurity additions
- Continue slow strain rate tests to better define role of strain rate anions, pH, and sensitization history on SCC susceptibility
- Investigate resistance of Type 316NG SS to crack propagation in BWR environments with impurity additions
- Complete pipe test facilities and begin parametric pipe tests
- Complete analytical studies on effect of loading on stress redistribution of weldments with IHSI
- Initiate study of effect of plastic strain on subsequent LTS kinetics
- Use Mode I/Mode III comparative tests to distinguish dissolution vs hydrogen embrittlement crack advance
- Continue stress/strain/strain-rate studies including effect of cyclic-loading histories

WORK OF THE ICCGR ON ENVIRONMENTALLY AFFECTED CRACK GROWTH

W. H. Cullen
Materials Engineering Associates, Inc.
Lanham, MD 20706 USA

INTRODUCTION

Fatigue and fatigue crack growth has long been a concern for pressure vessels and piping. The technology for conducting fatigue crack growth rate tests in reactor-typical environments was first developed in the late 1960's and early 1970's and the last five years have witnessed a rapid increase in the number of laboratories involved in the successful conduct of these tests. It was recognized early in these studies that it would be prohibitively expensive for one organization to address all the variables which enter the fatigue crack growth problem. For example, when realistic cyclic periods and load ratios are experimentally employed, a single fatigue crack growth rate test will require two to twelve months to complete.

This consideration stimulated the idea of assembling a group of representatives of sponsoring organizations and research laboratories, who were active in the field, would share both their techniques and experiences, and would assume various portions of the testing responsibilities so that more inroads could be made in this complex area.

FORMATION OF ICCGR

Under the guidance of K. Lynn (NRC) and K. Stahlkopf (EPRI) and with the organizational help of H. E. Watson of the Naval Research Lab -- at that time (1977) the prime contractor for the NRC-sponsored fatigue crack growth effort -- the fledgling ICCGR convened for the first time. Eighteen representatives from seven nations agreed to contribute their efforts to the goals of the group. From that start, the group has grown to include members from forty-one sponsoring or research organizations, representing eleven nations.

The timing of the formation of the group was coincident with the beginning of an exponential increase in the effort--facilities, personnel and financial resources--which has addressed environmentally assisted crack growth in pressure vessel and piping steels. In 1977, only a handful of laboratories had published any data at all, the range of variables which had been tested was small, and the data was often disjoint, filled with scatter due to the experimental difficulties, and, for the most part, without explanation. The growth and vitality of the ICCGR has both fueled and drawn from the concurrent growth and vitality of the world-wide environmentally-assisted crack growth effort.

MAJOR ACTIVITIES

During the intervening years, the interests of the group have been confined to primary boundary materials, and for the most part, pressure vessel steels. However, other types of testing which bear on the corrosion fatigue problem are now frequent topics of discussion. The group is divided into three sub-committees: Test Methods, Mechanisms, and Data Collection and Evaluation. Each subcommittee has organized inter-laboratory tasks directed at specific objectives. As the understanding of corrosion fatigue has improved, and the interaction of the corrosion and mechanics has been better understood, other allied topics have been included in the Group's discussions. The use of reference electrodes, measurement of redox potential, conduct of elastic-plastic fracture tests in high-temperature water, and conduct of constant-extension rate tests have received considerable attention from members of the group. Additionally, more refined test practices, data acquisition and processing methods, and techniques of post-test examination of specimens for oxide identification and fractographic features have been developed and described by members of the Group.

Participation of the NRC and its subcontractors in the ICCGR program affords an opportunity for keeping these groups in the world-wide mainstream of developments in the fatigue crack growth area. In this way, the NRC can take advantage of recent advances, tailor their programs to respond to areas of interest and importance, and/or to fill in the gaps in the research as necessary.

One of the true marks of progress in any research effort is denoted by the conduct of open forums -- work-shops, symposiums, etc. -- centered on the topic of interest. The ICCGR sponsored its first symposium on "Subcritical Crack Growth" in Freiburg, Germany on 13-15 May 1981. Thirty-one contributions, spanning allied topics from experimental fatigue crack growth results, fractographic and corrosion mechanism studies, and design applications of fatigue data, were delivered by scientists and engineers representing eight nations [1]. The group has begun the initial planning for a second symposium tentatively scheduled for 1984.

ROUND ROBIN TESTS

The group membership has initiated and completed several round robin test programs. The first was designed by the Data Collection and Evaluation Subcommittee and required the data processing of specific data sets of crack length vs cyclic count. The goal was to determine the variability among the data evaluation and processing procedures used by the participating laboratories. From the results of this round robin, together with subsequent work by the Subcommittee, a standarized method of data selection, processing and presentation has been evolved.

A major effort of the Group has been directed at the conduct of two experimental test (round robin) programs, one nearly complete, the second just underway. The objective of the first round robin was to assure that the participating laboratories were employing test practice, data acquisition and data processing methods which would yield comparable inter-laboratory results. This round robin consisted of testing A533B specimens in pressurized, high-temperature, deionized water in which impurity elements were to be kept very low (100 ppb) but dissolved oxygen content could be whatever a laboratory was accustomed to using. Specimens were tested under constant load amplitude (with two exceptions), using a load ratio (R) of 0.2 and an initial ΔK of 27.5 MPa$\sqrt{m}$, (25 ksi$\sqrt{in.}$). These conditions model the load ratio and expected ΔK range of a quarter-thickness flaw subjected to start-up/shut down transients. There were two phases to this program. The first required testing with 17 mHz sinusoidal waveforms. The second, prompted by the wide range of results generated by the first, required testing using 1 Hz sinusoidal waveforms.

The examination of the results of this experimental round robin has been especially informative to the ICCGR community, because it pointed out the high sensitivity of the results to the character of the environment and other variables relating to test practice. The basic findings of the round robin are summarized in the following statements and accompanying figures.

Figure 1 shows results from several laboratories, plotted without regard to the effects of their individual test practice or environmental parameters. This figure illustrates the sensitivity of the growth rate results to these supposedly small differences. Figure 2 shows results from laboratories which were judged to have nominally identical test practice and environmental control. This figure differs from Fig. 1 in that:

1) All laboratories maintained a very low level of dissolved oxygen (PWR-typical) throughout the course of the test ($\leq$ 2 ppb was the target for these laboratories). It is recognized that crack growth rates are quite dependent of dissolved oxygen content. In particular, high oxygen contents (> 200 ppb, BWR-typical) may result in high crack growth rates, often above the ASME reference line for the appropriate load ratio. [2,3]

2) All laboratories used a 17 mHz sinusoidal waveform. It is recognized that linearized waveforms (ramp/hold/reset, triangular) result in crack growth rates which are substantially reduced from those for sinusiodal waveforms, all other things being equal [4]. This is an important design and in-service inspection consideration, since many of the light water reactor normal and upset, pressure and temperature transients are characterized by essentially linear changes with time, but the more conservative crack growth rate data is generated using sinusoidal waveforms.

The second experimental round robin effort, now underway, involves testing of 2T-CT specimens, in idealized BWR and PWR environments. The test requirements call for a constant load amplitude, R=0.7, 17 mHz sinusoidal waveform, and an initial ΔK of 11 MPa $\sqrt{m}$. These conditions approximate the lower bound specifications of the more frequently occurring transients (reactor trips, turbine trips) in an operating reactor.

In support of these round robin efforts, there have been substantial, allied research efforts carried out by member laboratories. The Technical Research Centre of Finland (VTT) has carried out a detailed fractographic examination of the first round robin specimens [5,6]. Central Electricity Research Laboratory has examined the oxide formed on the fracture surfaces of several of the specimens [7]. The VTT work demonstrated that brittle appearing areas on the fatigue fracture surface were present on specimens tested in both BWR- and PWR- typical environments, and that these brittle appearing areas emanate from manganese sulfide inclusions. An example of the VTT findings is shown in Fig. 3. This, in turn, suggests that a hydrogen assistance mechanism is involved in both environments. In some cases this may also be coupled with a dissolution or active path mechanism.

In addition to the group-wide, organized round robin programs, several of the member laboratories are carrying out cooperative research in order to directly compare results or techniques, or to take advantage of individual areas of expertise. As examples:

1) Materials Engineering Associates, Inc. is forwarding selected groups of samples to CERL and VTT for oxide identification and fractographic studies.

2) Westinghouse-Nuclear Technology Division has exchanged specimens with UKAEA-Harwell Labs in order to help track down some consistent differences in results between the two laboratories.

3) Representatives of the UK have pooled their resources in a unified effort to address topics of concern which may arise in the forthcoming Inquiry, which is part of the licensing effort preceeding construction of the UK's first pressurized water nuclear steam supply system.

4) Westinghouse and Framatome are undertaking a cooperative research program on fatigue crack growth rates, with the Framatome effort addressing upset water chemistries.

MAJOR ACCOMPLISHMENTS

After its five years of existence, the group can point to several accomplishments which have evolved directly from its efforts and those of its members.

a) Several critical variables have been identified and their influence has been investigated. Among these are waveform, temperature, environment and material chemistry.

Figure 4 illustrates the dependence of the fatigue crack growth rates on waveform. These Creusot-Loire data show that triangular waveshapes yield lower fatigue crack growth rates than sinusoidal waveforms of equivalent peroiod [8]. This conclusion can generally be extended to include all linearized waveforms (ramp/reset, ramp/hold/reset).

Figure 5 shows an example of the effect of temperature on fatigue crack growth rates in PWR-typical environments. Work at Central Electricity Research Laboratory and at Materials Engineering Associates has confirmed that low alloy pressure vessel steels exhibit minimal crack growth rates at temperatures near 200°C [9,10]. Additional work at CERL on oxide identification indicates that the oxide on the fatigue fracture surface changes character from hematite at the lower temperatures (<180°C) to magnetite at the higher temperatures (> 180°C).

The recognition that material chemistry has a role in the level of fatigue crack growth rates has helped immensely in sorting out some of the other critical variables. This effect, which has been explored at Westinghouse and at Creusot-Loire, indicates the fatigue crack growth rates tend to increase with sulfur composition of the steel [8]. This is shown in Figure 6.

b) Significant advances in the understanding of mechanisms have been achieved, primarily through fractographic studies and corrosion potential measurements. An effort is underway at Centro Informazioni Studi Esperienze (CISE) to develop miniature corrosion potential probes to measure the electrochemical potential developed at the tip of a growing crack. This work offers great promise toward unraveling the mechanisms of corrosion fatigue crack growth [11]. Figure 7 shows the profile of the potential as a function of applied load during a fatigue load cycle.

c) Specific data reduction and presentation methods have been developed, to help refine crack growth data and establish a format for presentation which will allow easy and valid comparison of various data sets.

SUMMARY

The members of the ICCGR are continuing to evolve new, cooperative projects which will blend and employ the differing types of expertise drawn from the members of the group. Such diverse contributions often help to focus more quickly on the understanding of the importance of a particular variable or on the approach to a solution of a particular problem. Coordination of the efforts of the various laboratories has, and will continue to, shorten the time-to-solution of the research endeavors common to the nuclear industry.

REFERENCES:

1. Proceedings of the International Atomic Energy Agency Specialists' Meeting on Subcritical Crack Growth, 13-15 May 1981, Freiburg, FRG. Initial printing no longer available. To be released as a NUREG in early 1983.

2. Prater, T. A. and Coffin, L. F., "Crack Growth Studies on a Carbon Steel in Oxygenated High-Pressure Water at Elevated Temperatures," Proceedings of Specialists' Meeting on Subcritical Crack Growth, International Atomic Energy Agency, 1981, pp. 640-654.

3. Hale, D. A., Lange, C. H. and Kass, J. N., "Crack Growth Resistance of Low Alloy Steel in High Temperature Oxygenated Water," Proceedings of Specialists' Meeting on Subcritical Crack Growth, International Atomic Energy Agency, 1981, pp. 109-146.

4. Cullen, W. H., et al., "Fatigue Crack Growth of A508-2 Steel in High-Temperature, Pressurized Reactor-Grade Water," NUREG/CR-0969, 1979, Nuclear Regulatory Commission, Washington, D. C. 20555.

5. Torronen, K. and Kemppainen, M., "A Fractographic Study of the Effects of Varying Dissolved Oxygen Level on the Cyclic Crack Growth of A533B Steel in High-Temperature Reactor Grade Water" Report VTT-MET B32, Technical Research Centre of Finland, SF-02150 Espoo 15, Finland.

6. Torronen, K. and Kemppainen, M., "Fractography and Mechanisms of Environmentally Enhanced Fatigue Crack Propagation of a Reactor Pressure Vessel Steel," in Corrosion-Fatigue: Mechanics, Metallurgy, Electrochemistry and Engineering, ASTM STP 801, 1982.

7. Atkinson, J. D., Cole, S. T. and Forrest, J. E., "Oxide Identification on LWR Corrosion Fatigue Specimens From Several Laboratories" Report to ICCGR Group, Charlotte, NC Meeting, 26-28 October, 1981. Authors are affiliated with Central Electricity Generating Board, Leatherhead, Surry KT22 7SE, England.

8. Slama, G. and Rabbe, P., "French Approach and Results in Cyclic Crack Growth" in Proceedings of Post Conference Seminar of Structural Mechanics in Reactor Technology, August 1981.

9. Atkinson, J. D., Cole, S. T. and Forrest, J. E., "Corrosion Fatigue Mechanisms in Ferritic Pressure Vessel Steels Exposed to Simulated PWR Environments" Proceedings of Specialists' Meeting on Subcritical Crack Growth, International Atomic Energy Agency, 1981, pp. 459-483.

10. Cullen, W. H., "Effects of Loading Rate, Waveform and Temperature on Fatigue Crack Growth Rates of RPV Steels" in Aspects of Fracture Mechanics in Pressure Vessels and Piping, PVP-Vol. 58, Edited by S. S. Palusamy, and S. G. Sampath, The American Society of Mechanical Engineers, New York, N. Y. 10017.

11. Gabetta, G. and Rizzi, R., "Electrochemical Potential Measured at the Tip of a Fatigue Growing Crack in Demineralized Water at 93°C: Effects of Frequency, Waveform and Oxygen Content" in _Proceedings of the Conference on Low-Frequency, Cyclic-Loading Effects in Environment Sensitive Fracture_, 9-11 March, 1982, Milan, Italy.

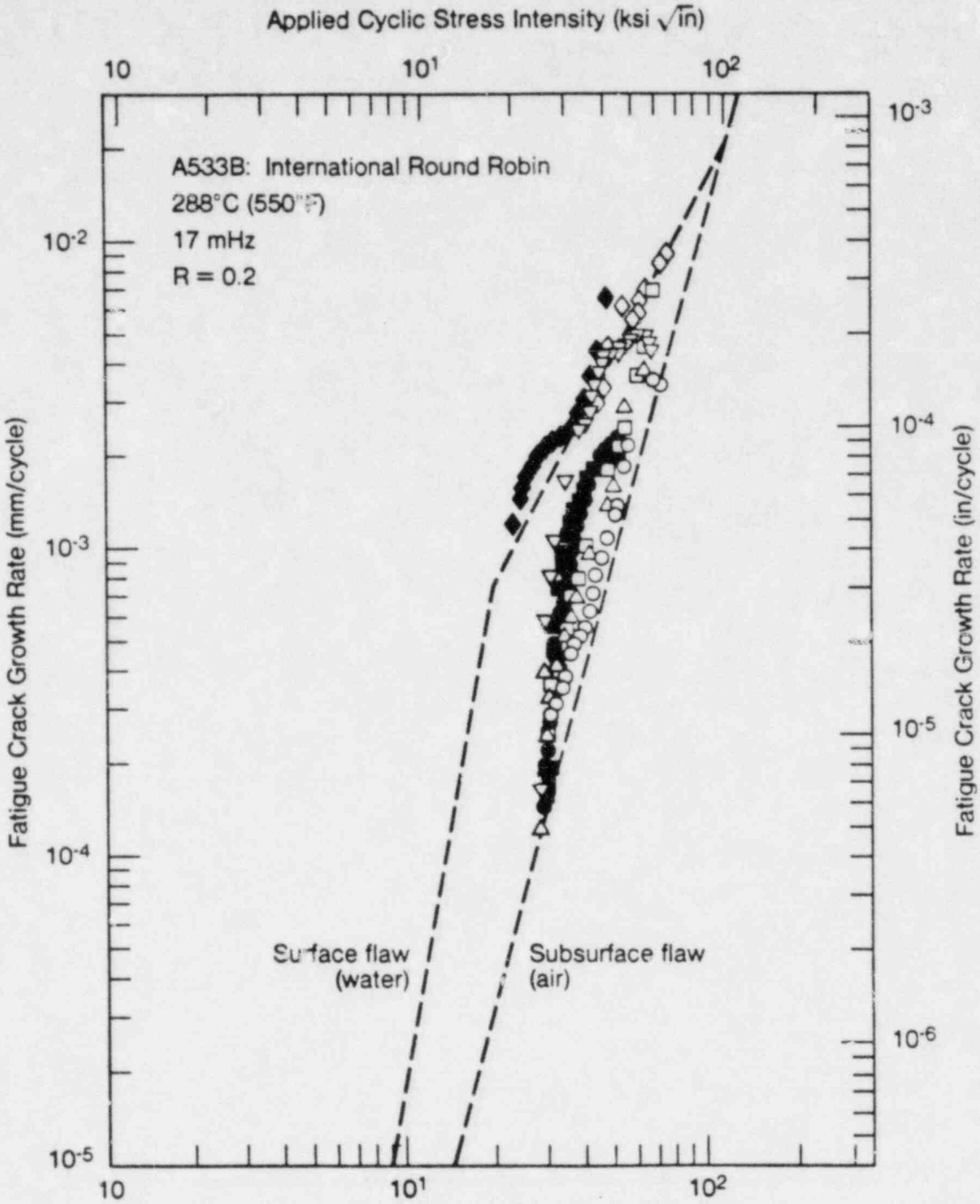

Figure 1. Fatigue crack growth rates vs applied cyclic stress intensity factor for A533B steel tested at a variety of laboratories using varying waveshapes and dissolved oxygen levels in deionized water. Ref. 1.

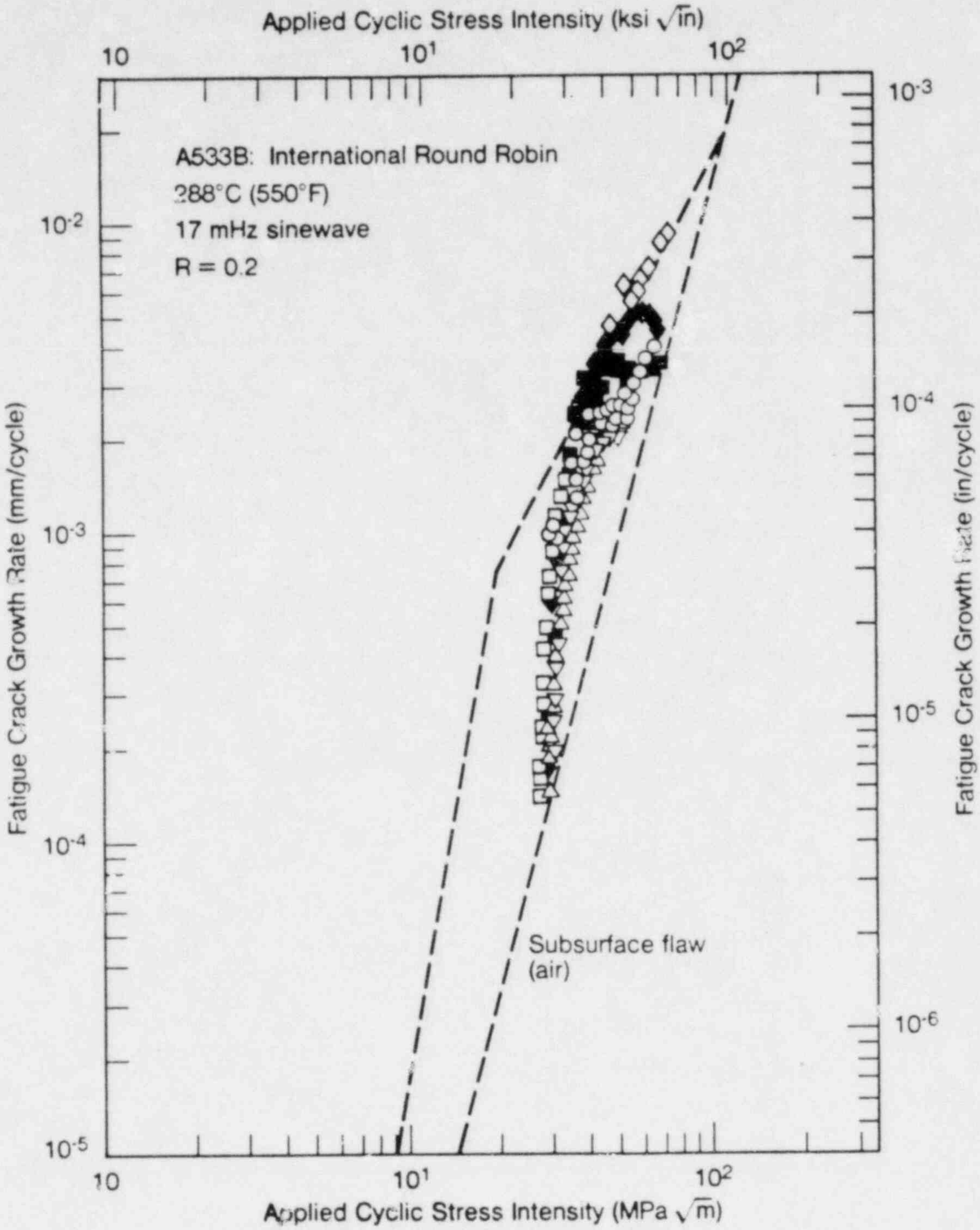

Figure 2. Fatigue crack growth rates vs applied cyclic stress intensity factor for A533B steel tested at a variety of laboratories using sinusoidal waveforms and low levels of dissolved oxygen. Ref. 1.

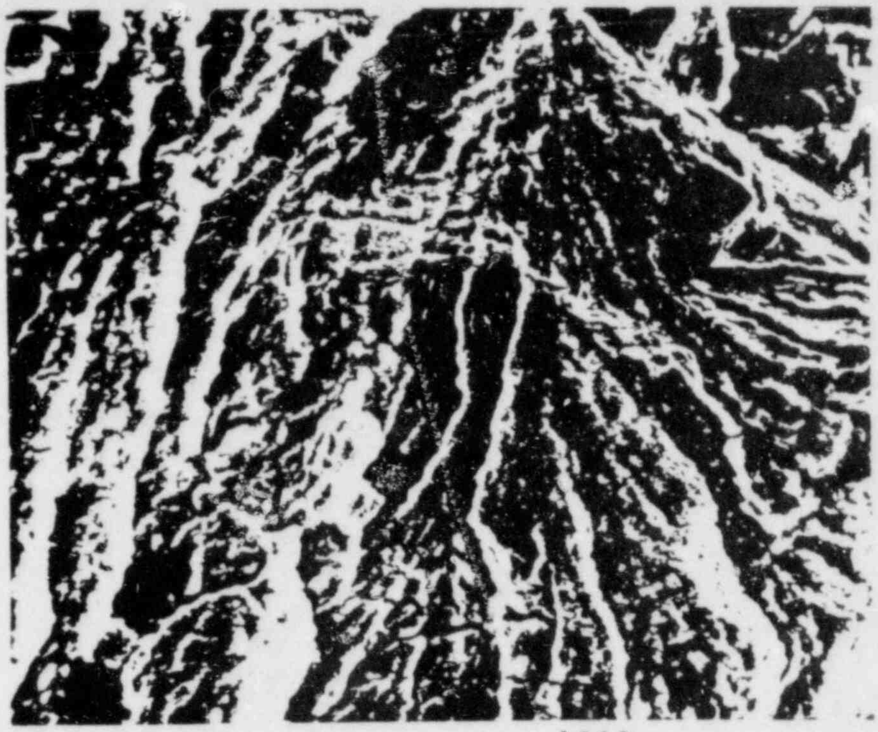

1000x

300x

Figure 3. Fractographic appearance of a specimen taken from the first round robin study showing evidence of brittle-appearing striations. The presence of these striations on environmentally assisted fatigue fracture surfaces suggests a hydrogen assistance crack growth mechanism may account for the increase in crack growth rates.

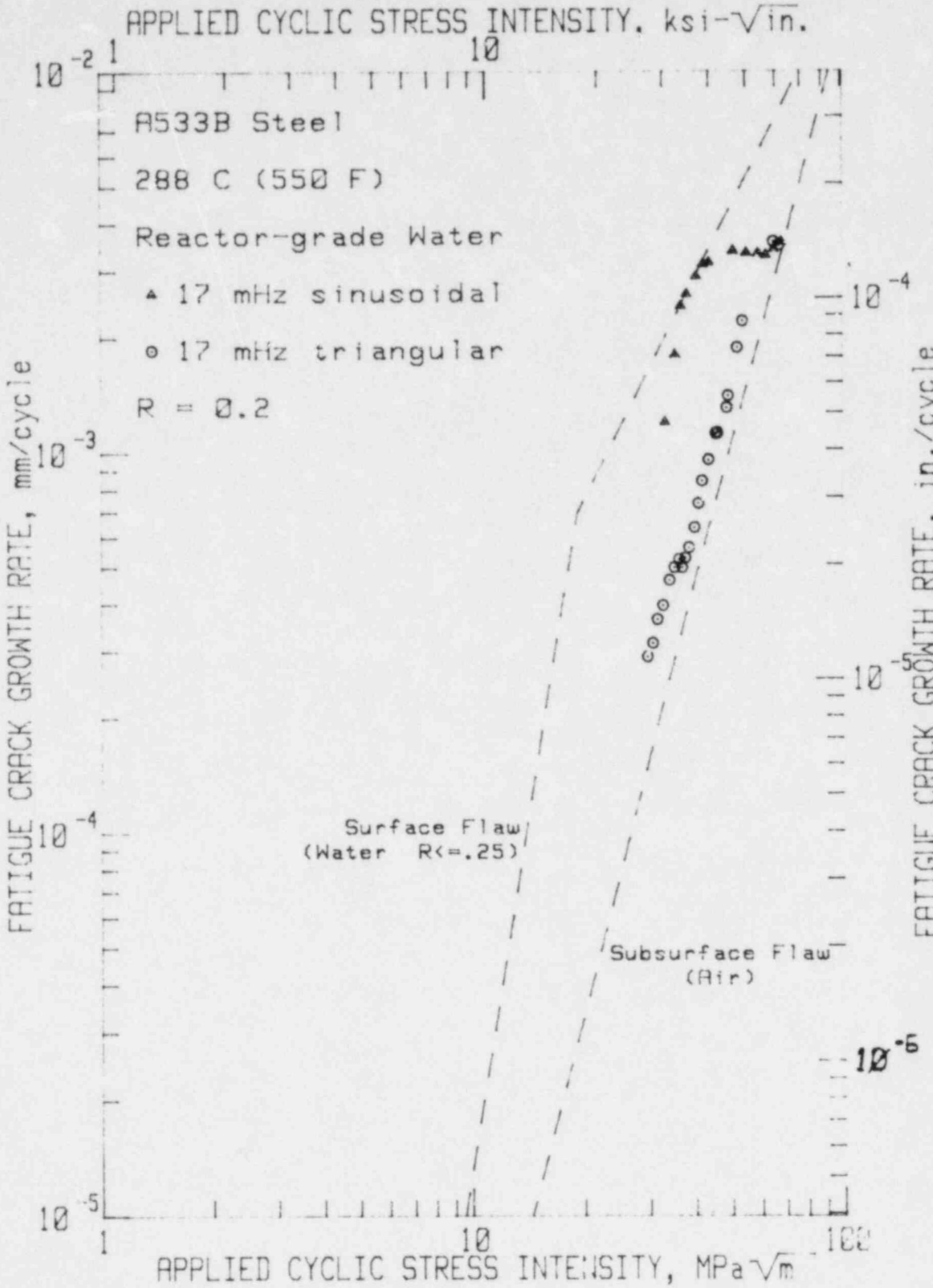

Figure 4. Fatigue crack growth rates vs applied cyclic stress intensity factor for A533B steel for two waveforms -- sinusoidal and triangular. This shows that the linearized waveforms result in lower crack growth rates than the sinusoidal waveforms.

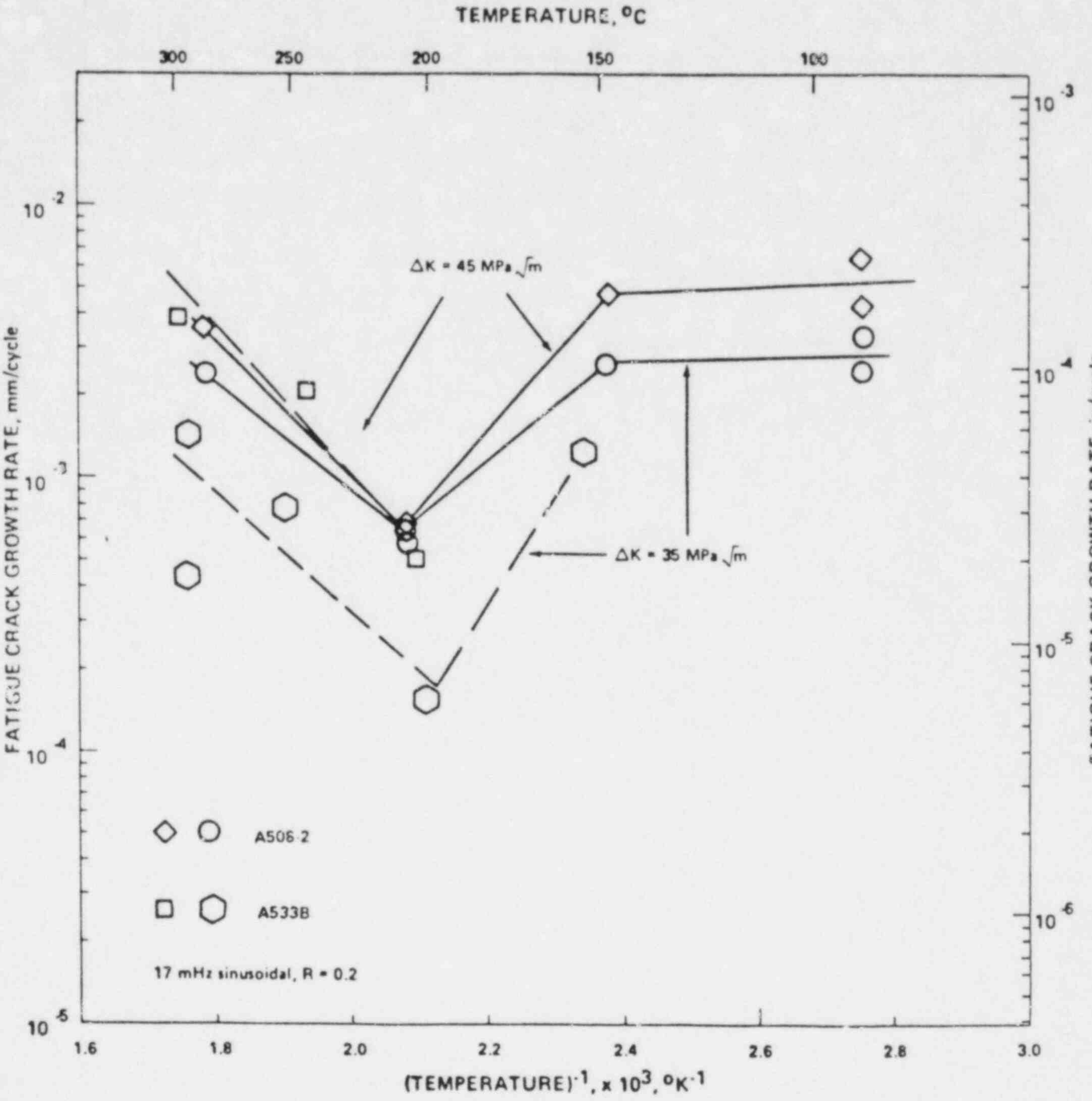

Figure 5. Fatigue crack growth rates at two ΔK levels as a function of temperature. This data shows that low alloy steels in a PWR-typical environment exhibit a minimum in growth rates at about 200°C.

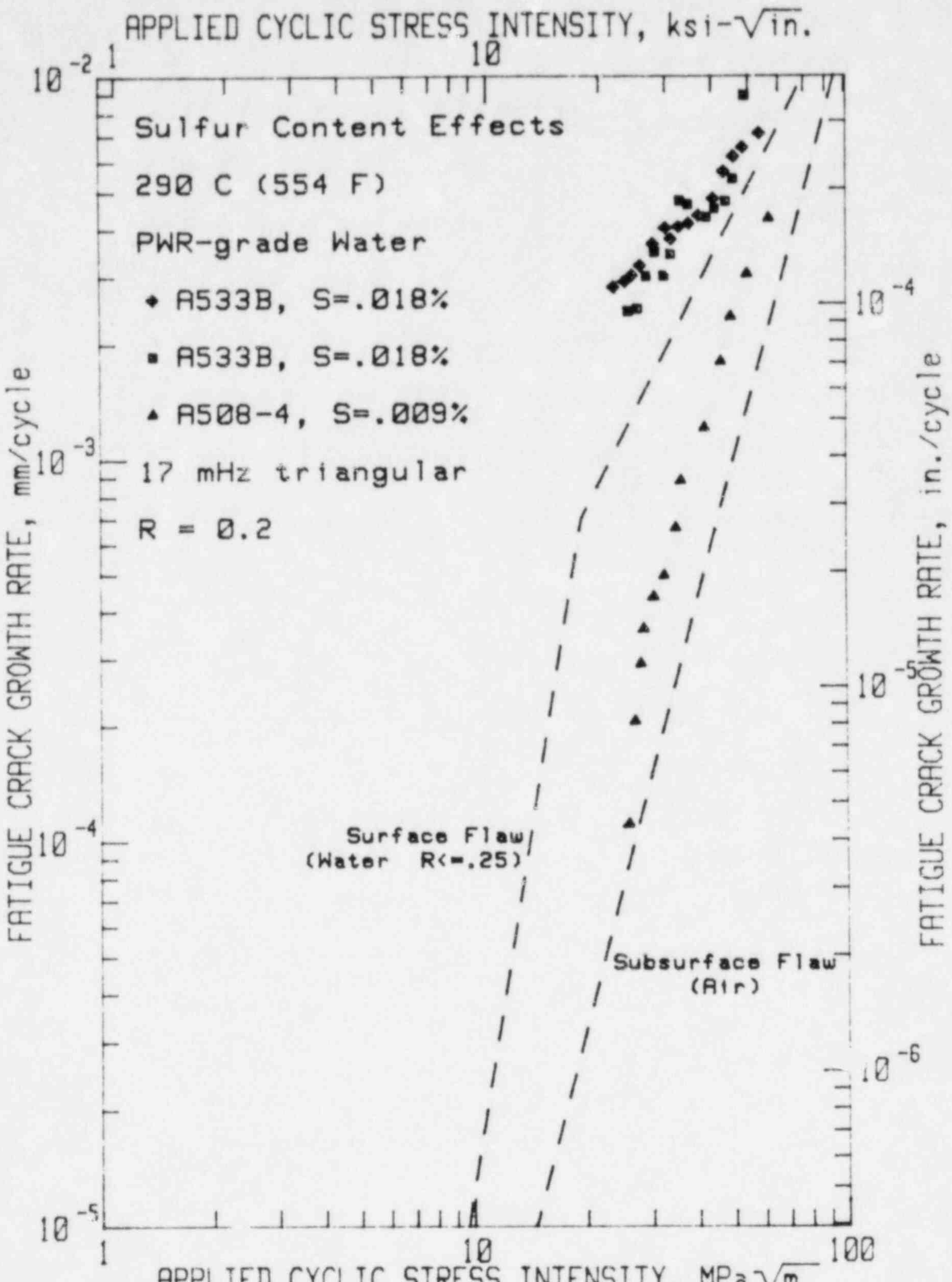

Figure 6. Fatigue crack growth rates vs applied cyclic stress intensity factor for two steels of different sulfur content, showing the increased crack growth rates for the higher sulfur level steel.

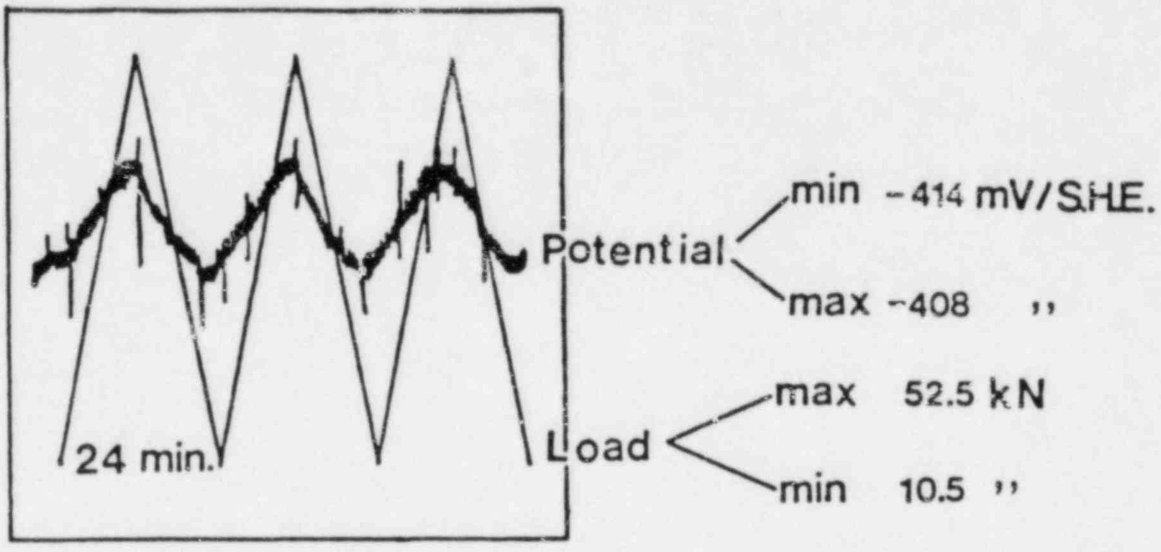

Figure 7. Applied load and free corrosion potential are plotted against time in this figure, showing that the potential increases as the load increases. These measurements were made with the CISE-developed crack tip potential probes.

PNL-SA-10804

STEAM GENERATOR INTEGRITY PROGRAM/ STEAM GENERATOR GROUP PROJECT

R.A. Clark, Project Manager
M. Lewis, Assistant Project Manager

Work Supported by
the U.S. Nuclear Regulatory Commission
NRC FIN No. B-2097
Dr. Joseph Muscara, Program Manager

Pacific Northwest Laboratory
Richland, Washington 99352

STEAM GENERATOR INTEGRITY PROGRAM/STEAM GENERATOR GROUP PROJECT

SUMMARY

The Steam Generator Integrity Program (SGIP) is a comprehensive effort addressing issues of nondestructive test (NDT) reliability, inservice inspection (ISI) requirements, and tube plugging criteria for PWR steam generators. In addition the program has interactive research tasks relating primary side decontamination, secondary side cleaning, and proposed repair techniques to nondestructive inspectability and primary system integrity. The program has acquired a service degraded PWR steam generator for research purposes.* This past year a research facility, the Steam Generator Examination Facility (SGEF), specifically designed for nondestructive and destructive examination tasks of the SGIP was completed. The Surry generator previously transported to the Hanford Reservation was then inserted into the SGEF. Nondestructive characterization of the generator from both primary and secondary sides has been initiated. Decontamination of the channelhead cold leg side was conducted. Radioactive field maps were established in the steam generator, at the generator surface and in the SGEF. Detailed planning and subcontracting was carried out for 1983 activities in eddy current examinations, tube unplugging, tube sheet section removal and secondary side characterization. Work was also continued on fabrication, nondestructive characterization, burst strength and leak rate determinations on stress corrosion cracked Inconel 600 tubing.

INTRODUCTION

Research in the SGIP began in 1976 with investigation into the remaining integrity of defected Inconel 600 steam generator tubes. Tubing specimens were fabricated with mechanically or chemically placed defects, simulating available knowledge on inservice defects. These specimens were subject to burst and collapse tests at steam generator operating temperature. Results from the mechanical integrity tests were used to derive constitutive equations relating remaining tube integrity to defect type and extent. Nondestructive characterization of the laboratory fabricated defect specimens utilized single and multifrequency eddy current techniques. Comparison with positive defect replicas allowed the establishment of confidence bands, associated with NDT accuracy, in the use of the constitutive integrity equations. However particular difficulties were encountered in the nondestructive characterization of laboratory fabricated stress corrosion cracks. The tightness of these cracks also precluded use of positive replication techniques. The lack of a definitive ability to precharacterize this type flaw has hampered efforts to conduct burst tests for correlation of the SCC defect with the constitutive integrity equation derived from tests employing an electro-discharge machined (EDM) notch, crack simulation. To resolve the characterization problem a round robin eddy

*The Surry 2A generator was obtained through the cooperation and assistance of the Virginia Electric and Power Company.

current examination was conducted on 10 SCC specimens with subsequent metallographic validation. The conclusions of this round robin have just recently become available and will allow completion of tube integrity testing for this defect type. One observation from the laboratory generated defect portion of the program is that present eddy current techniques exhibit deficiencies in the reliability of detection and accuracy of sizing for low volume defects, particularly stress corrosion cracks.

In addition to tube integrity tests and validation of NDT defect characterization, leak rate tests are conducted on failed or through wall defected steam generator tubing. These tests are conducted by pressurizing a tube with 300°C water which is leaked to air. The leak rates associated with a tube burst failure are established for pressure differentials up to 2500 psig, simulating a main steam line break (MSLB). Other specimens are not burst test prior to leak testing, but are fabricated with a through wall stress corrosion crack. Leakage is measured at normal operating pressure differentials then examined as a function of increasing pressure differential up to 2500 psig. Of particular concern is defect stability. Definitive information is sought on what a length through wall SCC, in terms of leakage at normal operating ΔP, becomes unstable under a MSLB pressure transient. Only the burst testing and leak rate tests on SCC tube specimens remain of the initial laboratory defect program elements.

Laboratory results on tube integrity models required confirmation on real service produced defects. Early program results indicated that current inservice inspection (ISI) eddy current techniques may have shortcomings in reliability of defect detection and accuracy of defect sizing. In addition there were attempts (under another NRC program) to provide an ISI inspection model. This model would determine frequency and extent of tube inspection necessary to provide a certain reliability of tubing between generator inspections. However necessary inputs, such as validated NDT accuracy on service defects and defect distribution, within a generator were missing. A search was initiated to obtain a suitable inventory of service defects. This led to the conclusion that the only source of sufficient suitable defects would be from a steam generator removed from service. At the time the Surry generators were the only units scheduled for removal. Investigations were conducted into suitability of these units for research use. Finding them suitable, studies were made on siting, transportion, options, and facilities availability, followed by licensing for transportation of a Surry generator to Hanford. Having obtained a service degraded steam generator for research purposes, program definition was expanded to maximize potential benefit from this unique resource. In addition an expanded sponsor base was sought as a condition for conducting parts of the expanded program. The research program as currently configured provides inputs not only into safety related issues, but also addresses items that concern operation and reliability. Figure 1 shows the task breakdown structure.

The primary objectives of SGIP activities utilizing the Surry steam generator are: 1) to provide a validated database on eddy current reliability of detection and accuracy of sizing for service induced flaws, 2) validate laboratory models on tube integrity through burst testing service degraded tubing, 3) provide an evaluation of the extent of ISI conducted versus probability of detecting potential tube failures during the subsequent operating period, 4) assess degradation in current potential problem areas, such as the tube sheet crevice, 5) study secondary side cleaning and primary side decontamination schemes for effectiveness, damage to steam generator components, effect on post application nondestructive characterization, radioactive waste generation, and health physics associated with application and radwaste handling, 6) test suggested repair methods for effectiveness, subsequent effect on NDT and operational safety, and health physics associated with application. Program provided results will serve as inputs to regulations on inservice inspection and tube plugging criteria. They may also assist on regulatory decisions regarding application of secondary side cleaning, primary side decontamination and repair techniques. From the operational and reliability standpoint, benefits include definition of effectiveness and safety associated with application of cleaning, decontamination or repair processes. Also potential improvements in NDT will be subject to validation. Improved NDT can lead to improved operational reliability.

ACCOMPLISHMENTS OF FY 1982

Steam Generator Examination Facility (SGEF)

The SGEF completed in December 1981 consists of a five story tower plus two story support area. The tower is designed to contain the research steam generator in its normal vertical operating position. The entire tower is double HEPA (High Efficiency Particle Acceptor) filtered. Services available in the tower include a 30,000 lb. bridge crane, a 2000 lb. jib crane, a portable rigid greenhouse for cutting operations, (with an independent third stage of HEPA filtration) breathing air, instrument air, vacuum inert gases and several voltage levels of power. The tower is also prewired for data transmission to an adjoining computer facility. A 2000 gallon liquid radwaste tank and transfer pump are located in the basement. The support structure contains a two story HEPA filtered truck lock, a laboratory with triple HEPA filtered hoods, change rooms, a central monitoring station, and a mechanical room with HVAC equipment, breathing air compressor, central vacuum system and heat recovery system. Operations in the facility can be monitored remotely from the central monitor station with audio, video, and radiation monitoring devices.

Placement of the Steam Generator into the SGEF

On January 11, 1982, the Surry generator was loaded through a removable roof panel into the SGEF tower. This task performed under subcontract by Neil F. Lampson, Co. involved transporting the generator from an interim storage site approximately 1 mile to the SGEF. The generator was then upended to a vertical position, using an excavated pit filled with sandbags as a pivot point to prevent damage to the generator. A 45 meter lift was then made using a single double-boom crane. The generator was then lowered into the SGEF tower and fastened to the support stand in the SGEF. The task was completed without incident and with less than 1.5 man-rem total exposure to workers.

Secondary Side Examination Through Preshipment Penetrations

Prior to transporting the generator from the Surry Nuclear Station, Surry, Virginia, to Hanford, Washington, an examination of the secondary side was conducted through three shell penetrations. These foot square penetrations were located in the tube lane astride the first support plate, just below the seventh (uppermost) support plate, and at ~45° from the tube lane on the hot leg side just below the fourth support plate. The intent of the examination was to document the generator condition at Surry, to assure that storage at Surry had not appreciably changed the units condition, and to assess if the unit was in transportable condition. Photographic documentation, corrosion product samples, and dimensional measurements were taken.

After placing the generator into the SGEF a repeat of the preshipment examination was conducted. Patches welded over the shell penetrations were ground off. Hinged shielding doors were then attached to the generator along with shielding plates adjacent to the openings. This provided three doors permanently available for secondary side generator access. Repeats of the preshipment photographic, corrosion product and dimensional documentation were conducted. Corrosion product composition remained the same in the two tube lane penetrations, indicating success of the inert gas (argon, helium) environment kept in the generator secondary side during transport and storage. Weld splatter from the off tube lane cut (at 45°), a low point in the horizontal transport mode, indicated by the presence of hematite that moisture had been present. In fact after transport the generator low point was tapped and several gallons of water removed. Analysis of this water showed a low Cl^- content. Thus condensation or water hidden in steam generator tubes was the probable source. Internal dimensions remained the same, i.e., measurements across flow slots. The generator internal structure moved slightly (~½") in the vertical direction relative to the shell. This is probably due to system elasticity since measurements at Surry were taken with the generator in a horizontal position and at Hanford in a vertical position. Photographic documentation indicated that loose corrosion scale had redistributed as expected. In addition inner-row U-bends that showed crack-like striations at Surry, had in a couple instances cracked open along those striations.

The generator visual observations made during the preshipment examination were extended further into the secondary side and photographically documented. These observations indicate that all support plate flow slots below the uppermost support plate, have essentially closed due to 'hourglassing'. Most of these flow slots are deformed only from the hot leg side with the cold leg remaining straight. Several flow slots have closed by cracking at the hot leg side corners. Pieces of support plate appear to be missing in several cracked flowslot corners. A couple small pieces of support plate have been found at non-support plate positions in the generator. Due to first support plate flow slot closure hot leg tubes in the flow slot tube columns exhibit what appears to be a bending at the tube sheet to tube intersection. Corrosion product samples indicate compositions of Fe-Ni-Cr spinels, and metallic copper.

Primary Side Examination

Primary side examinations have been limited to date to inspection of the hot and cold leg sides of the channelhead. These inspections revealed that several plugged tubes were still leaking water. Several liters of water were removed from both channelhead sides. The stainless steel strip clad on the channelhead bowl exhibited corrosion along the strip clad lap lines. The channelhead divider plate and the Inconel cladding on the tube sheet bottom showed no obvious corrosion.

Radioactivity Field Mapping

Field mapping was conducted on the steam generator surface, through the generator secondary side penetrations, into the channelhead manway and throughout the SGEF tower. These measurements were made as inputs to work procedure preparation to establish ALARA exposure for researchers. Measurements used strings of TLD's (thermo luminescent dosimeters) run along the generator surface, inserted into the generator via a plastic tube, and hung between floors in the SGEF. Portable ionization counting instruments were also used. Figure 2 illustrates a typical surface contact radiation field map of the steam generator. Maximum readings were ~150 mR/hr. Figure 3 shows a typical field map prepared for a region of the SGEF tower. Immediately inside the secondary side shell penetrations a field of 1-2 R/hr. exists. Mapping through the tube bundle the highest fields recorded were ~11 R/hr. The channelhead before decontamination remeasured between 3.5 and 5 R/hr. Shielded TLD's indicated the channelhead surface at 3-½ R/hr. Current measurements are determining vertical field distribution by insertion of TLD trains up through the primary side of selected steam generator tubes. A radionuclide mapping is planned, also through the primary side of steam generator tubes.

Channelhead Decontamination

The primary programmatic reason for channelhead decontamination is to reduce radiation exposure to researchers needing primary side access. However, it was realized that the availability of this unit might allow demonstration of the effectiveness of near commercial technologies, without the normal time constraint of operating reactors and with some ability to accept the risk of first time application. Based on response to a competitive bid procurement it was determined that two dilute reagent chemical decontamination schemes could be tried, one each on hot leg and cold leg sides of the channelhead. Chemical decontamination offers the opportunity for low radiation exposure during the application because there is no need to attach equipment the inside channelhead, and the operation is largely remote. Also there is potentially significant opportunity for reduced secondary waste volume compared with grit blasting methods. The element of first application risk involves the effects of the chemicals on generator materials and the ability to remove the chemicals from the system. Also in question is the effectiveness on PWR films. Two different techniques were chosen, a Candu process and a LOMI process, each applied by a commercial vendor. At the time of this writing we are just involved in the application of the first of these, and thus have no results to report. Prior to application, core samples were removed from the channelhead surfaces to allow predecontamination surface film characterization. Also a number of coupons have been placed in the channelhead to evaluate effects of the decontamination reagents. These coupons include stressed bend samples and various metal couples. In addition, a sample of steam generator tubing removed from just below the U-bend area is included to assess effects on the Inconel 600 tubing. A decontamination factor of 10 is the goal sought in these applications.

Nondestructive Examination and Data Analysis

Numerous preparations have been made for the extensive NDE to be conducted in the coming fiscal year. This included identifying and purchasing NDE primary side inspection probe positioning and indexing equipment and developing a computer interfaced probe pusher-puller that automatically indexes probe position with the eddy current or other NDE signal. Eddy current (EC) information will thus be locatable without having to listen to a voice track. Software has been completed that allows direct computer processing of EC data during inspection. This will provide readily accessible archives and also serve as data base for studies on computer aided EC signal interpretation, i.e., through pattern recognition techniques. During the year we have completed archiving historical information on the research generator. This includes data bases from Westinghouse, VEPCO, and the NRC, and contains histories for tube plugging, water chemistry, and operation. This database is initially being used to determine which of the plugged tubes should be unplugged to maximize the defect database for subsequent NDE validation studies.

Round Robin Eddy Current Examination

A round robin was conducted on ten specimens containing laboratory induced stress corrosion cracks. This round robin was initiated to determine if an adequate method of nondestructively characterizing stress corrosion cracks was available. Such a method could then be used to characterize SCC specimens allowing completion of burst and leak test studies on laboratory fabricated specimens. Results from 8 of the 10 round robin specimens are presented in Table 1, the other two specimens are undergoing metallographic characterization. Several specimens actually had multiple cracks, the worst case crack is listed. No team consistently sized all defects. However at this time a couple teams appear to be averaging better than the others, and one of these, Team F, is almost always conservative in their defect sizing. We plan to establish the best two overall team results, have these two teams inspect remaining specimens for burst and leak rate testing, and use an average defect characterization.

ACTIVITIES FOR FY83

The following task actions are planned in the order shown for FY 1983 research.

- Profilometry will be conducted on 150-200 tubes along the hot and cold leg sides of the generator. This will determine deformation state in the generator and allow acquisition of appropriate eddy current probes.

- Secondary side characterization via fiberoptic examination and corrosion product sampling/analysis.

- Approximately 500 of the 748 plugged tubes will be unplugged to maximize access for NDE and other studies.

- Post service baseline EC inspection of all accessible tube regions of the generator. Inspections will be conducted using a single frequency EC technique (Zetec EM3300), and two multifrequency techniques (Zetec MIZ12, Intercontrole IC3FA).

- A section of tube sheet will be removed for destructive characterization. Corrosion products will be characterized, tube and tube sheet degradation investigated, and NDE reliability validated for detection and sizing and any defects found.

- Completion of burst and leak rate tests on laboratory SCC specimens.

TABLE 1

STRESS CORROSION CRACKED SPECIMEN ROUND ROBIN TEST

TUBE NUMBER	TEAM A	TEAM B	TEAM C	TEAM D	TEAM E	TEAM F
B34-4 Actual- Maximum Depth 64%(1)	100% thru-wall	65% 52%	80%	ID Bobbin Coil-64% OD Absolute Coil-56%	40% 59% 40% 35%	82%
B49-4 Actual- Maximum Depth-81%	60%	72% 68%	10% 70%	ID Bobbin Coil-70% OD Absolute Coil-20-49%(2)	63% 40%	80%
B45-9 Actual Maximum Depth-52%	60-70%(2) (2 cracks)	26% 28% (multiple cracks)	20%	ID Bobbin Coil-40% OD Absolute Coil-52%	44% 36% (2 cracks)	84% (2 cracks)
B45-2 Actual Maximum Depth-63%	20-30% (2 cracks)	36% 25% (multiple cracks)	20%	ID Bobbin Coil-26% OD Absolute Coil-48%	58% 50%	74%

TABLE 1 (cont.)

B45-9 Actual Maximum Depth-66%	60-70% (2 cracks)	67% 68% (multiple cracks)	65% 15% (2 cracks)	ID Bobbin Coil-50% OB Abolsute Coil-15%, 45%, 20-56% (3 cracks)	56% 49%	84%
B46-10 Actual Maximum Depth-47%	20-30%	35% <20% (multiple cracks)	40%	ID Bobbin Coil-24% OD Absolute Coil-44%	40% 35%	32%
B61-8 Actual Maximum Depth-54%	20% 40% (2 or 3 cracks)	41% 37% (multiple cracks)	25% 40% (2 cracks)	ID Bobbin Coil-24% OD Absolute Coil-52%	44% 45% 44% (3 cracks)	50%
B63-2 Actual Maximum Depth-67%	50-60% (2 cracks) ~180° apart)	82% 50% (multiple cracks)	60% 80% 50% 20% (4 cracks)	ID Bobbin Coil-44% OD Absolute Coil-20-58%)	63% (multiple cracks)	85% (multiple cracks)

1) Only maximum depth of largest defect shown. Some specimens have multiple cracks.

2) Indicates range of depth of a given crack.

3) Multiple entries are for maximum depths of major cracks.

MILESTONE CHART
SURRY GENERATOR PROGRAM

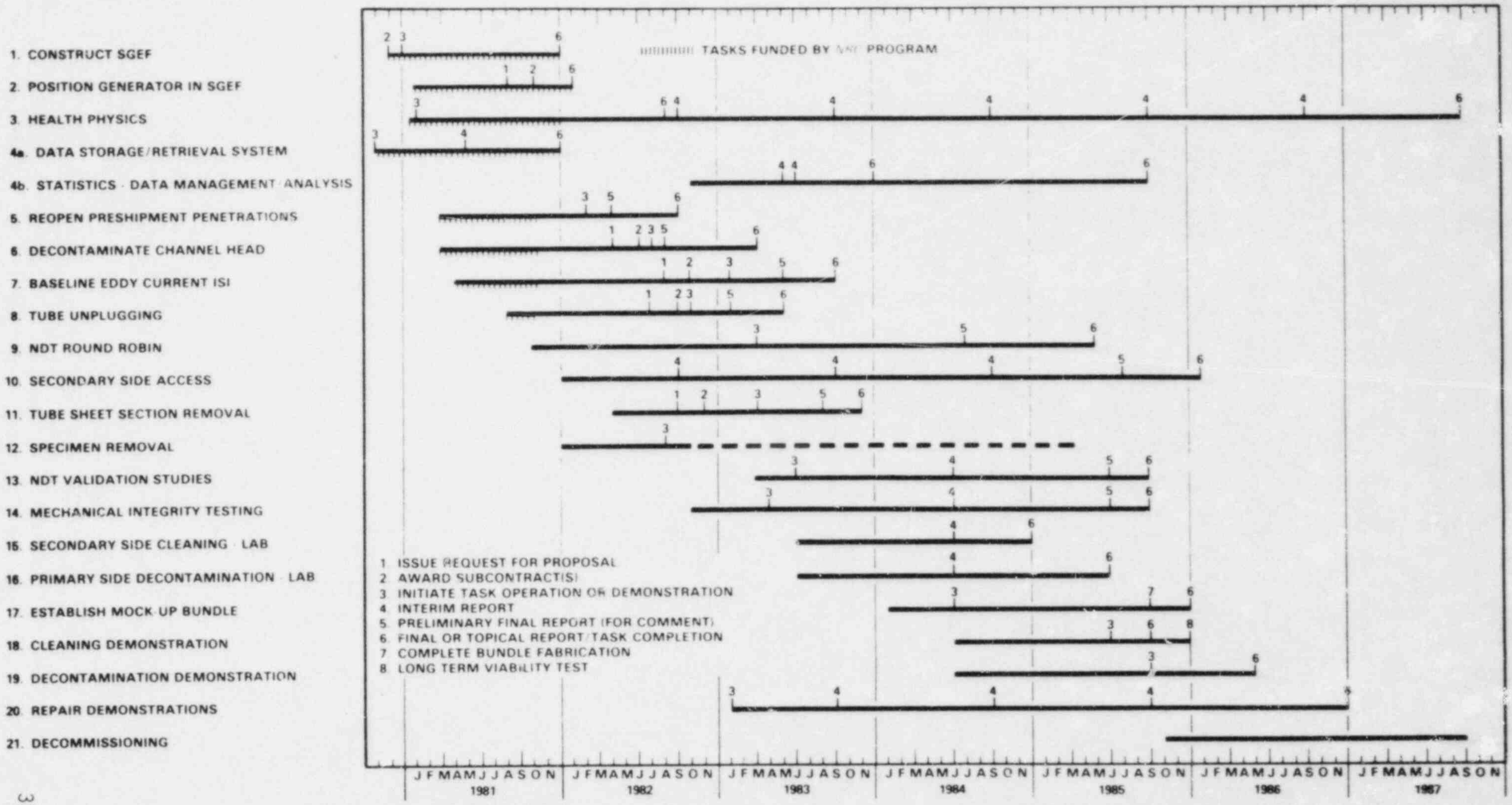

FIGURE 1

SURRY STEAM GENERATOR

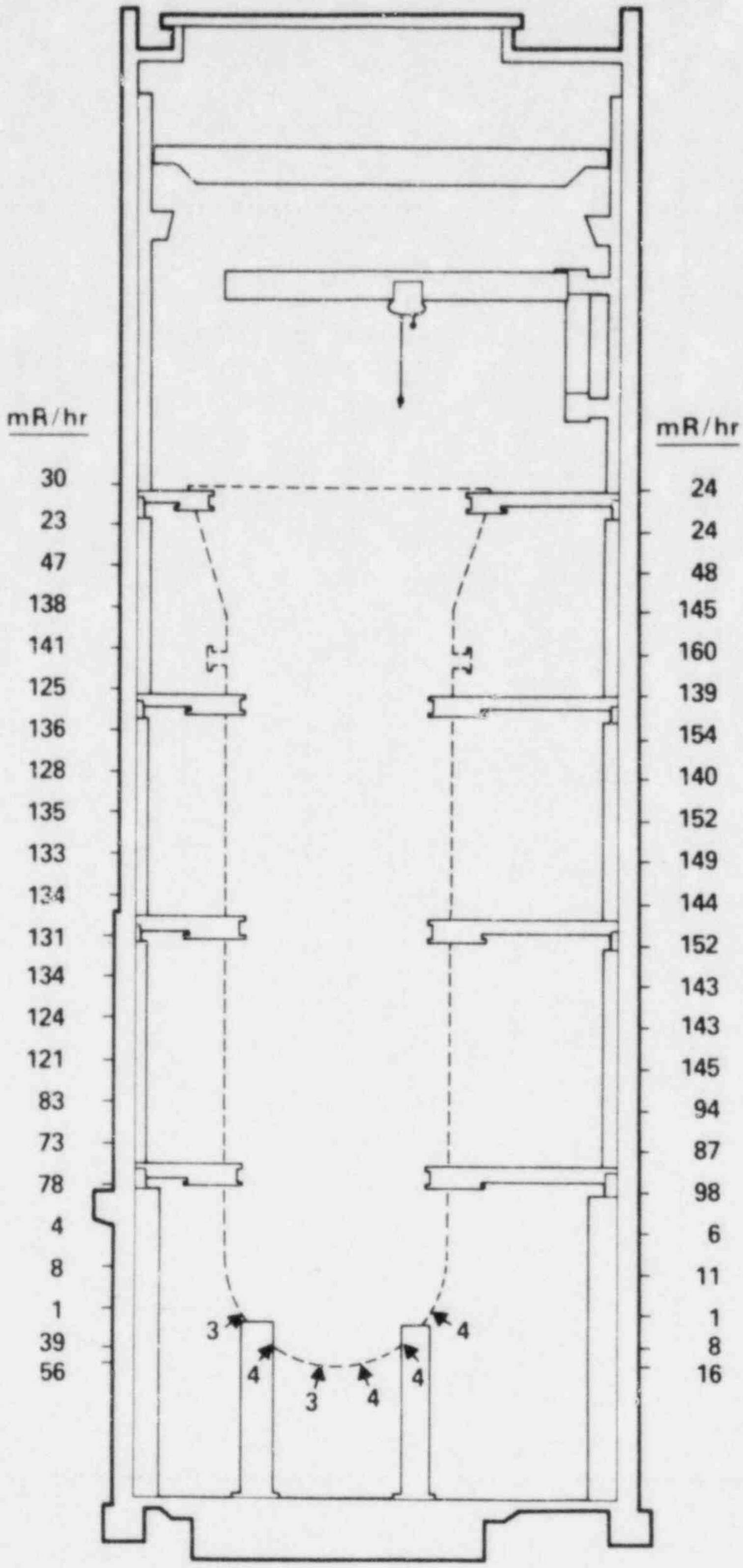

ALL EXPOSURES IN mR AT CONTACT

FIGURE 2

RADIOLOGICAL SURVEY DOSE PROFILE OF SURRY STEAM GENERATOR

LEVEL - 1st FLOOR

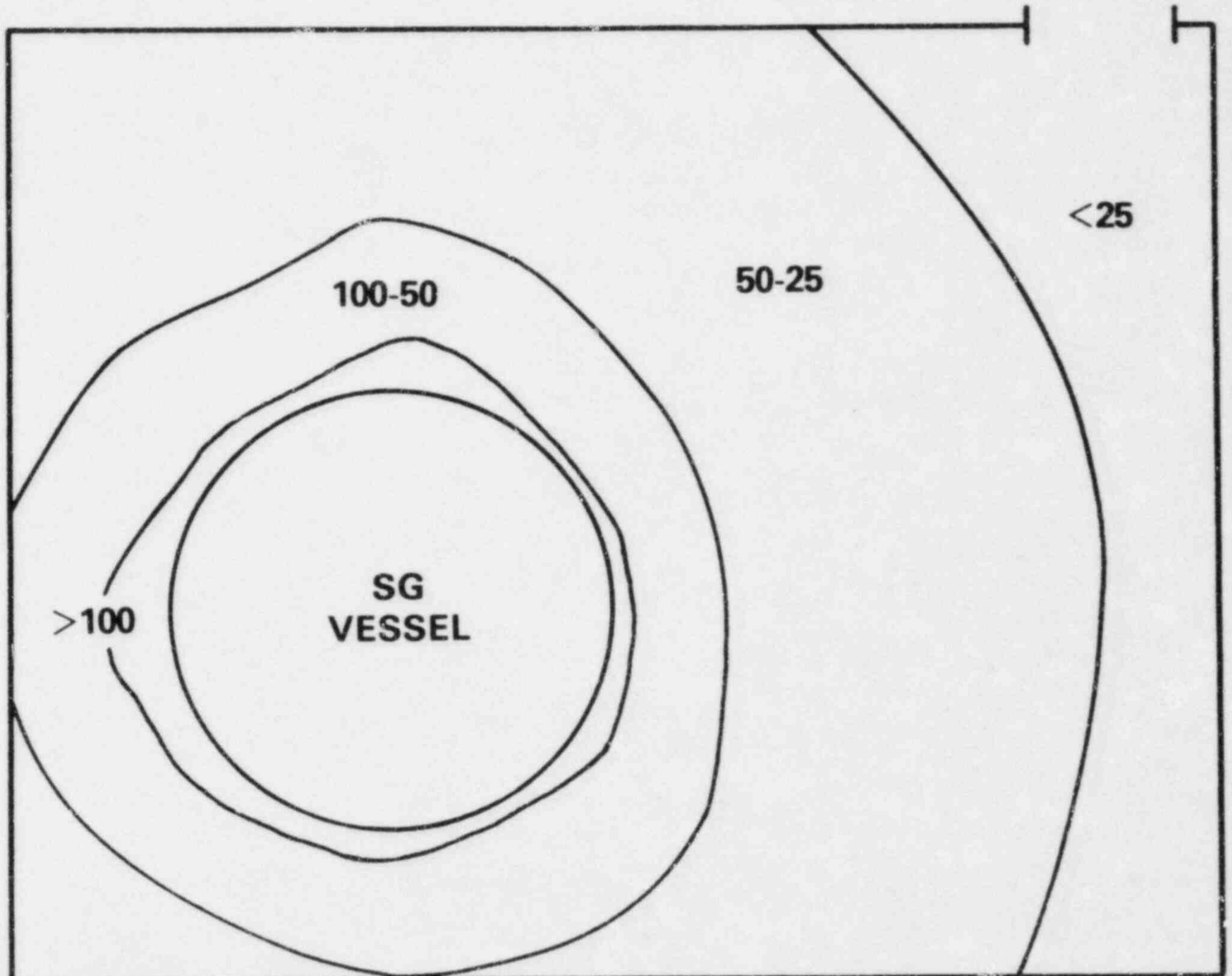

*DOSE RATES ARE IN mR/hr

FIGURE 3

BNL-NUREG-31814

TESTS WITH INCONEL 600 TO OBTAIN QUANTITATIVE STRESS CORROSION CRACKING DATA FOR EVALUATING SERVICE PERFORMANCE*

R. Bandy and D. van Rooyen

Corrosion Science Group
Department of Nuclear Energy
Brookhaven National Laboratory
Upton, New York 11973

NRC Program Manager: A. Taboada

*Work Supported by the U. S. Nuclear Regulatory Commission, Office of Nuclear Regulatory Research.

EXTENDED ABSTRACT

Inconel 600 tubes in pressurized water reactor (PWR) steam generators form a pressure boundary between radioactive primary water and secondary water which is converted to steam and used for generating electricity. Under operating conditions the performance of alloy 600 has been good, but with some occasional small leaks resulting from stress corrosion cracking (SCC), related to the presence of unusually high residual or operating stresses. The suspected high stresses can result from either the deformation of tubes during manufacture, or distortion during abnormal conditions such as denting. There have also been a few minor leaks that were not positively identified as stress corrosion cracks because the tubes were merely plugged without removal for examination. It is not yet certain what long-term effects are to be associated with lower stress levels that would be encountered during usual temperature cycles of a steam generator in service.

A primary to secondary leak causes contamination of the environment to some degree, and for this reason the Nuclear Regulatory Commission (NRC) is involved in a licensing decision whenever leaks are reported. In order to assist the NRC in making decisions concerning the licensing of a plant with SCC defects, data are necessary that could be used for predicting or estimating failure times when abnormal conditions are encountered. A program is active at present at Brookhaven National Laboratory to examine the factors involved in the SCC of Inconel 600 in high temperature deaerated water, with the objective of developing a model that will relate life expectancy of tubing to factors such as stress, strain, strain rate, environmental conditions, microstructure and cold work of the material. Such a model is intended to form the basis for determining a predicted life expectancy for an "unknown" by extrapolating one or two accelerated data points to operating conditions. This could then be used in various cases to assist in determining tube plugging or inspection criteria.

The present experimental program addresses two specific conditions, i.e., 1) where deformation occurs but is no longer active, such as when denting is stopped and 2) where plastic deformation of the metal continues, as would occur during denting. Laboratory media consist of pure water as well as solutions to simulate environments that would apply in service; tubing from actual production is used in carrying out these tests. The environments include both normal and "off" chemistries for primary and secondary water.

The results reported here were obtained in several different tests. The main ones are 1) split tube "reverse" U-bends, 2) constant extension rate tests (CERT), and 3) constant load. The temperature range covered is 290-365°C.

U-BENDS:

Split tube type U-bends have their inside surfaces exposed in tension. Using these specimens, a first series of experiments suggested a possibility that the carbon level of the Inconel influences the crack initiation/ temperature relationship. Specifically, activation energy seemed to increase with increasing carbon content. These data are based on cracks observed in the temperature range 325°C to 365°C, with most of the data from the highest temperature levels. Since the temperature range is small, it obviously remains important to verify that this effect persists down to operating temperatures. There is also some scatter in stress corrosion data in general, and the present tests are no exception; therefore, a statistical analysis was deemed necessary and tests were started in the first half of 1981 in which a larger number of replicate samples are exposed in water at 290 and 315°C. These U-bends had been in test for 60 weeks at the previous inspection without any observed cracking; it should be noted that little or no cracking is expected during such a short exposure. Figure 1 shows the data points in the U-bend tests, and Figure 2 shows the tentative activation energies plotted against carbon contents. For the 0.02% material, one test at 290°C and one at 315°C have now exceeded, without SCC, the times at which SCC would have been predicted by extrapolation. The expected failure times are shown in Table 1. At least for 0.02%C, therefore, the activation energy may be greater than 36 Kcal/mole over the lower temperature range, which includes operating temperatures. The other materials (.01, .03 and .05%C) have yet to reach points of intersection with the extrapolations of the high temperature portions of the curves. When sufficient data are available, we will use statistical methods (such as Weibull) to develop the final, quantitative model. The heats that are now exposed at 290 and 315°C, cover the range of 0.01 to 0.03% carbon, and a few (8) of the original specimens with 0.01, 0.02, 0.03 and 0.05%C also remain in the 290°C test. The latter 8 samples have reached 192 weeks without SCC.

CERT:

CERT data so far have shown a distinction between the initiation and propagation stages. Cracks do not initiate at the start of plastic deformation, but take a finite time (after that) to develop, and initiation times are much shorter than in the U-bend exposure. Extrapolations were made to determine the onset of SCC in CERT at temperatures of 325°C, 345°C and 365°C. These curves, shown in Figure 3, were obtained with specimens made from production tubing, flattened before cutting tensile specimens. For the present, corrections based on these curves also are used for calculating crack propagation rates in undeformed materials; similar initiation corrections are being developed for as-received tubing. Cracking in the CERT was achieved readily in cold worked or as-received material at strain rates in the vicinity of 2×10^{-7} sec^{-1}. As will be shown below in more detail, the activation energies for cold worked and non-cold worked Inconel 600 were found to be identical, suggesting that the mechanism is the same in the two cases, although the crack growth velocities for the types of specimens are different.

Figures 4 and 5 show the straight line Arrhenius plots of CERT data obtained to date. Several sets of points provide parallel curves that correspond to an activation energy of 33 Kcal/mole. Some additional observations based on the CERT data can be detailed as follows:

1. The slopes of the lines remain consistent with an activation energy of 33 Kcal/mole regardless of whether the material is cold worked, aged (365°C), or mill annealed.

2. Crack growth rates are faster in cold worked material due to a change in the constant k of the Arrhenius equation:

$$\text{Rate} = k.\exp\left(-\frac{Q}{RT}\right)$$

3. Environmental conditions may also affect the quantitative aspects of SCC. Hydrogen (added to pure water) increases the number of cracks as well as SCC growth rate of as-received material while H_3BO_3 does not appear to have this effect. Other combinations of the ingredients of primary and secondary water are in test now.

4. An "unknown" tube can now be tested in one accelerated test to establish its initiation and propagation rates, and data for other temperatures can be calculated from this determination.

5. Cold worked (flattened) specimens gave crack growth rates in simulated AVT and primary water consistent with rates observed in pure water. Tests with as-received material will be completed this year.

6. Specimens aged (furnace) at 365°C for several weeks before exposure in pure water (CERT) gave crack growth rates similar to fresh material.

7. Crack growth velocities in our work are in the same ranges as were found in published work for tests is sodium hydroxide solutions at elevated temperatures. (See Figure 4.)

8. Strain rates in the range 3×10^{-8} to 1×10^{-6} sec^{-1} were used for producing SCC, and it seems necessary to adjust the rate downwards in order to see SCC in the more resistant materials.

9. Temperature exerts a much greater influence on crack velocity in CERT than strain rate. The latter, within the range used, has had an effect of less than a factor of 2, and there are no plans now to examine the effects of strain rate any further. Most of the present tests are done at about 2×10^{-7} sec^{-1}.

10. Extrapolation of data from cold worked samples shows initiation at approximately 10% strain at operating temperature, as shown in Figure 6. This number appears to be in good agreement with what has been observed in the field when denting led to stress corrosion cracks in deformed Inconel tubing. A comparison of SCC times based on the laboratory data (using susceptible Inconel) with the field observations show considerable promise that the laboratory data can indeed be used to predict service performance. (See 11. below.)

11. An example of an extrapolation is as follows: Laboratory tests for as-received material in pure water indicate a crack velocity at 300°C of about 5×10^{-8} mm sec^{-1}. In order to achieve observable cracking in the CERT, strain rates at these low temperatures appear to be of the order of 1 to

5×10^{-8}. Assuming that a strain rate of 2.5×10^{-8} is observed, we can use this to show that it will take almost two months to reach 10% strain at which time cracks will initiate. At this temperature (for tubing that has not been cold worked), the crack velocity will be approximately 5×10^{-8} mm sec^{-1} based on presently available data, so that it would take approximately four to six months for cracks to propagate 60% through wall. A series of more accurate calculations will be made within the next few months when more refined data are available. However, it is evident that reasonable predictions can already be made for the case of active deformation.

12. A point to keep in mind is that the actual conditions of stress, strain and strain rate under operating conditions would have to be known, or calculated, in order to use the quantitative SCC data predictions to best advantage.

13. Figure 7 shows a comparison of the stress-strain curve for heat #2 in the as-received, mill annealed condition, with another that had first been subjected to a heat treatment of 20 hours in Ar at 700°C. This latter treatment is equivalent to the latest commercial method used to induce chromium carbide precipitation, which is believed to provide resistance to SCC in deaerated high temperature water. The as-received specimens showed intergranular failure, whereas the material after 700°C treatment showed a ductile fracture with only extremely shallow intergranular penetration at one point on the surface. This is an encouraging result, because the laboratory heat treatment was but a single step following after a processing procedure that obviously was quite "adverse" in terms of SCC resistance. In future production, we believe that the prior processing may be arranged to optimize the effects of the final 700°C heat treatment, and may well produce even greater resistance to this kind of SCC.

More tests are planned with samples of commercial (700°C treated) tubing, and these will include a range of strain rates to obtain comprehensive data, including primary coolant conditions.

<u>CONSTANT LOAD:</u>

For the case where denting or active deformation is no longer occurring, it is necessary to obtain data that relate the time to failure to the stress present in the surface of the material, i.e., the load on that part of the tube. These stress patterns can consist of residual plus operational stress, and may be complex. In the present test series, a first attempt at relating load to SCC failure time is made by means of tensile specimens under applied load. This will be compared with simulated dents in order to find out how the quantitative values compare for this type of failure in Inconel. Figure 8 shows the curves for stress versus failure time on logarithmic scales, including results for as-received and cold worked material. In the equation $T_F = k. \sigma^b$, the slope of the two parallel log-log curves correspond to a value of $b = -4.0$, in the range that has been studied so far. This is a much more reliable number than the previously reported value for b which was based on fewer data. Figure 9 shows 2 points of data obtained in simulated rimary water at 365°C, where the slope agrees with the pure water plots. Figure 10 is taken from the work of Theus (B&W) in caustic for comparison with our results.

In the cold worked material, the cold work resulted from the flattening of the tube specimens during the preparation of the tensile pieces. These cracked more readily than the as-received material, in agreement with the findings in CERT, but the stress dependence is the same.

One test has shown SCC at a stress level below the yield point in as-received Inconel 600, and relates to the important question whether the quantitative equation can be applied to stresses well below the yield point.

It is intended to combine the CERT data with the U-bend and or constant load results in one equation for translating exposure under known operating conditions into future performance, taking into account the spread to be expected within extrapolations.

Since cold work is an important parameter in accelerating SCC , although it is obviously not a prerequisite for cracking to occur, it will be examined in more detail. In practice, tubing is shaped, e.g., into U-bends, rolled into tube sheets, straightened without subsequent annealing during manufacture, and there are certain to be many other sources of residual stresses. Little is known about the influence of the degree of cold work on SCC, and for this reason it is included in the present BNL program. We are comparing the as-received condition with 5, 10, and 20% cold work in tests that include direct load and CERT. Environments include pure deaerated water as well as oxygen-free simulated primary and secondary water.

Capsule tests in which denting is being reproduced as well as tests in which cyclic stresses are applied to the specimens are due to resume in the near future. No new results are available for these experiments at present. They will be important in covering certain practical conditions.

HEAT TREATMENT:

Attempts have been made during the past two years to generate our own susceptible heats of Inconel by means of high temperature annealing of heavily cold worked Inconel 600. Annealing temperatures were chosen to simulate those that may possibly exist in tube mills. Earlier work had indicated no sucess in the temperature range of about 1600°F to 1850°F (approximately 870°C to 1,000°C), for times ranging from 15 to 30 minutes. In more recent work, the material has been held at an annealing temperature for relatively short times, and some success has been achieved by holding at temperature for about 2 minutes. At shorter or longer times than this we did not achieve susceptibility, as determined in CERT (by the presence of cracks and a maximum loss of ductility at 365°C in pure deaerated water) and also in U-bend tests (where cracking occurred only in the specimens that had been heated for about 2 minutes) as shown in Figure 11. It is stressed that these results may only apply to the specific heat that we used (0.03% carbon) and it is not suggested at this time that the specific temperature-time combination would be generally applicable to any heat of Inconel 600.

STRUCTURE:

The various heats of mill annealed Inconel 600 tubing used in this program are typical of nuclear grade production; however, only about half of these heats have shown evidence of intergranular SCC when U-bend specimens were exposed to pure deaerated water at high temperatures. It is difficult to establish what differences exist between these heats that account for the fact that some are susceptible while others appear to be immune. A susceptible structure is generally associated with carbide-free grain boundaries, while semi-continuous grain boundary precipitates are beneficial in preventing SCC in caustic and pure water environments. Electrolytic etching in phosphoric acid showed that all of the materials used in this program were relatively free of carbide precipitates in the grain boundary regions. The susceptibility of this alloy, therefore, cannot be judged on microstructural analysis alone. Small variations in processing history which occur within a mill or different mills must play an important role.

H_2 IN PURE H_2O:

A definite accelerating effect of H_2 has been observed on SCC in high temperature water in U-bends as well as tensile specimens. In the latter case, a heat (#11, 0.03%C) of commercially produced tubing did not crack in the as-received surface condition in pure water at 365°C in the CERT test as well as U-bends - although a basic tendency towards cracking was found in U-bends that were first pickled in HNO_3/HF. When tested as-received (resistant in water at 365°C) in CERT at 365°C in $H_2O + H_2$, intergranular SCC occurred.

Confirmation of a H_2 effect came from a comparison of 9 heats tested in pure H_2O and $H_2O + H_2$ as U-bends at 365°C. In water alone, as shown in Table 2, only 2% failures occurred in 12 weeks, compared to 83% in $H_2O + H_2$.

Table 1

Calculated Failure Times for Lab. U-Bend SCC

%C	Projected Weeks at: 315°C	290°C
0.05	150	1500
0.03	120	700
0.02	30*	150*
0.01	80	240

*Exceeded by ongoing tests, without visible SCC.

Table 2

Effect of the Presence of H_2 in H_2O at 365°C

Test duration:	12 weeks
Test medium:	Pure, deaerated water (with and without H_2)
Test temperature:	365°C
Test specimens:	U-bends
# Heats:	9

RESULTS

	Cracked	# Tested	% Failed
Pure H_2O	1	45	2
Pure H_2 + H_2O	15	18	83

(H_2 = amount found in primary H_2O).

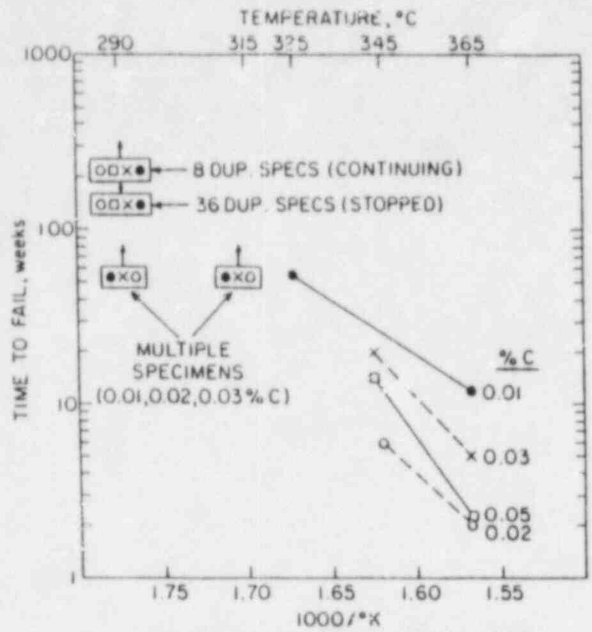

Fig. 1 SCC in pure water. U-bends of commercial tubing

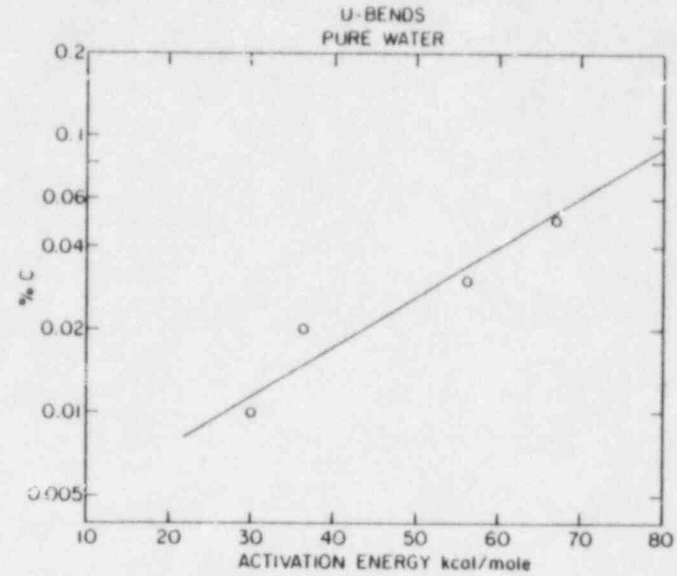

FIG. 2 TENTATIVE ACTIVATION ENERGIES (BASED ON HIGHER TEMPERATURE DATA)

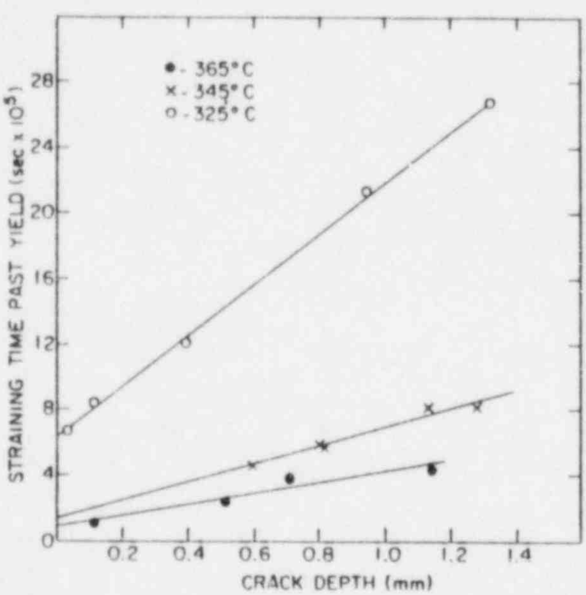

Fig. 3 Determination of Crack Initiation in CERT Specimens Machined from Heat #4 (.01%C) - Flattened Tube Tensile Pieces

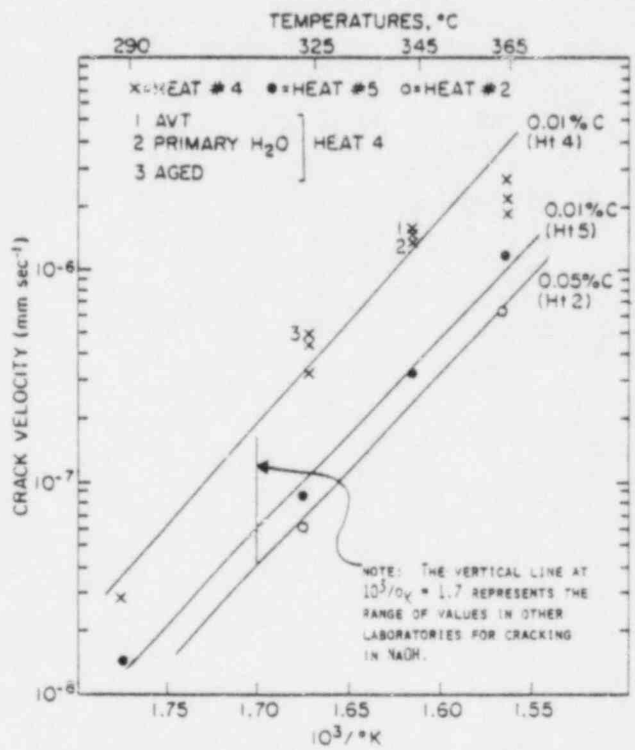

Fig. 4 Effect of Temperature on Crack Velocities Determined Using Cold Worked Inconel in CERT.

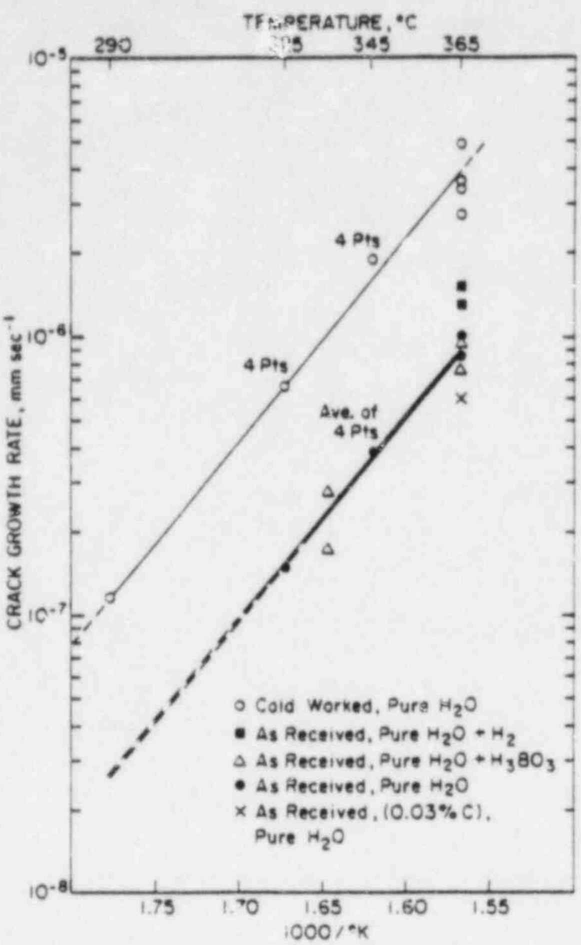

FIG. 5 CRACK GROWTH RATES, CERT EXPERIMENTS, 0.01%C

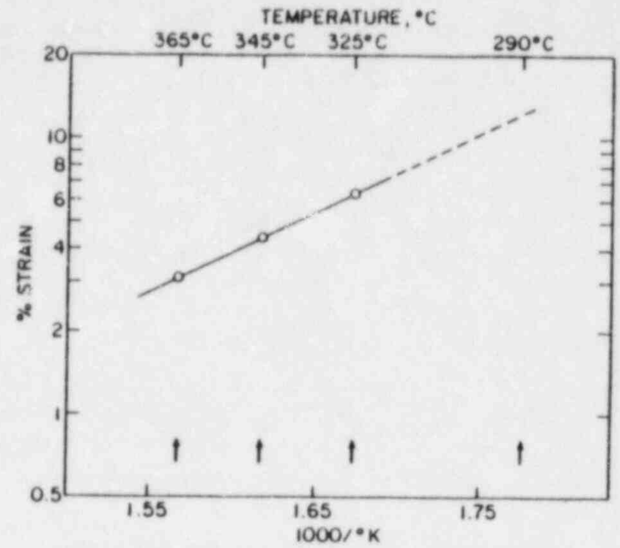

FIG. 6 EXTRAPOLATION OF SCC INITIATION STRAIN VALUES FROM FIG. 3

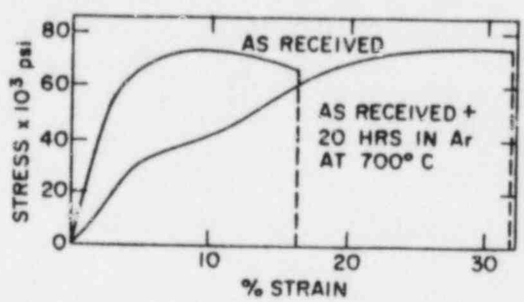

FIG. 7 COMPARISON OF STRESS STRAIN CURVES FOR HEAT #2 WITH AND WITHOUT HEAT TREATMENT AT 700°C FOR 20 HOURS

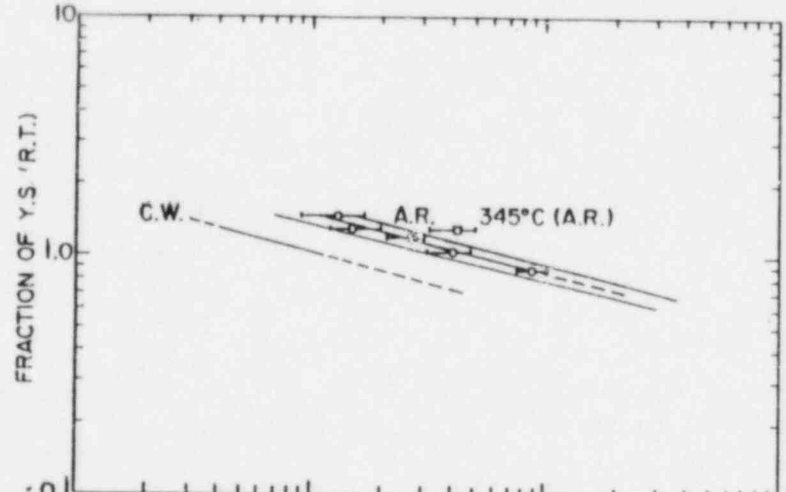

FIG. 8 FAILURE TIMES VS. STRESS, CONSTANT LOAD IN PURE H_2O, 365°C

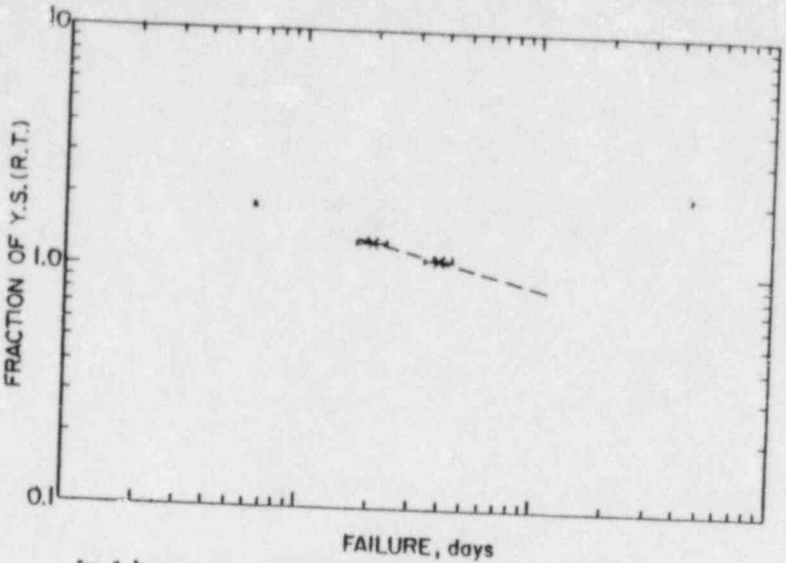

FIG. 9 FAILURE TIMES VS. STRESS, CONSTANT LOAD IN SIMULATED PRIMARY H_2O, 365°C

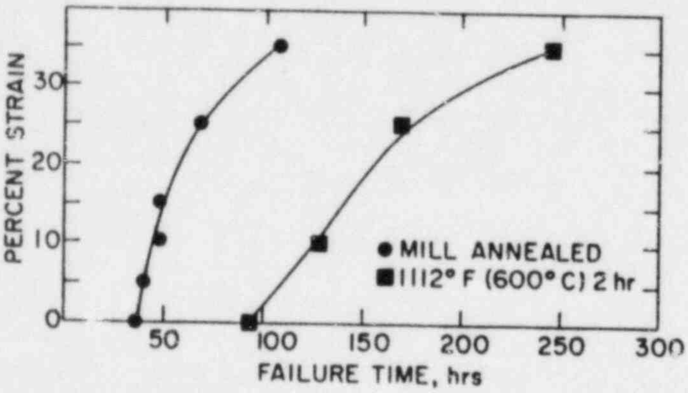

FIG. 10 PERCENT STRAIN VERSUS TIME TO FAIL - 550°F (10% NaOH) (FROM G. THEUS, B&W)

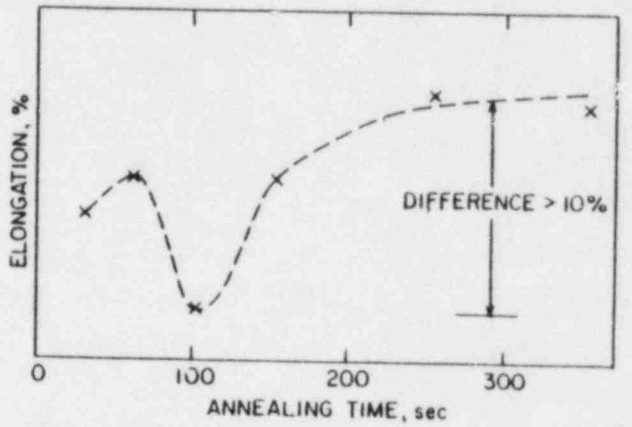

FIG. 11 CERT TEST; ANNEALING RESPONSE OF COLD WORKED INCONEL IN THE RANGE 1700°F TO 1775 F, INCONEL 600, 0.03%C, 365°C, PURE H_2O, DEAERATED.

NOTE: THE ONLY U-BENDS TO CRACK IN A SIMILAR TEST MEDIUM WERE ALSO THE ONES HEATED FOR 100 SECONDS

IMPROVED EDDY-CURRENT TESTING FOR LONGITUDINAL AND CIRCUMFERENTIAL FLAWS IN STEAM GENERATOR TUBING*

C. V. Dodd

Metals and Ceramics Division
OAK RIDGE NATIONAL LABORATORY
Oak Ridge, Tennessee 37830

ABSTRACT

The ORNL-developed multiple-frequency instrumentation is essentially complete and has been successfully tested in several different field applications. Improvements are being made in the software and the basic instrument is being applied to different test applications.

Due to recent steam generator failures, a major emphasis has been given to the design and development of pancake coil probes. Both analytical and dimensional analysis techniques have been applied. A pancake coil probe has been developed and tested that improves the signal-to-noise ratio to small defects by a factor of ten over the standard circumferential coil. In addition, the pancake coil probe can detect both axial and circumferential flaws, while the circumferential probe can only detect axial flaws. This type of probe will give a more sensitive inspection but will be more expensive to manufacture.

---

*Research sponsored by the Office of Nuclear Regulatory Research, U.S. Nuclear Regulatory Commission, under Interagency Agreement DOE 40-551-75 with the U.S. Department of Energy under contract W-7405-eng-26 with the Union Carbide Corporation.

GENERAL PROGRAM OBJECTIVES

1. Improve the state-of-the-art for steam generator inspection to meet the specific problems that are now present in steam generators.

2. Provide a broad technical base to allow quick response to new steam generator problems as they arise.

3. Provide NRC with an independent evaluation of the eddy-current inspections that the utilities and their vendors are performing.

ornl

SHORT-TERM PROGRAM OBJECTIVES

Develop eddy-current inspection techniques for steam generator tubing that will measure or discriminate against simultaneous variations in each of the following parameters:

1. tube diameter, including denting at the supports,
2. probe wobble,
3. presence of supports around the tube,
4. tube wall thickness,
5. location (radial and axial) of defects in the tube wall,
6. size of defects in the wall,
7. detect intergranular attack in the tubesheet crevice region and perform field inspections, and
8. design probes to detect defects with any type of orientation.

ornl

ORNL-DWG 80-19391

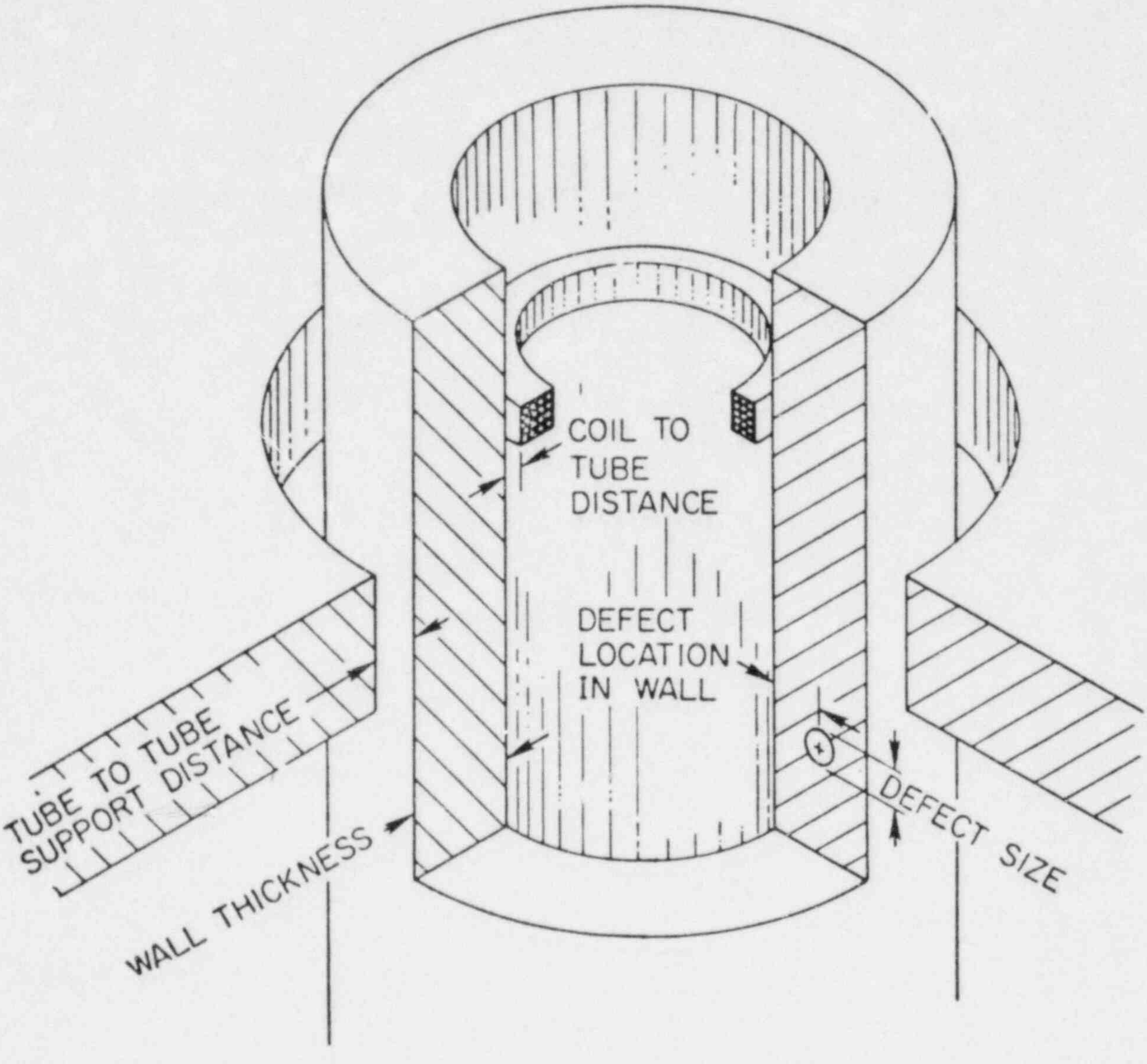

ornl

SOLUTION TO MULTIPLE PROPERTY PROBLEMS

There must be as many independent readings as there are test property variations.

Multifrequency/Pulse

Multicoil/Multiposition

ornl

ORNL–DWG 80-19392

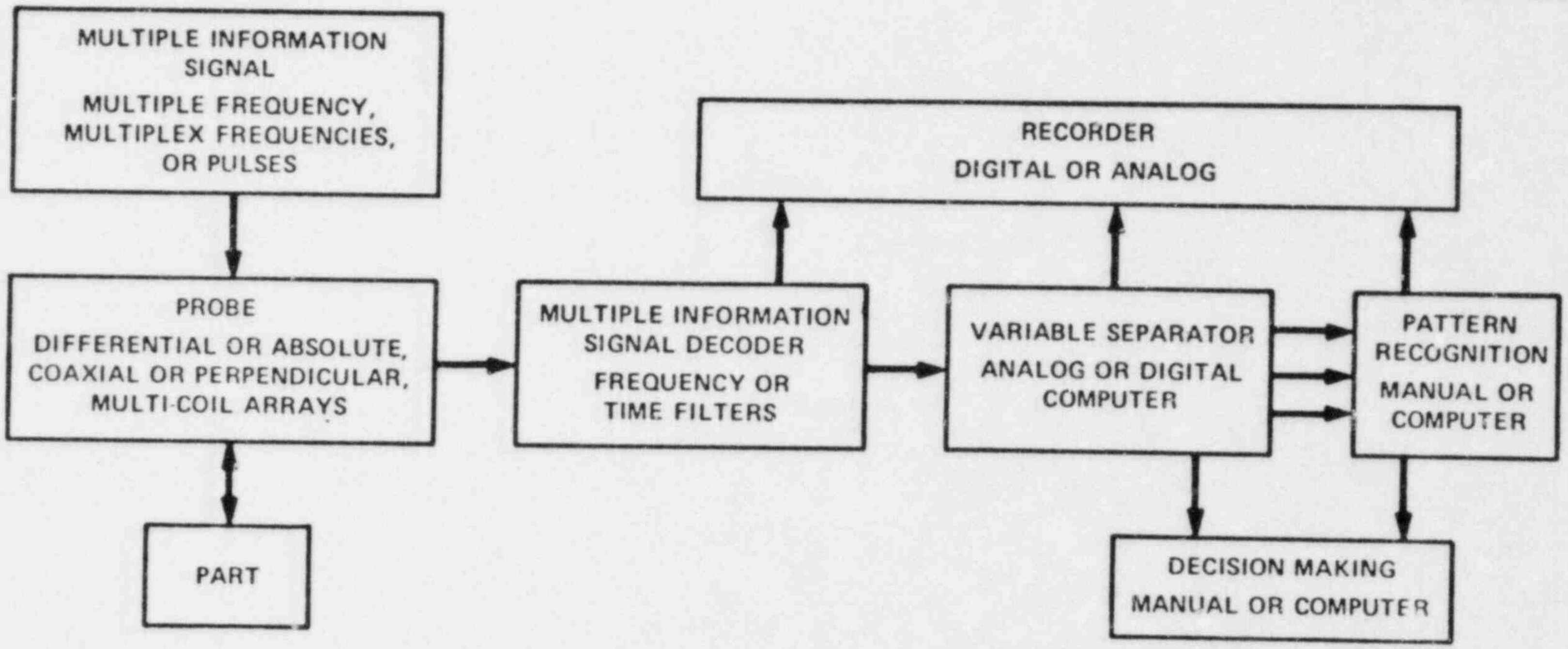

PANCAKE VERSUS CIRCUMFERENTIAL COIL

1. The pancake coil has higher sensitivity to small defects.

2. The pancake coil is able to ride the surface and has better coupling to the tube.

3. Property variations outside the tube have less effect on the pancake coil readings.

4. The pancake coil can detect both axial and circumferential cracks.

5. The pancake coil can measure different properties at different locations around the circumference.

6. The pancake coil array is a more complicated, expensive, and fragile probe.

7. The electronics and recording system for the pancake coil array is more complicated and expensive.

ornl

ORNL-DWG 82-12530

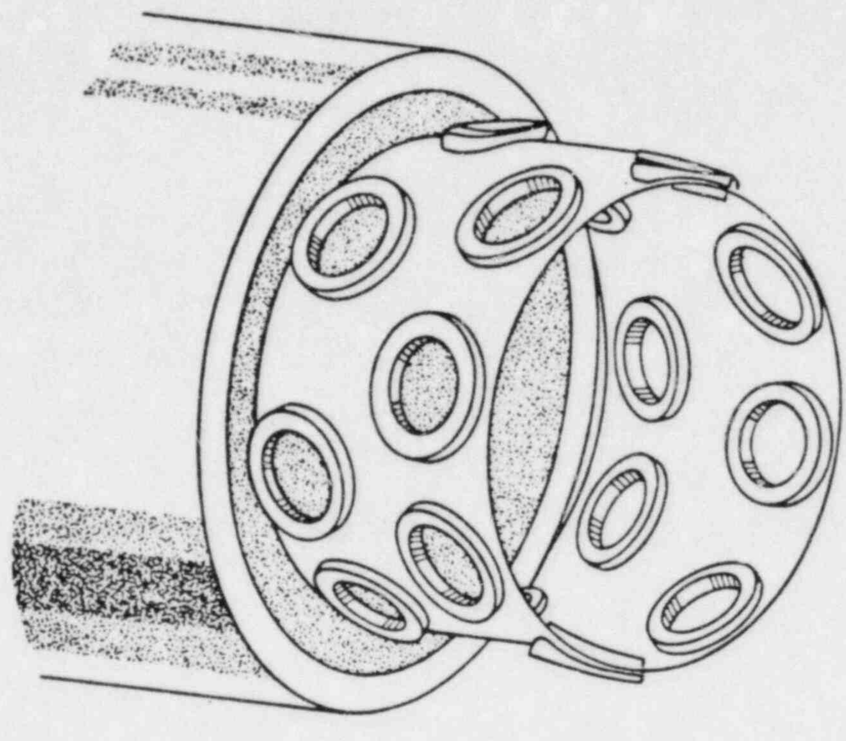

(a)

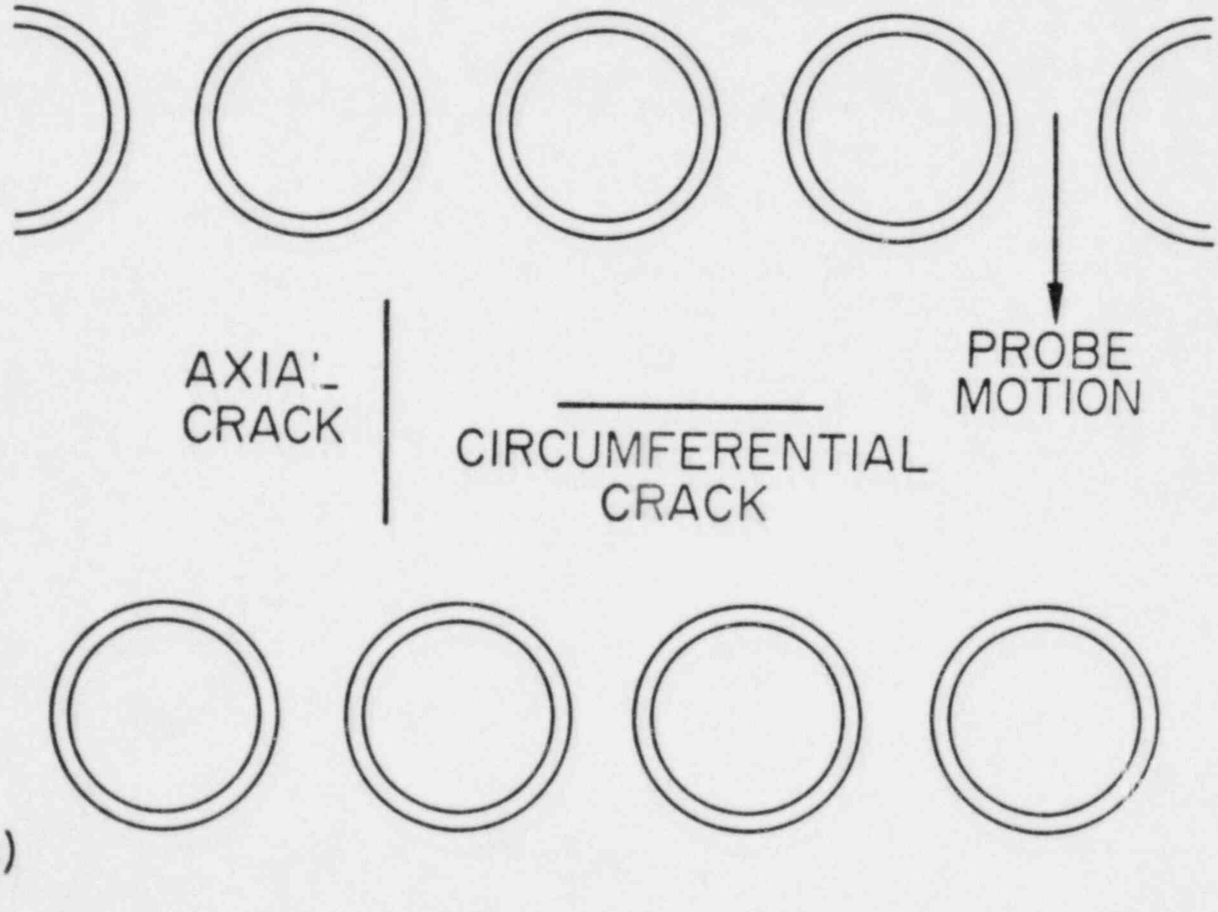

(b)

ORNL-DWG 82-12225R

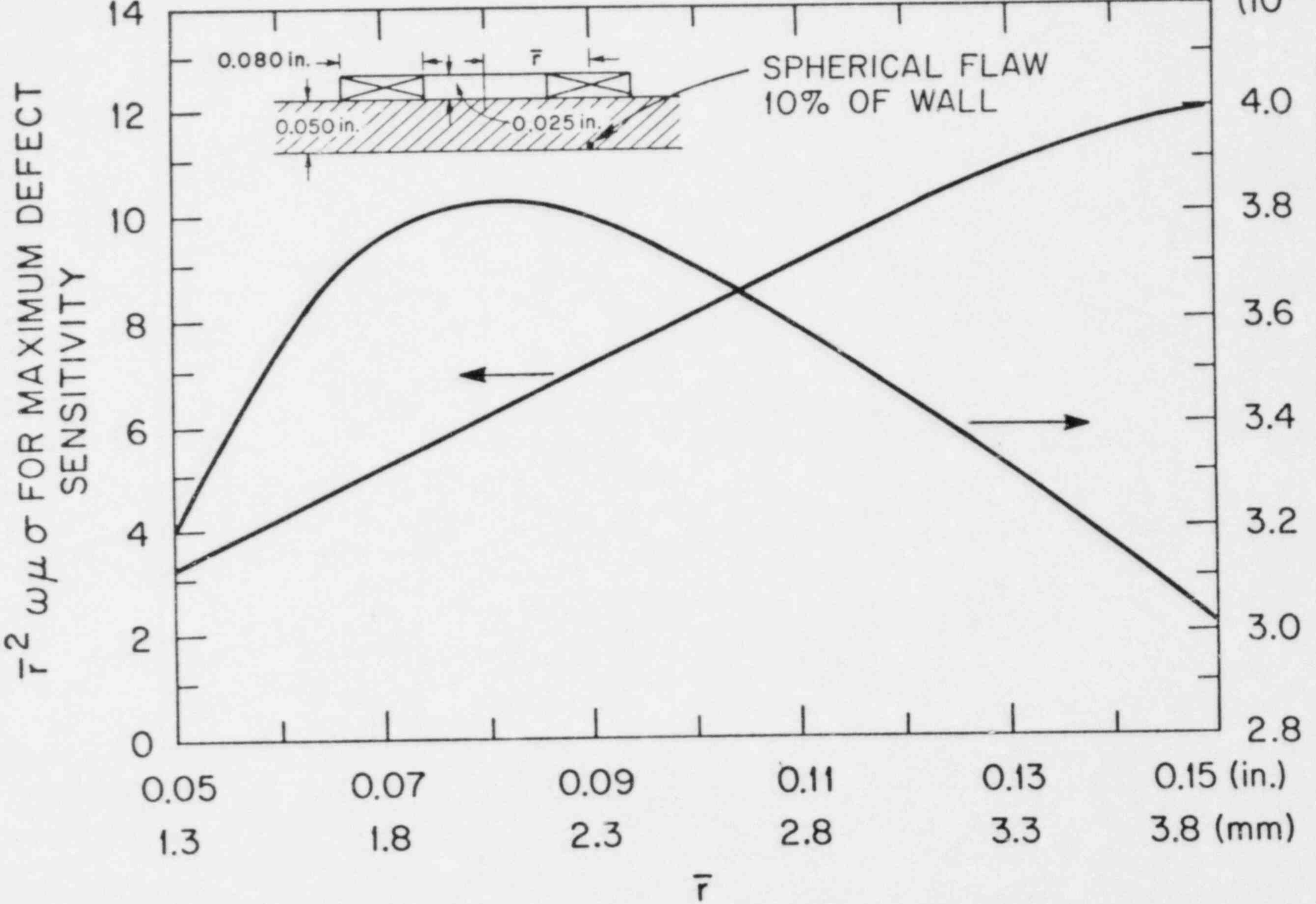

TECHNIQUE FOR CALCULATING TEST PROPERTIES FROM INSTRUMENT READINGS

1. Calculate instrument readings for many different test properties, including multiple frequency and multiple coil positions:

   $R = f(P)$.

2. Do a least squares fit of various nonlinear combinations of instrument readings to properties:

   $$P_{11} = C_0 + C_1R_{11} = C_2R_{12} + . . . + C_NR_{1N} .$$

   $$P_{12} = C_0 + C_1R_{21} + C_2R_{22} + . . . + C_NR_{2N} .$$

   .

   .

   .

   $$P_{1M} = C_0 + C_1R_{M1} + C_2R_{M2} + . . . + C_NR_{MN} .$$

   Let $P_{ij} - (C_0 + C_1R_{j1} + . . . + C_NR_{jN}) = \epsilon_j$.

   Determine $C_0, C_1, C_2, . . . , C_N$ to minimize $\sum_{j=1}^{M} \epsilon_j^2$.

   The R_{jk} can be functions or powers of the readings:

   $$\text{Thick} = C_0 + C_1(\ln M_1) + C_2(\ln M_1)^2 + C_3(Ph_1) + . . .$$

3. Calculate the errors due to lack of fit and instrument drift.

4. Repeat steps 1 through 3 for various coil and test designs.

ornl

ORNL-DWG 78-16168R

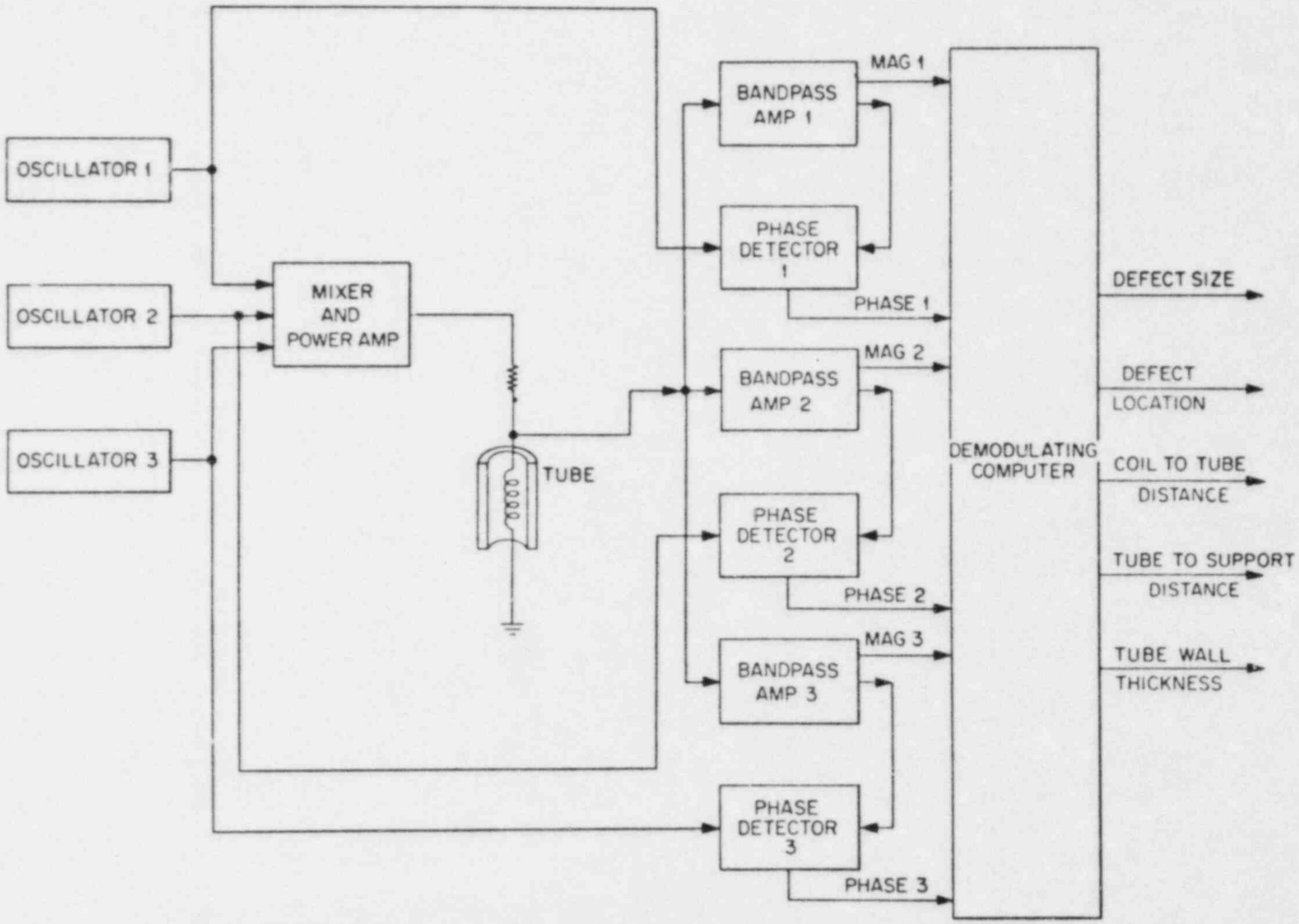

BLOCK DIAGRAM OF A THREE FREQUENCY INSTRUMENT

ORNL-DWG 80-11989

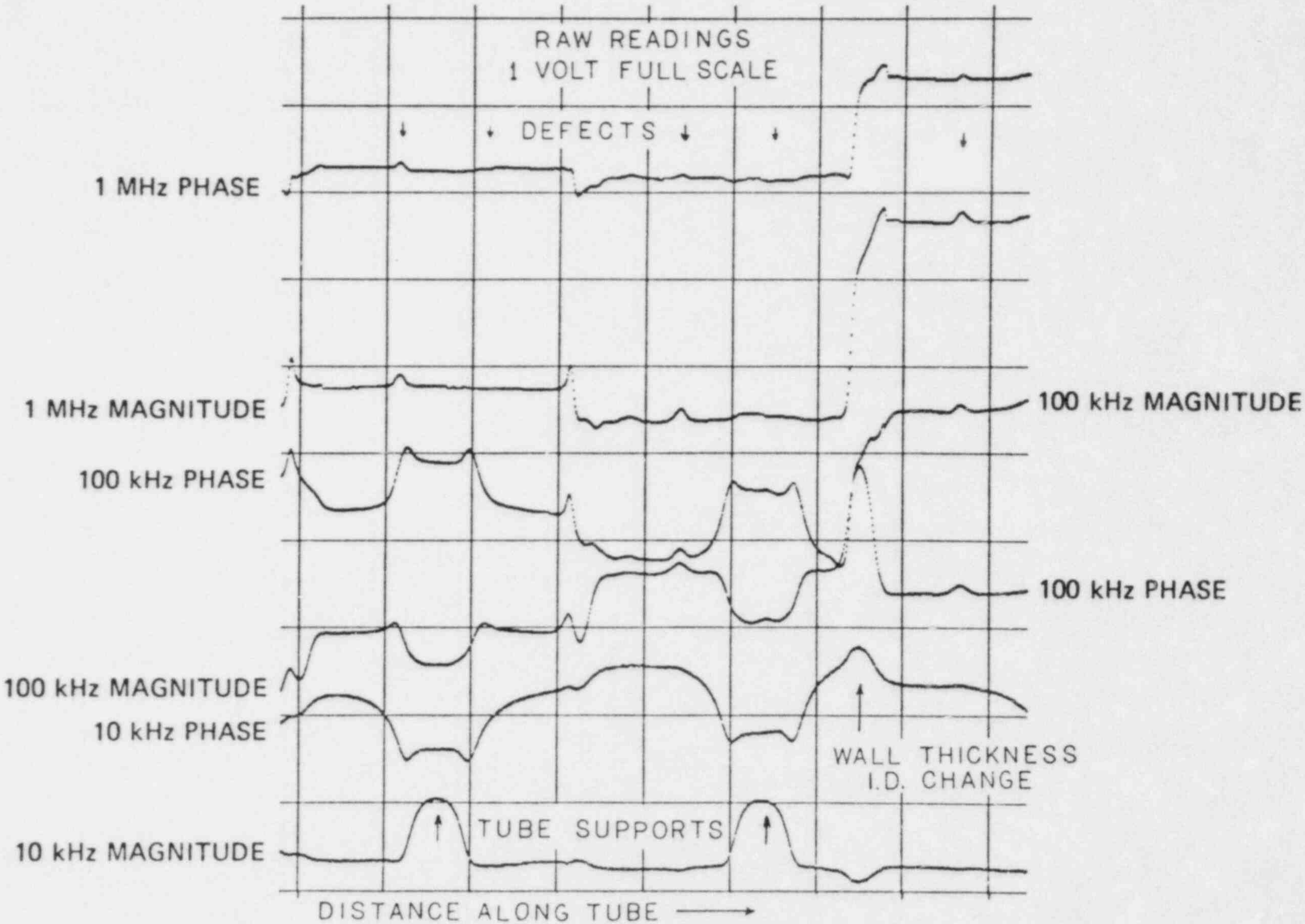

ORNL-DWG 80-11990R2

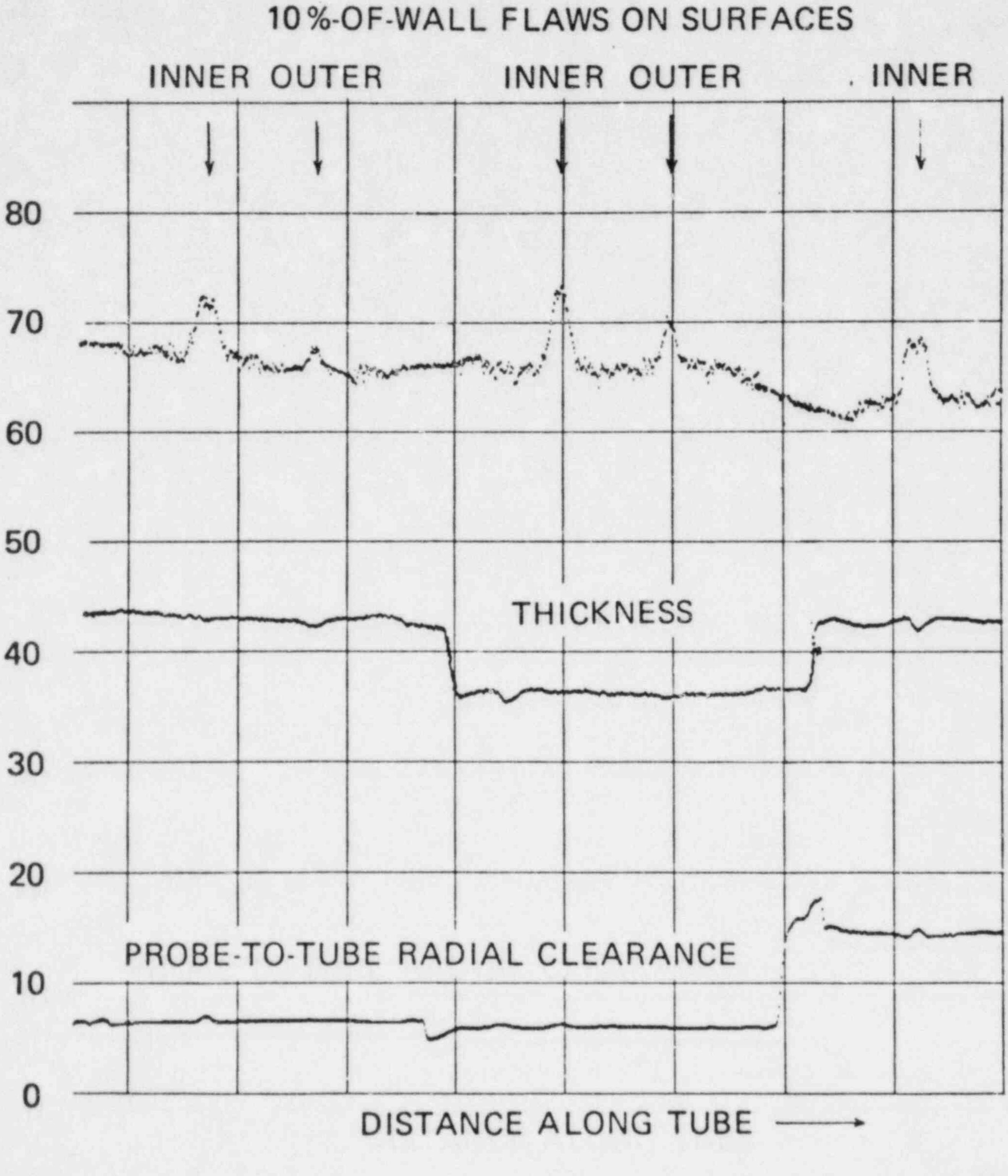

MULTIPLE PROPERTY EDDY-CURRENT TECHNIQUES CAN BE SUCCESSFULLY APPLIED TO STEAM GENERATOR INSPECTIONS

1. Steam generators represent a complex, changing problem that requires our best effort.

2. Modern computer and information processing techniques allow us to get more information and accuracy from our eddy-current tests.

3. The best solution for these tests requires considerable effort and attention to detail.

ornl

NRC-04-81-178

The Development of a Plan for the Assessment of Degraded Nuclear Piping by Experimentation and Tearing Instability Fracture Mechanics Analysis

M. F. Kanninen, G. M. Wilkowski, J. Pan, J. Ahmad,
C. W. Marschall, E. R. Gilbert, C. H. Popelar and D. Broek

Battelle's Columbus Laboratories
Columbus, Ohio 43201

Summary

Because nuclear plant pipe materials are very ductile and tough, even pipes with large cracks may have a considerable margin of safety against fracture. Ordinary linear elastic fracture mechanics is generally inadequate for these applications. This fact has led to the development of a nonlinear fracture mechanics approach known as a tearing instability analysis. But, while this approach is highly promising, it has yet to be validated for conditions that might occur in actual service. A two-phase effort was initiated to address this need.

The primary objective of this research is to critically examine the tearing instability fracture mechanics analyses for the flaw sizes and loads -- in both design and accident conditions -- that would be expected to occur in actual nuclear plant operation. The work that has so far been accomplished constitutes Phase I of the program. The approach that has been followed involves work in three main areas:

- identification and acquisition of in-service degraded piping (for possible use in Phase II), and accumulating relevant pipe fracture experimental results;
- development and application of tearing instability analysis procedures for the assessment of existing pipe fracture data;
- design and costing of a comprehensive experimental pipe fracture research program to be performed as Phase II.

Unnecessary duplication of experiments will be avoided in the Phase II effort, both by utilizing results already available and by becoming cognizant of the on-going and planned research activities of other agencies around the world.

The present research offers several conclusions. First, the extensive search for plant degraded piping and relevant pipe fracture data has turned up little of either that will assist the Phase II effort. While a great number of fracture experiments have been performed, until recently accurate measurements of the extent of stable crack growth preceding fracture instability were seldom made. This precludes a critical assessment of the tearing instability theory which focuses on this point. Moreover, the data that was available did not discriminate between tearing instability and net section collapse. The present plans of non-NRC agencies in the U.S., Europe and Japan will not provide substantially more information of this kind. Accordingly, it seems clear that the pipe fracture data needed for an assessment of the tearing instability approach must be generated in the Phase II program.

The second contribution of this research has been in the advancement of tearing instability techniques. Specifically, by use of the η-factor approach of Turner, it has been possible to broaden the applicability of existing analyses to include work-hardening stress-strain behavior and to remove the hithertofore necessary assumption of net section yielding in pipe fracture analyses. The resulting methodology contains all previously known J-estimation solutions as special cases. Further work was accomplished on tension and torsion loading conditions. It is expected that these results will play a key role in the detailed design and interpretation of the Phase II experiments.

The third achievement of this research is the development of a comprehensive pipe fracture experimental plan. Owing to the exhaustive efforts that were made to review and critique the efforts of others, this plan can be confidentially viewed as neither unnecessarily duplicative nor deficient in any vital aspects. The test matrix that has been evolved includes axially cracked pipes under pressure loading and circumferentially cracked pipes under bending, tension, torsion and combined loading conditions. Note that, because of the limited amount of in-service degraded piping that was found, it is expected that pipes with laboratory induced cracks will be used. The cost estimates were made in terms of three priority levels. Details are available in the final report on Phase I, in preparation at the time of this meeting.

PROGRAM OBJECTIVE

ESTABLISH THE APPLICABILITY OF THE TEARING INSTABILITY FRACTURE MECHANICS APPROACH FOR IN-SERVICE DEGRADED PIPING UNDER REALISTIC SERVICE LOADING CONDITIONS

PHASE I APPROACH

- EXTEND AND APPLY EXISTING ANALYSES FOR THE ASSESSMENT OF EXISTING PIPE FRACTURE DATA
- IDENTIFY AND ACQUIRE IN-SERVICE DEGRADED PIPE FRACTURE DATA
- DESIGN AND COST A COMPREHENSIVE EXPERIMENTAL PIPE FRACTURE PROGRAM TO BE CONDUCTED IN PHASE II

Battelle
Columbus Laboratories

OUTLINE OF PRESENTATION

- STATUS OF TEARING INSTABILITY ANALYSIS
- PROGRESS IN J/T ANALYSIS OF NUCLEAR PIPING
- ASSESSMENT OF EXISTING FRACTURE DATA FOR J/T VERIFICATION
- IDENTIFICATION OF IN-SERVICE DEGRADED PIPING
- DESIGN OF PHASE II EXPERIMENTAL PROGRAM

Battelle
Columbus Laboratories

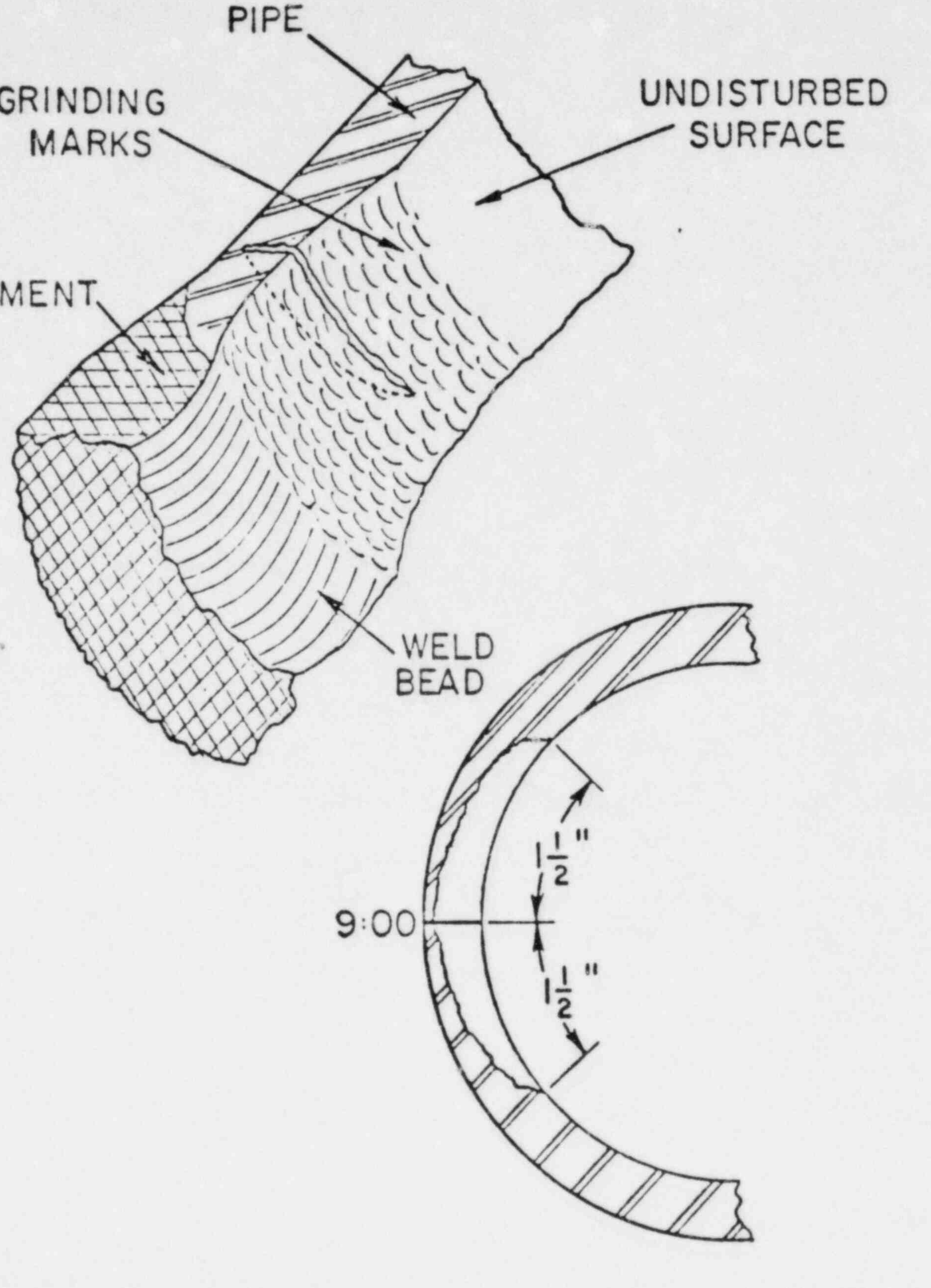

PROFILE OF CIRCUMFERENTIAL CRACK DETECTED IN 4-INCH (100-MM) DIAMETER RECIRCULATION BYPASS LINE (LOOP B) OF THE QUAD CITIES II BOILING WATER REACTOR

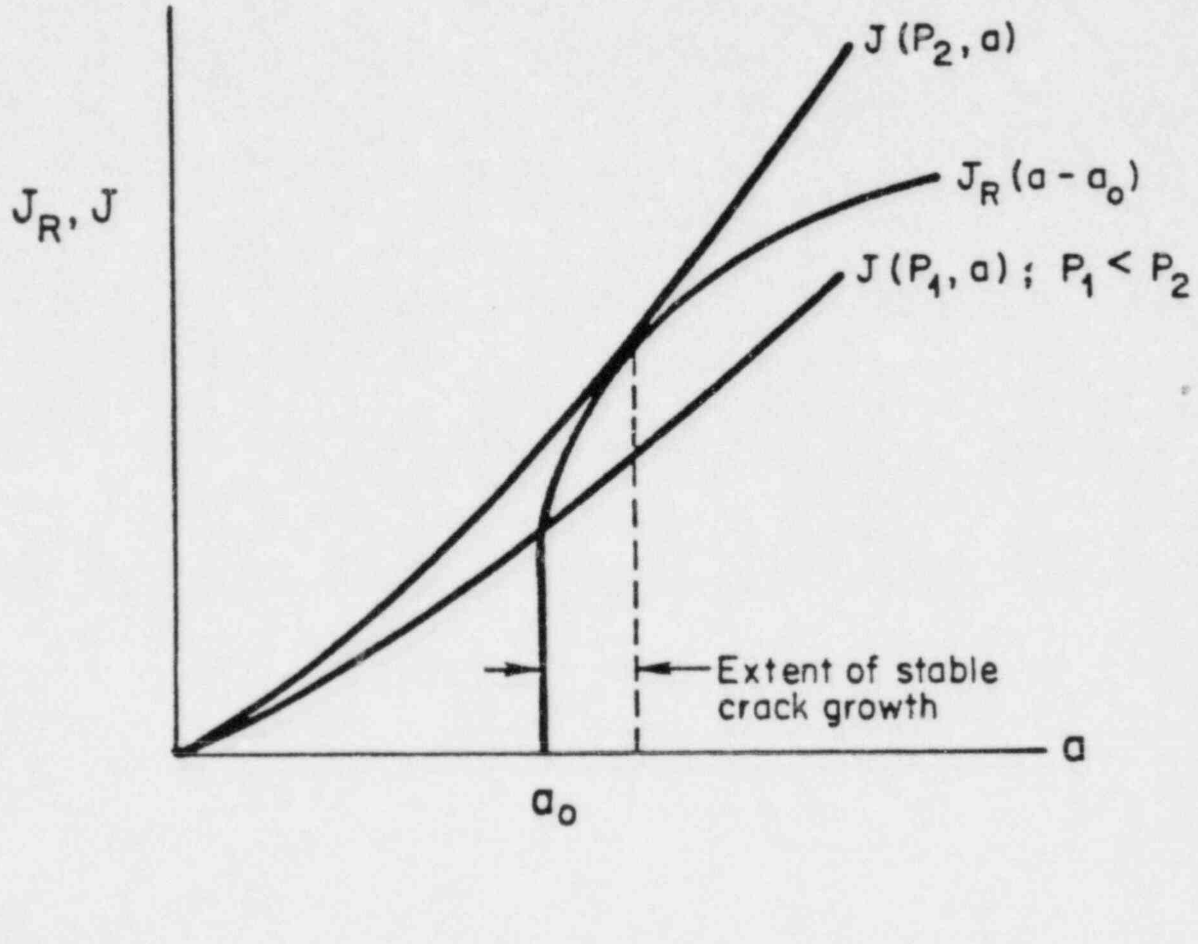

SCHEMATIC OF TYPICAL RESISTANCE CURVE ANALYSIS

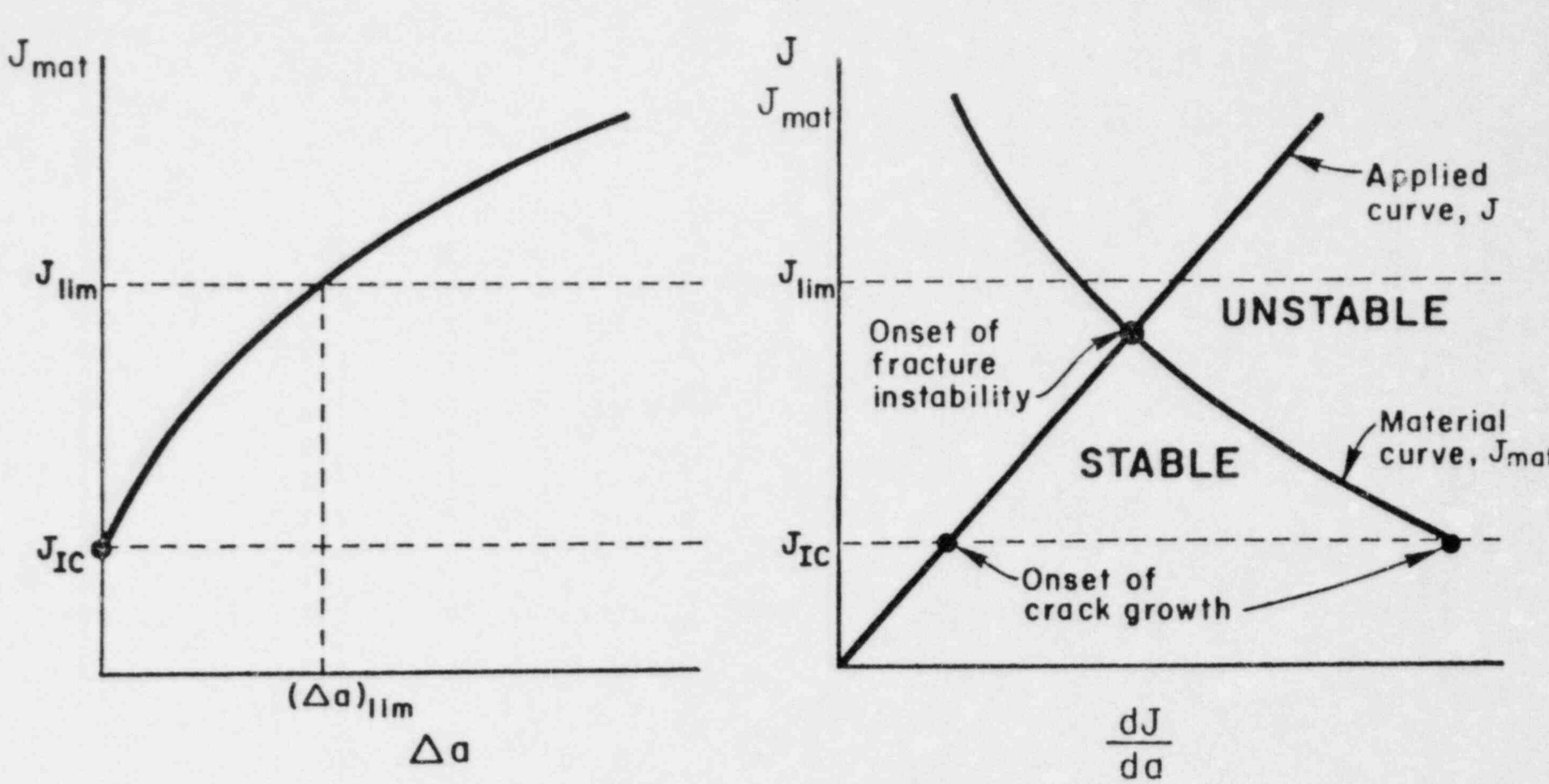

(a) Material J-Resistance Curve

(b) Fracture Instability Diagram

Figure 2-1. A conceptual illustration of the use of a plastic fracture mechanics approach to the prediction of fracture in a cracked structure.

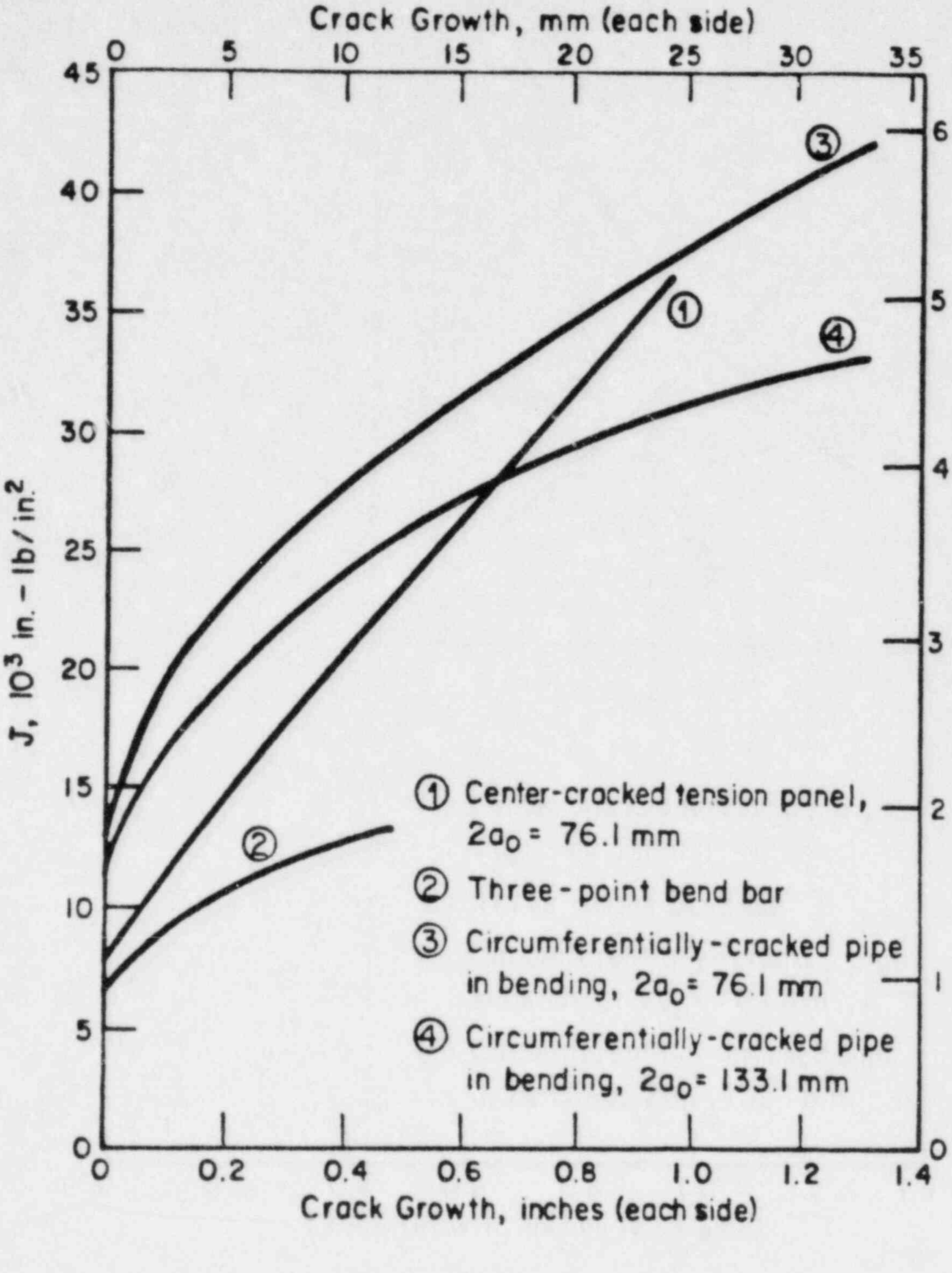

COMPARISON OF J-RESISTANCE CURVES FOR TYPE 304 STAINLESS STEEL INFERRED FROM EXPERIMENTS ON FOUR DIFFERENT CRACK/STRUCTURE GEOMETRIES

ISSUES IN ELASTIC-PLASTIC FRACTURE MECHANICS

1. LIMITATIONS ON VALIDITY OF J/T APPROACH:

- MAXIMUM PERMISSABLE EXTENT OF STABLE CRACK GROWTH

  $(b/J)(dJ/da) >> 1$

- UNIQUENESS OF J-RESISTANCE CURVE AS GEOMETRY-INDEPENDENT MATERIAL PROPERTY

- EXTENSION TO FULL-SCALE STRUCTURES UNDER REALISTIC SERVICE CONDITIONS (DYNAMIC AND MIXED MODE LOADING) AND CRACK LOCATIONS OBSERVED

- DUCTILE-BRITTLE TRANSITION BEHAVIOR

Battelle
Columbus Laboratories

ISSUES IN ELASTIC-PLASTIC FRACTURE MECHANICS

2. ANALYSIS OF CRACK GROWTH IN ELASTIC-PLASTIC CONDITIONS

- DETERMINATION OF J-RESISTANCE CURVES REQUIRES ANALYSIS MODEL
- J-ESTIMATION SCHEME VERSUS FINITE ELEMENT COMPUTATION
- EFFECT OF SIMPLIFYING ASSUMPTIONS (E.G. LIMIT LOAD CONDITIONS, PERFECTLY PLASTIC BEHAVIOR, SMALL DEFORMATION)
- THREE DIMENSIONAL CONDITIONS

Battelle
Columbus Laboratories

ISSUES IN ELASTIC-PLASTIC FRACTURE MECHANICS

3. EFFECT OF PRIOR LOADING AND CRACK GROWTH:

- SUBCRITICAL STRESS CORROSION OR FATIGUE CRACKING
- WELD-INDUCED RESIDUAL STRESS AND DEFORMATION
- TENSILE OVERLOAD (WARM PRESTRESS)
- ARRESTED UNSTABLE CRACK GROWTH

Battelle
Columbus Laboratories

CRITICAL CRACK EXPERIMENTS ON A106 GRADE B CARBON STEEL PIPE WITH THROUGH-WALL AXIAL FLAWS (CHANG ET AL, NUREG/CR 1119, JUNE 1980)

Pipe	Experiment	Test Temperature, F	Total Axial Crack Length, in.	σ_h, Nominal Hoop Stress at Failure, ksi	Tensile Data: Yield Stress, ksi	Tensile Data: Ultimate Stress, ksi	Outside Radius, in.	Wall Thickness, in.	Predicted Hoop Stress at Failure: J/T Analysis, ksi	Predicted Hoop Stress at Failure: Plastic Collapse, ksi
C1	3	575	24.5	13.49	33.0	75.4	12	1.735	13.6	14.3
C1	1	575	18.5	19.74	33.0	75.4	12	1.674	17.2	17.0
C1	2	587	18.5	18.03	32.8	75.0	12	1.593	17.2	17.3
C2	5	675	18.5	16.48	30.6	75.0	12	1.64	17.2	17.2
C2	7	670	18.5	17.05	30.6	75.0	12	1.635	17.2	17.2
C5	10	661	18.5	17.75	32.6	77.9	12	1.64	17.2	18.0
C5	15	639	18.5	19.85	32.6	77.9	12	1.64	17.2	18.0
C2	6	554	11.6	24.50	34.1	81.5	12	1.715	24.3	27.1
C2	17	642	6.0	33.94	33.6	82.3	12	1.65	35.5	38.1
				Averages	32.5	77.5				
					σ_o = 45.8					
C8	13	555	14.5	17.3	36.5	74.7	12	0.700	15.5	15.9
C8	11	547	10.25	23.55	36.5	74.7	12	0.705	20.5	21.0
C8	12	561	5.25	33.0	36.5	74.7	12	0.710	32.1	32.4
C7	16	581	2.5	42.8	36.5	74.7	12	0.700	41.0	41.6
				Averages	36.5	74.7				
					σ_o = 46.3					
C10	23	567	10.25	15.8	42.8	74.0	6.375	0.700	16.5	17.0
C10	22	538	5.25	24.8	42.8	74.0	6.375	0.707	27.0	28.1
C10	21	605	2.5	39.0	42.8	74.0	6.375	0.710	40.0	40.3
				Averages	42.8	74.0				
					σ_o = 48.7					

$\sigma_o = (\sigma_y + \sigma_u)/2.4$

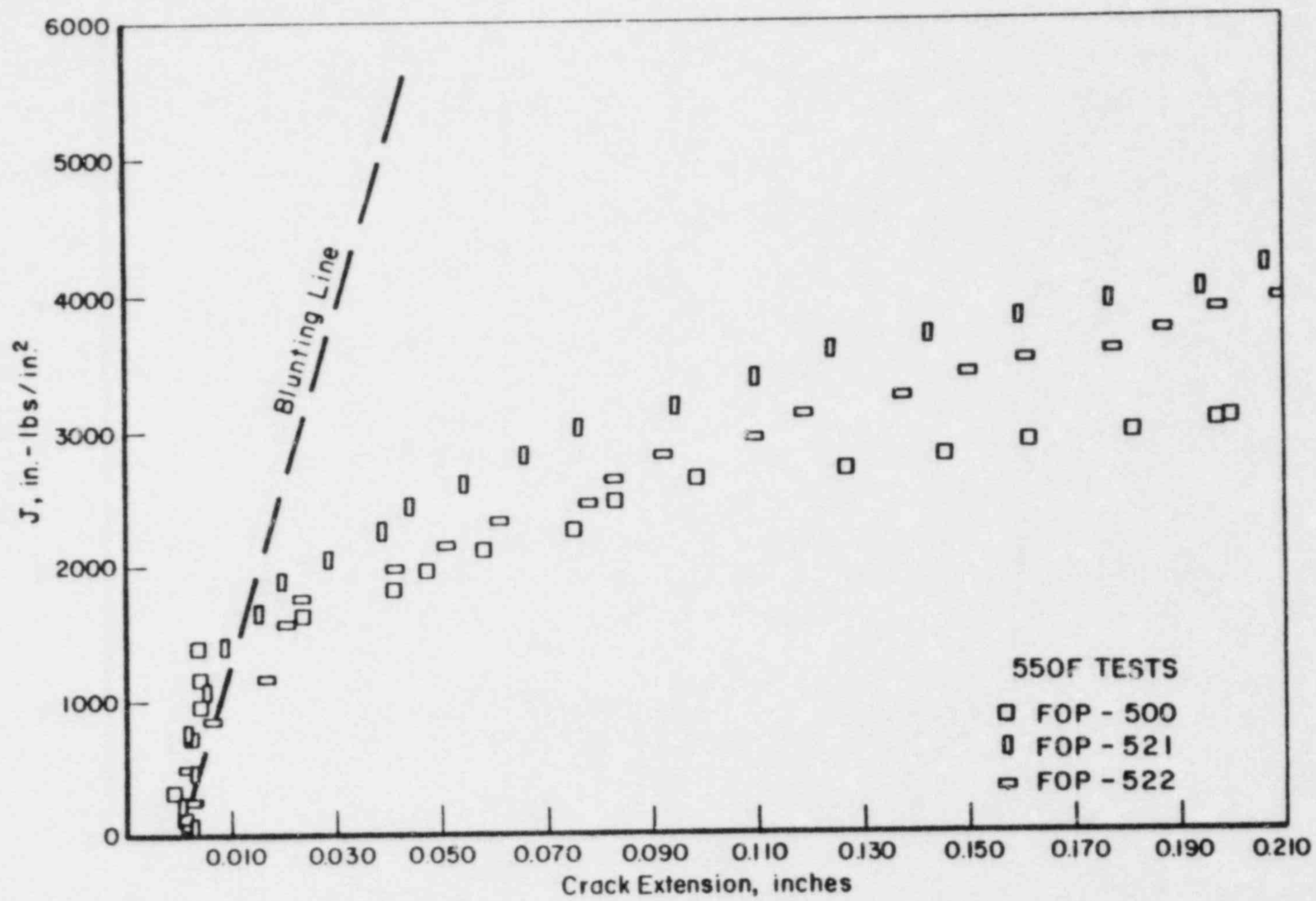

J VERSUS CRACK EXTENSION A106 (L-C ORIENT.)

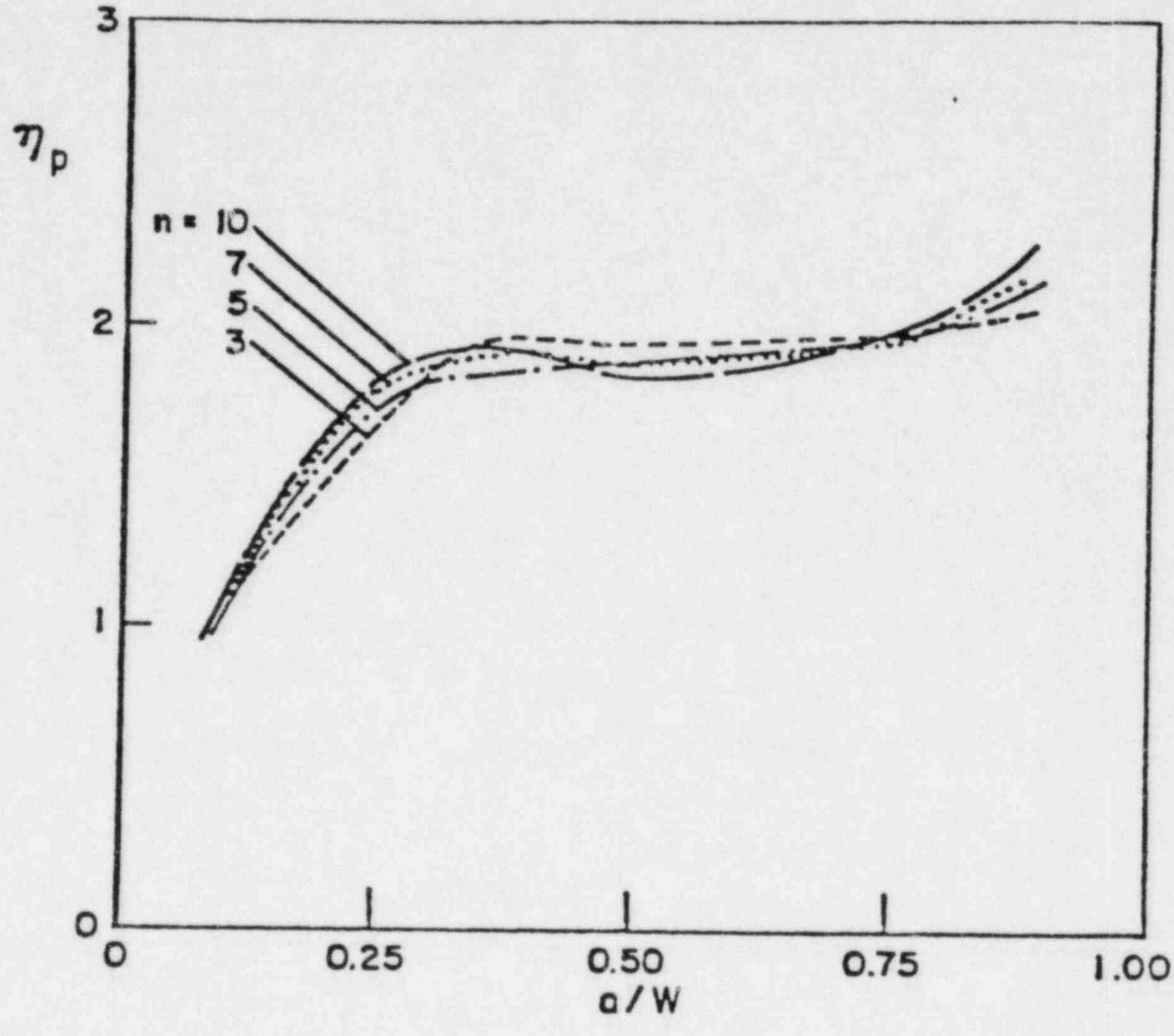

THE η_p FACTOR DEDUCED FROM THE GE/EPRI PLASTIC FRACTURE HANDBOOK AS A FUNCTION OF CRACK LENGTH AND HARDENING INDEX FOR A BEND SPECIMEN

J/T ANALYSIS FOR AXIAL CRACK IN A PRESSURIZED PIPE

MODIFIED DUGDALE MODEL

$$J = \frac{8a\sigma_o^2}{\pi E} \log \left[\sec \left(\frac{\pi}{2} \frac{MpR}{\sigma_o t} \right) \right]$$

WHERE

$$M = \left[1 + 1.255 \frac{a^2}{Rt} - 0.0135 \left(\frac{a^2}{Rt} \right)^2 \right]^{1/2}$$

NOTE THAT PLASTIC COLLAPSE IS GIVEN BY

$$\frac{MpR}{\sigma_o t} = 1$$

Battelle
Columbus Laboratories

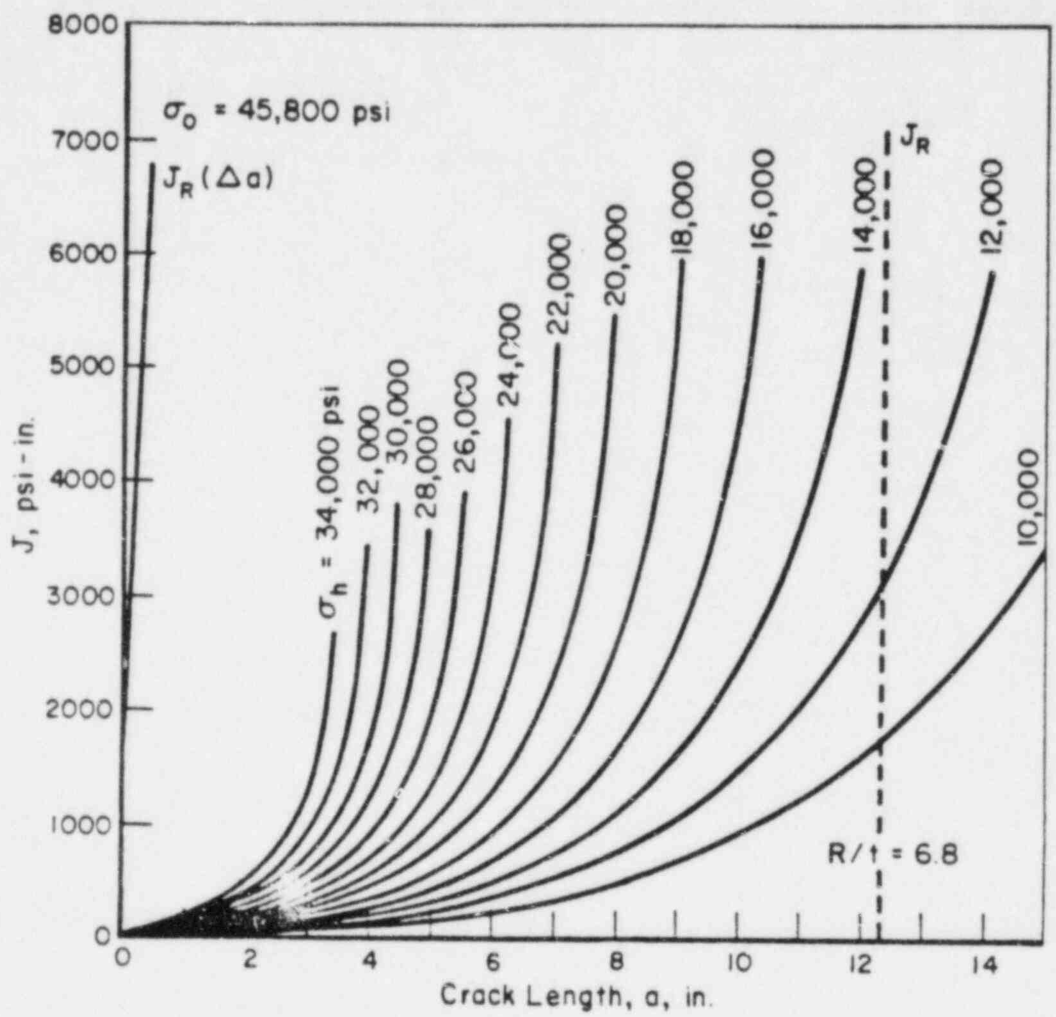

DRIVING FORCE VERSUS CRACK LENGTH
FOR FIRST SET OF DATA IN TABLE 1

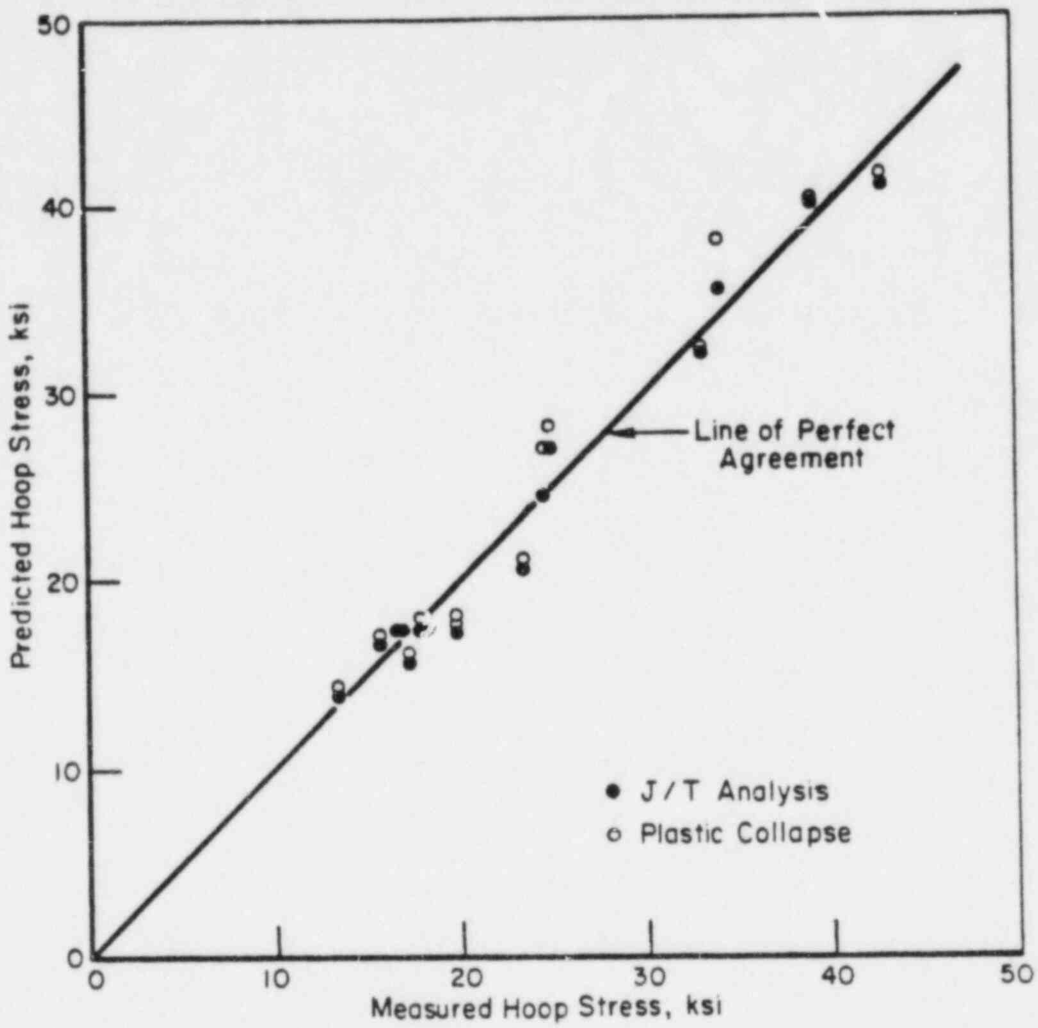

COMPARISON OF PREDICTED AND MEASURED HOOP STRESS AT FAILURE OF AXIALLY FLAWED A106B STEEL PIPES

GENERALIZED STABILITY ANALYSIS FOR J - CONTROLLED CRACK GROWTH

- Assumes existence of η-factor to relate J to strain energy and remaining ligament
- Considers strain hardening behavior (limit load assumption not necessary)
- Accounts for extent of stable crack growth
- Includes as special cases <u>all</u> current J - estimation analyses
- Can be used to extend GE/EPRI Elastic-Plastic Fracture Handbook Solutions

Battelle
Columbus Laboratories

GENERALIZED STABILITY ANALYSIS FOR J-CONTROLLED CRACK GROWTH

WHEN ELASTIC DEFORMATION CAN BE NEGLECTED:

$$J = \int_{0}^{\Delta_{cp}} \frac{\eta P}{b} \, d\Delta_{cp} + \int_{a_0}^{a} \frac{J}{b} \left[1 - \eta - \frac{b}{\eta} \frac{\partial \eta}{\partial b} \right] da$$

AND

$$\left(\frac{dJ}{da} \right)_{\Delta_T} = \frac{J}{b} \left[1 - \eta - \frac{b}{\eta} \frac{\partial \eta}{\partial b} \right] + C \left(\frac{\eta P}{b} \right)^2 \left[1 + C \left(\frac{\partial P}{\partial \Delta_{cp}} \right)_a \right]^{-1}$$

WHERE

$$C = C_M + d\Delta_{MC} \, dp$$

THIS CONTAINS CURRENT J-ESTIMATION ANALYSES FOR BEND SPECIMEN (HUTCHINSON AND PARIS), DEEPLY CRACKED CENTER-CRACKED PANEL (HUTCHINSON AND PARIS), COMPACT TENSION SPECIMEN (ERNST, ET AL) AND CIRCUMFERENTIALLY - CRACKED PIPE (ZAHOOR AND KANNINEN) AS SPECIAL CASES.

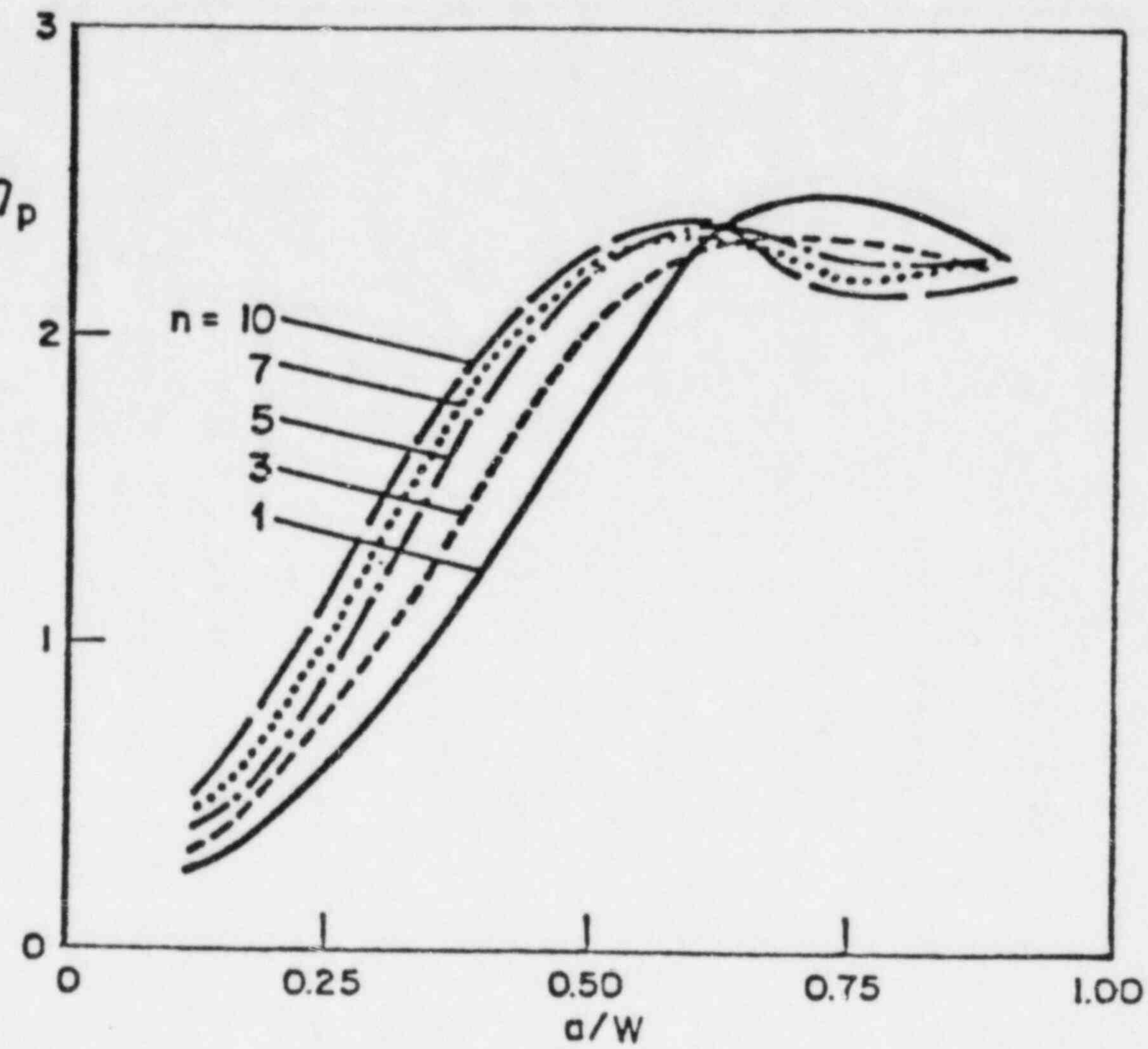

THE η_p FACTOR DEDUCED FROM THE GE/EPRI PLASTIC FRACTURE HANDBOOK AS A FUNCTION OF CRACK LENGTH AND HARDENING INDEX FOR A SINGLE EDGE CRACKED TENSION SPECIMEN

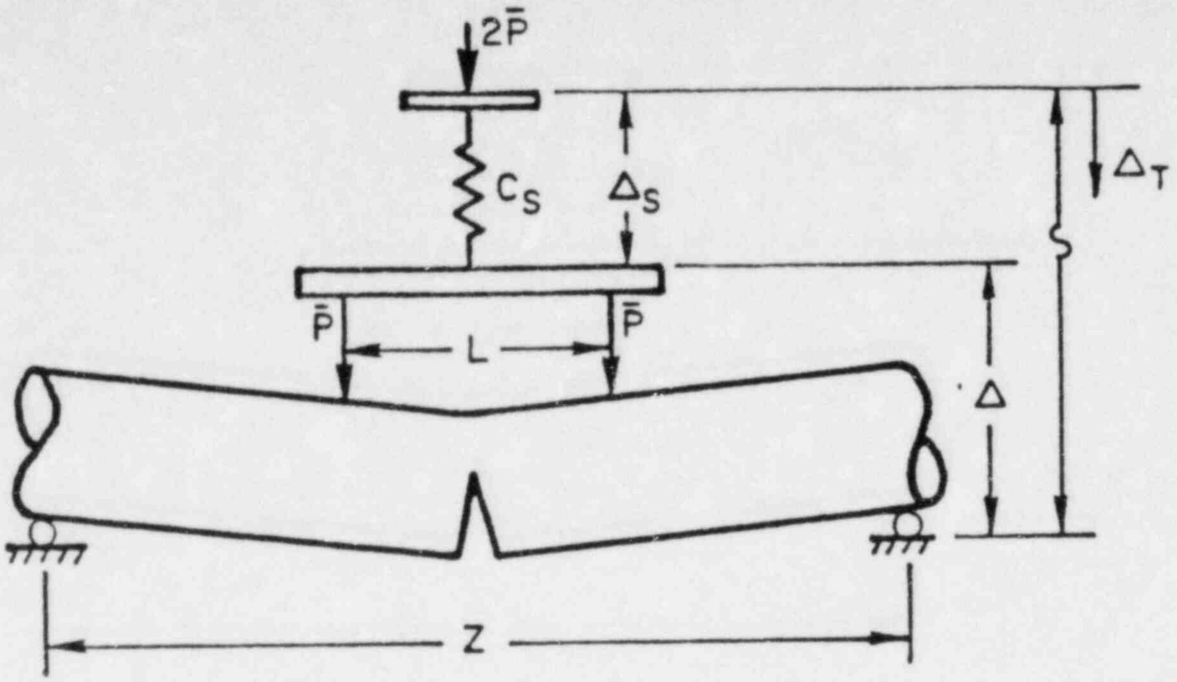

(a) Four-Point Bend Loading System

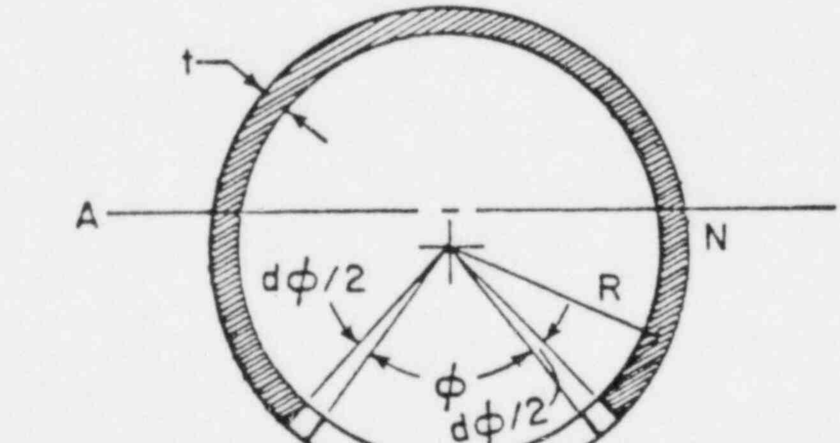

(b) Cross Section of a Through-Wall Cracked Pipe

COMPLIANT FOUR-POINT BEND LOADING OF A
CIRCUMFERENTIALLY CRACKED PIPE

DEGRADED PIPING IDENTIFIED

	MATERIAL	FIELD- OR LABORATORY-DEGRADED	STATUS
A.	10-INCH,TYPE 304 CORE SPRAY LINE	FIELD	STORED AT NATIONAL LABORATORY
B.	10-INCH, TYPE 304 CORE SPRAY LINE	FIELD	STORED AT NATIONAL LABORATORY
C.	10-INCH, TYPE 304 WATER CLEAN-UP LINES	FIELD	STORED AT NATIONAL LABORATORY
D.	4-INCH, TYPE 304 WATER CLEAN-UP LINES	FIELD	STORED AT REACTOR SITE
E.	4-INCH, TYPE A106 FROM RECOMBINER SECTION	FIELD	STORED AT REACTOR SITE
F.	28-INCH, TYPE 304 RECIRCULATION PIPES	FIELD	UNDERGOING REMOVAL FROM REACTOR
G.	8-INCH TYPE 304 PIPE FROM FEEDWATER SPARGER	FIELD	STORED AT REACTOR SITE
H.	12-INCH TYPE 304 PIPE FROM LEAK-RATE STUDIES	LABORATORY	STORED AT BATTELLE-COLUMBUS
I.	26-INCH TYPE 304 PIPE	LABORATORY	BEING CRACKED
J.	24-INCH TYPE 304 PIPES	LABORATORY	BIENG CRACKED
K.	5-INCH TYPE 304 PIPE	FIELD	STORED AT BATTELLE-COLUMBUS
L.	4-INCH TYPE 304 PIPE	LABORATORY	BEING CRACKED
M.	10-INCH TYPE 304 PIPES	LABORATORY	BEING CRACKED
N.	14- to 10-INCH TYPE 304 REDUCER	FIELD	STORED AT REACTOR VENDOR'S LABORATORY

DEGRADED PIPING IDENTIFIED FOR POSSIBLE TESTING IN PHASE II

	Material and Pipe Form	Field- or Laboratory-Degraded?	Crack Characterization	Status as of 9/15/82
A.	Two sections of 10-inch dia., Type 304, Sch. 80 core spray line: (a) 45° elbow, 3 ft. long, and (b) 90° elbow cut down to 45° for shipping, 1-1/2 ft. long	Field	Crack geometries have been characterized by NDE	Pipe is stored at a National Laboratory; utility has given written approval to use in Phase II
B.	10-inch dia., Type 304, Sch. 80 core spray line; two welds in a 20° elbow contain cracks; elbow is attached to 6-inch-long ends	Field	Crack geometries have been characterized by NDE	Pipe is stored at a National Laboratory; utility has given written approval to use in Phase II
C.	Three sections of 10-inch dia., Type 304 water cleanup lines; each has an elbow at the end of a 2-foot straight section	Field	Crack geometry not yet characterized	Pipe is stored at a National Laboratory awaiting crack characterization; it will probably be available for Phase II testing but written approval has not yet been granted
D.	Two sections of 4-inch dia., Type 304 water cleanup lines	Field	Crack geometry fairly well characterized by NDE	Pipe is stored at reactor site; utility and NRC resident inspectors are reviewing status; approval for use in Phase II is expected

DEGRADED PIPING IDENTIFIED FOR POSSIBLE TESTING IN PHASE II

Material and Pipe Form	Field- or Laboratory-Degraded?	Crack Characterization	Status as of 9/15/82
E. Several sections of 4-inch dia., Sch. 40, Type A106, Grade B pipe from a recombiner section	Field	Apparently, the crack geometries are well characterized by NDE	Pipe is stored at reactor site; verbal approval has been received for use in Phase II; written approval and additional details have been requested by Battelle
F. Several sections of 28-inch dia., Type 304 recirculation pipes	Field	Ultrasonic inspection revealed numerous crack-like indications near welds	Utility is making plans to remove cracked pipe; written permission has been received to transport and test the pipe in Phase II; shipment of pipe to Battelle for storage is expected to be completed within 60 days
G. 8-inch dia., Type 304 pipe from feedwater sparger	Field	Not known	Pipe is stored at reactor site; details of crack location, crack geometry, and availability for Phase II have been requested from utility
H. 12-inch dia., Type 304 straight pipe	Laboratory	Crack geometry is well characterized	Pipe was used in EPRI-sponsored leak-rate studies and is stored at Battelle; negotiations with EPRI to use pipe in Phase II are in progress
I. 26-inch dia., Type 304 straight pipe, 4 feet long, 1.3-inch-thick, with circumferential weld at midlength	Laboratory	Crack geometry is well characterized	Pipe is currently being cracked at B-PNL under EPRI sponsorship in a simulated BWR environment; exposure will continue through 1983; final disposition not yet decided; written request for use in Phase II has been submitted to EPRI

DEGRADED PIPING IDENTIFIED FOR POSSIBLE TESTING IN PHASE II

	Material and Pipe Form	Field- or Laboratory-Degraded?	Crack Characterization	Status as of 9/15/82
J.	Two sections of 24-inch, Type 304 straight pipe, 6-ft. long with circumferential welds at 1/3- and 2/3-length locations	Laboratory	Crack geometry is well characterized	Pipe is currently being cracked at B-PNL under EPRI sponsorship in a simulated BWR environment; exposure will continue through 1983; final disposition not yet decided: written request for use in Phase II has been submitted to EPRI
K.	5-inch dia.,Type 304 pipe; weld joining elbow to straight section contains cracks	Field	Cracks are visible but characterization is incomplete	Pipe is being stored at Battelle's West Jefferson Hot Laboratory
L.	One 4-inch dia., Type 304 pipe with a circumferential weld centered in the 16-inch length	Laboratory	Incomplete	Pipe is being cracked at B-PNL in simulated BWR environment using graphite wool; final disposition not yet decided
M.	Two sections of 10-inch dia., Type 304 Schedule 80 pipe welded to 10-inch dia. elbows; one section of 10-inch dia. pipe welded to conical transition piece	Laboratory	Incomplete	Pipes are being cracked at B-PNL in autoclave using graphite wool; final disposition not yet decided
N.	14-inch to 10-inch diameter reducer; Type 304	Field	Reducer contains weld defect; degree of characterization unknown	Reducer is being stored at a laboratory operated by a reactor vendor

STATUS OF COOPERATIVE EFFORTS

ORGANIZATION	FRACTURE DATA EXCHANGED	ANALYSES EXCHANGED	PIPE SPECIMENS CONTRIBUTED	COOPERATION ON TEST MATRIX	COST SHARING
UNITED STATES					
EPRI	X			X	
GENERAL ELECTRIC	X	X		X	
WESTINGHOUSE	X	X		X	
BABCOCK & WILCOX		X			
COMBUSTION ENGINEERING		X			
EUROPE					
FRAMATONE	X	X	X	X	
MPA - STUTTGART	X	X		X	
CEGB	X	X		X	
EDEA	X	X		X	
KRAFTWERK UNION	X	X		X	
TÜV	X	X			
NIT	X	X			
JAPAN					
JAERI	X	X			
HITACHI	X	X			

Battelle
Columbus Laboratories

RECOMMENDED REQUIREMENTS FOR PHASE II PROGRAM

FACILITIES

- LABORATORY-SCALE FRACTURE TESTING EQUIPMENT
- MULTI-LOAD PIPE FRACTURE SET-UP
- HIGH ENERGY RELEASE CONTAINMENT
- HOT CELL FOR FRACTURE TESTING AND CLEAN-UP

CAPABILITIES

- LABORATORY-INDUCED CRACK FORMATION
- CRACK GROWTH LENGTH MEASUREMENTS
- DYNAMIC INSTRUMENTATION AND DATA ACQUISITION

BACKGROUND EXPERIENCE

- TEARING INSTABILITY ANALYSIS DEVELOPMENT
- PIPE FRACTURE EXPERIMENTATION
- ANALYTICAL/EXPERIMENTAL INTERACTION

Battelle
Columbus Laboratories

RECOMMENDED TEST MATRIX FOR PHASE II PROGRAM

NUMBER	PRIMARY VARIABLE	PRIORITY
	AXIAL CRACKS - PRESSURE LOADING	
A-1	LOW TOUGHNESS MATERIALS	1
A-2	SUSTAINED LOAD/ENVIRONMENT EFFECTS	2
A-3	WATERHAMMER RESPONSE	2
A-4	EXTENT OF AXIAL INSTABILITY AT OPERATING CONDITIONS	3
	CIRCUMFERENTIAL CRACKS - BENDING LOADING	
CB-1	EFFECT OF INITIAL FLAW CONDITION	1
CB-2	EFFECT OF PIPE DIAMETER (THROUGH WALL CRACKS)	1
CB-3	EFFECT OF WALL-THICKNESS (SURFACE CRACKS)	1
CB-4	SURFACE CRACK CONSTRAINT	1
CB-5	THROUGH-WALL CRACK INSTABILITY WITH SURFACE CRACKS	1
CB-6	INSTABILITY OF LONG SURFACE CRACKS	1
CB-7	LOW TOUGHNESS MATERIALS	1
CB-8	SUSTAINED LOAD/ENVIRONMENTAL EFFECTS	2
	CIRCUMFERENTIAL CRACKS - TENSILE LOADING	
CA-1	CRACK SIZE (THROUGH-WALL, PART THROUGH)	2
CA-2	INSTABILITY BEHAVIOR	3
CA-3	WATERHAMMER RESPONSE	2
	CIRCUMFERENTIAL CRACKS - TORSION LOADING	
CT-1	MIXED MODE RESPONSE	2
	CIRMFERENTIAL CRACKS - COMBINED PRESSURE AND BENDING	
CPB-1	MIXED CONTROL CONDITIONS	1
CPB-2	OPERATING CONDITIONS	2

Battelle
Columbus Laboratories

RECOMMENDED NUMBER OF EXPERIMENTS FOR PHASE II PROGRAM

CRACK ORIENTATION - LOADING	GROUP NUMBERS	LOW ENERGY SMALL DIA.	LOW ENERGY MED. DIA.	LOW ENERGY LGE. DIA.	HIGH ENERGY SMALL DIA.	HIGH ENERGY MED. DIA.	HIGH ENERGY LGE. DIA.	COMMENTS
AXIAL-PRESSURE ONLY	A1	2	2					AMBIENT-WATER
	A2	4	4					LWR-SUSTAINED LOAD
	A3	2	2					DYNAMIC
	A4				4	4	2	LWR-WATER
CIRCUMFERENTIAL-BENDING	CB-1		4					NOTCH ACUITY
	CB-2		1	2				DIA. EFFECT ON T.W.
	CB-3	5	5					DIA. & THICKNESS ON S.F.
	CB-4	6						J/T OF T.W.C./S.C.
	CB-5	2	2					INSTAB. T.W.C./S.C.
	CB-6	4	4					INSTAB. S.F.
	CB-7	3	3					WELD METAL, LOW TOUGHNES MATERIALS
	CB-8	2	2					HIGH TEMP-SUSTAINED LOAD
CIRCUMFERENTIAL-AXIAL	CA-1a	3	1					T.W. GROWTH
	CA-1b	7	1					S.F. GROWTH
	CA-2	CONTINGENT ON JAPANESE DATA						INSTABILITY
	CA-3	3						DYNAMIC-WATERHAMMER
CIRCUMFERENTIAL-TORSION	CT-1	8						T.W. & S.F. SCOPING
CIRCUMFERENTIAL-PRESSURE AND EXCESSIVE BENDING	CPB-1		3	4				INSTABILITY-OIL
	CPB-2a				4			INSTABILITY, LWR WATER
	CPB-2b						4	INSTABILITY, LWR-WATER
	SUBTOTAL	51	34	6	8	4	6	/TOTAL = 109 EXPERIMENTS

Battelle
Columbus Laboratories

ESTIMATED PIPE TEST COSTS

GROUP NUMBER	APPROXIMATE COST, $1,000 PRIORITY 1	PRIORITY 2	PRIORITY 3
A-1	$ 60	$ -	$ -
A-2	-	200	-
A-3	-	80	-
A-4	-	-	730
CB-1	200	-	-
CB-2	140	-	-
CB-3	200	-	-
CB-4	120	-	-
CB-5	150	-	-
CB-6	300	-	-
CB-7	210	-	-
CB-8	-	140	-
CA-1	-	200	-
CA-2	-	-	150
CA-3	-	70	-
CT-1	-	160	-
CPB-1	300	-	
CPB-2	-	640	-
TOTAL	$1,680	$1,490	$880

Battelle
Columbus Laboratories

ESTIMATED ASSOCIATED COSTS

DESCRIPTION	COST, $1,000		
	PRIORITY 1	PRIORTY 2	PRIORTY 3
• SHIPPING AND ADDITIONAL HANDLING PROBLEMS FOR DEGRADED PIPE	100	-	-
• SPECIMEN PREPARATION			
- PIPE COST	150	100	100
- WELDING (LARGER DIAMETER)	50	30	30
- LABORATORY SIMULATED CRACKS	150	30	50
• FIXTURING/FACILITY CONSTRUCTION			
- LOW ENERGY EXPERIMENTS (PRIORITY 1)	300	-	-
- HIGH ENERGY EXPERIMENTS (PRIORITY 2,3)	-	750	-
• ANALYSIS AND COMPUTOR TIME	400	200	100
• LABORATORY SPECIMEN TESTING	300	20	20
TOTAL	1450	1130	300

Battelle
Columbus Laboratories

TOTAL COST ESTIMATE

	COST, $1000		
	PRIORITY 1	PRIORITY 2	PRIORITY 3
PIPE TESTS	1680	1490	880
ASSOCIATED COSTS	1450	1130	300
TOTAL	3,130	2,620	1,180

GRAND TOTAL 6,930

Battelle
Columbus Laboratories

CONCLUSIONS AND ACHIEVEMENTS

- ONLY LIMITED AMOUNT OF SERVICE DEGRADED PIPE IS AVAILABLE FOR PHASE II
- MOST EXISTING DATA FOUND TO BE INADEQUATE FOR J/T ASSESSMENT
- GENERALIZATION OF J-ESTIMATION PROCEDURE WAS MADE TO INCLUDE WORK HARDENING
- COMPREHENSIVE PIPE FRACTURE EXPERIMENTAL PROGRAM WAS DESIGNED AND COSTED

Battelle
Columbus Laboratories

COMPACT SPECIMEN GEOMETRY AND ELASTIC COMPLIANCE TEST METHOD EFFECTS ON THE J-INTEGRAL R-CURVE

JOHN P. GUDAS
D.A. DAVIS
M.G. VASSILAROS
G.E. SUTTON

DAVID TAYLOR NAVAL SHIP R&D CENTER
ANNAPOLIS, MD. 21401

OBJECTIVE

EVALUATE SENSITIVITY OF THE
J-INTEGRAL R-CURVE

— COMPACT SPECIMEN GEOMETRY

— ELASTIC UNLOADING RANGE

2T COMPACT SPECIMEN

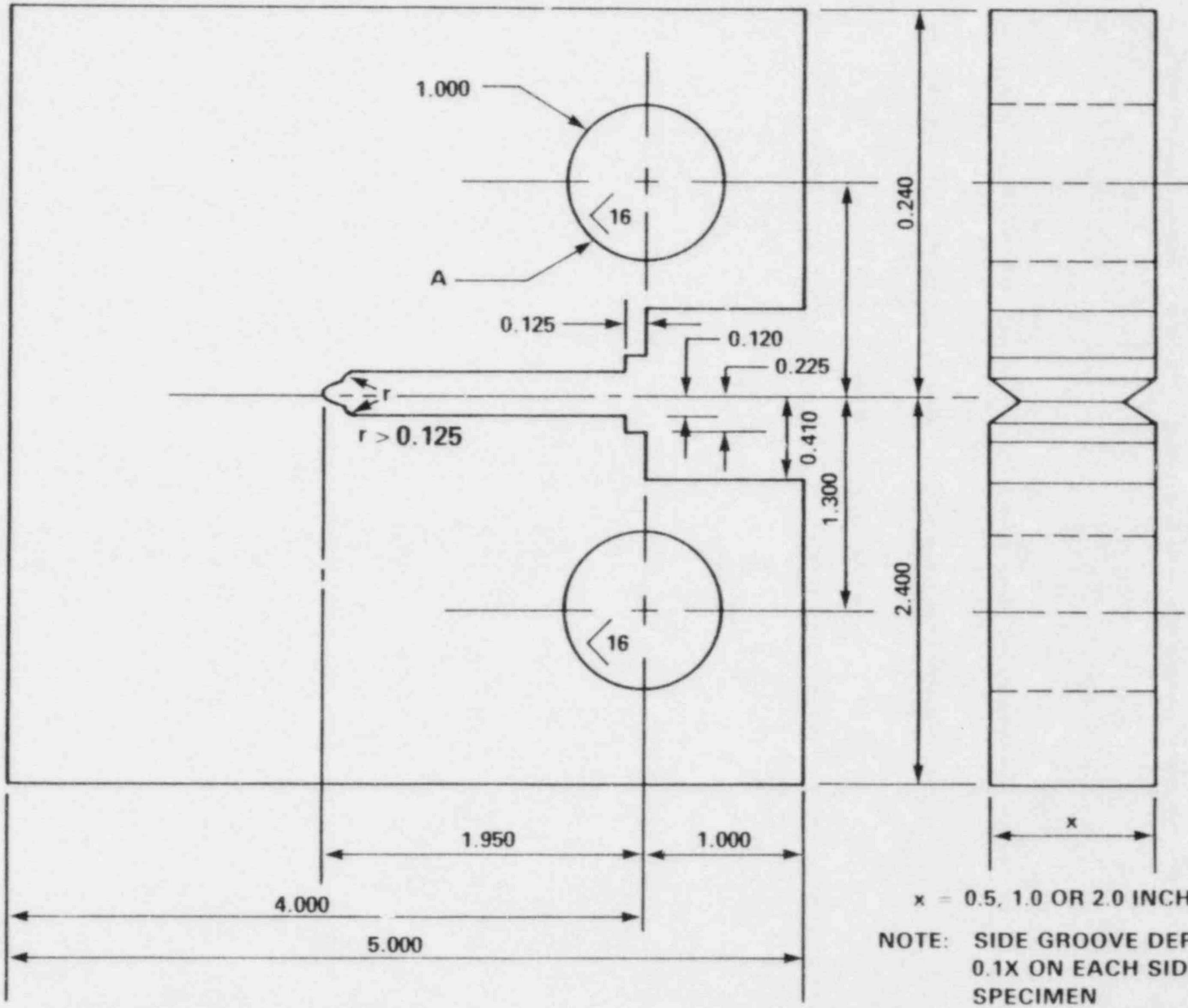

x = 0.5, 1.0 OR 2.0 INCHES

NOTE: SIDE GROOVE DEPTH IS 0.1X ON EACH SIDE OF SPECIMEN

• ALL DIMENSIONS IN INCHES

TEST MATRIX FOR EVALUATING THICKNESS/LIGAMENT GEOMETRY EFFECTS

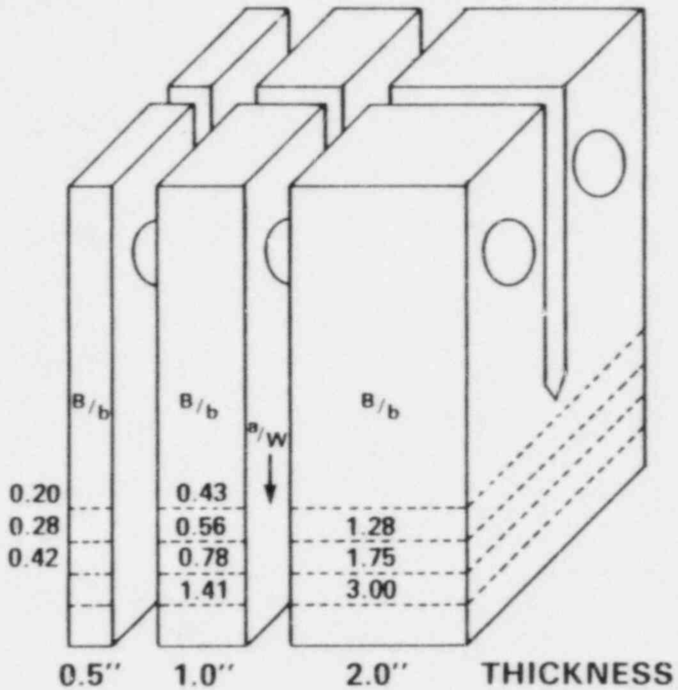

(A) ASTM A533B HSST-03 STEEL

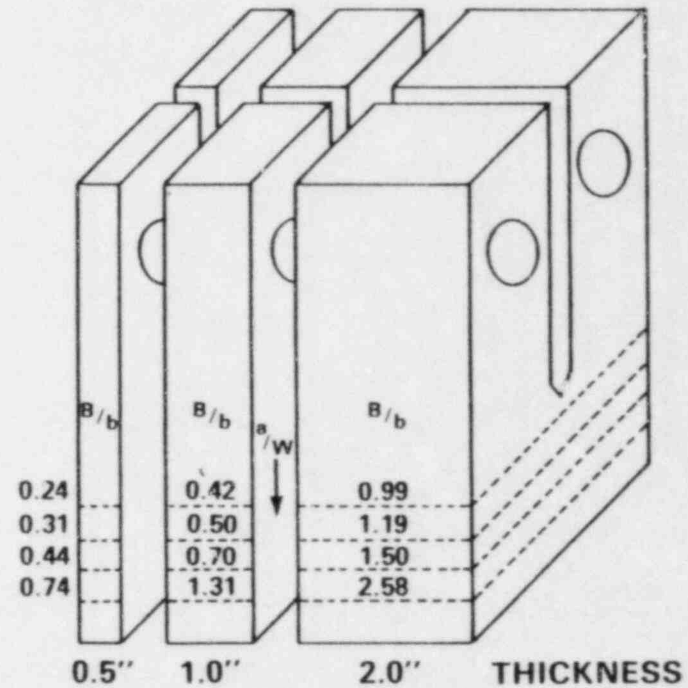

(B) HY-130 STEEL

HY 130 STEEL; 12.5 mm THICK 2T COMPACT SPECIMENS

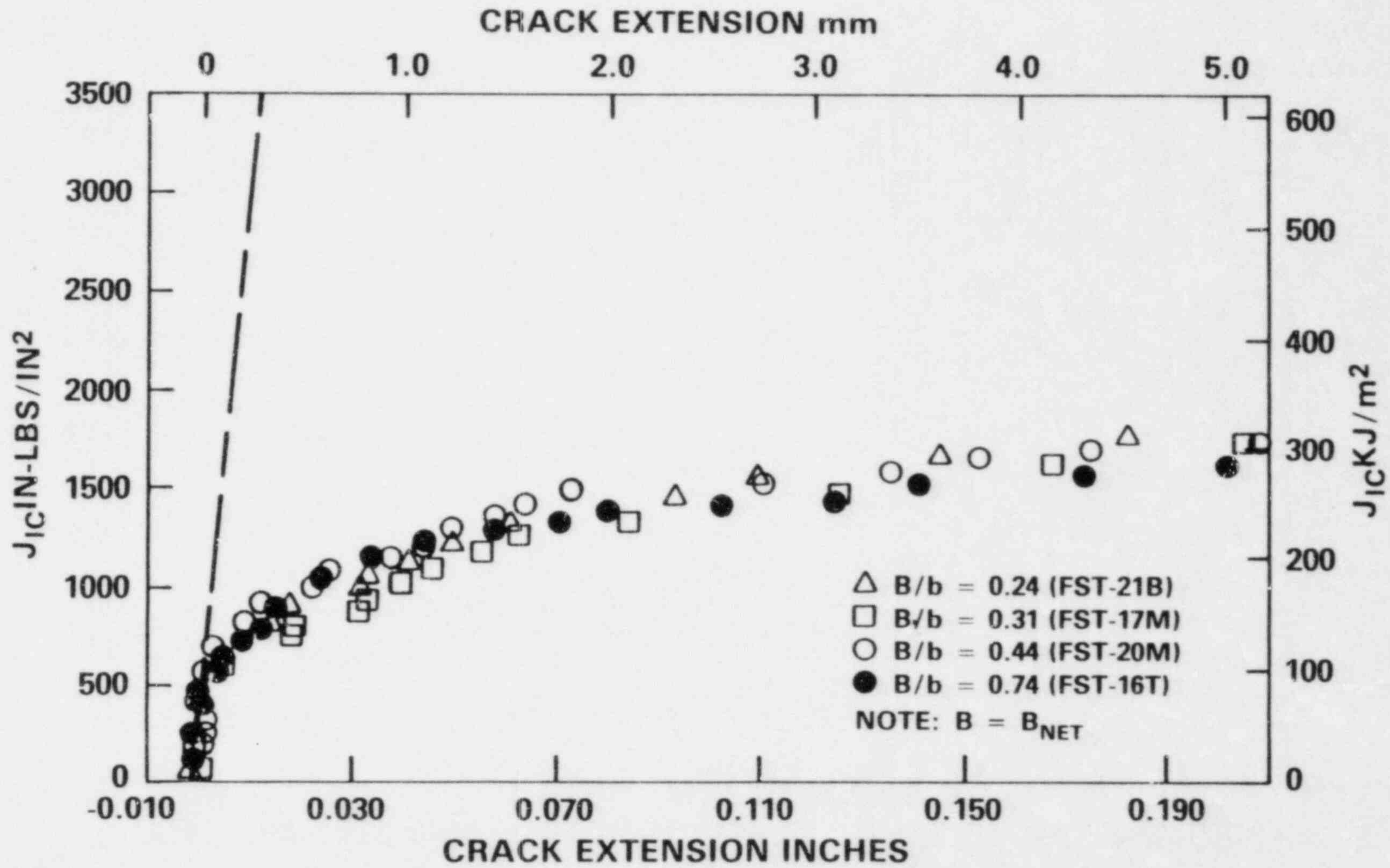

HY 130 STEEL; 25 mm THICK 2T COMPACT SPECIMENS

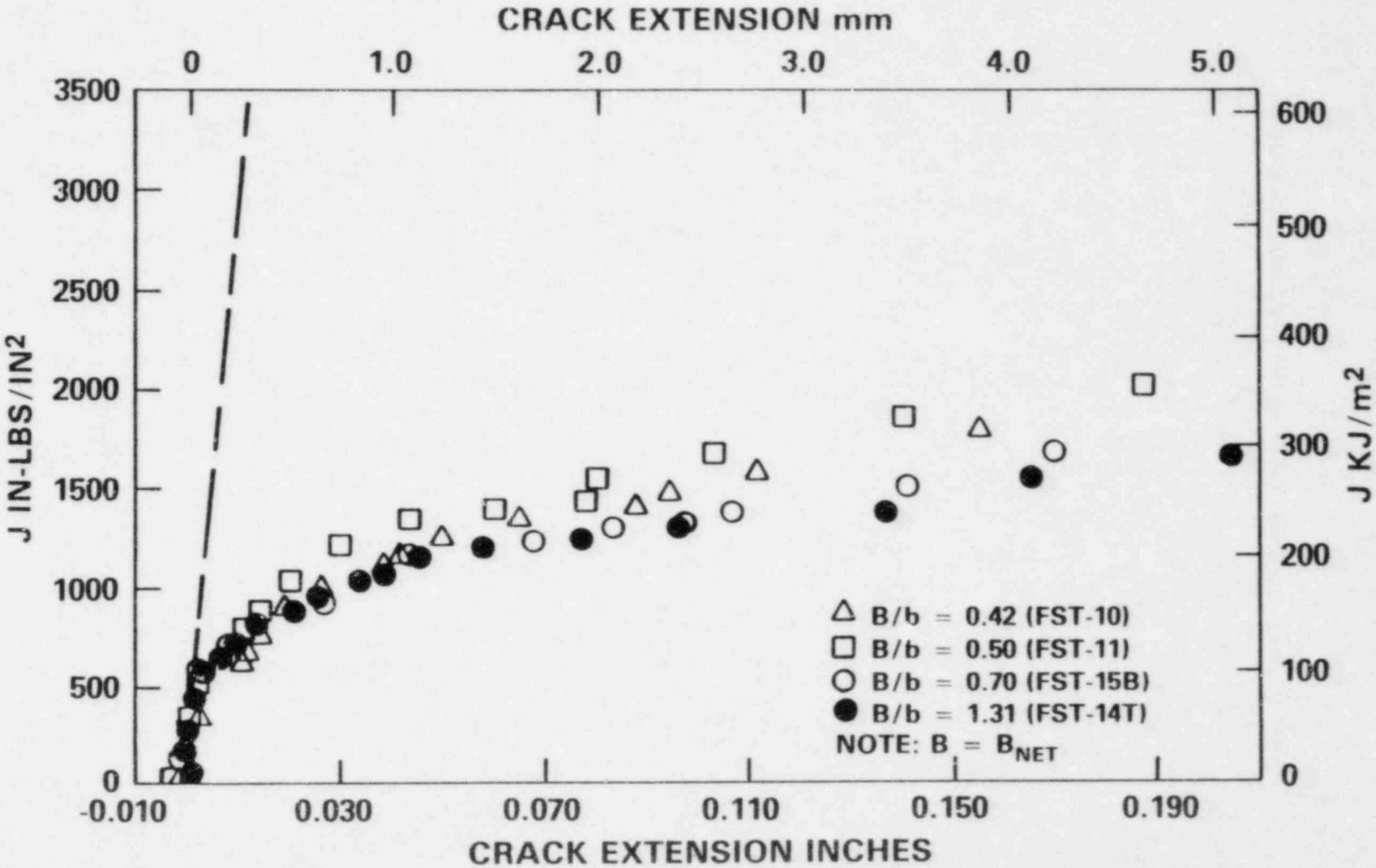

HY 130 STEEL; 2T COMPACT SPECIMENS

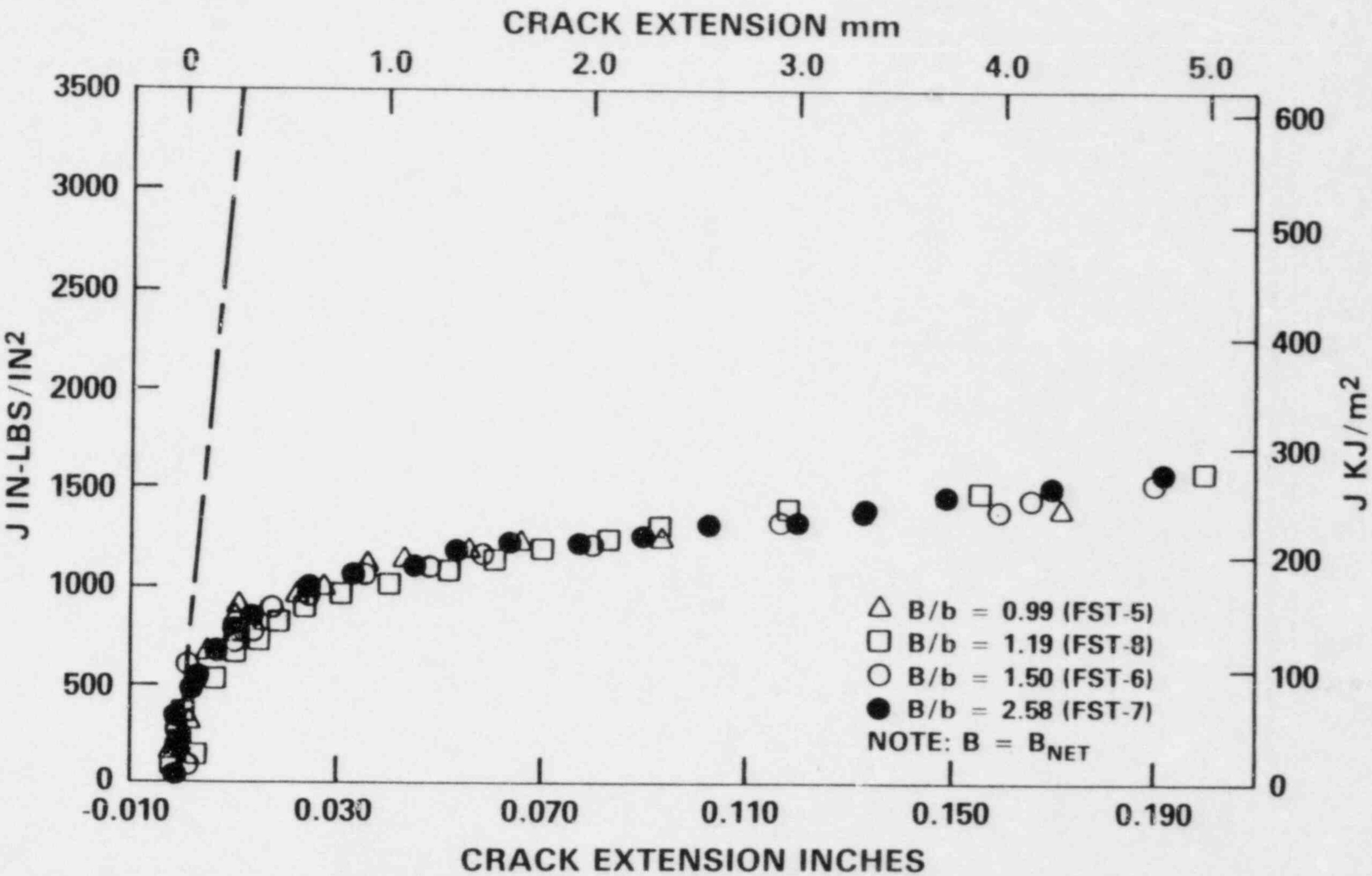

HY 130 STEEL

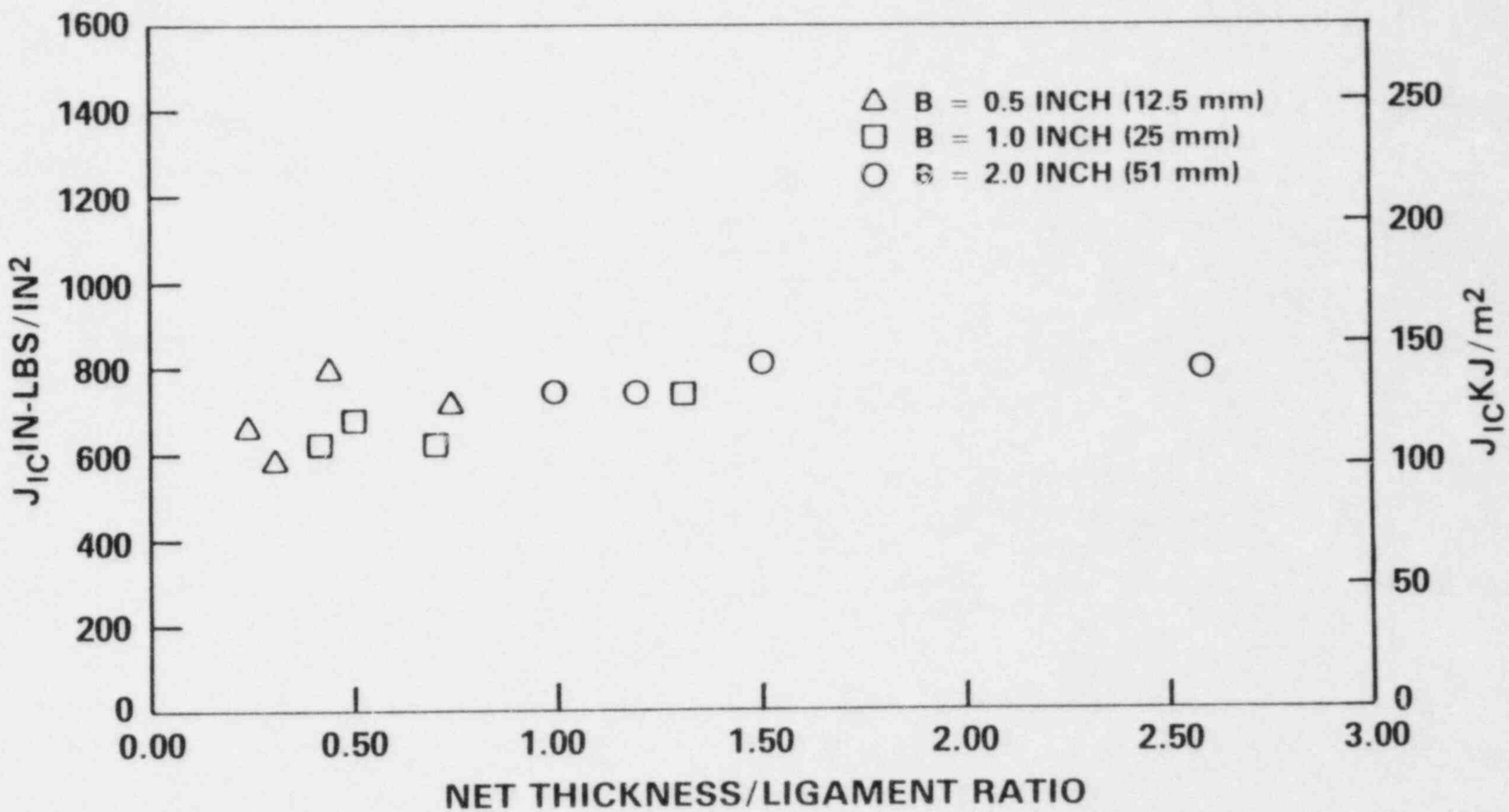

101

HY 130 STEEL
T EVALUATED OVER 1.5 mm CRACK EXTENSION

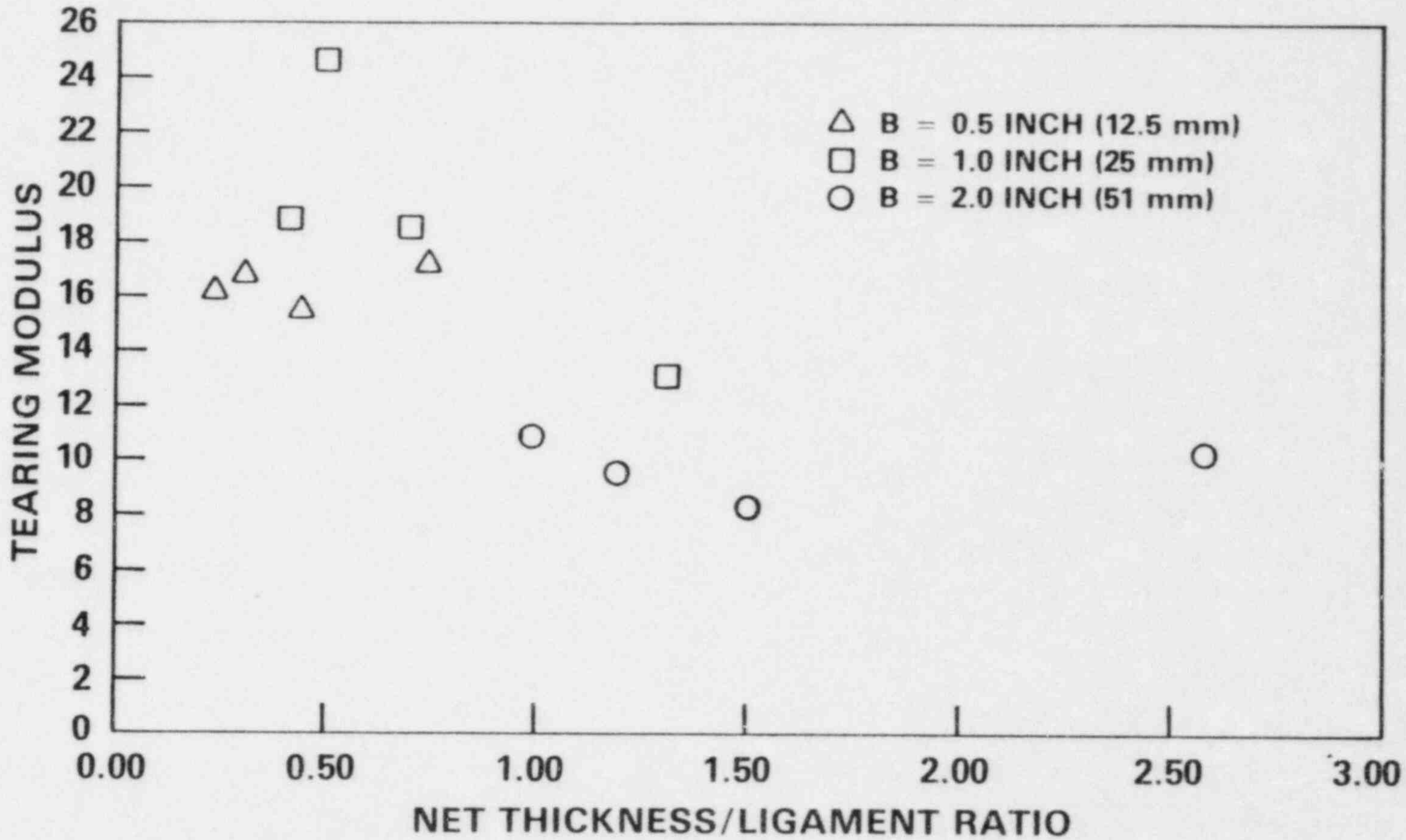

HY 130 STEEL
T EVALUATED OVER 5.0 mm CRACK EXTENSION

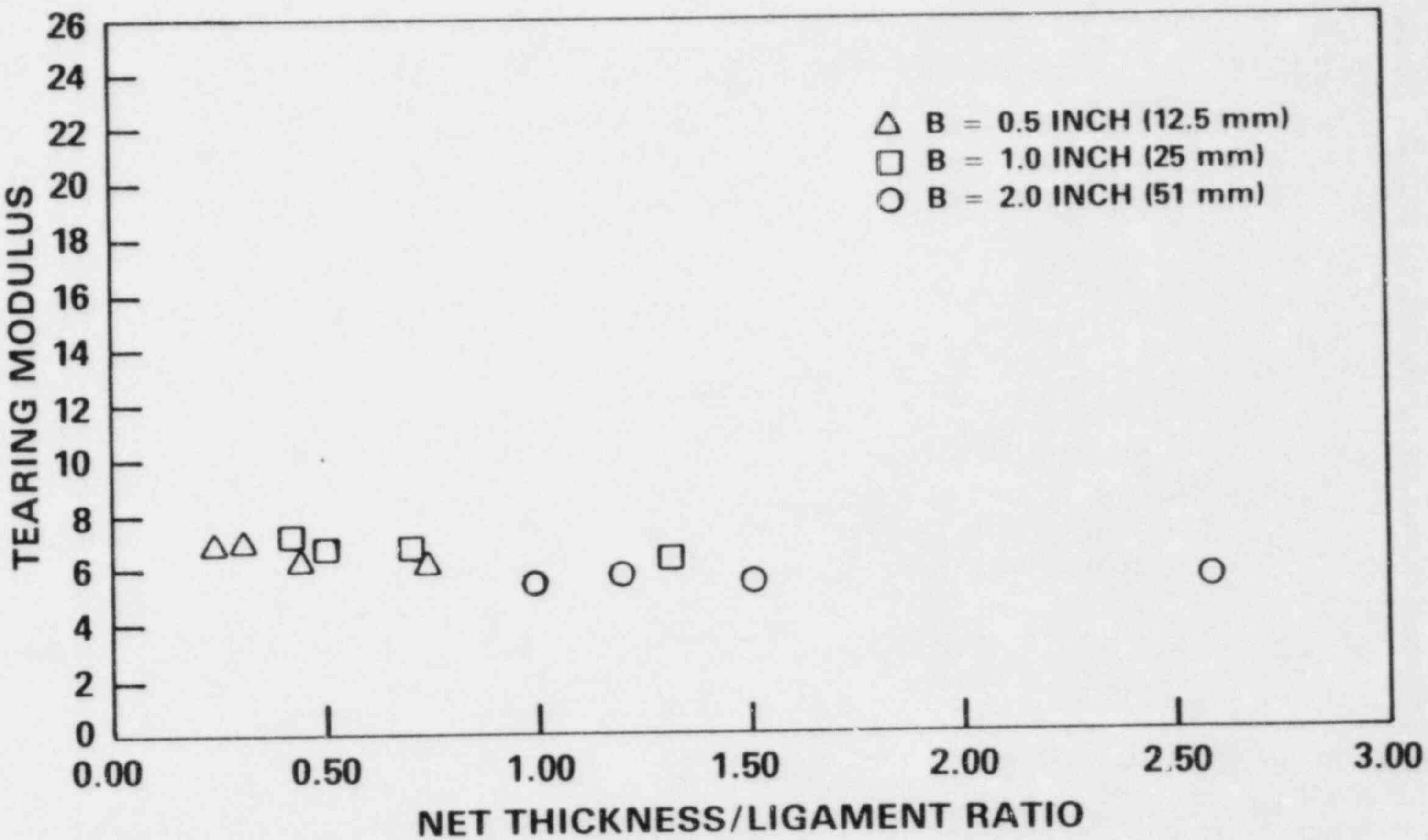

HY 130 STEEL

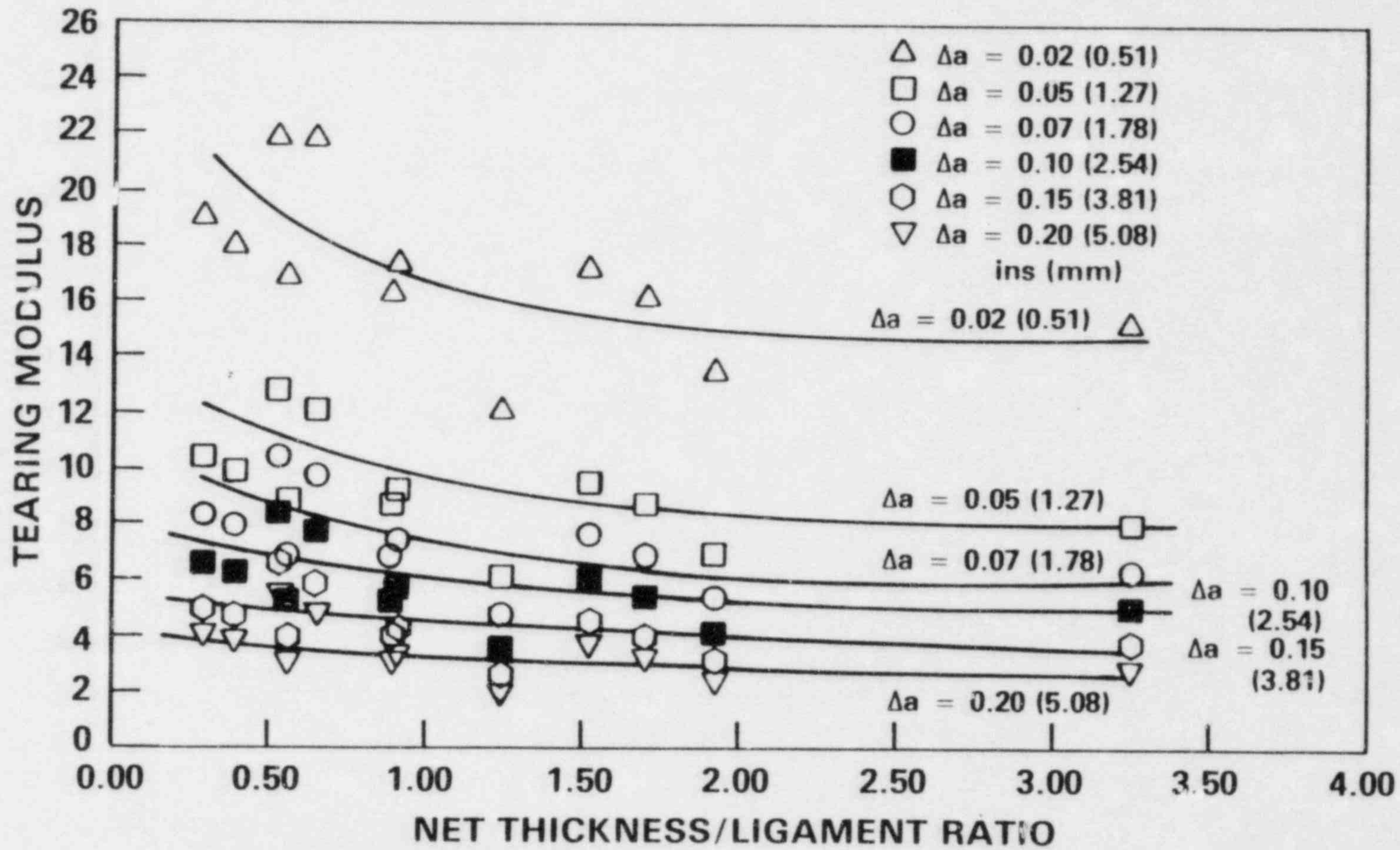

TEARING MODULUS
NET THICKNESS/LIGAMENT RATIO
0
2
4
6
8
10
12
14
16
18
20
22
24
26
0.00
0.50
1.00
1.50
2.00
2.50
3.00
3.50
4.00
Δa = 0.02 (0.51)
Δa = 0.05 (1.27)
Δa = 0.07 (1.78)
Δa = 0.10 (2.54)
Δa = 0.15 (3.81)
Δa = 0.20 (5.08)
ins (mm)
Δa = 0.02 (0.51)
Δa = 0.05 (1.27)
Δa = 0.07 (1.78)
Δa = 0.10 (2.54)
Δa = 0.15 (3.81)
Δa = 0.20 (5.08)

ASTM A533 B STEEL; 12.5 mm THICK
2T COMPACT SPECIMENS

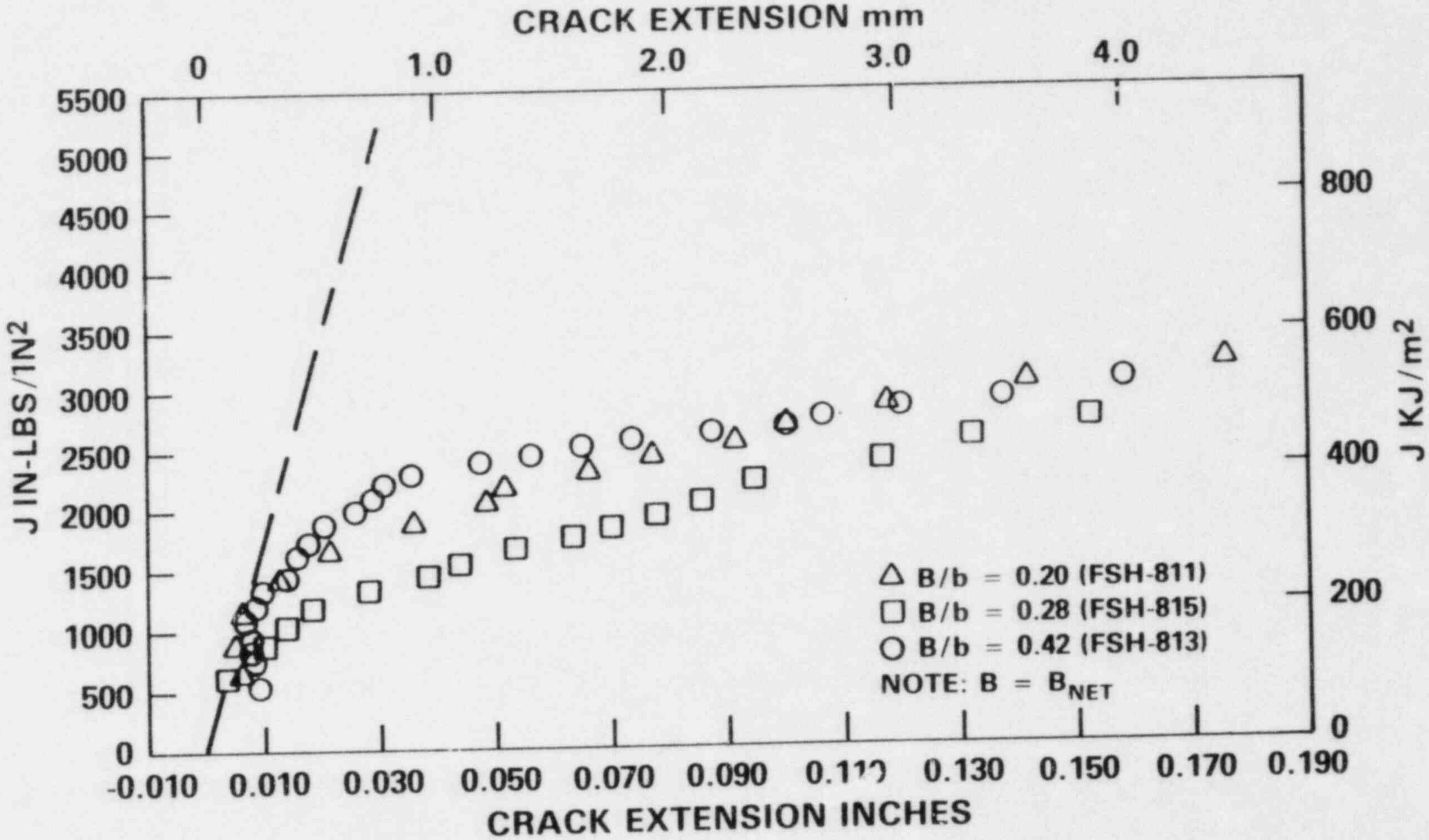

105

ASTM A533 B STEEL; 25 mm THICK
2T COMPACT SPECIMENS

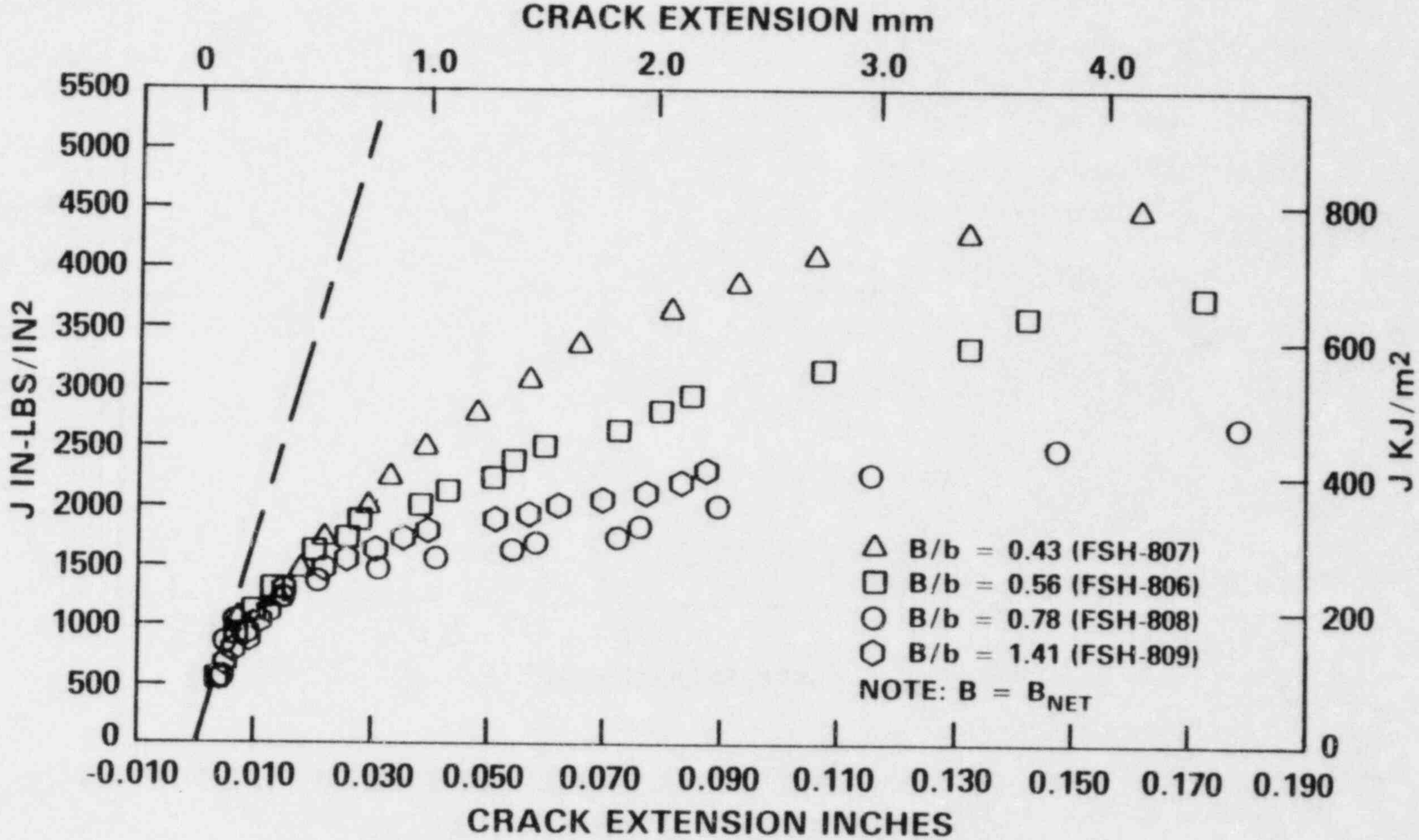

106

ASTM A533 B STEEL; 2T COMPACT SPECIMENS

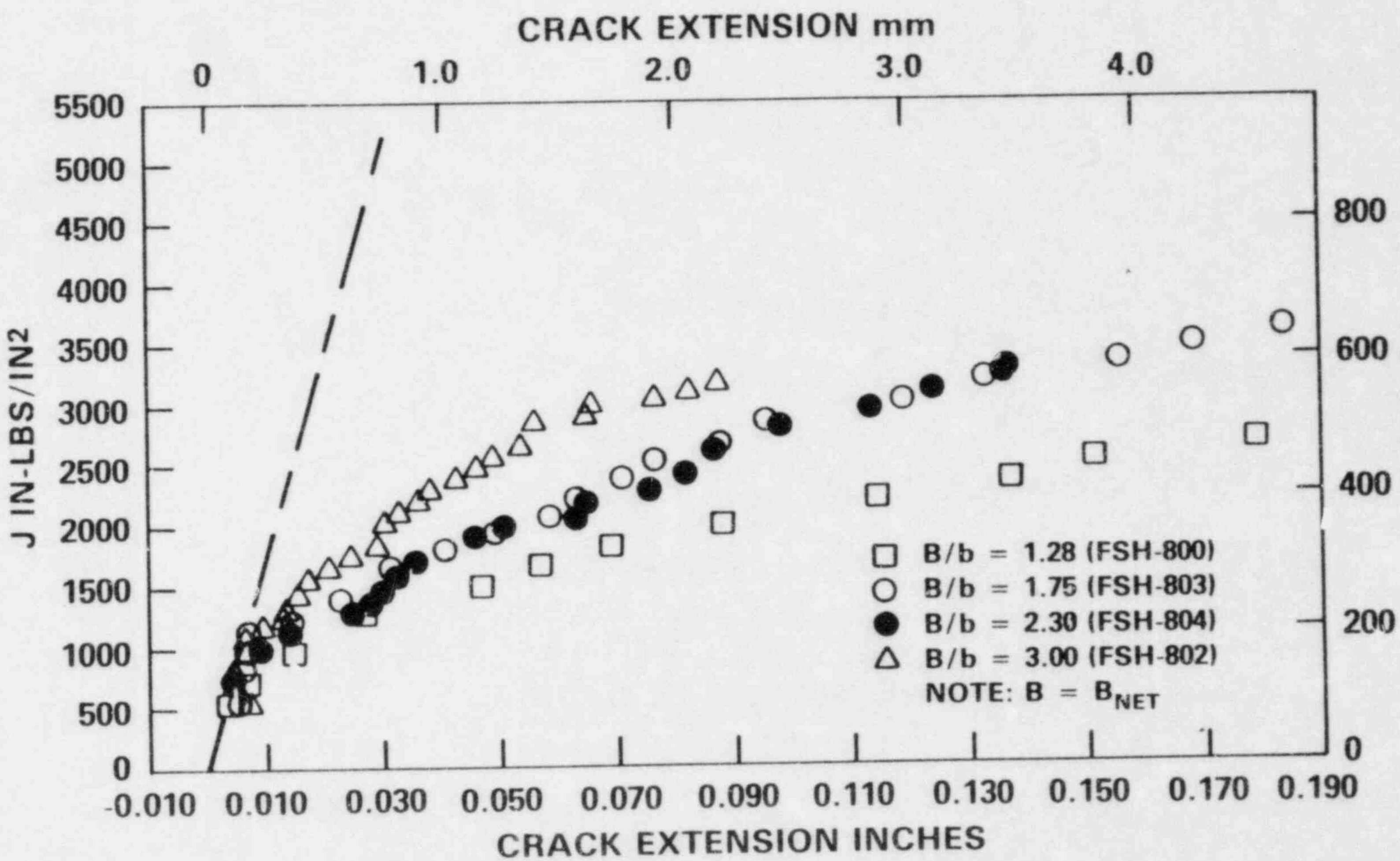

ASTM A533 B STEEL; VALID SPECIMENS ONLY

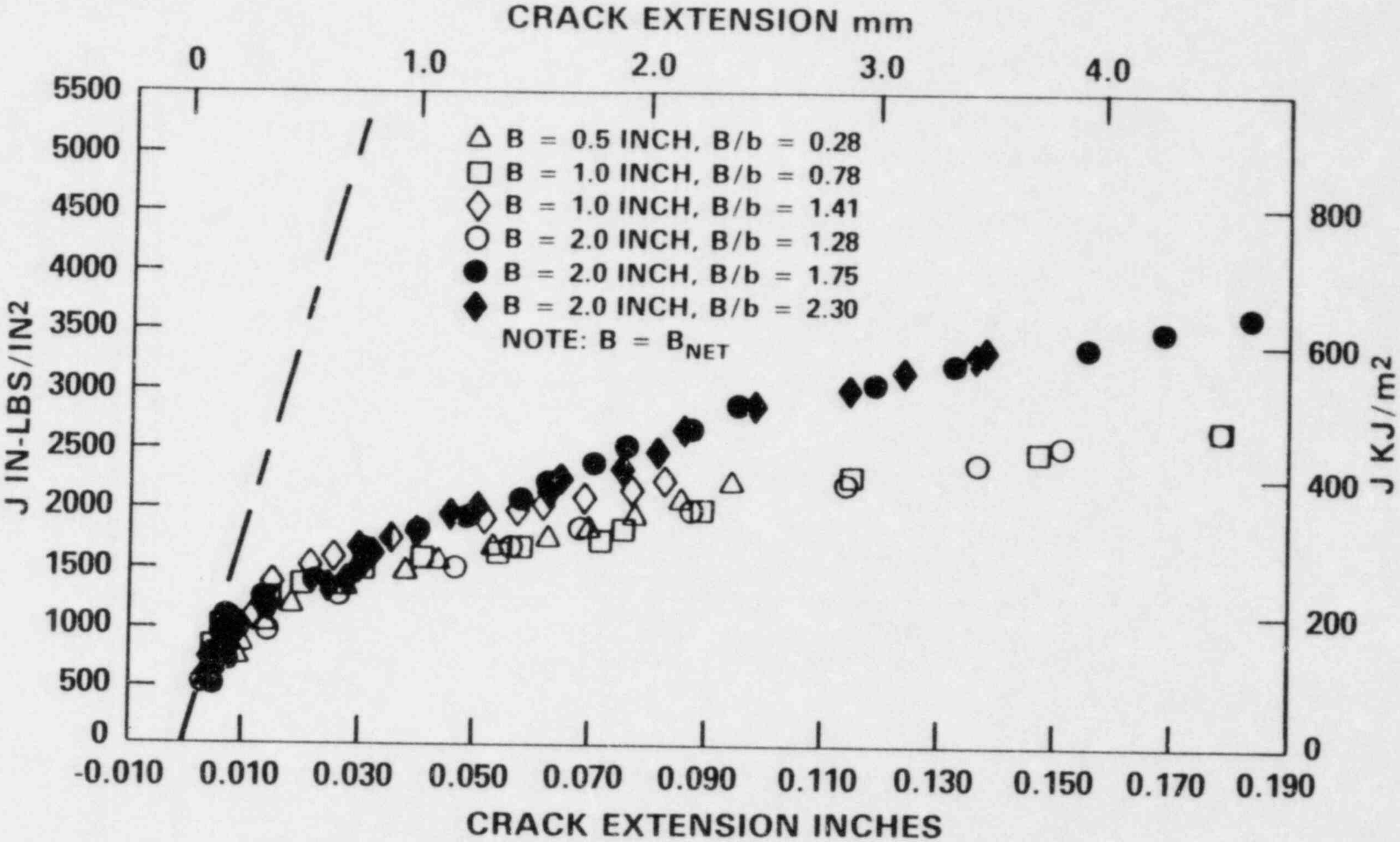

108

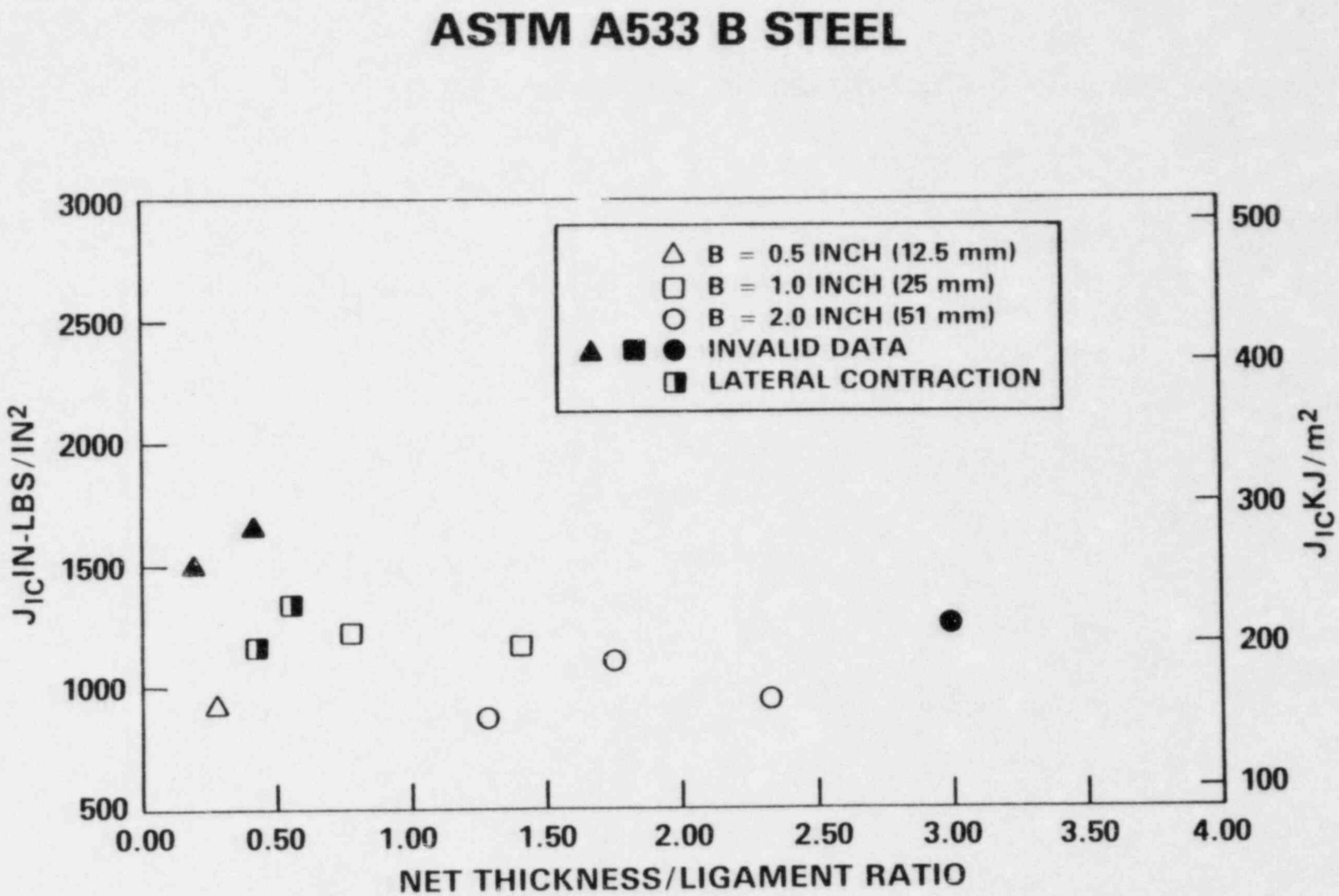
ASTM A533 B STEEL
B = 0.5 INCH (12.5 mm)
B = 1.0 INCH (25 mm)
B = 2.0 INCH (51 mm)
INVALID DATA
LATERAL CONTRACTION
J_{IC} IN-LBS/IN^2
J_{IC} KJ/m^2
NET THICKNESS/LIGAMENT RATIO
3000
2500
2000
1500
1000
500
500
400
300
200
100
0.00
0.50
1.00
1.50
2.00
2.50
3.00
3.50
4.00

109

ASTM A533 B STEEL
T EVALUATED OVER 1.5 mm CRACK EXTENSION

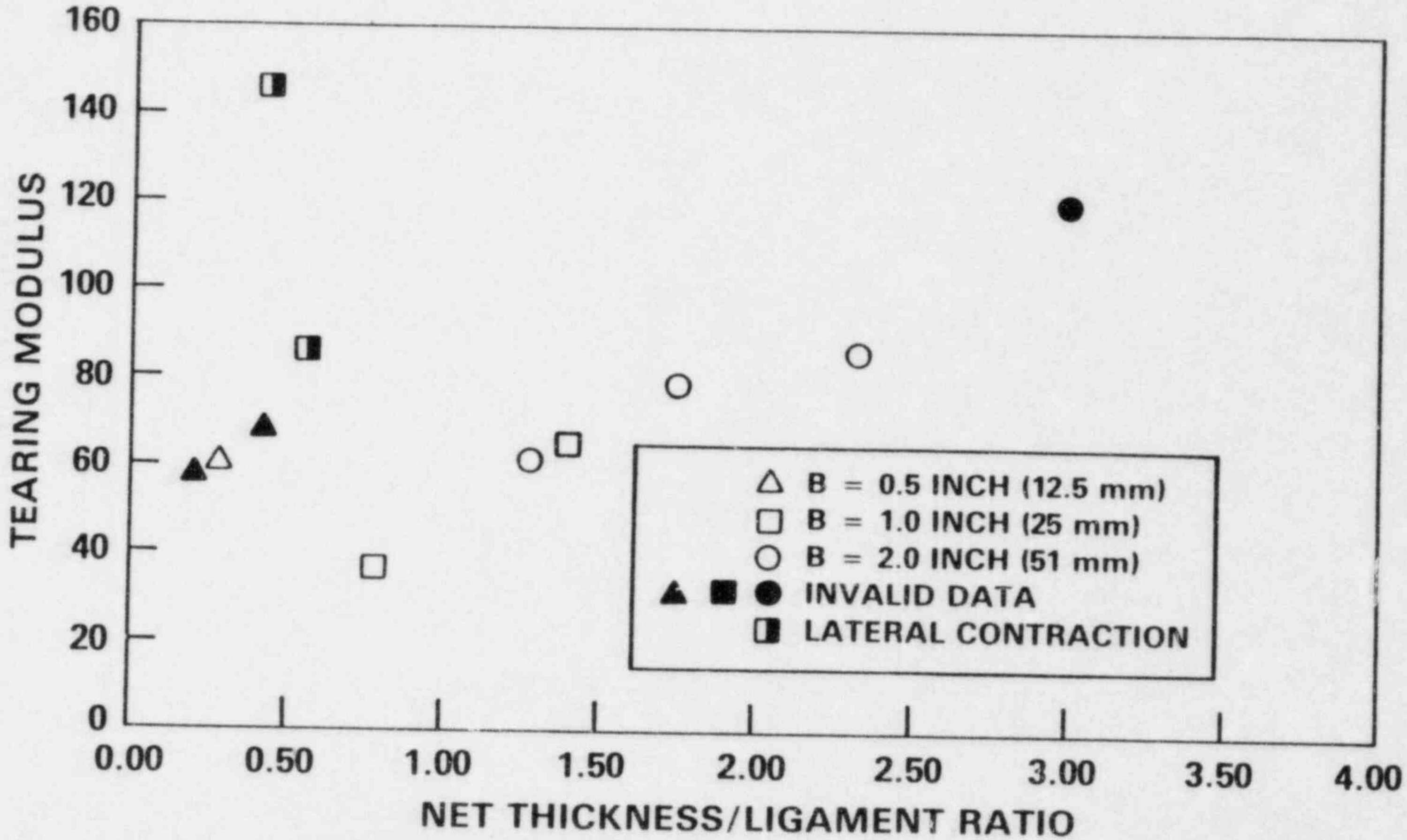

CONCLUSIONS

- J_{IC} IS GEOMETRY INDEPENDENT WHEN VALIDITY CRITERIA ARE MET

- J_I-R-CURVE IS DEPENDENT ON B/b AND Δa

ELASTIC UNLOADING TEST PROGRAM

MATERIAL: ASTM A106 CLASS C STEEL

TEST TEMPERATURE: 275° F

SPECIMEN GEOMETRY: 1T COMPACT; L-C ORIENTATION

TEST METHOD: COMPUTER INTERACTIVE, ELASTIC COMPLIANCE

TARGET UNLOADING RANGES: $\% \; P_{MAX}$ 10, 20, 30, 40, 50, 60, 70, 80, 90, 95

ASTM A106 CLASS C STEEL:
55% UNLOADING

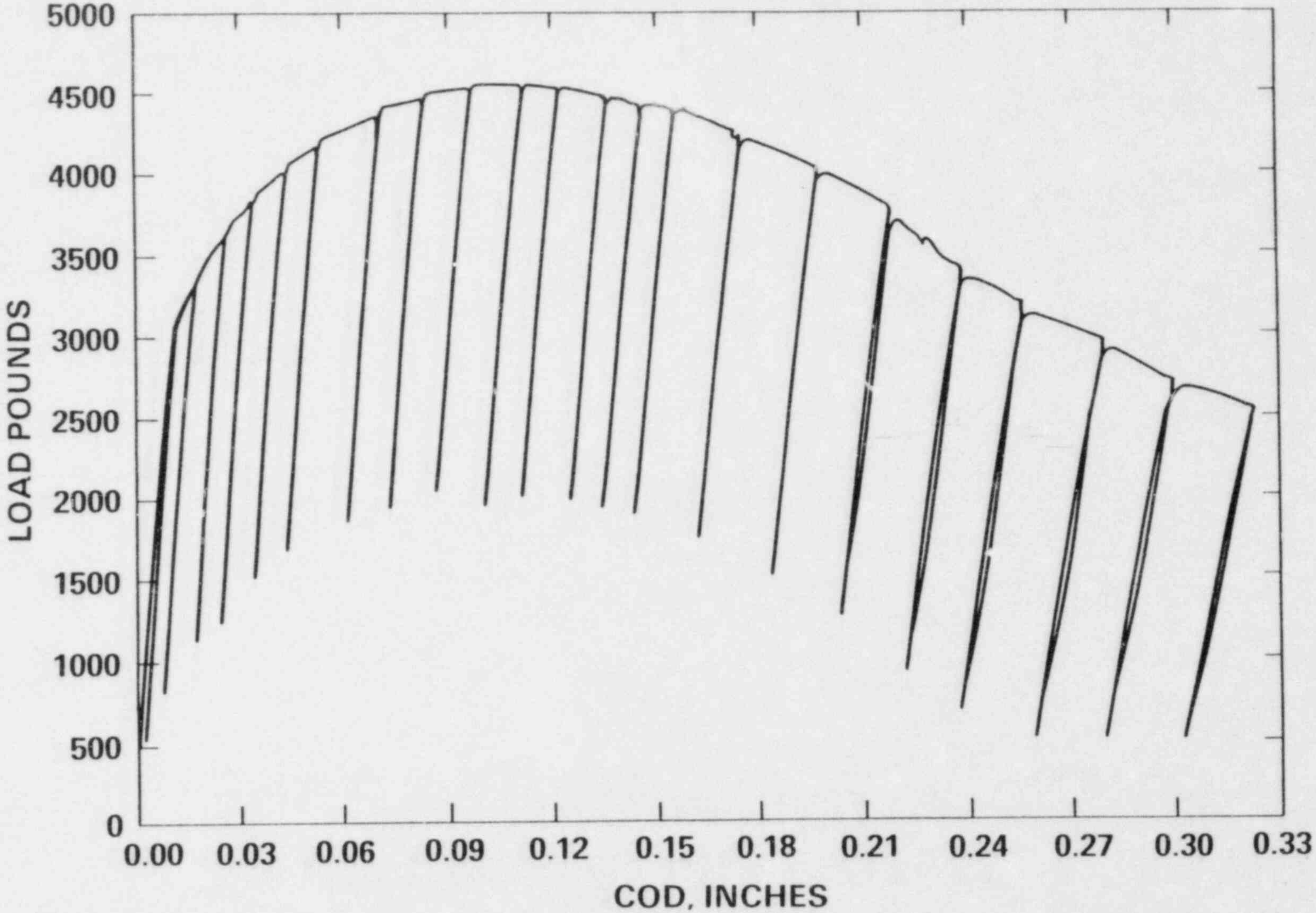

ASTM A106 CLASS C STEEL; 89% UNLOADING

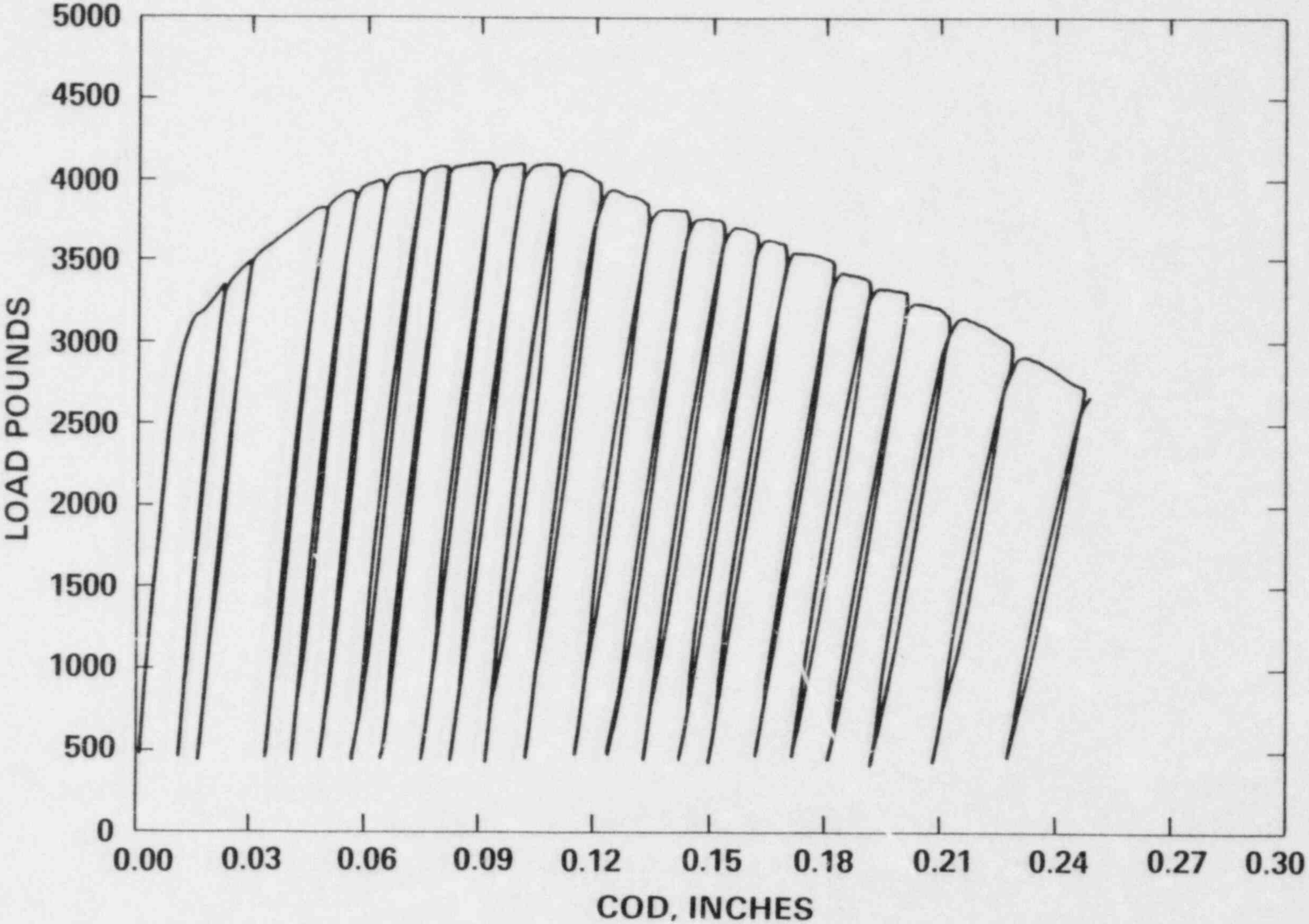

ASTM A106 STEEL; ITCT; 89% UNLOADING

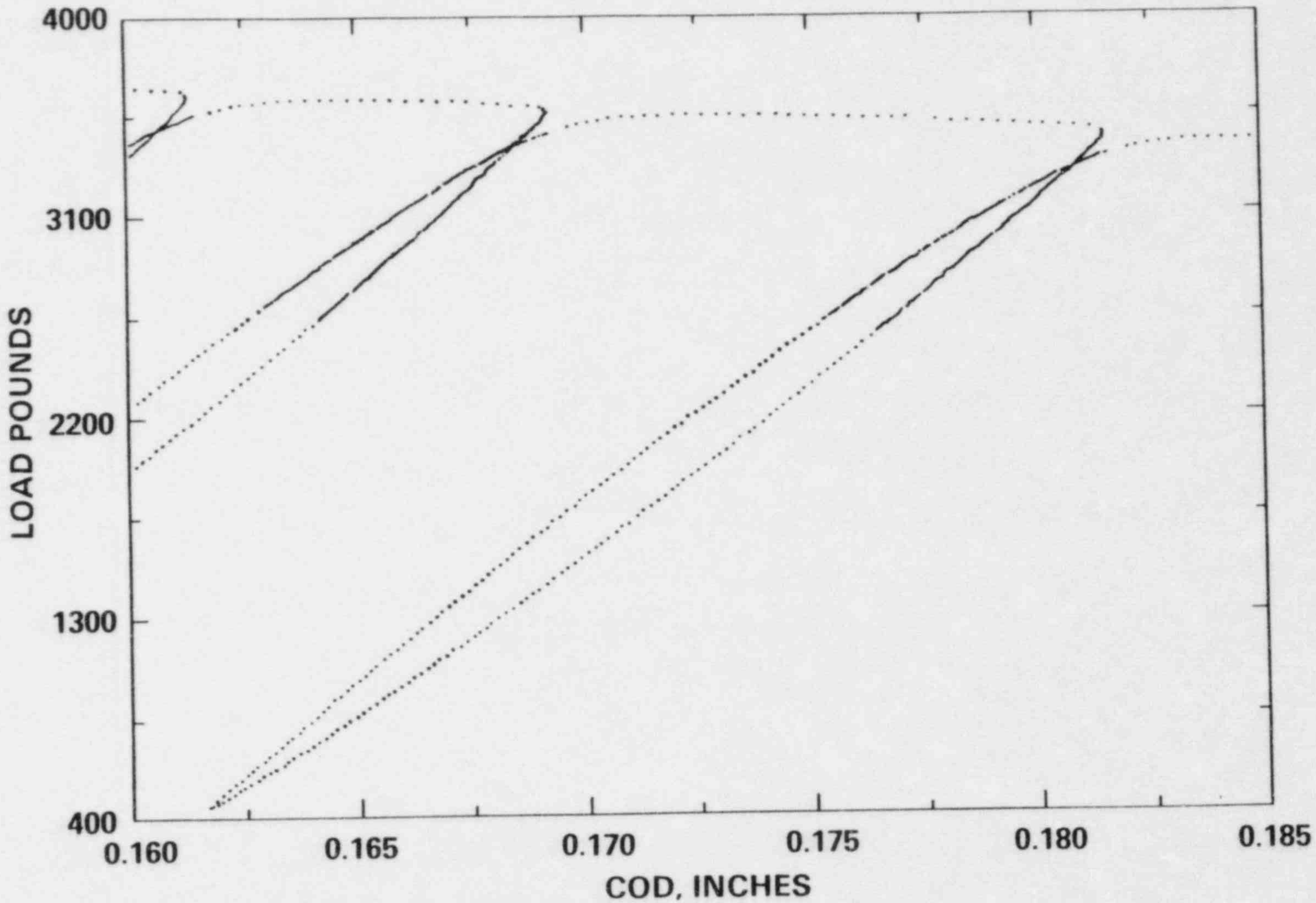

ASTM A106 CLASS C STEEL

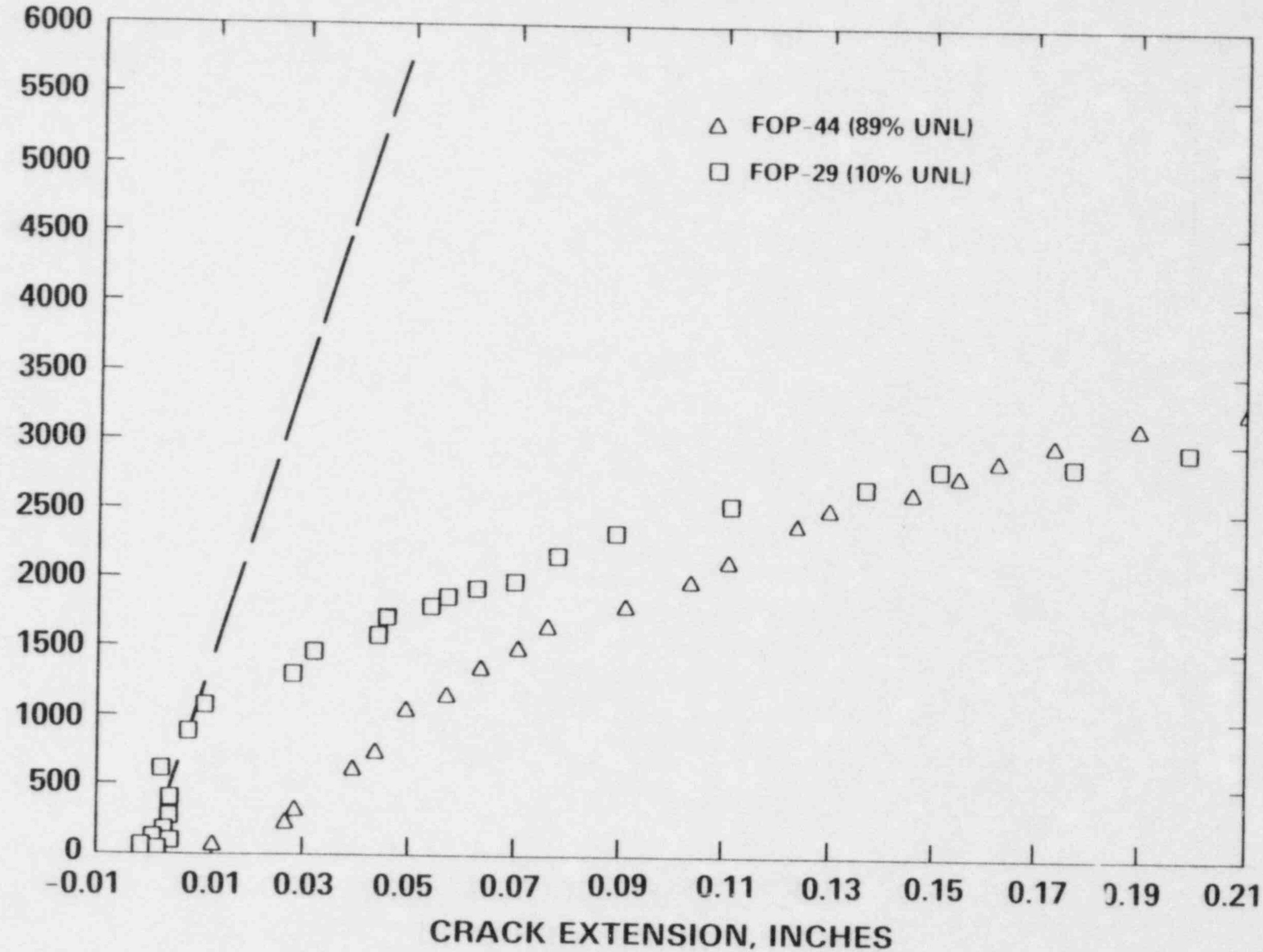

ASTM A106 CLASS C STEEL

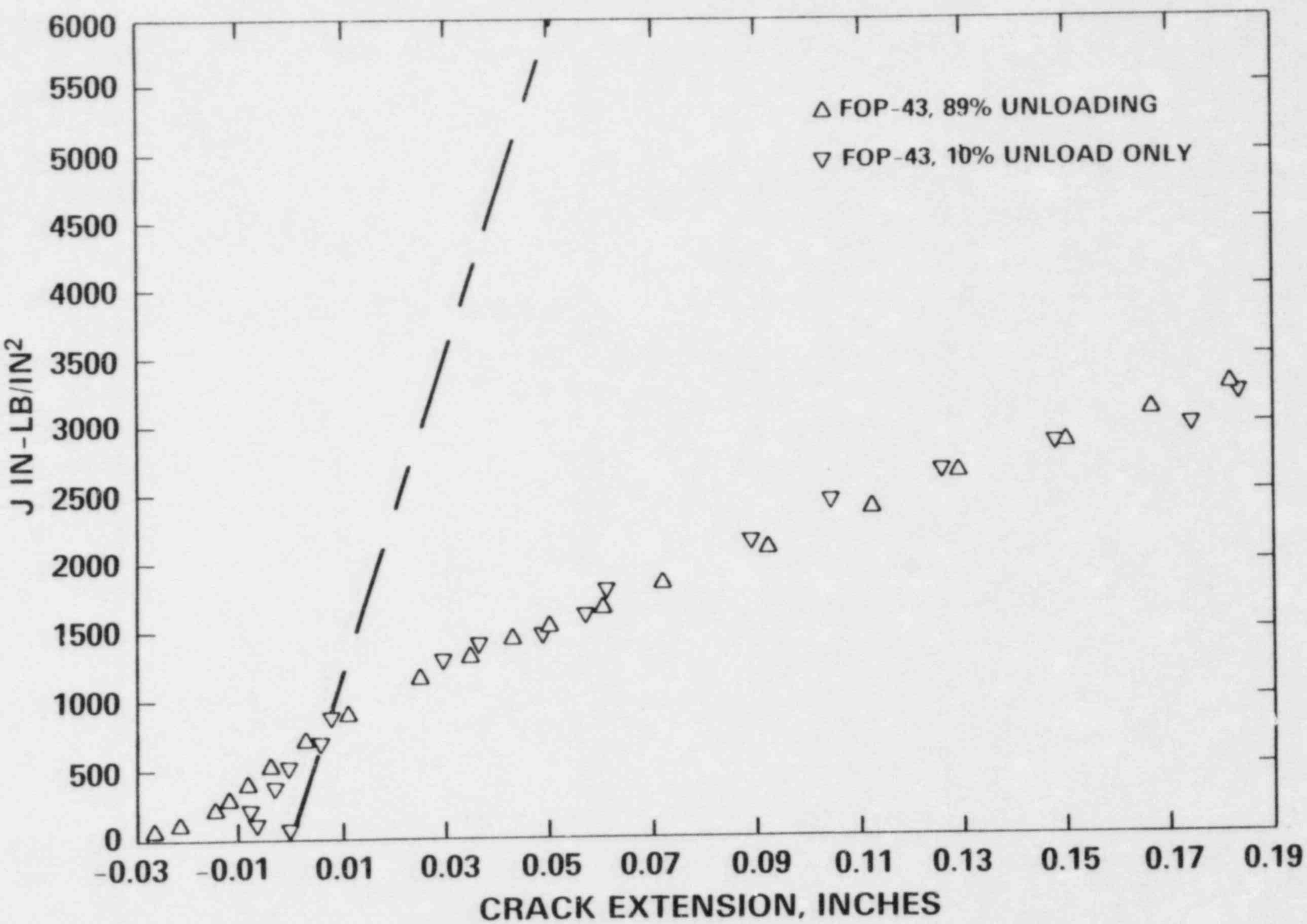

ASTM A106 CLASS C STEEL; 1TCT SPECIMENS

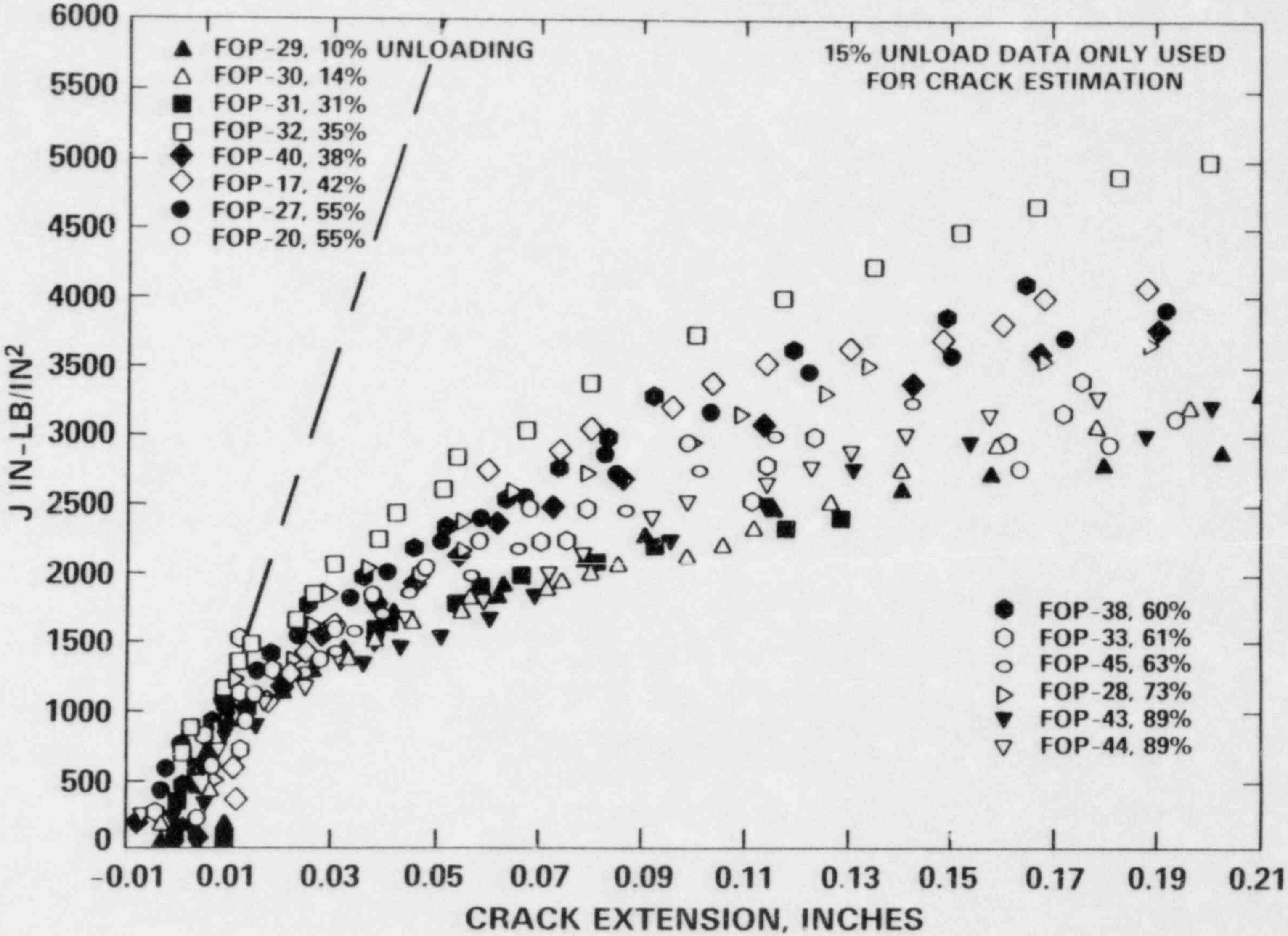

DEGRADED PIPE EXPERIMENTAL PROGRAM

JOHN P. GUDAS
MICHAEL G. VASSILAROS

DAVID TAYLOR NAVAL SHIP R&D CENTER
ANNAPOLIS, MD. 21402

PROGRAM OBJECTIVES

120

- EVALUATE J-INTEGRAL RESISTANCE CURVES FROM 8 INCH DIAMETER A106 CLASS C STEEL PIPE AND COMPACT SPECIMENS
- EVALUATE TEARING INSTABILITY ANALYSIS WITH A106 CLASS C PIPES IN BENDING

APPROACH

A. PROCURE 8-INCH SCHEDULE 80, ASTM A106 STEEL, AND CHARACTERIZE ROOM TEMPERATURE MECHANICAL PROPERTIES, TOUGHNESS AND J-INTEGRAL DUCTILE FRACTURE PROPERTIES;

B. BUILD TEST FIXTURES FOR CLOSED-LOOP TEST MACHINE TO PRODUCE $T_{APPLIED}$ VALUES UP TO 200;

C. DEVELOP AND VALIDATE CRACKED CYLINDER COMPLIANCE FORMULATIONS WITH Al 6061 AND A106 CYLINDERS OF PROPORTIONAL GEOMETRIES;

D. DEVELOP OR MODIFY EXISTING J-INTEGRAL FORMULATIONS FOR CRACKED CYLINDERS;

E. PERFORM J-INTEGRAL R-CURVE TESTS WITH CRACKED CYLINDERS OF A106 AT ROOM TEMPERATURE WITH VERY LOW $T_{APPLIED}$ VALUES;

F. PERFORM J-INTEGRAL R-CURVE TESTS WITH CRACKED CYLINDERS OF A106 AT 125° F WITH $T_{APPLIED}$ VALUES VARYING UP TO 200;

G. CORRELATE CRACK STABILITY OBSERVED IN TESTS WITH J-INTEGRAL R-CURVE PREDICTIONS FROM COMPACT SPECIMENS AND CRACKED CYLINDERS.

EIGHT INCH SCHEDULE 80 PIPE

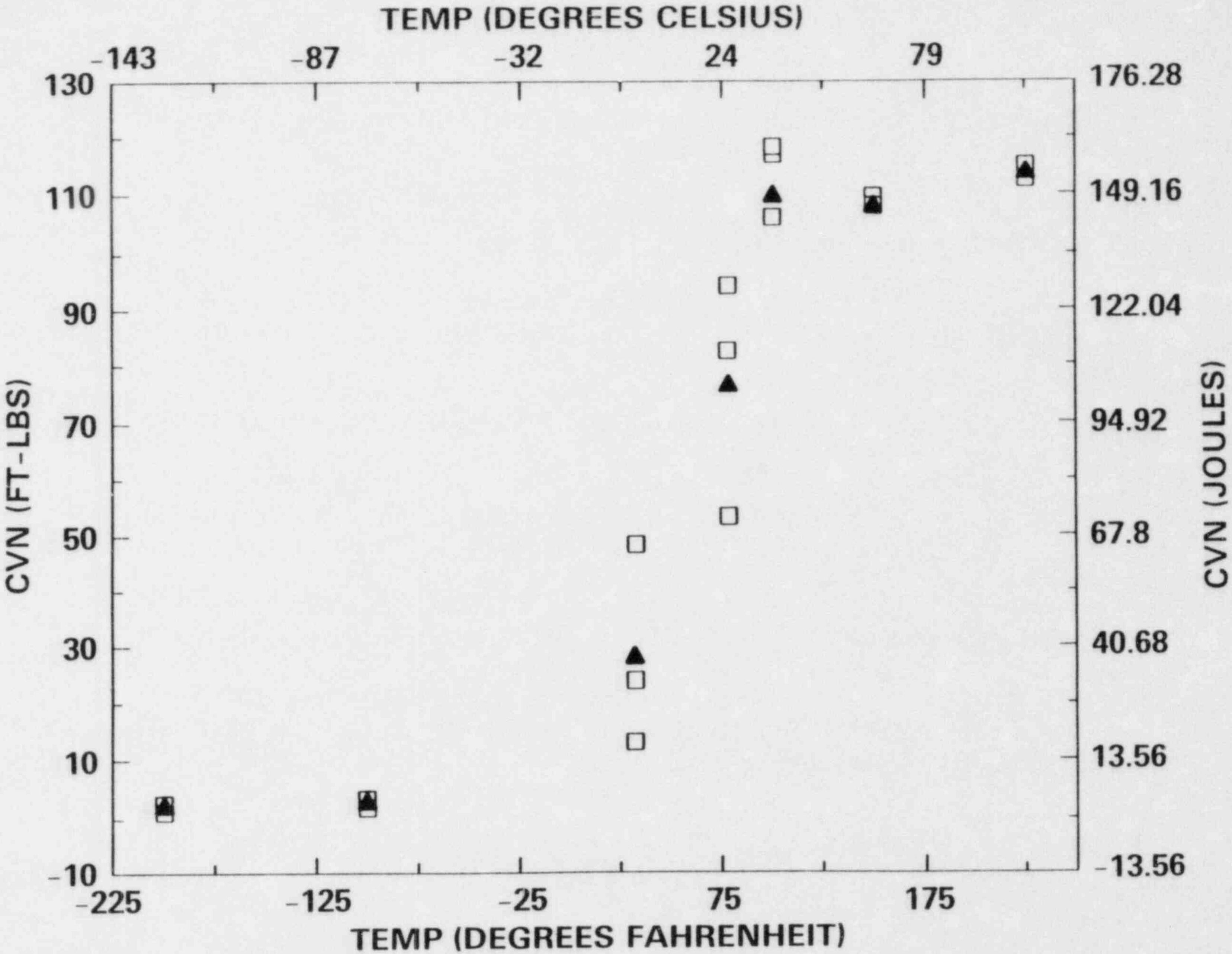

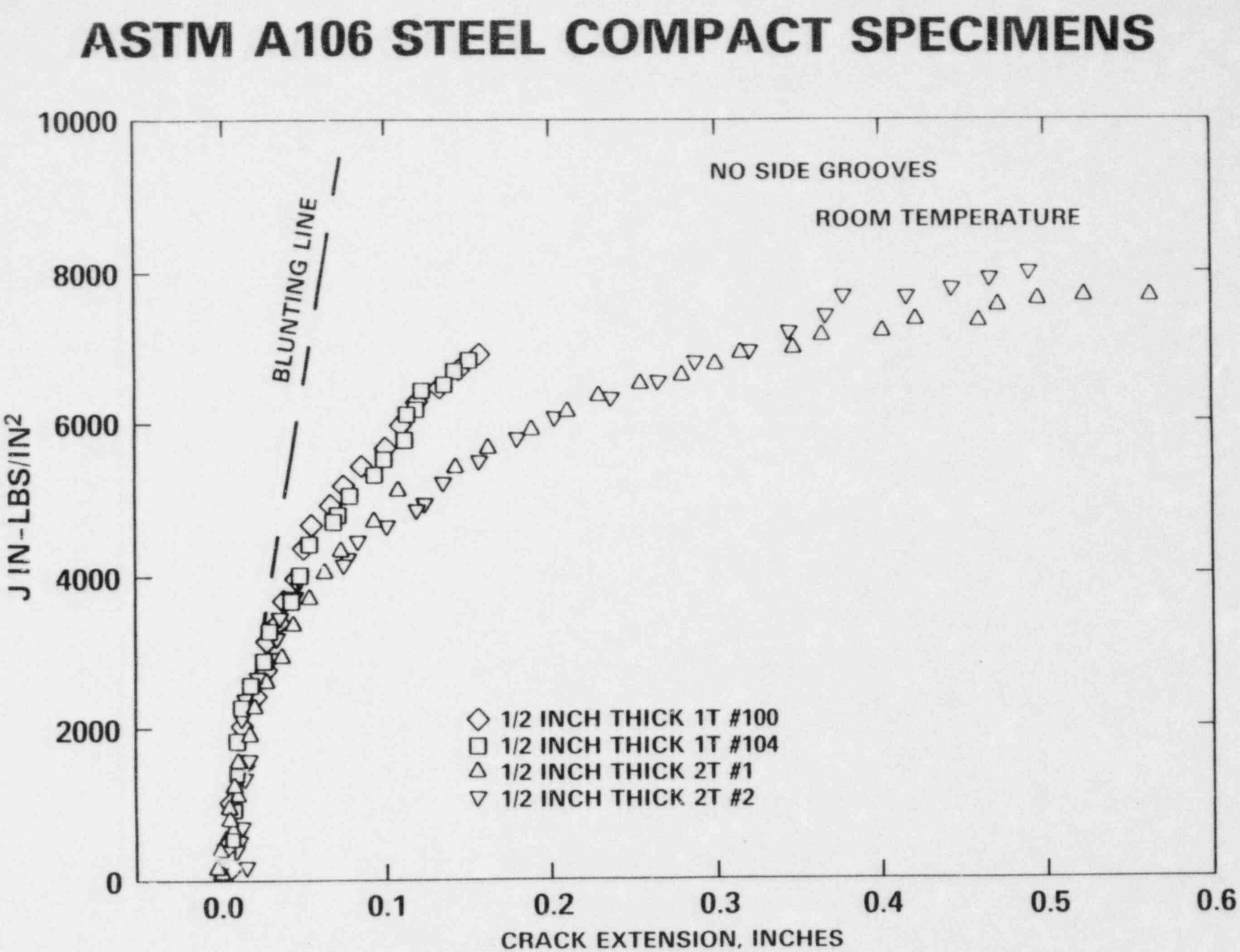
ASTM A106 STEEL COMPACT SPECIMENS
NO SIDE GROOVES
ROOM TEMPERATURE
BLUNTING LINE
J IN-LBS/IN²
CRACK EXTENSION, INCHES
10000
8000
6000
4000
2000
0
0.0
0.1
0.2
0.3
0.4
0.5
0.6
1/2 INCH THICK 1T #100
1/2 INCH THICK 1T #104
1/2 INCH THICK 2T #1
1/2 INCH THICK 2T #2

123

1/2 INCH THICK 2T COMPACT SPECIMENS

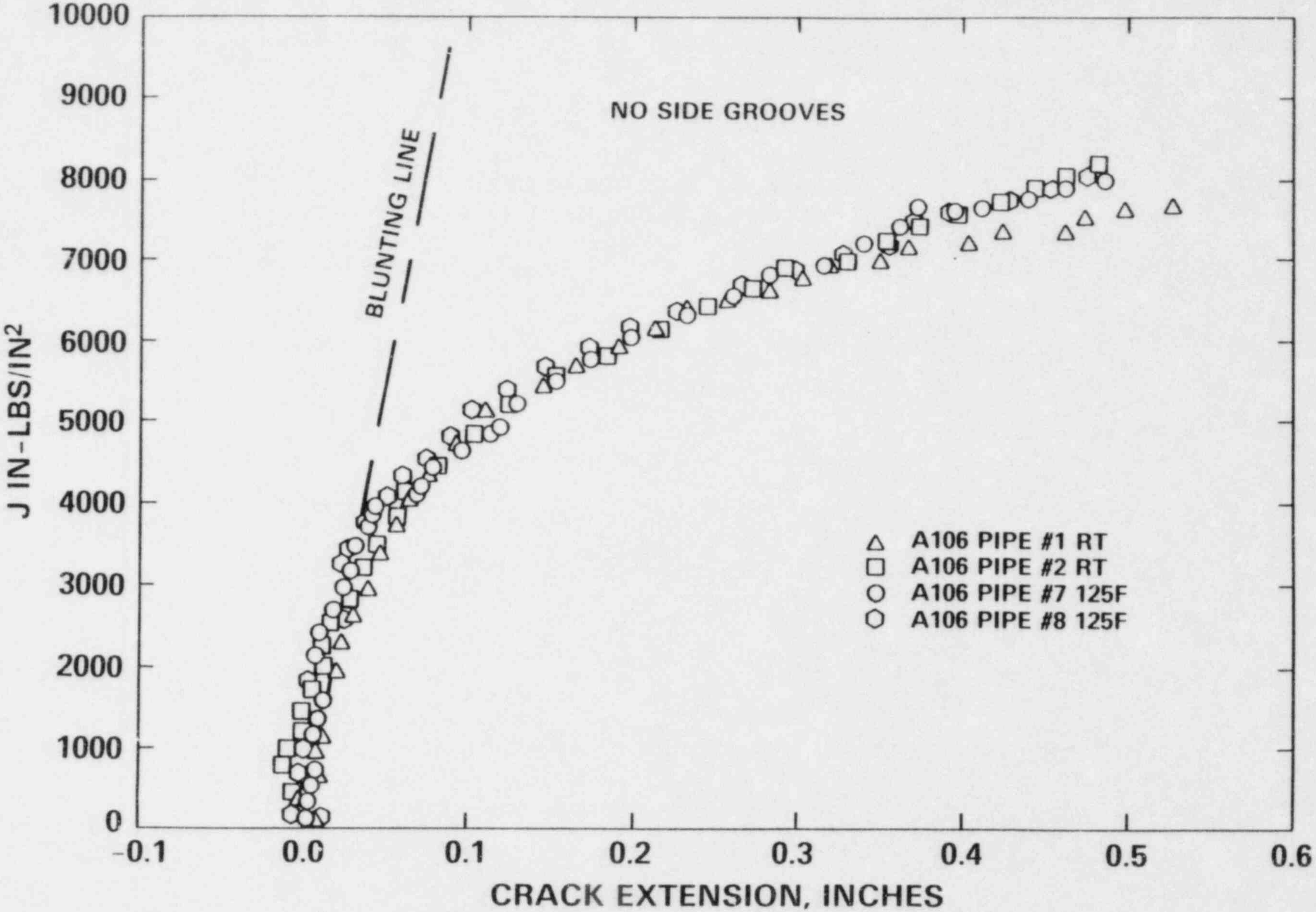

124

SCHEMATIC OF TESTING APPARATUS FOR LARGE PIPE TEARING INSTABILITY TESTS

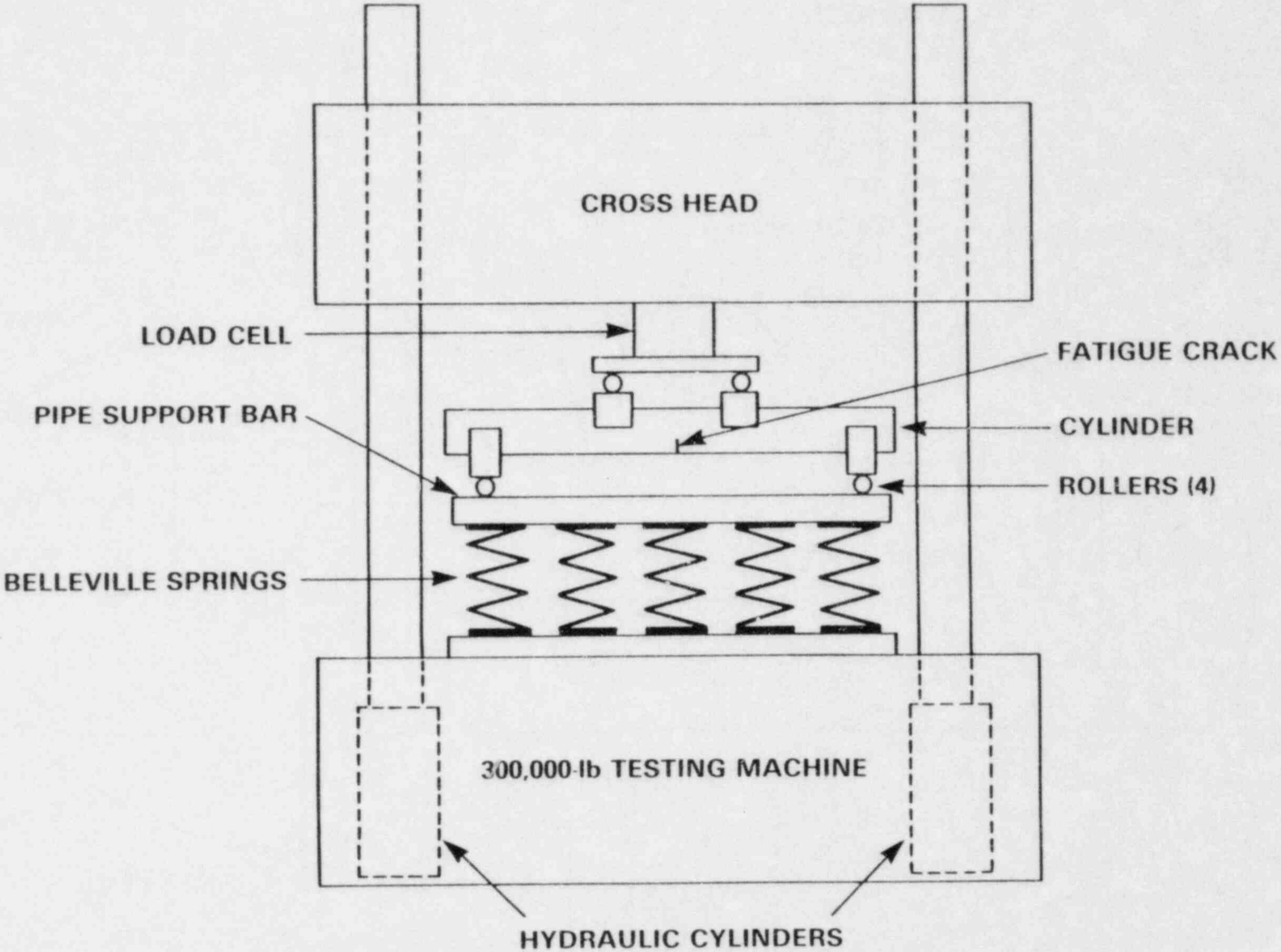

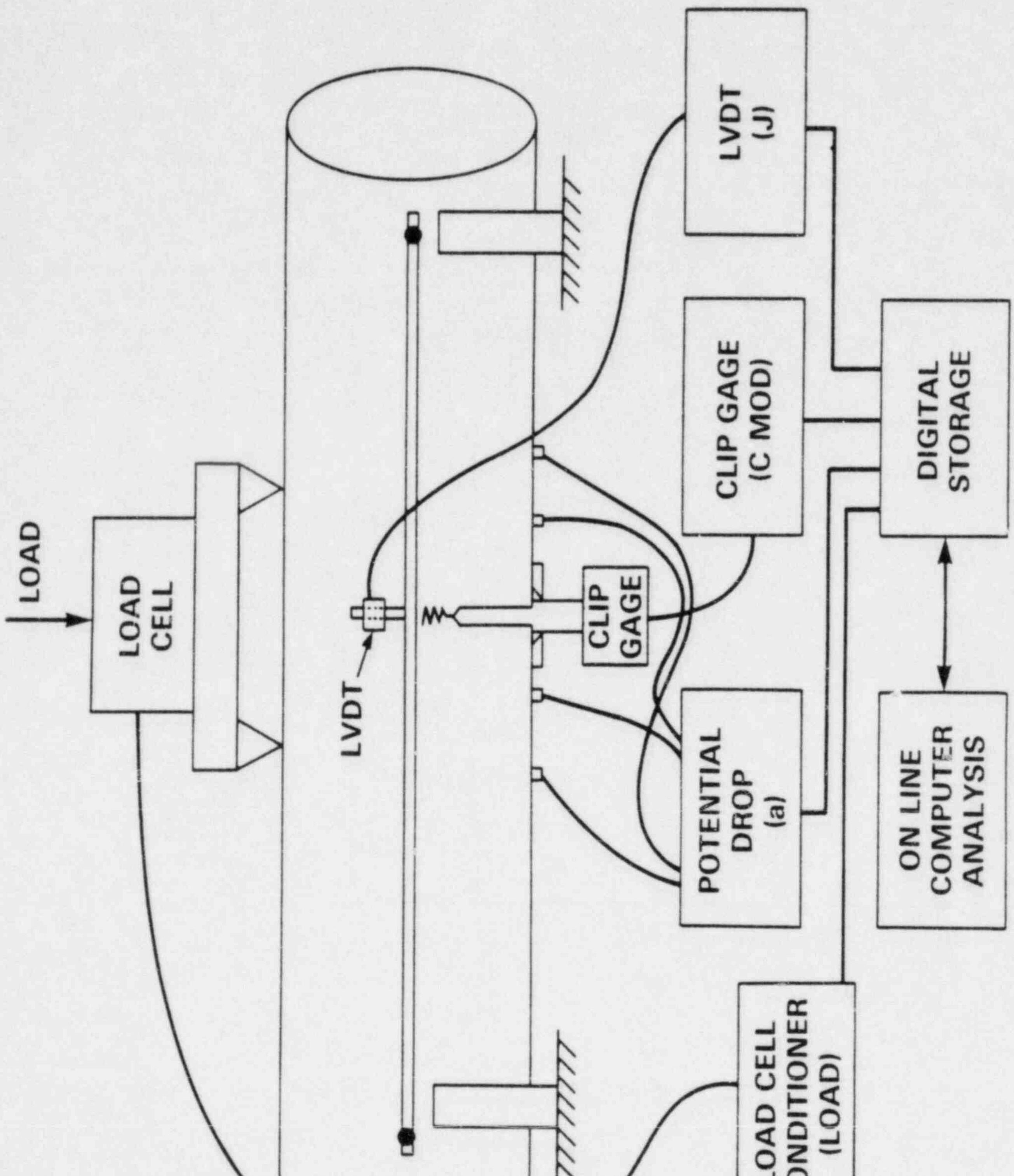

LOAD
LOAD CELL
LVDT
CLIP GAGE
LVDT (J)
CLIP GAGE (C MOD)
POTENTIAL DROP (a)
DIGITAL STORAGE
ON LINE COMPUTER ANALYSIS
LOAD CELL CONDITIONER (LOAD)

FORMULATIONS FOR J AND $T_{APPLIED}$ IN A PIPE

ZAHOOR AND COWORKERS	TADA AND COWORKERS
J_Z = f (ACTUAL LOAD AND DISPLACEMENTS)	J_T = f (ASSUMED FLOW STRESS AND MEASURED BEND ANGLE
$T_{APPLIED}$ = f (J_Z, K_M AND MEASURED HARDENING OF PIPE MATERIAL)	$T_{APPLIED}$ = f (J_T, K_M)

K_M = TOTAL SYSTEM COMPLIANCE,

= TEST MACHING STIFFNESS + FIXTURE STIFFNESS + SPRING STIFFNESS

J_I-R CURVES FROM 8 INCH DIAMETER A106 STEEL PIPE USING UNLOADING COMPLIANCE

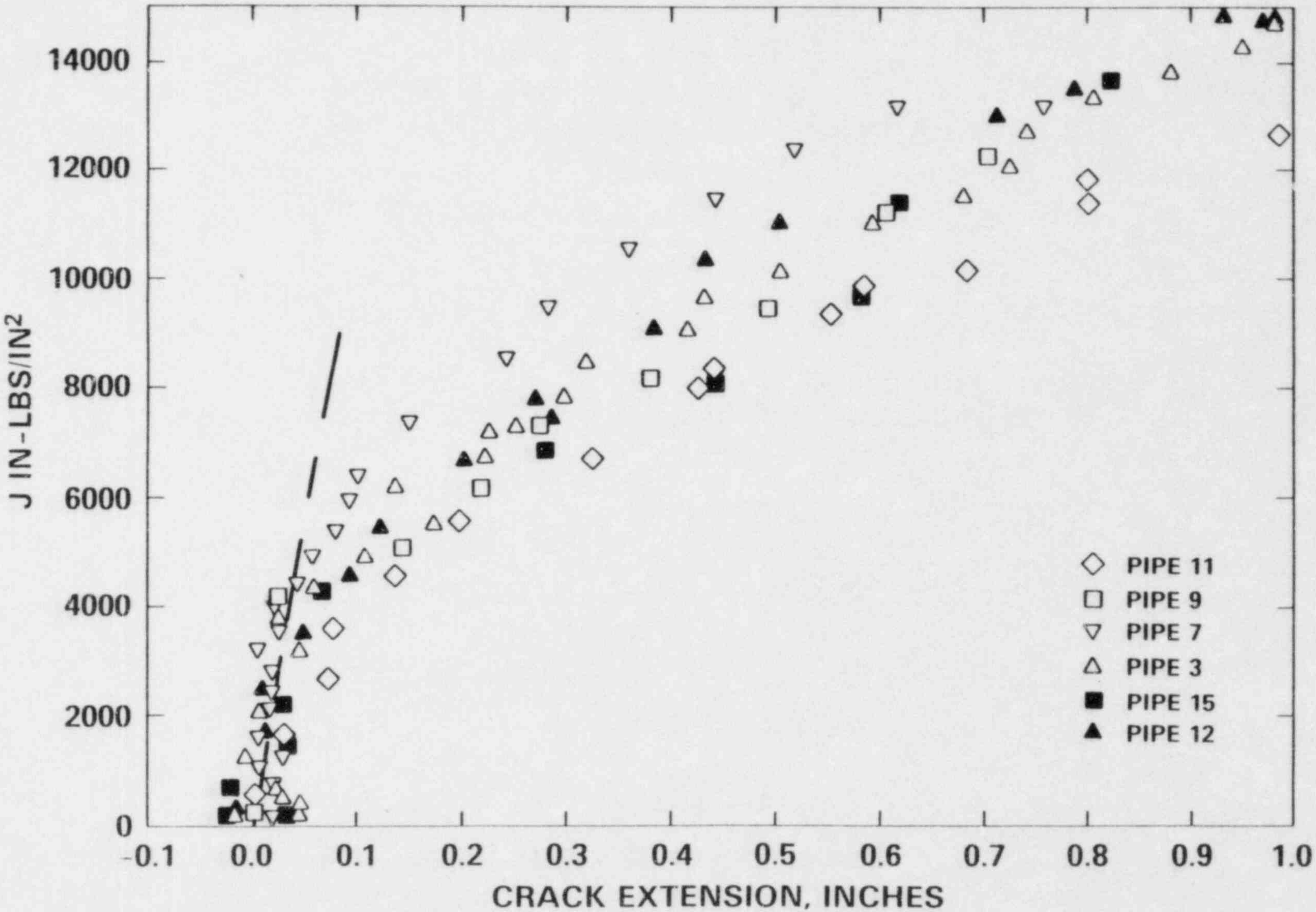

J_I-R CURVES FROM 8 INCH DIAMETER PIPE SPECIMENS D.C. POTENTIAL DROP TECHNIQUE

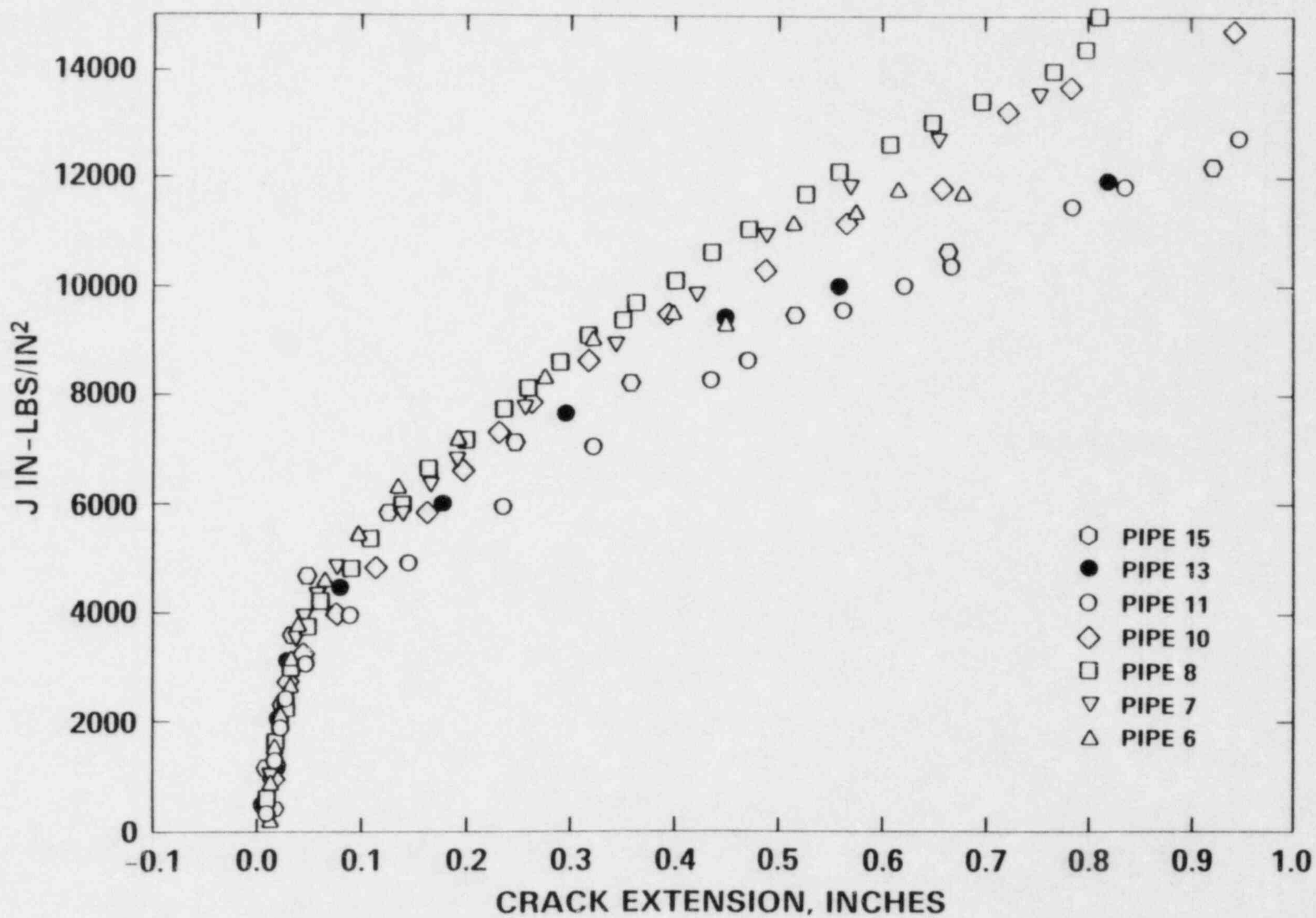

J_I-R CURVES FOR 8 INCH DIAMETER PIPE SPECIMENS AND A 1/2 INCH THICK 1T COMPACT SPECIMEN

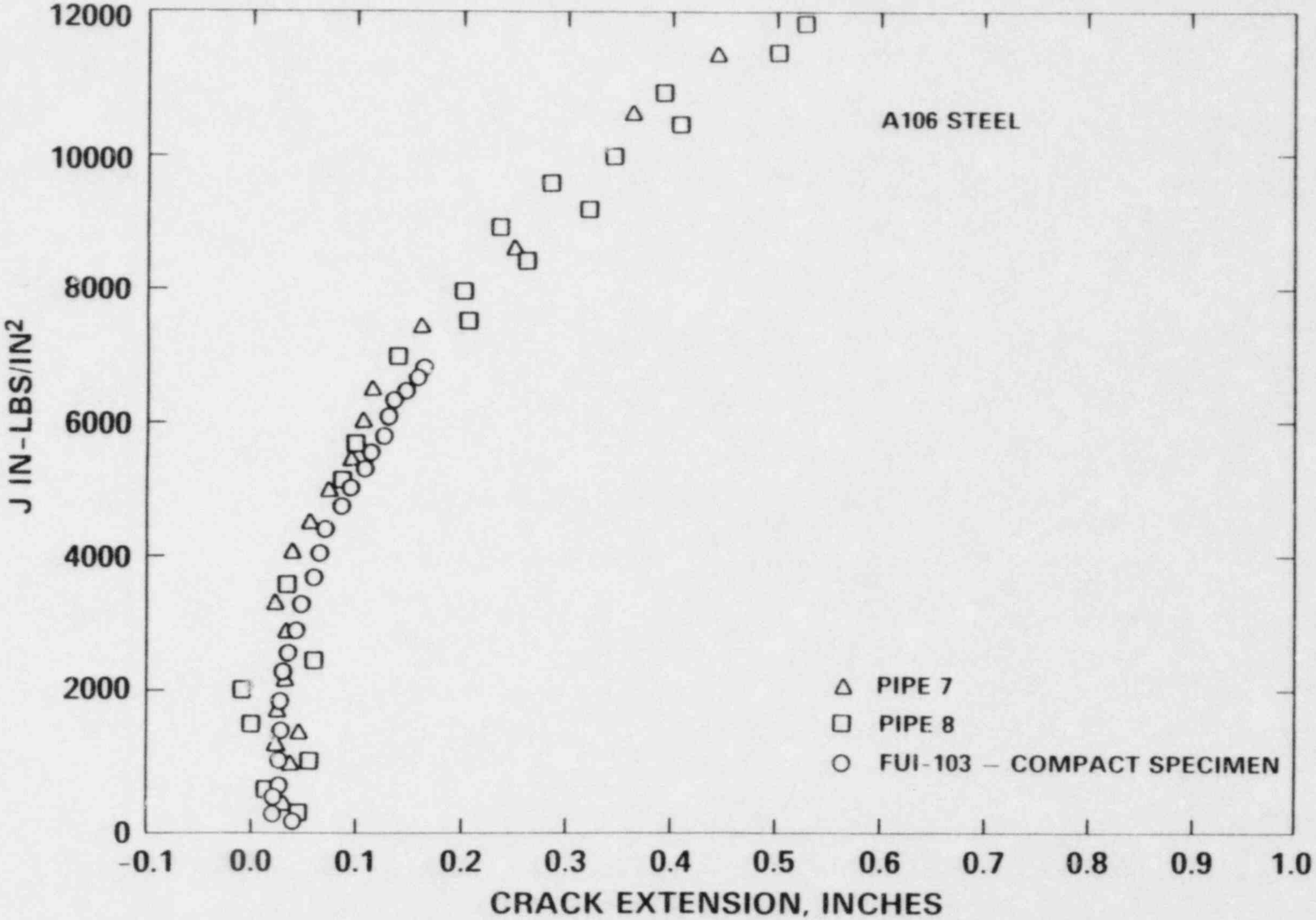

J_I-R CURVES FROM 8 INCH DIAMETER PIPE SPECIMENS AND 1/2 INCH THICK 2T COMPACT SPECIMENS USING UNLOADING COMPLIANCE

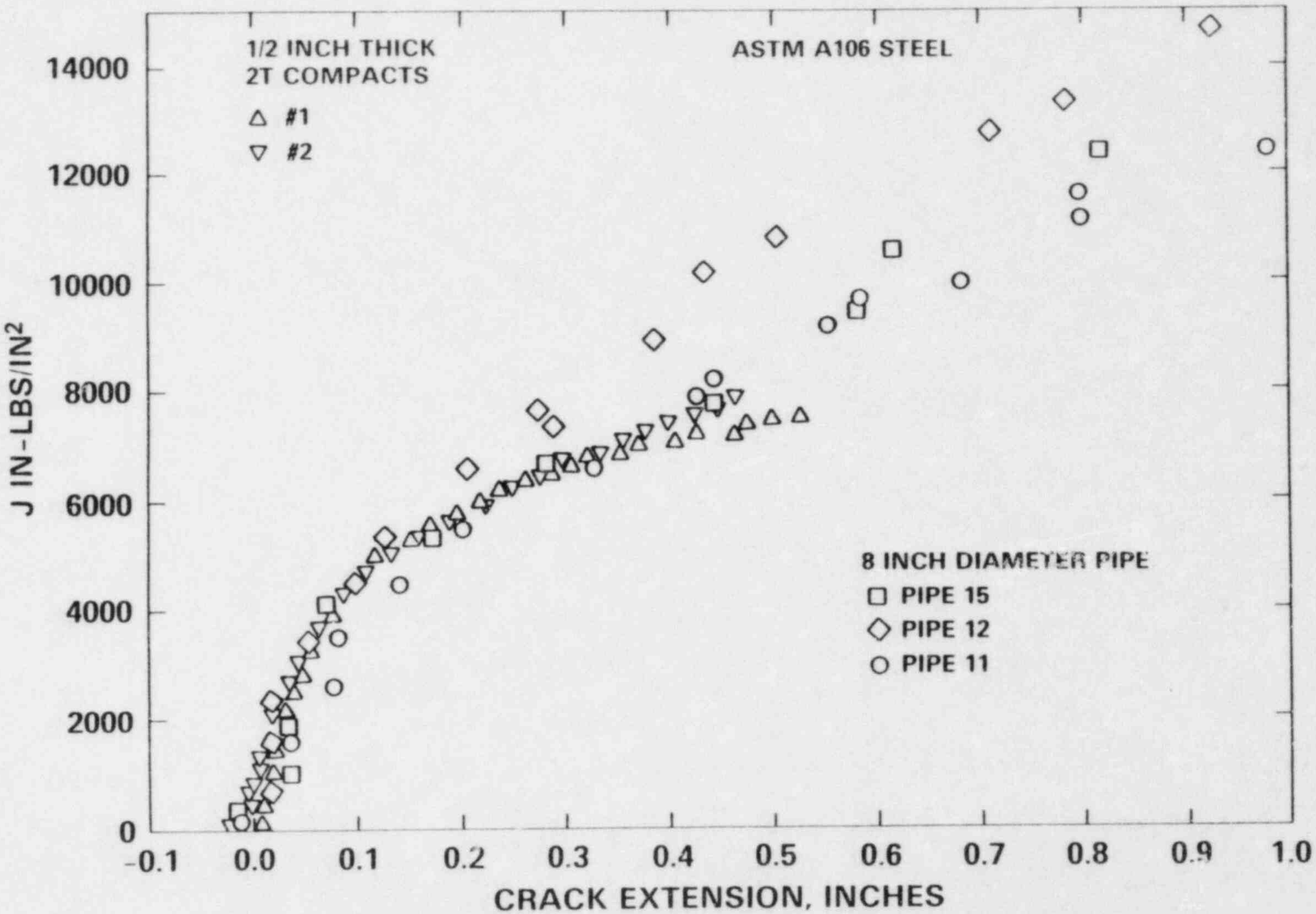

J_I-R CURVES FROM 8 INCH DIAMETER PIPE SPECIMENS AND 1/2 INCH THICK 2T COMPACT SPECIMEN USING D.C. POTENTIAL DROP TECHNIQUE

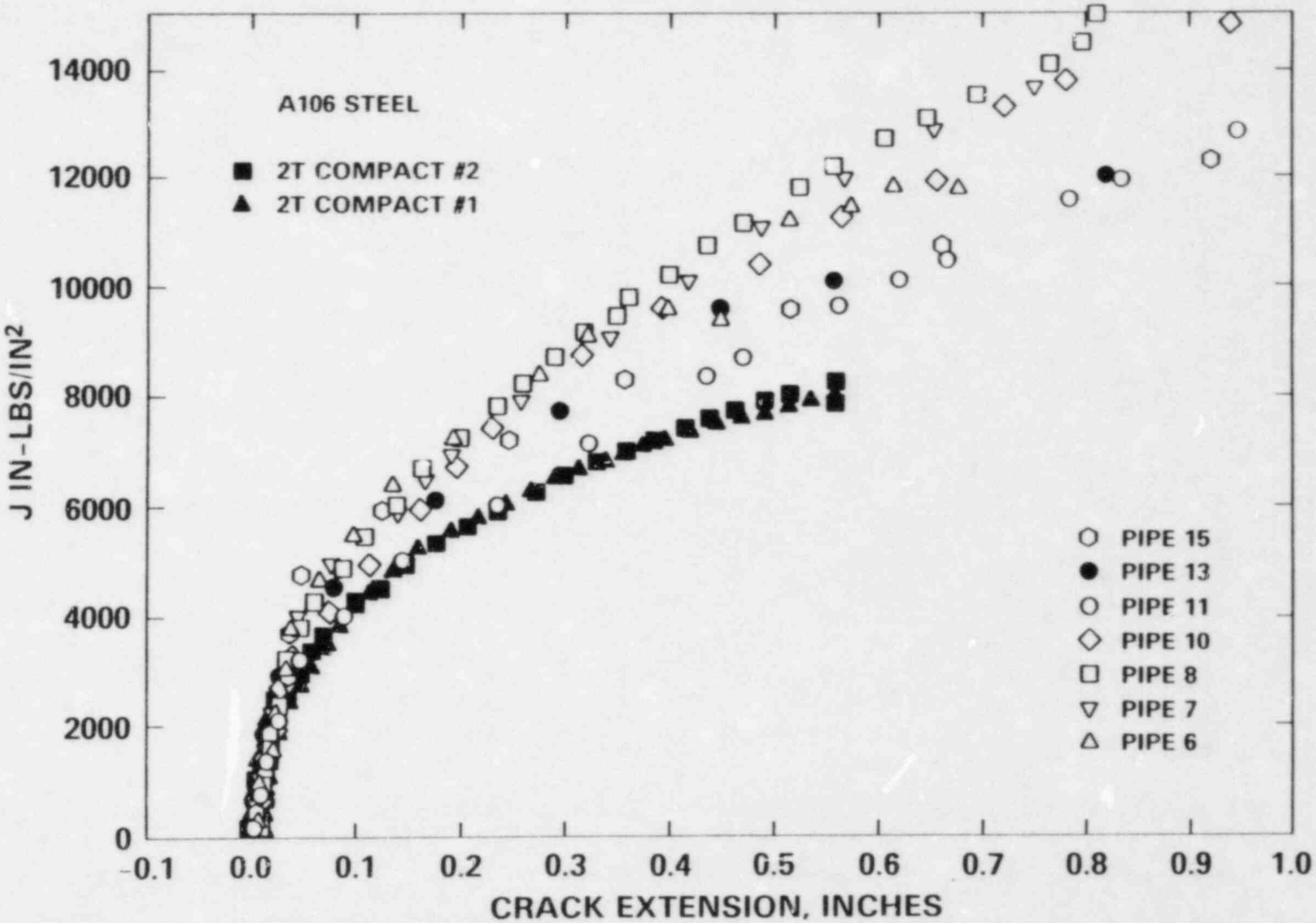

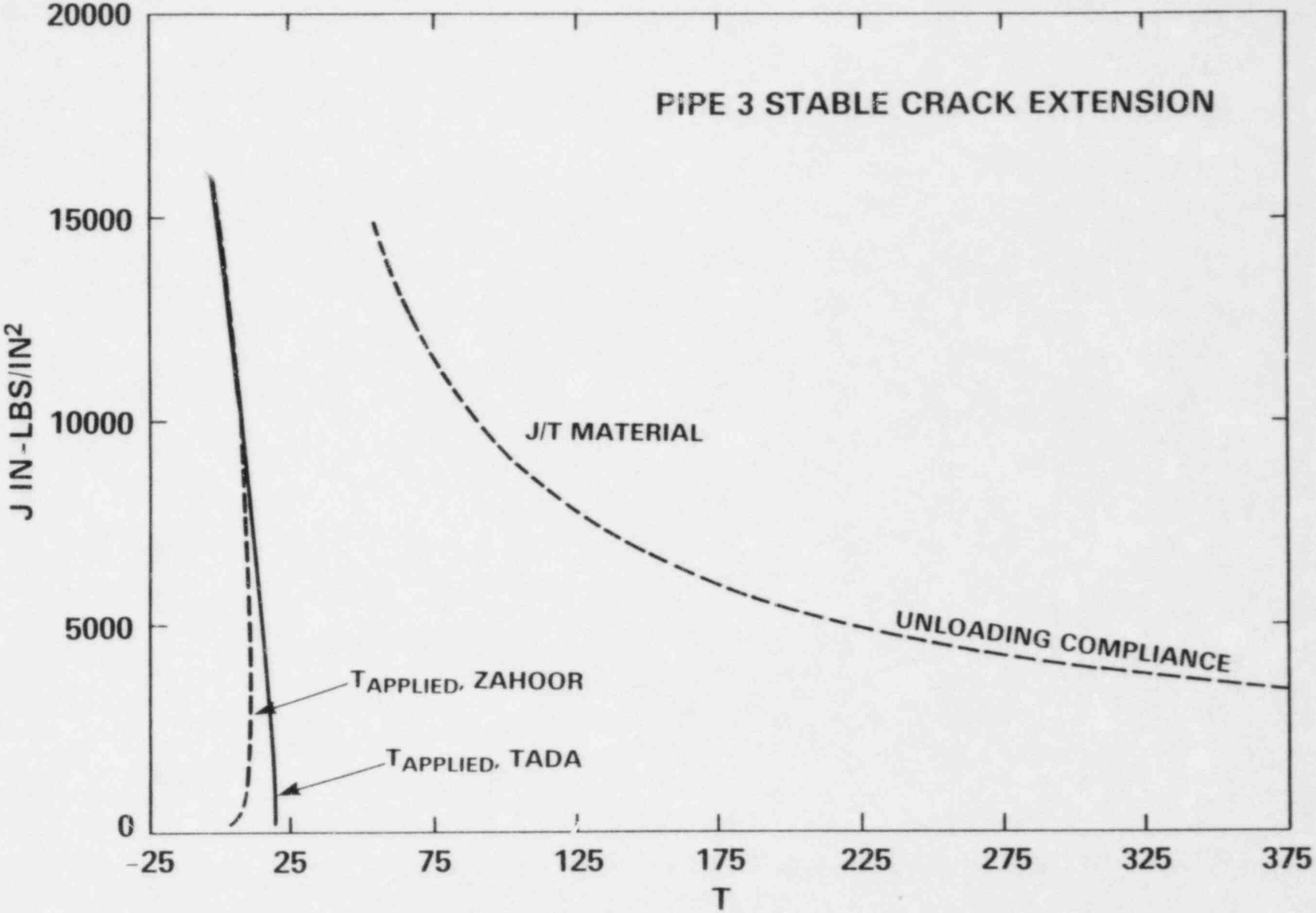
PIPE 3 STABLE CRACK EXTENSION
J IN-LBS/IN²
20000
15000
10000
5000
0
-25
25
75
125
175
225
275
325
375
T
J/T MATERIAL
UNLOADING COMPLIANCE
T APPLIED, ZAHOOR
T APPLIED, TADA

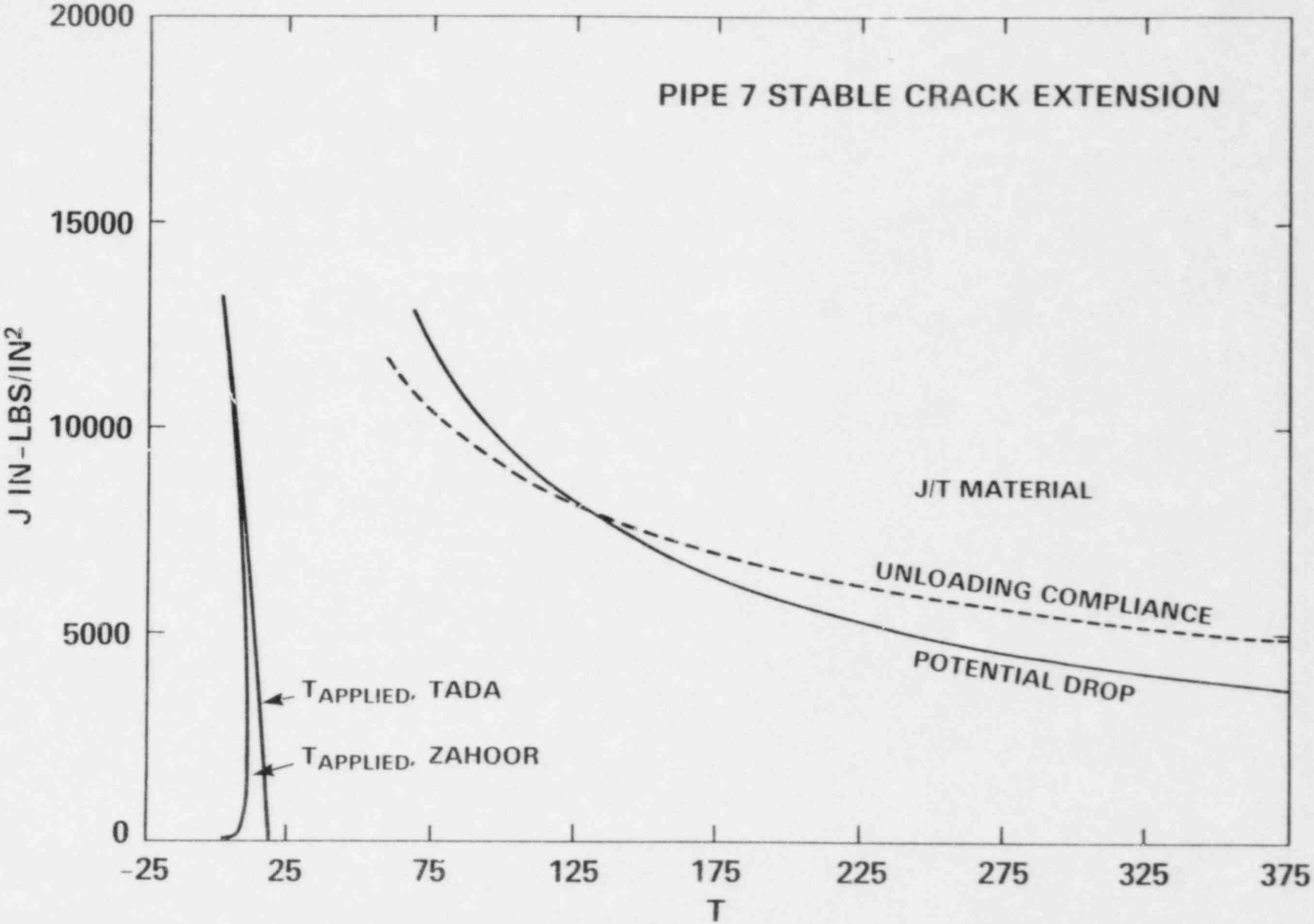
PIPE 7 STABLE CRACK EXTENSION
J IN-LBS/IN²
T
20000
15000
10000
5000
0
-25
25
75
125
175
225
275
325
375
J/T MATERIAL
UNLOADING COMPLIANCE
POTENTIAL DROP
TAPPLIED, TADA
TAPPLIED, ZAHOOR

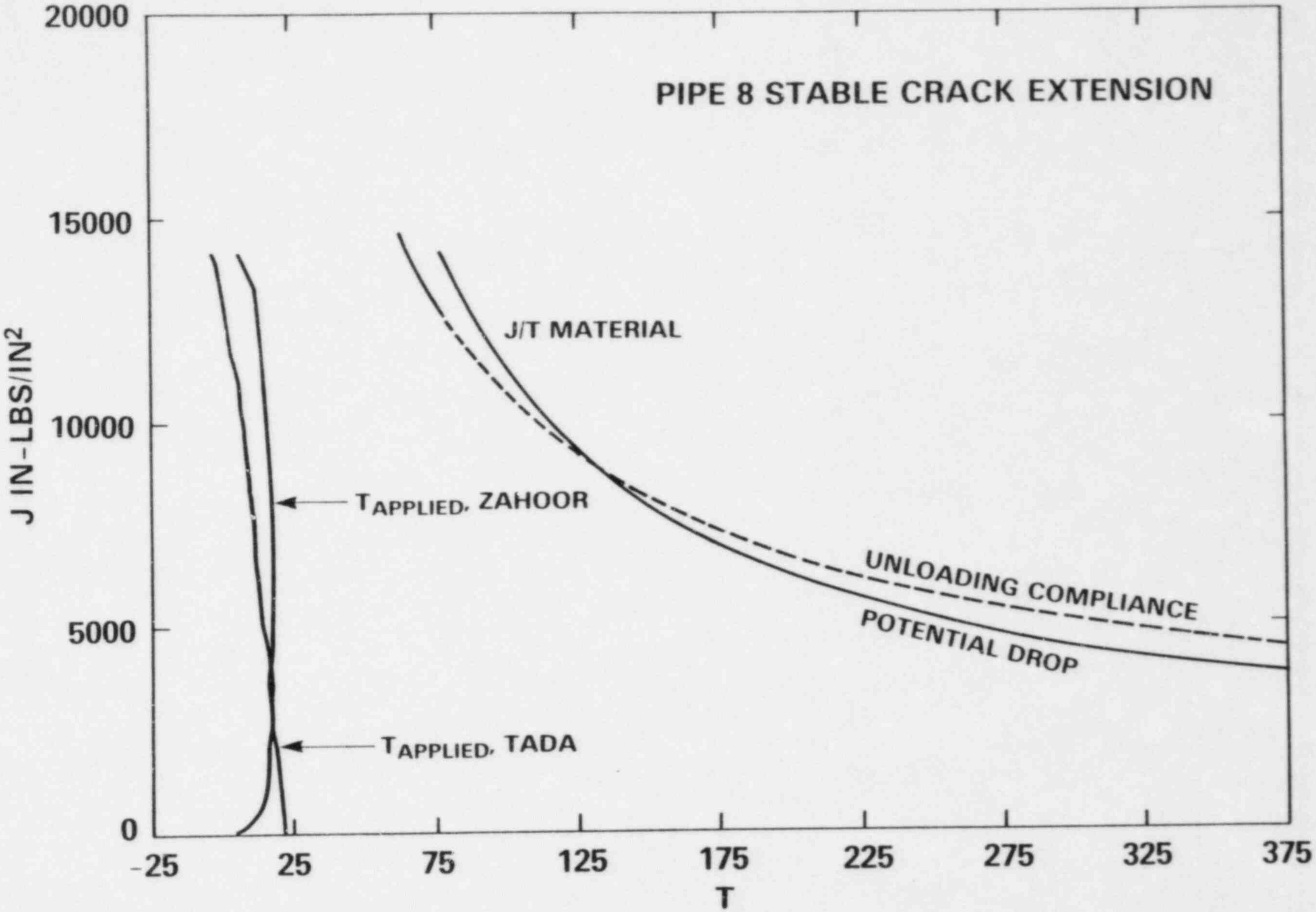

PIPE 8 STABLE CRACK EXTENSION
J/T MATERIAL
$T_{APPLIED}$, ZAHOOR
UNLOADING COMPLIANCE
POTENTIAL DROP
$T_{APPLIED}$, TADA
J IN-LBS/IN^2
20000
15000
10000
5000
0
-25
25
75
125
175
225
275
325
375
T

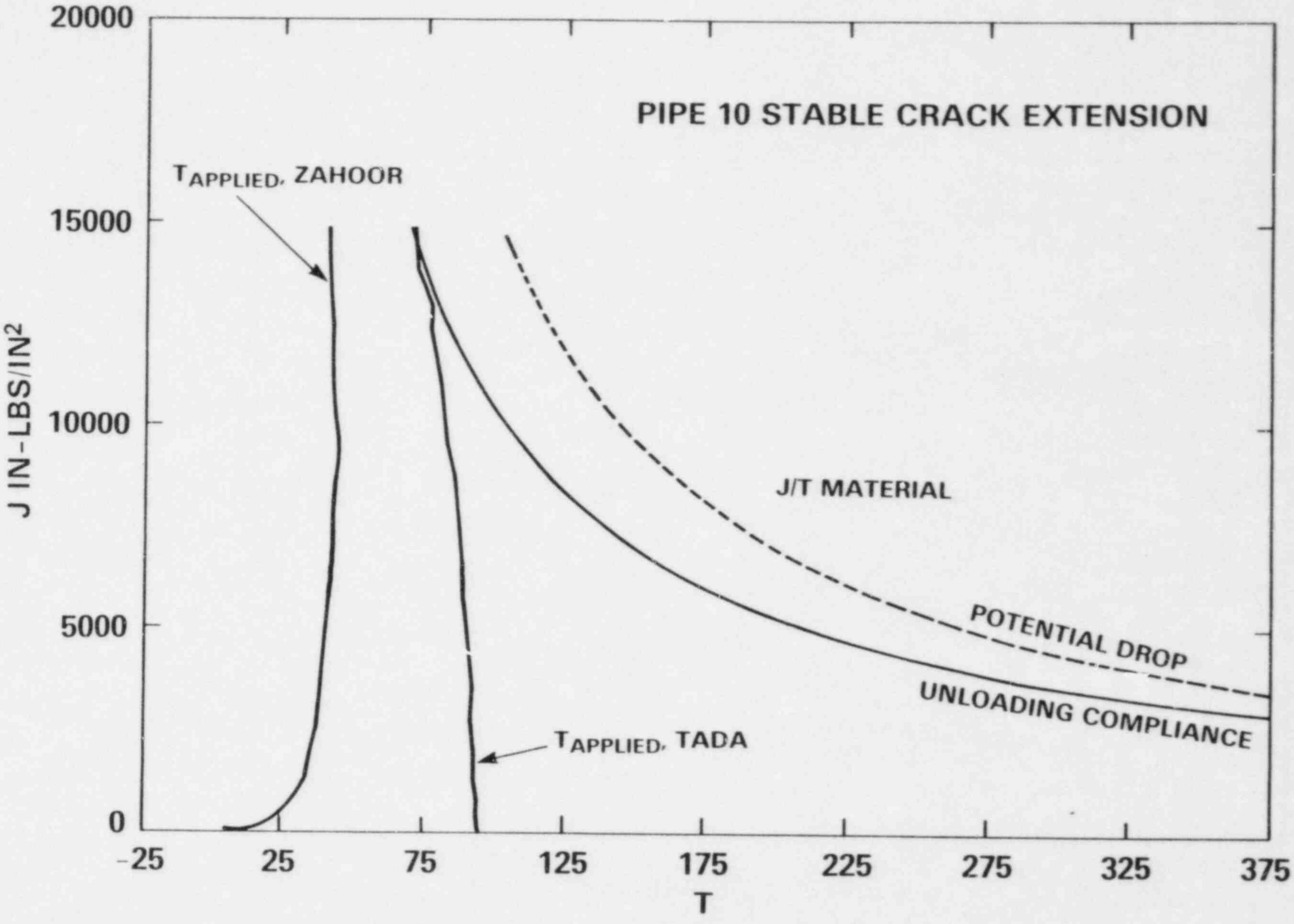
PIPE 10 STABLE CRACK EXTENSION
T APPLIED, ZAHOOR
T APPLIED, TADA
J/T MATERIAL
POTENTIAL DROP
UNLOADING COMPLIANCE
J IN-LBS/IN²
T
20000
15000
10000
5000
0
-25
25
75
125
175
225
275
325
375

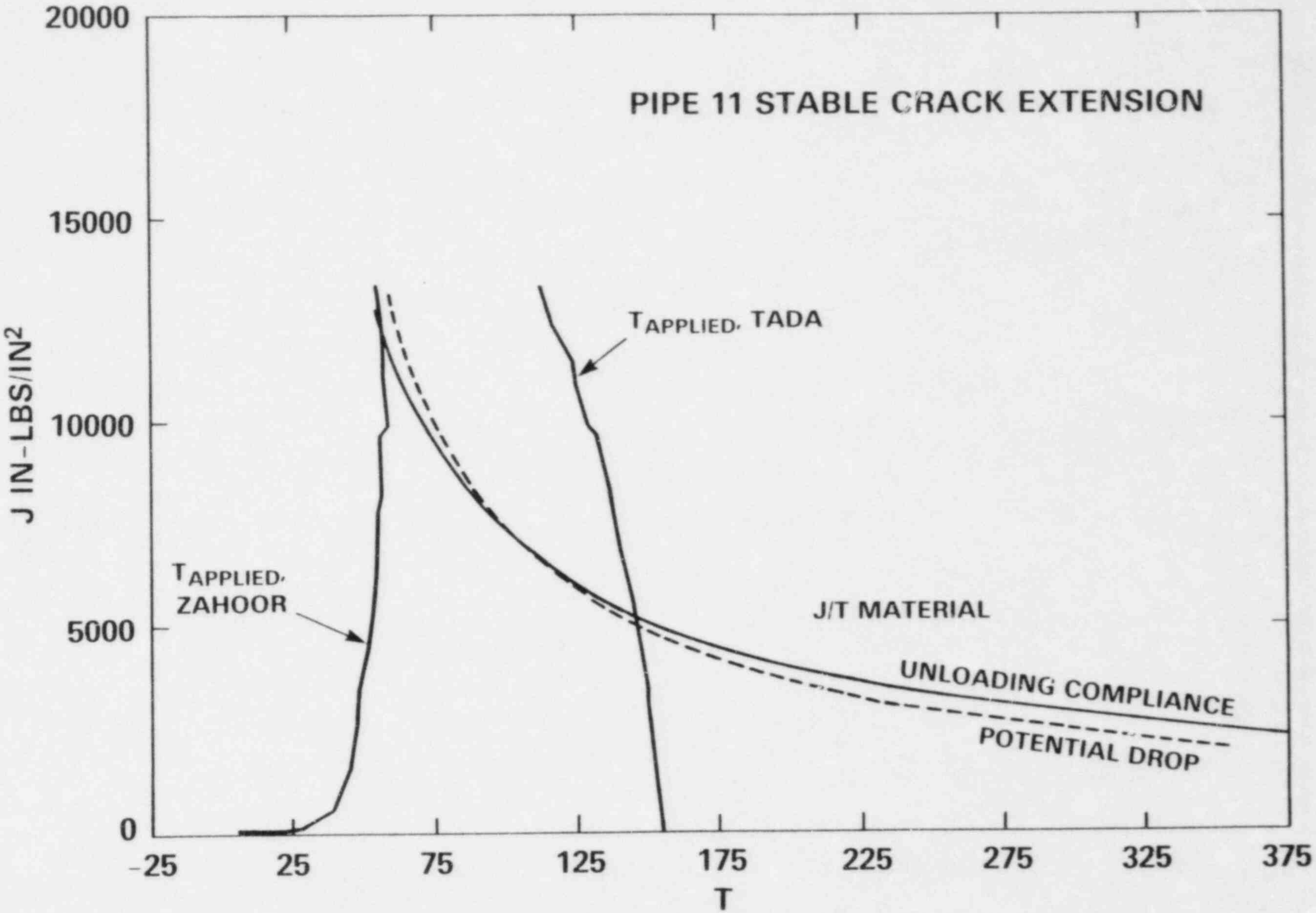
PIPE 11 STABLE CRACK EXTENSION
J IN-LBS/IN²
T
20000
15000
10000
5000
0
-25
25
75
125
175
225
275
325
375
T APPLIED, TADA
T APPLIED, ZAHOOR
J/T MATERIAL
UNLOADING COMPLIANCE
POTENTIAL DROP

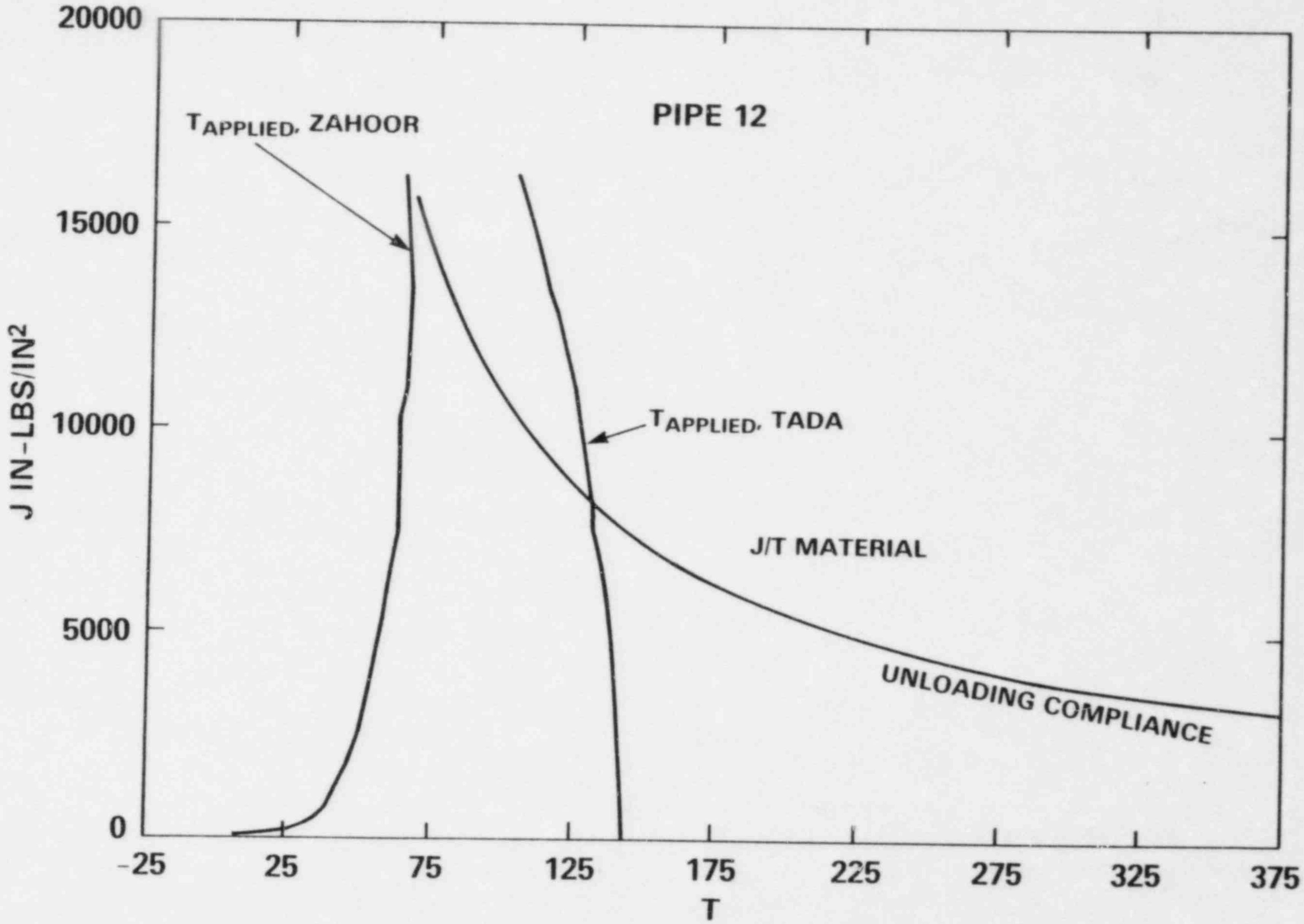
PIPE 12
$T_{APPLIED}$, ZAHOOR
$T_{APPLIED}$, TADA
J/T MATERIAL
UNLOADING COMPLIANCE
J IN-LBS/IN^2
20000
15000
10000
5000
0
-25
25
75
125
175
225
275
325
375
T

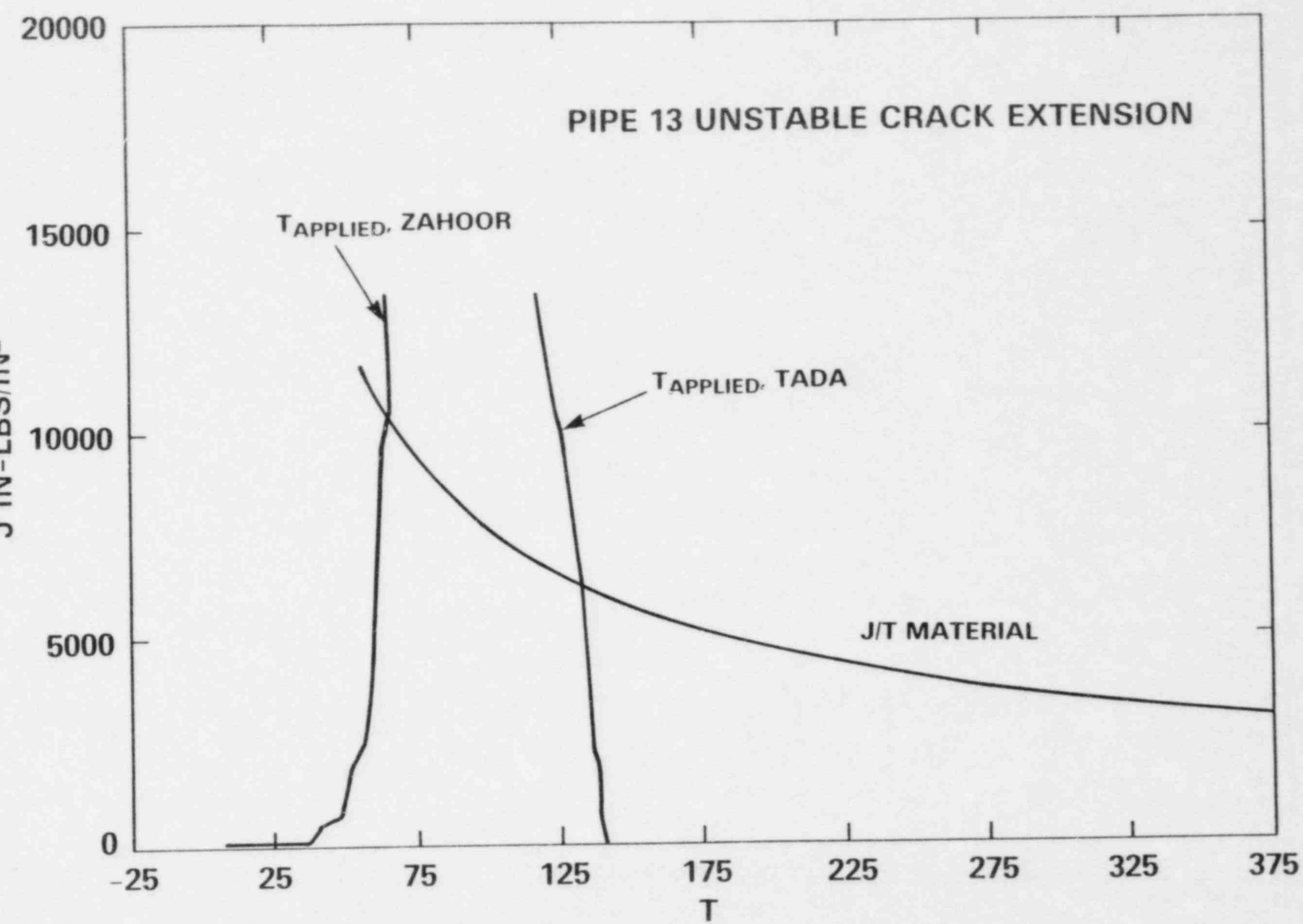
PIPE 13 UNSTABLE CRACK EXTENSION
$T_{APPLIED}$, ZAHOOR
$T_{APPLIED}$, TADA
J/T MATERIAL
J IN-LBS/IN^2
20000
15000
10000
5000
0
-25
25
75
125
175
225
275
325
375
T

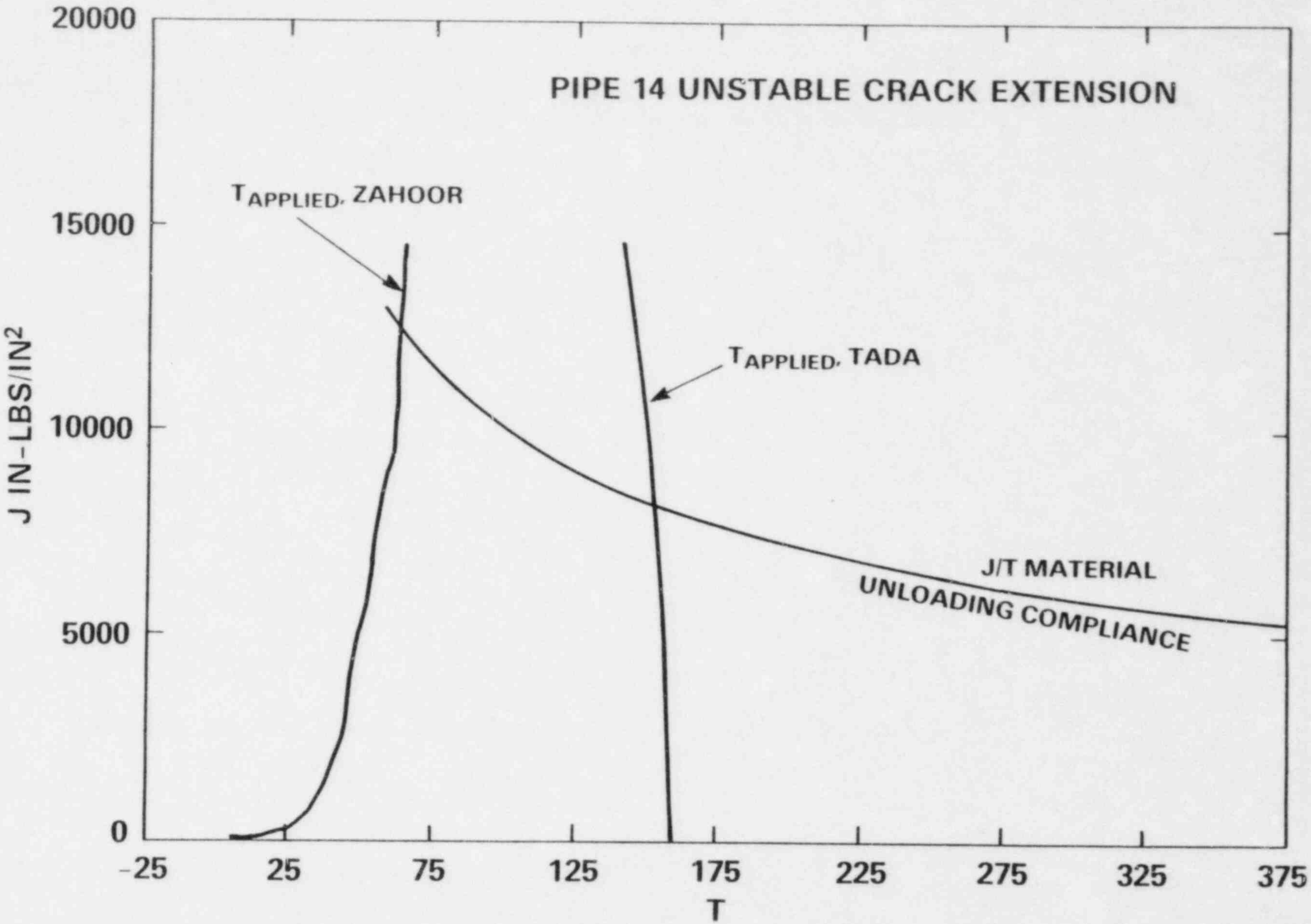
PIPE 14 UNSTABLE CRACK EXTENSION
T APPLIED, ZAHOOR
T APPLIED, TADA
J/T MATERIAL
UNLOADING COMPLIANCE
J IN-LBS/IN²
T
20000
15000
10000
5000
0
-25
25
75
125
175
225
275
325
375

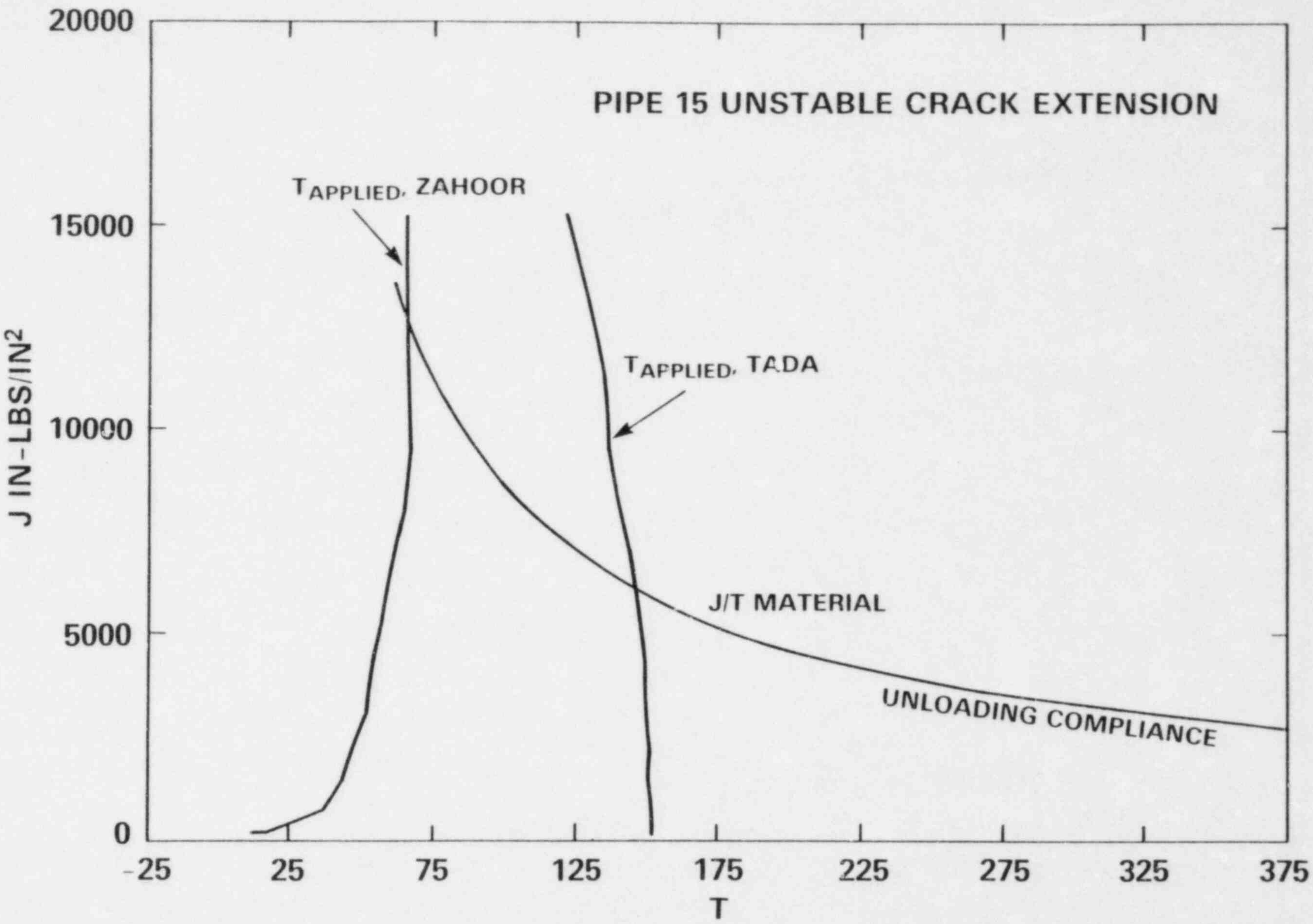

PIPE 15 UNSTABLE CRACK EXTENSION
$T_{APPLIED}$, ZAHOOR
$T_{APPLIED}$, TADA
J/T MATERIAL
UNLOADING COMPLIANCE
J IN-LBS/IN^2
T
20000
15000
10000
5000
0
-25
25
75
125
175
225
275
325
375

J/T PLOT A106 STEEL 1/2 INCH 2T COMPACTS

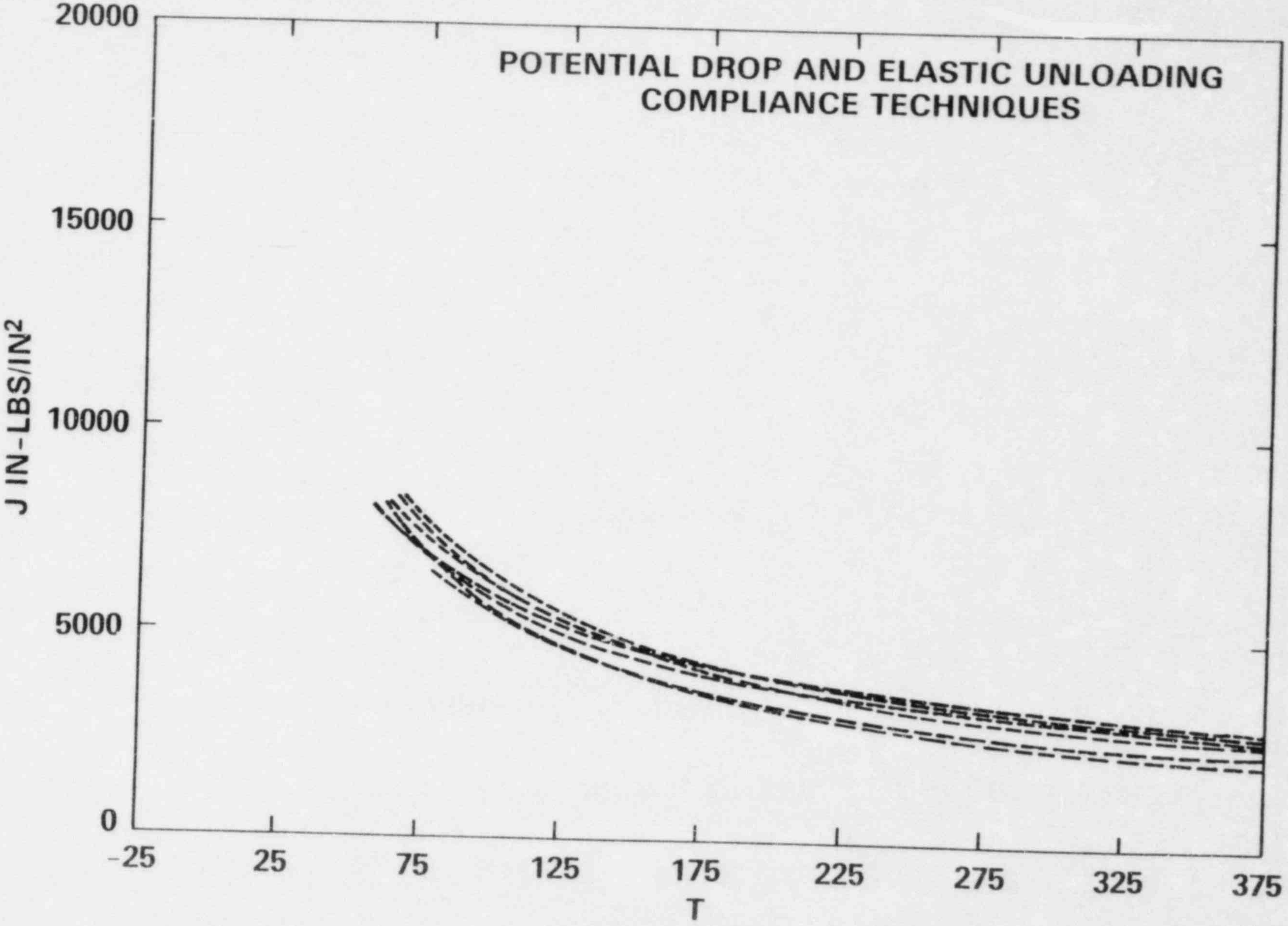

J/T PLOT 1/2 INCH THICK 1T COMPACTS

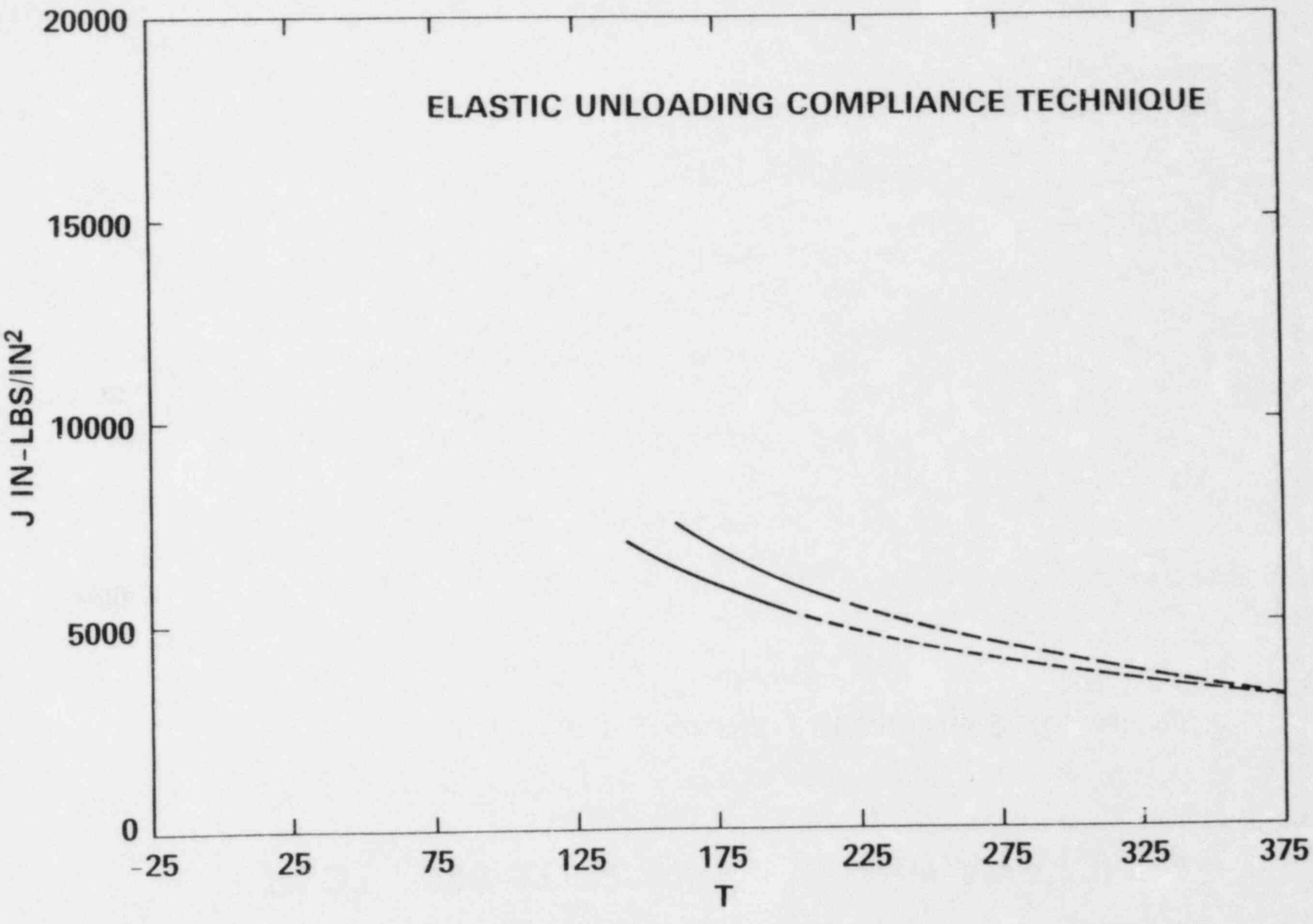

J/T PLOT A106 STEEL PIPE 8 INCH DIAMETER

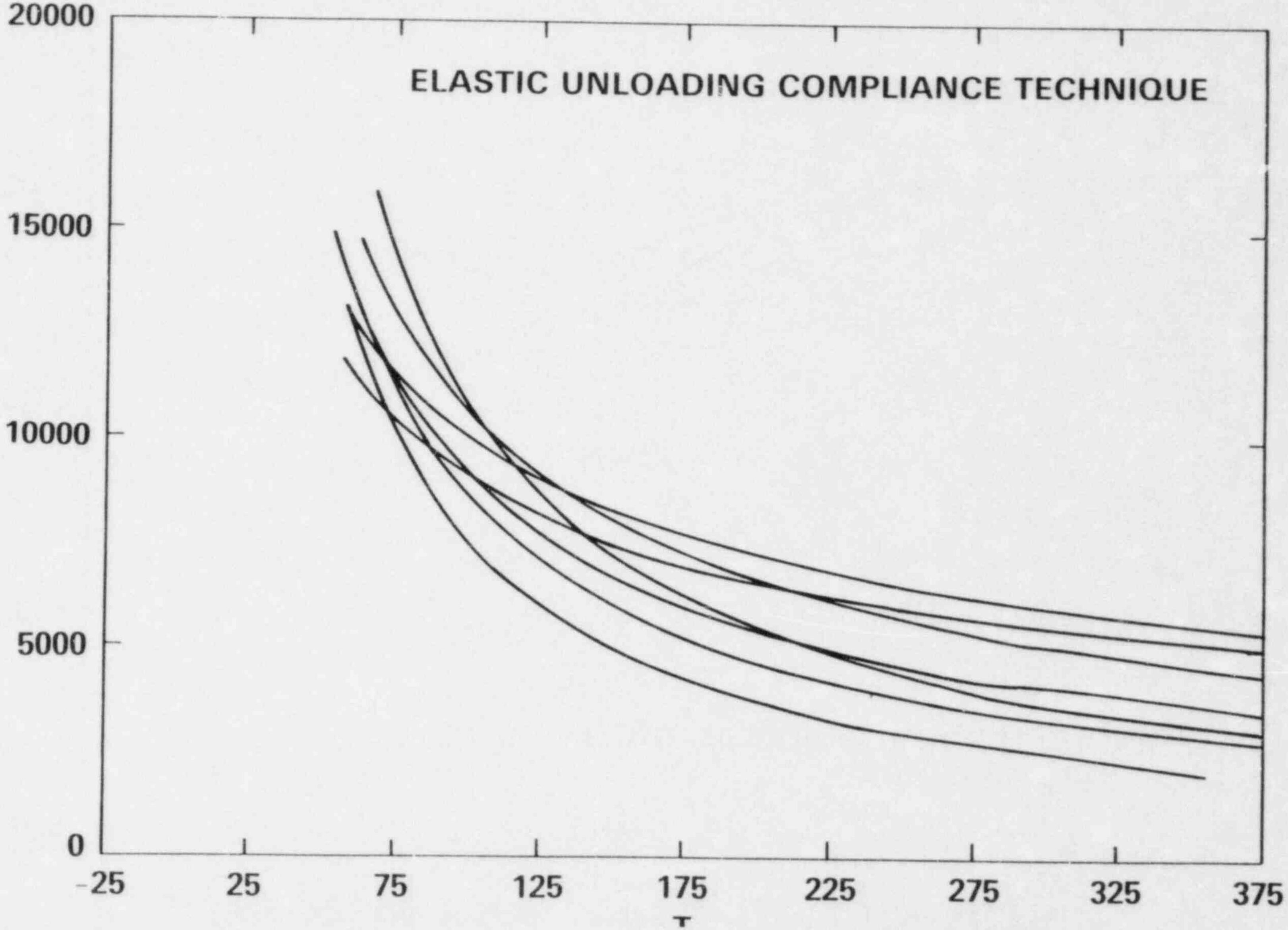

J/T PLOT A106 STEEL PIPE 8 INCH DIAMETER SPECIMENS

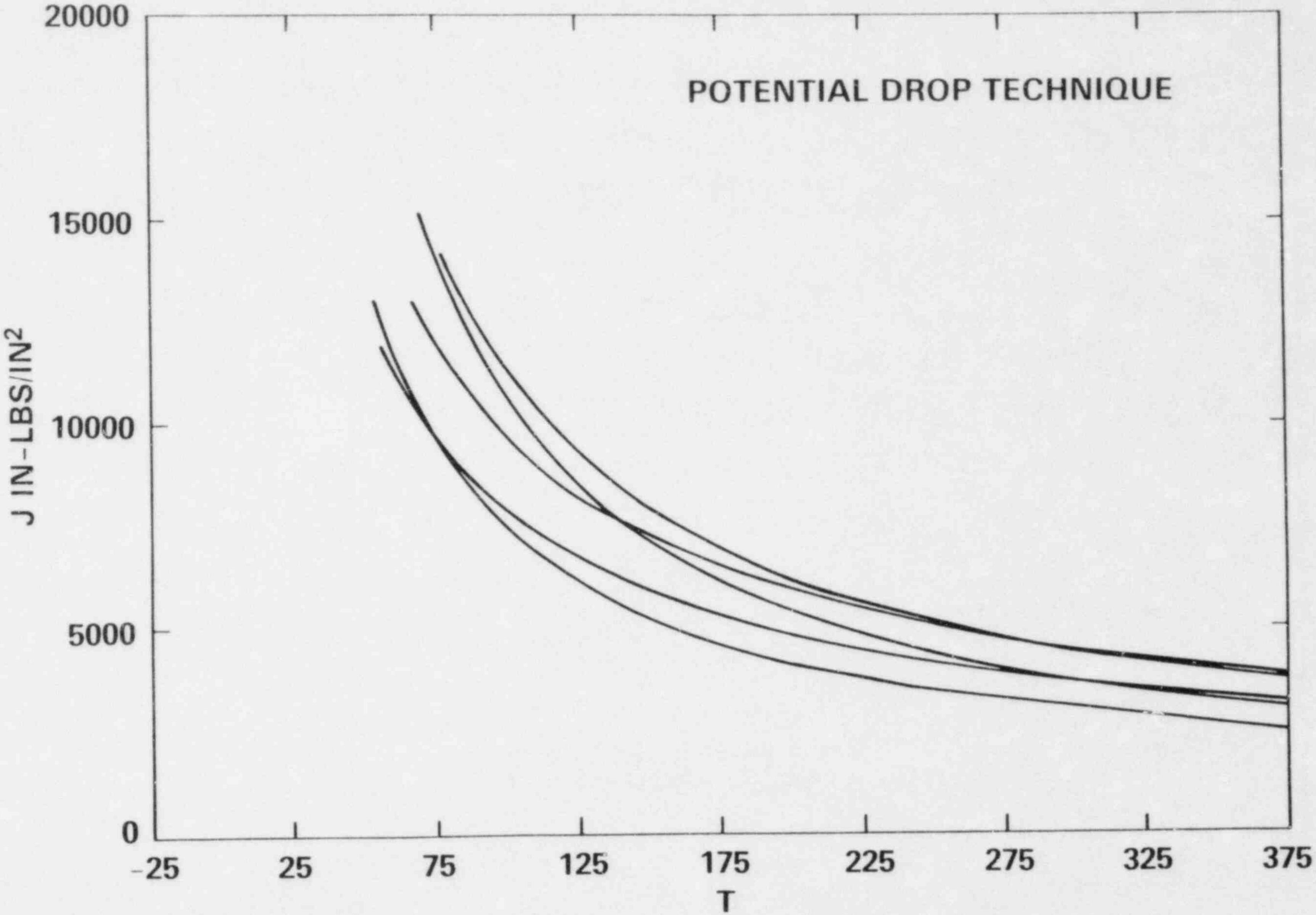

SUMMARY

- J-R CURVES FROM COMPACT SPECIMENS CAN BE USED TO PREDICT J-R CURVES FROM 8 INCH DIAMETER PIPE

- $T_{APPLIED}$ ANALYSIS USING PIPE BEHAVIOR CAN ACCURATELY DESCRIBE TEARING INSTABILITY IN A106 STEEL PIPES

- $T_{APPLIED}$ ANALYSIS USING ASSUMED MATERIAL BEHAVIOR WAS CONSERVATIVE IN PREDICTING INSTABILITY BEHAVIOR

PIPING RELIABILITY MODEL DEVELOPMENT, VALIDATION AND ITS APPLICATIONS TO LIGHT WATER REACTOR PIPING*

H. H. Woo, Ph.D., P. E.
Lawrence Livermore National Laboratory
University of California
P.O. Box 808, L-90
Livermore, California 94550 USA

SUMMARY

This summary provides a brief description of a three-year effort undertaken by the Lawrence Livermore National Laboratory for the piping reliability project. The ultimate goal of this project is to provide guidance for nuclear piping design so that high-reliability piping systems can be built.

The Code of Federal Regulations requires that structures, systems, and components affecting the safe operation of nuclear power plants be designed to withstand combinations of loads that may result from natural phenomena, normal operating conditions, and postulated accidents. Conventional methods of structural design through the use of safety factors allow for variability in loads, material strengths, in-service environments, the fabrication process, etc. However, the subjective manner in which these safety factors have been determined result in variable and nonuniform reliability. Reliability is defined as the probability that a structure or component will maintain its design functions during its designed lifetime.

In contrast to these conventional methods, the probabilistic (reliability) approach, which considers the stochastic nature of loads and variations in material properties, can better provide us with an assessment of the safety and performance of structures. Both the NRC and the nuclear industry are moving toward a greater use of reliability analysis for safety evaluations.

In response to an NRC request, the Lawrence Livermore National Laboratory initiated a Piping Reliability Project in 1980 which was based on the reliability approach. A piping reliability model was developed during fiscal year (FY) 1980 and was immediately applied to analyze the influence of seismic events on the probability of failure in the primary coolant system of a PWR. The results were accepted favorably by the Advisory Committee on Reactor Safeguards (ACRS) and the NRC. Details of the model were documented in the report, NUREG/CR-2189, Probability of Pipe Fracture in the Primary Coolant Loop of a PWR Plant.

The FY 82 and 83 scope of work for the piping reliability project consists of three major tasks: (1) the development of fracture mechanics models for assessing piping reliability in LWR; (2) the validation of the models; and (3) the establishment of a technical basis for modifying Regulatory Guide 1.46, Protection Against Pipe Whip Inside Containment. Task 1 results are reported in the report, NUREG/CR-2301, Fracture Mechanics Models Developed for Piping Assessment in Light Water Reactors. Some results for Tasks (2) and (3) can be found in the report, NUREG/CR-2801, Piping Reliability Model Validation and Potential Use for Licensing Regulation Development.

*This work was supported by the United States Nuclear Regulatory Commission under a Memorandum of Understanding with the United States Department of Energy.

The success of the validation work for the piping reliability model relies on the results of a comparison between analytical predictions and documented failure cases. Two failure cases were chosen for comparison with the results based on the piping reliability model. The first case was for PWR feedwater line cracking incidents. The failure mode was found to be thermal fatigue. For one PWR plant at the end of 11 months of commercial service, the leak probability was estimated to be 0.9; this estimate correlates very well with the leaking observed in the plant at that time. The second case was a BWR recirculation line safe-end cracking incident. Investigation of the incident led to the conclusion that stress corrosion was the cause of the pipe cracking. The piping reliability results indicated that the cumulative leak probability at the end of 3.5 years (the approximate length of time the plant has been operating prior to the incident) is about 20% if we consider the performance of preservice inspection. This result correlates favorably with the observation that at the end of 3.5 years operating time, only one safe end out of eight at one BWR plant was found to be leaking.

The failure probability of the postulated pipe break locations was also evaluated, as required by Regulatory Guide 1.46. A PWR surge line was selected for the study. The result showed that the leak and rupture probabilities for the weld joints are on the order of 10^{-5} and 10^{-9}, respectively.

Based on the results studied so far, we conclude that the reliability approach can undoubtedly help us understand not only how to assess and improve the safety of the piping systems but also how to design more reliable piping systems.

nSSP NUCLEAR SYSTEMS SAFETY PROGRAM 1

PIPING RELIABILITY MODEL DEVELOPMENT, VALIDATION, AND ITS APPLICATIONS TO LIGHT WATER REACTOR PIPING

PRESENTED BY

H. H. WOO

AT

10TH WATER REACTOR SAFETY RESEARCH INFORMATION MEETING
GAITHERSBURG, MARYLAND
OCTOBER 13, 1982

nSSP NUCLEAR SYSTEMS SAFETY PROGRAM 2

OUTLINE OF PRESENTATION

0 LLNL PIPING RELIABILITY PROJECT

0 OVERVIEW OF PIPING RELIABILITY MODEL

0 VALIDATIONS AND APPLICATIONS

0 RECOMMENDATIONS FOR FUTURE WORK

LLNL PIPING RELIABILITY PROJECT AND MODEL DEVELOPMENT

0 PROJECT OBJECTIVES

- TO ASSESS RELIABILITY OF LIGHT WATER REACTOR PIPING
- TO RECOMMEND HOW TO IMPROVE RELIABILITY OF NUCLEAR PIPING
- TO PROVIDE GUIDANCE FOR HIGH-RELIABILITY NUCLEAR PIPING DESIGN

0 MODEL DEVELOPMENT

- FISCAL YEAR '80: THERMAL FATIGUE
- FISCAL YEAR '81: THERMAL FATIGUE AND STRESS CORROSION

OVERVIEW OF PIPING RELIABILITY MODEL

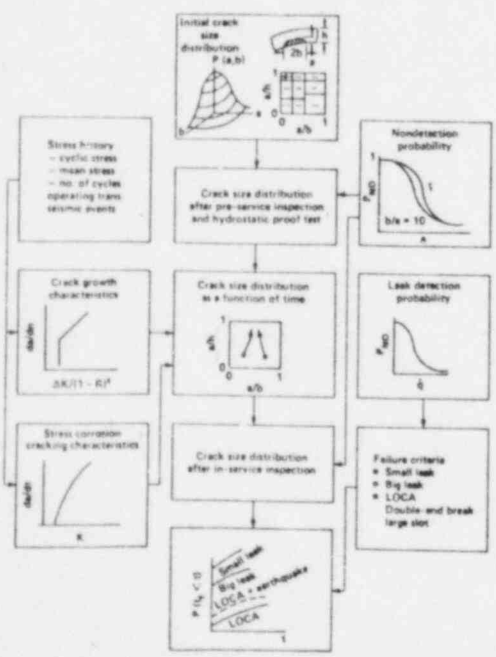

0 PROBABILISTIC FRACTURE MECHANICS

0 TWO-DIMENSION CRACK

0 CRACK GROWTH
- FATIGUE
- STRESS CORROSION

0 PRESERVICE AND INSERVICE INSPECTIONS

0 LEAK DETECTION

0 LEAK AND LOCA ASSESSMENT

NSSP NUCLEAR SYSTEMS SAFETY PROGRAM

5

MODEL VALIDATIONS AND APPLICATIONS

VALIDATIONS

- O PWR FEEDWATER LINE CRACKING INCIDENT
- O BWR RECIRCULATION-INLET-NOZZLE SAFE END CRACKING INCIDENT

APPLICATIONS

- O PWR PRIMARY COOLANT LOOPS LEAK AND RUPTURE PROBABILITY STUDY
- \- WESTINGHOUSE ZION-I PLANT

- O REGULATORY GUIDE 1.46 STUDY
"PROTECTION AGAINST PIPE WHIP INSIDE CONTAINMENT"

NSSP NUCLEAR SYSTEMS SAFETY PROGRAM

6

VALIDATION CASE I: PWR FEEDWATER LINE CRACKING INCIDENT

- O D. C. COOK 2 PLANT, MICHIGAN, MAY, 1979
- O THERMAL FATIGUE
- O PIPE SIZES 16~19 INCHES, A106 GRADES B OR C

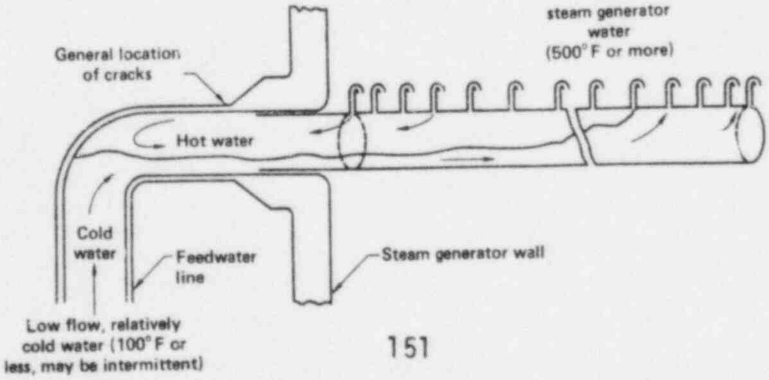

RELIABILITY ANALYSIS RESULTS FOR PWR FEEDWATER LINE CRACKING INCIDENT

Plant	Time up to inspection since service T_o^1(yr)	Max crack depth A (in)	Counter bore thickness T(in)	A/T	Leak probability at T_o^1: [2]With ISI, PSI	Leak probability at T_o^1: Without ISI, PSI
A	11 mos	0.57	0.57	1.0	0.60	0.9
B	2 yrs 9 mos	0.235	0.875	0.27	0.32	0.63
C	4 yrs 3 mos	0.028	0.75	0.04	0.0022	0.074
D	9 yrs	0.75	1.21	0.62	0.08	0.29
E	10 yrs	0.107	0.843	0.13	0.55	0.92

[1] Leaking was discovered at Plant A in 5/79, and the balance was reported in 3/80 (Ref. 2).

[2] ISI (In-service Inspection) PSI (Pre-service Inspection)

ISI was based on ASME XI Inspection Program A, 1980.

VALIDATION CASE II: BWR RECIRCULATION-INLET-NOZZLE SAFE END CRACKING INCIDENT

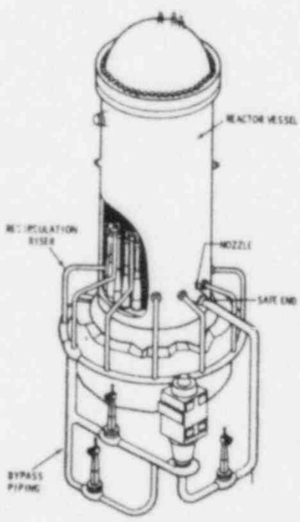

BWR Recirculation System

- 0 DUANE ARNOLD PLANT, IOWA, JUNE, 1978
- 0 STRESS CORROSION CRACKING
- 0 PIPE SIZE 10 INCHES, INCONEL 600

THERMAL SLEEVE

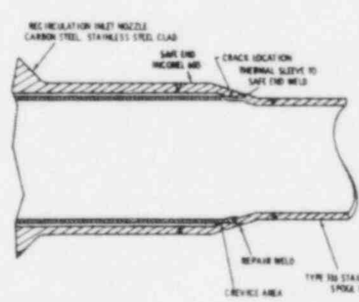

Duane Arnold Recirculation—Inlet-Nozzle Safe End Configuration

nSSP NUCLEAR SYSTEMS SAFETY PROGRAM

9

RELIABILITY ANALYSIS RESULTS FOR BWR RECIRCULATION LINE CRACKING INCIDENT

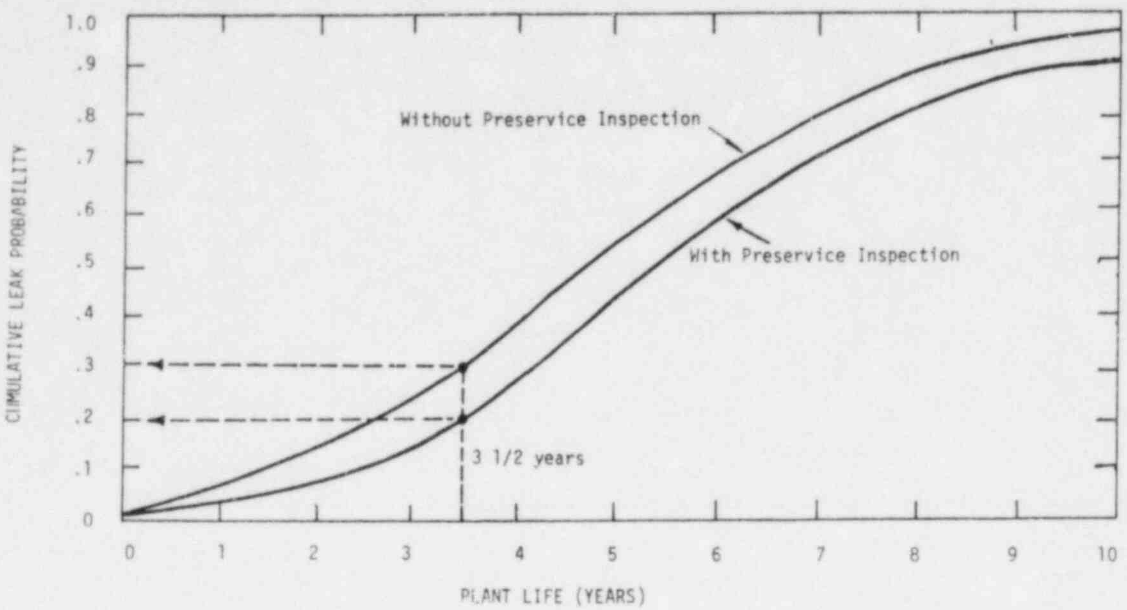

nSSP NUCLEAR SYSTEMS SAFETY PROGRAM

10

APPLICATION CASE I: SSE-LOCA ASSESSMENT FOR ZION-1 PRIMARY COOLANT LOOPS

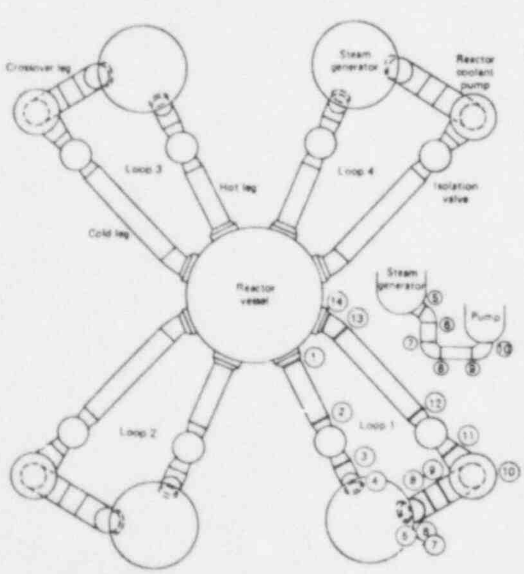

- O FOUR (4) LOOPS
- O FOURTEEN (14) CIRCUMFERENTIAL WELD JOINTS IN EACH LOOP
- O FAILURE PROBABILITY ASSESSMENT
  - LEAK: ORDER OF 10^{-9}
  - LOCA: ORDER OF 10^{-15}
  - LEAK BEFORE BREAK

nSSP
NUCLEAR SYSTEMS SAFETY PROGRAM

11

APPLICATION CASE II: REGULATORY GUIDE 1.46 STUDY

- 0 RELIABILITY APPROACH VERSE ASME BOILER AND PRESSURE VESSEL CODE. SECTION III APPROACH
- 0 WE CONTACTED A/E FIRMS AND GOT COMMITMENTS FROM:
  - BECHTEL POWER CORPORATION, L.A.
  - STONE & WEBSTER ENGINEERING CORPORATION (S&W)
  - SARGENT & LUNDY ENGINEERS
  - UNITED ENGINEERS & CONSTRUCTORS
  - EBASCO SERVICE INC.
  - GIBSON & HILL, INC.
- 0 PIPING DESIGN DATA HAVE BEEN RECEIVED:
  - TWO (2) SURGE LINES
  - FOUR (4) MAIN STEAM LINES
  - THREE (3) LOW & ONE (1) HIGH HEAD SAFETY INJECTION SYSTEMS
  - FOUR (4) RESIDUAL HEAT REMOVAL SYSTEMS
  - THREE (3) PRESSURIZER SPRAY SYSTEMS
  - ONE (1) PRESSURIZER SAFETY & RELIEF VALVE SYSTEM

nSSP
NUCLEAR SYSTEMS SAFETY PROGRAM

12

FIRST SYSTEM STUDIED: A PWR SURGE LINE

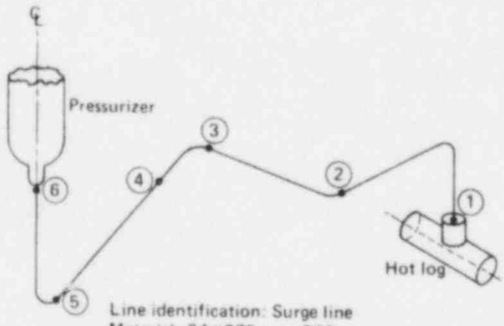

Line identification: Surge line
Material: SA#376 type 304
Pipe outer diameter: 12.75''
Wall thickness: SCH# 160 (1.312'')
Design temperature: 700°F
Design pressure: 2485 psi
Operating temperature: 653°F
Operating pressure: 2250 psi

• Field weld joints

RELIABILITY ANALYSIS RESULTS FOR A PWR SURGE LINE

WELD JOINT	PROBABILITY OF FAILURE*										USAGE FACTOR^X
	LEAK (10^{-5})					LOCA (10^{-9})					
	0	10	20	30	40	0	10	20	30	40	
1	.15	.78	.92	1.1	1.2	3.1	3.9	4.2	4.2	4.5	.00199
2	.16	1.9	2.5	3.0	3.3	1.3	2.4	2.4	4.0	6.2	.00235
3	.41	3.6	4.9	6.2	6.8	1.9	6.7	9.5	9.7	10.	.01630
4	.22	1.6	2.0	2.4	2.7	2.0	3.1	3.9	3.9	4.3	.01630
5	.43	4.2	6.3	7.6	8.3	3.1	6.2	7.4	12.	15.	.01492
6	.07	.55	.64	.81	.96	4.5	4.6	5.2	5.3	5.3	.00900

* ONLY PRE-SERVICE INSPECTION IS INCLUDED

\+ VALUES AT THE END OF THE YEAR

X FROM A/E FIRM

SUMMARY FOR REGULATORY GUIDE 1.46 STUDY

0 WE HAVE COMPLETED ANALYSES FOR TWO SURGE LINES AND TWO MAIN STEAM LINES (INSIDE CONTAINMENT)

- LEAK: ORDER OF 10^{-5}
- RUPTURE: ORDER OF 10^{-9}

0 BECAUSE OF INCOMPLETE RESULTS. WE ARE NOT ABLE TO MAKE RECOMMENDATIONS FOR MODIFYING REG. GUIDE 1.46 AT THIS MOMENT

NSSP NUCLEAR SYSTEMS SAFETY PROGRAM

15

RECOMMENDATIONS FOR FUTURE WORK

IN ORDER TO MAKE FINAL RECOMMENDATIONS, WE NEED:

0 AT LEAST TEN (10) PIPING SYSTEMS FOR EACH OF ASME CLASSES I, II AND III PIPING

0 MORE PIPING DESIGN DATA FROM A/E FIRMS
- COOPERATION FROM INDUSTRY

0 CONTINUING EFFORTS TO COMPLETE RELIABILITY ANALYSIS
- SUPPORT FROM NRC

NSSP NUCLEAR SYSTEMS SAFETY PROGRAM

16

NUREG REPORTS AND DOCUMENTS GENERATED BY LLNL IN THE AREA OF PIPING RELIABILITY STUDY

0 PROBABILITY OF PIPE FRACTURE IN THE PRIMARY COOLANT LOOP OF A PWR PLANT (9 VOLUMES) NUREG/CR-2189

0 FRACTURE MECHANICS MODELS DEVELOPED FOR PIPING RELIABILITY ASSESSMENT IN LIGHT WATER REACTORS NUREG/CR-2301

0 PIPING RELIABILITY MODEL VALIDATION AND POTENTIAL USE FOR LICENSING REGULATION DEVELOPMENT NUREG/CR 2801

0 PIPING RELIABILITY ANALYSIS FOR PRESSURIZED WATER REACTOR FEEDWATER LINES. <u>RELIABILITY AND SAFETY OF PRESSURE COMPONENTS</u>. ASME. PVP-62. 1982

0 PARAMETRIC STUDY ON IN-SERVICE INSPECTION PROGRAM FOR PWR FEEDWATER NOZZLE (IN PREPARATION)

0 A PROBABILISTIC ASSESSMENT OF THE PRIMARY COOLANT LOOP PIPE FRACTURE DUE TO FATIGUE CRACK GROWTH FOR A TYPICAL COMBUSTION ENGINEERING PLANT (IN PREPARATION)

0 DUANE ARNOLD STRESS CORROSION CRACKING ANALYSIS (IN PREPARATION)

IRRADIATION AND ANNEALING SENSITIVITY STUDIES

J. R. Hawthorne
Materials Engineering Associates, Inc.
Lanham, MD 20706 USA

Summary

Current concerns on service irradiation effects on the brittle/ductile transition temperature and the upper shelf toughness level of early production reactor vessels reinforce the need for a clear understanding of the metallurgical factors influencing irradiation response and annealing/reirradiation response. For new construction, the development and usage of radiation resistant steels precludes such concerns. Steels and welds produced in the USA to ASTM and AWS guidelines on composition (impurities) restrictions for nuclear service, for example, have been found to have high radiation resistance. That is, transition temperature elevations typically are 100°F or less at $5x10^{19}n/cm^2$.

This report describes an evaluation of foreign steel production made to USA guidelines for improved radiation resistance (new vessel forms) and investigations on variable radiation sensitivity and postirradiation annealing for embrittlement relief (vessels produced 1971 or earlier) (Fig. 1).

In the study of foreign steels, investigations coordinated by the IAEA IWG-RRPC and involving steels produced in West Germany, France and Japan have confirmed the adequacy of the USA developed specifications and guidelines for worldwide production of radiation resistant steel. Findings at Materials Engineering Associates are compared to the upper bound embrittlement prediction for low Cu, low P steels of RG 1.99 in Fig. 2.

The study on Cu vs Ni effects, reported in part at the 1981 WRSIM, provided experimental confirmation of the suspect synergism between Cu impurities and Ni alloying in radiation sensitivity development and annealing response (Fig. 3). Recent additional findings show that, with a 0.7% nickel content, transition temperature recoveries are greater with 399°C annealing but that residual embrittlement levels are about the same as those for a 0.3 percent nickel content (at an equivalent copper level) (Fig. 4, 5). The results further suggest that a high nickel content can make the recovery process more sluggish. For long term 399°C treatments, only copper level appears to influence the magnitude of the residual embrittlement.

A new study (MEA-HEDL Cooperative) which is evaluating additional binary combinations and selected tertiary combinations is described. Postirradiation data are not yet available although initial irradiation experiments (2) have been completed for this study.

Progress of the Irradiation-Anneal-Reirradiation (IAR) investigations is also described. The objectives of this phase 2 effort are to assess the

reembrittlement path upon reirradiation, i.e. after annealing, (Figure 6) and to test the effect on reembrittlement rates of material composition and/or weld flux type. Comparisons are being developed between C_v and 0.5T CT test performances in the interest of evolving correlations of notch ductility and fracture toughness behavior under IAR. Research materials include a 8" thick Linde 80 weld (60 ft-lb C_v USE, -10F C_v 30 ft-lb temperature) and a 8" thick Linde 0091 weld (120 ft-lb C_v USE, -80F C_v 30 ft-lb temperature) produced for MEA by Lukens Steel Company under contract.

The PVI Surveillance Dosimetry Improvement Program has primary application to the more radiation sensitive vessels. MEA is a participating laboratory with responsibilities for C_v, CT and tensile specimen evaluations. Three steels representing USA production and three steels representing overseas production were irradiated for the program in the Oak Ridge Research Reactor (ORR) Pool Side Facility (PSF); however, only two of the materials were irradiated in the form of 1T-CT and 0.5T-CT specimens along with the tensile and C_v specimens. MEA has tested the C_v specimens (Fig. 7) and the CT specimens from capsules SSC-1 and SSC-2 (simulated surveillance capsules) and determined fracture toughness changes (Fig. 8, 9). Companion specimens from the PSF capsules representing through-wall locations (surface, 1/4T and 1/2T) in a vessel have just been received and will be tested this year. The SSC capsule results indicate a reasonable agreement between C_v 41J transition temperature increase and CT K_{J_c} 100 MPa$\sqrt{m}$ transition temperature increase; however the former tends to underpredict the 100 MPa$\sqrt{m}$ temperature elevation somewhat.

References

J. R. Hawthorne, "Status of Knowledge of Radiation Embrittlement in USA Reactor Pressure Vessel Steels," NUREG/CR-2511, Nuclear Regulatory Commission, Feb., 1982.

J. R. Hawthorne, "Evaluation of IAEA Coordinated Program Steels and Welds for 288°C Radiation Embrittlement Resistance," NUREG/CR-2487, Nuclear Regulatory Commission, Feb. 1982

J. R. Hawthorne, "Significance of Nickel and Copper Content to Radiation Sensitivity and Postirradiation Heat Treatment Recovery of Reactor Vessel Steels," NUREG/CR-2948, Nuclear Regulatory Commission (to be published).

TOPICS

- IAEA IMPROVED STEELS vs RG 1.99
- %Cu + %Ni vs %RECOVERY BY ANNEALING
- MEA/HEDL COOPERATIVE
- IAR PROGRAM
- PVI SURVEILLANCE DOSIMETRY PROGRAM

Figure 1

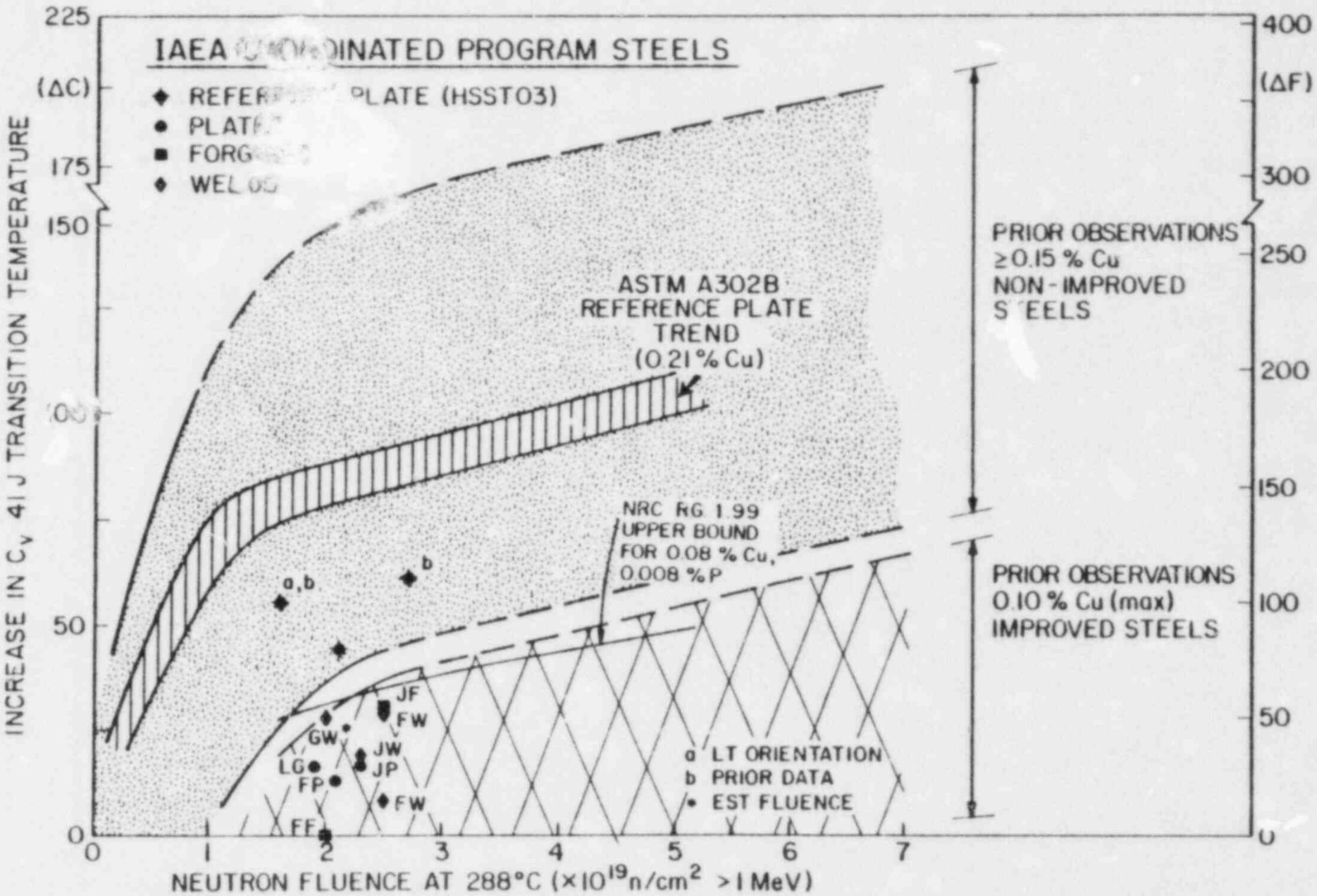

DINATED PROGRAM STEELS
PLATE (HSST03)
PRIOR OBSERVATIONS
≥0.15 % Cu
NON-IMPROVED
STEELS
ASTM A302B
REFERENCE PLATE
TREND
(0.21 % Cu)
NRC RG 1.99
UPPER BOUND
FOR 0.08 % Cu,
0.008 % P
PRIOR OBSERVATIONS
0.10 % Cu (max)
IMPROVED STEELS
a LT ORIENTATION
b PRIOR DATA
• EST FLUENCE
JF
FW
GW
JW
LG
JP
FP
FF
INCREASE IN C_V 41 J TRANSITION TEMPERATURE
(ΔC)
(ΔF)
NEUTRON FLUENCE AT 288°C ($\times 10^{19}$ n/cm^2 >1 MeV)

Figure 2

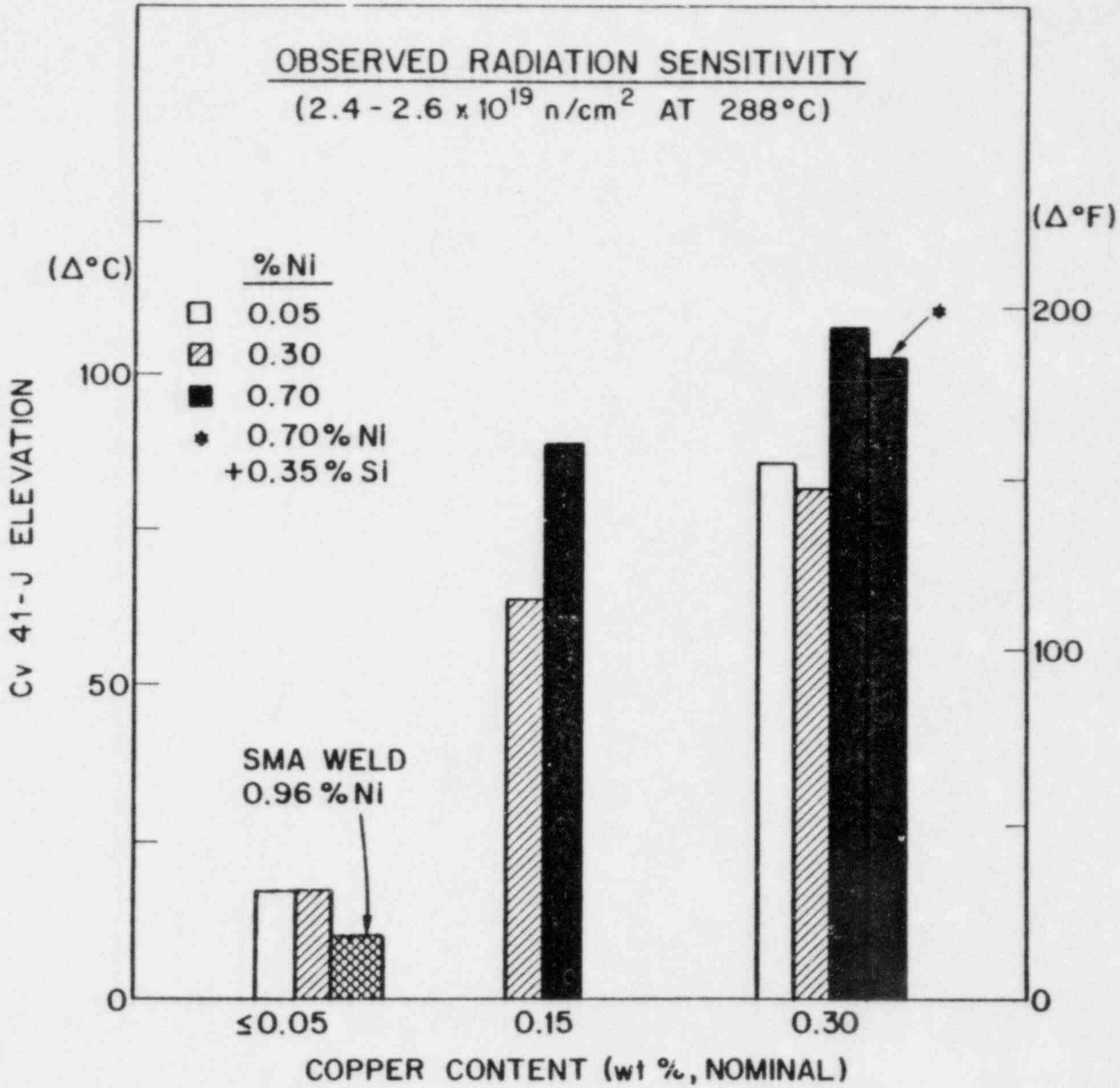
OBSERVED RADIATION SENSITIVITY
(2.4 - 2.6 x 10^19 n/cm^2 AT 288°C)
(Δ°C)
(Δ°F)
% Ni
0.05
0.30
0.70
0.70 % Ni
+0.35 % Si
SMA WELD
0.96 % Ni
Cv 41-J ELEVATION
100
50
0
200
100
0
≤0.05
0.15
0.30
COPPER CONTENT (wt %, NOMINAL)

Figure 3

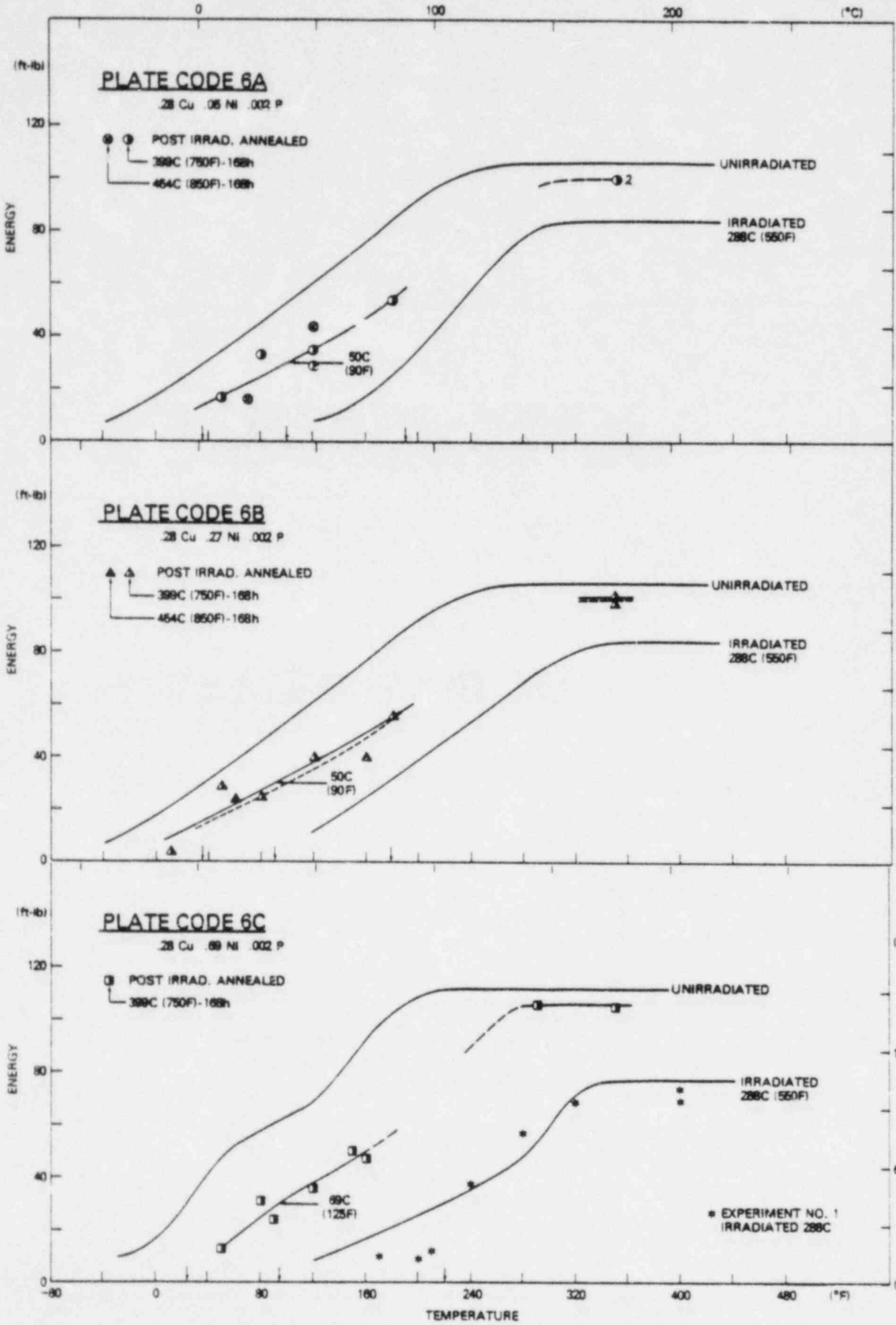

(°C)
0
100
200
PLATE CODE 6A
.28 Cu .06 Ni .002 P
POST IRRAD. ANNEALED
399C (750F)-168h
454C (850F)-168h
UNIRRADIATED
IRRADIATED
288C (550F)
50C
(90F)
PLATE CODE 6B
.28 Cu .27 Ni .002 P
POST IRRAD. ANNEALED
399C (750F)-168h
454C (850F)-168h
UNIRRADIATED
IRRADIATED
288C (550F)
50C
(90F)
PLATE CODE 6C
.28 Cu .69 Ni .002 P
POST IRRAD. ANNEALED
399C (750F)-168h
UNIRRADIATED
IRRADIATED
288C (550F)
69C
(125F)
* EXPERIMENT NO. 1
IRRADIATED 288C
ENERGY
(ft-lb)
(J)
TEMPERATURE
(°F)

Figure 4

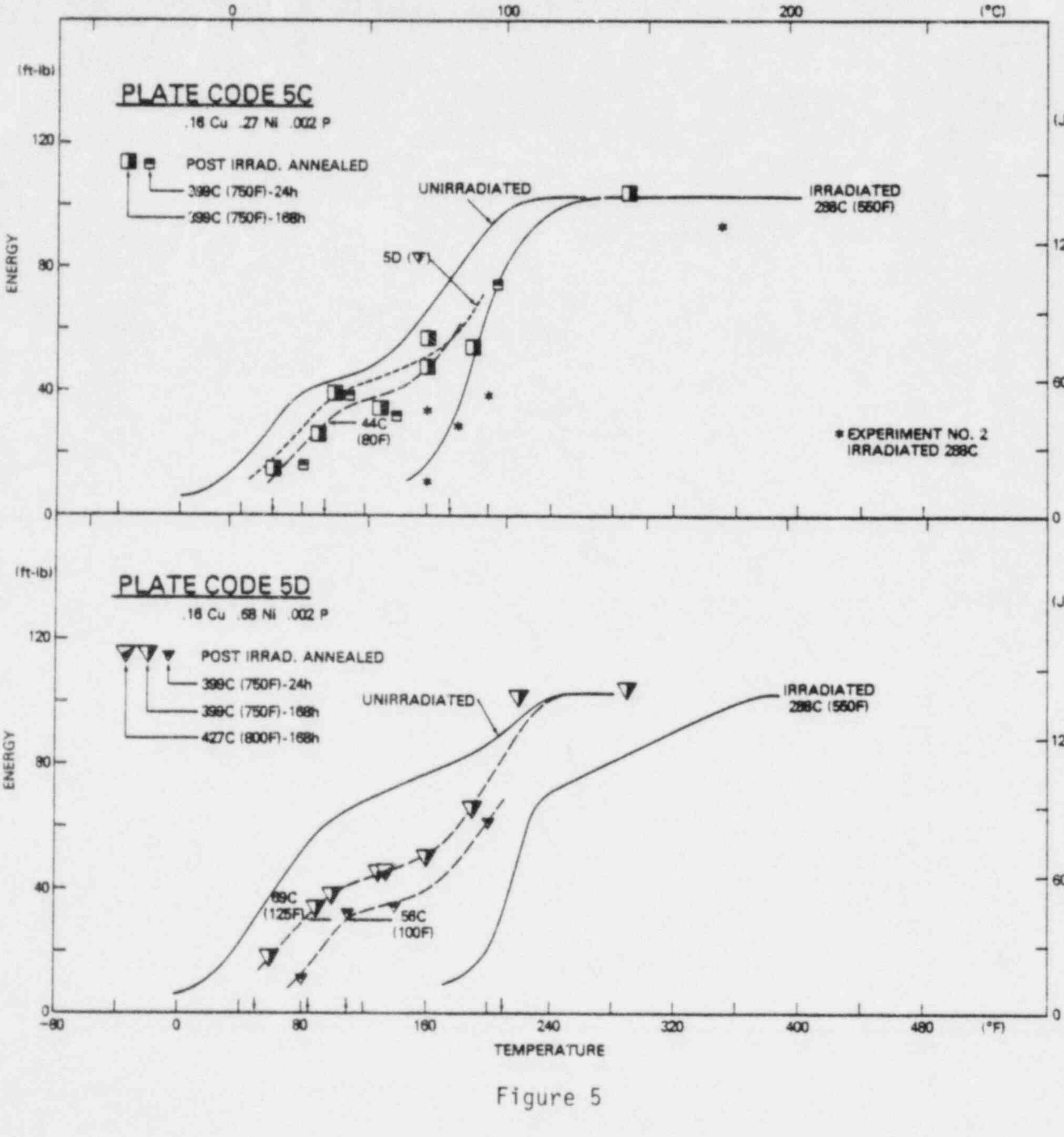

PLATE CODE 5C
.16 Cu .27 Ni .002 P
POST IRRAD. ANNEALED
399C (750F)-24h
399C (750F)-168h
UNIRRADIATED
IRRADIATED
288C (550F)
5D (▽)
44C
(80F)
* EXPERIMENT NO. 2
IRRADIATED 288C
PLATE CODE 5D
.16 Cu .58 Ni .002 P
POST IRRAD. ANNEALED
399C (750F)-24h
399C (750F)-168h
427C (800F)-168h
UNIRRADIATED
IRRADIATED
288C (550F)
69C
(125F)
56C
(100F)
ENERGY
(ft-lb)
(J)
TEMPERATURE
(°C)
(°F)

Figure 5

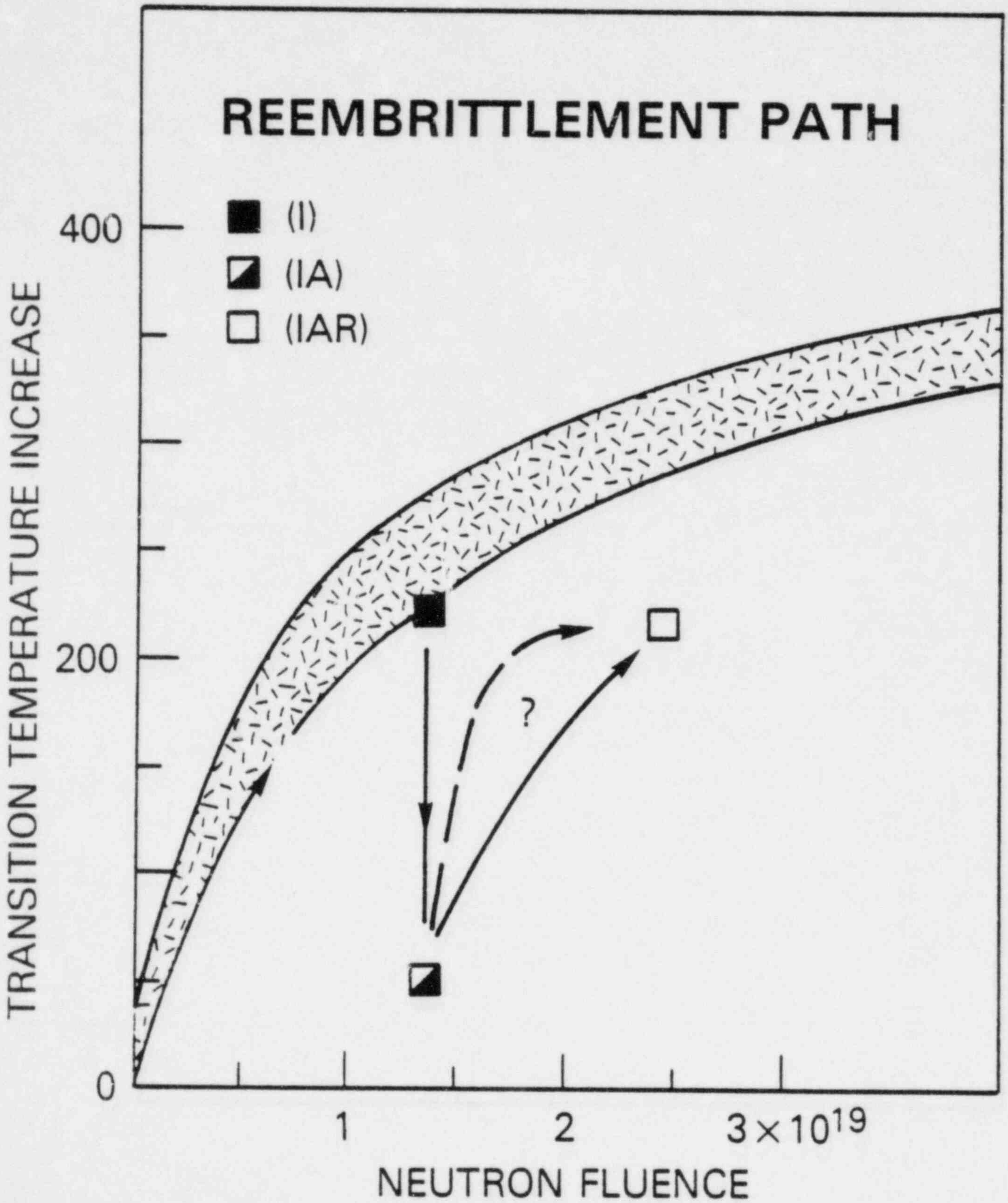
REEMBRITTLEMENT PATH
(I)
(IA)
(IAR)
400
200
0
?
1
2
3×10^19
TRANSITION TEMPERATURE INCREASE
NEUTRON FLUENCE

Figure 6

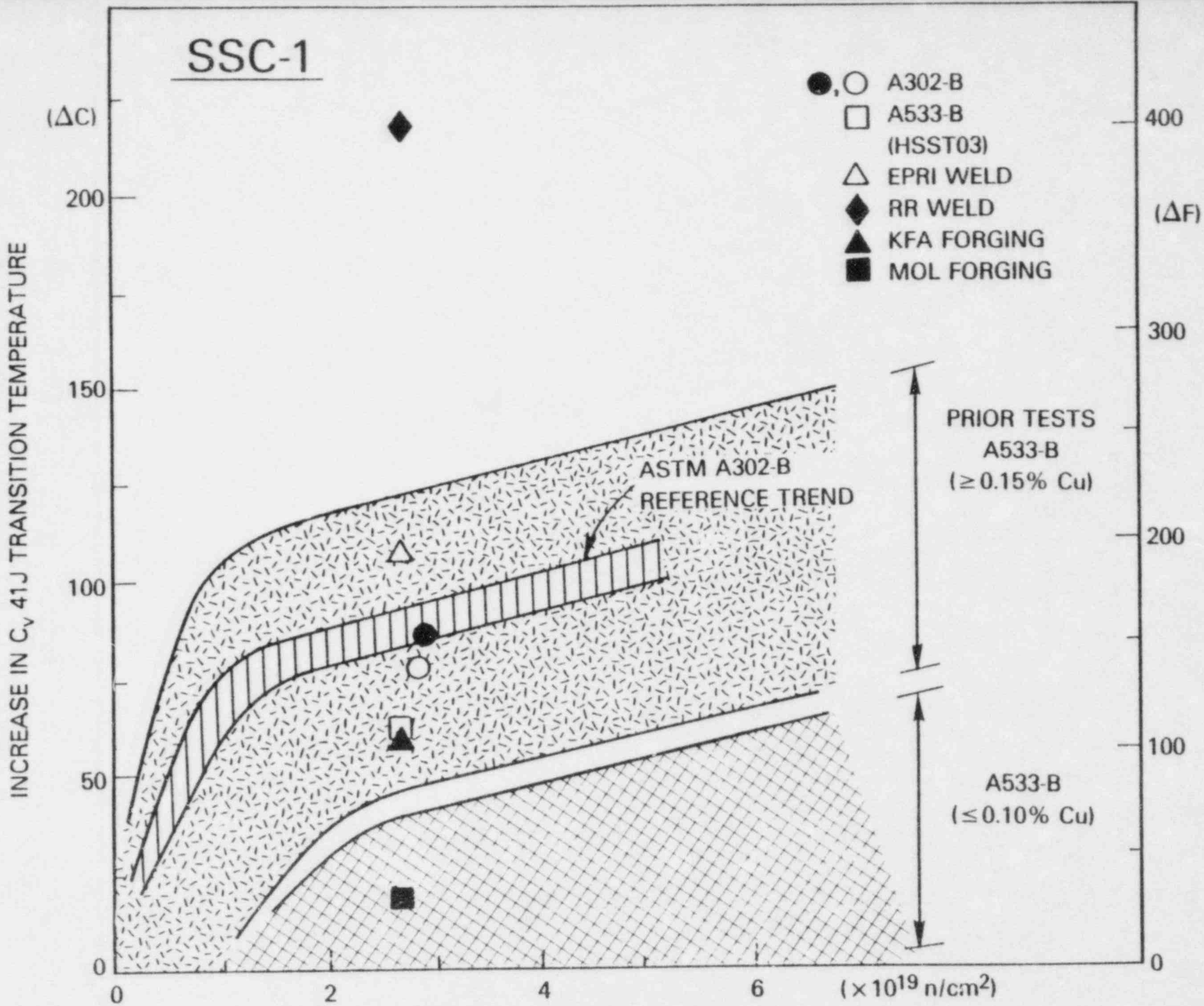

SSC-1
A302-B
A533-B
(HSST03)
EPRI WELD
RR WELD
KFA FORGING
MOL FORGING
(ΔC)
(ΔF)
PRIOR TESTS
A533-B
(≥0.15% Cu)
ASTM A302-B
REFERENCE TREND
A533-B
(≤0.10% Cu)
INCREASE IN C_v 41J TRANSITION TEMPERATURE
NEUTRON FLUENCE AT 288°C
($\times 10^{19}$ n/cm^2)
0
50
100
150
200
0
100
200
300
400
0
2
4
6

Figure 7

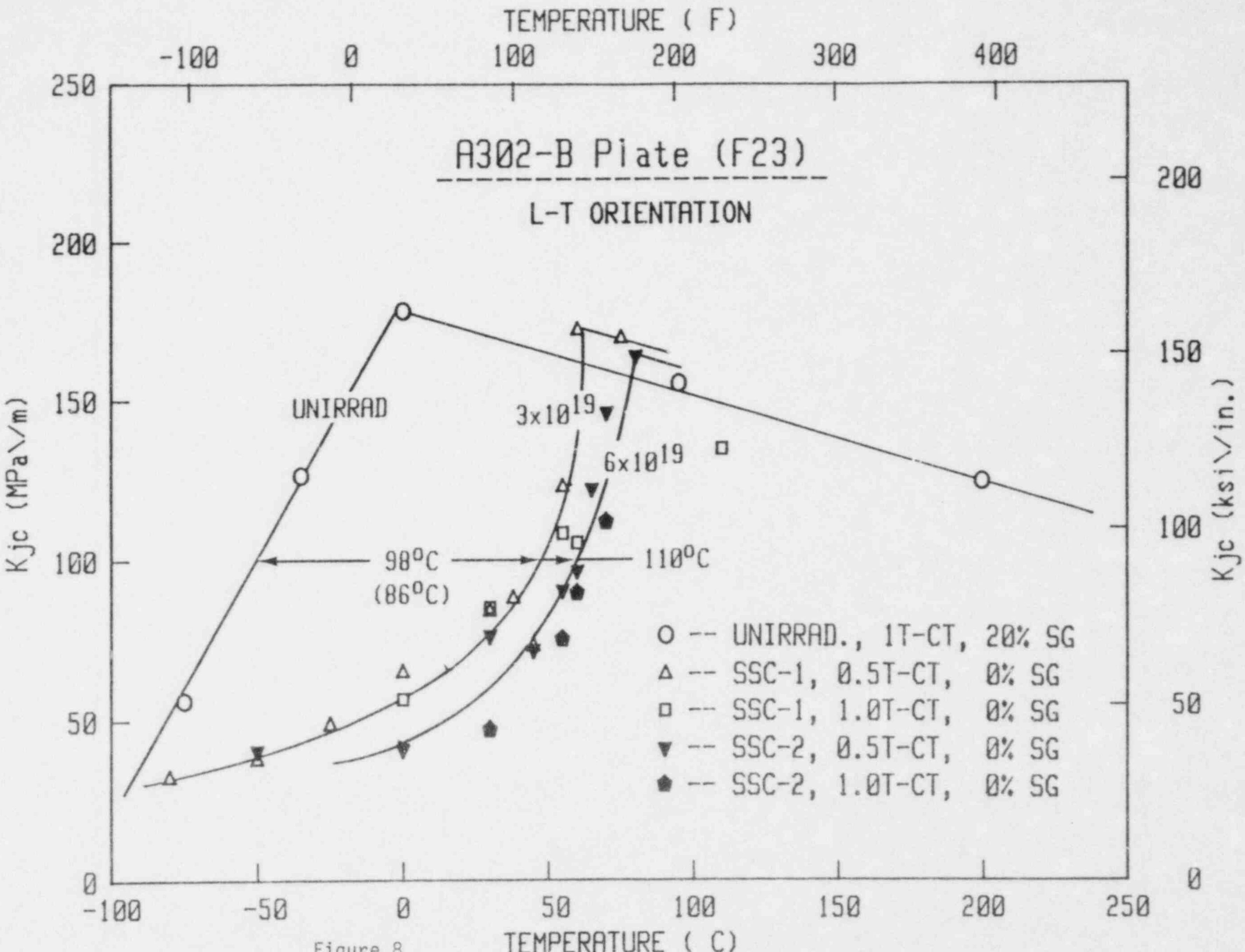

TEMPERATURE (F)
A302-B Plate (F23)
L-T ORIENTATION
UNIRRAD
3x10^19
6x10^19
98°C
(86°C)
110°C
O -- UNIRRAD., 1T-CT, 20% SG
△ -- SSC-1, 0.5T-CT, 0% SG
□ -- SSC-1, 1.0T-CT, 0% SG
▼ -- SSC-2, 0.5T-CT, 0% SG
⬟ -- SSC-2, 1.0T-CT, 0% SG
Kjc (MPa√m)
Kjc (ksi√in.)
TEMPERATURE (C)

Figure 8

166

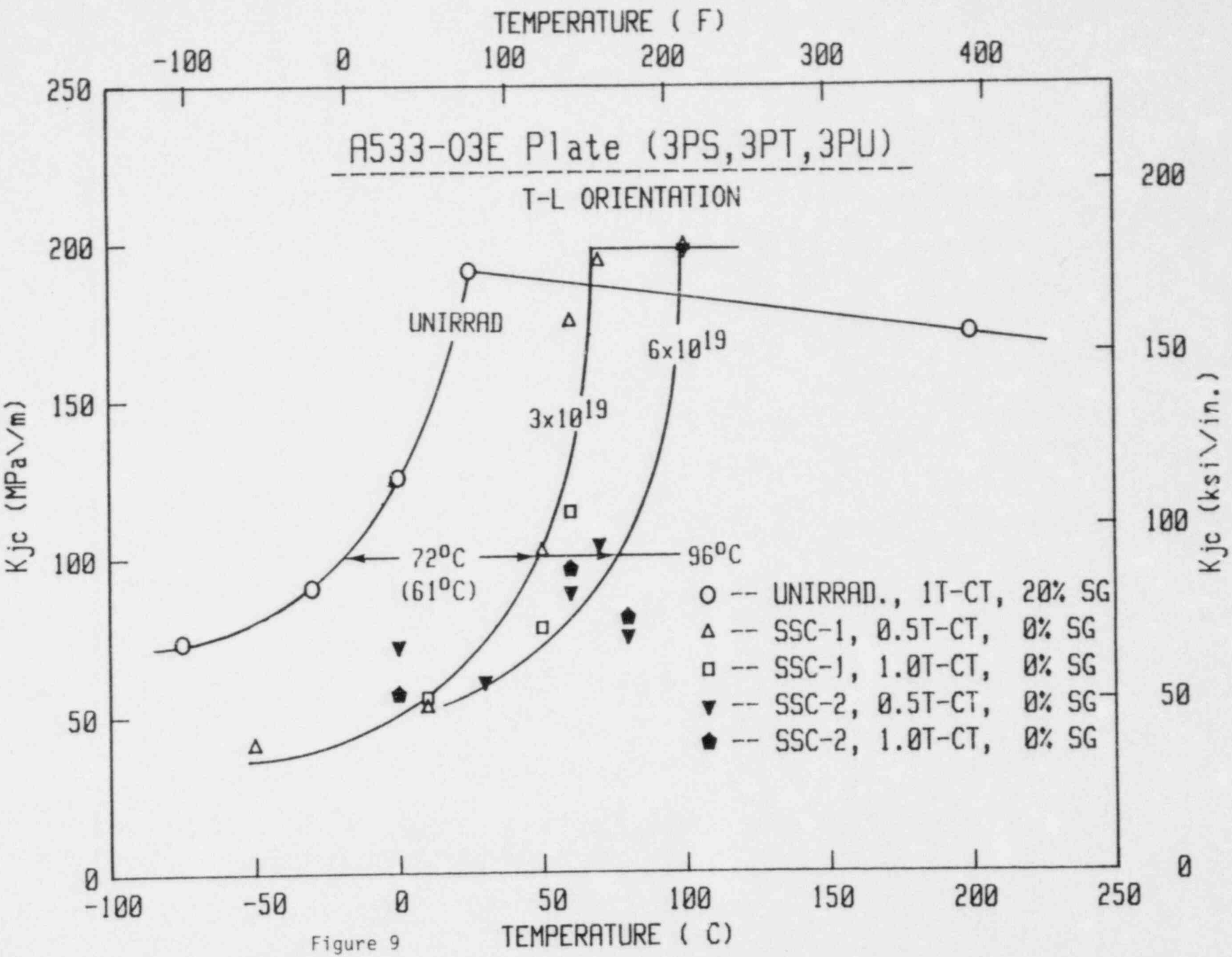
TEMPERATURE (F)
-100
0
100
200
300
400
A533-03E Plate (3PS,3PT,3PU)
T-L ORIENTATION
UNIRRAD
6x10^19
3x10^19
72°C
(61°C)
96°C
O -- UNIRRAD., 1T-CT, 20% SG
Δ -- SSC-1, 0.5T-CT, 0% SG
□ -- SSC-1, 1.0T-CT, 0% SG
▼ -- SSC-2, 0.5T-CT, 0% SG
⬟ -- SSC-2, 1.0T-CT, 0% SG
Kjc (MPa√m)
Kjc (ksi√in.)
250
200
150
100
50
0
-100
-50
0
50
100
150
200
250
TEMPERATURE (C)

Figure 9

FRACTURE TOUGHNESS CHARACTERIZATION OF IRRADIATED, LOW-UPPER SHELF WELDS

F. J. Loss, B. H. Menke, A. L. Hiser
Materials Engineering Associates
Lanham, MD 20706

BACKGROUND

Previous studies have shown that A533-B submerged arc weld deposits of the type used in the beltline region of some commercial, light water reactor vessels can exhibit low Charpy-V (C_v) upper shelf energy levels after irradiation, that is, energies which lie below 68J (50 ft-lb). In this event, Federal regulations (10 CFR Part 50) require, as one option, the performance of a fracture mechanics analysis that conservatively demonstrates the existence of adequate margins of safety for continued operation. In the upper shelf region the vessel is assumed to exhibit elastic-plastic behavior so that a linear elastic fracture mechanics approach would be inappropriate. The question of a suitable fracture mechanics analysis procedure to quantify the margin against fracture is addressed through Generic Safety Issue A-11 on Reactor Vessel Materials Toughness [1]. In resolving this issue the NRC has suggested that under elastic-plastic conditions the vessel can be properly evaluated in terms of the tearing instability concept of Paris and others [2]. Currently, this concept is being verified through intermediate vessel tests at Oak Ridge National Laboratory (ORNL) under the Heavy Section Steel Technology (HSST) Program.

The fracture toughness property required for a tearing instability analysis is the J-R curve. The NRC is therefore establishing a data base of J-R curve trends for irradiated pressure vessel steels of low shelf toughness. Of primary interest is A533-B submerged arc weld deposit made with Linde 80 flux and containing a high copper impurity level. The high sensitivity to irradiation associated with the copper impurity, coupled with a low preirradiation toughness associated with the Linde 80 flux, can result in a low upper shelf behavior. Seven welds (61W-67W) of this type were irradiated in the HSST Program. All of the welds are essentially identical to those in operating plants in which the material may exhibit a low upper shelf behavior. The experimental capsules containing compact toughness (CT) specimens of several sizes (e.g. 0.5T-, 0.8T-, 1.6T- and 4T-CT) as well as C_v and tensile specimens, were irradiated to fluence levels of 0.6 to 1.5 x 10^{19} n/cm^2 > 1 MeV to produce C_v upper shelf levels of 54 to 81J (40 to 60 ft-lb). The J-R curve characterization of these welds was undertaken by the Naval Research Laboratory (NRL); this work was later continued by Materials Engineering Associates (MEA). All other phases of the materials characterization were completed by ORNL. A summary of the results from this program is presented here.

J-R CURVE METHODOLOGY

A modified version of the J integral known as J_M [3], has been used in this study:

$$J_M = J_D - \int_{a_o}^{a} \left. \frac{\partial [J - G]}{\partial a} \right|_{\delta_{pl}} da \qquad (1)$$

where J_D is the deformation theory J, G the Griffith linear elastic energy release rate, a_o and a the initial and current crack lengths, $J_D - G = J_{pl}$ the plastic part of the deformation theory and δ_{pl} the plastic part of the displacement.

J-R curves have been obtained by means of the single specimen compliance (SSC) technique [4, 5]. The CT specimens used in this study were side-grooved by 20% in order to achieve a straight crack-front extension. A typical R curve produced with the SSC method, as illustrated in Fig. 1, is normally restricted to a small crack extension (Δa) in order to maintain a region of "J dominance." This requirement has been formulated by Hutchinson and Paris [6] as $\omega >> 1$ where $\omega = (b/J)(dJ/da)$ and b is the unbroken ligament. However, R curves exhibiting a longer crack extension, which would violate the ω criterion, may be necessary for a given structural analysis. Therefore, R curves have been developed in this program which sometimes exceed current crack extension limitations with the expectation that the data may prove useful for future analyses.

The R curve format of Fig. 1 is in accordance with ASTM Standard E813 for J_{Ic} whereby J_{Ic} is defined by the intersection of a linear regression fit to the data (i.e., the dashed line between the 0.15 mm and 1.5 mm exclusion lines) with the blunting line, $J = 2\ \sigma_f\ \Delta a$ where σ_f is the flow stress. Using the SSC technique, however, Loss and co-workers [7] have demonstrated that the R curve is nonlinear for small amounts of crack extension (e.g., 2 mm) in structural steels. Consequently, the R curve in the region between the 0.15 mm and 1.5 mm exclusion lines has been described in terms of a power law, $J = C\ \Delta a^n$, where C and n are constants chosen to optimize the curve fit. To circumvent the potential difficulties associated with the ASTM least squares procedure, Loss and co-workers [7] have formulated a new indexing procedure for J_{Ic} which more clearly represents the physical behavior. Specifically, J_{Ic} is taken as that value of J where the power-law R curve crosses the 0.15 mm exclusion line. This is an engineering approach, analogous to that used for the 0.2% yield stress, and it permits a small, but measurable crack extension at the J_{Ic} point. However, it should be noted that for the reactor vessel steels discussed here the magnitude of J_{Ic} given by the authors' method is nearly identical to that of the ASTM procedure for reactor vessel steels, as illustrated in Fig. 1.

As a consequence of the power-law R curve it is clear that the tearing modulus of the material, T_m, defined as $(E/\sigma_f^2)(dJ/da)$, where E is Young's modulus, is not constant for small crack extension as was originally envisioned. Consequently, an average value of tearing modulus, T_{avg}, for the portion of the R curve between the exclusion lines was chosen to represent the material behavior.

Normally, a single clip gage mounted within the notch (on the load line) is used to determine both the specimen load vs. deflection as well as the crack extension. With the 0.5T- and 0.8T-CT specimens, however, insufficient room was available in the irradiated specimens to mount such a gage. Therefore, a new technique using two clip gages was devised, with one clip gage providing load vs. deflection data and the other providing crack length information (Fig. 2). At that time, it was not known if one gage, mounted on the crack mouth, would produce the required accuracy since load-line displacements are necessary to compute J. Since that time it has been found that each of the gages can be used individually for load vs. deflection and crack extension assessments to produce R curves identical to that obtained with the double clip gage technique (Fig. 3).

Application of the tearing instability concept is illustrated schematically in Fig. 4 in terms of structural parameters (applied J_a and T_a) and a material parameter (J-R curve). The material resistance curve reflects the power-law behavior depicted in Fig. 1. The structural loading line represents a simple case of a surface flaw in a cylindrical shell, where a is the crack depth. The loading of the cylinder and the related response of the material are illustrated by the arrows; instability is achieved when $T_a > T_m$, as denoted by the intersection of the two curves. Although the verification of the tearing instability concept for low upper shelf behavior in pressure vessels is still in progress, the concept illustrated in Fig. 4 provides valuable insight as to the structural significance of changes in the R curve behavior associated with radiation embrittlement.

SUMMARY OF RESULTS

The majority of R curve tests in the program were conducted at 200°C to ensure ductile behavior for both the irradiated and unirradiated materials. A summary of the R curve trends at this temperature, obtained with 4T-CT specimens is illustrated in Fig. 5. The results for pre- and post irradiation conditions exhibit a relatively small scatter considering the fact that the data include tests from seven different welds and a fluence variation by more than a factor of two. Upon closer examination we have found that J_{Ic} is reduced by 0-50% with irradiation whereas a larger change (50-75%) is exhibited by T_{avg}. In these tests $\omega = 1$ at 15-20mm of crack extension, thereby indicating that the region of J dominance may have been exceeded at longer crack extensions.

The C_v shelf energy levels for the irradiated and unirradiated conditions are also shown in Fig. 5. Because of the relatively small variation in C_v energy for both the irradiated and unirradiated materials, it is difficult to associate changes in C_v energy directly with changes in the R curve. However, a correlation between C_v energy and both J_{Ic} and T_{avg} from 1T-CT specimen tests has been observed by the authors in other NRC-sponsored programs as well as in a program sponsored by the Electric Power Research Institute (EPRI) [8] (Fig. 6-7). In terms of these correlations, the HSST data show a similar correlation with C_v shelf energy even though some data lie outside of the correlation bands. While an explanation for the latter is not currently available, the possibility exists of a size effect between CT specimens of different thickness, since the correlation bands are based on only 1T-CT data. In Fig. 7 it is primarily the larger specimens (1.6T- and 4T-CT) which lie outside of the band. Nevertheless, these correlations provide added significance to C_v data from surveillance specimens in terms of the tearing instability concept.

All the data shown thus far have been derived at 200°C. The effect of test temperature on J_{Ic} and T_{avg} is illustrated in Figs. 8 and 9, respectively. Both quantities exhibit a 30-40% drop within 100°C. This phenomenon is sufficiently pronounced that it must be taken into account in structural integrity assessments. This inverse relationship was unexpected on the basis of the C_v upper shelf energy performance. The latter exhibits an apparent invariance with upper shelf temperature (Fig. 10). This difference in behavior between the two specimen types is believed to be a strain aging phenonemon resulting from the rapid loading of the C_v specimen vis a vis the quasi-static loading of the J-R curve specimen. While a correlation exists between C_v shelf energy and the R curve, this relationship must be adjusted to reflect the test temperature.

Figure 11 presents a summary of all the data obtained at 200°C from the four different specimen sizes in terms of a J vs T plot. A trend of increasing R curve level with C_v shelf energy is apparent, reflecting the correlations shown in Fig. 6-7. The plot also contains an applied loading line for a flawed cylinder having a slope of 8.8 kJ/m^2 (50 $in.lb/in.^2$). This loading line was suggested by the NRC select committee that drafted a resolution to Generic Issue A-11 [1]. This line has been constructed with a slope that is a factor of 10 less than that expected in an actual vessel containing an axial flaw (1/4T deep) in the beltline region. The arrows labeled A and B represent estimates of the applied J values for this flawed condition with the vessel loaded to design pressure and to twice design pressure, respectively. The latter is taken to represent a faulted condition. It can be seen that under the higher of the two loading conditions the margin of safety provided by the indicated loading line would be exceeded by only the two lowest R curves. Since the lowest R curves are associated with a ~68J (50 ft-lb) C_v shelf energy, caution is suggested in operating a vessel containing beltline material having less than this C_v energy if a loading as high as twice the design level is anticipated.

CONCLUSIONS

The principal conclusions of this study are:

- The SSC technique has been demonstrated as an effective method to characterize the J-R curve of irradiated steels.

- The J-R curves for reactor vessel steels of low upper shelf energy obey a power-law relationship for crack extension increments less than 2 mm.

- The first R-curve data base has been developed for irradiated vessel steels having low shelf energy.

- A correlation has been suggested between the R curve parameters (J_{IC} and T_{avg}) and C_v upper shelf energy. If further verified, this finding could enhance the significance of C_v reactor surveillance data with respect to structural integrity.

- The R curve parameters (J_{Ic} and T_{avg}) exhibit an inverse relationship with temperature which is not reflected by the C_v upper shelf trend. Therefore, the correlation between C_v energy and R curve must be adjusted to reflect the test temperature.

REFERENCES

1. R. E. Johnson, ed., "Resolution of Reactor Vessel Materials Toughness Safety Issue, Task Action Plan A-11", NUREG-0744, Nuclear Regulatory Commission, Sept. 1981.

2. P. C. Paris, H. Tada, A. Zahoor and H. Ernst, "Instability of the Tearing Mode of Elastic-Plastic Crack Growth", ASTM STP 668 (1979), pp 5-36.

3. H. A. Ernst, "Material Resistance and Instability Beyond J-Controlled Crack Growth", Scientific Paper 81-1D7-JINTF-P6, Westinghouse R & D Center, Dec. 3, 1981.

4. F. J. Loss, ed., "Structural Integrity of Water Reactor Pressure Boundary Components - Quarterly Progress Report, April-June 1979", NUREG/CR-0943, NRL Memorandum Report 4064, Sept. 28, 1979.

5. F. J. Loss, ed., "Structural Integrity of Water Reactor Pressure Boundary Components, Annual Report, Fiscal Year 1979", NUREG/CR-1128, NRL Memorandum Report 4122, Dec. 31, 1979.

6. J. W. Hutchinson, P. C. Paris, "The Theory of Stability Analysis of J-Controlled Crack Growth", ASTM STP 668, (1979), pp. 37-64.

7. F. J. Loss, B. H. Menke, R. A. Gray, Jr., H. E. Watson, "J-R Curve Characterization of A533-B Weld Metal with Irradiated and Postirradiated Annealing", ASTM STP 725, (1981), pp. 77-91.

8. J. R. Hawthorne, et. al. "The NRL-EPRI Research Program (RP886-2), Evaluation and Prediction of Neutron Embrittlement in Reactor Pressure Vessel Materials," Electric Power Research Institute (in press).

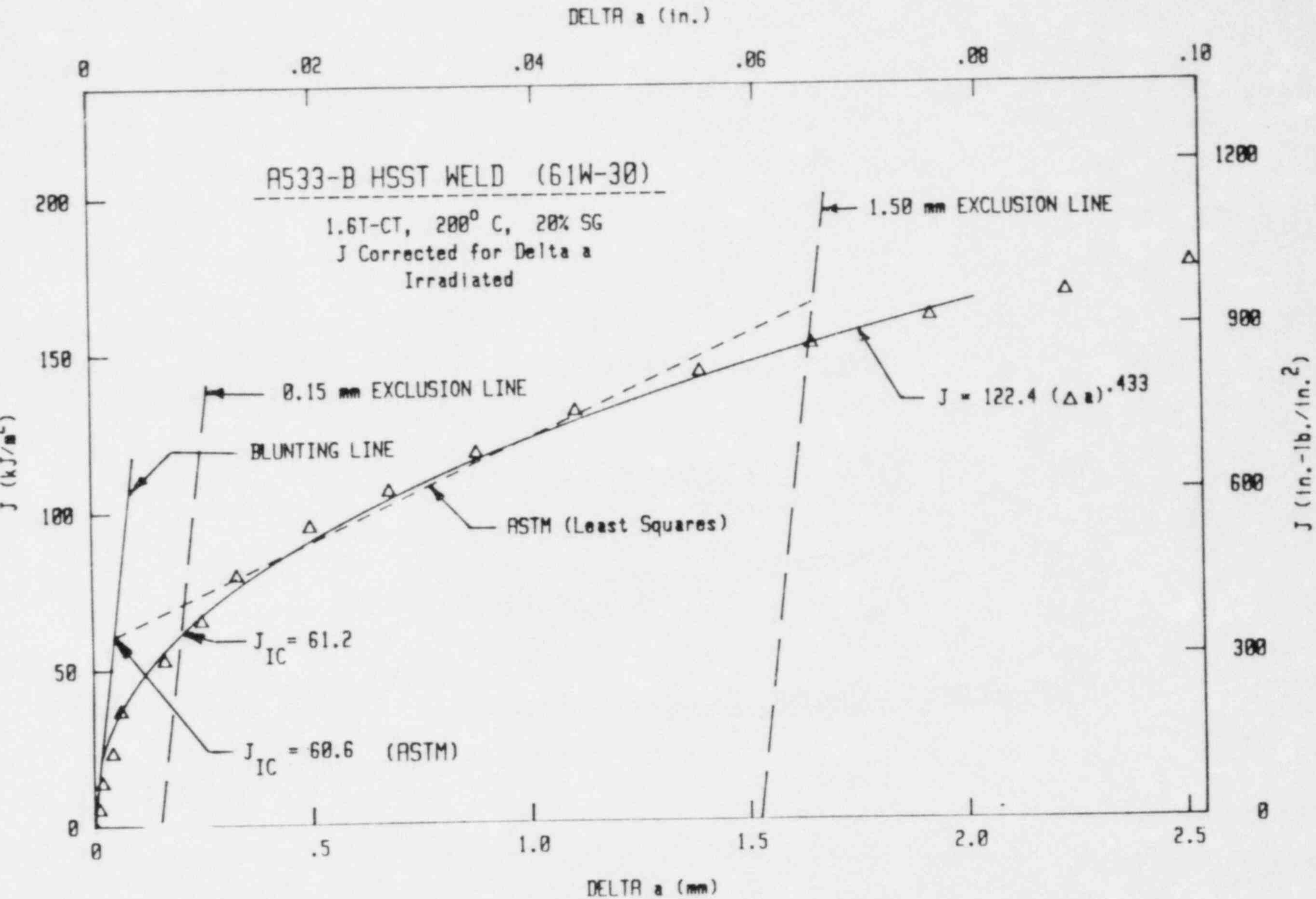

Fig. 1 - Expanded R curve illustrating the power-law behavior exhibited at small crack extension. With the MEA procedure, J_{Ic} is taken as that value where the R curve intersects the 0.15 mm exclusion line. Conversely, J_{Ic} is defined by ASTM Standard E813 as the intersection of the least squares fit of the data (between exclusion lines) with the blunting line.

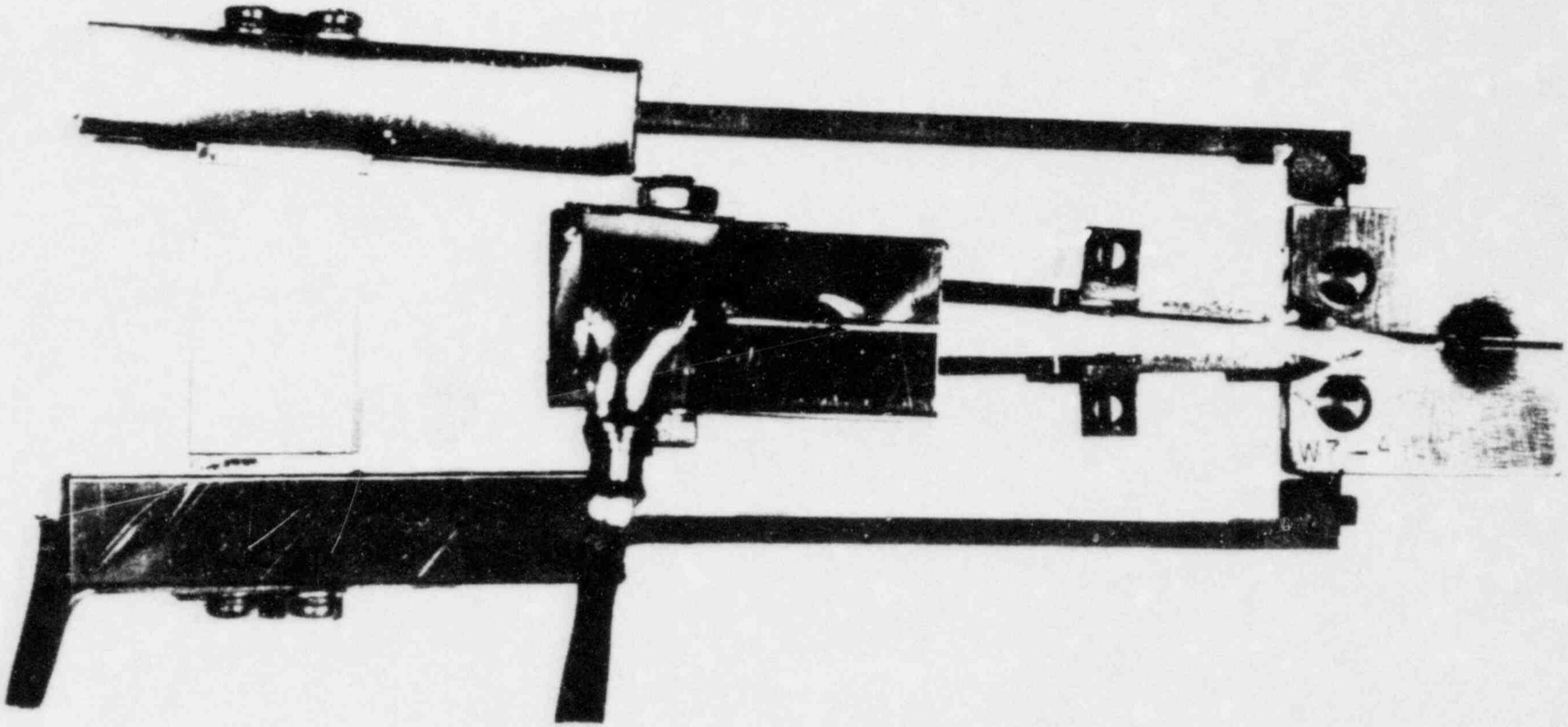

Fig. 2 - Double clip gage arrangement for testing 0.5T- and 0.8T-CT specimens by the SSC technique. The outer (load line) and inner (front face) gages are used to measure load-line deflection and specimen compliance changes, respectively.

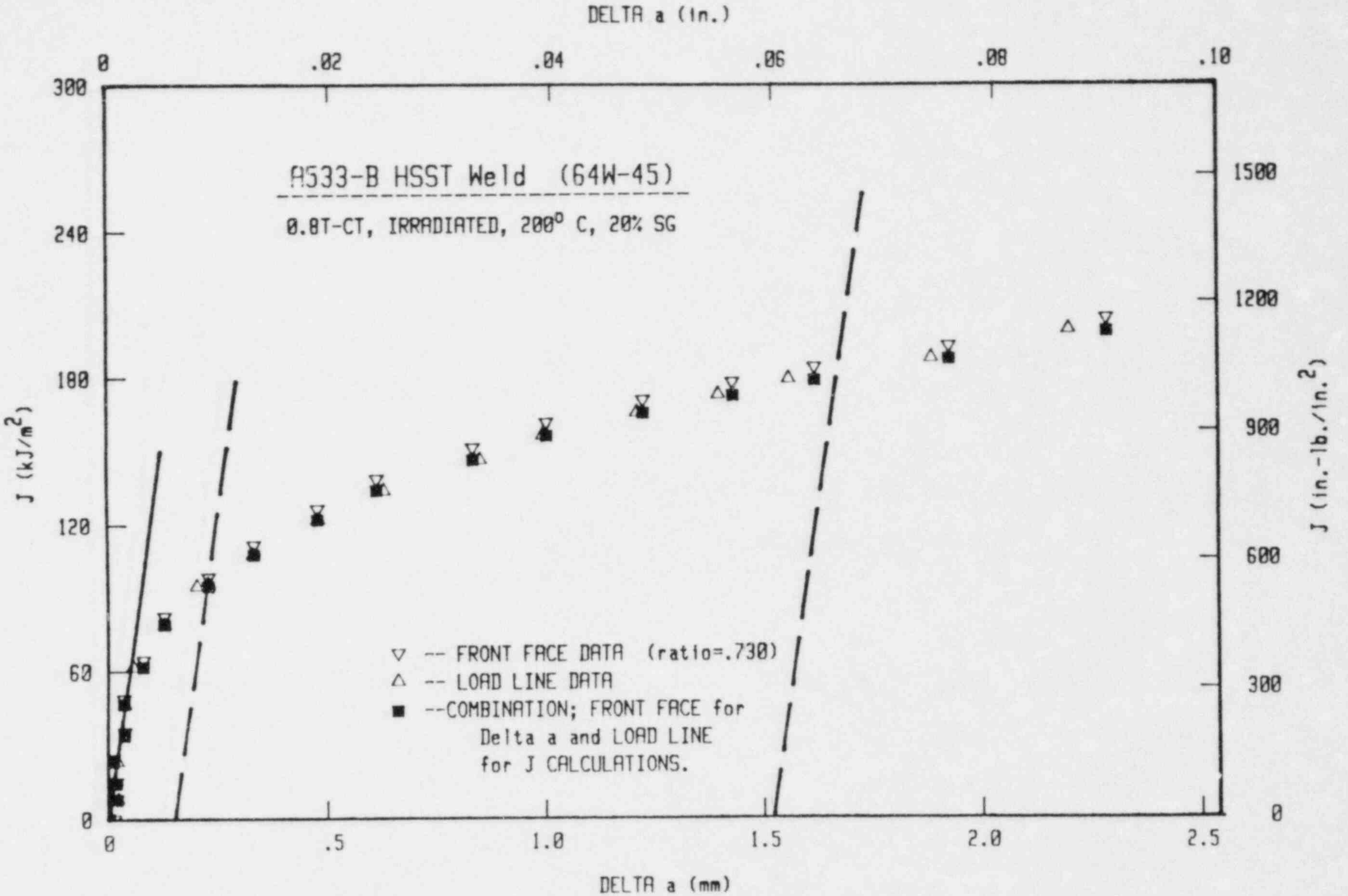

Fig. 3 - R curve developed with the double clip gage technique (Fig. 2) compared with R curves developed independently from each of the two gages. A ratio of 0.73 was used to convert front face deflection to load-line deflection.

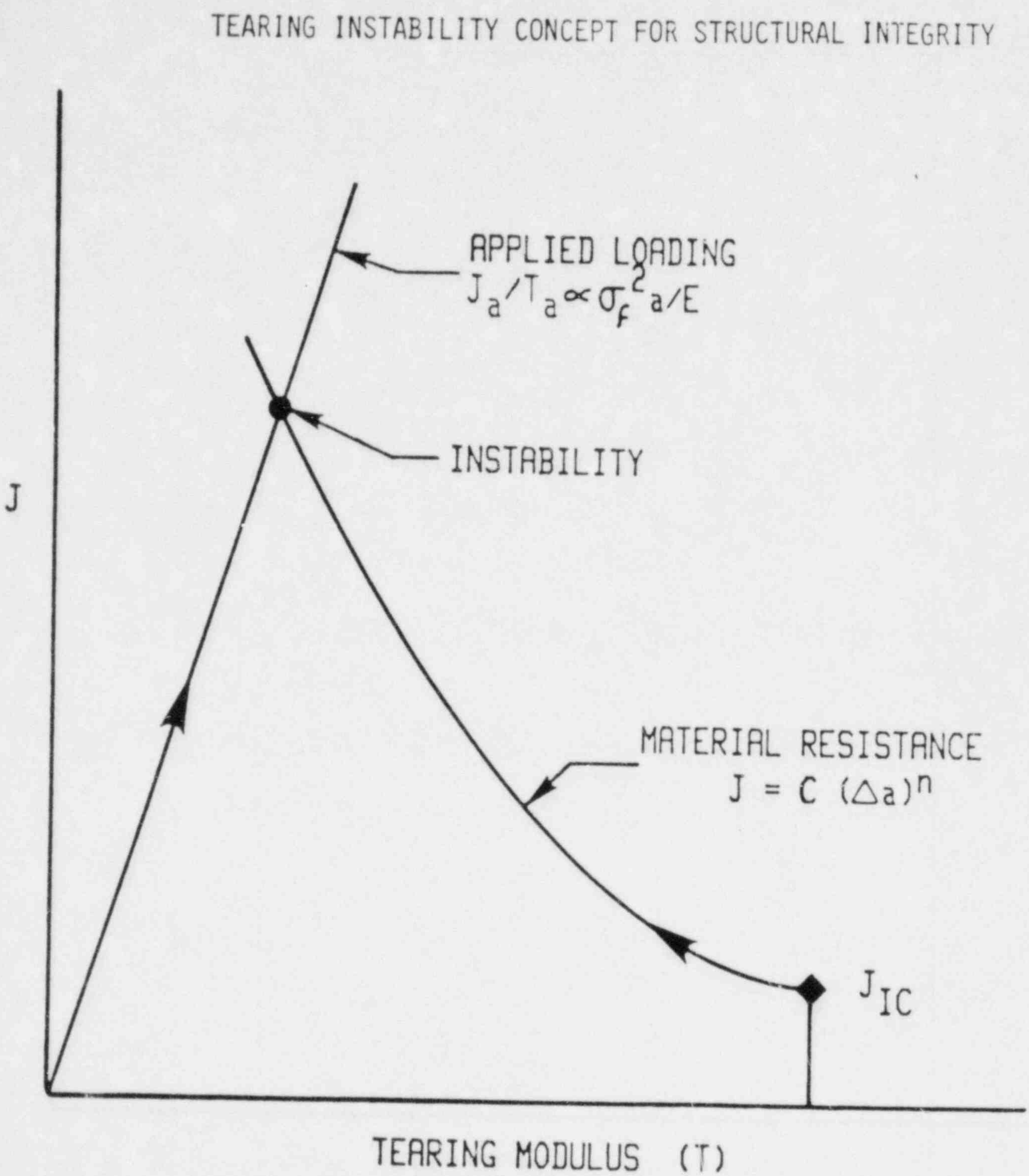

Fig. 4 Instability diagram illustrating the interaction of material and structural parameters.

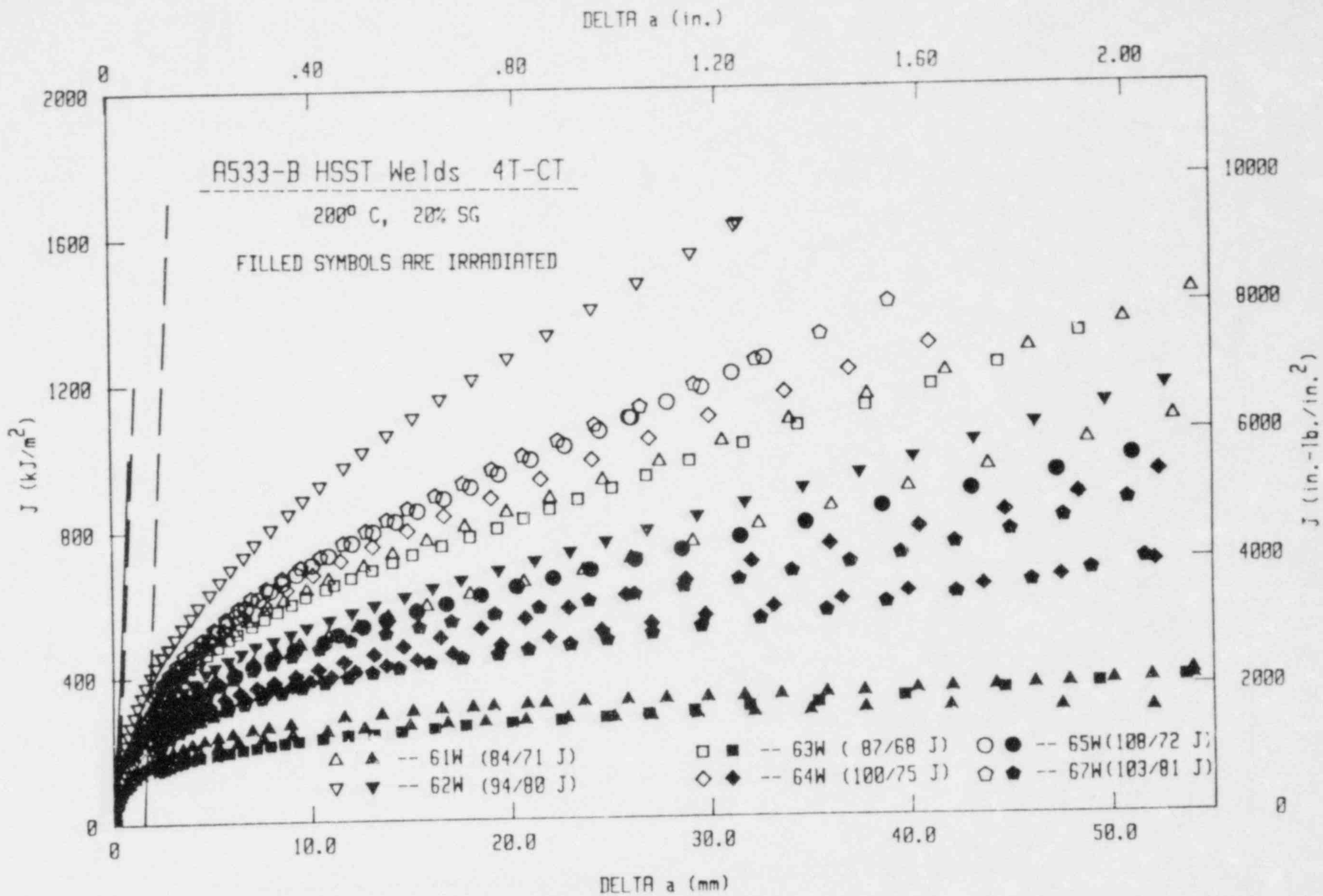

Fig. 5 - Pre- and postirradiation R curve trends measured with 4T-CT specimens. Average values of Charpy-V upper shelf energy levels in the unirradiated/irradiated conditions are indicated adjacent to the material heat codes (61W-67W).

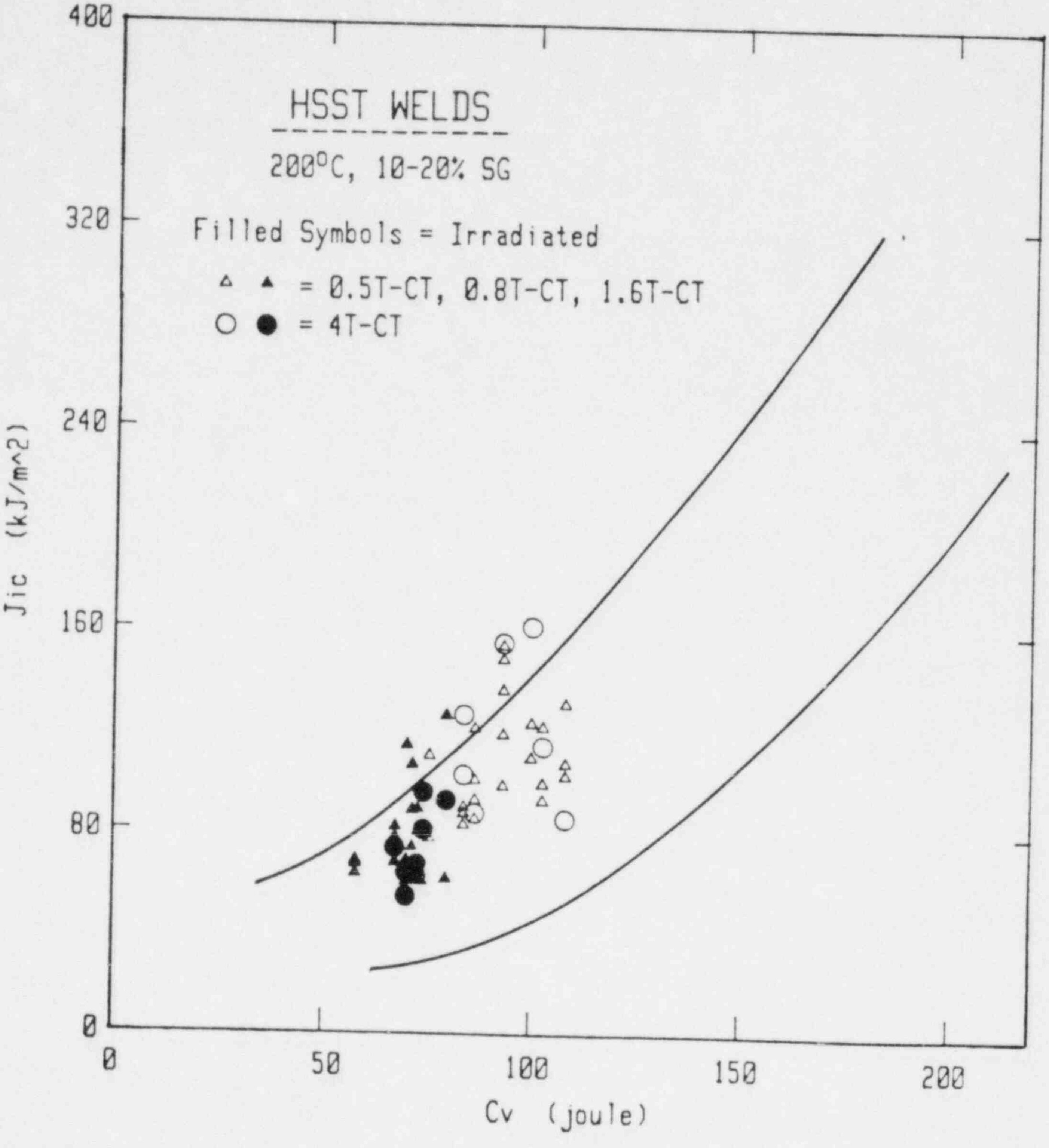

Fig. 6 - Trend of J_{Ic} vs C_v upper shelf energy for the HSST welds. The band was taken from a previous correlation of these two quantities [5,8].

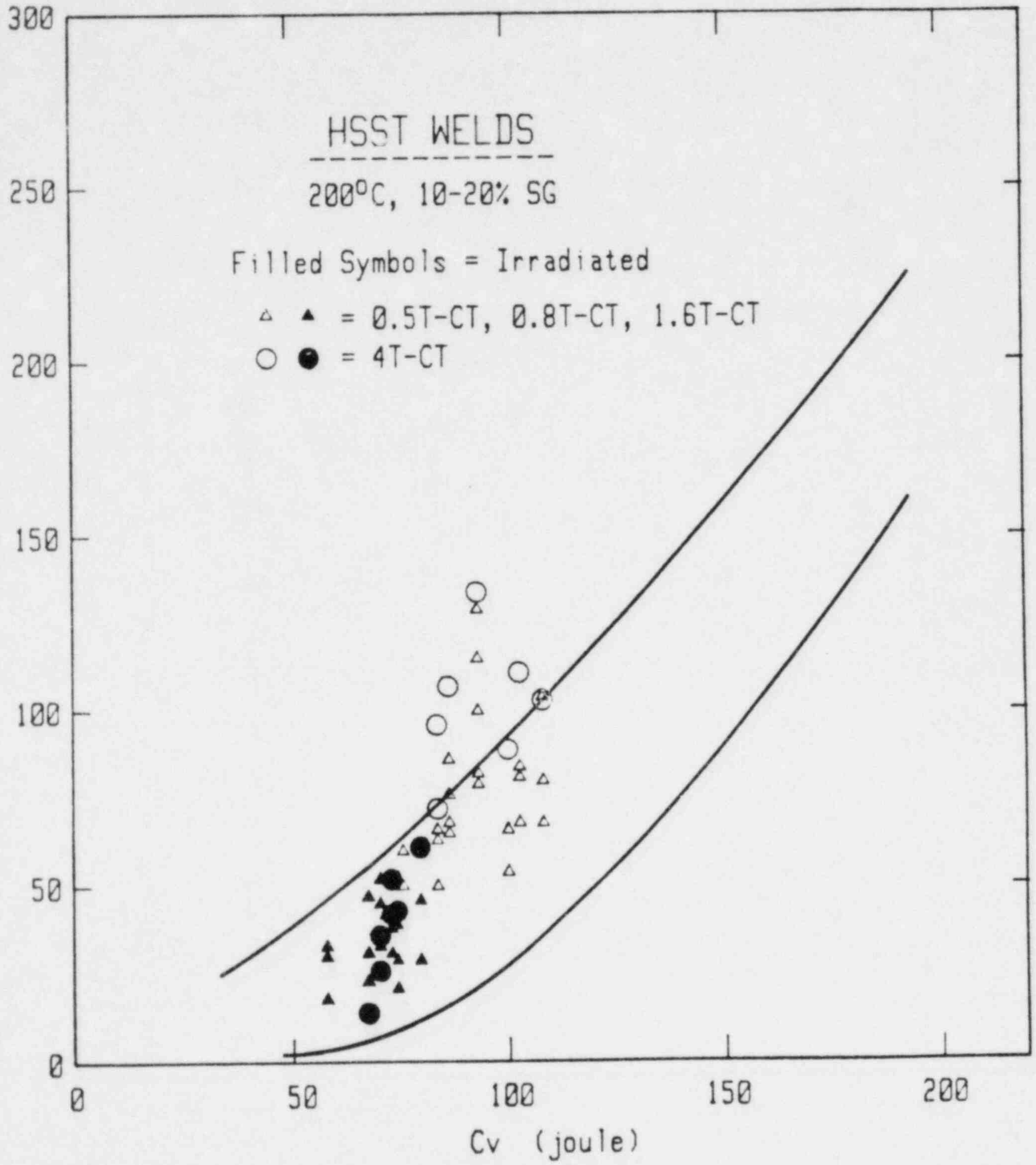

Fig. 7 - Trend of T_{avg} vs C_v upper shelf energy for the HSST welds. The band was taken from a previous correlation of these two quantities [5,8].

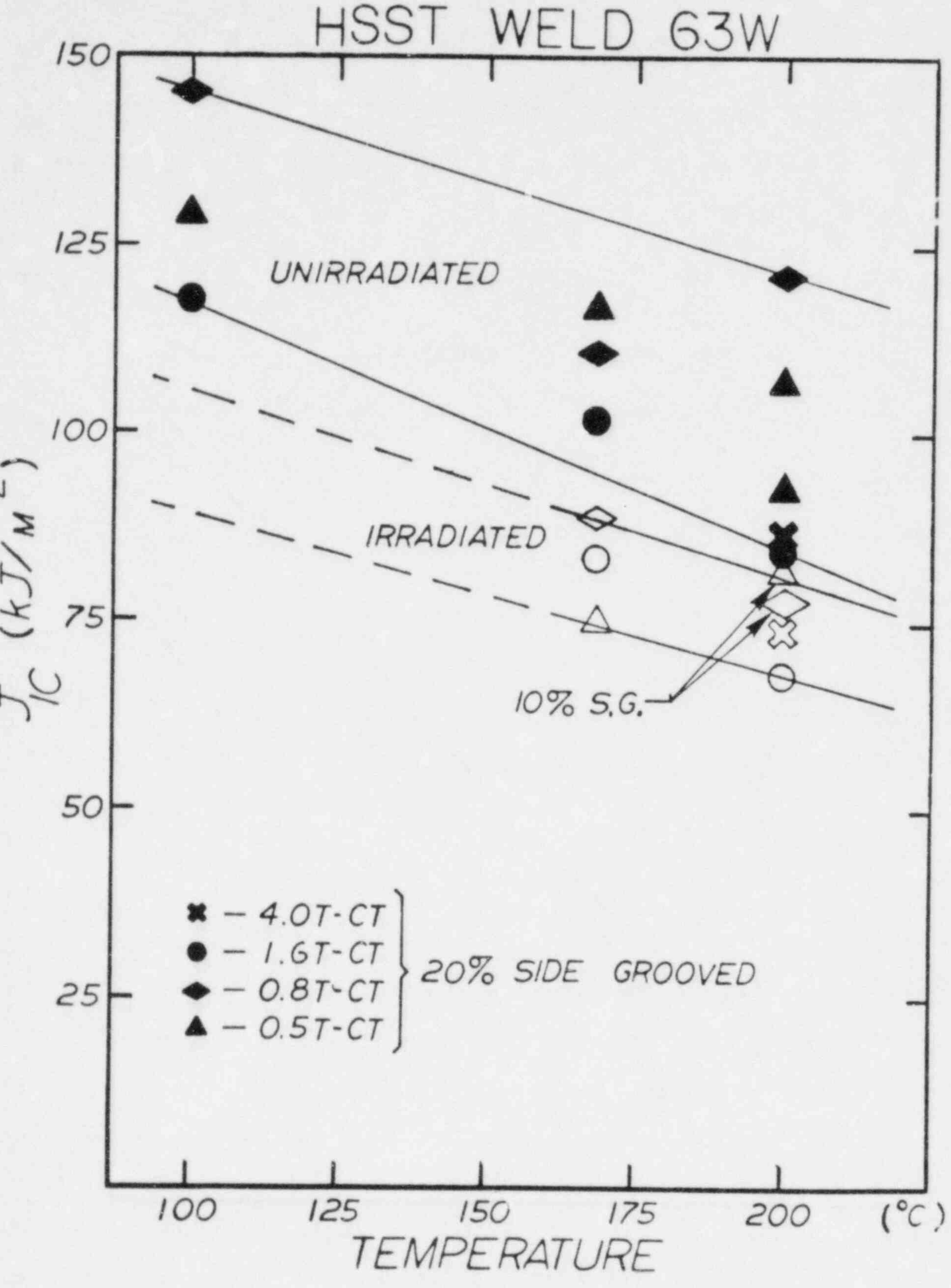

Fig. 8 - Variation of J_{Ic} with temperature

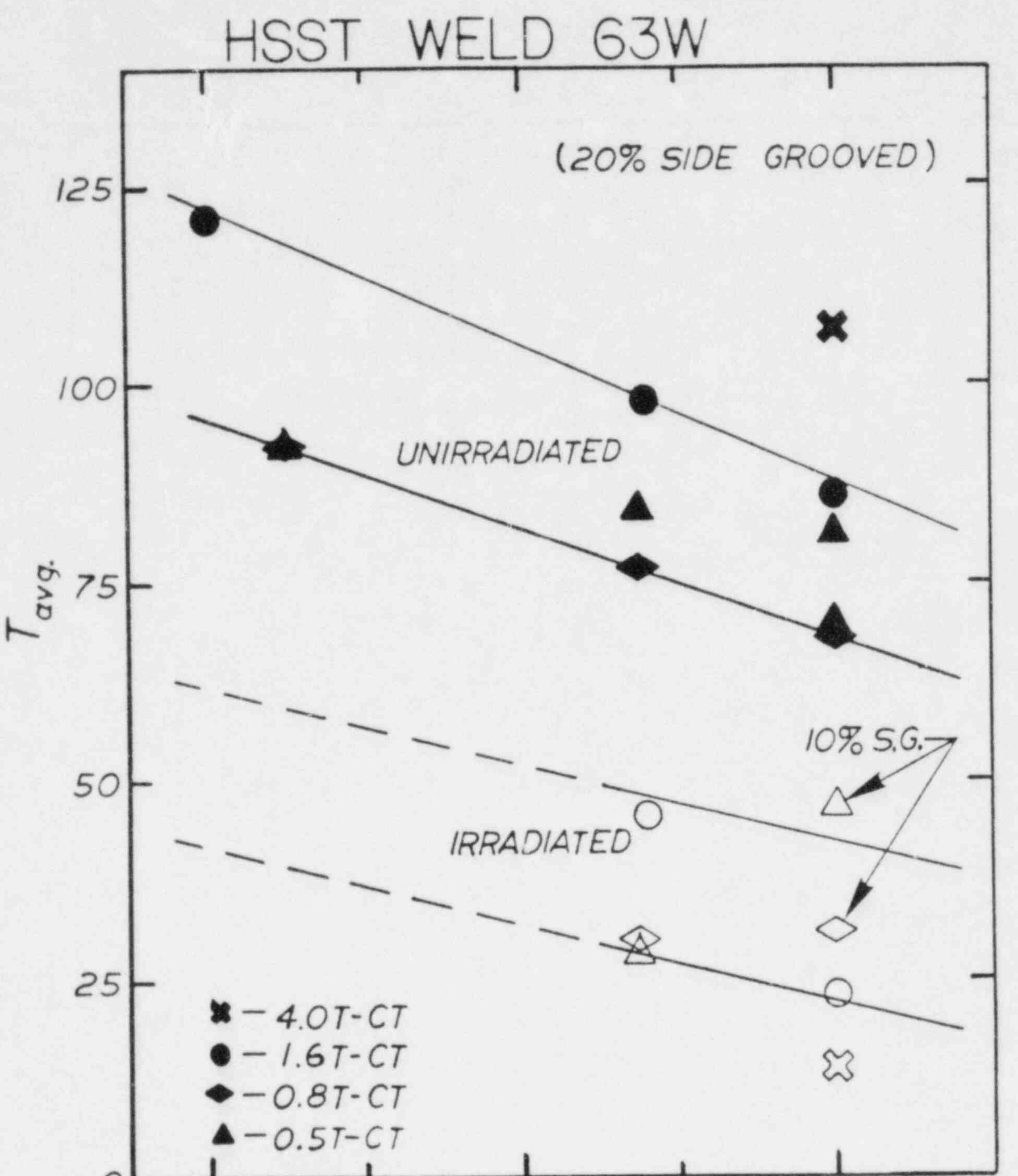

Fig. 9 - Variation of T_{avg} with temperature

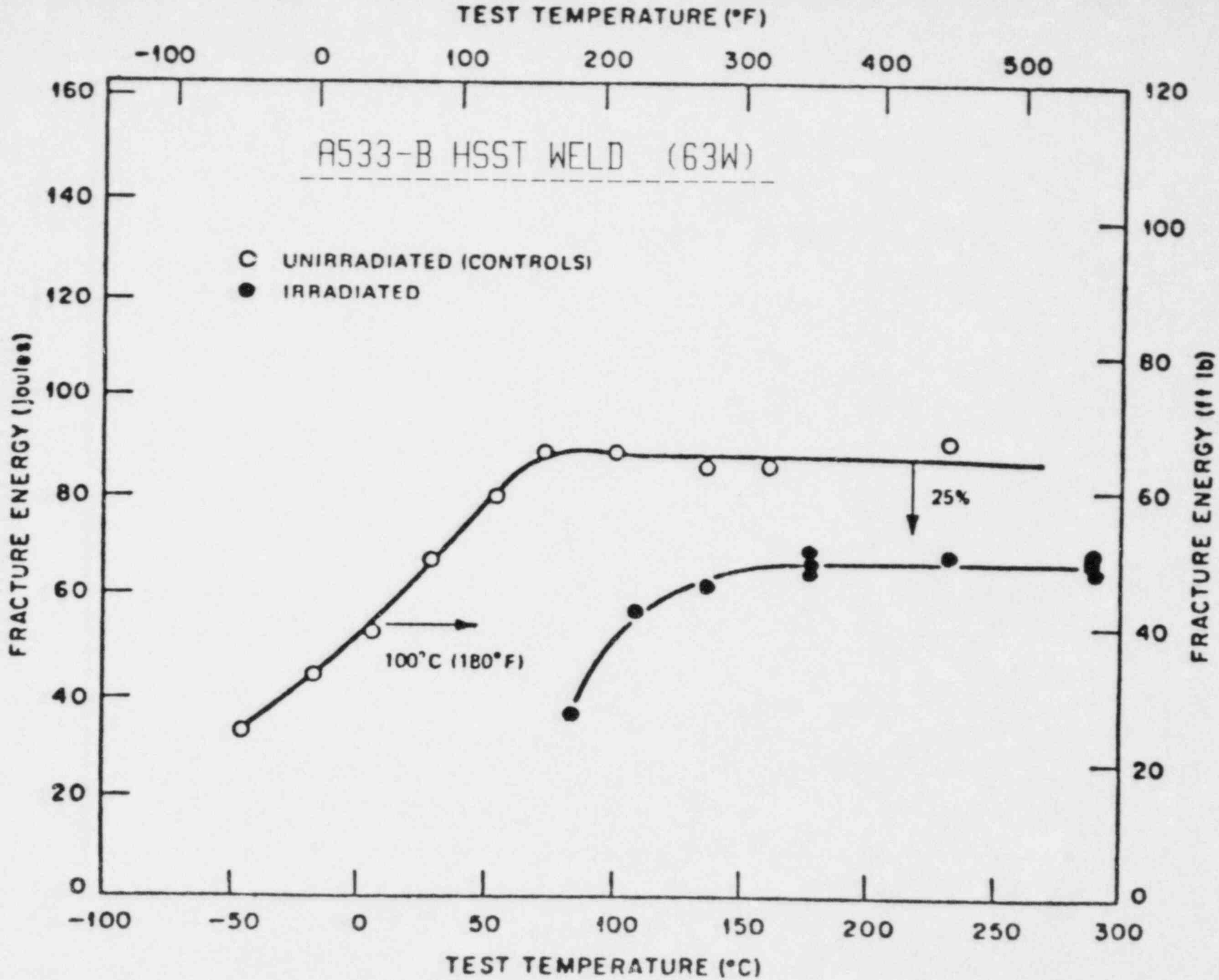

Fig. 10 - Charpy-V trend illustrating an invariance with temperature in the upper shelf regime (ORNL data).

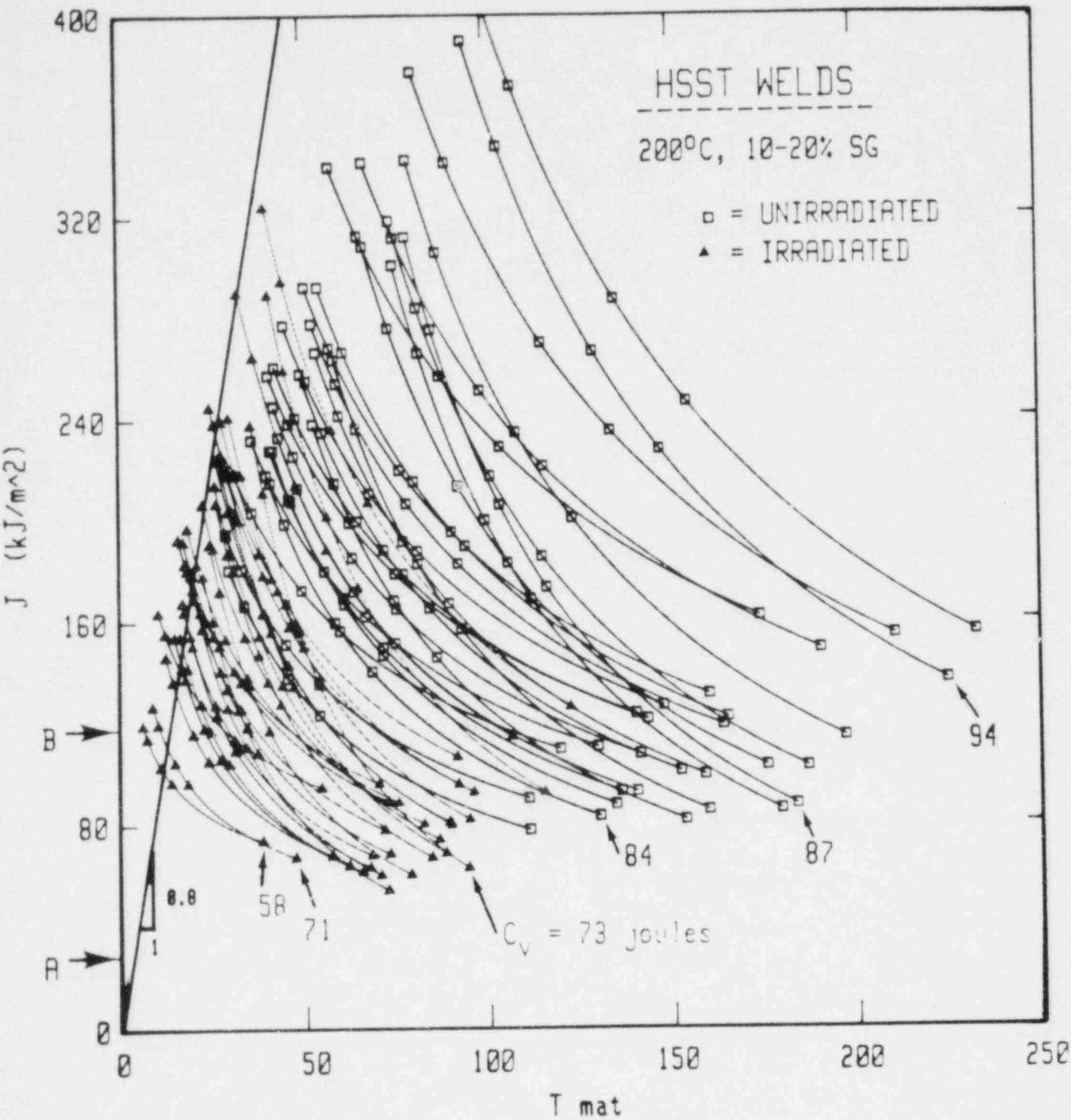

Fig. 11 - R curve trends for HSST welds. The arrows (A and B) denote approximate applied J levels in a cylindrical reactor vessel having a 1/4T axial flaw and loaded to design pressure and to twice design pressure, respectively.

HEDL-SA-2791

VERIFICATION OF EFFECTS OF FUEL MANAGEMENT SCHEMES ON THE CONDITION OF PRESSURE VESSELS AND THEIR SUPPORT STRUCTURES

W. N. McElroy, R. Gold, L. S. Kellogg, E. P. Lippincott,
W. Y. Matsumoto, F. H. Ruddy, R. L. Simons and J. A. Ulseth
(Hanford Engineering Development Laboratory)
J. A. Grundl and E. D. McGarry (National Bureau of Standards)
F. B. K. Kam (Oak Ridge National Laboratory)
A. Fabry and H. Tourwé (Centre de l'Etude de l'Energie Nucleaire)
M. Austin and A. Thomas (Rolls-Royce & Associates, Limited)
A. J. Fudge (Atomic Energy Research Establishment, Harwell)
H. Farrar IV and B. M. Oliver (Rockwell International)
S. L. Anderson (Westinghouse Electric Corporation)
A. L. Lowe Jr., R. H. Lewis and C. L. Whitmarsh (Babcock & Wilcox Company)
S. Grant (Carolina Power & Light Company)
H. F. Jones (Maine Yankee Atomic Power Company)

1. INTRODUCTION

A number of potential methods exist for assuring the adequacy of fracture control of reactor pressure vessel (PV) beltlines under normal and accident loads.[1-9] One of these methods, involving the use of fuel management schemes for reducing the rate of neutron damage accumulation at points of high neutron exposure, shows considerable promise.[10-12] Practices for assessing and controlling the condition of PV beltlines and their support structures follow the recommendations in the US Code of Federal Regulations 10CFR50 (App. G and H) and 10CFR21, respectively, as well as those of the ASME Boiler and Pressure Vessel Code, Sec. III and XI.[13-16]

In summary fashion, this paper reviews the methods for fracture behavior assessment and control and the interfaces with physics-dosimetry-metallurgy. It then reviews the calculated effects of new fuel management schemes on derived exposure parameter values for a representative PWR power plant. This is followed by a review of recent results of LWR Pressure Vessel Surveillance Dosimetry Improvement Program (LWR-PV-SDIP) interlaboratory efforts. This work is directed towards the verification of the effects of old and new fuel management schemes using new physics-dosimetry-metallurgy methods, procedures and data being developed and recommended in a new set of ASTM Standards.[17] Also provided is an updated set of references[18-59] to the literature that is most relevant to the LWR-PV-SDIP work through September 1982.

2. ASTM STANDARDS AND FRACTURE BEHAVIOR ASSESSMENT AND CONTROL

The interrelationships, preparation, validation and calibration schedule for the ASTM standards are shown in Figures 1 and 2 and they all should be in place for routine use by the nuclear industry by the end of fiscal year 1984. Tables 1 and 2 summarize: 1) the licensing and regulatory requirements; and 2) the procedures for the analysis and interpretation of nuclear reactor surveillance results for the assessment and control of the fracture toughness of reactor pressure vessels and their support structures. The information contained in these two tables is rather detailed and does not require further discussion here.[18,39] It is sufficient to note that the appropriate interfaces between licensing and regulatory requirements and physics-dosimetry-metallurgy and fracture analysis are being established for the ASTM standards and on an international basis.[31] With this in mind, we turn our attention to fuel management effects on neutron exposure parameters.

3. FUEL MANAGEMENT EFFECTS ON EXPOSURE PARAMETERS

The benefits of low neutron leakage fuel management schemes have been studied rather extensively by the nuclear industry. At the request of NRC, HEDL has performed such a study to determine the benefits of replacing selected outer row fuel with stainless steel assemblies for reducing pressure vessel wall neutron exposures at points of high accumulated neutron damage.[10,11] Further, the NRC staff has conducted a survey of eight licensees, vendors and several foreign reactors for methods of lowering neutron exposures to pressure vessels.[12] They find that two methods in current use are 1) low neutron leakage core loading and 2) fuel assembly substitution. Based on the survey, reduction of neutron exposure of up to a factor of $\sim$5 appears feasible for Method (1) and up to a factor of $\sim$10 or more for Method (2).

As stated above the Method (2) technique of fuel assembly substitution has been investigated by HEDL. Calculations were run for six types (A through F) of commercial generic PWRs. The reactor types were chosen primarily on the basis of the immediate availability of required information. For the purposes of this review, it will suffice to illustrate results with just the Type A PWR. The information presented is taken directly from Ref. 10.

Particular core fuel assemblies were identified as the heaviest contributors to the flux at the point on the vessel wall with the highest damage accumulation rate. A 2-D transport calculation was used to determine the benefit to be gained by replacing a few fuel assemblies by stainless steel (SS) dummies, with appropriate water fractions to account for the coolant. The core power distribution in the remaining fuel assemblies was assumed to be unchanged except for a renormalization factor that maintained the same total power output.

For the Type A PWR reactor with both accelerated and wall surveillance capsules, reactor physics calculations were made for 3 conditions: (a) full fuel, capsules in, (b) modified fuel, capsules in, and (c) full fuel, capsules out. The R and theta meshes were the same for the three cases. The core map in (x,y) geometry is shown in Figure 3. The calculations used as-built dimensions for a particular reactor installation. Figure 4 shows the Type A reactor in an (R,θ) map, which indicates the mesh detail in the DOT calculation. A comparison of Figures 3 and 4 shows that two outer fuel assemblies (a and b) in the region near $(0° < \theta < 10°)$ were replaced by SS dummies with appropriate water fractions in the modified-fuel DOT calculation. For the case of surveillance capsules out, all three capsules were removed and a normal fuel load was assumed.

Figure 5 compares the dpa[17,30] damage exposure dose on the front face of the pressure vessel after 32 years of full-power operation for two cases: (a) a full fuel load is assumed and (b) two fuel assemblies were replaced by SS dummies with power distribution renormalized to return to full power. The reduction in dpa damage exposure rate at the $\theta = 0°$ position is 13.6/1.0, but the peak damage accumulation is shifted to the 29° angular position. The ratio of normal to modified fuel in maximum-damage rate is 1.58/1.0.

Using dpa is an attempt to express radiation damage in a unit that can be applied to a wide variety of neutron spectra. Fluence greater than some selected energy level (e.g., $E > 1.0$ MeV) does not correctly account for lower energy neutrons and differences in spectral shapes in general. The significance of this consideration to the neutron exposure of pressure vessels throughout their thickness is indicated in Figure 6. In this figure we have taken a radial sweep from the core out through a surveillance capsule at the $\theta = 35°$ angular position. We have calculated dpa/ϕt ($E > 1.05$ MeV), normalized to unity at the capsule center. As can be seen from Figure 6, the dpa/ϕt ratio at the 1/4 T position is similar to the ratio at the surveillance capsule position; but the dpa/ϕt ratio varies by a factor of 2.23 going from the PV front to the rear. Therefore, if ϕt ($E > 1.0$ MeV) information is used with surveillance capsule mechanical properties data to develop in-vessel material property change trend curves, the conclusions drawn from such information will be nonconservative. Also exposures will be nonconservative by a factor of two if the trend curve is used with ϕt ($E > 1.0$ MeV) exposure information for positions near the PV rear wall. More information on this subject is provided in Table 3 of Ref. 17 for PWR, BWR and Test Reactor neutron fields.

For the Type A Reactor accelerated and wall surveillance capsules, each capsule was modeled as a 15 region rectangle (3 theta regions x 5 radial regions). The center lines of the capsules are located at 3°, 35° and 45°. The capsule perturbation effect can be seen in Figures 7 and 8, in which radial traverse values of dpa are plotted at the 3° and 35° angular positions; capsule in is compared with capsule out for the 32-year full-power dpa exposure. The capsule's presence causes an increase in neutron exposure, measured either in dpa or in fluence (E > 1.0 MeV) units. At the capsule center, its presence causes an increase of about 24% in the dpa exposure value or an increase of about 23% for the fluence (E > 1.05 MeV) for the wall capsule located at an angular position of 3°. For the accelerated capsule located on the core side of the thermal shield, the similar increases are about 27% for the dpa exposure and about 24% for the fluence (E > 1.05 MeV). These types of calculated perturbation effects have been verified for the Westinghouse and Combustion Engineering perturbation and the first ORR-SDMF RM sensor certification test (Figures 20 and 21). For this type of power plant and surveillance capsule configuration, transport code solutions obtained without explicit capsule modeling will require corrections of the magnitude indicated above, when the transport solution is used directly to provide a "lead factor."

From the information provided in Figures 1 through 8 and in Table 1, the significance to the nuclear industry of the determination and verification of the effects of using old and new fuel management schemes and different exposure parameters on the assessment and control of the condition of PV and support structure steels is readily apparent. That is, timely reduction of vessel wall exposure by fuel management methods (low leakage cores) provides a practical and perhaps relatively inexpensive approach to reducing or eliminating the risk of fracture associated with pressurized thermal shock. It should be noted that low leakage core designs were initially proposed for economic reasons (increased fuel burnup), and their effect on ex-core component neutron exposure has since been recognized. The following section deals with the results and status of work on verifying the effects of using different fuel management schemes and exposure parameters by application of the new physics-dosimetry-metallurgy methods, procedures and data being developed and recommended in the set of 21 ASTM LWR standards (Figures 1 and 2).

4. LWR-PV-SDIP VERIFICATION STUDIES FOR OLD AND NEW FUEL MANAGEMENT SCHEMES

Figure 9 shows the interrelationship of the new ASTM standard methods for the application and analysis of radiometric (RM), solid state track recorder (SSTR), helium accumulation fluence monitor (HAFM), and damage monitors (DM) to the determination and verification of neutron exposure parameter values. Using these new ASTM recommended procedures and data, the results of LWR-PV-SDIP verification studies are summarized by the information presented in Figures 10 and 11 and Table 3 for the period up to September 1982.

New H. B. Robinson, Maine Yankee and Crystal River (or Davis Besse) benchmark tests have been designed to provide direct experimental verification of the accuracy of reactor physics-dosimetry predictions for new low leakage core fuel management schemes. Table 4 lists the power reactors being used by LWR-PV-SDIP participants to benchmark physics-dosimetry procedures and data for pressure vessel and support structure surveillance for both old and new fuel management schemes.

The planning (P), selection [Y for yes, N for not desired or cannot be used, and any of the forenamed letters (P, Y, N) within parantheses suggest some doubt], and fabrication of RM, SSTR, HAFM, and DM sensor sets for H. B. Robinson and Maine Yankee are completed. The placement of the sensor sets for H. B. Robinson has been completed and the one (or more) cycle, low leakage core, irradiation has started. Figures 12 thorugh 15 show photographs of as-built dosimetry and the locations for placement in the in-vessel physics-dosimetry surveillance capsule and the reactor cavity. This placement was completed in June 1982.

For Maine Yankee, the placement and start of irradiations has yet to be accomplished. Figures 16 through 19 show photographs of the as-built dosimetry for a replacement physics-dosimetry-metallurgy surveillance capsule and the reactor cavity. The new surveillance capsule, which is planned for irradiation in a previously removed surveillance capsule wall location, will be held in reserve for future use, pending the establishment of an equilibrium low leakage core burnup distribution. The one or more cycle irradiation for the cavity RM, SSTR, HAFM and DM sensor sets is expected to start in November or December 1982.

Planning for the Crystal River (or David Besse) benchmark studies has been init ted and actual selection, fabrication, and placement of sensors and metallurgical specimens could be accomplished in early 1983.

In support of these old and new type fuel management verification studies are a series of planned benchmark studies in the Mol Belgium VENUS and United Kingdom NESDIP benchmark fields.[18,29] Related to these benchmark studies, two considerations will be briefly discussed: core management benchmarking pl ns and lead factor assessment.

The lead factor between surveillance capsule and vessel wall is a complex parameter to determine at the required goal accuracy of 10 to 20% (1σ). If combined with a surveillance capsule accuracy of, say, 15%, this translates to a corresponding PV weld fluence accuracy of 18 to 25% (1σ). It can be conceptually separated into four parts or factors:

$$\text{Radial}\cdot\text{Azimuthal}\cdot\text{Vertical}\cdot\text{Perturbation}\cdot\begin{bmatrix}\text{Exposure value with uncertainty}\\ \text{for each surveillance capsule}\end{bmatrix}$$

In this regard, neutronic exposures are needed for all the "limiting" weld or other materials; the "beltline region of the reactor vessel" is defined as encompassing indeed any weld or materials for which the predicted adjustment of reference temperature at the end of its service life exceeds 50°F.[13]

The vertical correction is derived from dosimetry traverses within the surveillance capsule or from 2D(R,Z) transport theory when the limiting material is significantly outside the vertical range of the dosimeters. It is noted that uncertainties of ~10% or less may arise within the vertical range of the active fuel. This problem becomes more difficult for support structures and is particularly important in the case of water shield tanks

(Maine Yankee, Connecticut Yankee, Surry, BR3) for which the NDT temperature may be elevated by irradiation to equal or even exceed the service temperature.[57] This will be addressed as part of the NESDIP Program.[29]

Benchmarking the neutron field perturbation by the surveillance capsule and RM sensor counting laboratory certification tests is an important part of the ORR-SDMF program. As shown in Figures 20 and 21, significant results have already been obtained for Westinghouse and Combustion Engineering type capsules; and the ORR-SDMF irradiation is complete for Babcock and Wilcox type capsules (Figure 22). Results of recent service laboratory RM sensor counting certification tests for four reactor vendors and two other service laboratories in the U.S. and four laboratories in Europe are presented in Tables 5, 6, and 7. HEDL and CEN/SCK served as the reference counting laboratories for these tests, respectively. RM sensor counting results in the 5 to 10% (1σ) range must be obtained routinely to achieve derived exposure parameter values (fluence E > 1.0 MeV, dpa, etc.) in the 10 to 20% (1σ) range desired for fracture analysis studies.

The radial in-vessel projection, exclusive of surveillance capsule perturbation effects, has been addressed by the PCA blind test[23] and is reasonably well understood. Three main areas of discrepancies or inconsistencies remain:

1. Integral C/E ratios at deep penetration and high neutron energy indicate that calculations underpredict the flux; this is traced to iron cross-section inadequacies in current nuclear data files.[23,58]

2. Differences between fission chamber and SSTR[23] measurement results have been observed; further benchmark-field referencing work is expected to largely resolve this problem.

3. Neutron spectrometry versus integral measurement and calculation studies are in progress: Comparison of current transport theory with the envelope (Figure 23) of all $^6Li(n,\alpha)$ energy-dependent flux spectrum attenuations as function of steel penetration (PCA 8/7 and 12/13,

1/4 T versus 1/2 T, and 1/2 T versus 3/4 T ratios) displays overall trends compatible with the ones under Figure 24, but inconsistencies are claimed at the level of more detailed confrontations.[23]

Figure 24 was also prepared to illustrate the transferability of neutronic benchmark observations to power reactor environments. From an applied RPV engineering viewpoint, the primary program goals have been reached; R&D improvement of the current PCA blind test results is not considered a high priority, but should be useful for: (a) the analysis of pressurized thermal shock insofar as more accurate dpa steel traverses would ensue (the critical crack arrest depth after initiation of shallow flaws is relatively sensitive to these traverses, but a host of other uncertainties may be more critical at present); and (b) the interpretation of ex-vessel physics-dosimetry, both in the context of a better understanding of lead factor uncertainties and in assessing support structure embrittlement.[57]

The benchmarking of azimuthal neutron flux spectrum gradient predictions for in-vessel locations is addressed in the VENUS zero-power engineering mockup of a PWR core-baffle-barrel-thermal shield configuration.[18] These predictions depend on:

1. Correct and detailed estimates of core fission source distributions in the last core fuel rows relative to the plant power output.

2. Correct modeling of core boundary heterogeneity effects.

The first aspect is a particularly important focus for investigation because usual core management considerations do not call for an accuracy as great as needed for in-vessel RPV surveillance projections. Current lead factor uncertainties are, therefore, likely to be dominated by core fission source uncertainties and are likely to be the most significant in plants displaying large azimuthal effects (Westinghouse, Combustion Engineering); these effects are not (or are less) sensitive to fuel burnup,[59] which enhances the value of results from a zero-power benchmark. On another hand, in-vessel azimuthal gradients are attenuated by scattering within the vessel and distorted by the cavity. This may be related to vessel exposure [fluence ($E > 1.0$ MeV) and dpa] when sufficient data and techniques are available from benchmark and in-reactor tests. The VENUS and NESDIP programs are expected to provide verification for in-vessel azimuthal gradient calculations and a better understanding and verification of in- and ex-vessel neutron and gamma field predictive methods. Thus, the VENUS and NESDIP programs will contribute to the development and verification of a fracture analysis predictive methodology for RPV application and ex-vessel dosimetry, which otherwise could never become quantitative and comprehensive. Two other essential aspects of the VENUS effort, as already discussed in Ref. 18, are the investigation of pressurized thermal shock mitigation by core management techniques and the investigation of PWR gamma heating.

Further discussion of the VENUS and NESDIP programs is provided in papers being presented at this 10th NRC Water Reactor Research Information meeting. It is useful to mention that the experimental and analytical program is interlaboratory and open to more participants than the ones already engaged in the U.S., Belgium and the United Kingdom. In this regard, the active participation of reactor vendors, architect/engineers, and utilities is deemed essential.

5. CONCLUSIONS

Fuel management schemes provide practical and perhaps relatively inexpensive ways of reducing the risk of PV fracture associated with pressurized thermal shock. Assessment and control of the conditions of LWR pressure vessels and support structures are related problems. The regulatory demand(7) is for assurance (verification)

1) that errors in neutron exposure values (fluence $E > 1.0$ MeV) of a factor of two are a thing of the past; i.e., that there are no more technical surprises, for instance, due to a lack of knowledge of the effects of old and new fuel management schemes,

2) that an improved neutron exposure parameter (such as dpa) be used to account for neutron spectral effects,

3) that gamma heating be better understood to account for steel metallurgy time-temperature effects, and

4) that all of the physics-dosimetry-metallurgy information correlates properly with the embrittlement of the reactor vessel and support structure materials.

To meet the above challenge, a new series of ASTM standards is being developed, tested, verified, and applied for LWR pressure vessel and support structure surveillance. It is expected that all of these standards will be in place by late 1984, with appropriate revisions thereafter. Routine and careful application of these recommended ASTM physics-dosimetry-metallurgy methods, procedures and data will allow verification at the required accuracy level (10 to 30%, 1σ) of the effects of old and new fuel management schemes on the estimated current and end-of-life condition of pressure vessel and support structure steels.

ACKNOWLEDGMENTS

The success of the LWR PV Surveillance Dosimetry Improvement Program (LWR-PV-SDIP) continues to depend on the efforts and the free exchange of ideas and views by representatives of a large number of research, service, regulatory, vendor, architect/engineer and utility organizations. The information reported herein could not have been developed without the continuing support of the respective funding organizations and their management and technical staffs. Special acknowledgment is due to C. Z. Serpan of NRC for having identified the need for such an international program as the LWR-PV-SDIP and for making it possible by taking a strong overall support and management lead position.

Additional acknowledgment is due to D. G. Doran and W. F. Sheely of HEDL for their technical reviews and constructive comments related to the subject material and preparation of this paper. The contributions of G. L. Guthrie, B. J. Kaiser, J. P. McNeece, C. C. Preston, J. H. Roberts, J. M. Ruggles and F. A. Schmittroth of HEDL and to G. C. Martin of General Electric, G. P. Cavanaugh, J. D. Varsik and S. T. Byrne of Combustion Engineering, and W. C. Hopkins of Bechtel Power Corporation to this multilaboratory program work are gratefully acknowledged.

Very special acknowledgment is given to J. M. Dahlke, who edited this document, and to the HEDL Publications Services, Word Processing, Graphics, and Duplicating personnel who contributed to its preparation.

REFERENCES

1. ASTM Standard E509-74, "Recommended Guide for In-Service Annealing of Water-Cooled Nuclear Reactor Vessels," 1979 Annual Book of ASTM Standards, ASTM, Philadelphia, PA, 1979.

2. T. U. Marston and T. R. Mager, "EPRI Thermal Anneal Program RP1021-1," Report to ASME Section XI Subcommittee on Repairs and Replacements, and to NRC, February 1982.

3. T. U. Marston and K. E. Stahlkopf, "Radiation Embrittlement: Significance of its Effects on Integrity and Operation of LWR Pressure Vessels," Nuclear Safety 21 (6), p. 724, November-December 1980.

4. U.S. Nuclear Regulatory Commission, Task Action Plan A-11 Report: Resolution of the Reactor Vessel Materials Toughness Safety Issue, NUREG-0744, Nuclear Regulatory Commission, Washington, DC, September 1981.

5. Standard Review Plan and Branch Technical Position MTEB 5.2: Fracture Toughness Requirements, NUREG-75/087, U.S. Nuclear Regulatory Commission, Office of Nuclear Regulation, Washington, DC, 1981.

6. P. N. Randall, "The Status of Trend Curves and Surveillance Results in USNRC Regulatory Activities," Proceedings of an IAEA Specialists' Meeting, Vienna, Austria, October 20, 1981.

7. P. N. Randall, "Status of Regulatory Demands in the U.S. on the Application of Pressure Vessel Dosimetry," Proceedings of the Fourth ASTM-EURATOM Symposium on Reactor Dosimetry, NUREG/CP-0029, p. 1011, July 1982.

8. Regulatory Guide 1.99, Effects of Residual Elements on Predicted Radiation Damage to Reactor Vessel Materials, Rev. 1, U.S. Nuclear Regulatory Commission, Washington DC, April 1977.

9. W. Schneider, Ed., "CAPRICE 79: Correlation Accuracy in Pressure Vessel Steel as Reactor Component Investigation of Change of Material Properties with Exposure Data," Proceedings of the IAEA Technical Committee Meeting, Julich, Federal Republic of Germany, JUL-Conf-37, International Atomic Energy Agency, Vienna, Austria, 1980.

10. G. L. Guthrie, W. N. McElroy and S. L. Anderson, "Investigation of Effects of Reactor Core Loadings on PV Neutron Exposure," NUREG/CR-2345, Vol. 4 and HEDL-TME 81-36, Section E Appendix, September 1982.

11. G. L. Guthrie, W. N. McElroy and S. L. Anderson, "A Preliminary Study of the Use of Fuel Management Techniques for Slowing Pressure Vessel Embrittlement," Proceedings of the Fourth ASTM-EURATOM Symposium on Reactor Dosimetry, NUREG/CP-0029, p. 111, July 1982.

12. NRC Staff, Presentation to Advisory Committee on Reactor Safety, Metal Components Subcommittee, Meeting on Reactor Vessel Integrity (RVI), Washington, DC, May 11-12, 1982.

13. "Domestic Licensing of Production and Utilization Facilities," Code of Federal Regulations, 10CFR50; "General Design Criteria for Nuclear Power Plants," Appendix A; "Fracture Toughness Requirements," Appendix G; "Reactor Vessel Material Surveillance Program Requirements," Appendix H; US Government Printing Office, Washington, DC, Current Edition.

14. "Reporting of Defects and Noncompliance," Code of Federal Regulations, 10CFR21 U.S. Government Printing Office, Washington, DC, Current Edition.

15. "Rules for Inservice Inspection of Nuclear Power Plant Components," ASME Boiler and Pressure Vessel Code, Section XI, ASME, New York, NY, Current Edition.

16. "Nuclear Power Plant Components: General Requirements," Section III, ASME Boiler and Pressure Vessel Code, Division 1 and Appendix G, "Protection Against Nonductile Failure," ASME, New York, NY, Current Edition.

17. ASTM Standard E706-81a, "Master Matrix for LWR Pressure Vessel Surveillance Standards," 1982 Annual Book of ASTM Standards, Part 45, ASTM, Philadelphia, PA, 1982.

18. A. Fabry et al., "Improvement of LWR Pressure Vessel Steel Embrittlement Surveillance: Progress Report on Belgian Activities in Cooperation with the USNRC and other R&D Programs," Proceedings of the Fourth ASTM-EURATOM Symposium on Reactor Dosimetry, NUREG/CP-0029, p. 45, July 1982.

19. Regulatory Guide 1.150, Ultrasonic Testing of Reactor Vessel Welds During Preservice and Inservice Examinations, U.S. Nuclear Regulatory Commission, Washington, DC, June 1981.

20. S. K. Iskander, R. R. Cheverton and D. G. Ball, OCA-I, A Code for Calculation of the Behavior of Flaws on the Inner Surface of a Pressure Vessel Subject to Temperature and Pressure Transients, NUREG/CR-2113, ORNL/NUREG-84, Oak Ridge National Laboratory, Oak Ridge, TN, August 1981.

21. R. C. Kryter et al., Evaluation of Pressurized Thermal Shock, Initial Phase Study, NUREG/CR-2083, ORNL/TM-8072, Oak Ridge National Laboratory, Oak Ridge, TN, 1982.

22. R. D. Cheverton, "A Brief Account of the Effect of Overcooling Accidents on the Integrity of PWR Pressure Vessels," Proceedings of the Fourth ASTM-EURATOM Symposium on Reactor Dosimetry, NUREG/CP-0029, p. 1061, July 1982.

23. W. N. McElroy, Ed., LWR Pressure Vessel Surveillance Dosimetry Improvement Program: PCA Experiments and Blind Test, NUREG/CR-1861, HEDL-TME 80-87, Hanford Engineering Development Laboratory, Richland, WA, July 1981.

24. W. N. McElroy et al., "Surveillance Dosimetry of Operating Power Plants," Proceedings of the Fourth ASTM-EURATOM Symposium on Reactor Dosimetry, NUREG/CP-0029, p. 3, July 1982, also in LWR-PV-SDIP 1981 Annual Report, HEDL-SA-2546, 1982.

25. R. Gold, B. J. Kaiser and J. P. McNeece, "Gamma-Ray Spectrometry in Light Water Reactor Environments," Proceedings of the Fourth ASTM-EURATOM Symposium on Reactor Dosimetry, NUREG/CP-0029, p. 267, July 1982.

26. N. Maene, R. Menit and G. Minsart, "Gamma Dosimetry and Calculations," Proceedings of the Fourth ASTM-EURATOM Symposium on Reactor Dosimetry, NUREG/CP-0029, p. 355, July 1982.

27. J. A. Mason, "Development of Sensitive Microcalorimeters for Absorbed Dose Measurements in Benchmark Radiation Fields," Proceedings of the Fourth ASTM-EURATOM Symposium on Reactor Dosimetry, NUREG/CP-0029, p. 365, July 1982.

28. A. Fabry et al., "The Mol Cavity Fission Spectrum Standard Neutron Field and Its Applications," Proceedings of the Fourth ASTM-EURATOM Symposium on Reactor Dosimetry, NUREG/CP-0029, p. 665, July 1982.

29. M. Austin, "Sense of Direction: An Observation of Trends in Materials Dosimetry in the United Kingdom," Proceedings of the Fourth ASTM-EURATOM Symposium on Reactor Dosimetry, NUREG/CP-0029, p. 461, July 1982.

30. ASTM Standard E693-79, "Recommended Practice for Characterizing Neutron Exposures in Ferritic Steels in Terms of Displacements per Atom (dpa)," Annual Book of ASTM Standards, Part 45, ASTM, Philadelphia, PA, Current Edition.

31. F. B. K. Kam, Ed., Proceedings of the Fourth ASTM-EURATOM Symposium on Reactor Dosimetry, NUREG/CP-0029, Vols. 1 and 2, July 1982.

32. J. A. Grundl et al., NRC-EPRI Studies of Pressure-Vessel-Cavity Neutron Fields, presented at the NRC Ninth Water Reactor Safety Information Meeting, October 26-30, 1981, National Bureau of Standards, Washington, DC, 1981.

33. R. A. Shaw, "Brown's Ferry and Arkansas Nuclear One Pressure Vessel Neutron Fluence Benchmarks," Proceedings of the Fourth ASTM-EURATOM Symposium on Reactor Dosimetry, NUREG/CR-0029, p. 513, July 1982.

34. G. C. Martin, "Brown's Ferry Unit-3 Cavity Neutron Spectral Analysis," Proceedings of the Fourth ASTM-EURATOM Symposium on Reactor Dosimetry, NUREG/CR-0029, p. 555, July 1982, and EPRI NP-1997, August 1981.

35. W. E. Brandon et al., "Neutron Dosimetry in the Pressure Vessel Cavity of Two Pressurized Water Reactors," Proceedings of the Fourth ASTM-EURATOM Symposium on Reactor Dosimetry, NUREG/CR-0029, p. 533, July 1982.

36. N. Tsoulfanidis et al., "Calculation of Neutron Spectra at the Pressure Vessel and Cavity of a PWR," Proceedings of the Fourth ASTM-EURATOM Symposium on Reactor Dosimetry, NUREG/CR-0029, p. 519, July 1982.

37. M. Petilli, "A New Analysis of the Experiment for Measurement of Φ > 1 MeV in Pressure Vessel Cavity of U.S. Light Water Power Reactor Arkansas," Proceedings of the Fourth ASTM-EURATOM Symposium on Reactor Dosimetry, NUREG/CR-0029, p. 545, July 1982.

38. W. E. Selph and J. MacKenzie, Passive Neutron Dosimetry for Measurements at the McGuire Reactor, EPRI NP-2570, September 1982.

39. ASTM E853-81, "ASTM Standard Practice for Analysis and Interpretation of Light-Water Reactor Surveillance Results," 1982 Annual Books of ASTM Standards, Part 45, ASTM, Philadelphia, PA, 1982.

40. R. L. Simons et al., "Re-Evaluation of the Dosimetry for Reactor Pressure Vessel Surveillance Capsules," Proceedings of the Fourth ASTM-EURATOM Symposium on Reactor Dosimetry, NUREG/CR-0029, p. 903, July 1982.

41. H. Tourwé and G. Minsart, "Surveillance Capsule Perturbations Studies in the PSF 4/12 Configuration," Proceedings of the Fourth ASTM-EURATOM Symposium on Reactor Dosimetry, NUREG/CR-0029, p. 471, July 1982.

42. L. S. Kellogg and E. P. Lippincott, "PSF Interlaboratory Comparison," Proceedings of the Fourth ASTM-EURATOM Symposium on Reactor Dosimetry, NUREG/CR-0029, p. 929, July 1982.

43. H. Tourwé et al., "Interlaboratory Comparison of Fluence Neutron Dosimeters in the Frame of the PSF Start-Up Measurement Programme," Proceedings of the Fourth ASTM-EURATOM Symposium on Reactor Dosimetry, NUREG/CR-0029, p. 159, July 1982.

44. ASTM E854-81, "ASTM Standard Method for Application and Analysis of Solid State Tracks Recorder (SSTR) Monitors for Reactor Surveillance," 1982 Annual Book of ASTM Standards, Part 45, Philadelphia PA, 1982.

45. W. N. McElroy et al., LWR PV Surveillance Dosimetry Improvement Program: 1979 Annual Report, NUREG/CR-1291, HEDL-SA 1949, February 1980.

46. A. Fabry et al., "Results and Implications of the Initial Neutronic Characterization of Two HSST Irradiation Capsules and the PSF Simulated LWR Pressure Vessel Irradiation Facility," presented at the NRC Eighth Safety Research Information Meeting, at National Bureau of Standards, Washington, DC, October 27-31, 1980.

47. G. P. Pells et al., "An Investigation into the Use of Sapphire as a Fast Neutron Damage Monitor," Proceedings of the Fourth ASTM-EURATOM Symposium on Reactor Dosimetry, NUREG/CR-0029, p. 331, July 1982.

48. A. Alberman et al., "Nouveaux Developpements de la Dosimetrie des Dommages par Technique Tungstene (W)," Ibid., p. 321, July 1982.

49. P. Mas and R. Perdreau, "Characterisation d'Emplacements d'Irradiation en Spectres Neutroniques et en Dommages," Ibid., p. 847, July 1982.

50. S. De Leeuw and R. Menil, "Silicon P.I.N. Diode Neutron Damage Monitors," Ibid., p. 387, July 1982.

51. F. H. Ruddy et al., "Light Water Reactor Pressure Vessel Neutron Spectrometry with Solid State Tracks Recorders," Ibid., p. 293, July 1982.

52. R. Gold et al., "Computer Controlled Scanning Systems for Quantitative Tracks Measurements," Ibid., p. 281, July 1982.

53. J. G. Bradley et al., "Threshold Response of Helium Accumulation Fluence Monitors for Fast Breeder Reactor Dosimetry," Ibid., p. 195, July 1982.

54. B. M. Oliver et al., "Spectrum-Integrated Helium Generation Cross Sections for ^{6}Li and ^{10}B in the Sigma Sigma and Fission Cavity Standard Neutron Fields," Ibid., p. 889, July 1982.

55. W. N. McElroy et al., LWR Pressure Vessel Surveillance Dosimetry Improvement Program: 1980 Annual Report, NUREG/CR-1747, HEDL-TME 80-73, April 1981.

56. A. Alberman et al., "Influence des Neutrons Thermiques sur la Fragilisation de l'Acier de Peau d'Etancheite des Reacteurs a Haute Temperature (H.T.R.)," Proceedings of the Fourth ASTM-EURATOM Symposium on Reactor Dosimetry, NUREG/CR-0029, p. 839, July 1982.

57. J. R. Hawthorne and J. A. Sprague, Radiation Effects to Reactor Vessel Support Structures, Report by Task C of Interagency Agreement NRC-03-79-148, October 22, 1979.

58. R. E. Maerker, J. J. Wagshal and B. L. Broadhead, Development and Demonstration of an Advanced Methodology for LWR Dosimetry Applications, EPRI-NP 2188, Interim Report, 1981.

59. S. L. Anderson, "Sensitivity of Vessel Exposure to Power Distribution Uncertainties," Presented at the Fourth ASTM-EURATOM Symposium on Reactor Dosimetry, March 1982.

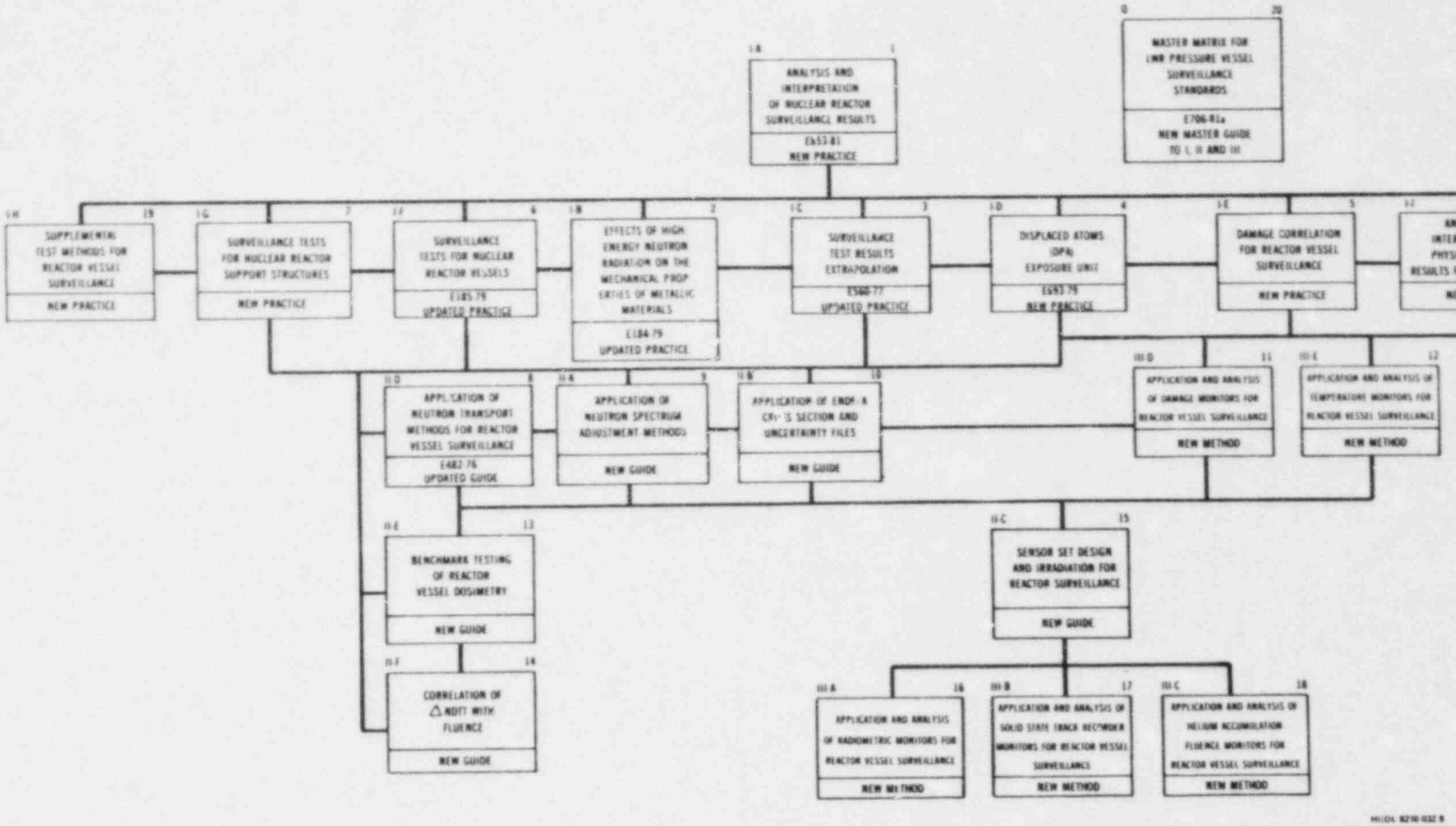

FIGURE 1. ASTM Standards for Surveillance of LWR Nuclear Reactor Pressure Vessels and Support Structures.

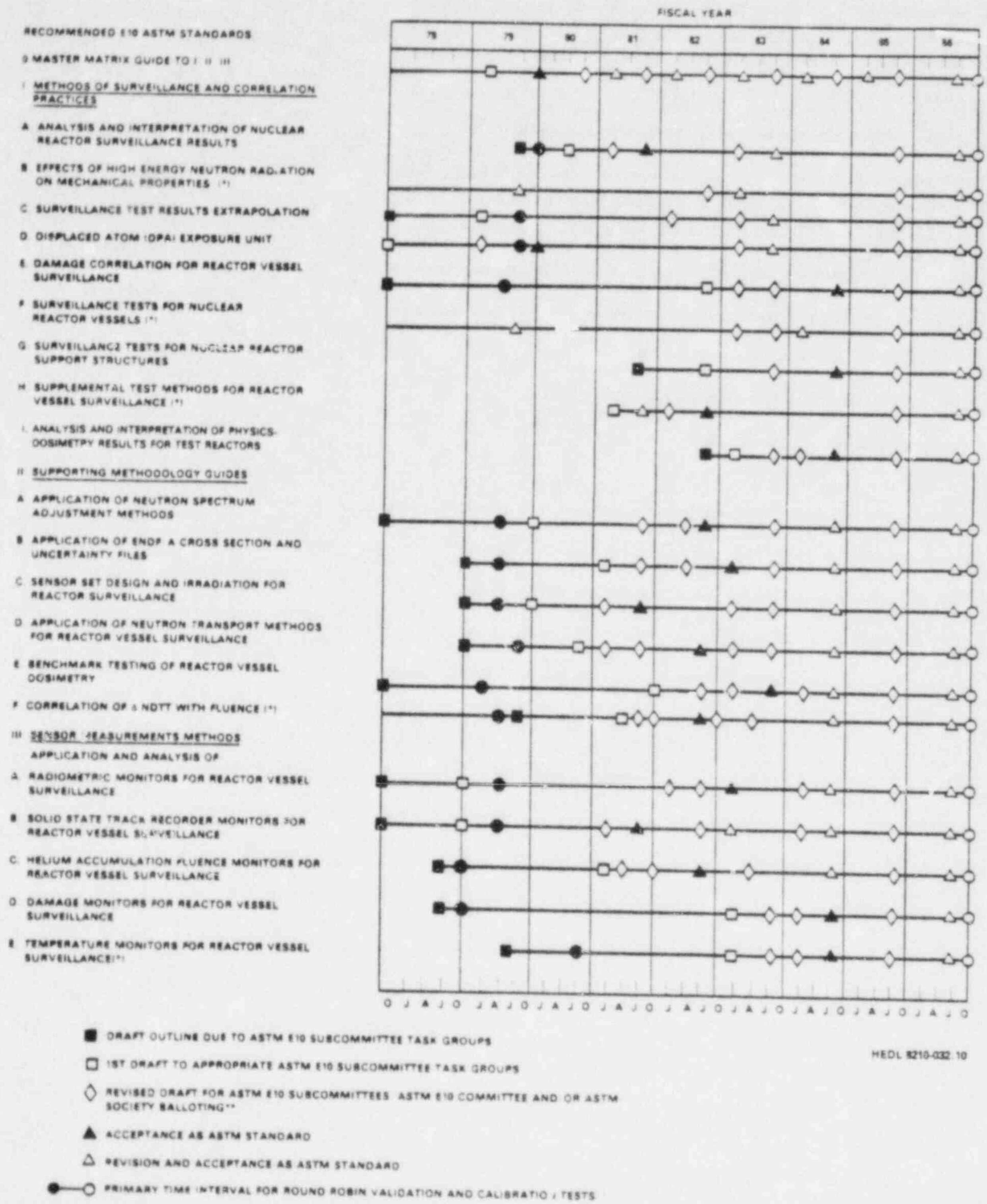

*AN ASTERISK INDICATES THAT THE LEAD RESPONSIBILITY IS WITH SUBCOMMITTEE E10.02 INSTEAD OF WITH SUBCOMMITTEE E10.05
**THE 1985-1986 REVISIONS WILL PRIMARILY ESTABLISH STANDARD TO STANDARD SELF CONSISTENCY

FIGURE 2. Preparation, Validation and Calibration Schedule for LWR Pressure Vessel and Support Structure Surveillance Standards.

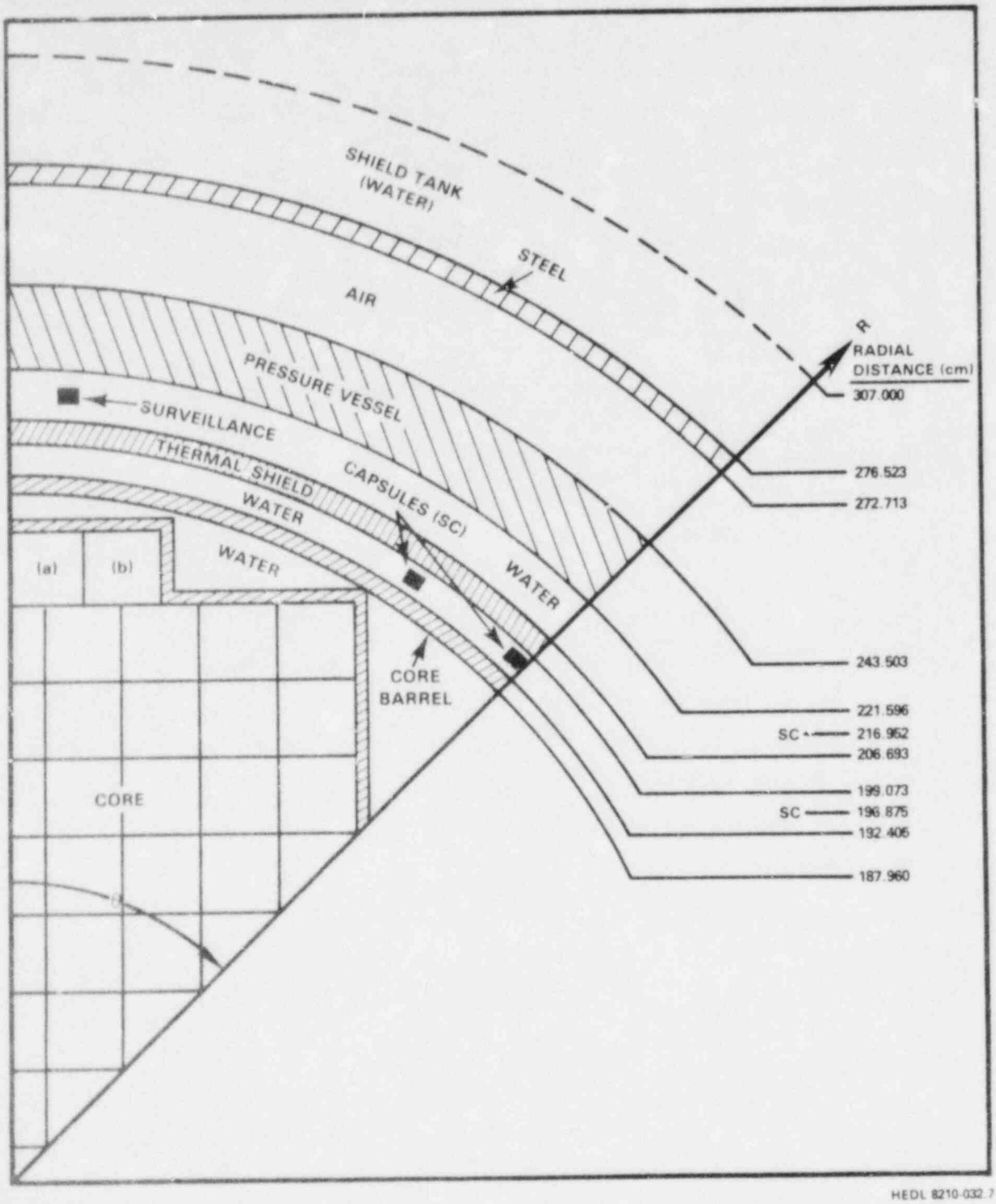

FIGURE 3. Schematic Representation-Type A PWR with Two Types of Surveillance Capsules (taken from Reference 10).

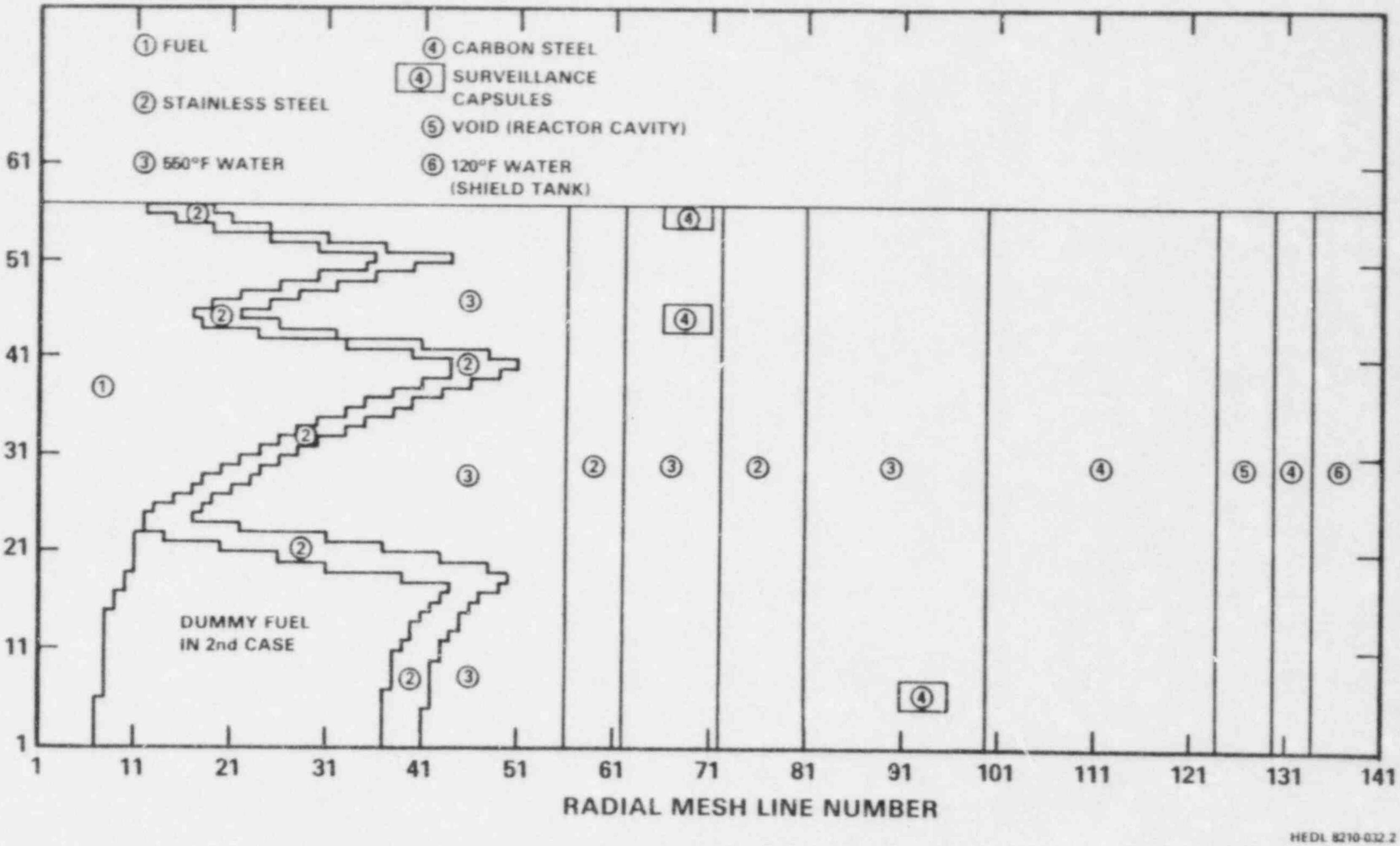

FIGURE 4. Mesh Line Description for R,θ Analysis of the Type A Reactor with Two Types of Surveillance Capsules (taken from Reference 10).

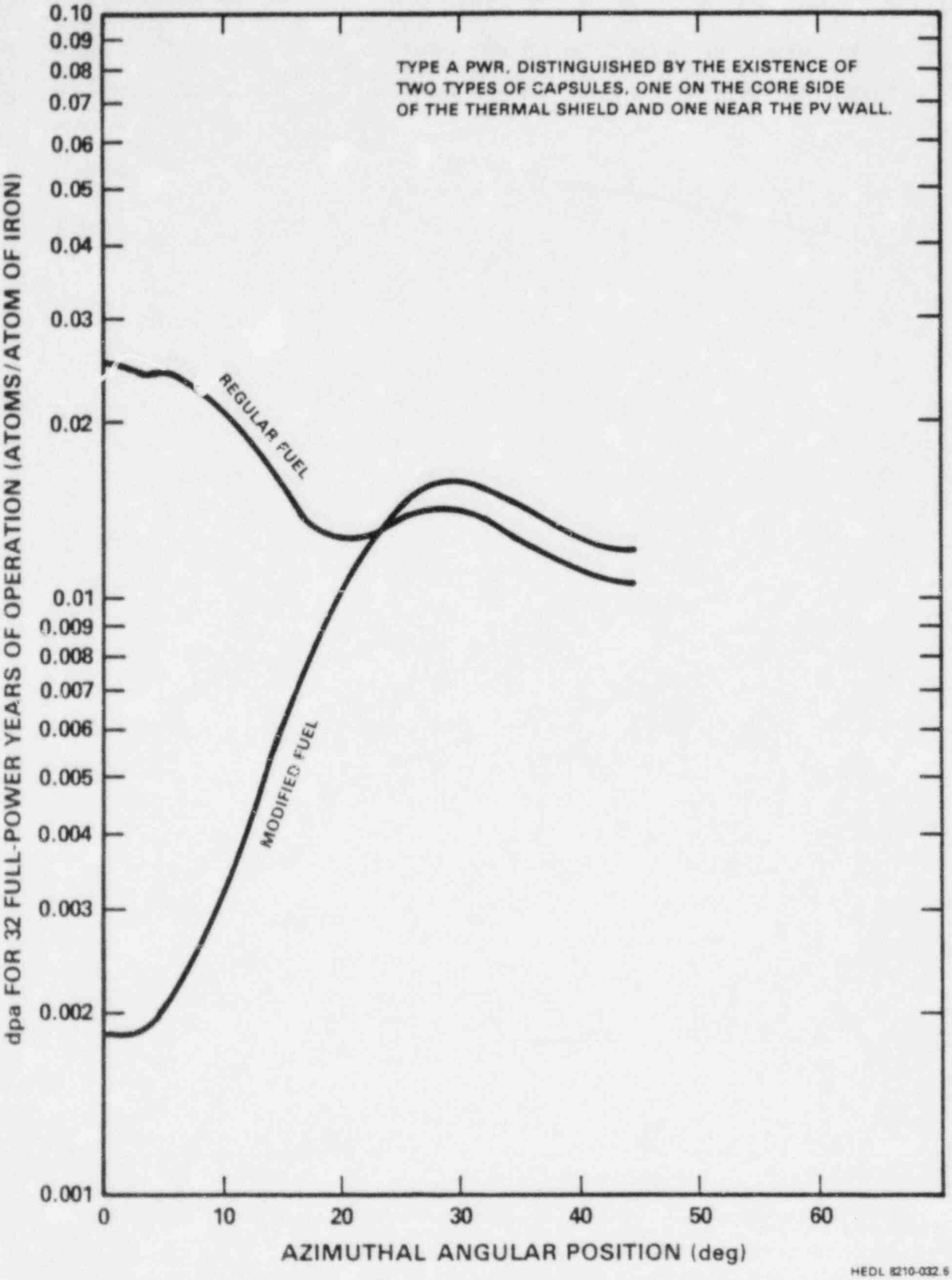

FIGURE 5. Dpa for 32 Years Full Power Exposure on the Front Face of the Pressure Vessel, Plotted as a Function of Angular Position (taken from Reference 10).

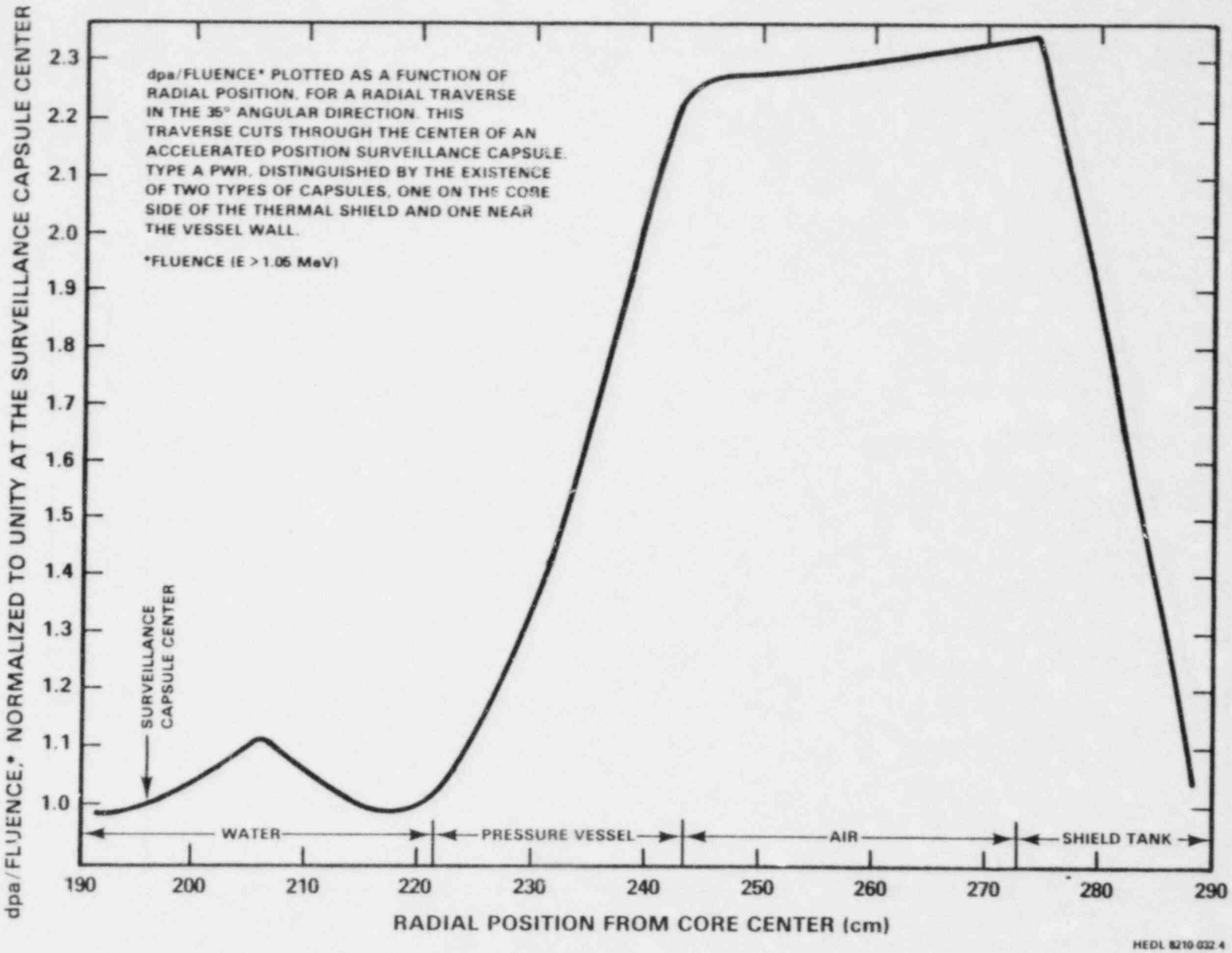

FIGURE 6. Dpa/Fluence Radial Traverse for Type A PWR (taken from Reference 10).

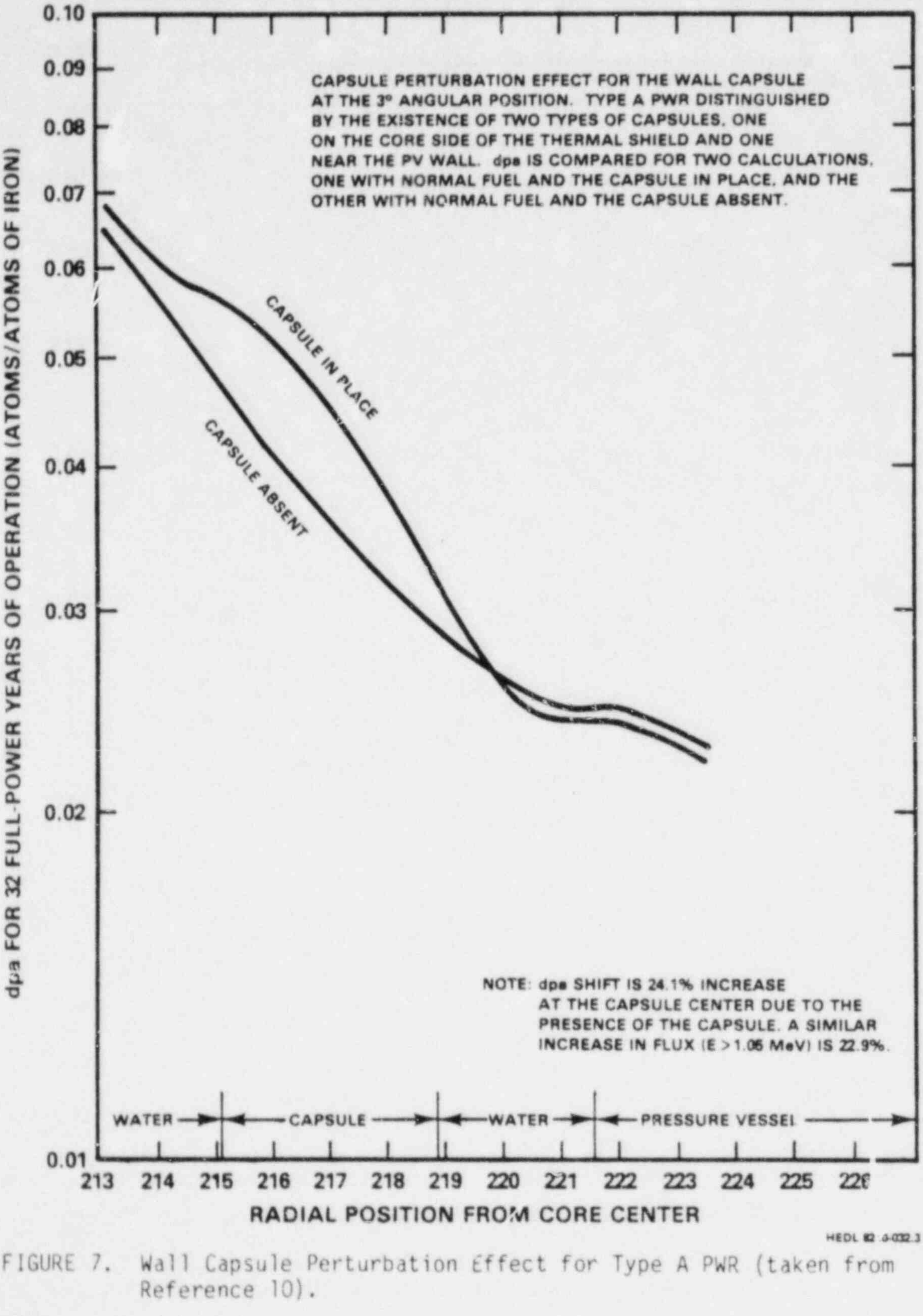

FIGURE 7. Wall Capsule Perturbation Effect for Type A PWR (taken from Reference 10).

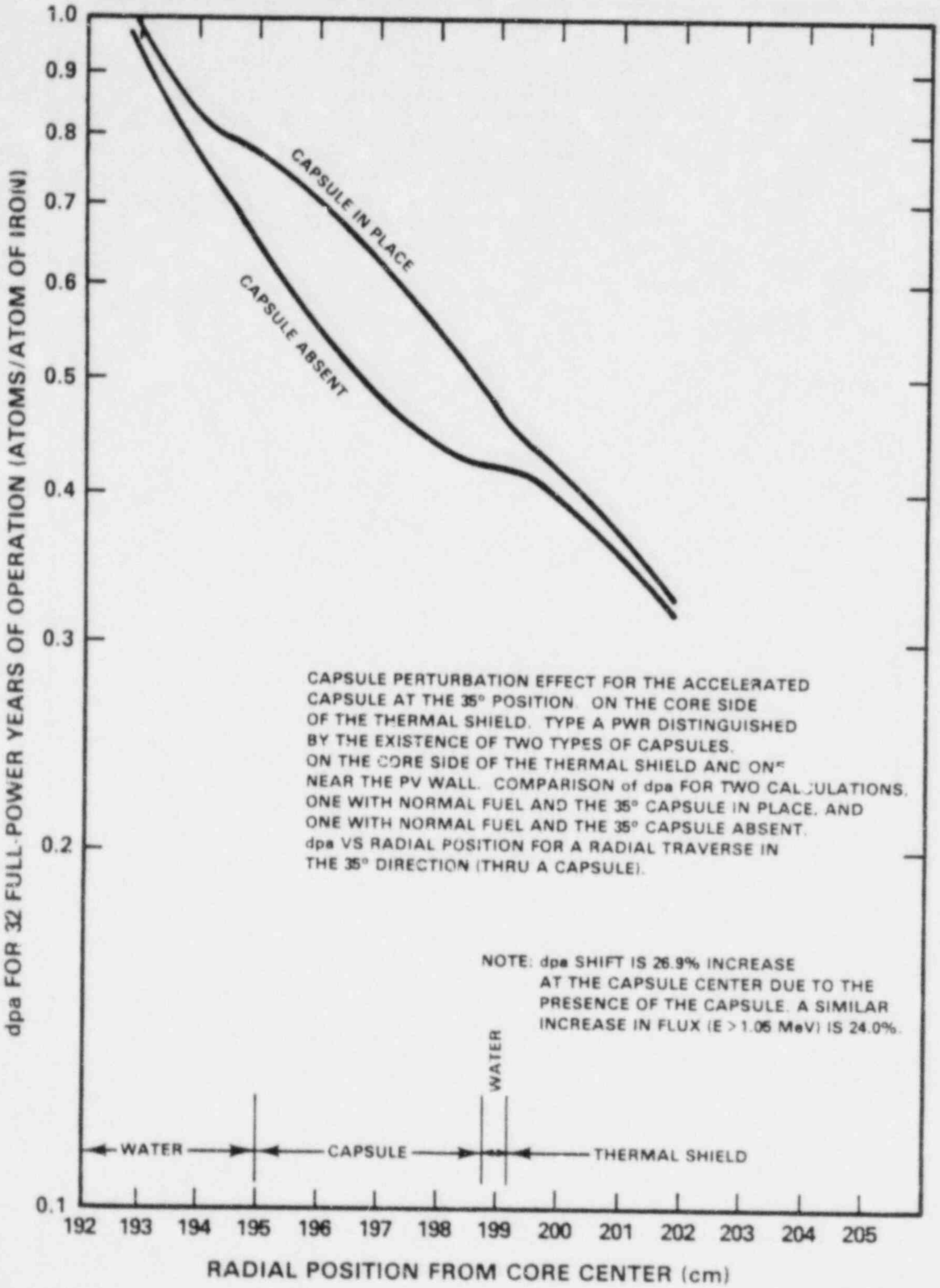

FIGURE 8. Accelerated Capsule Perturbation Effect for Type A PWR (taken from Reference 10).

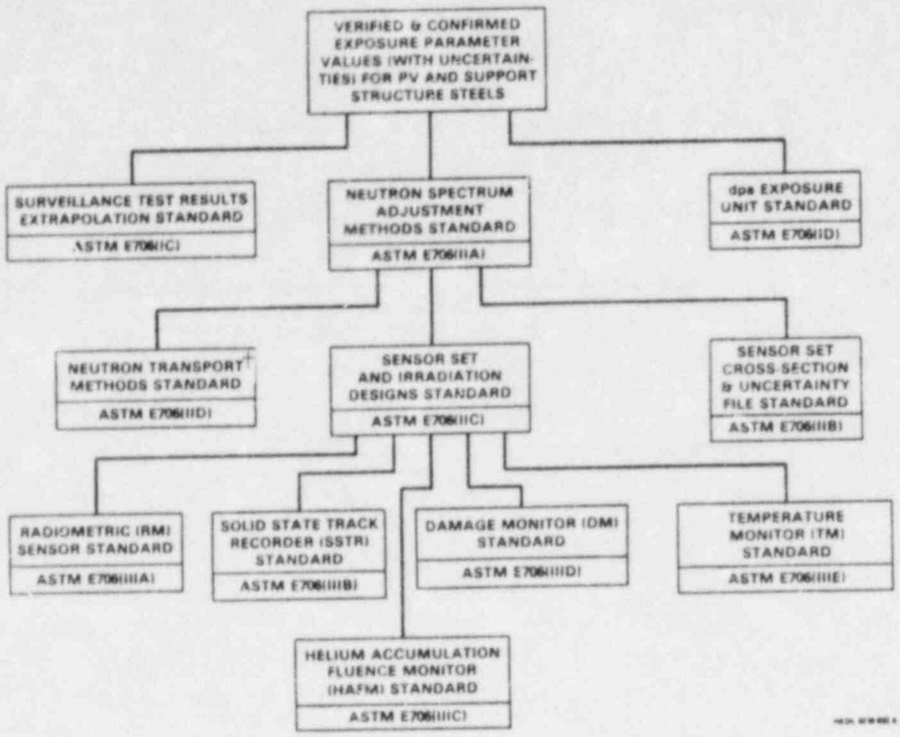

FIGURE 9. Interrelationship of ASTM Physics-Dosimetry Standards to Determination of Exposure Values.

+CURRENT ANALYSIS PROCEDURES AND DATA USED BY A NUMBER OF US LABORATORIES AND VENDORS

Analyst	Transport Code Used	Transport Code Cross-Section Data	Sensor Cross-Section Data	Adjustment Code	Currently Reported Exposure Values
Westinghouse	DOT IIIW	ENDF/B-II, -III & -IV adjusted in-house	ENDF/B-IV	SACSBOT*	E > 1.0 MeV Fluence Thermal Fluence dpa
General Electric	DOT II Variant (SN2D)	ENDF/B-IV	ENDF/B-V	GE-RD-M02	E > 1.0 MeV Fluence E > 0.1 MeV Fluence Thermal Fluence Some use of dpa
Combustion Engineering	DOT III Changing to IV.2	DLC-23E (Cask)	SAND-II Library	SAND-II	E > 1.0 MeV Fluence Thermal Fluence dpa
Babcock & Wilcox	Previously DOT III.5 now IV.2	DLC-23E (Cask)	ENDF/B-V	Equivalent to SACSBOT*	E > 1.0 MeV Fluence E > 0.1 MeV Fluence Thermal Fluence
Brookhaven	DOT III.5	ENDF/B-IV	Collapsed Version of ENDF/B-V	SACSBOT*	E > 1.0 MeV Fluence E > 0.1 MeV Fluence Thermal Fluence dpa
SWRI	DOT III.5 Changing to IV.2	DLC-23E (Cask) Changing to DCL-75 BUGLE-80 (ENDF/B-IV)	ENDF/B-IV Changing to ENDF/B-V	Previously SAND-II now SACSBOT*	E > 1.0 MeV Fluence E > 0.1 MeV Fluence Thermal Fluence
BMI	DOT III.5 Changing to IV.2	DLC-23E (Cask) Changing to DCL-75 BUGLE-80 (ENDF/B-IV)	SAND-II Library	SACSBOT*	E > 1.0 MeV Fluence E > 0.1 MeV Fluence Thermal Fluence dpa

*SACSBOT = Individual Sensor Spectrum Averaged Cross Sections Based On Transport Calculations.

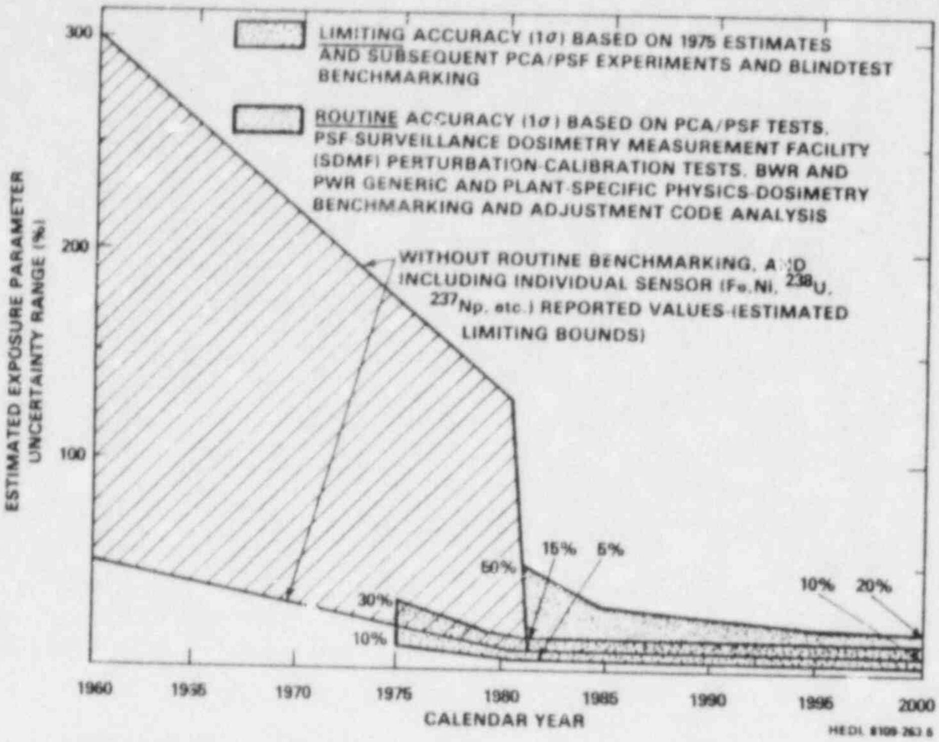

FIGURE 10. Estimated Exposure Parameter Uncertainties Obtained from FSAR and Surveillance Capsule Reports (taken from Reference 24).

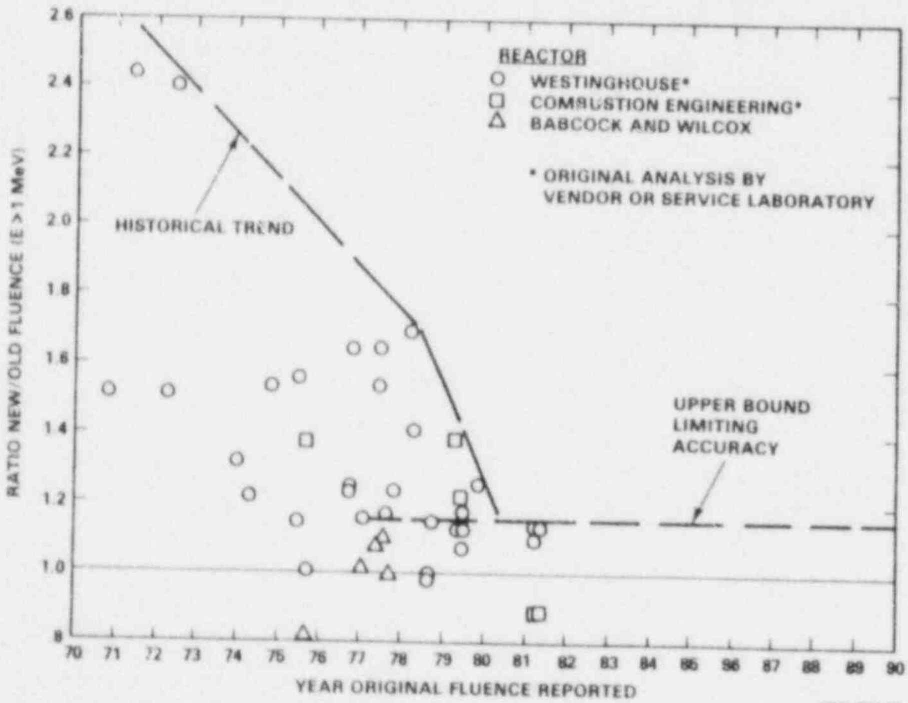

FIGURE 11. Ratio of New Fluence/Old Fluence as a Function of Date That Old Fluence was Reported (revision of Reference 40 data).

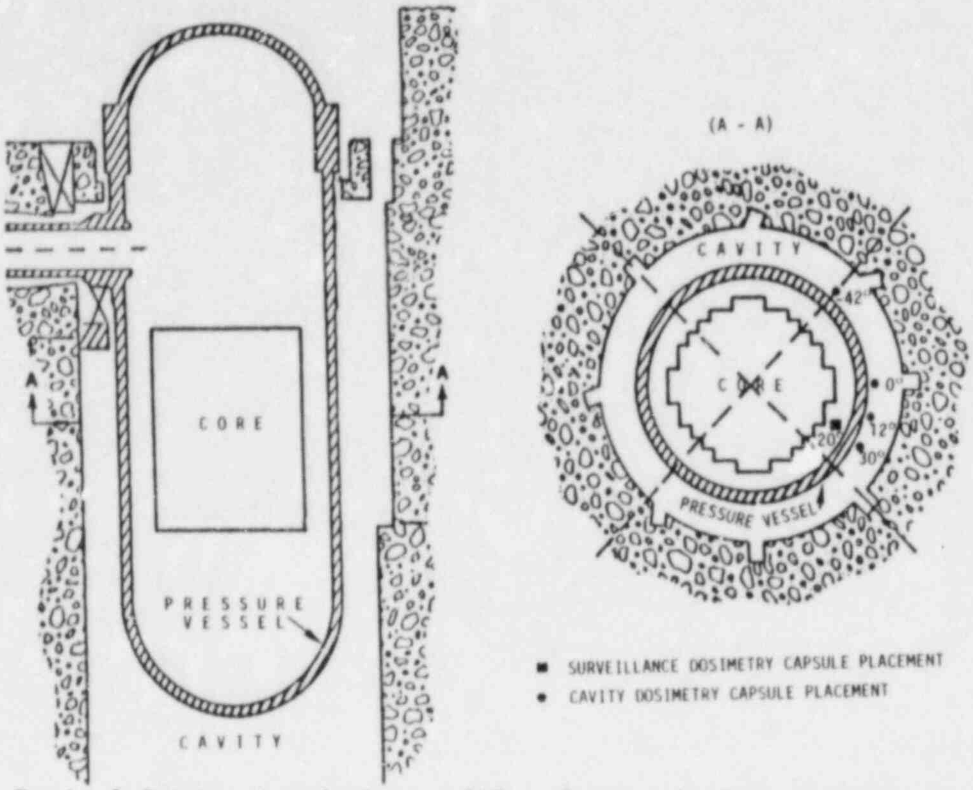

FIGURE 12. Typical 3-Loop Westinghouse PWR: Schematic Representation for H. B. Robinson Surveillance and Cavity Dosimetry Capsule Placement.

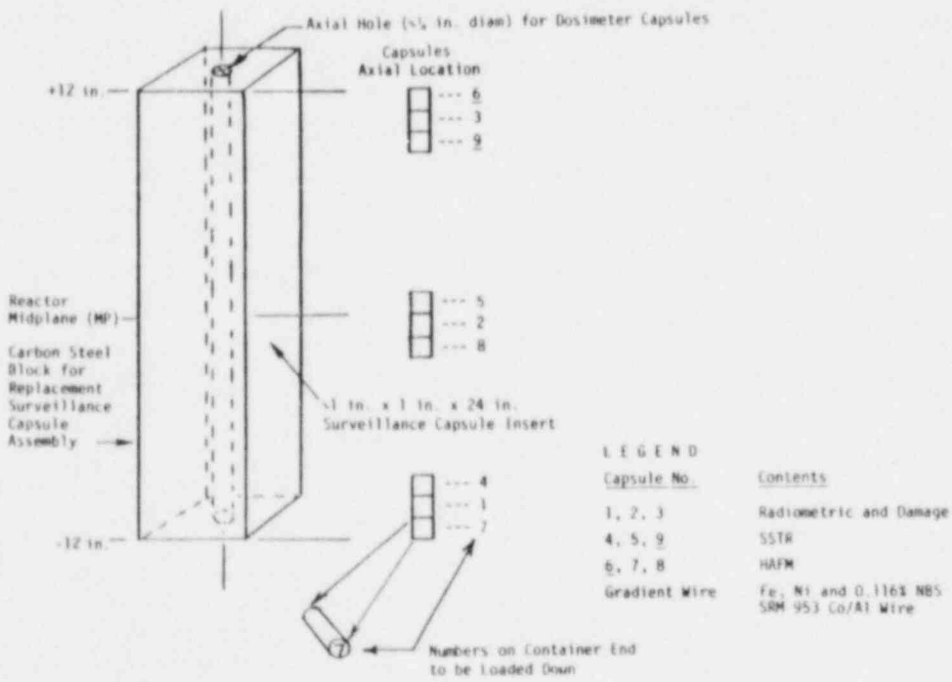

FIGURE 13. H. B. Robinson Surveillance Capsule Dosimetry.

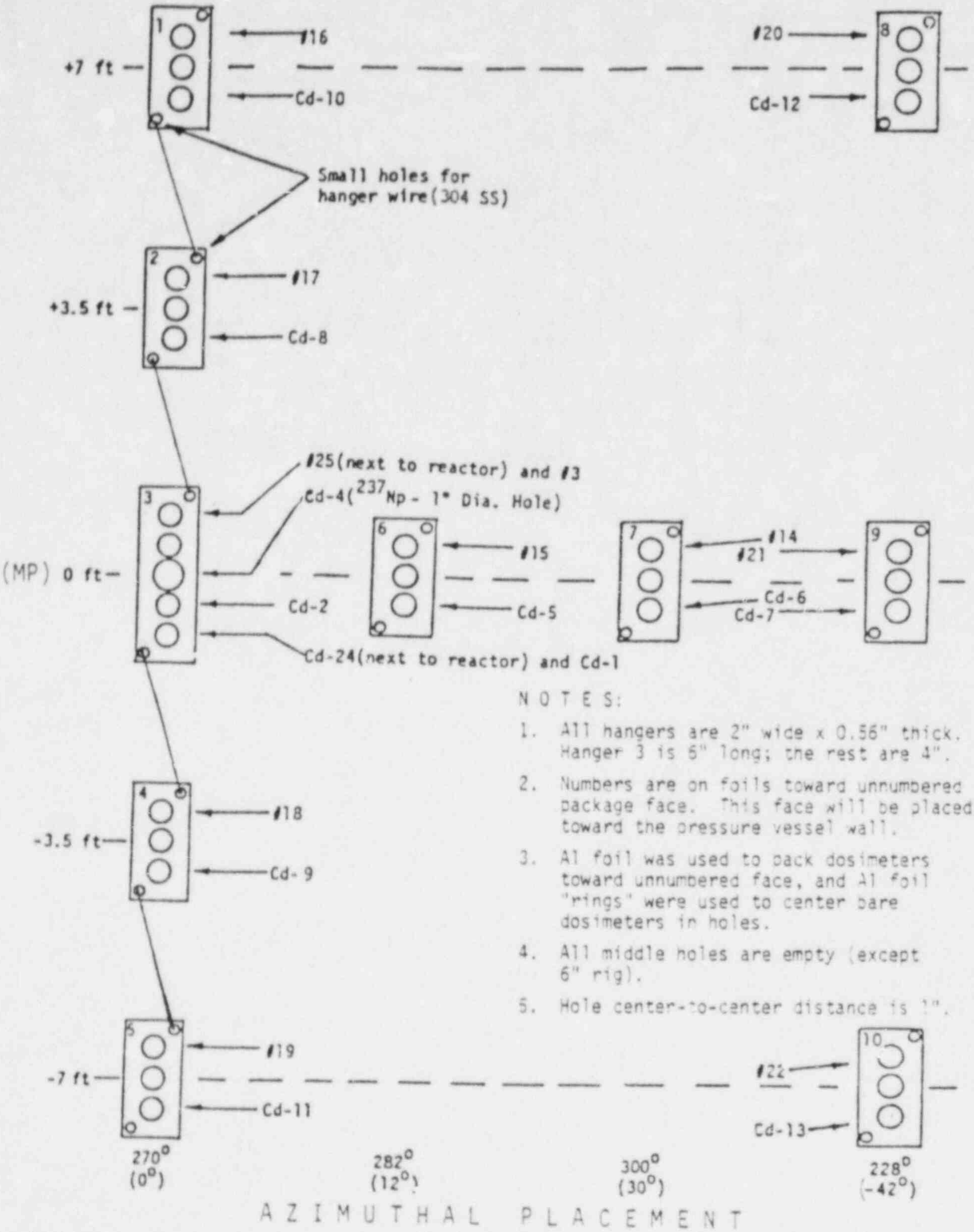

N O T E S:

1. All hangers are 2" wide x 0.56" thick. Hanger 3 is 6" long; the rest are 4".
2. Numbers are on foils toward unnumbered package face. This face will be placed toward the pressure vessel wall.
3. Al foil was used to back dosimeters toward unnumbered face, and Al foil "rings" were used to center bare dosimeters in holes.
4. All middle holes are empty (except 6" rig).
5. Hole center-to-center distance is 1".

FIGURE 14. H. B. Robinson Cavity Dosimetry Hanger Rigs. (Individual dosimeter sensors are identified in Table 4).

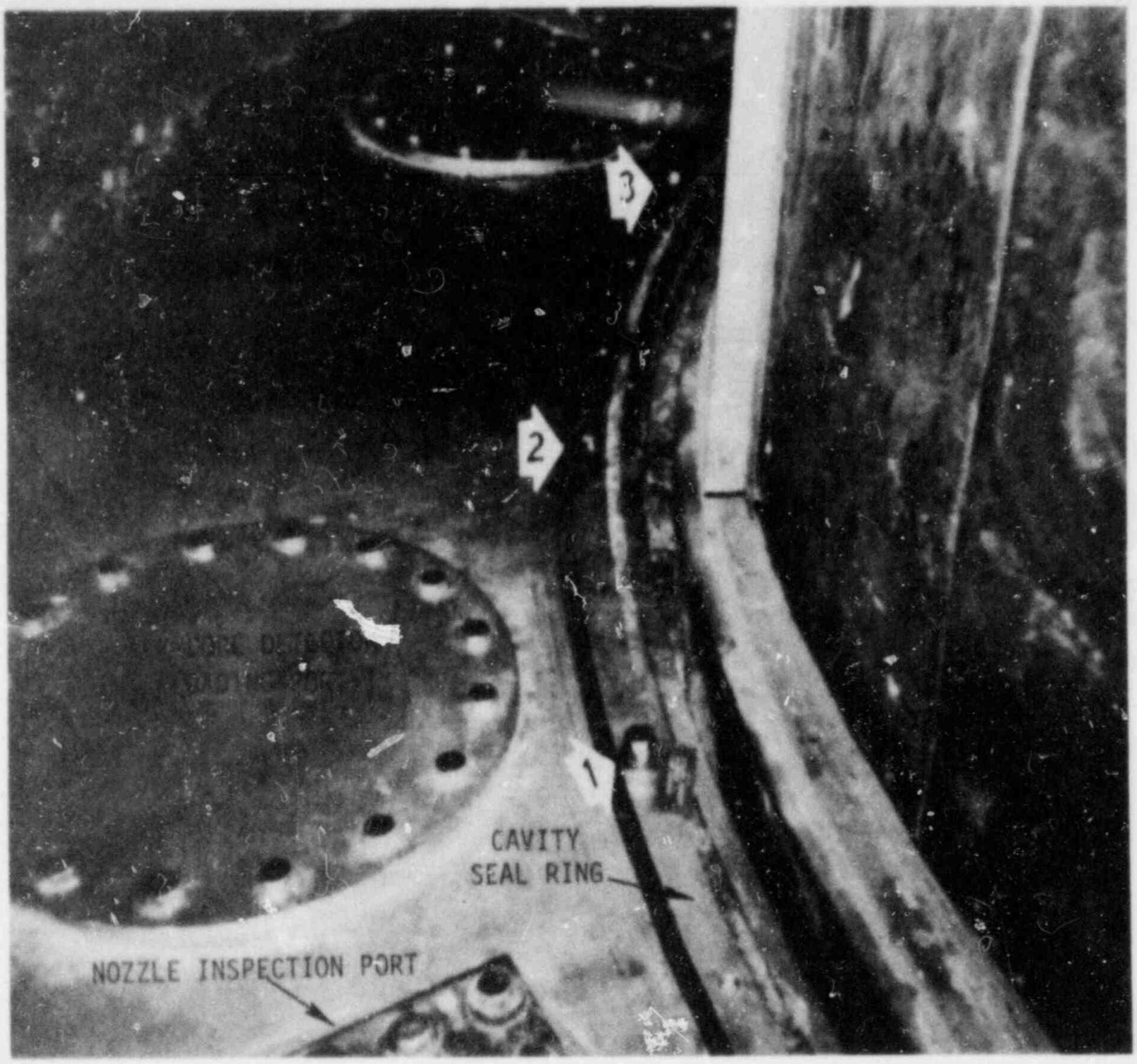

1) 0° Dosimetry String (1 SSTR & 5 RM Sets) [270° Azimuthal]

2) 12° Dosimetry String (1 RM Set) [282° Azimuthal]

3) 30° Dosimetry String (1 RM Set) [300° Azimuthal]

4) -42° Dosimetry String (3 RM Sets) [228° Aximuthal] Out of View

FIGURE 15. Actual Placement of Cavity Dosimetry Hanger Rigs for H. B. Robinson. Neg 8205833-2cn

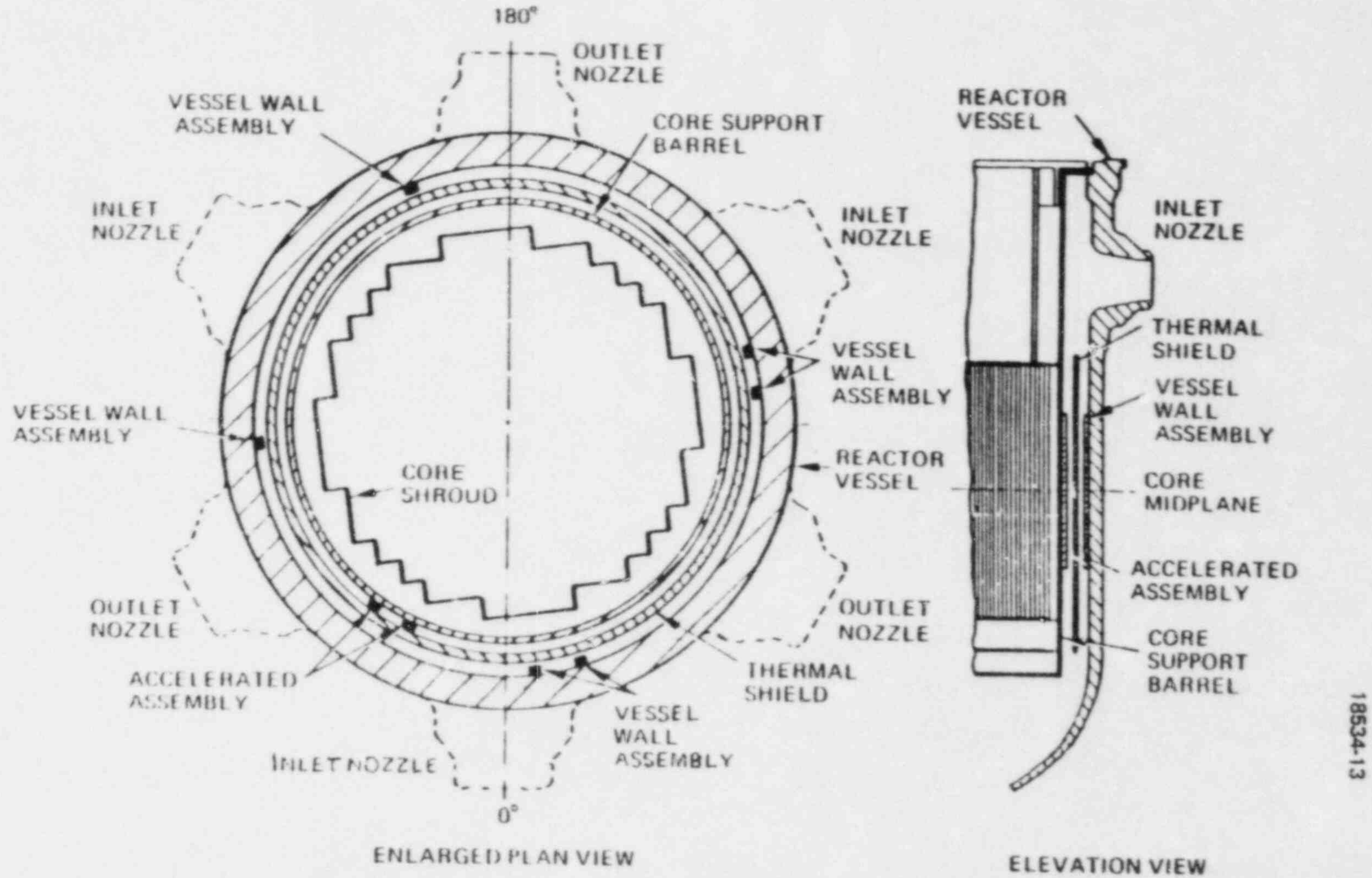

FIGURE 16. Typical Locations of Maine Yankee Surveillance Capsule Assemblies. (The three selected cavity locations are not shown, and actual placement has yet to be accomplished.)

FIGURE 17. Maine Yankee Midplane RM and SSTR Dosimetry Capsule with Gd Shield. (There are 3 Gd-shielded and 3 unshielded capsules for the top, midplane and bottom locations.)

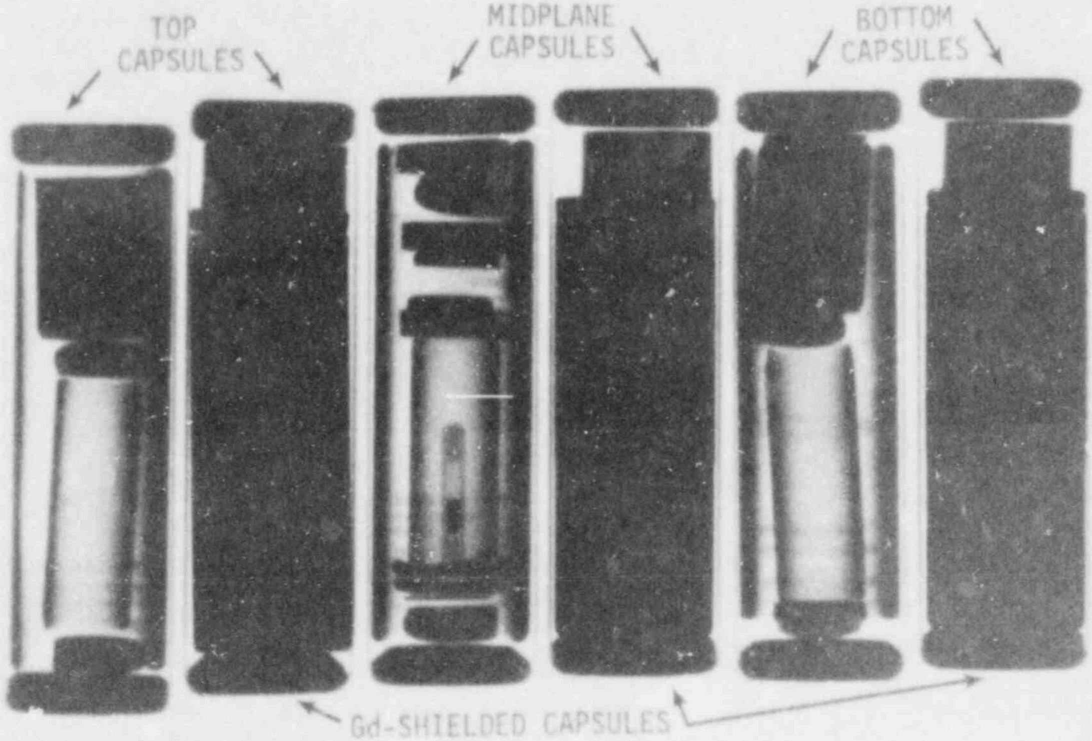

FIGURE 18. Maine Yankee Surveillance Capsules: Quality Assurance Radiographs for Capsule Weld Integrity and Sensor Placement Verification.

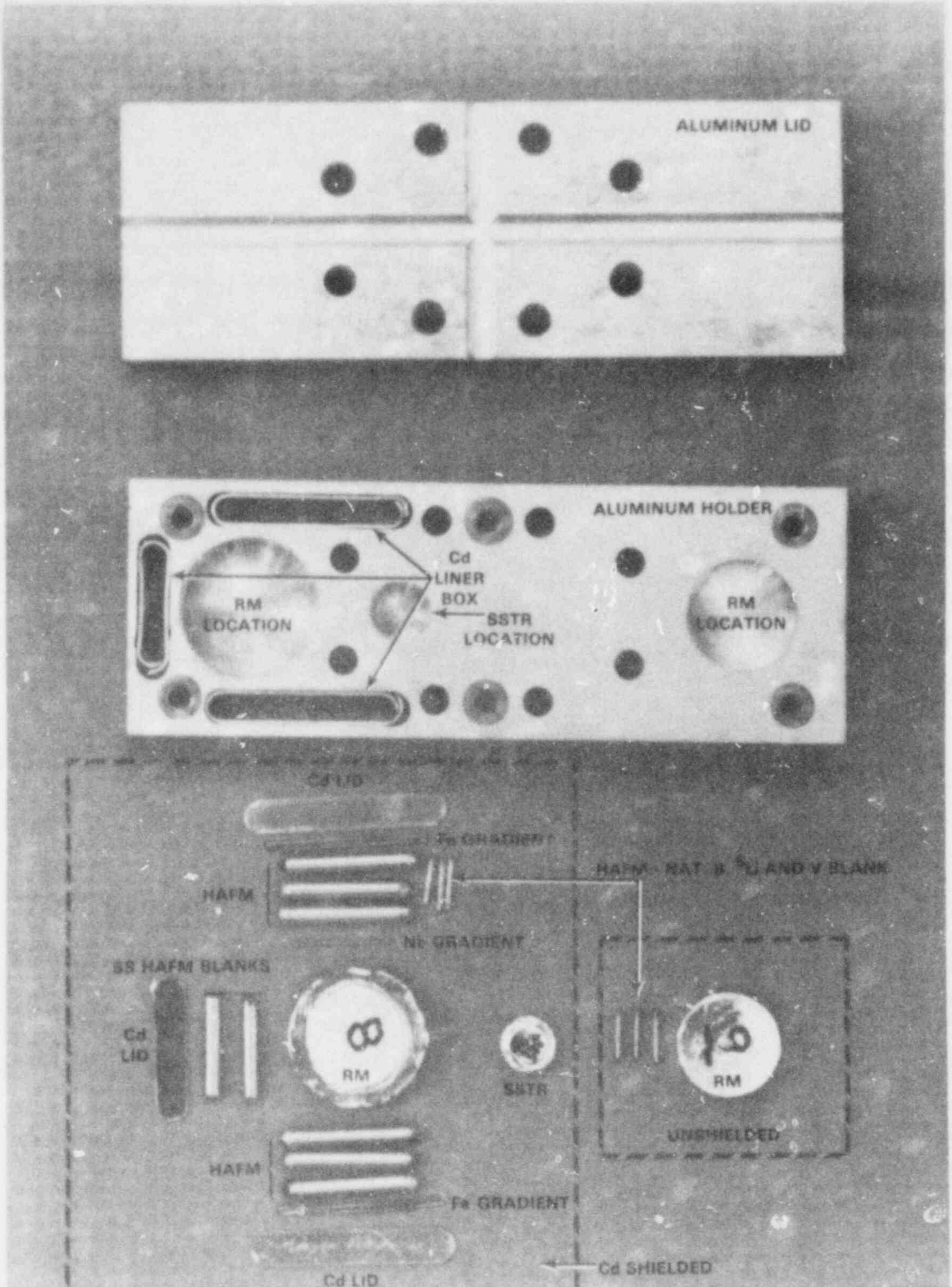

FIGURE 19. Maine Yankee 15° and 30° Cavity Dosimetry Holder with RM, SSTR, HAFM and Gradient Wires Before Assembly. Neg P14116-1

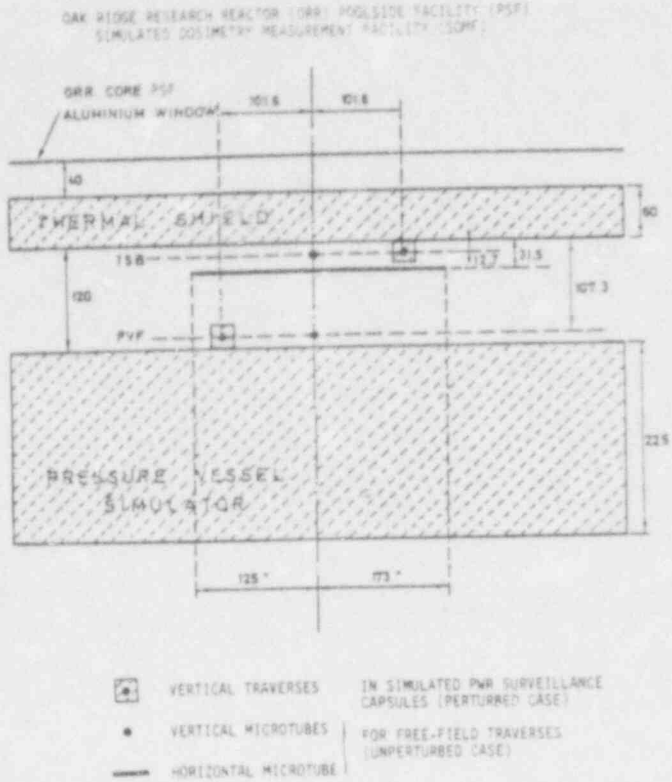

FIGURE 20. As-Build Experimental Configuration for (1) Westinghouse and Combustion Engineering Type Surveillance Capsule Perturbation Test and (2) the First ORR-SDMF RM Sensor Certification Test (taken from References 24 and 41).

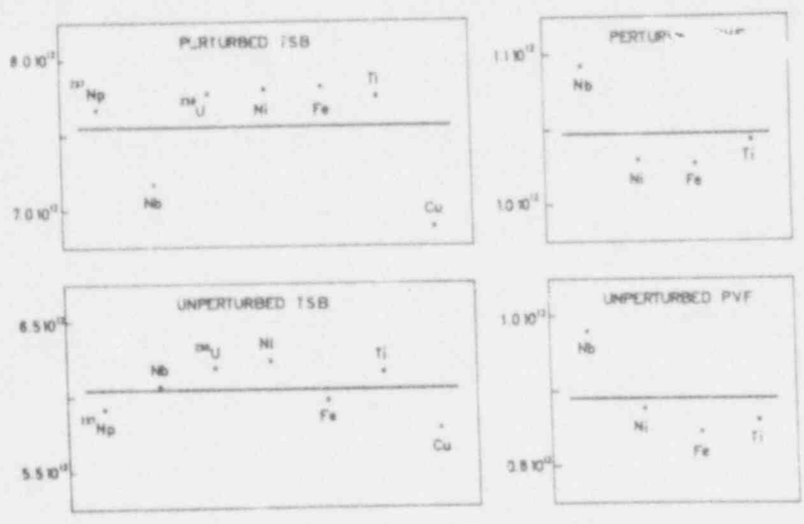

FIGURE 21. $\emptyset$ (>1 MeV) in n $s^{-1}cm^{-2}$ at the Thermal Shield Back (TSB) and Pressure Vessel Front (PVF) Positions for the Westinghouse and Combustion Engineering Type Surveillance Capsule Perturbation Test (taken from Reference 41).

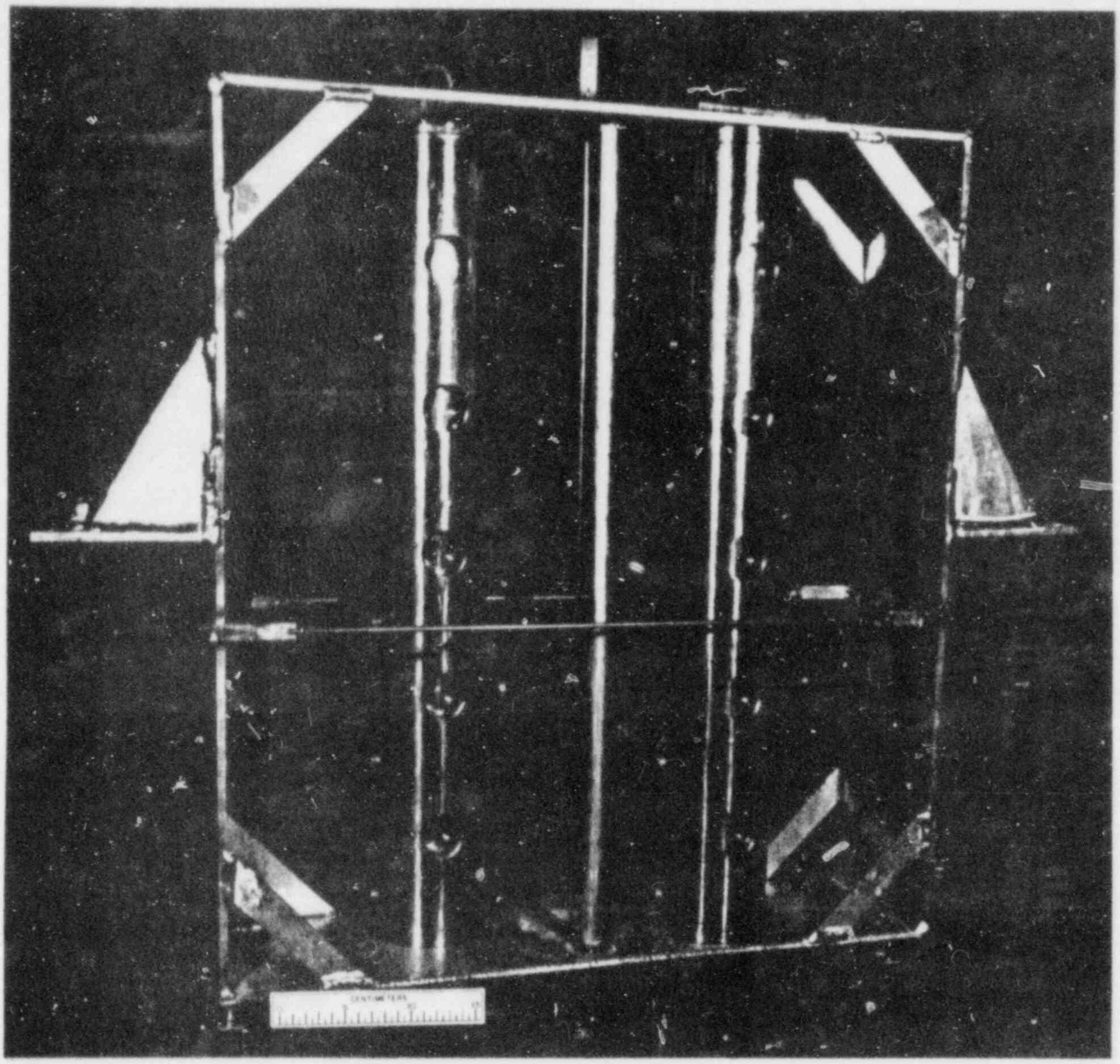

FIGURE 22. As-Build Experimental Configuration for the Babcock & Wilcox Type Surveillance Capsule Perturbation Test and Third RM Sensor Certification Test, Fluence ($E > 1$ MeV) of $\sim 1.0 \times 10^{18}$ n/cm^2.

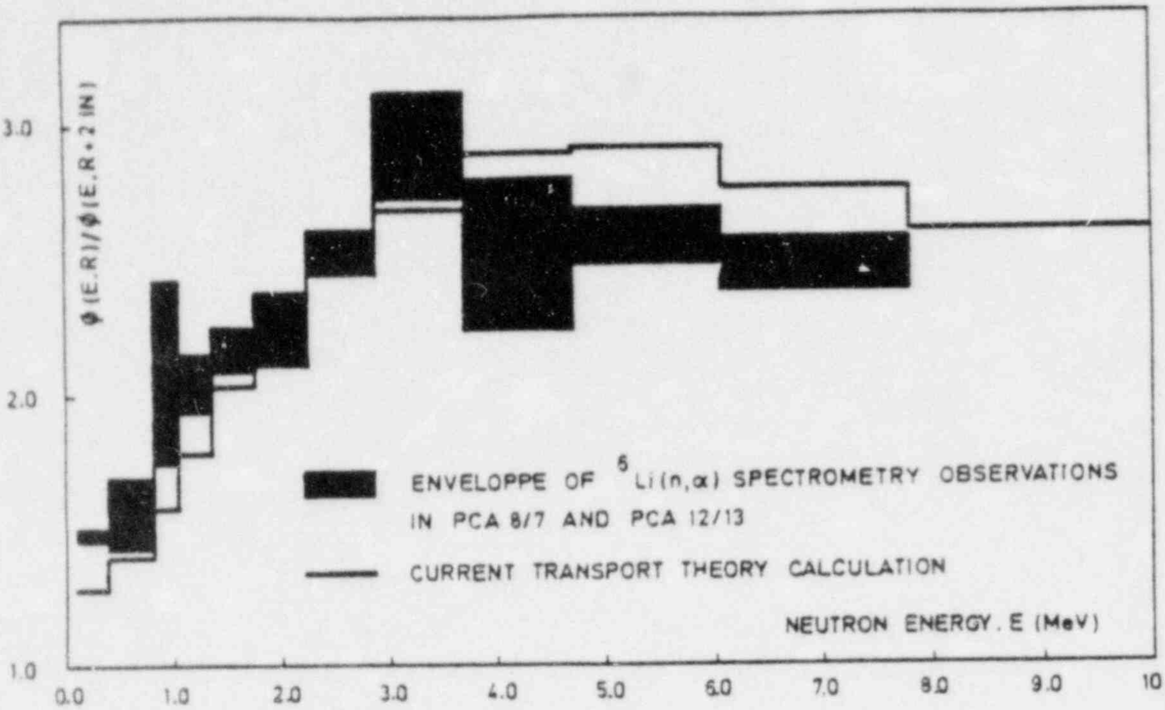

FIGURE 23. Radial Neutron Flux Spectrum Attenuation by Steel in Simulated LWR Pressure Vessel Environments (taken from Reference 46).

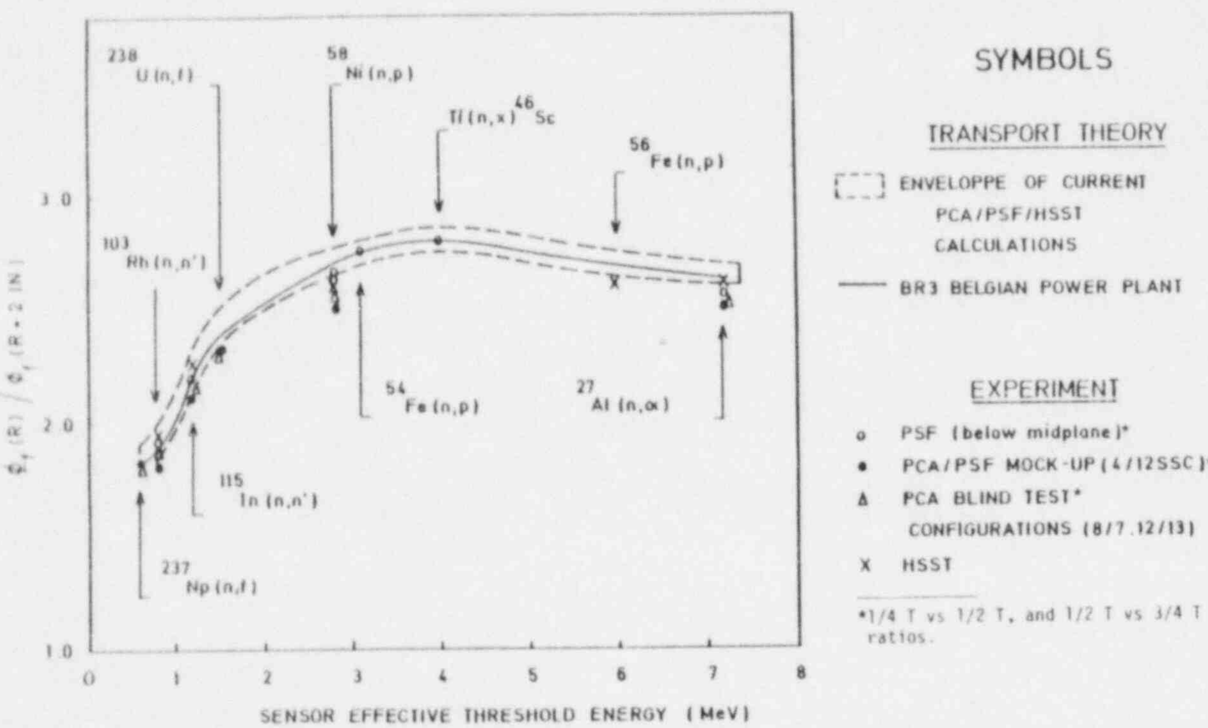

FIGURE 24. Radial Fission Flux Attentuation by Steel in Typical LWR Pressure Vessel Environments (taken from Reference 46).

TABLE 1

LICENSING AND REGULATORY REQUIREMENTS RELATED TO THE ASSESSMENT AND CONTROL OF THE FRACTURE TOUGHNESS OF REACTOR PRESSURE VESSELS

A. Two distinct licensing requirements form the backbone of the latest regulations related to the fracture toughness of reactor pressure vessels:*

1. Protection against failure by tearing instability: (Ductile regime, 100% shear fracture)

$$USE \geq 50 \text{ ft-lb } (67.8 \text{ joules}) \quad (1)$$

(USE is the Upper Shelf Energy absorbed in the C_v-impact test at the vessel operating temperature)

2. Protection against non-ductile failure:

$$\text{Applied Load} \times \text{Safety Margin} \leq \text{Material Strength} \quad (2)$$

$$2\,K_{IP} + K_{IT} \leq K_{IR}\,(T\text{-}RT_{NDT})$$

Pressure + Thermal + + (Calculated Stress Intensity Factors)	Reference Fracture Toughness K_{IR} = Lower Bound of Valid K_{Ic}, K_{Ia}, K_{Id} Measurements (Indexed to reference temperature, $T\text{-}RT_{NDT}$)[7]

where RT_{NDT} = (unirradiated nil-ductility temperature) + (ΔRT_{NDT}). From this relationship are derived the pressure versus temperature heat-up and cool-down limit curves P(T); at core criticality, these limits must, furthermore, be shifted conservatively by an additional margin of 40°F.

B. Surveillance-capsule physics-dosimetry measurement results enter into the application of requirements of Eq. (1) and (2) at two stages:

1. Mechanical testing and physics-dosimetry data are used to consolidate plant-specific "trend curves":

$$USE = \text{function of neutron exposure and other variables} \quad (3)$$

$$\Delta RT_{NDT} = \text{function of neutron exposure and other variables} \quad (4)$$

The neutron exposure is expressed as fluence of neutrons with energy greater than 1 MeV or, more appropriately, as dpa.[30]**

2. Dosimetry data are used to consolidate reactor physics calculations of in-vessel neutron exposure projections (lead factors) at the end of the considered plant service cycle: The derived exposures are then input to Eqs. (3) and (4) in order to apply Eqs. (1) and (2); in this regard, ex-vessel dosimetry measurements[32-38] are a particularly relevant supplement to surveillance capsule dosimetry and to the extensive low power benchmarking studies in PCA,[23] VENUS[18] and NESDIP.[29]**

---

*In addition, screening criteria to sort out plants for which more extensive analysis of thermal shock risk is needed have recently been proposed by the NRC.

**Physics-dosimetry licensing requirements are as yet unspecified, but the technology and the ASTM Standards are at hand for the use of dpa and ex-vessel measurements, see Refs. 17, 30 and 39.

TABLE 2*

PROCEDURES FOR ANALYSIS AND INTERPRETATION
OF NUCLEAR REACTOR SURVEILLANCE RESULTS

PROCEDURAL STEPS:

1. Establish the basic surveillance test program for each operating power plant. Currently Practice E185 is available and is used. However, updated versions of this standard should include the following:

2. Determination of surveillance capsule spatial flux-fluence-spectral and DPA maps for improved correlation and application of measured property change data (upper shelf, NDTT, etc.). Measured surveillance capsule fission and nonfission monitor reaction and reaction rate data should be combined with reactor physics computations to make necessary adjustments for capsule perturbation effects.

3. As appropriate, use of measured/calculated DPA damge for normalization of Charpy to Charpy (and other metallurgical specimen) variations in neutron flux, fluence, and spectra. Here, an increased use of a larger number of metallurgical specimen iron drillings may be appropriate for dosimetry.

4. Establish a reactor physics computational method applicable to the surveillance program. Currently Practices E 482 and E 560 provide general guidance in this area. However, updated versions of these standards should include the following:

5. Determination of core power distributions applicable to long-term (30 to 40 year) irradiation. Associated with this is the need for the use of updated FSAR (Final Safety Analysis Report) reactor physics information at startup.

6. Determination of potential cycle-to-cycle variations in the core power distributions. This will establish bounds on expected differences between surveillance measurements and design calculations. Ex-vessel dosimetry measurements should be used for verification of this and the previous step.

7. Determination of the effect of surveillance capsule perturbations and photofission on the evaluation of capsule dosimetry. Adjustment codes should be used, as appropriate, to combine reactor physics computations with dosimetry measurements.

8. Benchmark validation of the analytical method.

9. Establish methods for relating dosimetry, metallurgy, and temperature data from the surveillance program to current and future reactor vessel and support structure conditions. Currently, Practice E 560 provides general guidance in this area. An updated version of this standard should include the following considerations:

10. Differences in core power distributions that may be expected during long-term operation and that may impact the extrapolation of surveillance results into the future. As previously stated, ex-vessel dosimetry should be used for verification.

11. Establish methods to verify Steps 2 - 10 and to determine uncertainty and error bounds for the interpretation of the combined results of dosimetry, metallurgical and temperature measurements. Currently, Practice E185 provides general guidance in this area. An updated version of this standard should more completely address the separate and combined accuracy requirements of physics, dosimetry, metallurgy, and temperature-measurement techniques.

*Taken from ASTM Standard E 853-81.[39]

TABLE 3

RE-EVALUATED EXPOSURE VALUES AND THEIR UNCERTAINTY FOR LIGHT WATER REACTOR PRESSURE VESSEL SURVEILLANCE CAPSULES (revision of Reference 40 data)

			Fluence (ϕt > 1 MeV) (n/cm^2)						
Plant	Unit	Capsule	Old	New [% (1σ)]	New/Old	dpa [% (1σ)]	dpa/ϕt New	dpa/s	Exposure* Time (s)
Westinghouse									
Conn. Yankee		A	2.08 + 18	3.17 + 18 (12)**	1.52	4.89-03 (12)	1.54-21	9.18-11	5.233 + 07
Conn. Yankee		F	4.04 + 18	6.17 + 18 (24)	1.53	9.70-03 (27)	1.57-21	1.27-10	7.651 + 07
Conn. Yankee		H	1.79 + 19	2.06 + 19 (25)	1.15	3.38-02 (28)	1.64-21	1.42-10	2.390 + 08
San Onofre		A	1.20 + 19	2.93 + 19 (22)	2.44	5.04-02 (27)	1.72-21	8.66-10	5.824 + 07
San Onofre		D	2.36 + 19	5.66 + 19 (26)	2.40	9.51-02 (29)	1.68-21	1.07-09	8.881 + 07
San Onofre		F	5.14 + 19	5.81 + 19 (14)	1.13	9.79-02 (21)	1.69-21	4.02-10	2.438 + 08
Turkey Pt.	3	S	1.41 + 19	1.66 + 19 (25)	1.18	2.65-02 (27)	1.60-21	2.42-10	1.095 + 08
Turkey Pt.	3	T	5.68 + 18	7.05 + 18 (10)	1.24	1.09-02 (12)	1.55-21	4.74-10	2.302 + 07
Turkey Pt.	4	S	1.25 + 19	1.34 + 19 (25)	1.07	2.22-02 (27)	1.66-21	2.06-10	1.079 + 08
Turkey Pt.	4	T	6.05 + 18	7.58 + 18 (13)	1.25	1.32-02 (13)	1.74-21	3.53-10	3.728 + 07
H. B. Robinson	2	S	3.02 + 18	3.99 + 18 (24)	1.32	6.99-03 (27)	1.75-21	1.66-10	4.209 + 07
H. B. Robinson	2	V	4.51 + 18	7.43 + 18 (22)	1.65	1.19-02 (25)	1.60-21	1.14-10	1.050 + 08
Surry	1	T	2.50 + 18	2.88 + 18 (9)	1.15	4.56-03 (12)	1.58-21	1.35-10	3.378 + 07
Surry	2	X	3.02 + 18	3.05 + 18 (11)	1.01	4.81-03 (13)	1.58-21	1.30-10	3.687 + 07
North Anna	1	V	2.49 + 18	2.74 + 18 (9)	1.10	4.17-03 (11)	1.52-21	1.17-10	3.570 + 07
Pr. Island	1	V	5.21 + 18	6.09 + 18 (11)	1.17	1.05-02 (16)	1.72-21	2.46-10	4.248 + 07
Pr. Island	2	V	5.49 + 18	6.80 + 18 (10)	1.24	1.19-02 (13)	1.75-21	2.71-10	4.394 + 07
R. E. Ginna	1	R	7.60 + 18	1.17 + 19 (10)	1.54	2.18-02 (14)	1.86-21	2.62-10	8.328 + 07
R. E. Ginna	1	V	4.90 + 18	5.98 + 18 (14)	1.22	1.02-02 (22)	1.71-21	2.22-10	4.612 + 07
Kewaunee		V	5.59 + 18	6.46 + 18 (10)	1.16	1.16-02 (13)	1.80-21	2.86-10	4.057 + 07
Pt. Beach	1	S	--	8.51 + 18 (10)	--	1.48-02 (13)	1.74-21	1.27-10	1.163 + 08
Pt. Beach	1	R	2.22 + 19	2.17 + 19 (10)	0.98	4.41-02 (14)	2.03-21	2.70-10	1.632 + 08
Pt. Beach	2	T	9.45 + 18	9.47 + 18 (10)	1.00	1.59-02 (13)	1.68-21	1.46-10	1.087 + 08
Pt. Beach	2	V	4.74 + 18	7.33 + 18 (11)	1.56	1.23-02 (13)	1.68-21	2.56-10	4.805 + 07
Pt. Beach	2	R	2.01 + 19	2.54 + 19 (10)	1.26	4.68-02 (14)	1.84-21	2.85-10	1.640 + 08
D. C. Cook	1	T	1.80 + 18	2.78 + 18 (22)	1.54	4.61-03 (26)	1.66-21	1.16-10	3.991 + 07
Indian Pt.	2	T	2.02 + 18	3.34 + 18 (22)	1.65	5.49-03 (27)	1.64-21	1.23-10	4.473 + 07
Indian Pt.	3	T	2.92 + 18	3.30 + 18 (22)	1.13	5.38-03 (26)	1.63-21	1.28-10	4.211 + 07
Zion	1	T	1.80 + 18	3.06 + 18 (10)	1.70	4.97-03 (12)	1.62-21	1.31-10	3.789 + 07
Zion	1	U	8.92 + 18	1.02 + 19 (10)	1.14	1.68-02 (13)	1.65-21	1.49-10	1.123 + 08
Zion	2	U	2.00 + 18	2.82 + 18 (9)	1.41	4.54-03 (12)	1.61-21	1.13-10	4.007 + 07
Salem	1	T	2.56 + 18	2.91 + 18 (22)	1.14	4.77-03 (26)	1.64-21	1.39-10	3.426 + 07
Combustion Engineering									
Palisades		A240	4.40 + 19	6.10 + 19 (23)	1.39	9.77-02 (28)	1.60-21	1.37-09	7.130 + 07
Fort Calhoun		W225	5.10 + 18	6.22 + 18 (15)	1.22	9.20-03 (18)	1.48-21	1.12-10	8.191 + 07
Maine Yankee		1	1.30 + 19	1.79 + 19 (19)	1.38	2.43-02 (23)	1.64-21	1.05-09	2.777 + 07
Maine Yankee		2	8.84 + 19	7.85 + 19 (13)	0.89	1.25-01 (18)	1.59-21	8.61-10	1.446 + 08
Maine Yankee		W263	6.90 + 18	6.12 + 18 (13)	0.89	9.21-03 (15)	1.50-21	6.37-11	1.446 + 08
Babcock & Wilcox									
Oconee	1	F	8.70 + 17	7.10 + 17 (21)	0.82	9.83-04 (20)	1.38-21	3.74-11	2.629 + 07
Oconee	1	E	1.50 + 18	1.50 + 18 (10)	1.00	2.11-03 (10)	1.41-21	4.07-11	5.186 + 07
Oconee	2	C	9.43 + 17	1.02 + 18 (10)	1.08	1.50-03 (11)	1.47-21	3.95-11	3.802 + 07
Oconee	3	A	7.39 + 17	8.10 + 17 (10)	1.10	1.15-03 (11)	1.42-21	3.85-11	2.983 + 07
Three Mile Is.	1	E	1.07 + 18	1.09 + 18 (9)	1.02	1.53-03 (9)	1.40-21	3.80-11	4.036 + 07

*Equivalent constant power level exposure time.
**3.17 + 18 reads 3.17×10^{18} with a 12% (1σ) uncertainty.

TABLE 4

POWER REACTORS BEING USED BY LWR-PV-SDIP PARTICIPANTS
TO BENCHMARK PHYSICS-DOSIMETRY PROCEDURES AND DATA
FOR PRESSURE VESSEL AND SUPPORT STRUCTURE SURVEILLANCE*

(Plant name; reactor type/supplier; reactor operator; ex-vessel cavity (C) and in-vessel (V) surveillance positions available)

Energy Range (MeV)	Type of Dosimeter	Dosimetry Reaction	Nuclear One-1 PWR/B&W Arkansas Power & Light		Nucleur One-2 PWR/CE Arkansas Power & Light		Brown's Ferry-3 BWR/GE Tennessee Valley Authority		H.B. Robinson PWR/WEC Carolina Power & Light		Maine Yankee PWR/CE Maine Yankee Atomic Power		Point Beach-2 PWR/WEC Wisconsin Electric Power		McGuire PWR/WEC Duke Power		CR or DB PWR/B&W		Oconee 1,2&3 PWR/B&W Duke Power		BR-3 PWR/WEC Belgium	
			C	V	C	V	C	V	C	V	C	V	C	V	C	V	C	V	C	V	C	V
>1.5	RMs	$^{63}Cu(n,\alpha)^{60}Co^f$	Y		Y	Y	Y	Y	Y	Y	Y	Y		Y	Y	Y	P	Y	P		Y	Y
		$^{46}Ti(n,p)^{46}Sc^f$	Y		Y	Y	Y	Y	Y	Y	Y	Y			Y		P	P	PYJ		Y	Y
		$^{54}Fe(n,p)^{54}Mn^f$	Y	Y	Y	Y	Y	Y	Y	Y	Y	Y		Y	Y	Y	P	Y	PY	Y	Y	Y
		$^{58}Ni(n,p)^{58}Co^f$	Y	Y	Y	Y	Y	Y	Y	Y	Y	Y		Y	Y	Y	P	Y	PY	Y	Y	Y
		$^{238}U(n,f)^{140}Ba\text{-}La$	Y	(N)	Y	(N)	Y	Y	(N)	(N)	(N)	(N)	(N)	(N)	(N)	(N)	(N)	(N)	(N)	(N)	(N)	(N)
		$^{238}U(n,f)^{103}Ru$	(Y)	Y	(Y)	(Y)	Y	Y	Y	Y	Y	Y			Y	Y	P	Y	P	Y	Y	Y
		$^{238}U(n,f)^{95}Zr\text{-}Nb$	(Y)	Y	(Y)	(Y)	Y	Y	Y	Y	Y	Y			Y	Y	P	Y	P	Y	Y	Y
		$^{238}U(n,f)^{137}Cs$	(Y)	Y	(Y)	Y	Y	Y	Y	Y	Y	Y			Y	Y	P	Y	P	Y	Y	Y
>0.4		$^{232}Th(n,f)^{140}Ba\text{-}La$		(N)		(N)	(N)	(N)	(N)	(N)	(N)	(N)	(N)	(N)	(N)	(N)	(N)	(N)	(N)	(N)	(N)	
		$^{232}Th(n,f)^{95}Zr\text{-}Nb$					Y	Y									P	P				
		$^{232}Th(n,f)^{137}Cs$					Y	Y									P	P				
		$^{237}Np(n,f)^{140}Ba\text{-}La$	Y	(N)	Y	(N)	Y	Y	(N)	(N)	(N)	(N)	(N)	(N)	(N)	(N)	P	(N)	(N)	(N)		(N)
		$^{237}Np(n,f)^{103}Ru$	(Y)	Y	(Y)	(Y)	Y	Y	Y	Y	Y	Y			Y	Y	P	Y	P	Y		Y
		$^{237}Np(n,f)^{95}Zr\text{-}Nb$	(Y)	Y	(Y)	(Y)	Y	Y	Y	Y	Y	Y			Y	Y	P	Y	P	Y		Y
		$^{237}Np(n,f)^{137}Cs$	(Y)	Y	(Y)	Y	Y	Y	Y	Y	Y	Y		Y	Y	Y	P	Y	P	Y		Y
		$^{93}Nb(n,n')^{93m}Nb$								Y	Y	Y					P	P	P			Y
5×10^{-7} to 0.5^b		$^{59}Co(n,\gamma)^{60}Co^e$	Y	Y	Y	Y	Y	Y	Y	Y	Y	Y		Y	Y	Y	P	Y	PY	Y	Y	Y
		$^{109}Ag(n,\gamma)^{110m}Ag^e$	Y		Y	Y	Y	Y	Y	Y	Y	Y			Y		P	P	P		Y	Y
		$^{58}Fe(n,\gamma)^{59}Fe$	Y	Y	Y	Y	Y	Y	Y	Y	Y	Y			Y		P	Y	PY	Y	Y	Y
		$^{45}Sc(n,\gamma)^{46}Sc^e$	Y		Y	Y	Y	Y	Y		Y	Y			Y		P	P	PY		Y	Y
		$^{235}U(n,f)^{140}Ba\text{-}La$	Y	(N)	Y	(N)	Y	Y	(N)	(N)	(N)	(N)	(N)	(N)	(N)		(N)	(N)	(N)	(N)		(N)
		$^{235}U(n,f)^{103}Ru$	(Y)		(Y)		Y	Y	Y	Y	Y	Y			Y		P	P	P			Y
		$^{235}U(n,f)^{95}Zr\text{-}Nb$	(Y)		(Y)		Y	Y	Y	Y	Y	Y			Y		P	P	P			Y
		$^{235}U(n,f)^{137}Cs$	(Y)		(Y)		Y	Y	Y	Y	Y	Y			Y		P	P	P			Y
As Above[a]	SSTRs[g]	$^{238}U(n,f)FP$					Y		Y	Y	Y	Y			Y		P	P	P			
		$^{232}Th(n,f)FP$					Y								Y		P	P	P			
		$^{237}Np(n,f)FP$					Y		Y	Y	Y	Y			Y		P	P	P			
		$^{235}U(n,f)FP$					Y		Y	Y	Y	Y			Y		P	P	P		Y	
		$^{239}Pu(n,f)FP$					Y										P	P	P			
<0.1		$^{6}Li(n,\alpha)$															P	P	P			
		$^{10}B(n,\alpha)$															P	P	P			
>0.3		H(n,p) as CR-39		N		N		N		N		N	(N)	N		N	(P)	N	(P)			N
>4	HAFMs[d]	Ni(n,He) as metal[f]							(Y)	Y	(Y)	Y		Y	(Y)	Y	(P)	P	(Y)		(Y)	(Y)
		Al(n,He) as metal[f]	N		N		N		N	Y	(N)	Y		Y	N	Y	N	P	N		N	(Y)
		Cu(n,He) as metal[f]	N		N		N		N	Y	(N)	Y		Y	N	Y	N	P	N		N	(Y)
		Fe(n,He) as metal[f,h]	N		N		N		N	Y	(N)	Y		Y	N	Y	N	P	N		N	(Y)
>0.1[b]		$^{7}Li(n,He)$ as LiF															P	P				
		Be(n,He) as metal								Y	Y						P	P				(Y)
		S(n,He) as PbS									Y						P	P				
		F(n,He) as PbF_2									Y						P	P				
		Ca(n,He) as CaF_2									Y						P	P				
		N(n,He) as NbN or TiN									Y						P	P				(Y)
		Cl(n,He) as $PbCl_2$									Y						P	P				
		O(n,He) as GeO_2															P	P				
<0.1		$^{6}Li(n,He)$ as LiF or alloy								Y	Y						P	P				(Y)
		$^{10}B(n,He)$ nat. or alloy								Y	Y						P	P				(Y)
>0.1	DMs[c]	Quartz															P	P				
		Sapphire								Y							P	P				
		A302B[f,k]								Y				Y			P	P				
		A533B[f,k]								Y				(Y)		Y	P	P				
		Other Steel[f]								Y		Y				Y	P	P				P

*See footnotes for this table on next page. B & W, CE, GE, and WEC are Babcock and Wilcox, Combustion Engineering, General Electric, and Westinghouse Electric Company, respectively.

FOOTNOTES* for Table 4:

Power Reactors Being Used by LWR-PV-SDIP Participants

---

[a]Energy ranges for the solid state track recorders (SSTRs) are the same as those given for the fissionable radiometric sensors.

[b]Generally these reactions are used with cadmium, cadmium-oxide or gadolinium filters to eliminate their sensitivity to neutrons having energies less than 0.5 eV. The cavity measurements in the Arkansas Power & Light reactors have also included intermediate-energy measurements using thick (1.65 g/cm^2) boron-10 filters (shells) for the ^{235}U, ^{238}U and ^{237}NP fission sensors.

[c]DM means damage monitors (damage to the sensor crystal lattice, such as A302B and A533B or other steels with high copper content and high sensitivity to damage).

[d]HAFM means helium accumulation fluence monitors.

[e]Generally cobalt and silver are included as dilute alloys with aluminum. Scandium is normally ScO_2, and more recently as a $\sim$1% ScO_2-Al_2O_3 ceramic wire.

[f]Frequently when there is no specific HAFM dosimetry package, some of the radiometric sensors and some of the steel damage monitors serve as HAFMs after they have been analyzed for their principal function.

[g]Ni and/or Fe gradient disks were also included in the SSTR capsule, as required.

[h]Iron from RM sensors or Charpy specimens.

[i]Note that power plant CR is Crystal River-3 (Florida Power Corp.) and DB is Davis Besse-1 (Toledo Edison Co.).

[j]The Y following the P refers to a previous Oconee 2 test.

[k]Surveillance capsule reference correlation material (ASTM reference steel plates).

[l]The determination (or feasibility) of using any of the Oconee plants for future benchmark studies has yet to be made.

TABLE 5

RELATIVE RATIO FIRST ORR-SDMF RM SENSOR CERTIFICATION TEST*
(X/HEDL)-1 (%) (taken from Reference 42)

Set ID	Reaction	LABORATORY** A	B	C	D	E	F
HNF-1***	$^{58}Ni(n,p)$	2.38	- 7.05	-3.99	2.10	-1.60	-1.77
-3		2.16	- 6.34	-3.63	1.37	-2.60	0.24
-2		2.33	- 8.59	0.15	-0.93	-2.82	2.69
-4		3.34	- 9.24	-0.84	0.47	-2.03	3.90
HNF-1	$^{46}Ti(n,p)$	2.33	-10.6	3.60	1.43	-0.71	2.16
-3		1.10	-13.9	4.72	2.23	-2.11	1.82
-2		5.72	-7.52	6.98	5.76	-0.85	5.26
-4		4.56	-1.33	7.84	4.56	0.27	3.98
HNF-1	$^{63}Cu(n,\alpha)$	1.76	-3.38	8.59	-1.12	-2.27	8.05
-3		2.63	1.61	3.05	1.81	-2.00	2.01
-2		1.06	1.40	8.37	3.00	0.59	5.73
-4		4.66	1.85	6.50	2.00	2.14	6.85
HNF-1	$^{54}Fe(n,p)$	3.02	-6.31	1.95	-3.73	0.39	-5.37
-3		0.56	-10.26	0.11	-2.27	-3.35	-4.13
-2		2.19	-7.63	1.76	1.30	-3.96	0.24
-4		6.49	-7.53	4.69	1.52	0.68	-1.94
HNF-1	$^{58}Fe(n,\gamma)$	1.54				1.19	
-3		3.29				0.81	
-2		-4.87				-2.97	
-4		1.96				3.25	
HNF-3	$^{59}Co(n,\gamma)$	2.84	-1.55	7.45	1.09	1.83	-1.07
-5		0.06	-7.42	6.36	-1.00	-1.61	-0.52
-4		2.28	-1.84	7.74	1.56	2.82	1.28
-6		1.95	-9.21	6.76	3.72	-0.49	2.35

Set ID	Reaction	LABORATORY** A	B	C	D	E	F
HF-3	$^{235}U(n,f)^{140}Ba$	0.00			- 4.35	- 6.68	
HF-5		9.46			- 9.40	- 4.26	
HF-4		9.39			- 7.42	- 5.36	
HF-6		-2.92			-14.79	-13.08	
HF-3	$^{235}U(n,f)^{103}Ru$	5.27		-13.09	- 3.18	0.88	
HF-5		8.27		6.21	- 9.00	1.54	
HF-4		3.31		- 5.59	- 2.57	3.17	
HF-6		6.39		- 6.37	- 8.18	0.99	
HF-3	$^{235}U(n,f)^{95}Zr$	0.76	0.00	-13.49	4.99	- 2.84	
HF-5		5.67	-14.40	9.29	2.26	- 3.31	
HF-4		-2.40	- 6.49	-11.47	- 0.10	- 8.36	
HF-6		3.16	- 1.78	- 6.99	1.54	- 5.22	
HF-1	$^{237}Np(n,f)^{140}Ba$	1.27			- 6.38	-11.28	-5.58
HF-2		3.29			- 0.91	-13.29	-3.05
HF-1	$^{237}Np(n,f)^{103}Ru$	3.06		-31.26	- 4.37	- 0.92	-4.06
HF-2		4.11		- 6.94	2.91	- 3.28	-2.38
HF-1	$^{237}Np(n,f)^{95}Zr$	-0.22	10.59	- 9.06	4.12	- 4.40	-1.46
HF-2		1.99	5.38	- 4.76	10.83	- 2.80	-1.24
HF-1	$^{238}U(n,f)^{140}Ba$	2.96			- 2.19	- 5.60	-0.35
HF-2		0.65			- 0.40	- 7.05	-1.33
HF-1	$^{238}U(n,f)^{103}Ru$	5.48		- 4.29	- 1.93	0.46	-5.17
HF-2		3.74		1.65	2.08	- 2.51	-1.79
HF-1	$^{238}U(n,f)^{95}Zr$	1.72	2.60	- 5.81	8.55	- 2.56	1.37
HF-2		-1.58	4.41	- 3.83	5.35	- 6.62	-3.48

*The first RM sensor certification test and the Westinghouse and Combustion Engineering type surveillance capsule perturbation test; fluence (E > 1.0 MeV) of $\sim 6 \times 10^{18}$ n/cm^2 for the thermal shield back (TSB) and $\sim 9 \times 10^{17}$ n/cm^2 for the pressure vessel front (PVF) locations.

**Four vendors and two service laboratories in the U.S. participated in this test. All laboratories remain anonymous for these intercomparisons and are identified only as Laboratories A, B, C, D, E and F.

***HNF-1 and -3 and HF-1, -3 and -5 are the TSB and HNF-2 and -4 and HF-2, -4 and -6 are the PVF locations, respectively.

TABLE 6

RELATIVE RATIO SECOND ORR-SDMF RM SENSOR CERTIFICATION TEST*
(X/HEDL)-1 (%) (taken from Reference 42)

Reaction		Laboratory**						
		A	B	C-1	C-2	D	E	F
$^{58}Ni(n,p)$		1.40		- 9.57	- 6.85	-0.96		
$^{63}Cu(n,\alpha)$		0.88		- 3.71	- 2.04	1.84		
$^{54}Fe(n,p)$		1.98		- 7.38	- 3.42	0.75		
$^{58}Fe(n,\gamma)$		0.11		- 2.51	0.22	2.17		
$^{59}Co(n,\gamma)$		1.30		- 4.32	- 1.44	1.65		
$^{237}Np(n,f)$	^{103}Ru	3.42		- 9.70	-10.4			
	^{95}Zr	- 1.58		-10.9	- 5.6			
	^{137}Cs			- 7.83	- 1.34	1.73		
$^{238}U(n,f)$	^{103}Ru	2.09		-11.9	- 8.86			
	^{95}Zr	- 0.78		-11.6	1.58			
	^{137}Cs			-16.8	-7.96	1.38		

*The second RM sensor certification test and the ORR-PSF first simulated surveillance capsule (SSC-1) metallurgical irradiation; fluence (E > 1.0 MeV) of $\sim 2 \times 10^{19}$ n/cm^2.

**Four vendors and two service laboratories in the U.S. participated in this test. All laboratories remain anonymous for these intercomparisons and are identified only as Laboratories A, B, C, D, E and F.

TABLE 7

SPECIFIC ACTIVITIES MEASURED BY THE DIFFERENT LABORATORIES
FOR THE ORR-SDMF STARTUP TEST
AND FIRST EUROPEAN LABORATORY RM SENSOR CERTIFICATION TEST
(taken from Reference 43)

	REACTION	SPECIFIC ACTIVITIES RELATIVE TO SCK/CEN				RECOMMENDED SPECIFIC ACTIVITIES ($Bq\ g^{-1}$)	σ (%)
		INTERLABORATORY CAPSULE		AERE/RR & A CAPSULE			
		ECN	PTB	$(AERE)_1$ (1)	$(AERE)_2$ (1)		
SSC	$^{93}Nb(n,n')$	1.17			1.02	$2.062\ 10^7$	9.0
	$^{58}Ni(n,p)$		1.01	1.09	1.05	$7.242\ 10^8$	3.9
	$^{54}Fe(n,p)$	1.01	1.00	1.07	1.10	$1.103\ 10^7$	4.3
	$^{46}Ti(n,p)$	0.99	1.02	1.12	1.07	$8.508\ 10^6$	5.3
	$^{63}Cu(n,\alpha)$	1.02	1.01	0.99(2) (1.29)	(1.05)	$1.201\ 10^5$	1.4
1/4 T	$^{237}Np(n,f)$ ^{95}Zr	0.97	0.98			$3.437\ 10^7$	1.6
	$^{237}Np(n,f)$ ^{137}Cs	0.96	0.98			$2.522\ 10^5$	2.0
	$^{238}U(n,f)$ ^{95}Zr	0.95	0.98			$3.508\ 10^6$	2.6
	$^{238}U(n,f)$ ^{137}Cs	0.99	0.97			$2.738\ 10^4$	1.4
	$^{93}Nb(n,n')$				1.00	$1.330\ 10^6$	0.3
	$^{58}Ni(n,p)$	1.00	1.00	1.07	1.03	$4.472\ 10^7$	3.1
	$^{54}Fe(n,p)$	1.00	0.98	1.11	1.09	$6.956\ 10^5$	6.0
	$^{46}Ti(n,p)$	1.00	1.01	1.12	1.04	$5.851\ 10^5$	4.9
	$^{63}Cu(n,\alpha)$	1.01	1.01	1.01(2) (1.15)	(1.08)	$9.206\ 10^3$	0.5
1/2 T	$^{93}Nb(n,n')$				0.85	$6.643\ 10^5$	11.3
	$^{58}Ni(n,p)$	0.99		1.09	1.02	$1.721\ 10^7$	4.4
	$^{54}Fe(n,p)$	0.97	1.00	1.10	1.10	$2.606\ 10^5$	6.0
	$^{46}Ti(n,p)$	0.98	1.02	1.13	1.07	$2.161\ 10^5$	5.8
	$^{63}Cu(n,\alpha)$	1.03	1.02	1.02(2) (1.37)	(1.30)	$3.465\ 10^3$	1.0
3/4 T	$^{93}Nb(n,n')$				0.84	$3.338\ 10^5$	11.9
	$^{58}Ni(n,p)$	1.00	0.99	1.07	1.00	$6.310\ 10^6$	3.3
	$^{54}Fe(n,p)$	1.00	1.00	1.10	1.07	$9.306\ 10^4$	4.7
	$^{46}Ti(n,p)$	0.96	0.98	(0.76)	1.01	$7.566\ 10^4$	2.2
	$^{63}Cu(n,\alpha)$	1.00	1.01	1.02(2) (1.46)	(1.27)	$1.245\ 10^3$	0.9

(1) $(AERE)_1$: MEASUREMENTS PERFORMED AT HARWELL; $(AERE)_2$: MEASUREMENTS PERFORMED AT WINFRITH

(2) Cu FOIL FROM INTERLABORATORY CAPSULE

UNITED STATES NUCLEAR REGULATORY COMMISSION

TENTH WATER REACTOR SAFETY RESEARCH INFORMATION MEETING

(Held at the National Bureau of Standards, Washington DC, October 12 - 15 1982)

DESCRIPTION AND STATUS OF THE NESTOR DOSIMETRY IMPROVEMENT PROGRAMME (NESDIP)

Author: M Austin, Rolls-Royce and Associates Ltd, Derby, England.

1. NESTOR DOSIMETRY IMPROVEMENT PROGRAMME OBJECTIVES

The NESTOR Dosimetry Improvement Programme (NESDIP) comprises a series of experiments in which, in conditions broadly representative of current Light Water Reactor designs, some outstanding problems of Pressure Vessel (PV) dosimetry and monitoring can be explored. The objectives of the programme are as follows:-

1) To provide 'benchmark' quality measurements of neutron and gamma-ray fields against which calculational methods for predicting damage to PV and reactor internals can be validated. In addition provision will be made for the further development or refinement of necessary dosimetry measurement techniques.
2) To ensure that the programme complements, and where necessary extends, the scope of other international programmes in the PV dosimetry area - for example the USNRC/SDIP and the VENUS programmes.
3) To incorporate, as part of this complementary role, the requirements of external calculational and experimental groups in the development of the NESDIP. (This requirement has to conform to the overall level of time and resources available to the programme).
4) To provide reports of calculational and experimental data derived as part of the programme in an available form, in a manner similar to those provided as part of the USNRC/SDIP.

2. INTENDED SCOPE OF THE NESDIP

The NESDIP is being carried out on the ASPIS facility of the NESTOR reactor situated at the United Kingdom Energy Authority Establishment, Winfrith, England. Reference has been made elsewhere, (1,2) to the main differences between the UK facility and its US counterpart at the Oak Ridge National Laboratory, (the Pool Critical Assembly). In essence the radiation source for ASPIS is a fission-plate rather than a volume-distributed core thereby ensuring a precise definition of source terms in experiment and calculation. In addition the 'cave' facilities of ASPIS provide a convenient environment in which the proposed experiments may be performed, thus facilitating their easy mounting and dissembly. As will be further explained below it is also possible to extend the ASPIS cave facility to "mock-up" features such as the PV 'Cavity' which have not to date been amenable to benchmark quality experimental investigation. As mentioned in Section 1 the programme development depends to a large extent on input from interested parties, so that, at present, the following three broad phases of the NESDIP have been identified. These are:-

Phase 1 - the 'Replica' experiment
Phase 2 - Pressure Vessel Cavity Simulation studies
Phase 3 - Pressure Vessel Support-structure and Streaming studies

Of these, Phase 1 of the programme has been started and is initially supporting UK methods development work in the dosimetry area and measurements to aid the evaluation of UK specimens irradiated in the ORNL Poolside Facility experiment. Detailed proposals for Phases 2 and 3 have not yet been agreed and the opportunity for input from groups other than the UK participants has yet to be formally examined. it is hoped that such planning can proceed within the next few months.

However it is possible to describe briefly the work envisaged under the phases given above and reference should be made to the accompanying figures (Figs 3 - 8).

2.1 The Replica Experiment

As is evident from Figs 3, 6, 7 and 8, the purpose of this phase is to essentially reproduce the features of the Oak Ridge PCA measurement arrays with the important difference that the core source of radiation is replaced by a fission-plate. In addition full use will be made of the Winfrith experience in active neutron spectrometry to derive full range-of-interest (0.1 – 10 MeV) neutron spectra in measurement positions of interest. (It is possible within this arrangement to produce any of the arrays used for the US PCA measurements). In the initial experiments attention will be concentrated on the "12/13" configuration. The UK programme planned for this phase will aim at providing detailed neutron measurements for the development and validation of adjustment techniques currently under investigation in the UK and linked to PV Cavity measurements. Some work in the "4/12" array will be carried out to facilitate the analysis of the UK metallurgical specimens irradiated in off-axis positions of the ORNL/PSF experiment.

2.2 PV Cavity Simulation Studies

It is possible to provide, in the ASPIS cave, a "roof slot" facility which may be used very effectively to simulate PV Cavity arrangements, representative of LWR plants, (see Fig. 4). In this phase of the work it will be possible to measure not only relevant reaction-rates and spectra in the cavity, but also to investigate the effect of varying associated design parameters such as a range of cavity dimensions and structural materials, in validating calculational and measurement techniques. This is seen as an ideal experimental arrangement for the investigation of the application of cavity-monitoring techniques to the prediction of damage-rates within the PV itself.

2.3 PV Support Structures and Streaming Studies

This phase may be seen as an extension of the investigation into the practical problems of carrying out cavity-monitoring measurements with high accuracy, but further, as a means of investigating the effects of neutron spectrum and streaming upon other features to which attention has been drawn as part of the USNRC/SDIP, (for example the reactor pressure vessel support structure). Fig. 5 merely serves to indicate the potential present in the ASPIS facility for "mocking-up" such support structure arrangements.

Succeeding sections of this paper deal with current progress and proposed future activity but it should be stressed that the detailed planning of later phases of the NESDIP are intended to reflect as wide a range of design and analysis requirements as possible, and that early input is sought from interested groups who may intend to participate.

3. MEASUREMENTS TO BE PERFORMED IN THE NESDIP

ASPIS is a penetration-benchmark facility in which the power is restricted in order to reduce background activation and maintain a clean environment for spectrometry measurements. Thus reaction-rate measurements will be obtained with indium, rhodium, sulphur and nickel foils at a representative range of positions throughout the arrays to be studied. These results will be supplemented by active spectrometry measurements using the well-established Winfrith hydrogen proportional-counter techniques (covering the energy range 0.1 - 2 MeV) and the NE213 spectrometer (covering the range 2 - 10 MeV). Experience has demonstrated the feasibility of using individual proportional counters as "integral detectors" in their own right in regions where low sensitivity precludes the use of activation monitors. Moreover consistency between spectrum measurements and activation techniques is always sought by 'predicting' reaction-rates from the measured spectrum and the activation cross-sections. In addition to the neutron measurements the NESDIP will place more emphasis on the evaluation of the gamma-ray environment within the chosen experimental arrays. These measurements will include the estimation of integral quantities using thermoluminescent dosimeter techniques, and, it is hoped, assessment of the gamma-spectra at key positions. The environment and access would be very suitable for such a characterisation using the HEDL JANUS probe.

It is intended to reference the measurement techniques (both neutron and gamma-ray) by making use of the NESSUS facility of the NESTOR reactor (see Fig. 10) although such "benchmark-referencing" can be usefully extended in principle to include any other benchmark field which may be suggested by participants. Particular attention is being paid to the development of niobium as a fluence monitor: measurements of the cross-section are being made and integral checks carried out by irradiation in NESSUS, British MTR's, and other standard fields.

4. CURRENT NESDIP STATUS

As mentioned above, only Phase 1 of the programme has been planned in detail and this is currently being carried out. The timescales envisaged for this stage of the programme are outlined on Fig. 11 and cover the period from September 1982 to March 1983. Significant effort has been invested in careful characterisation of the source distribution in the fission-plate and this is now substantially complete. First measurements in the Phase 1 programme are concentrated on the "12/13" array and in this configuration foil measurements have been carried out at all centre-line locations and spectral information obtained at the T/4 and Cavity positions using the hydrogen proportional counters. As shown by Fig. 11 the remainder of the currently planned NESDIP period will be devoted to completing centre-line activation foil measurements, checking off-axis locations and performing first irradiations of gamma-ray detectors.

As mentioned, a real advantage of the ASPIS cave facility is the ease with which experiments can be mounted and dismantled. Thus although it will be necessary to re-assemble the 'Replica' experiment during 1983 for further measurements this poses no difficulties in terms of run-to-run reproducibility. It is hoped that during these operating periods the first opportunity will be taken to irradiate detectors from other participating groups (at present principally Mol and HEDL) and proposals for further measurements by other potential participants are welcomed.

5. NESDIP: THE COMPLEMENTARY CONTEXT

As explained in Section 1 NESDIP is seen as part of a complementary cycle of benchmark experiments which includes the PCA programme and the VENUS programme at Mol in Belgium. These are aimed, in their entirety, at a comprehensive investigation of current problems and techniques for pressure vessel dosimetry (see Fig. 12). It should be noted that each programme possesses its own, independent, features. Thus the PCA was able to present an extended core source and pressure vessel array capable of a wide dynamic range in terms of activation and fission-foil measurements.

As a result of this programme the importance of calculation and representation of core sources was recognised together with some features of the transport calculation of penetrating neutrons within the PV array. The purpose of NESDIP therefore is to provide first a replica of the PCA PV array driven by a fission-plate in which source representation uncertainties were reduced to a minimum (by virtue of the thin plate source) and secondly to extend the PCA "Cavity-box" concept to include a full-range, full-depth cavity facility. In the VENUS programme the cycle will be completed by an experimental array which will concentrate heavily upon the representation of a typical LWR core in which core physics calculations and fuel-management strategies can, in principle, be investigated.

By means of such a cyclic programme, and the international collaboration which typified the USNRC/SDIP it is hoped that these projects will achieve their common goal of resolving outstanding PV dosimetry problems and of standardising the solution techniques.

6. REFERENCES

1. Minutes of the 8th LWR-PV Surveillance Dosimetry Improvement Programme Meeting (published November 10, 1981)
2. 'Sense of Direction: An Observation of Trends in Materials Dosimetry in the United Kingdom', M. Austin; Proceedings of the 4th ASTM-EURATOM Symposium on Reactor Dosimetry (March 22 - 26, 1982)

NESDIP

NESTOR DOSIMETRY IMPROVEMENT PROGRAMME

OBJECTIVES

1. To provide a 'clean-source' UK PV-Steels benchmark experiment for methods-testing.
2. To extend scope of US-NRC/SDIP benchmark programme in important areas of interest.
3. To complement information from other international dosimetry programmes.

Fig. 1

SCOPE OF **NESDIP** PROGRAMME

PHASE 1	ORNL-PCA 'REPLICA' (Neutronics checks; PSF methods checks; extended γ ray measurements)
PHASE 2	SIMULATED PV - CAVITY (Development of Cavity-monitoring and interpolation; Cavity size effects; neutron streaming corrections)
PHASE 3	SIMULATED PV - SUPPORT STRUCTURE (PV - nozzle effects; support structure dosimetry)

Fig. 2

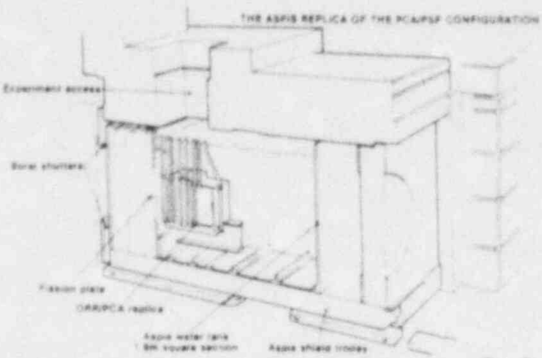

Fig. 3

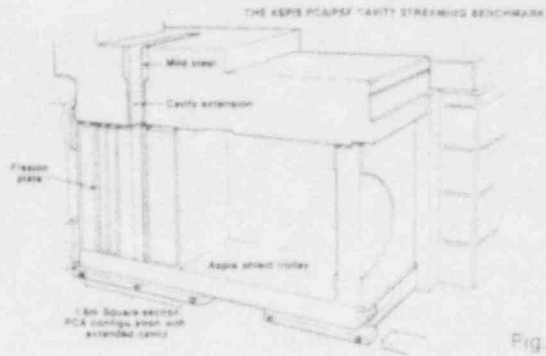

Fig. 4

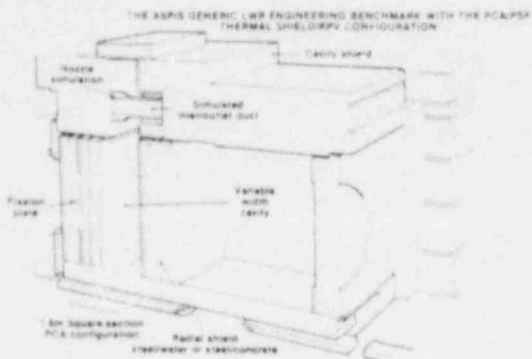

Fig. 5

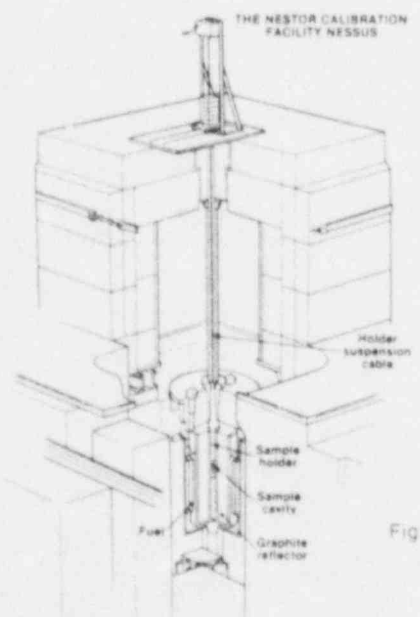

Fig. 10

NESDIP

PROPOSED MEASUREMENT TECHNIQUES

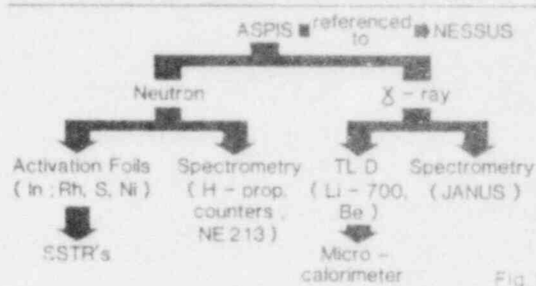

Fig. 9

NESDIP

DRAFT PROGRAMME PROPOSALS

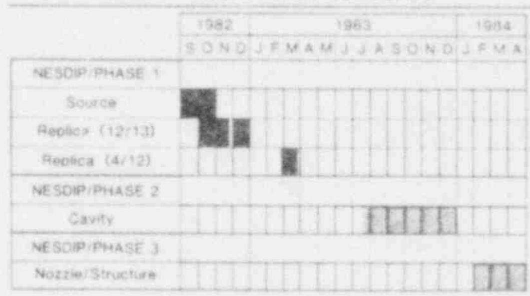

Fig. 11

NESDIP

PROGRAMME CONTEXT

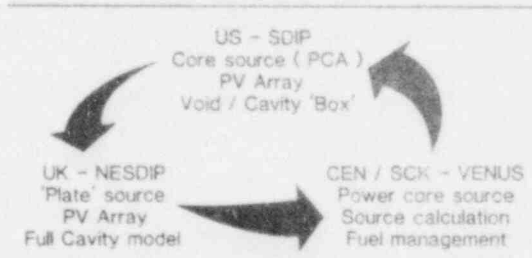

Fig. 12

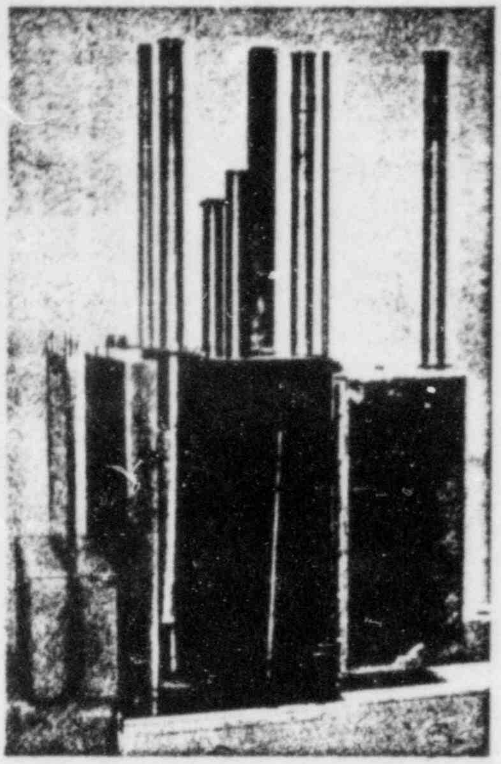

Fig. 6

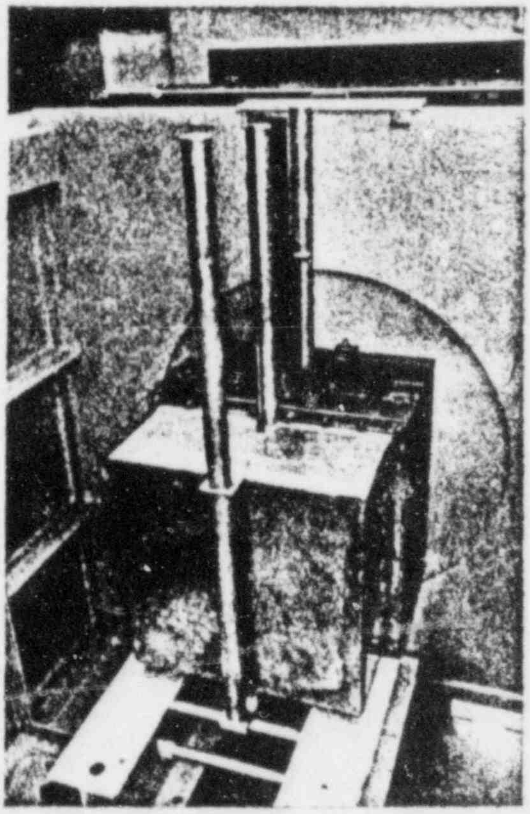

Fig. 7

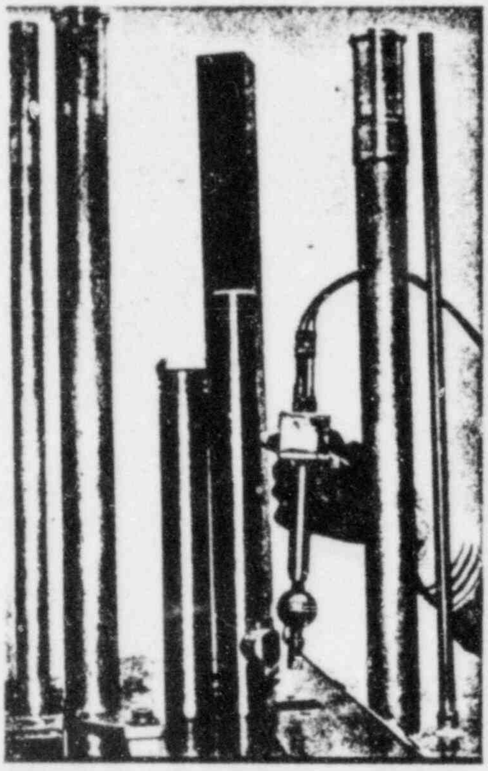

Fig. 8

THE INTEGRITY OF PWR PRESSURE VESSELS DURING OVERCOOLING ACCIDENTS*

R. D. Cheverton S. K. Iskander G. D. Whitman

Oak Ridge National Laboratory
Oak Ridge, Tennessee 37830, U.S.A.

ABSTRACT

The reactor pressure vessel in a pressurized water reactor is normally subjected to temperatures and pressures that preclude propagation of sharp, crack-like defects that might exist in the wall of the vessel. However, there is a class of postulated accidents, referred to as overcooling accidents, that can subject the pressure vessel to severe thermal shock while the pressure is substantial. As a result of such accidents vessels containing high concentrations of copper and nickel, which enhance radiation embrittlement, may possess a potential for extensive propagation of preexistent inner surface flaws prior to the vessel's normal end of life.

For the purpose of evaluating this problem a state-of-the-art fracture-mechanics model was developed and has been used for conducting parametric analyses and for calculating several recorded PWR transients. Results of the latter analysis indicate that there may be some vessels that have a potential for failure in a few years if subjected to a Rancho Seco-type transient. However, the calculational model may be excessively conservative, and this possibility is under investigation.

INTRODUCTION

The reactor pressure vessel in a pressurized water reactor (PWR) is normally subjected to temperatures and pressures that preclude propagation of sharp, crack-like defects (flaws) that might exist in the wall of the vessel. However, there is a class of postulated accidents, referred to as overcooling accidents (OCA's), that allow cool water to come in contact with the inner surface of the vessel wall, resulting in high thermal stresses and a reduction in fracture toughness near the inner surface. This introduces the possibility of propagation of preexistent inner-surface flaws, and this possibility increases with reactor operating time because of the additional reduction in fracture toughness that results from exposure of the vessel material to fast neutrons.

Thermal loading (thermal shock) by itself presumably cannot drive a flaw all the way through the wall; however, if the primary-system pressure is substantial, a

*Research sponsored by the Office of Nuclear Regulatory Research, U.S. Nuclear Regulatory Commission under Interagency Agreements 40-551-75 and 40-552-75 with the U.S. Department of Energy under contract W-7405-eng-26 with the Union Carbide Corporation.

potential for vessel failure could exist; that is, a preexistent flaw, under proper circumstances, could penetrate the vessel wall and provide a large enough opening to prevent flooding of the reactor core. The nuclear industry has been aware of this problem for quite some time, [1,2,3] but the probability of the existence of the requisite conditions for significant flaw propagation seemed very remote. In recent years however, several PWR OCA initiating events have occurred, [4,5,6] and there has also been a growing awareness that copper and nickel significantly enhance radiation damage in the vessel. [7,8] As a result a reevaluation of the integrity of PWR pressure vessels during OCA's has been undertaken.

A complete evaluation of the OCA problem in terms of its threat to pressure vessel integrity requires consideration of a number of factors, including postulated accident initiating events, reactor system and operator response to these events, specific design features of the reactor vessel and core that affect fluence-rate and coolant-temperature distributions adjacent to the inner surface of the vessel wall, sensitivity of the vessel material to radiation damage, size and orientation of preexistent flaws, and remedial measures. This paper examines primarily the fracture-mechanics-related conditions that could lead to a potential for vessel failure.

THE TENDENCY FOR INNER-SURFACE FLAWS TO PROPAGATE DURING THERMAL-SHOCK LOADING ONLY

The tendency for inner-surface flaws to propagate as a result of thermal-shock loading is illustrated in Fig. 1, which shows the temperature, resultant thermal stress, and fracture toughness distributions through the wall of the vessel (exclusive of cladding) at a particular time during a postulated large-break loss-of-coolant accident (LBLOCA). Also included in the figure for the same time in the transient are the stress intensity factors (K_I) for long axial flaws of different depths and the radial distribution of the fast neutron fluence. As indicated, the positive gradient in temperature and the steep attenuation of the fluence result in positive gradients in the crack initiation toughness (K_{Ic}) and the crack arrest toughness (K_{Ia}), and these positive gradients tend to limit crack propagation. However, K_I for the assumed long axial flaw also increases with flaw depth, except near the back surface, and for the particular case and time analyzed it is evident that both shallow and deep flaws can initiate; that is, $K_I \geq K_{Ic}$ for a broad range of crack depths. As the crack tip moves through the wall it encounters higher toughness material and for this particular case eventually arrests.

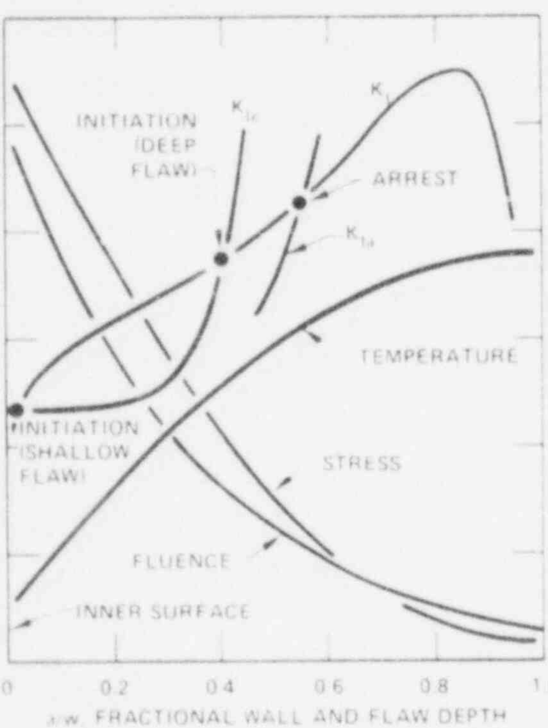

Fig. 1. Radial distributions in a vessel wall of several fracture-mechanics-related parameters at a specific time during a PWR LOCA.

If the crack depths corresponding to the initiation and arrest events are plotted as a function of the times in the transient at which the events take place, a set of curves referred to as the critical-crack-depth curves is obtained that indicates the behavior of the flaw during the entire transient. A typical set of critical-crack-depth curves for a LBLOCA is shown in Fig. 2. As indicated by the dashed lines the long axial flaw would propagate in a series of initiation-arrest events and, if a phenomenon referred to as warm prestressing (WPS) were not effective, would penetrate deep into the wall.

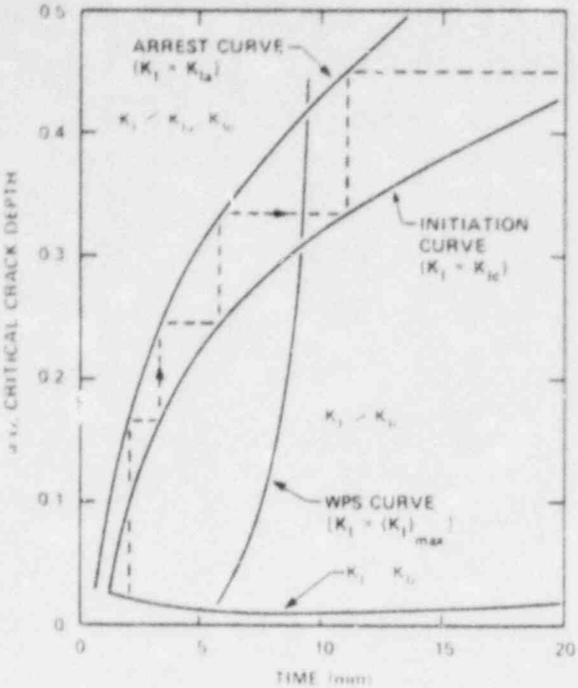

Fig. 2. Critical-crack-depth curves for a PWR LOCA assuming a long axial flaw, high concentrations of copper and nickel, and normal end-of-life fluence.

Warm prestressing, as referred to above, is a term used to describe a situation where K_I is decreasing with time (t) when K_I becomes equal to K_{Ic} by virtue of a decrease in temperature. It has been postulated[9] and demonstrated experimentally[9,10] that under these conditions a flaw will not propagate; that is, a flaw will not initiate while K_I is decreasing. In Fig. 2 the WPS curve is the locus of points for $K_I = (K_I)_{max}$ ($dK_I/dt = 0$). To the left of the WPS curve $dK_I/dt > 0$ and thus crack initiation can take place, but to the right of the WPS curve $dK_I/dt < 0$, and crack initiation will not take place. For the particular case illustrated in Fig. 2, WPS limits crack propagation to ~40% of the wall thickness.

Even if WPS were not effective, the flaw could not completely penetrate the wall under thermal-shock loading conditions only. This is a result of the substantial decrease in K_I as the crack tip approaches the outer surface (see Fig. 1) and has been demonstrated recently in a thermal-shock experiment.[11] However, when pressure is applied in addition to the thermal loading, the possibility of vessel failure (complete penetration of the wall) exists for some assumed conditions.

FRACTURE MECHANICS CALCULATIONAL MODEL

Linear elastic fracture mechanics (LEFM)[12] has been used thus far to analyze the behavior of a flaw during the postulated overcooling accidents. The initial flaw was assumed to be quite long on the vessel surface, to be oriented either in an axial or circumferential direction and to extend radially through the cladding into the base material. The thin layer of stainless steel cladding on the inner surface was included as a discrete region, in which case its effect on temperature and stress and thus K_{Ic}, K_{Ia}, and K_I were accounted for.

Fracture toughness data (K_{Ic} and K_{Ia} vs T − RTNDT, where T is the temperature and RTNDT is the reference nil ductility temperature) were taken from ASME Section XI,[13] and the reduction in toughness due to radiation damage was estimated using Eq. 1, which was recently proposed (tentatively) by Randall[8] as a revision to Reg. Guide 1.99, Rev. 1.[14]

$$\Delta RTNDT = f\,(Cu, Ni, F) \propto (F)^{0.27} , \qquad (1)$$

where

$2 \times 10^{17} \leq F \leq 6 \times 10^{19}$ neutrons/cm^2 ,

ΔRTNDT = change in RTNDT at tip of flaw due to fast neutron exposure,

Cu, Ni = copper and nickel concentrations, wt %

F = fast neutron fluence ($E \geq 1$ MeV) at tip of flaw

A typical attenuation of the fluence through the wall of the vessel that includes a correction for the effect of displaced atoms (DPA) on radiation damage was also recently proposed by Randall[8] and is being used in the ORNL studies. The relation is

$$F = F_o e^{-0.0094a\ mm^{-1}} , \tag{2}$$

where

F = fast neutron fluence at tip of flaw

F_o = fast neutron fluence at inner surface of vessel

a = depth of flaw

It is of interest to note that the use of Eq. 1 as oppo:ed to Reg. Guide 1.99, Rev. 1, and the inclusion of the effects of DPA in the fluence attenuation equation result in relatively greater estimated values of radiation damage (ΔRTNDT) deep in the wall of the vessel.

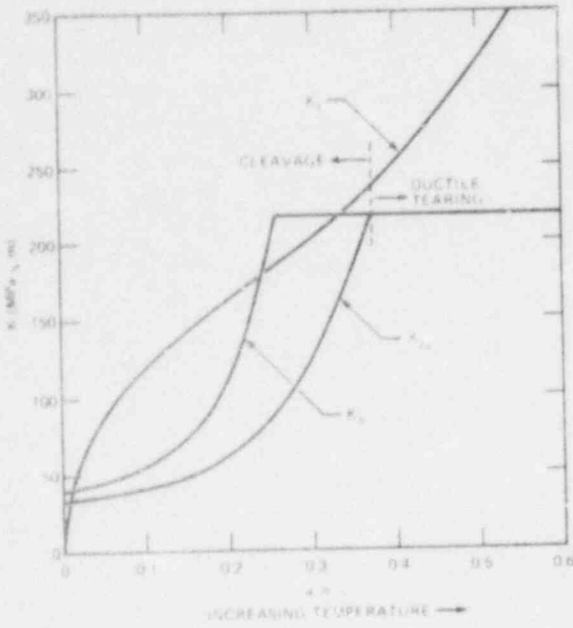

Fig. 3. Plots of K_I, K_{Ic} and K_{Ia} vs fractional crack depth at a specific time in an OCA transient, indicating initiation but no arrest unless on the upper shelf.

For some postulated OCA's, following crack initiation the tip of the fast-running crack will encounter upper-shelf-toughness temperatures prior to crack arrest, as illustrated in Fig. 3. Since techniques are not yet well established for evaluating flaw behavior under these conditions, it was assumed that crack arrest would not occur if K_I was above an arbitary upper-shelf toughness value of 220 MPa $\sqrt{m}$ prior to a calculated arrest event.

The procedure used for evaluating the integrity of a pressure vessel was to calculate, using the above model, the threshold or critical values of RTNDT corresponding to incipient initiation (II) of a flaw and incipient failure (IF) of the vessel (extension of the flaw through the wall) and then compare these critical values with the estimated actual values for a particular PWR pressure vessel. To obtain the critical values of RTNDT it is necessary to specify a transient, the fracture-mechanics model, a failure criterion and an initial (zero fluence) value of RTNDT ($RTNDT_o$), although the results are not very sensitive to the latter parameter. To obtain the actual value of RTNDT for a specific plant it is necessary to have a consistent set of values for the fluence, Cu, Ni and $RTNDT_o$ that corresponds to an area of the vessel wall that is most likely to experience propagation of a flaw; that is, the area in which the worst combination of the four parameters exists.

For convenience the particular values of RTNDT that are compared with each other are the values corresponding to the inner surface of the vessel wall, using material properties for the base material rather than for the cladding. These values of RTNDT are referred to herein as $(RTNDT_s)_c$, the critical value, and $(RTNDT_s)_A$, the actual value.

The critical value of RTNDT is the minimum value, with respect to both time in the transient and crack depth, that results in $K_I = K_{Ic}$ and/or crack penetration of the wall (no arrest). Since K_{Ic} = f (T, $RTNDT_o$, ΔRTNDT) only,[13] where T is the temperature at the crack tip, it is only necessary to determine these three parameters and K_I to perform the analysis. Values of ΔRTNDT are calculated from Eq. 3, which was obtained by combining Eqs. 1 and 2.

$$\Delta RTNDT = \Delta RTNDT_s \; e^{-2.54 \times 10^{-3} a \; mm^{-1}} \tag{3}$$

The complete analysis for obtaining $(RTNDT_s)_c$ was performed with the computer code OCA-II,[15] which accepts as input the downcomer-coolant-temperature and primary-system-pressure transients and automatically searches for $(\Delta RTNDT_s)_c$. For some OCA's $(\Delta RTNDT_s)_c$ corresponds to incipient initiation followed by crack arrest and no reinitiation, as shown in Fig. 4 assuming WPS to be ineffective. However, increasing $\Delta RTNDT_s$ will eventually result in failure (no arrest), and the corresponding minimum value is $(\Delta RTNDT_s)_c$ for incipient failure. For other OCA's, $(\Delta RTNDT_s)_c$ corresponds to both incipient initiation and incipient failure because, as shown in Fig. 5, there is no arrest following initiation of a shallow flaw. This latter situation tends to be typical of high-pressure transients and the former of low-pressure transients.

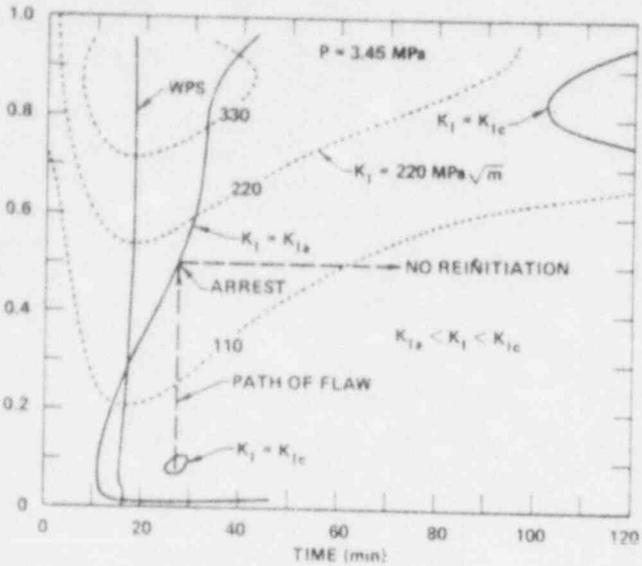

Fig. 4. Critical-crack-depth curves for an OCA illustrating incipient initiation followed by arrest and no reinitiation.

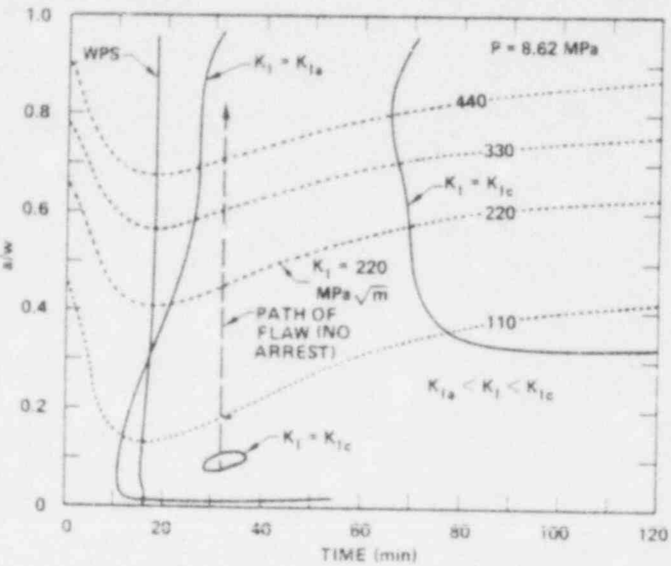

Fig. 5. Critical-crack-depth curves for an OCA illustrating incipient initiation and failure (no arrest unless on the upper shelf).

The sets of critical-crack-depth curves in Figs. 4 and 5 include the locus of points for constant values of K_I. This allows one to determine if arrest takes place in accordance with a maximum specified value for K_{Ia} (220 MPa $\sqrt{m}$ for these studies). In Fig. 4 it does and in Fig. 5 it does not. [The initiation and arrest curves in Figs. 4 and 5 were extended beyond points corresponding to existing maximum values for K_{Ic} and K_{Ia} (~200 MPa $\sqrt{m}$) using the K_{Ic} and K_{Ia} equations in Ref. 13 for extropolation purposes; thus, the extensions of the initiation and arrest curves beyond these points are fictitious to some extent but nevertheless allow one to apply different upper-shelf toughness values when using the critical-crack-depth curves to evaluate flaw behavior.]

The existence of two initiation loops (locus of points for $K_I = K_{Ic}$) in Figs. 4 and 5 suggests additional criteria for calculating $(\Delta RTNDT_s)_c$. One is a reasonable range of depths for initial flaws, and the other is the duration of the transient (t_{max}). For the cases depicted by Figs. 4 and 5, specification of a maximum initial fractional flaw size of 0.15 made a difference, because for lower values of $\Delta RTNDT_s$ the small initiation loop (actually just a point for incipient initiation) would disappear, and $(\Delta RTNDT_s)_c$ would be determined by the other initiation loop in accordance with some other criteria such as a greater critical flaw depth.

EVALUATION OF THE FM MODEL

The validity of LEFM for application to thermal-shock problems has been verified in a series of thermal-shock experiments with thick-walled steel cylinders.[10,11,16] These experiments were designed to exhibit flaw behavior trends calculated to exist during OCA's and thus included initiation and arrest of long axial shallow and deep flaws, a stepwise progression of the flaw deep into the wall, arrest in a rising K_I field ($dK_I/da>0$) and WPS with $dK_I/dt<0$. There are still some areas of uncertainty, but in each of these areas the FM model described above is believed to be conservative. The degree of conservatism is not known at this time, but programs are underway to obtain such information. The presumed conservative features in the model include (1) consideration of long flaws that extend through the cladding, (2) no arrest on the upper shelf, and (3) to some extent a disregard for the beneficial effects of warm prestressing. Long surface flaws have a greater potential than others for penetrating deep into the wall, but the probability of a long flaw existing as an initial flaw and of any length flaw extending through the cladding presumably is very small. One justification for assuming long flaws was that under thermal-shock loading conditions and in the absence of cladding short flaws tend to extend on the surface to become long flaws.[17] However, it may be that the cladding will prevent short flaws from extending on the surface and if so would limit radial growth of the flaw.[18]

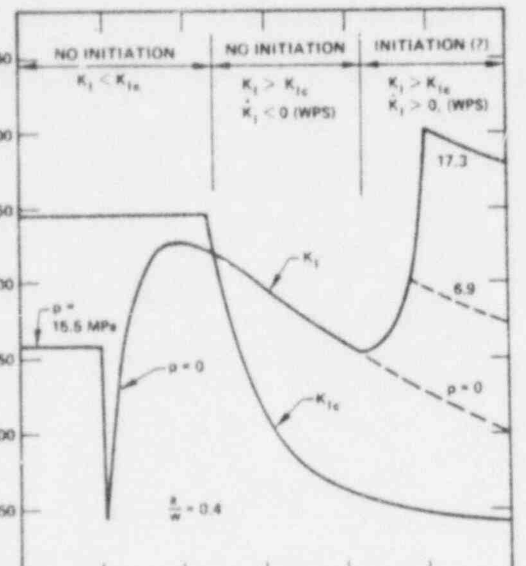

Fig. 6. Illustration of an OCA transient involving repressurization and two types of WPS.

If long flaws through the cladding must be considered, there is still the possibility that the tearing resistance of the material will be sufficient to permit arrest on the upper shelf, and it is also possible that WPS effects in addition to the one mentioned earlier will help to limit flaw propagation. For instance, Fig. 6, which compares K_I and K_{Ic} for a particular crack depth during a postulated transient involving loss of pressure and then repressurization, indicates two types of WPS. During normal operation of the reactor ($t<o$), the material toughness corresponds to upper shelf conditions and K_I is relatively low, as indicated. The transient starts at time zero, and as it progresses K_I becomes equal to K_{Ic}, but only after K_I has begun to decrease with time. Thus, crack initiation would not take place even though K_I becomes substantially greater than K_{Ic}. When repressurization finally takes place, K_I increases with time again, but WPS experiments conducted by Loss, Grey and Hawthorne[9] indicate that because of the particular thermal and loading history that the stationary flaw was exposed to the effective value of K_{Ic} would be elevated, perhaps to a value equal to the previous maximum value of K_I. Thus, presumably some repressurization would be possible, but this particular beneficial effect of WPS was not included in the FM model. (There is some hesitancy at this time to take advantage of WPS even with $dK_I/dt<0$ because there is no assurance that dK_I/dt will remain negative.)

OCA PARAMETRIC ANALYSIS

To obtain a better understanding of the sensitivity of $(RTNDT_s)_c$ to the many parameters involved in an OCA FM analysis, a parametric study was conducted, assuming a constant pressure and an exponential decay of the downcomer coolant temperature.

The temperature transient is expressed as

$$T_c = T_f + (T_i - T_f)e^{-nt} \quad , \tag{4}$$

where

T_c = downcomer coolant temperature,

T_i = initial temperature of vessel wall and coolant,

T_f = final (asymptotic) temperature of coolant,

n = decay constant,

t = time in transient.

The fluid-film heat transfer coefficient (h_f) which is a necessary input to OCA-II, was assumed to be independent of time and for most cases was assigned a value that is achieved with the main circulating pumps running (5680 $W \cdot m^{-2} \cdot {}^\circ C^{-1}$). In order to determine the sensitivity of $(RTNDT_s)_c$ to h_f a relatively low value corresponding to natural convection cooling (1700) was also used for a few calculations.

A list of pertinent input data for the parametric analysis is included in Table 1, and a summary of results of the analysis is presented in Fig. 7, which shows the relation between $(RTNDT_s)_c$ and pressure (p) for $RTNDT_o = -7°C$ and for several values of T_f and n, ignoring the beneficial effects of WPS. The dashed lines in Fig. 7 correspond to both incipient initiation (II) and incipient failure (IF), the latter corresponding to no crack arrest following crack initiation. The solid line corresponds to II only; however, as indicated, only a small increase in $RTNDT_s$ is required for failure, except as the pressure approaches zero. As already mentioned, thermal shock alone will not drive the flaw completely through the wall.

Table I. Input data for parametric analysis

Vessel dimensions, mm	
Outside diameter	4800
Inside diameter	4370
Cladding thickness	5.4
Flaw type	Long, axial, through clad
T_i, °C	288
T_f, °C	66, 93, 121, 149
n, min^{-1}	0.015 – ∞
t_{max}, h	2, 1^a
h_f, $W \cdot m^{-2} \cdot {}^\circ C^{-1}$	5680, 1700^a
p, MPa	0–17.2 in 1.72 increments
$RTNDT_o$, °C	−29, −7, 4

[a]Used in a few cases for comparison purposes.

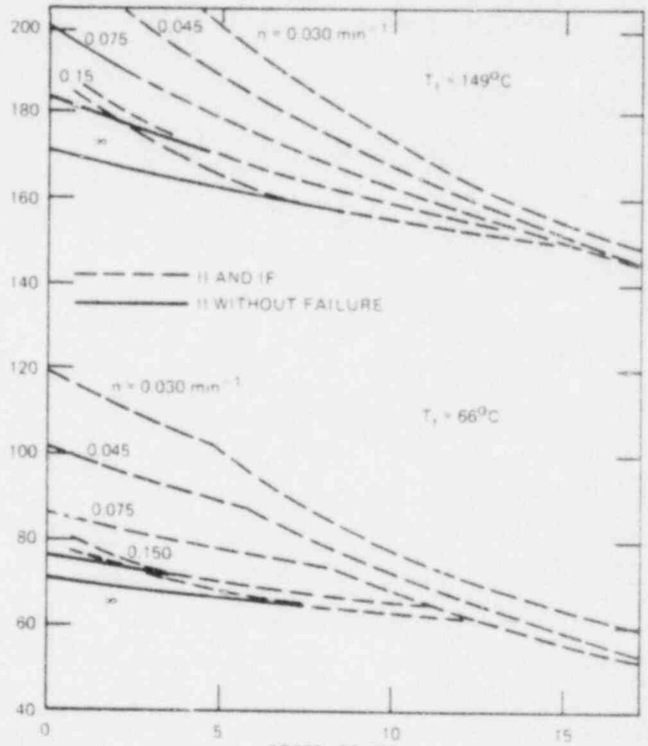

Fig. 7. Summary of results for OCA parametric analysis showing $(RTNDT_s)_c$ vs p for two values of T_f and three values of n and ignoring the beneficial effects of WPS.

The results in Fig. 7 show that at high pressure and for . ˙J.030 min^{-1}, $(RTNDT_s)_c$ is insensitive to the rate at which the coolant temperature decreases; and for the highest pressure considered (17.2 MPa, which is approximately the safety-valve setting) it was found that over the range of T_f values considered (66–149°C)

$$(RTNDT_s)_c \approx 1.10\ T_f - 22°C \quad . \tag{5}$$

Equation 5 might be used for obtaining a conservative maximum permissible value of $RTNDT_s$ by specifying a reasonable minimum value of T_f. Suppose such a value of T_f is 120°C. Then the maximum permissible value of $RTNDT_s$ would be ~110°C.

The sensitivity of $(RTNDT_s)_c$ to $RTNDT_o$ was found to be rather small (~3°C) over the range of $RTNDT_o$ values considered. Furthermore, the sensitivity to t_{max} over the range of 1 to 2 h and to h_f over the range of 1700 to 5680 $W \cdot m^{-2} \cdot °C^{-1}$ was found to be small except for a few cases involving a sensitivity to t_{max} as shown in Table II. For very slow transients (n = 0.015 min^{-1}), $(RTNDT_s)_c$ decreased significantly with the decrease in t_{max}. Of course for cases where II takes place prior to 1 h (see Figs. 4 and 5), changing t_{max} from 2 to 1 h would make no difference. This tends to be the case for the more rapid transients.

Table II. Effect of h_f and t_{max} on critical values of $\Delta RTNDT_s$ corresponding to II without WPS

Case			$(\Delta RTNDT_s)_c$, °C			
T_f	n	p	h_f, $W \cdot m^{-2} \cdot °C^{-1}$ / t_{max}, hr			
°C	min^{-1}	MPa	5680/2	1700/2	5680/1	1700/1
66	0.015	3.4	152	157	196	208
66	0.015	17.2	101	107	163	173
66	0.15	3.4	79	95	79	95
66	0.15	17.2	58	61	61	71
149	0.015	3.4	>220	>220	>220	>220
149	0.015	17.2	177	181	216	>220
149	0.15	3.4	180	194	180	194
149	0.15	17.2	151	153	151	157

Another sensitivity investigated was that of $(RTNDT_s)_c$ to the imposed limit on the maximum critical crack depth. Decreasing this limit tends to increase $(RTNDT_s)_c$, and the increase is larger for high-pressure cases since the critical crack depths are greater for higher-pressure transients. Calculations were made for two limiting fractional crack depths of 0.15 and 0.076 and for n = 0.015 and 0.15 min^{-1}, T_f = 66 and 149°C, and for p = 17.2 MPa. The differences in $(RTNDT_s)_c$ associated with the two limits on critical crack depth were small, the maximum values being 8°C.

ANALYSIS OF SEVERAL RECORDED PWR OCA's

Several PWR OCA's have occurred in recent years, and recordings of the pressure and temperature transients have been used as input to fracture-mechanics analyses, using the FM model described herein. The temperature transients were measured upstream of the injection point for the emergency core coolant and thus do not necessarily reflect the temperature of the coolant in the downcomer. However, in the absence of more accurate data the recorded transients were used so as to obtain some indication of the severity of actual OCA's in terms of pressure vessel integrity.

Table III. Values of $(RTNDT_s)_c$ for several recorded PWR OCA's

Plant (date)		$(RTNDT_s)_c$ w/o WPS, °C	
		Flaw Orientation	
		Long.	Cir.
Robinson	(1970)	161 (F)[a]	177 (A)
Robinson	(1972)	193 (F)	>249
Robinson	(1975)	179 (F)	189 (A)
Rancho Seco	(1978)	146	165 (A)
TMI-2	(1979)	98 (F)	124 (F)
R. E. Ginna	(1982)	—	192 (F)

[a]A and F in parentheses indicate arrest (with no reinitiation) and failure.

The accidents analyzed and the results obtained are shown in Table III. The values of $(RTNDT_s)_c$ correspond to either incipient initiation followed by crack arrest and no reinitiation or to incipient initiation and failure, as indicated; WPS was ignored, and the imposed limits on critical fractional crack depth were 0.025 and 0.15, the lower limit disallowing crack initiation in the cladding. Because copper and nickel concentrations can be very much different in the circumferential and axial welds, $(RTNDT_s)_c$ was calculated for both crack orientations for the plate-type vessels.

Estimates[14] of $(RTNDT_s)_A$ for all PWR pressure vessels in service today indicate that at this time (September 1982) a few vessels have values approaching 120°C for axial welds and 140°C for circumferential welds. Thus, assuming appropriate flaws to exist in the welds, the analysis indicates that these few unidentified vessels would have a potential for failure today, if the reactor facilities were subjected to a TMI-2-type OCA; however, the Rancho Seco-type transient would not be a threat for several more years.

SUMMARY

A state-of-the-art fracture-mechanics model has been developed that is based on LEFM, includes recent modifications to the radiation-damage trend curves and to the fluence attenuation curve, and is believed to be conservative. The results of an OCA parametric analysis indicate that crack propagation will not take place under the most severe accident conditions if $RTNDT_s < 1.10\ T_f - 22°C$, and it was determined that this relation was not sensitive to $RTNDT_o$, h_f or the assumed duration of the transient over a reasonable range of values.

A fracture-mechanics analysis was also performed for several PWR recorded OCA's, and it was determined, based on preliminary estimates of actual values of $RTNDT_s$ for existing PWR vessels, that a few vessels may have a potential for failure in a few years if subjected to the 1978 Rancho Seco-type transient.

Presumed conservatisms in the fracture-mechanics model are associated with arrest on the upper shelf, the effects of cladding on surface extension of short flaws and warm prestressing. These areas are being investigated to determine the degree of conservatism and to see if the model can be modified to remove excessive conservatism, should it exist.

ACKNOWLEDGMENTS

These studies were sponsored by the Office of Nuclear Regulatory Research, U.S. Nuclear Regulatory Commission (NRC). The authors wish to acknowledge the direction and encouragement provided by Milton Vagins, NRC Project Manager.

REFERENCES

1. W. H. Tuppeny, Jr., W. F. Siddall, Jr., and L. C. Hsu, *Thermal Shock Analysis of Reactor Vessels Due to Emergency Core Cooling System Operation*, Combustion Engineering, Inc., Report A-68-9-1, March 15, 1968.

2. R. C. Hutto, C. D. Morgan, and W. A. Van De Sluys, *Analysis of the Structural Integrity of a Reactor Vessel Subjected to Thermal Shock*, Babcock & Wilcox Power Generation Division, Topical Report BAW10018, May 1969.

3. D. J. Ayres, W. F. Siddall, Jr., *Finite-Element Analysis of Structural Integrity of a Reactor Pressure Vessel During Emergency Core Cooling*, Combustion Engineering Report A-70-19-2, January 1970.

4. (March 20, 1978, Rancho Seco) Nuclear Safety Information Center Accession #0020-138830).

5. (February 26, 1980 Crystal River 3) Nuclear Safety Information Center Accession #0020-160846.

6. (April 23, 1979 Three Mile Island 2) Nuclear Safety Information Center Accession #0020-137918, 137919, 139931.

7. L. E. Steele, *Neutron Irradiation Embrittlement of Reactor Pressure Vessel Steels*, Technical Report Series No. 163, International Atomic Energy Agency, Vienna, 1975.

8. Personal communication with P. N. Randall, U.S. Nuclear Regulatory Commission, 1982.

9. F. J. Loss, A. A. Gray, Jr. and J. R. Hawthorne, *Significance of Warm Prestress to Crack Initiation During Thermal Shock*, Naval Research Laboratory, Washington, DC, NRL/NUREG 8165, September 1977.

10. R. D. Cheverton, et al., "Thermal Shock Investigations," *Heavy-Section Steel Technology Program Quart. Prog. Rep. for October—December 1980*, NUREG/CR-1951 (ORNL/NUREG/TM-437), March 1981, pp. 37—54.

11. R. D. Cheverton et al., "Thermal Shock Investigations," *Heavy-Section Steel Technology Program Quart. Prog. Rep. for October—December 1981*, NUREG/CR-2141, Vol. 4 (ORNL/TM-8252), April 1982, pp. 52—80.

12. S. T. Rolfe and J. M. Barsom, *Fracture and Fatigue Control in Structures, Applications of Fracture Mechanics*, Prentice-Hall, Inc., 1977.

13. T. U. Marston (editor), *Flaw Evaluation Procedures: ASME Section XI*, EPRI NP-719-SR, August 1978.

14. USNRC, "Effects of Residual Elements on Predicted Radiation Damage to Reactor Pressure Vessel Materials," *Reg. Guide 1.99*, Rev. 1 (Sept. 16, 1976).

15. S. K. Iskander, R. D. Cheverton, D. G. Ball, *OCA-I, A Code for Calculating the Behavior of Flaws on the Inner Surface of a Pressure Vessel Subjected to Temperature and Pressure Transients*, ORNL/NUREG-84, August 1981. OCA-II is a modification of OCA-I. A report is in preparation.

16. R. D. Cheverton, et al., "Thermal Shock Investigations," *Heavy-Section Steel Technology Program Quart. Prog. Rep. for July—September 1981*, NUREG/CR-1197 (ORNL/NUREG/TM-370), April 1980, pp. 52—80.

17. R. D. Cheverton, et al., "Thermal Shock Investigations," *Heavy-Section Steel Technology Program Quart. Prog. Rep. for October—December 1979*, NUREG/CR-1305 (ORNL/NUREG/TM-380), May 1980, pp. 67-70.

18. G. C. Robinson and J. G. Merkle, "Stainless Steel Cladding Investigations," *Heavy-Section Steel Technology Program Quart. Prog. Rep. for October—December 1981*, NUREG/CR-2141, Vol. 4 (ORNL/TM-8252), April 1982, pp. 118—123.

Failure Probability of a PWR Pressure Vessel

Subjected to Pressurized Thermal Shock

by

Jack Strosnider, NRC

1.0 INTRODUCTION

Reactor pressure vessels (RPV) in nuclear power plants have traditionally been considered extremely reliable structural components. Indeed, studies completed in the United States and Europe have concluded that the disruptive failure rate (loss of the pressure retaining boundary) for nuclear pressure vessels is less than 10^{-6} at a 99% confidence level for RPVs designed, fabricated, inspected, and operated in accordance with the Boiler and Pressure Vessel Code of the American Society of Mechanical Engineers. However, recent results from surveillance and research programs and operating experience suggest that the issue of RPV failure probability should be reassessed. The renewed interest in RPV failure probability is due to the observation that thermal hydraulic transients occuring in commercially operating nuclear power plants are subjecting RPVs to unanticipated loadings which could contribute significantly to the failure probability of RPVs. In addition, operating experience and research programs over the past few years have provided additional information that more clearly defines both material property variations in RPVs and the effect of neutron irradiation on the material's resistance to fracture. The objective of this study is to assess the contribution to RPV failure probability of recently observed thermal hydraulic transients using the most recent material property data.

In this study, Monte Carlo simulation techniques have been used because of the ability to consider a greater number of significant random variables and to perform a wide spectrum of sensitivity studies. The results of extensive sensitivity studies which have been conducted are extremely important because they quantify the effect of uncertainties in the input parameters, thereby providing an estimate of the accuracy of the calculated failure probabilities, and they identify the significant variables and variable interactions. The results are best applied in a relative sense, and extreme caution must be exercised in applying the results in an absolute sense.

2.0 RPV FAILURE PROBABILITY MODEL

Figure 1 illustrates the simulation model developed for RPV failure probability. The left hand column in the figure is the deterministic analysis which includes the heat transfer, thermal and pressure stress, and applied stress intensity value calculations for a range of crack depths at ten time steps in the transient. The K_I values are calculated for two dimensional (infinitely long) surface cracks oriented in the longitudinal direction. Matrices of temperature and K_I values are stored for use later in the simulation analysis.

The variables designated "simulate" in the diagram are treated as random variables, and their values are sampled, using Monte Carlo techniques, from appropriate statistical distributions. Crack depth, a; fluence, F; initial RT_{NDT}, RT_{NDTo}; copper content , Cu; K_{Ic}; and K_{Ia} were treated as random variables in this study. On each pass through the loop a flaw size is simulated and the corresponding applied stress intensity, K_I, value retrieved from the K_I matrix. The mean K_{Ic} value is then calculated using the temperature corresponding to the time step and simulated crack depth and an RT_{NDT} based on the values of copper content, fluence, and RT_{NDTo} sampled from their corresponding statistical distributions. Since the K_{Ic} data exhibits significant variability, the K_{Ic} value is simulated by sampling from a distribution about the mean K_{Ic} value.

If crack initiation is predicted, the crack is allowed to advance through the RPV wall in discrete steps of 0.25 inches, and a check for crack arrest is made at each crack advance. K_{Ia} is treated in a similar fashion to K_{Ic} as mentioned above. If crack arrest is predicted, the code continues to analyze successive time steps in the transient using the arrested crack depth. Since the applied K values and material temperature at the crack tip are a function of time in the transient, reinitiation of the crack may occur.

Each pass through the simulation loop depicted in Figure 1 represents a single computer experiment conducted to determine if RPV failure will occur. Up to a million passes through this loop can be made. The code keeps track of the number of crack initiations and RPV failures and the probabilities of crack initiation and RPV failure are estimated by dividing these values by the total number of trials. Thus, the code actually performs millions of deterministic calculations with each set of calculations based on a different set of values selected from the appropriate statistical distributions for the significant variables. This is equivalent to subjecting a population of up to a million operating reactor pressure vessels to the pressurized thermal shock transient of interest and then inferring the failure probability based on the number of observed failures.

3.0 INPUT DISTRIBUTIONS

Unfortunately, very little information exists in the literature regarding the required statistical inputs, and the time frame of this initial study was not sufficient to allow the necessary research and analysis to develop rigorous statistical inputs. Therefore, many of the statistical distributions associated with the random variables in the model are based on expert opinion and have somewhat ill-defined "levels of confidence." Table I presents the statistical distributions that were defined for the reference case analyses.

4.0 RESULTS

The simulation model has been used to evaluate a reference case defined by an idealized representation of the March 20, 1978 Rancho Seco transient, illustrated in Figure 2 and the reference case statistical distributions shown in Table I. Sensitivity studies were then performed to determine the sensitivity of the calculated results to assumptions regarding input distributions and modelling assumptions. Finally, a set of idealized transients characterized by an exponential decay of the primary coolant temperature and constant pressure was analyzed. The results presented are conditional probabilities; that is, the probability of failure of a RPV weld given that the pressurized thermal shock transient under consideration occurs. To convert the results into failure rates, the frequency of the transient considered must be defined. Since the results presented are for an individual weld in the RPV beltline, the total conditional failure probability of the RPV beltline welds is the appropriate summation of the failure probabilities for each weld. If these values are sufficiently low and independence is assumed, the failure probabilities for the six welds can simply be summed. If the failure probabilities become high, the intersection of the weld failure probabilities must be subtracted.

4.1 REFERENCE CASE

The reference case analysis was conducted for an idealized representation of the March 20, 1978 Rancho Seco transient and the reference case statistical distributions shown in Table I. Figure 3 presents the failure probability versus the mean fluence for a specified mean copper content of 0.34% and for three mean values of RT_{NDTo}. Also, plotted across the top of the figure, is the ΔRT_{NDT} calculated using the mean HEDL curve. These shifts are based on the mean copper content and fluence value in each figure. A set of curves like this for various mean copper contents makes it possible to estimate the failure probability for the beltline region of a PWR for which the mean values of the random variables can be estimated.

4.2 SENSITIVITY STUDIES

Sensitivity studies were conducted on the distribution for copper content, initial RT_{NDT}, fluence, and fracture toughness. In addition, conditional failure probabilities were calculated assuming that specific flaw sizes exist with a probability of 1.0.

4.2.1 COPPER CONTENT

Figure 4 illustrates the results of the sensitivity study on copper content. When the standard deviation for the copper distribution was increased from 0.025% to 0.07%, the calculated failure probabilities increased by approximately a factor of 5.

4.2.2 INITIAL RT

Figure 5 illustrates the results of the sensitivity study on RT_{NDTo}. When the standard deviation for the RT_{NDTo} distribution was increased from 15°F to 25°F, the calculated failure probabilities were increased by a factor of approximately 3.

4.2.3 FLUENCE

Figure 6 illustrates the results of the sensitivity study on fluence. The standard deviation for the fluence distribution was increased from 30% to 50% and decreased to 15%. The increased standard deviation resulted in approximately a factor of three increase in calculated failure probabilities, while the decrease in the standard deviation had little effect on the calculated failure probabilities.

4.2.4 FRACTURE TOUGHNESS

Figure 7 illustrates the results of the sensitivity study on fracture toughness. Three different representations of the fracture toughness distribution were considered. In the first two cases the normal distribution about the mean fracture toughness values for K_{Ic} and K_{Ia} was maintained, but the standard deviation was increased to 15% and then 20% of the mean value. In the third case, K_{Ic} and K_{Ia} were treated deterministically using the lower bound fracture toughness curves from Section XI of the American Society of Mechanical Boiler and Pressure Vessel Code. The sensitivity study was conducted for a mean copper content of 0.34% and a mean initial RT_{NDT} of 0°F. Assuming the large standard deviations resulted in less than a factor of three difference from the reference case failure probabilities for a mean RT_{NDT} of 236°F or less. At higher values of RT_{NDT} the calculated failure probabilities for the assumed standard deviations of 15% and 20% were a factor of [illegible] and over an order of magnitude greater than the reference case, respectively. When the lower bound fracture toughness curves from Section XI of the Code were used, the calculated failure probabilities were one order of magnitude to almost two orders of magnitude higher than the reference case.

Figure 8 presents the failure probabilities calculated when copper content, fluence, and initial RT_{NDT} were assumed to show the increased variances used in sensitivity studies, including one case where K_{Ic} and K_{Ia} were treated as random variables and one case where they were modelled using the lower bound curves. For the first case, the calculated failure probabilities were approximately an order of magnitude greater than the reference case, while for the second case (lower bound K_{Ic} and K_{Ia}) the calculated failure probabilities were almost three orders of magnitude higher.

4.2.5 FLAW DISTRIBUTION

Figure 9 presents the conditional failure probabilities calculated assuming that flaw sizes ranging from 0.125 inches to 2.0 inches exist with a probability of 1.0 and for several different mean fluence values and values of RT_{NDT}. These curves are useful because they can be used to calculate failure probabilities for different assumed crack distributions.

4.2.6 HEAT TRANSFER COEFFICIENT

Figure 10 presents the results of a sensitivity study conducted on heat transfer coefficient. The two curves in the figure present RPV failure probability versus heat transfer coefficient, h in BTU/hr ft^2 °F, for two different hypothetical exponential cooldowns. One has a final transient temperature of 150°F while the other has a final transient temperature of 200°F. A constant pressure level of 1000 psig was assumed and the RPV material was assumed to have an adjusted RT_{NDT} of 250°F. When the thermal conductivity of the cladding is considered, the range of the effective heat transfer coefficient for the thermal hydraulic transients under consideration is between 200 BTU/hr ft^2°F and 400 BTU/hr ft^2°F. The results indicate that over that range, the assumed heat transfer coefficient can make as much as an order of magnitude difference in the calculated RPV failure probabilities. The results presented in this study were generated assuming an effective heat transfer coefficient of approximately 300 BTU/hr ft^2°F.

4.3 Transient Sensivity Studies

In addition to the reference Rancho Seco transient, a set of hypothetical pressurized thermal shock transients with assumed exponential temperature decays and constant pressure levels was analyzed to determine the sensitivity of failure probability to the minimum temperature reached in the transient, rate of temperature drop, and pressure level. The temperature time history in each transient is assumed to follow an exponential decay defined by

$$T(t) = T_F + (550 - T_f)e^{-\beta t}$$

where T is the temperature in °F, t is time in minutes, T_f is the final temperature of the transient in °F, and β is the decay constant in min^{-1}. Three values of T_f, 150°F, 225°F, and 300°F; three values of β, 0.05 min^{-1}, 0.15 min^{-1}, and 0.50 min^{-1}; and five constant pressure levels, 0 psig , 500 psig, 1000 psig, 1500 psig, and 2000 psig were considered for a total of 45 different transients. Each of these transients was evaluated for five levels of fluence, 0.5 x 10^{19} neut/cm^2, 1.0 x 10^{19} neut/cm^2, 2.0 x 10^{19} neut/cm^2, 3.0 x 10^{19}neut/cm^2, and 4.0 x 10^{19} neut/cm^2 assuming a mean copper content of 0.30% and a mean initial RT_{NDT} of 20°F.

Figure 11 presents failure probability versus $T_f - RT_{NDT}$ for the three different values of β considered and a constant pressure of 1000 psig.

Figure 11 indicates a much greater increase in failure probabilities when β is increased from 0.05 to 0.15 than when β is increased from 0.15 to 0.50. This observation is more clearly illustrated in Figure 12 where failure probability is plotted as a function of β for several values of T_f-RT_{NDT} and 1000 psig constant pressure. The curves illustrate that failure probability is very sensitive to β in the range below 0.15 min^{-1} while increasing β beyond 0.15 min^{-1} increases the failure probability by less than a factor of five. This result is related to the assumed thermal inertia of the system, and the sensitivity curves will change if different thermal characterisitics are assumed in the heat transfer analysis.

Figure 13 is a plot of failure probability versus pressure for several values of the parameter T_f-RT_{NDT}. The figure illustrates increasing sensitivity to pressure as the parameter T_f-RT_{NDT} increases.

5.0 CONCLUSIONS

The results presented indicate that the most significant random variables in the reactor vessel pressurized thermal shock analyses are flaw distribution, fracture toughness, and heat transfer coefficient.

Further work is underway to develop more rigorous statistical distributions and to better define the uncertainties associated with the estimated failure probabilties. In addition, other refinements are going to be incorporated in the model. These include factors such as cladding effects on crack initiation and growth, finite shaped flaws, and warm prestressing. At this point in time, it is suggested that the results presented be used in a relative sense for studying the significance of certain variables in reactor vessel analysis and that the results not be applied in an absolute sense until the levels of confidence associated with the failure probability estimates are more rigorously defined.

TABLE I: REFERENCE CASE RANDOM VARIABLES

- OCTAVIA FLAW DISTRIBUTION[2]

- COPPER CONTENT $\sim N(\mu, 0.025\%)$, $0.08\% \leq Cu \leq 0.40\%$

- $RT_{NDT_0} \sim N(\mu, 15°F)$

- FLUENCE $\sim N(\mu, 30\%)$[1]

- ΔRT_{NDT} CALCULATED BY MEAN TRENDLINE DEVELOPED BY HEDL

- $K_{Ic} \sim N(\mu, 0.10\ )$

$$\mu = \begin{cases} 36.2 + 49.4\ \mathrm{EXP}\ (0.0104\ (T-RT_{NDT}))\ , & T-RT_{NDT} \leq -50°F \\ 55.1 + 28.0\ \mathrm{EXP}\ (0.0214\ (T-RT_{NDT})), & T-RT_{NDT} > -50°F \end{cases}$$

- $K_{IA} \sim N(\mu, 0.10\ )$

$$\mu = \begin{cases} 19.9 + 43.9\ \mathrm{EXP}\ (0.00993\ (T-RT_{NDT}))\ , & T-RT_{NDT} \leq 50°F \\ 70.1 + 6.5\ \mathrm{EXP}\ (0.0196\ (T-RT_{NDT}))\ , & T-RT_{NDT} > 50°F \end{cases}$$

1. McElroy, et al., Surveillance Dosimetry of Operating Power Plants, NRC 9th Water Reactor Safety Information Meeting, October 16, 1981.

2. W. E. Vesely, E. K. Lynn, and F. F. Goldberg, The OCTAVIA Computer Code: PWR Reactor Pressure Vessel Failure Probabilities Due to Operationally Caused Pressure Transients, U.S. Nuclear Regulatory Commission Report, NUREG-0258, 1978.

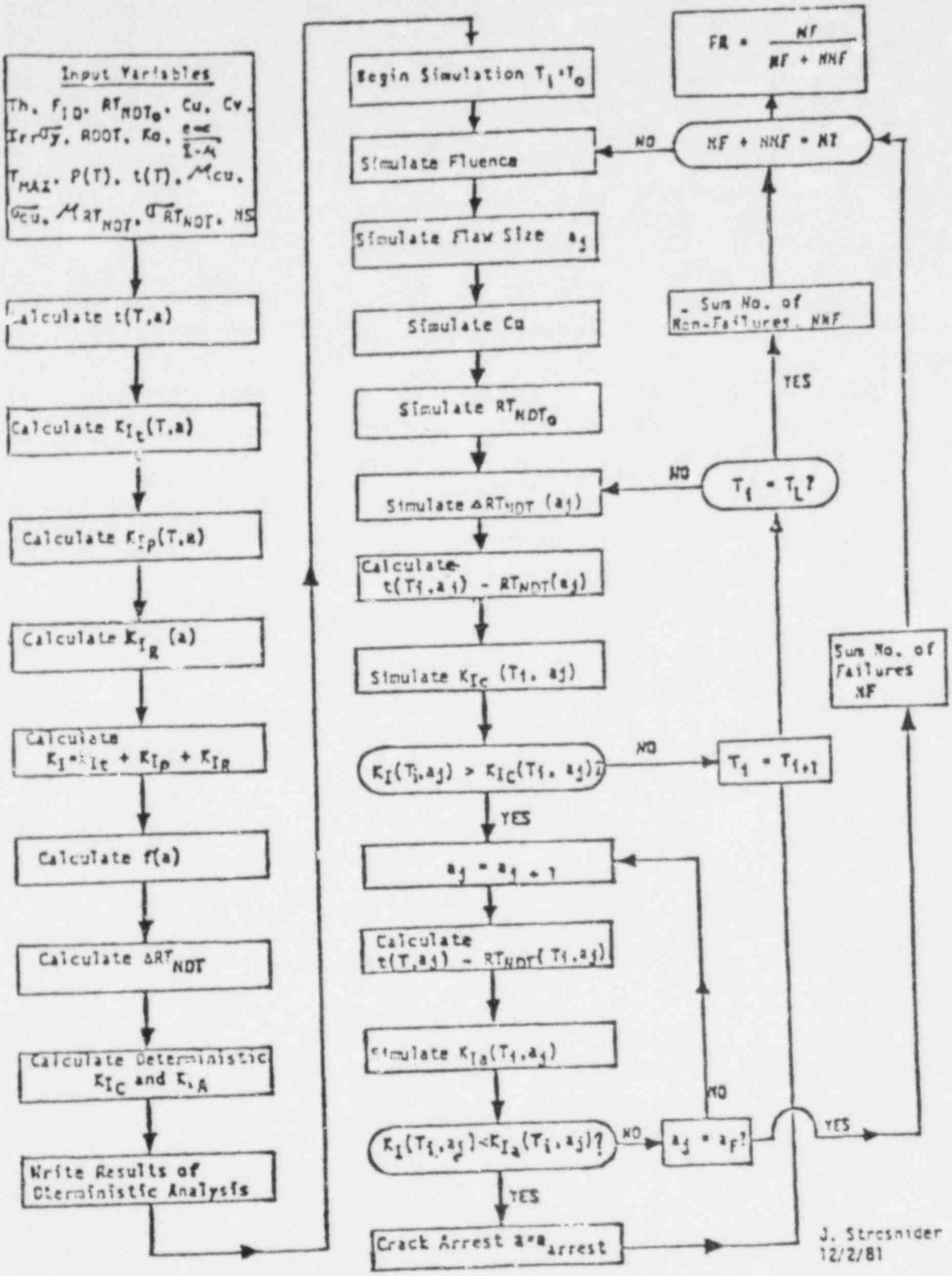

FIGURE 1: RPV FAILURE PROBABILITY SIMULATION MODEL

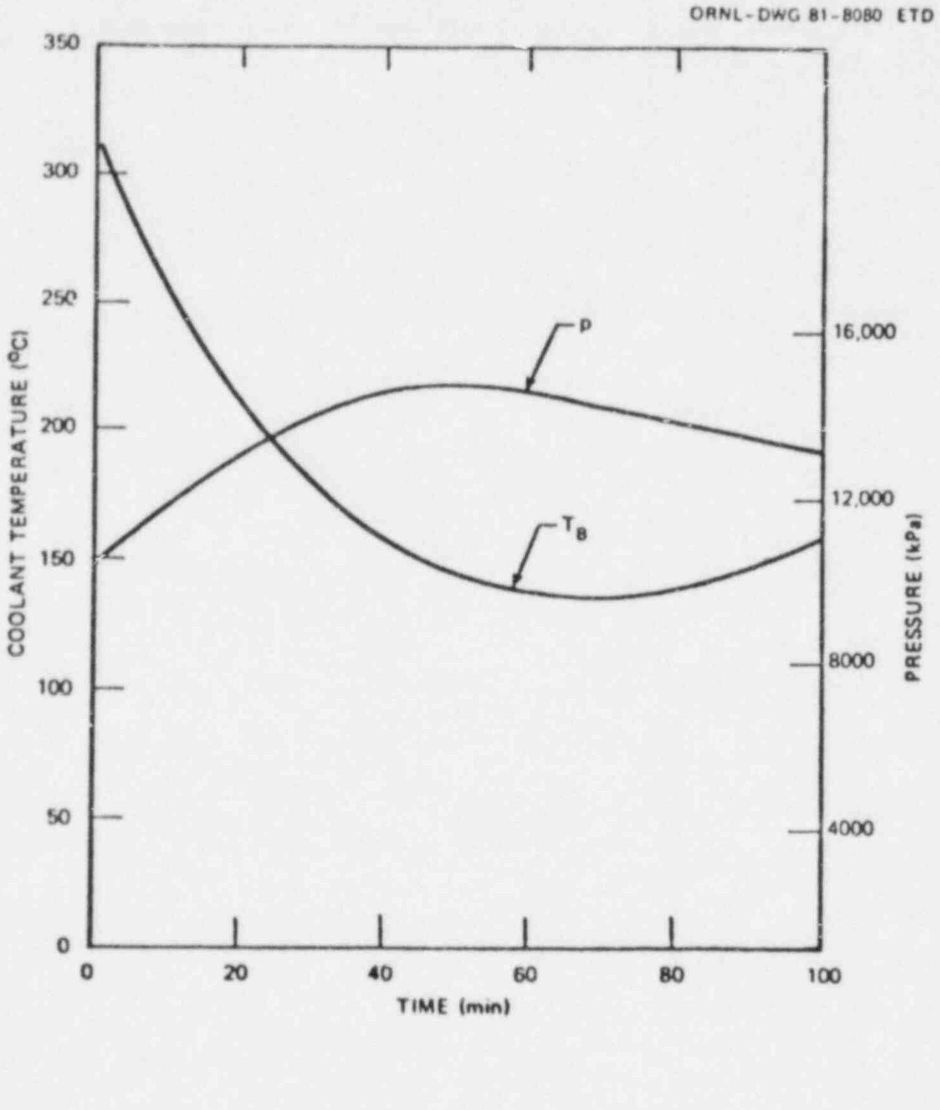

FIGURE 2: IDEALIZED RANCHO SECO PRESSURE AND TEMPERATURE TIME HISTORIES

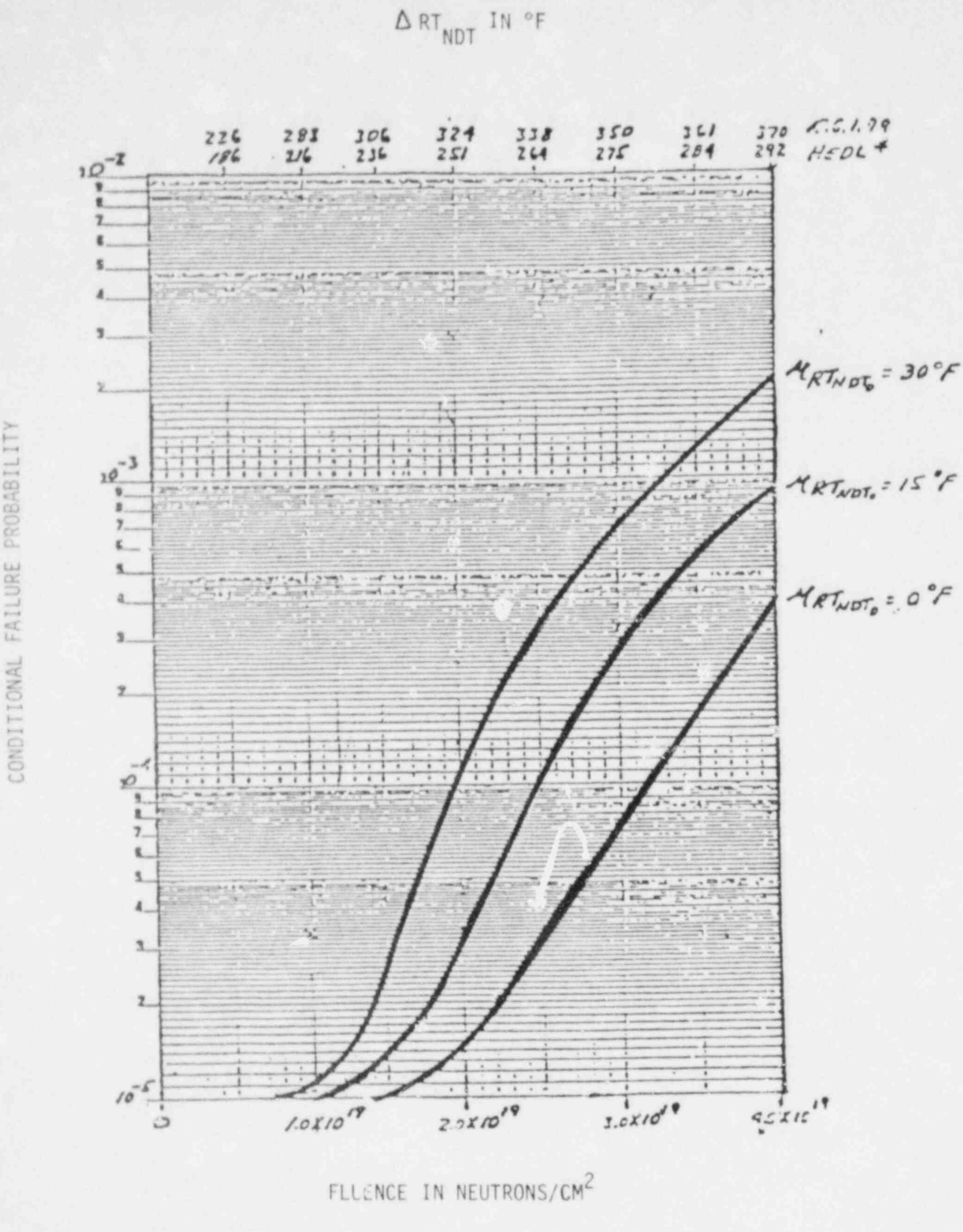

FIGURE 3: CONDITIONAL FAILURE PROBABILITY FOR THE RANCHO SECO TRANSIENT MEAN Cu = 0.34%

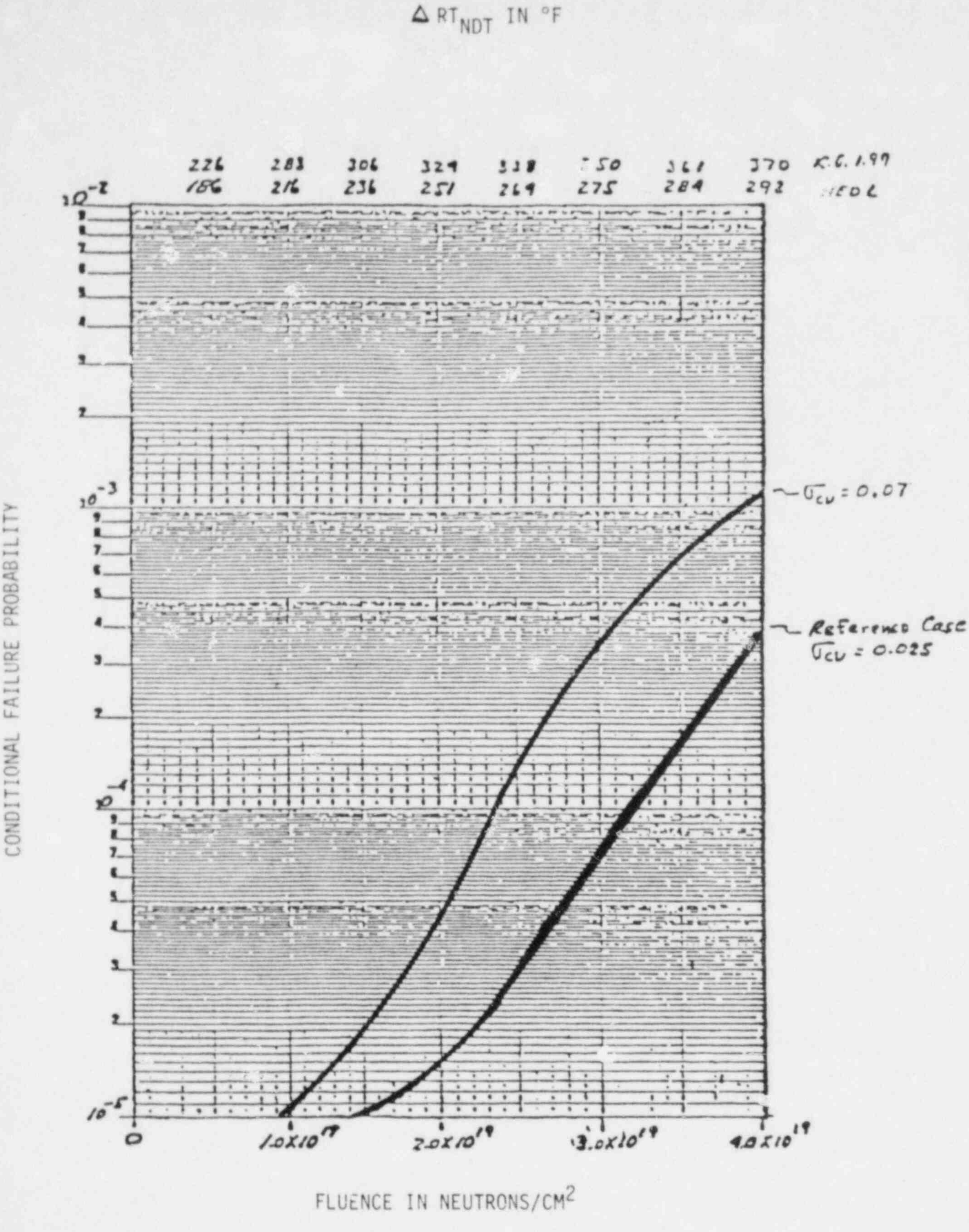

FIGURE 4: COPPER CONTENT SENSITIVITY STUDY MEAN Cu = 0.34%
MEAN RT_{NDT_O} = 0°F

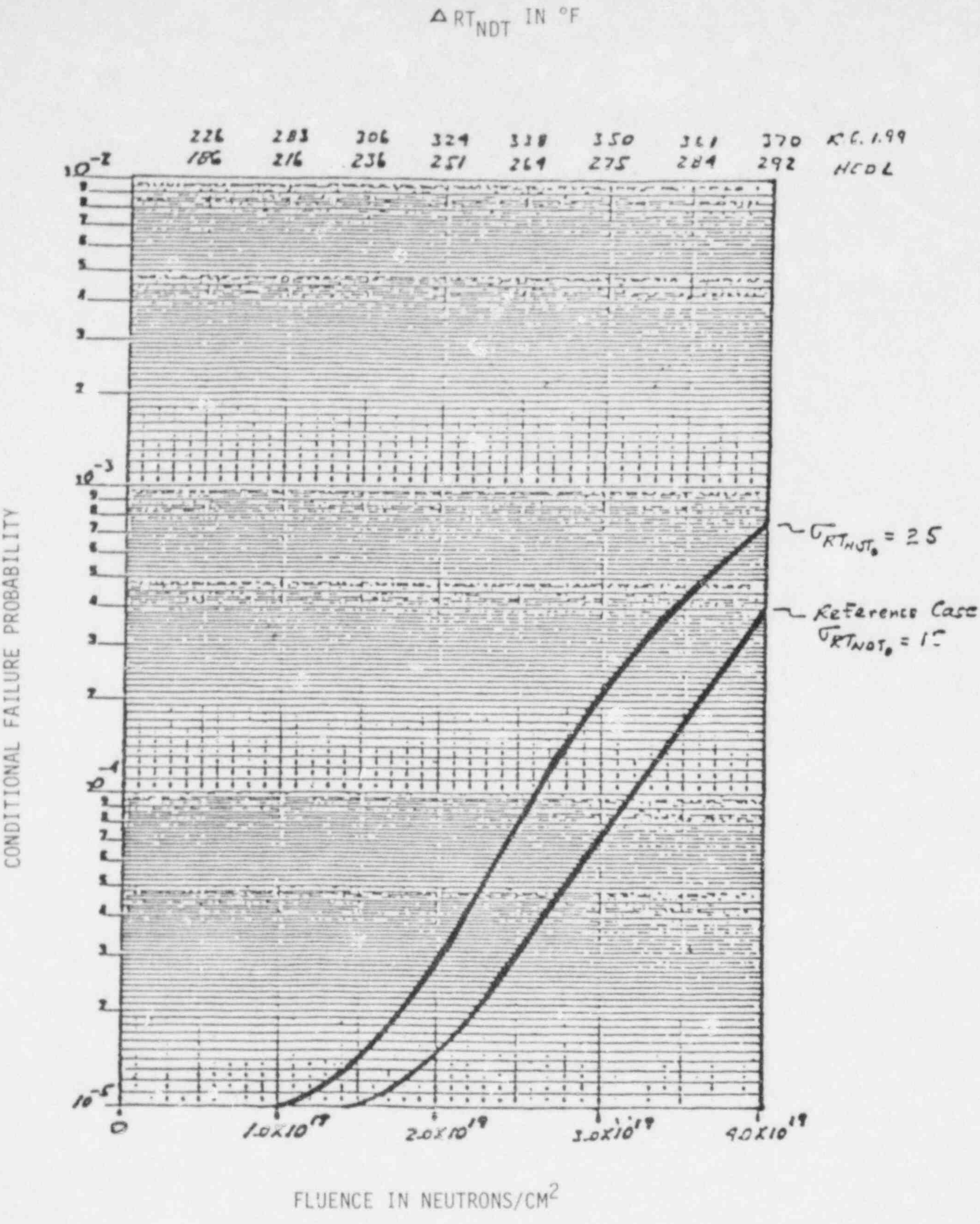

FIGURE 5: INITIAL RT_{NDT} SENSITIVITY STUDY MEAN Cu = 0.34%
MEAN RT_{NDTo} = 0°F

ΔRT_{NDT} IN °F

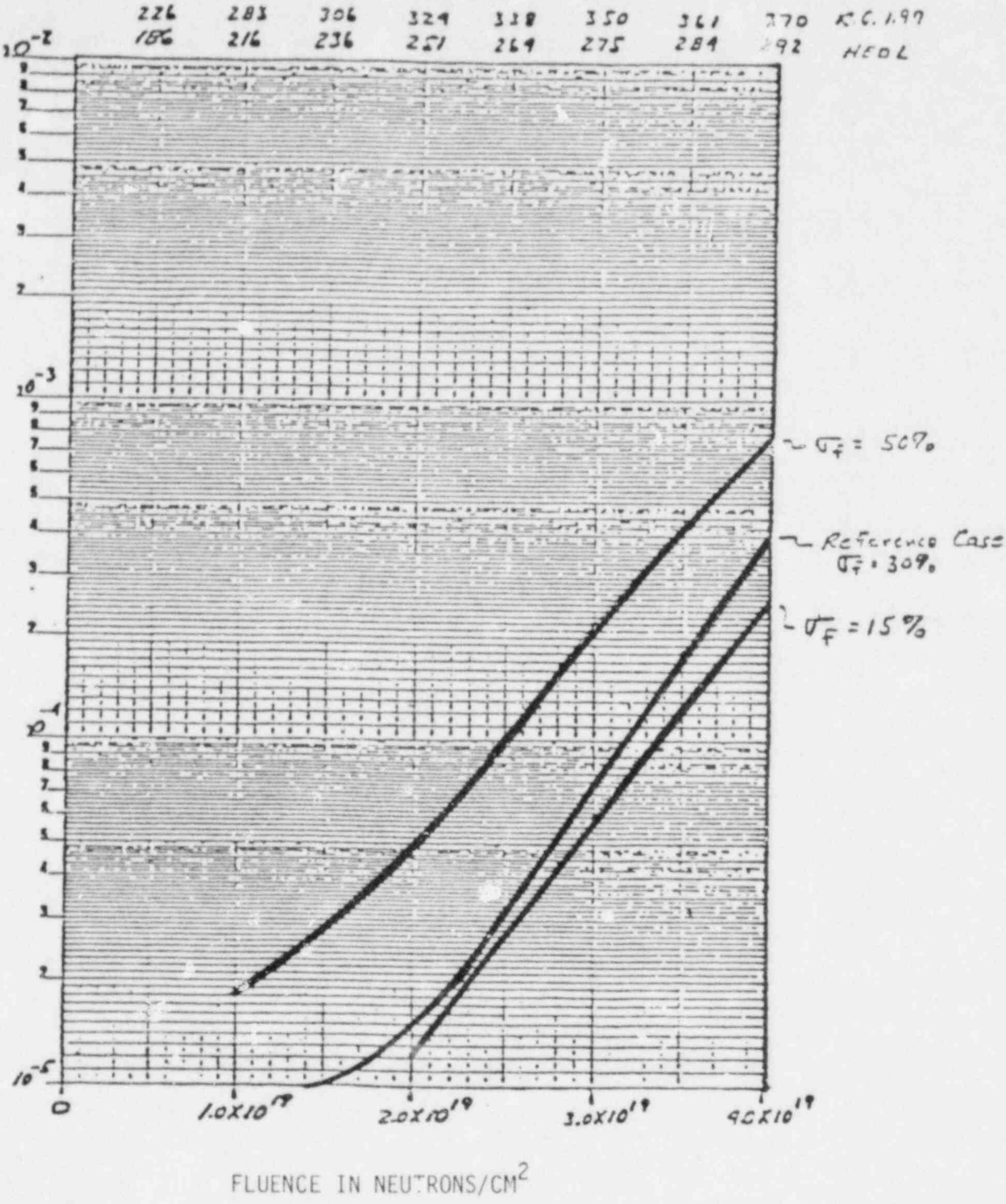

FIGURE 6: FLUENCE SENSITIVITY STUDY MEAN Cu = 0.34%
MEAN RT_{NDTo} = 0°F

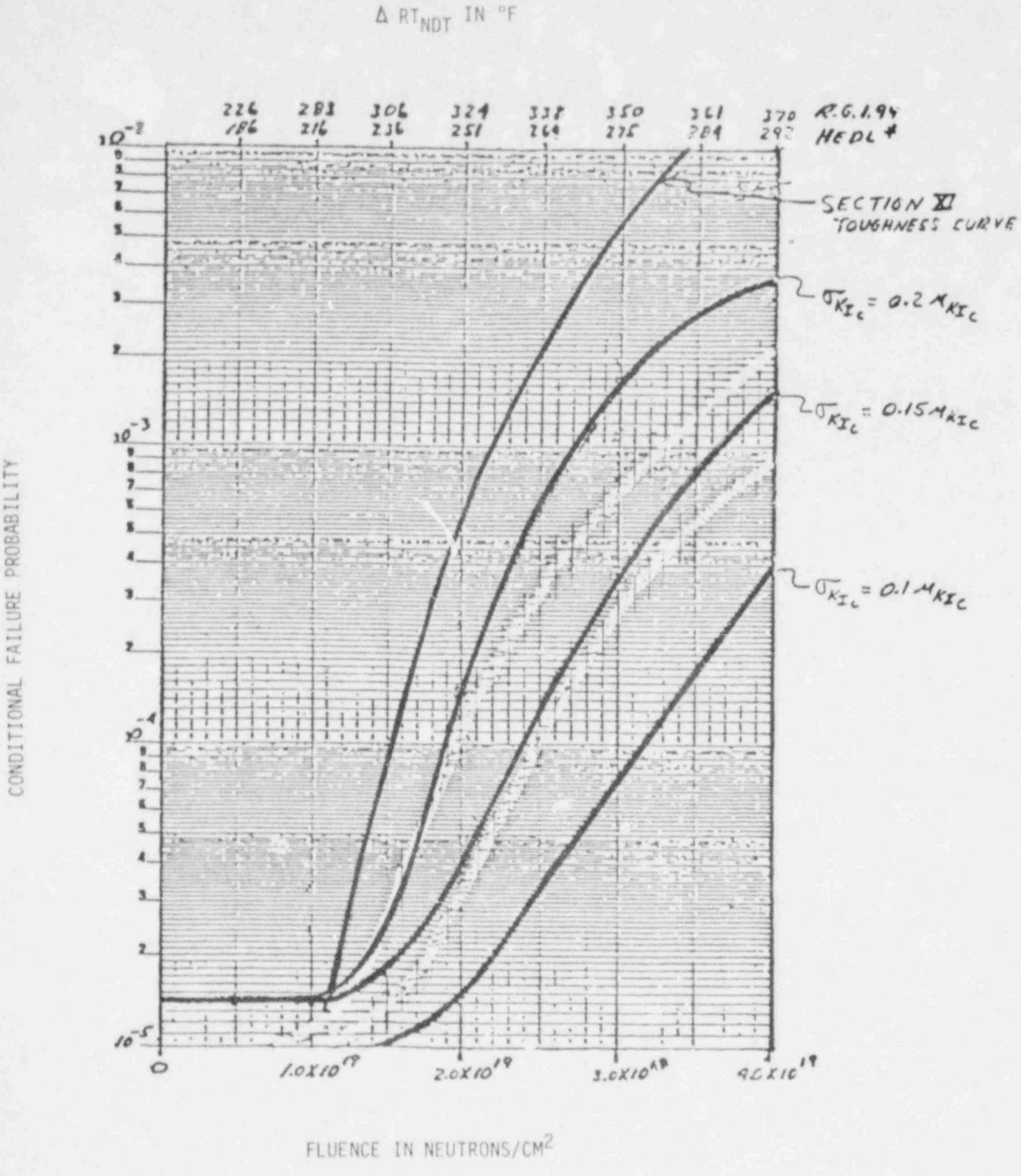

FIGURE 7: FRACTURE TOUGHNESS DISTRIBUTION SENSITIVITY STUDY
MEAN Cu = 0.34% MEAN RT_{NDTo} = 0°F

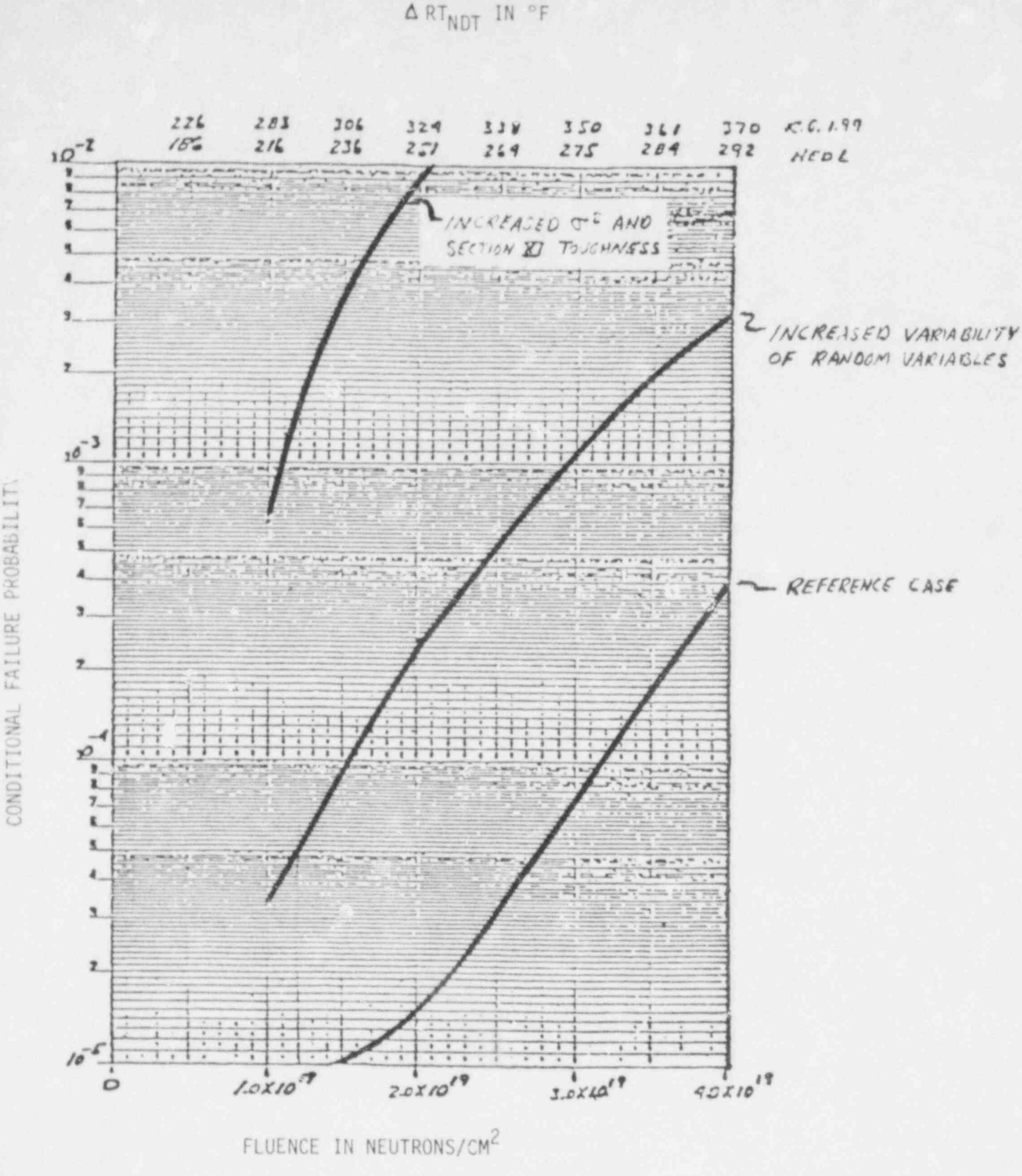

FIGURE 8: SIMULTANEOUS INCREASE IN THE VARIABILITY OF THE RANDOM VARIABLES MEAN Cu = 0.34% MEAN RT_{NDTo} = 0°F

FIGURE 9: CONDITIONAL FAILURE PROBABILITY P(F/a) FOR THE RANCHO SECO TRANSIENT
MEAN Cu = 0.34% MEAN RT_{NDTo} = 0°F

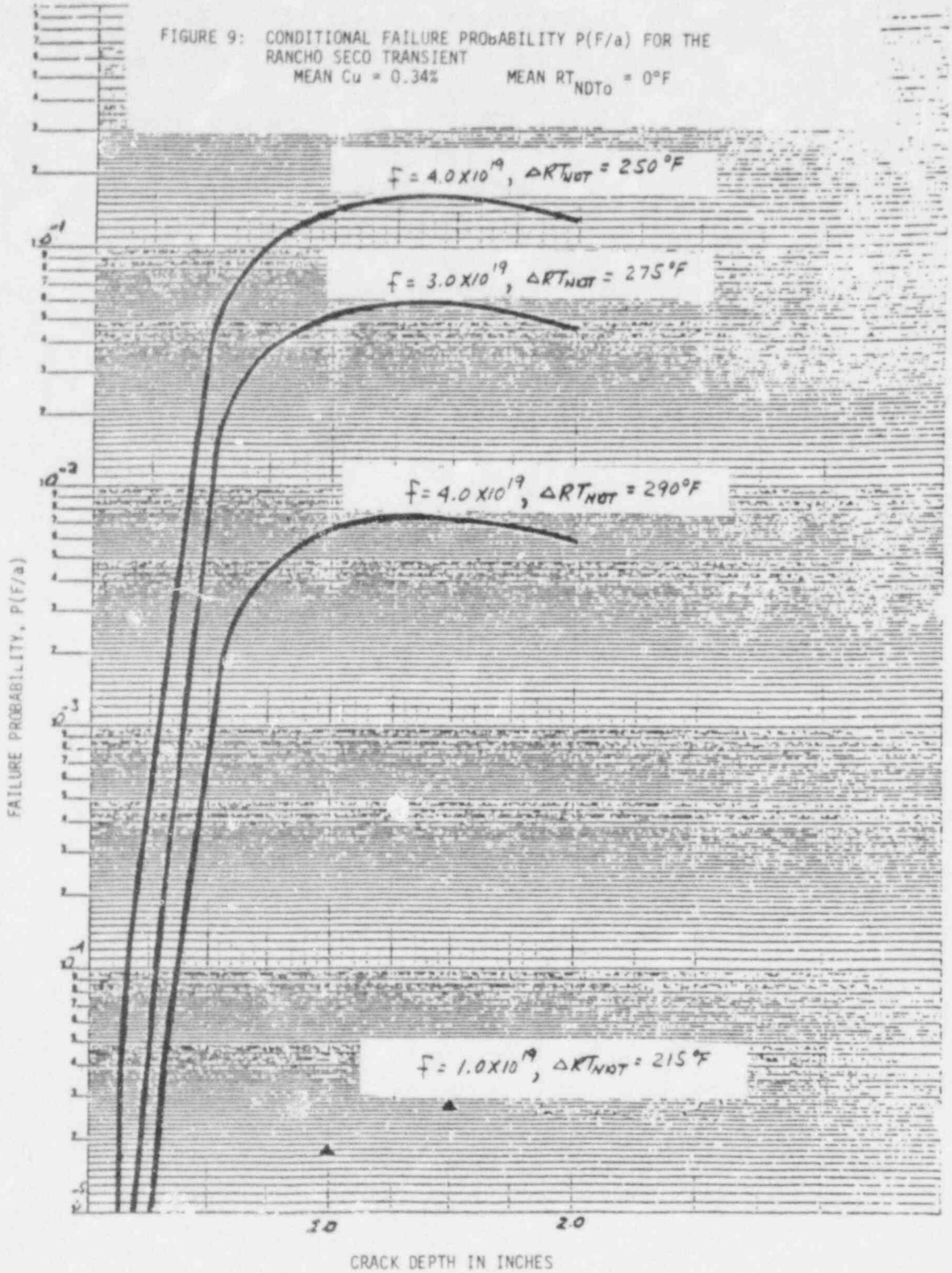

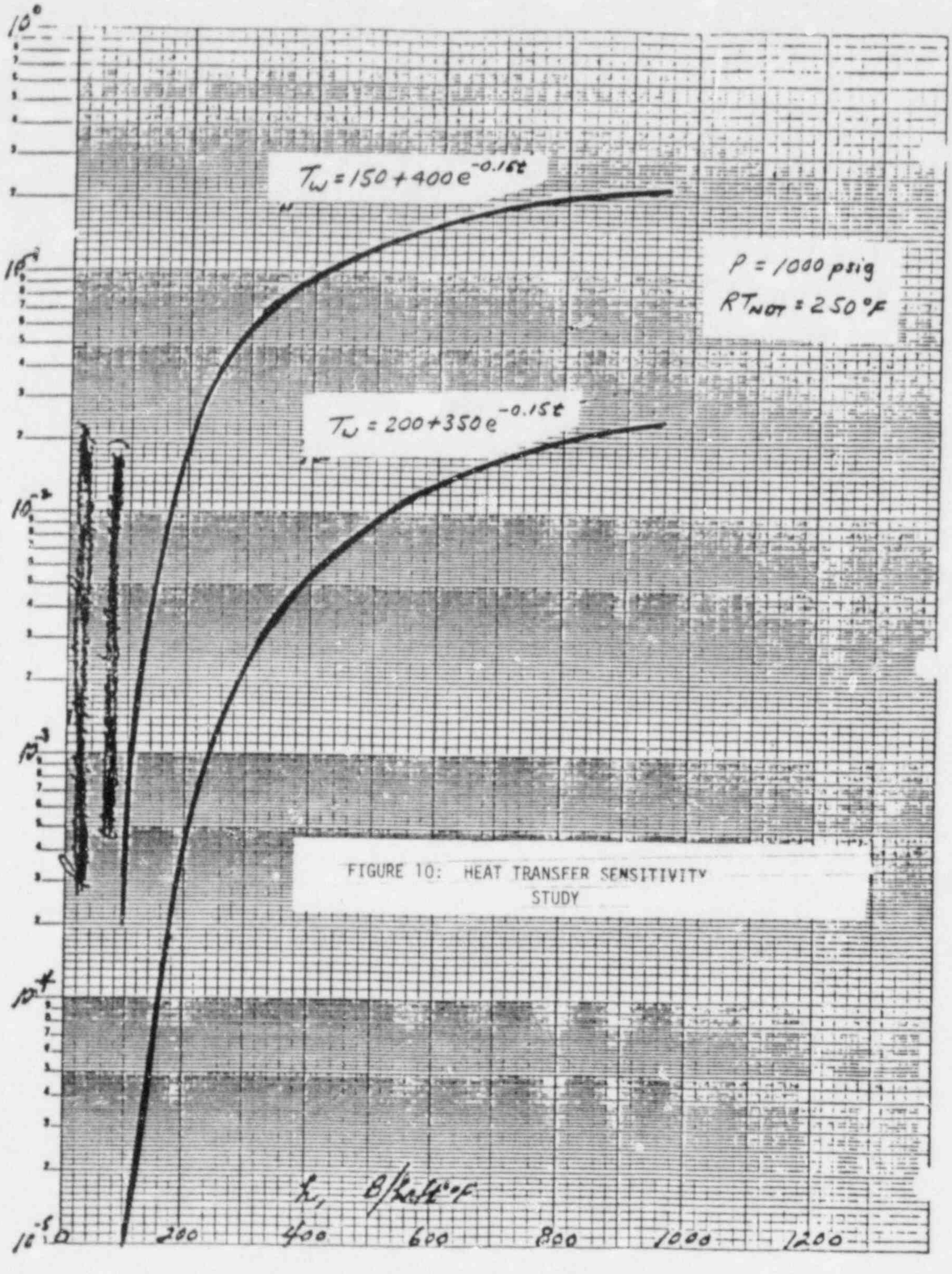

FIGURE 10: HEAT TRANSFER SENSITIVITY STUDY

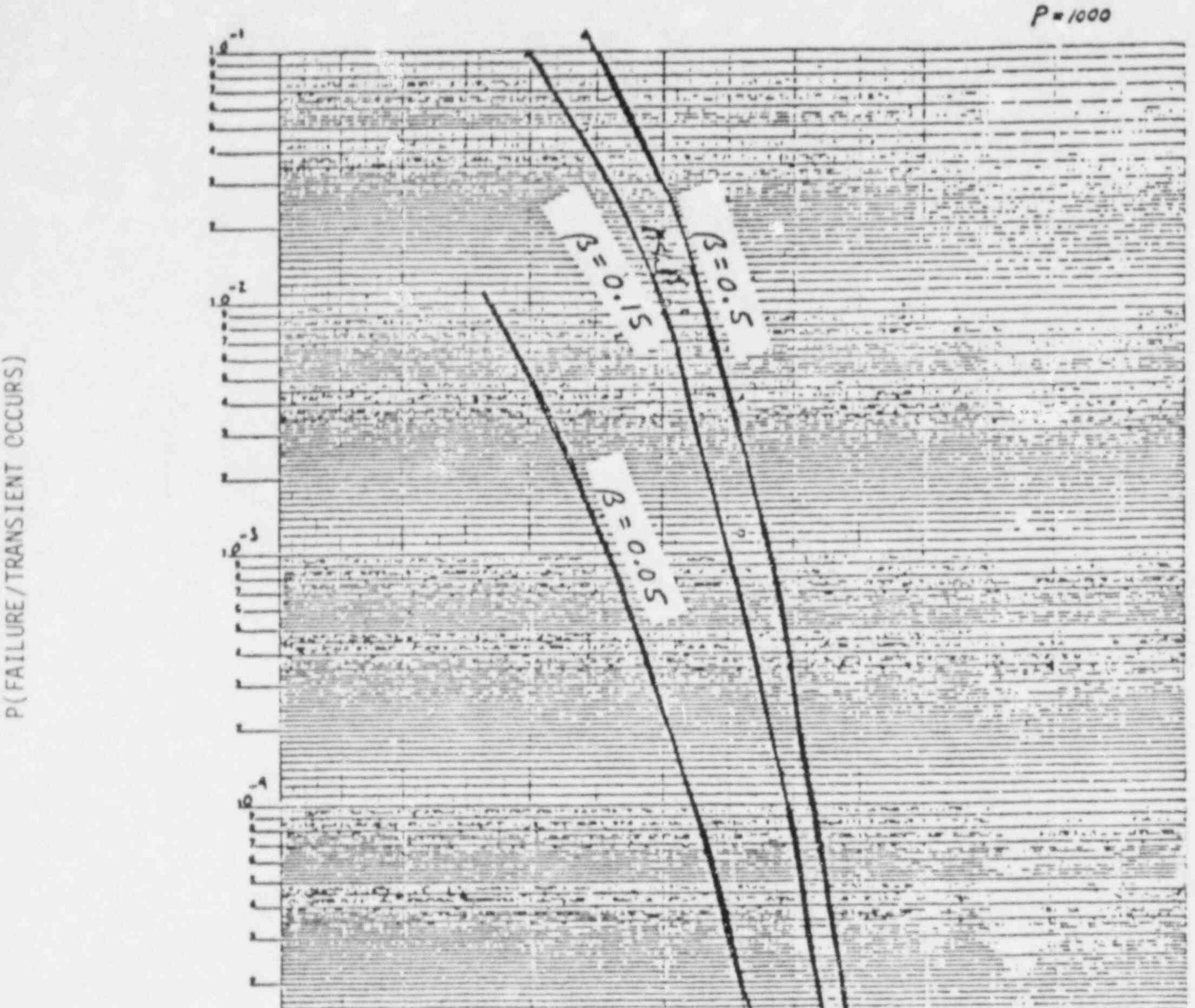

FIGURE 11: SENSITIVITY OF CONDITIONAL FAILURE PROBABILITY TO $T_f - RT_{NDT}$

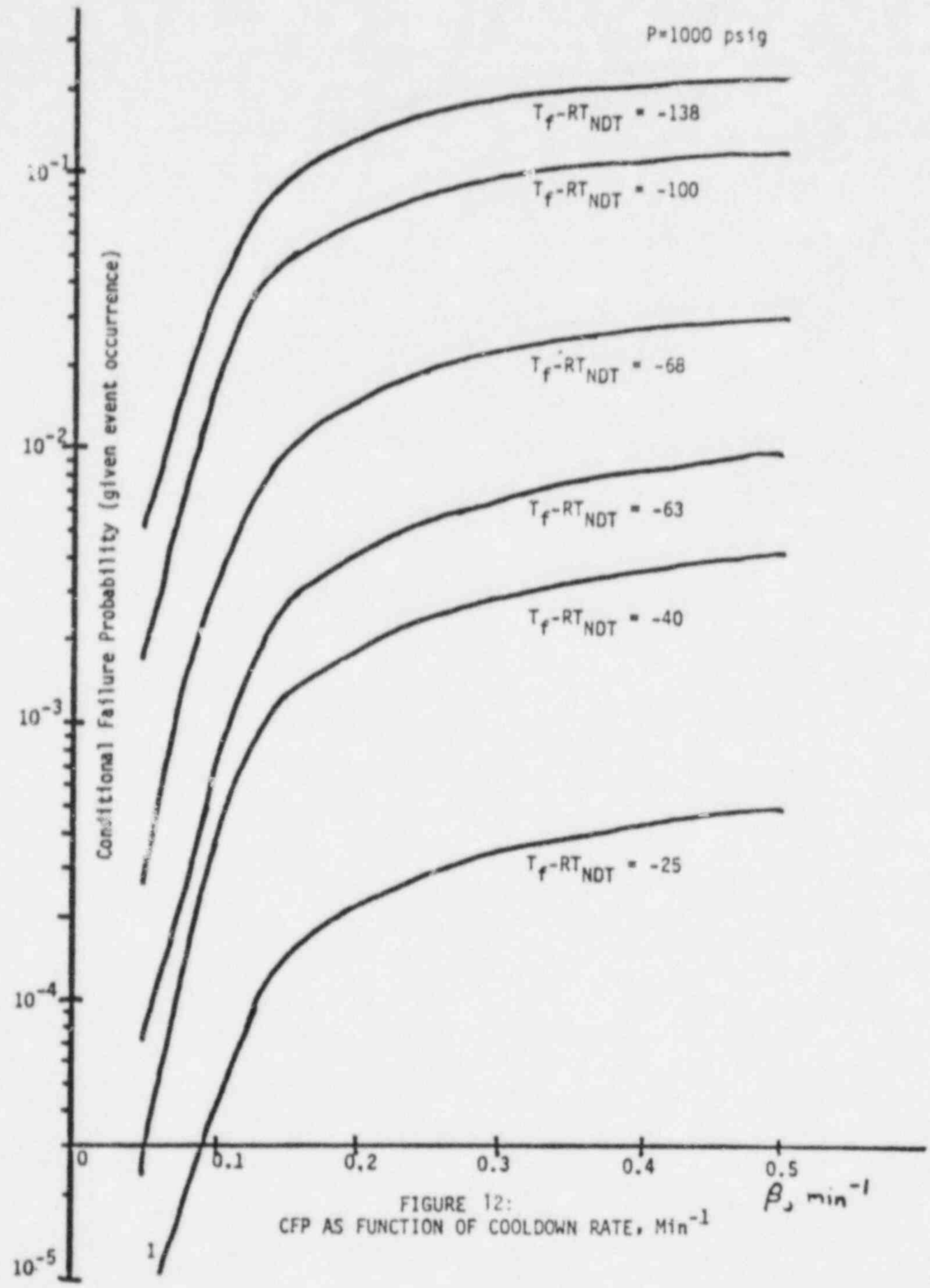

FIGURE 12:
CFP AS FUNCTION OF COOLDOWN RATE, Min^{-1}

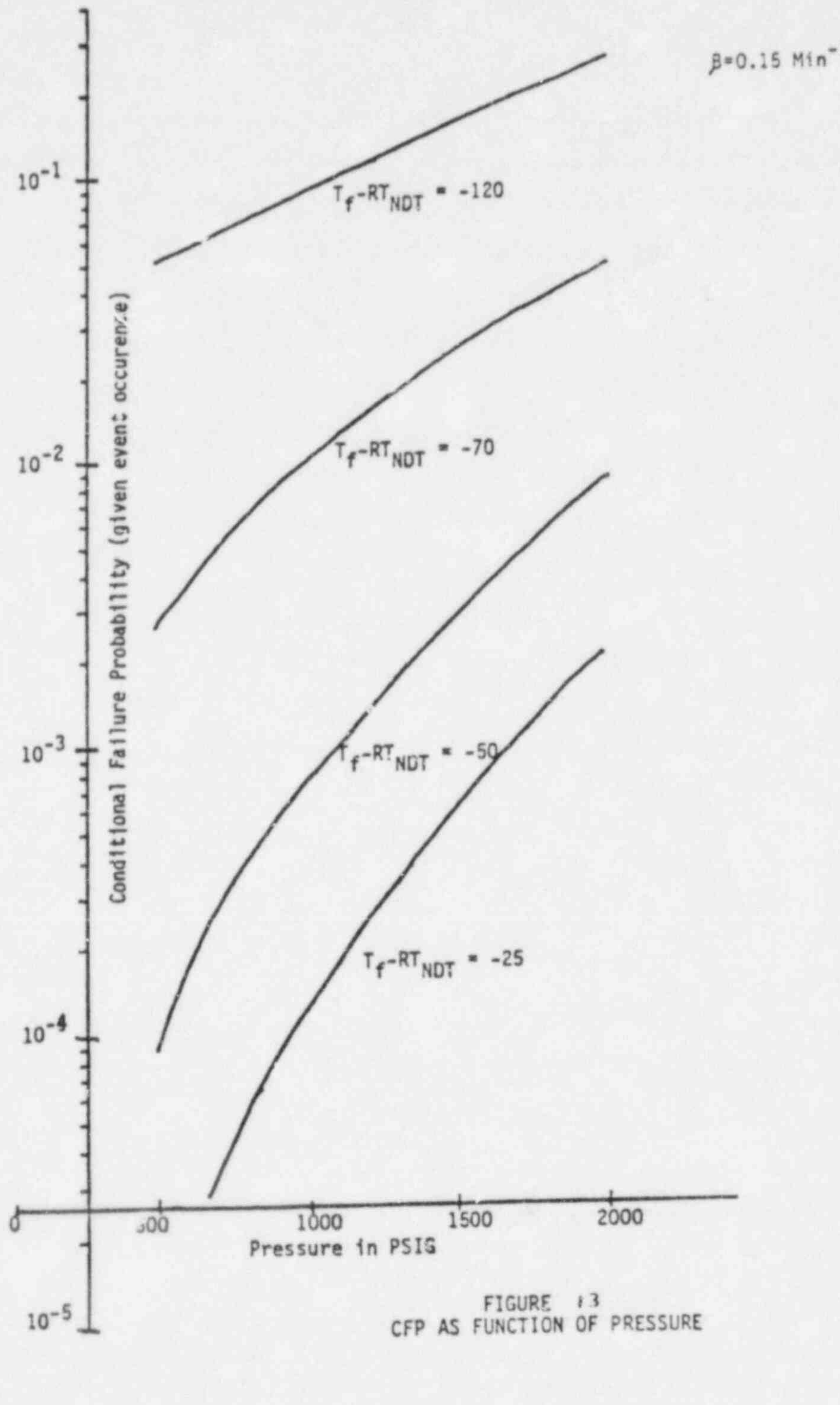

FIGURE 13
CFP AS FUNCTION OF PRESSURE

PRESSURIZED-THERMAL-SHOCK EXPERIMENTS*

G. D. Whitman R. W. McCulloch

Oak Ridge National Laboratory
Oak Ridge, Tennessee 37830

The reactor pressure vessel in a pressurized water reactor is normally subjected to temperatures and pressures that preclude propagation of sharp, crack-like defects that might exist in the wall of the vessel. However, there is a class of postulated accidents, referred to as overcooling accidents, that can subject the pressure vessel to severe thermal shock while the pressure is substantial. As a result of such accidents vessels containing high concentrations of copper and nickel, which enhance radiation embrittlement, may possess a potential for extensive propagation of preexistent inner-surface flaws prior to the vessel's normal end of life.

The primary objective of the ORNL pressurized-thermal-shock (PTS) experiments is to verify analytical methods that are used to predict the behavior of pressurized-water-reactor vessels under these accident conditions involving combined pressure and thermal loading. The criteria on which the experiments are based are:

(a) Scale large enough to attain effective flaw border triaxial restraint and a temperature range sufficiently broad to produce a progression from frangible to ductile behavior through the wall at a given time.

(b) Use of materials that can be completely characterized for analysis.

(c) Stress states comparable to the actual vessel in zones of potential flaw extension.

(d) Range of behavior to include cleavage initiation and arrest, cleavage initiation and arrest on the upper shelf, arrest in a high K_I gradient, warm prestressing, and entirely ductile behavior.

---

*Research sponsored by the Office of Nuclear Regulatory Research, U.S. Nuclear Regulatory Commission under Interagency Agreements 40-551-75 and 40-552-75 with the U.S. Department of Energy under contract W-7405-eng-26 with the Union Carbide Corporation.

(e) Long and short flaws with and without stainless steel cladding.

(f) Control of loads to prevent vessel burst, except as desired.

A PTS test facility is under construction which will enable the establishment and control of wall temperature, cooling rate, and pressure on an intermediate test vessel (ITV) in order to simulate stress states representative of an actual reactor pressure vessel. The facility, to be completed in June of 1983, will house an ITV in a heated shroud, which will also serve to establish sufficient flow of a precooled water-alcohol mixture to thermally shock the flawed ITV outer surface. The ITV will be pressurized internally during the test and will contain instrumentation to enable on-line data acquisition and control. Vessel wall temperatures, initiation and arrest fracture toughness, and stress intensity will be calculated and displayed during the tests.

Three experiments are presently planned. The first will address warm prestressing effectiveness and arrest on the ductile upper shelf. The second will examine arrest on a low-toughness ductile upper shelf, and the last will evaluate stainless steel cladding effectiveness in restricting small flaw growth. The test matrix and first two experiments are discussed in detail and the third experiment is summarized.

References

1. W. R. Corwin, "Pressurized-Thermal-Shock Studies," *Heavy-Section Steel Technology Program Quart. Prog. Rep. July–September 1980*, NUREG/CR-1806 (ORNL/NUREG/TM-419), pp. 53–60.

2. R. H. Bryan and G. C. Robinson, "Pressurized-Thermal-Shock Studies," *Heavy-Section Steel Technology Program Quart. Prog. Rep. October–December 1980*, NUREG/CR-1941 (ORNL/NUREG/TM-437), pp. 57–60.

3. S. K. Iskander et al., *OCA-I, A Code for Calculating the Behavior of Flaws on the Inner Surface of a Pressure Vessel Subjected to Temperature and Pressure Transients*, NUREG/CR-2113 (ORNL/NUREG-84), July 1981.

4. R. H. Bryan and G. C. Robinson, "Pressurized-Thermal-Shock Studies," *Heavy-Section Steel Technology Program Quart. Prog. Rep. January–March 1981*, NUREG/CR-2141, Vol. 1 (ORNL/TM-7822), pp. 102–111.

5. G. C. Robinson, "Pressurized Thermal Shock," *Heavy-Section Steel Technology Program Quart. Prog. Rep. April–June 1981*, NUREG/CR-2141, Vol. 2 (ORNL/TM-7955), pp. 74–85.

6. G. C. Robinson, "Pressurized-Thermal-Shock Studies," *Heavy-Section Steel Technology Program Quart. Prog. Rep. July–September 1981*, NUREG/CR-2141, Vol. 3 (ORNL/TM-8195), pp. 105–108.

7. R. H. Bryan and J. W. Bryson, "Pressurized-Thermal-Shock Studies and Fracture Analysis," *Heavy-Section Steel Technology Program Quart. Prog. Rep. July–September 1981*, NUREG/CR-2141, Vol. 3 (ORNL/TM-8195), pp. 108–122.

8. R. H. Bryan, J. W. Bryson and B. R. Bass, "PTS Test Studies," *Heavy-Section Steel Technology Program Quart. Prog. Rep. October–December 1981*, NUREG/CR-2141, Vol. 4 (ORNL/TM-8252), pp. 107–113.

9. G. C. Robinson and R. W. McCulloch, "Pressurized-Thermal-Shock Studies," *Heavy-Section Steel Technology Program Quart. Prog. Rep. January–March 1982*, NUREG/CR-2751, Vol. 1 (ORNL/TM-8369, Vol. 1), pp. 109–120.

10. R. W. McCulloch, "Pressurized-Thermal-Shock Studies," *Heavy-Section Steel Technology Program Quart. Prog. Rep. April–June 1982*, NUREG/CR-2751, V2 (ORNL/TM-8369, V2), (in preparation).

UNION CARBIDE ORNL

PRESSURIZED–THERMAL–SHOCK EXPERIMENTS

G. D. WHITMAN   R. W. McCULLOCH
OAK RIDGE NATIONAL LABORATORY

PRESENTED AT THE
TENTH WATER REACTOR SAFETY RESEARCH
INFORMATION MEETING

GAITHERSBURG, MARYLAND

OCTOBER 12–15, 1982

UNION CARBIDE ORNL

SUMMARY

- STATEMENT OF THE PROBLEM
- CRITERIA FOR PRESSURIZED–THERMAL–SHOCK EXPERIMENTS
- PRESSURIZED–THERMAL–SHOCK TEST FACILITY
- PLANNED PRESSURIZED–THERMAL–SHOCK EXPERIMENTS

UNION CARBIDE ORNL

OCA'S REPRESENT A CHALLENGE TO THE INTEGRITY OF PWR PRESSURE VESSELS

UNION CARBIDE ORNL

CRITICAL CRACK DEPTH CURVES FOR A REFERENCE PWR VESSEL INDICATE DEEP PENETRATION OF A FLAW UNDER SOME PRESSURIZED–THERMAL–SHOCK LOADINGS

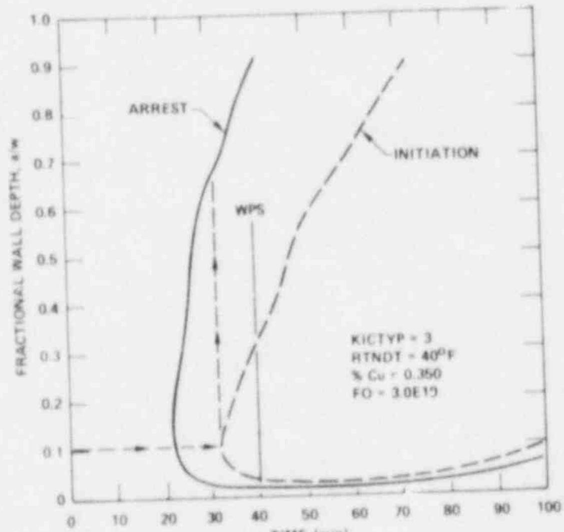

UNION CARBIDE
ORNL

CRITERIA FOR PRESSURIZED–THERMAL–SHOCK EXPERIMENT

- TEST TO VALIDATE METHODS OF ANALYSIS APPLICABLE TO FULL–SCALE RPV'S UNDER COMBINED LOADING
- SCALE LARGE ENOUGH TO ATTAIN EFFECTIVE FULL–SCALE RESTRAINT
- USE CHARACTERIZED MATERIAL IN FLAW REGION (INCLUDING CLADDING)
- TEST CONDITIONS AND MATERIALS PRODUCE

  (1) REALISTIC (PWR) STRESS FIELDS AND GRADIENTS

  (2) REALISTIC FRACTURE TOUGHNESS CONDITIONS IN ZONE OF ACTION

UNION CARBIDE
ORNL

CRITERIA FOR PRESSURIZED–THERMAL–SHOCK EXPERIMENT (CONTINUED)

- TEST CONDITIONS ARE CAPABLE OF PRODUCING

  (1) CLEAVAGE INITIATION (SMALL AND LONG FLAWS)

  (2) CLEAVAGE INITIATION AND ARREST BELOW UPPER SHELF

  (3) CLEAVAGE INITIATION WITH ARREST ON UPPER SHELF

  (4) ARREST IN HIGH K GRADIENT

  (5) WPS STATES, MARGINAL, RELIEF WITH LOW AND HIGH K_I, SECONDARY WPS

- LOADING CONDITIONS AND CONTROLS ARE CAPABLE OF PREVENTING VESSEL BURST (EXCEPT WHEN DESIRED)

UNION CARBIDE
ORNL

PRESSURIZED–THERMAL–SHOCK ISSUES WHICH THE PRESSURIZED–THERMAL–SHOCK TEST FACILITY CAN ADDRESS INCLUDE

- INTERVENTION OF DUCTILE UPPER SHELF IN CRACK ARREST
- EFFECTIVENESS OF WARM PRESTRESSING
- ARREST IN A RAPIDLY RISING K_I FIELD
- BEHAVIOR OF SMALL FLAWS WITH AND WITHOUT SS CLADDING

UNION CARBIDE
ORNL

THE FUNCTION OF THE PTSTF IS TO ESTABLISH AND CONTROL

- MAXIMUM TEMPERATURE – T_{max}
- SINK TEMPERATURE – T_{sink}
- HEAT TRANSFER COEFFICIENT – h
- PRESSURE – p

THE METHOD OF TESTING INCLUDES

- USING EXISTING HSST INTERMEDIATE TEST VESSELS (ITV'S)
- EXTERNAL FLAW, EXTERNAL COOLING, INTERNAL PRESSURE
- COMPLETE PRETEST MATERIALS CHARACTERIZATION
- PRETEST ANALYSIS AND PREDICTION
- HIGHLY INSTRUMENTED ITV
- ON–LINE CONTROL AND MONITORING
- POSTTEST FAILURE ANALYSIS

PRESSURIZED–THERMAL–SHOCK TEST FACILITY

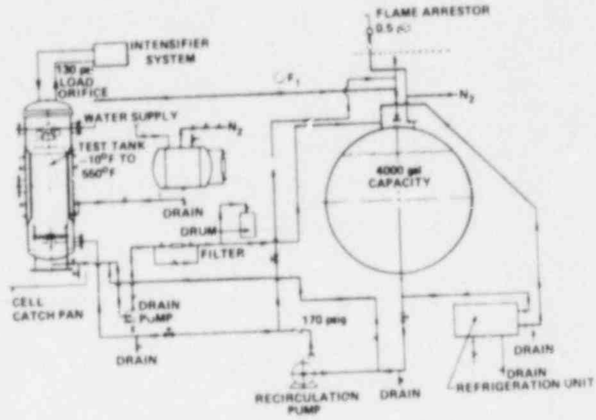

SECTION ELEVATION OF HSST PROGRAM PRESSURIZED–THERMAL–SHOCK FACILITY

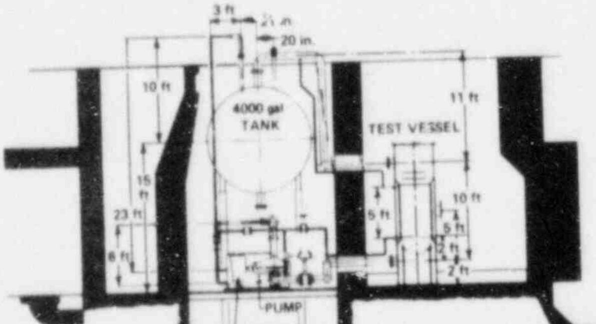

THE MAJOR OBJECTIVES OF A PRESSURIZED–THERMAL–SHOCK EXPERIMENT ARE

- SIMULATION OF CONDITIONS OF MATERIAL TOUGHNESS AND STRESS STATE REPRESENTING A COMBINATION OF PRESSURE AND THERMAL LOADINGS IN A REACTOR VESSEL
- DEVELOPMENT OF DATA FOR VALIDATION OF ANALYTICAL MODELS OF FLAW BEHAVIOR FOR THE CONDITIONS OF INTEREST

UNION CARBIDE ORNL

LONG FLAW CONFIGURATION FOR PRESSURIZED–THERMAL–SHOCK EXPERIMENTS

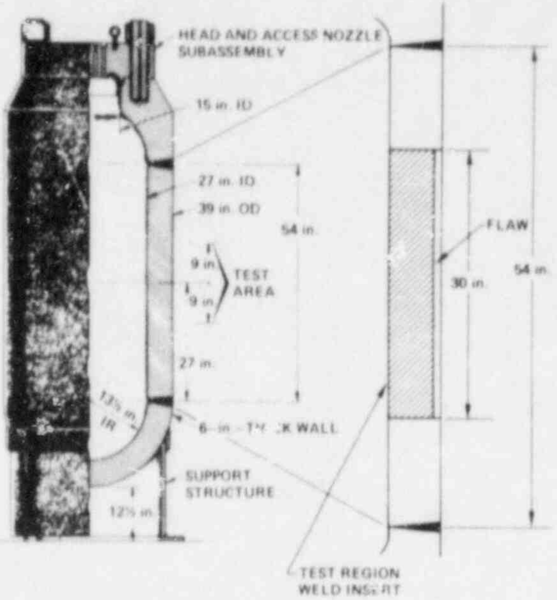

UNION CARBIDE ORNL

3D ANALYSIS SHOWS THE MIDSECTION OF THE FLAW HAS UNIFORM STRESS INTENSITY

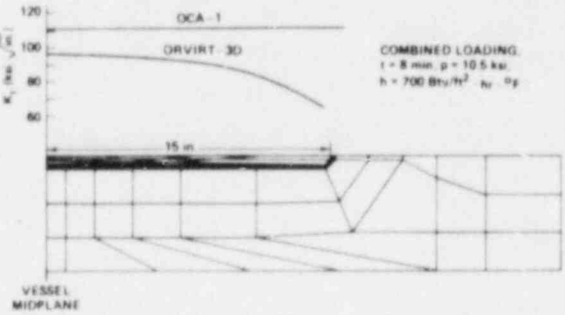

UNION CARBIDE ORNL

BURST PRESSURE VS CRACK LENGTH FOR HSST INTERMEDIATE VESSEL

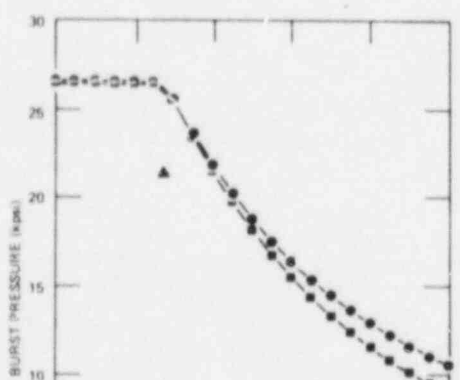

UNION CARBIDE ORNL

PRESSURIZED–THERMAL–SHOCK TRANSIENTS PRODUCE CONDITIONS THAT MAY RESULT IN PROPAGATION OF INNER–SURFACE FLAW

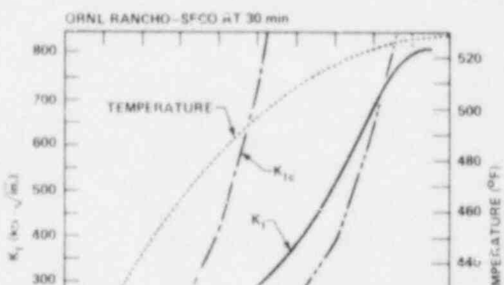

UNION CARBIDE ORNL

CONDITIONS IN HSST INTERMEDIATE VESSEL ARE SIMILAR TO PWR VESSEL UNDER PRESSURIZED–THERMAL–SHOCK TRANSIENT

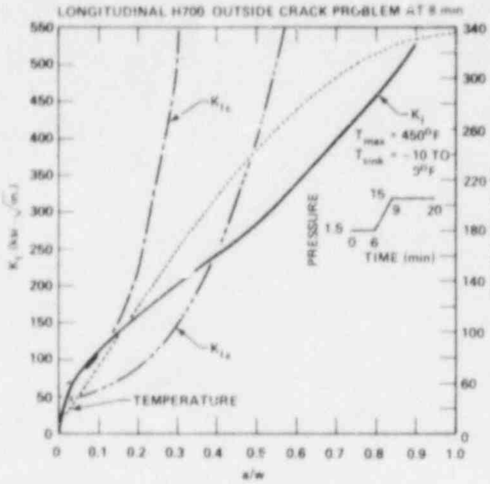

UNION CARBIDE ORNL

RANCHO–SECO PRESSURIZED THERMAL SHOCK, K_I VERSUS a/w AT 30 MINUTES

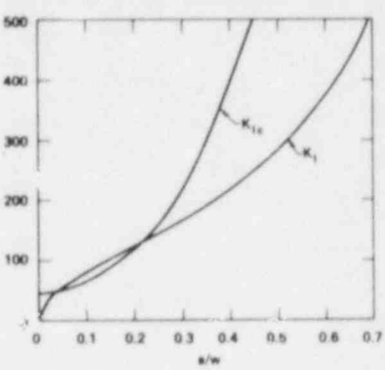

UNION CARBIDE ORNL

ORNL PTS, K_I VERSUS a/w AT 8 MINUTES

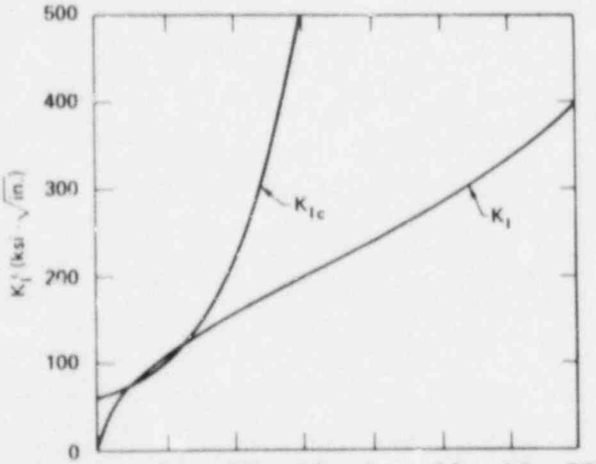

UNION CARBIDE ORNL

PRESSURIZED–THERMAL–SHOCK EXPERIMENT INVOLVES TESTS ON THREE VESSELS TO VALIDATE PREDICTIONS OF FLAW BEHAVIOR UNDER COMBINED LOADS

EXPERIMENT	OBJECTIVE
PTS–1	WARM PRESTRESSING EFFECTIVENESS AND ARREST ON DUCTILE SHELF
PTS–2	ARREST ON DUCTILE SHELF IN LOW UPPER SHELF MATERIAL
PTS–3	STAINLESS STEEL CLADDING EFFECTIVENESS IN RESTRICTING SMALL FLAW GROWTH

UNION CARBIDE ORNL

PRESSURIZED–THERMAL–SHOCK TEST MATRIX

TEST NO.	MATERIAL TOUGHNESS	WPS EFFECTS	ARREST CONDITION	FLAW GEOMETRY	CLADDING
PTS–1	HIGH SHELF	YES	TRANSITION AND DUCTILE SHELF IN RISING K FIELD	LONG	NO
PTS–2	LOW SHELF	NO	DUCTILE SHELF IN RISING K FILED	LONG	NO
PTS–3	HIGH SHELF	NO	TRANSITION	SHORT	YES

UNION CARBIDE ORNL

PTS–1 WILL DEMONSTRATE WARM PRESTRESSING EFFECTIVENESS

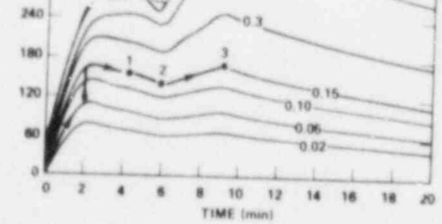

UNION CARBIDE ORNL

WPS (LOAD AND THERMAL HISTORIES) AFFECTS CRITICAL VALUES OF K_I FOR CRACK INITIATION

- K_{Ic}: $\dot{K}_I > 0$, $\dot{T} = 0$
- DURING OCA, K_I VARIES AND $\dot{T} < 0$

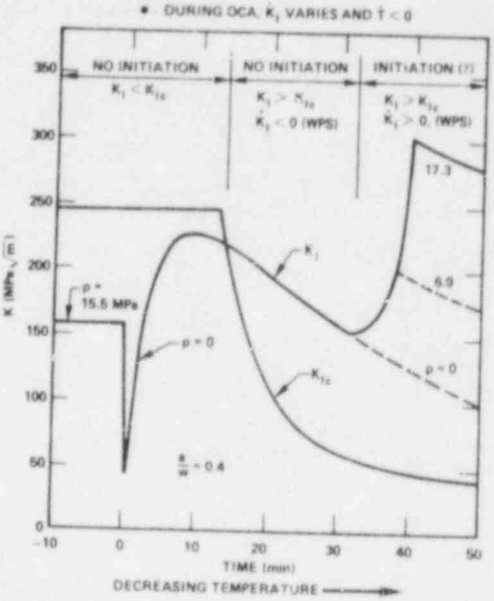

UNION CARBIDE ORNL

CRITICAL CRACK DEPTH CURVES FOR LONGITUDINAL OUTSIDE CRACK, PTS–1

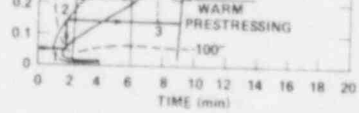

CRITICAL CRACK DEPTH CURVES FOR LONGITUDINAL OUTSIDE CRACK, PTS–2

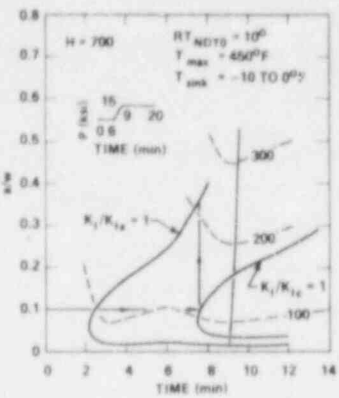

SHORT FLAW CONFIGURATION WITH STAINLESS STEEL CLADDING

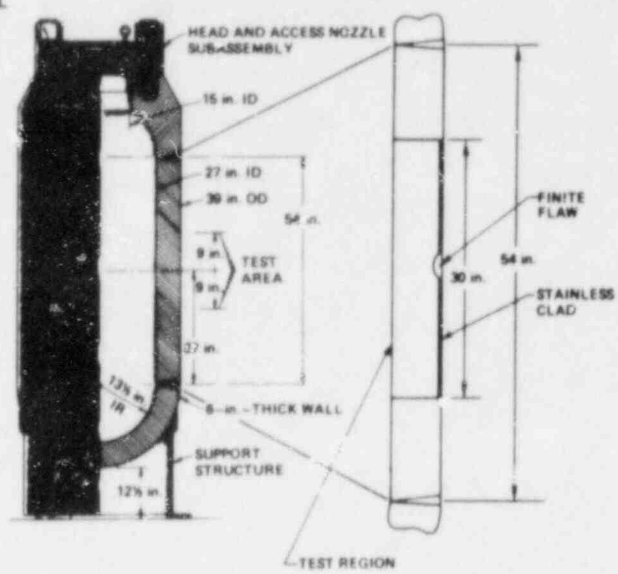

THE FLEXIBILITY OF THE INTERMEDIATE VESSEL TEST CONCEPT WILL PRODUCE DATA ON MAJOR PTS ISSUES

- ARREST
- WARM PRESTRESSING
- FLAW GEOMETRY
- CLADDING

SMALL-SCALE CLAD EFFECTS STUDY*

G. C. Robinson

Oak Ridge National Laboratory
Oak Ridge, Tennessee 37830

The Small-Scale Clad Effects Study of the HSST Program was initiated to study the interaction of stainless cladding with flaws initiated in and propagating in base metal. From the designer's viewpoint stainless cladding is primarily viewed as a corrosion- and crud-prevention measure in light-water reactor vessel design, and except for its effect upon fatigue in thermal transients, its effect upon structural integrity has heretofore been largely disregarded. With the more recent focus of safety studies upon LOCA scenarios that emphasize the behavior of small flaws, it has become evident that stainless cladding may have a key role in the propagation and/or arrest of propagating flaws. A complicating factor in understanding the role of stainless cladding in this setting is its fracture toughness as a function of radiation dose and as a function of fabrication process for which meager data exist. The initial phase of this study has attempted to address this question by testing stainless-clad specimens that had been subjected to heat treatments to simulate "beginning-of-life" and "end-of-life" toughness conditions to fast-running cracks.

A survey of fabrication processes employed on reactor vessels revealed that the majority of light-water reactor vessels have employed either three-wire or strip-clad processes with the three-wire process being predominantly used on early vessels, strip on later vessels. Because of the pressing need for data, the mothballing by vendors of their three-wire equipment and the attendant difficulty in obtaining timely contracts for vendor preparation of specimens, we elected to prepare specimens in-house by using a single wire welding procedure.

---

*Research sponsored by the Office of Nuclear Regulatory Research, U.S. Nuclear Regulatory Commission under Interagency Agreements 40-551-75 and 40-552-75 with the U.S. Department of Energy under contract W-7405-eng-26 with the Union Carbide Corporation.

The specimens were designed as rectangular parallelepipeds with stainless cladding on one face. Grooves were machined in the cladding with the intent to provide a plane surface at the bottom of the groove at the stainless-base metal interface. An electron beam (EB) weld was then applied to the bottom groove surface. Specimens were cooled to the testing temperature and were loaded by four-point, constant-moment loading to the stress state required. Hydrogen charging of the EB weld was initiated and presented the stainless cladding with a relatively fast-running crack. A matrix of specimens was planned that varied the parameters: flaw size, run distance from EB weld to cladding, cladding type, and stress state in order to elucidate cladding arrest behavior.

Problems were experienced with groove machining to obtain the stainless base metal interface, in some cases the groove was too shallow, in others too deep. On specimens where stainless remained below the groove, premature popping of the EB weld prior to hydrogen charging was a common phenomenon, preventing a proper control of the stress state. On specimens with too deep grooves, the geometry caused premature arrest and prevented the flaw from running to the cladding. In addition, the specimens prepared by sigma-phase heat treatment were too brittle and, based on limited data, are not representative, as intended, of end-of-life conditions.

The tests completed to date under the initial phase of this study indicate that the cladding employed to represent beginning-of-life conditions has sufficient arrest toughness to stop running cracks, but the upper and lower bounds of crack arrest are not yet determined. Analyses of the tests by two approximate techniques and by the ORVIRT finite-element methods have not been completely consistent. The fabrication techniques employed for this first series of tests have resulted in conditions that have prevented control of the stress state at pop-in of the hydrogen-charged EB welds. Consequently, bounding of the arrest toughness of the stainless cladding has been prevented.

Preparations are now under way to redesign and fabricate a new series of specimens that will eliminate the problems presented by the groove/EB weld design of the first series. In addition, this series will employ a three-wire weld cladding technique typical of many early reactor vessel designs.

UNION CARBIDE ORNL

SMALL-SCALE CLAD EFFECTS STUDY

G. C. ROBINSON
OAK RIDGE NATIONAL LABORATORY

PRESENTED AT
TENTH WATER REACTOR SAFETY RESEARCH
INFORMATION MEETING

NATIONAL BUREAU OF STANDARDS
GAITHERSBURG, MARYLAND

OCTOBER 14, 1982

UNION CARBIDE ORNL

OBJECTIVE OF CLADDING EFFECTS EXPERIMENTS

TO DEMONSTRATE THE EFFECT OF STAINLESS STEEL WELD CLADDING ON THE EXTENT OF CRACK PROPAGATION, FOR A SMALL FINITE LENGTH SURFACE CRACK SUBJECTED TO A STRESS GRADIENT SIMILAR TO THAT PRODUCED BY THERMAL SHOCK

UNION CARBIDE ORNL

RATIONALE FOR TEST SERIES

AN UNCLAD SPECIMEN IN P[illegible] BENDING SUBJECTED TO A FAST RUNNING CRACK WILL FAIL CATASTROPHICALLY, WHEREAS, IF THE CLADDING IS SUFFICIENTLY TOUGH, THE PROPAGATING FLAW WILL BE [illegible]INNED BY THE STAINLESS

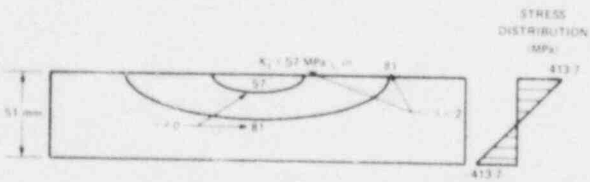

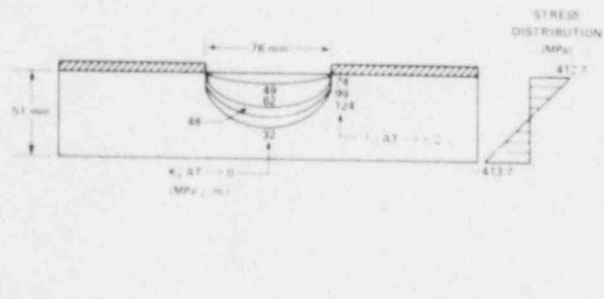

UNION CARBIDE ORNL

A TEST MATRIX WAS PLANNED TO INVESTIGATE THE ABILITY OF CLADDING TO ARREST A PROPAGATING FLAW AS A FUNCTION OF FLAW SIZE, RUN DISTANCE AND CLADDING TYPE

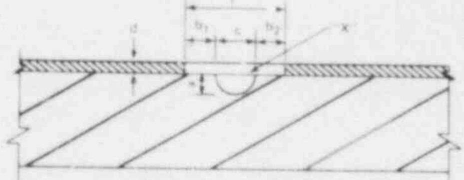

UNION CARBIDE ORNL

A SINGLE PLATE, HSST PLATE 07B, WAS USED TO FABRICATE CLAD PLATE TEST SPECIMENS TO SIMPLIFY CHARACTERIZATION OF MATERIAL PROPERTIES AND TO IMPROVE DATA CORRELATION

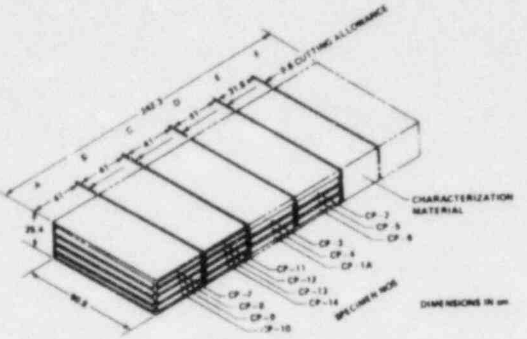

UNION CARBIDE ORNL

TO EXPEDITE PERFORMANCE OF THE FIRST PHASE OF THE TASK, IN-HOUSE SINGLE-WIRE, SUBMERGED-ARC WELD EQUIPMENT WAS USED TO APPLY CLADDING

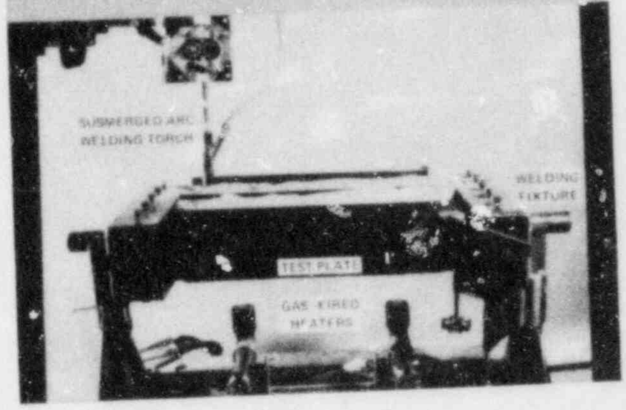

UNION CARBIDE ORNL

THREE TYPES OF PLATES HAVE BEEN TESTED IN THIS PROGRAM

- UNCLAD PLATES
- PLATES CLAD WITH A MODERATE TOUGHNESS WELD METAL
- PLATES CLAD WITH A LOW TOUGHNESS WELD METAL

UNION CARBIDE ORNL

THE TEST PLATES ARE COMPOSED OF FOUR MATERIALS

MATERIAL	USE
A533 GRADE B CLASS 1	ENTIRE TEST PIECE IN UNCLAD TEST PLATES
	BASE METAL FOR PLATES CLAD WITH T308/309
A533 GRADE B CHEMISTRY, NORMALIZED AND TEMPERED	BASE METAL FOR PLATES CLAD WITH T312
T308/309 WELD METAL	MODERATE TOUGHNESS CLADDING
T312 WELD METAL, SIGMATIZED	LOW TOUGHNESS CLADDING

UNION CARBIDE
ORNL

THE MATERIALS USED IN THE MODERATE TOUGHNESS CLAD PLATES ARE GENERALLY LESS STRONG AND MORE DUCTILE THAN THOSE IN THE LOW TOUGHNESS CLAD PLATES AT TEST TEMPERATURE

MATERIAL	TEMPERATURE (°C)	STRESSES (MPa)		DUCTILITY (%)	
		YIELD	ULTIMATE	ELONGATION	REDUCTION OF AREA
A533, GRADE B CLASS 1	−40	490.8	685.4	20.7	61.7
	−73	529.0	697.0	23.8	68.0
A533B, N + T	−62	645.2	804.7	17.8	60.1
308/309 WELD METAL	−40	324.7	874.7	43.7	47.0
	−73	323.0	974.6	40.7	40.3
312 WELD METAL	−62	484.5	904.0	27.2	20.3

UNION CARBIDE
ORNL

THE RELATIVE TOUGHNESS OF THE WELD METAL TO THE BASE METAL IS REVERSED IN THE LOW AND MODERATE TOUGHNESS CLAD PLATES

MATERIAL	TEMPERATURE (°C)	K_J (MPa$\sqrt{m}$)
A533 GRADE B CLASS 1	−40	69
	−73	46
A533B, NORMALIZED AND TEMPERED	−62	161
T308/309 WELD METAL	−40	192
	−73	148
T312 WELD METAL	−62	85

UNION CARBIDE
ORNL

THE CHARPY ENERGIES OF THE A533 GRADE B CLASS 1 ARE TYPICAL OF REACTOR PRESSURE VESSEL STEELS

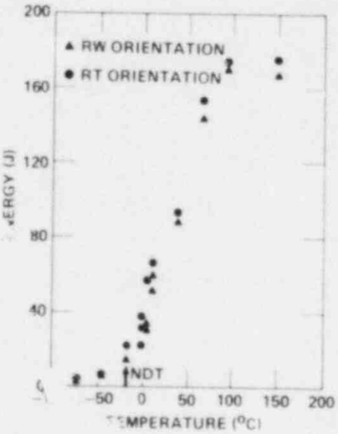

UNION CARBIDE
ORNL

THE CHARPY RESULTS OF THE NORMALIZED AND TEMPERED A533 GRADE B CHEMISTRY MATERIAL SHOW LOWER UPPER–SHELF AND TRANSITION TEMPERATURE THAN STANDARD A533 GRADE B CLASS 1

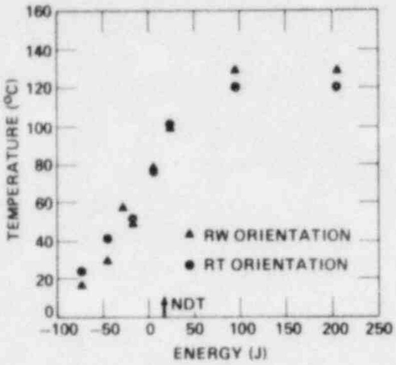

UNION CARBIDE
ORNL

THE CHARPY ENERGY OF THE T308/309 WELD METAL IS A STRONG FUNCTION OF TEMPERATURE

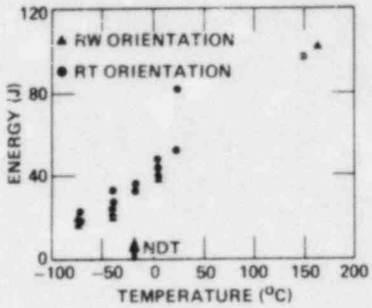

UNION CARBIDE
ORNL

THE CHARPY ENERGIES OF THE T312 WELD METAL ARE MUCH LOWER THAN THAT OF THE T308/309

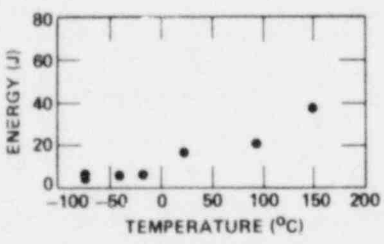

UNION CARBIDE
ORNL

AN EXISTING TESTING MACHINE WAS MODIFIED TO PERMIT COOLING, HYDROGEN CHARGING AND LOADING OF THE CLAD PLATE SPECIMEN

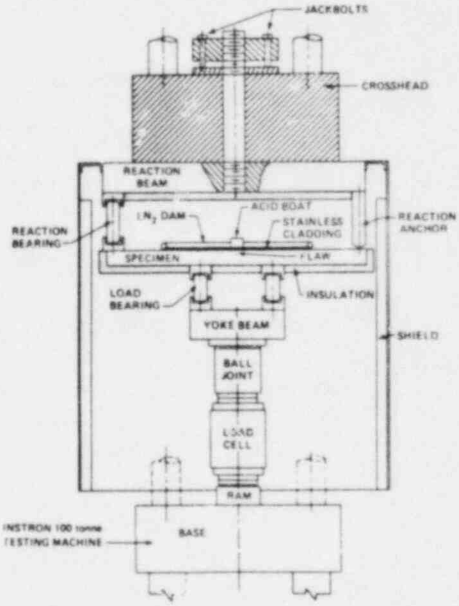

UNION CARBIDE ORNL

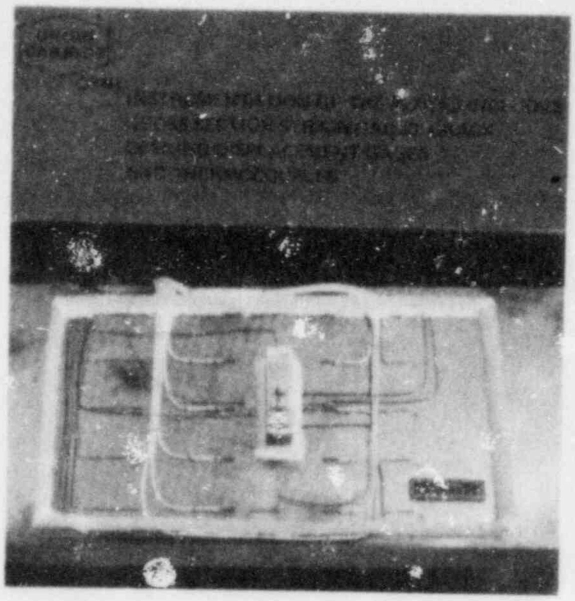

UNION CARBIDE ORNL

SPECIMEN DIMENSIONS HAVE VARIED SIGNIFICANTLY FROM INITIAL INTENT

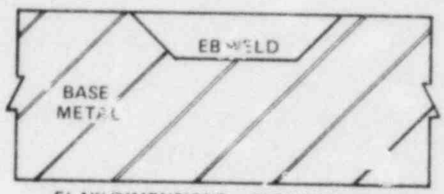

FLAW DIMENSIONS – SPECIMEN CP–1A

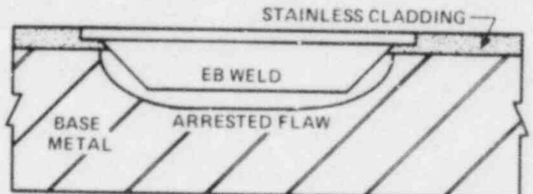

FLAW DIMENSIONS – SPECIMEN CP–3

UNION CARBIDE ORNL

SPECIMEN DIMENSIONS HAVE VARIED SIGNIFICANTLY FROM INITIAL INTENT

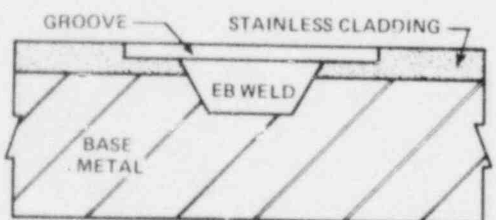

FLAW DIMENSIONS – SPECIMEN CP–5

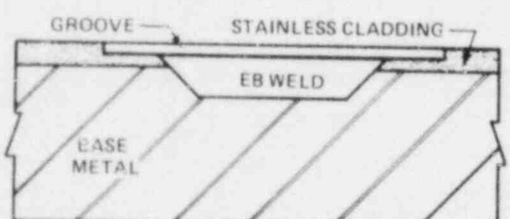

FLAW DIMENSIONS – SPECIMEN CP–7

UNION CARBIDE ORNL

SPECIMEN DIMENSIONS HAVE VARIED SIGNIFICANTLY FROM INITIAL INTENT

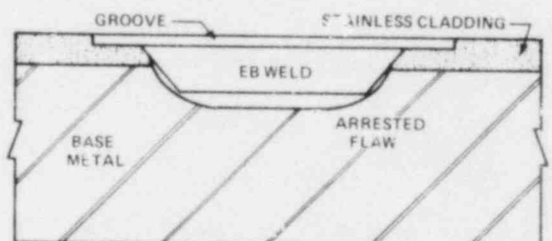

FLAW DIMENSIONS – SPECIMEN CP–8

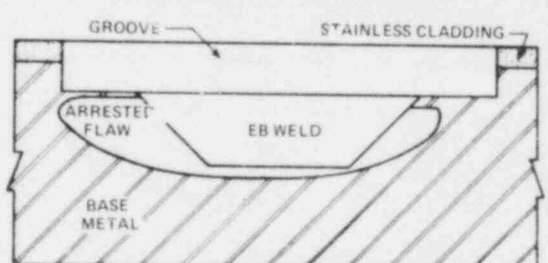

FLAW DIMENSIONS – SPECIMEN CP–9

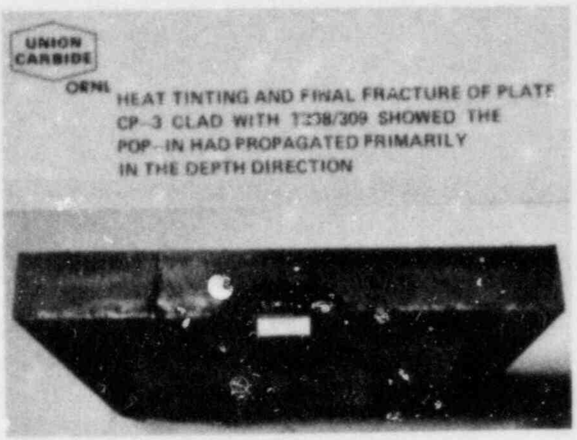
UNION
CARBIDE
ORNL
HEAT TINTING AND FINAL FRACTURE OF PLATE
CP-3 CLAD WITH T308/309 SHOWED THE
POP-IN HAD PROPAGATED PRIMARILY
IN THE DEPTH DIRECTION

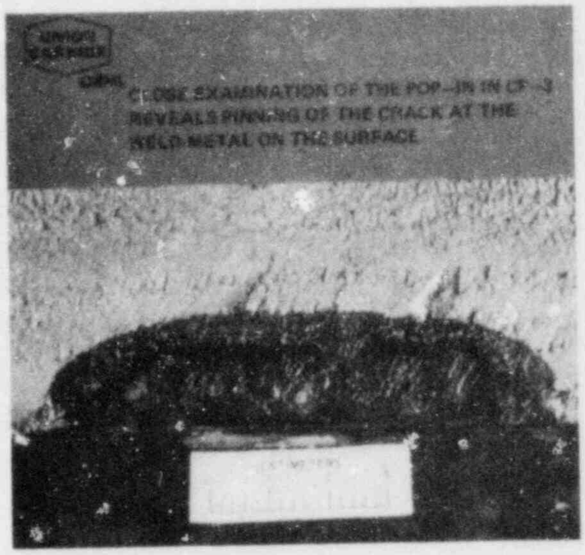
CLOSE EXAMINATION OF THE POP-IN IN CP-3
REVEALS PINNING OF THE CRACK AT THE
WELD METAL ON THE SURFACE

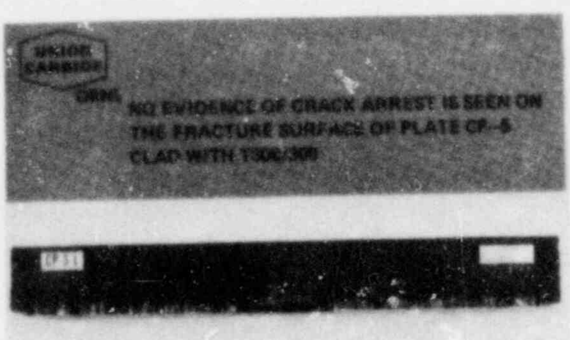
UNION
CARBIDE
ORNL
NO EVIDENCE OF CRACK ARREST IS SEEN ON
THE FRACTURE SURFACE OF PLATE CP-5
CLAD WITH T306/309

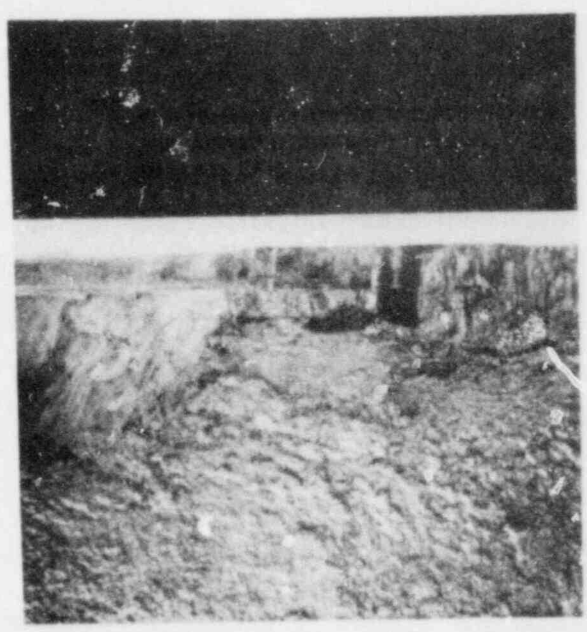

UNION CARBIDE
ORNL

STRESS INTENSITIES CALCULATED BY SEVERAL METHODS ARE GENERALLY CONSISTENT EXCEPT NEAR BASE METAL/CLADDING INTERFACE

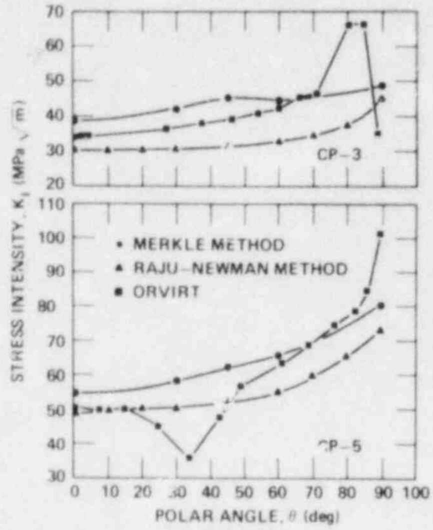

UNION CARBIDE
ORNL

STRESS INTENSITIES CALCULATED BY SEVERAL METHODS ARE GENERALLY CONSISTENT EXCEPT NEAR BASE METAL/CLADDING INTERFACE

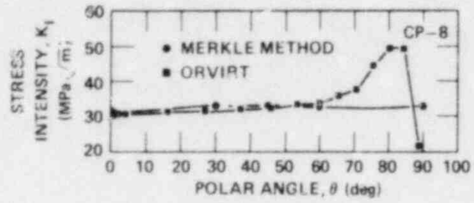

UNION CARBIDE
ORNL

STRESS INTENSITIES CALCULATED BY SEVERAL METHODS ARE INCONSISTENT

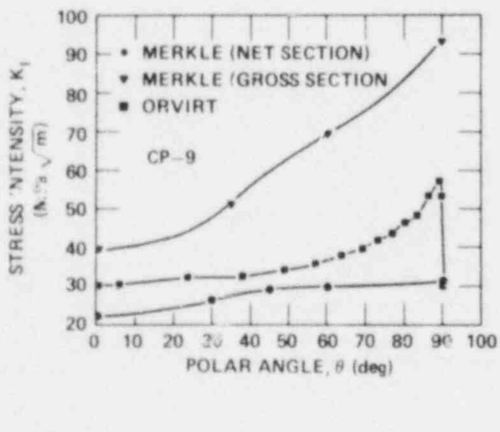

UNION CARBIDE
ORNL

BOUNDS FOR FLAW ARREST BY STAINLESS CLADDING ARE STILL UNDETERMINED

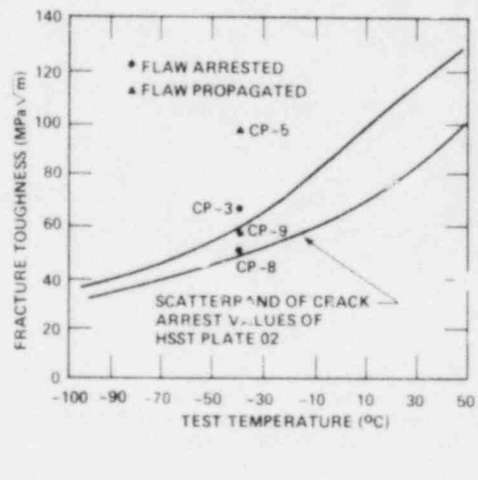

UNION CARBIDE
ORNL

TEST RESULTS TO DATE HAVE SHOWN

- CLADDING OF MODERATE TOUGHNESS DOES HAVE A LIMITED ABILITY TO ARREST A RUNNING CRACK ON THE SURFACE
- A WIDE RANGE OF ARREST/LACK-OF-ARREST CONDITIONS HAS BEEN IDENTIFIED. THIS RANGE NEEDS TO BE BETTER DEFINED
- TO PROVIDE BETTER DEFINITION, EXPERIMENTAL PROCEDURE NEEDS TO BE MODIFIED BY REDESIGNING PLATE SPECIMENS TO ELIMINATE PROBLEMS PRESENTED BY GROOVE DESIGN

RESULTS OF THERMAL-SHOCK EXPERIMENT TSE-6*
and
PROPOSAL FOR TSE-7, 8, 9*

R. D. Cheverton

Oak Ridge National Laboratory
Oak Ridge, Tennessee 37830

Results of Thermal-Shock Experiment TSE-6

In the event of a PWR large-break loss-of-coolant accident, and provided there has been a substantial reduction in the fracture toughness of the pressure vessel material due to radiation damage, a potential could exist for deep penetration of a preexistent long axial flaw. According to an LEFM analysis, there could be a long crack jump followed by arrest deep in the wall without the tip of the crack encountering upper-shelf toughness conditions. The proximity of the arrest point to the outer surface of the vessel wall and the possibility of dynamic effects associated with the long crack jump introduced uncertainties in the analysis that required experimental investigation. A thermal-shock experiment, TSE-6, was conducted for that purpose.

The desired conditions for TSE-6 were achieved with an A508 class-2-chemistry test cylinder tempered at 613°C and having dimensions of 991-mm OD x 76-mm wall x 1.2-m length. The initial flaw was on the inner surface and extended the full length of the cylinder; it was generated by means of the EB-weld technique and had a depth equal to ten percent of the wall thickness. During the experiment, the test cylinder, initially at ~96°C, was subjected to a severe thermal shock by exposing the inner surface of the cylinder to liquid nitrogen.

Prior to the experiment the required tempering temperature for the test cylinder was determined through a combination of fracture toughness determinations for different tempering temperatures and fracture-mechanics analyses of the proposed experiment for different fracture toughness-vs-temperature curves. Once the specific tempering temperature was determined, the test-cylinder material was completely characterized using a prolongation of the test cylinder as a source of test specimen material.

As a result of the severe thermal-shock loading during TSE-6, there were two initiation-arrest events. The first took place at 69 s into the transient with arrest at a fractional crack depth (a/w) = 0.27, and the second event took

*Research sponsored by the Office of Nuclear Regulatory Research, U.S. Nuclear Regulatory Commission under Interagency Agreements 40-551-75 and 40-552-75 with the U.S. Department of Energy under contract W-7405-eng-26 with the Union Carbide Corporation.

place at 137 s at a/w = 0.93. The second event included the desired long crack jump with arrest near the outer surface and demonstrated, in agreement with the LEFM analysis, the inability of the crack to completely penetrate the wall under thermal-shock-loading conditions only.

The first arrest event took place in a steeply rising K_I field ($dK_I/da > 0$), and the corresponding critical value of K_I fell within the scatter band of the lab K_{Ia} data. This indicated that there are no significant differences between arrest in a rising K_I field, which is calculated to take place during thermal-shock loading, and arrest in a falling K_I field ($dK_I/da < 0$), which is characteristic of a lab measurement of K_{Ia}.

The K_I value corresponding to the second arrest event also fell within the scatter band of the lab K_{Ia} data, and thus it appears that dynamic effects at arrest were negligible; that is, they were not discernible by comparing values of K_{Ia}.

With TSE-6 completed, all of the K_{Ic} and K_{Ia} values deduced from TSE-5, 5A and 6 were compared with the ASME Section XI K_{Ic} and K_{Ia} vs T − RTNDT lower-bound curves. All of the data points from the thermal-shock experiments fell to the left of the ASME curves, indicating perhaps that the latter curves are indeed conservative.

Proposal for TSE-7, 8, 9

The purpose of thermal-shock experiments TSE-7, 8, and 9 is to investigate the effect of cladding on the surface extension of short flaws that extend through the cladding into the base material. If the cladding can prevent significant surface extension of a short flaw in a PWR vessel during an overcooling accident, and if the probability of initial through-clad cracks being long is small enough, then the concern over vessel failure as a result of overcooling accidents may vanish.

The proposed thermal-shock experiments would be similar to TSE-5, 5A and 6, although the initial flaws would be short, and at least one of the tests would be conducted with a test cylinder clad on the inner surface. The first test, TSE-7, would be conducted without cladding to demonstrate the ability of a short axial flaw to extend the length of the test cylinder under severe thermal-shock loading and in the absence of cladding. The second test, TSE-8, would be very similar but with cladding on the inner surface of the test cylinder. The specific purpose of TSE-9 will depend on the results of TSE-8 and may include cladding that is degraded to simulate radiation damage effects.

Publications

1. R. D. Cheverton, HSST Thermal-Shock Program Quick-Look Report for TSE-6, ORNL/TSP-1008, December 1981.

2. R. D. Cheverton et al., "Thermal-Shock Investigations," *Heavy-Section Steel Technology Program Quart. Prog. Rep. for October—December 1981*, ORNL/TM-8252, April 1982, pp. 52—81.

3. R. D. Cheverton et al., "Fracture Mechanics Data Deduced from Thermal-Shock and Related Experiments with LWR Pressure Vessel Material," *Aspects of Fracture Mechanics in Pressure Vessels and Piping*, ASME special publication, PVP-Vol. 58, July 1982, pp. 1—17, edited by S. S. Palusamy and S. G. Sampath.

RESULTS OF THERMAL–SHOCK EXPERIMENT TSE–6 AND PROPOSAL FOR TSE–7, 8, 9

R. D. CHEVERTON
HSST THERMAL–SHOCK PROGRAM
OAK RIDGE NATIONAL LABORATORY

PRESENTED AT
TENTH WATER REACTOR SAFETY RESEARCH
INFORMATION MEETING

NATIONAL BUREAU OF STANDARDS
GAITHERSBURG, MARYLAND

OCTOBER 14, 1982

PURPOSE OF TSE–6: EXAMINE FLAW BEHAVIOR FOR

- LONG CRACK JUMP (POSSIBLE DYNAMIC EFFECTS)
- ARREST (?) DEEP IN WALL ($a/w \approx 0.9$)
- GREATER WALL FLEXIBILITY THAN FOR TSE–5 AND 5A

R_o/w = 11.1 (PWR)
= 6.5 (TSE–6)
= 3.3 (TSE–5, 5A)

PWR LBLOCA MAY RESULT IN LONG CRACK JUMP WITH ARREST AT $a/w \approx 0.9$ (LEFM)

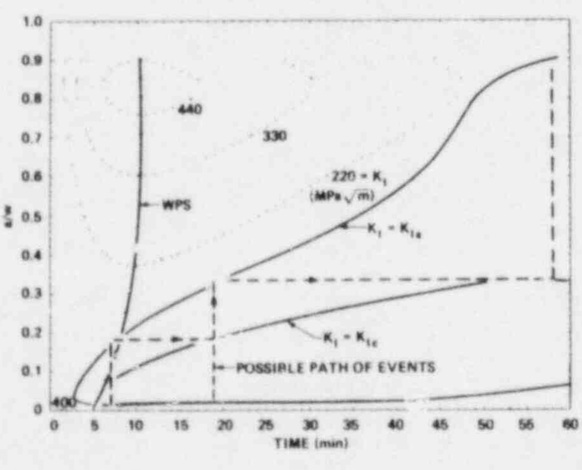

APPROPRIATE EXPERIMENTAL CONDITONS WERE ACHIEVED FOR TSE–6

- 991–mm OD x 76–mm WALL x 1.2–m LENGTH
- A508 CLASS–2 CHEMISTRY
  - TEMPERED AT 613°C
  - RTNDT = 66°C
- SAME THERMAL SHOCK AS FOR TSE–5, 5A
- LONG AXIAL FLAW (a/w = 0.1)

UNION CARBIDE

ORNL TSE-6 TEST CYLINDER INSTRUMENTATION INCLUDED 180 THERMOCOUPLES, 9 COD GAGES, 7 UT CRYSTALS

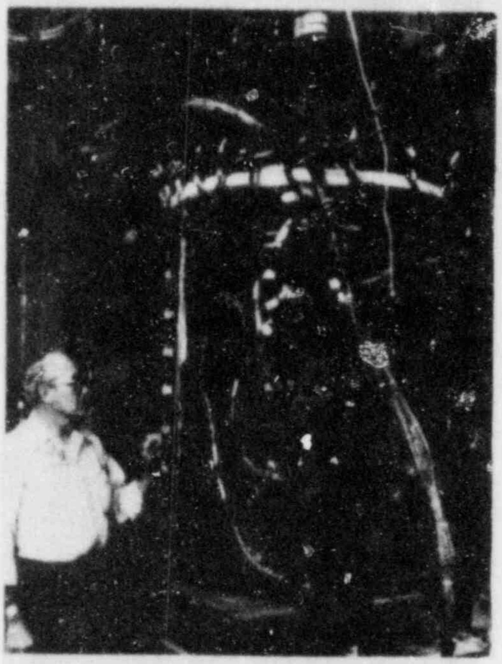

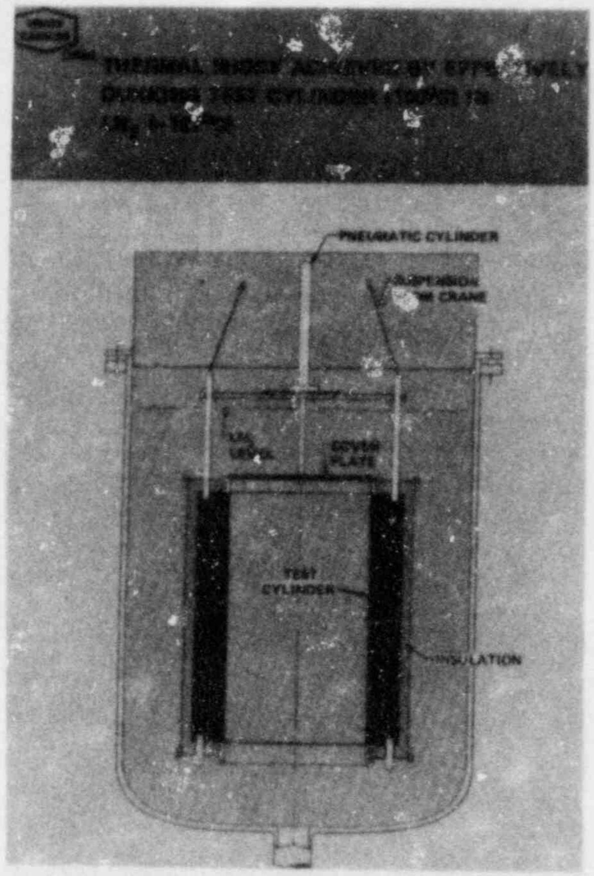

UNION CARBIDE

ORNL FRACTURE TOUGHNESS OF TEST-CYLINDER MATERIAL DETERMINED FOR EXPERIMENT DESIGN AND EVALUATION PURPOSES

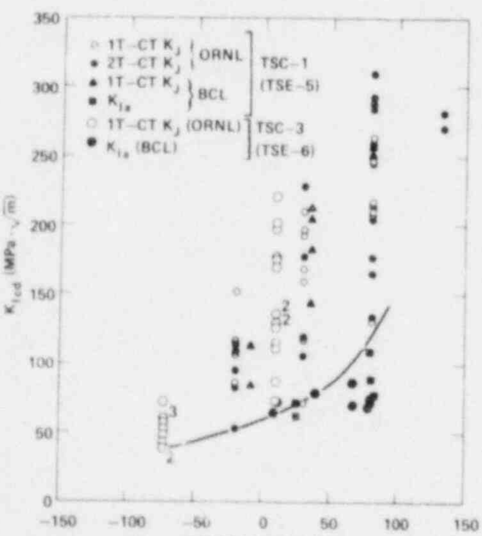

UNION CARBIDE

ORNL PRETEST ANALYSIS, USING TSE-5 TOUGHNESS CURVES, INDICATED DESIRED LEFM FLAW BEHAVIOR ACHIEVABLE

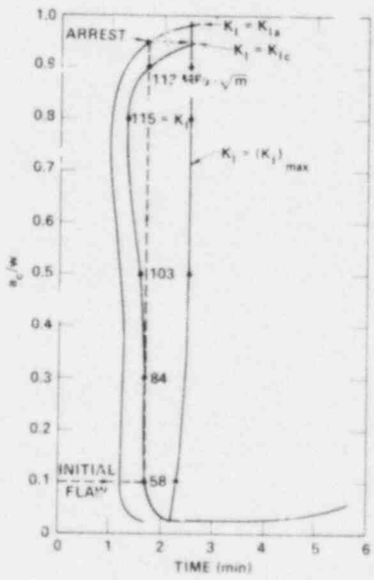

UNION CARBIDE

ORNL DURING TSE–6, DEEP PENETRATION WITH ARREST AT a/w = 0.93 WAS ACHIEVED

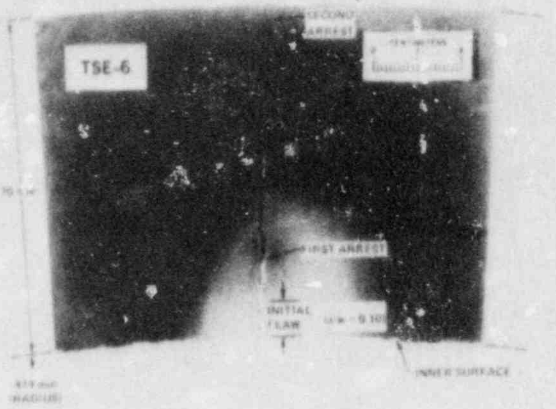

UNION CARBIDE

ORNL COD DATA INDICATE TWO INITIATION ARREST EVENTS

TIME (s)	EVENT	a/w	TEMPERATURE (°C)	K_I (MPa·$\sqrt{m}$) TSE–6	LAB[a]
69	INITIATION	0.10	–12	46[b]	55[c]
	ARREST	0.27	34	63	72
137	INITIATION	0.27	–28	87	50
	ARREST	0.93	106	105	77

[a]K_{Ic} (LOWER BOUND), K_{Ia} (MEAN)

[b]EB–WELD RESIDUAL STRESSES NOT INCLUDED

[c]DOES NOT ACCOUNT FOR EB–WELD EFFECTS

UNION CARBIDE

ORNL FRACTURE SURFACES REVEAL A THIRD AND THUS DYNAMIC EVENT

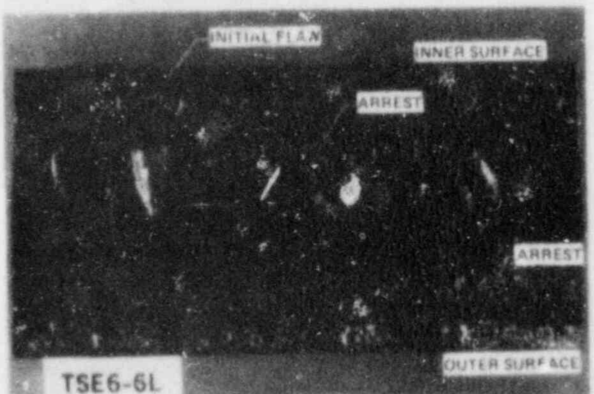

UNION CARBIDE

ORNL TSE–6 DEMONSTRATED

- INABILITY OF CRACK TO PENETRATE WALL AFTER LONG JUMP
- ARREST IN RISING K_I FIELD ($dK_I/da > 0$)

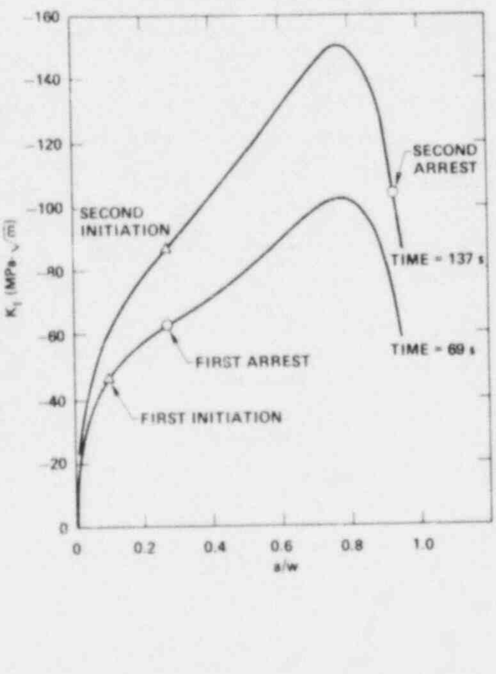

COMPARISON OF TSE–6 AND LAB K_{Ic} AND K_{Ia} DATA INDICATES (FOR THERMAL–SHOCK LOADING)

- LEFM VALID
- DYNAMIC EFFECTS AT ARREST NEGLIGIBLE

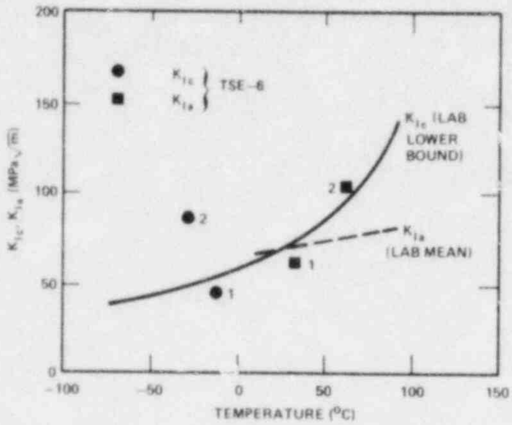

COMPARISON OF TSE K_{Ic} AND K_{Ia} VALUES WITH ASME XI CURVES INDICATES ASME XI CONSERVATIVE

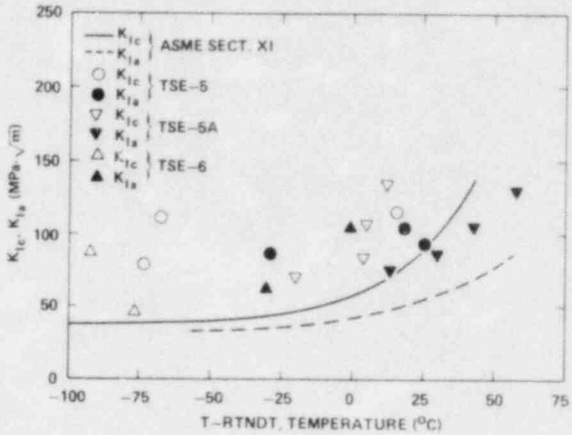

THERMAL–SHOCK EXPERIMENTS HAVE CONFIRMED VALIDITY OF CALCULATIONAL TECHNIQUES WITHIN LEFM REGIME

- LEFM VALID FOR SHALLOW AND DEEP FLAWS
- LEFM VALID FOR SERIES OF INITIATION–ARREST EVENTS
- DEMONSTRATED ARREST WITH $dK_I/da > 0$
- DEMONSTRATED WPS WITH $dK_I/dt < 0$
- DYNAMIC EFFECTS IN TSE'S NEGLIGIBLE
- THERMAL SHOCK ALONE WILL NOT DRIVE CRACK THROUGH WALL
- BASED ON COMPARISON WITH TSE DATA, ASME XI K_{Ic} AND K_{Ia} CURVES CONSERVATIVE

PURPOSE OF TSE–7, 8 AND 9: EVALUATE EFFECT OF CLADDING ON SURFACE EXTENSION OF SHORT, THROUGH–CLAD CRACKS

- TSE–7: SHORT AXIAL FLAW, NO CLADDING, SURFACE EXTENSION EXPECTED
- TSE–8: SHORT AXIAL FLAW, CLADDING
- TSE–9: DEPENDS ON RESULTS OF TSE–8
- TEST CONDITIONS SIMILAR TO THOSE FOR TSE–5, 5A, 6

RESULTS OF LOW DUCTILE SHELF INTERMEDIATE VESSEL TEST V-8A*

R. H. Bryan

Oak Ridge National Laboratory
Oak Ridge, Tennessee 37830

Intermediate test vessel V-8A was pressure tested hydraulically at 150°C on August 11, 1982, in the twelfth test of a flawed 152-mm-thick steel vessel. The purpose of the test was to investigate the tearing behavior of material having low upper-shelf toughness similar to the toughness of irradiated high-copper seam welds in some existing reactor pressure vessels. A primary objective of the test was to induce and interrupt a tearing instability so as to obtain experimental data by which the application of methods of elastic-plastic fracture mechanics to large structures could be evaluated. This objective was attained. Posttest examinations and evaluations of data are progressing. A preliminary assessment of results follows.

All of the previous intermediate vessel tests involved material with high-upper-shelf toughness typical of steels in reactor pressure vessels of current design, while some vessels in operating plants contain high-copper welds of lower toughness and greater sensitivity to neutron embrittlement. After some period of operation, the toughness of these welds is expected to be degraded to the extent that practical operating temperature limits may not be definable in accordance with present regulatory guidelines. However, no one has actually demonstrated that a vessel with low toughness does not have adequate resistance to tearing.

Vessel V-8A had previously been tested as vessel V-8 in 1978.[1] It is a cylindrical vessel fabricated of ASTM A533, grade B, class 1 steel plate. The original V-8 flaw was removed, and the Babcock and Wilcox Company (B&W) repaired and placed a special seam weld in the vessel.[2] B&W used an automatic submerged-arc process with ma[illegible] nd postweld heat treatment selected to produce the desired upper-sh[illegible] ss properties. The tearing resistance properties (J_R vs crack exte[illegible] of characterization welds produced by this process compared favorab[illegible] the resistance of irradiated high-copper welds.[3,4]

The flaw in vessel V-8A was placed in the special seam weld by first machining a notch and then cyclically pressurizing it to extend the notch by fatigue. The location of the tip of the fatigue crack during the fatiguing process was determined by ultrasonic measurements. Our pretest estimate of the pretest crack dimensions was that the flaw was 93-mm deep by 280-mm long.

---

*Research sponsored by the Office of Nuclear Regulatory Research, U.S. Nuclear Regulatory Commission under Interagency Agreements 40-551-75 and 40-552-75 with the U.S. Department of Energy under contract W-7405-eng-26 with the Union Carbide Corporation.

The vessel was instrumented inside and outside with thermocouples and strain gages. Seven ultrasonic transducers were mounted on the inside surface in the plane of the flaw to observe changes in crack depth. Displacement gages were mounted across the mouth of the flaw to provide data for posttest estimates of flaw size at all stages of the test.

Stress and fracture mechanics analyses were performed by ORNL prior to machining the initial notch, as a basis for selecting an initial flaw geometry, and after flaw sharpening for planning test operation and predicting flaw behavior during the test. Five types of analyses were made. Gross yield pressure of an unflawed cylinder was calculated, and local plastic instability pressure vs crack size was determined. Calculations of J_I vs pressure and Δa were made by two simplified methods: the Raju-Newman equations[5,6] for linear-elastic conditions and the tangent modulus method for elastic-plastic conditions.[7,8] Results of these calculations and linear-elastic finite element computations suggested a range of parameters to be considered by three-dimensional, elastic-plastic finite-element analyses using the ADINA-ORVIRT-3D computer programs.[8,9] Elastic-plastic calculations of J_I vs Δa were compared with the J_R curves to predict the pressures and flaw sizes prior to and at instability.

Vessel V-8A was maintained at about 150°C during pressurization. Pressure was increased slowly with intermittent small decrements introduced so as to record the elastic response of crack-opening displacement even after yielding. An instability was observed between 135 and 140 MPa for a period of a few minutes. The vessel restabilized when the pressure decreased slightly. Pressure was subsequently increased to about 143 MPa; and the vessel again became unstable, at this time between about 139 and 143 MPa. After several seconds of instability the vessel was depressurized in order to preserve evidence of the final crack geometry for posttest evaluation.

After the test, visual examinations indicated that the initial flaw was, as intended, well sharpened by fatigue along the entire crack front and that the flaw grew in size during pressurization. Tearing appears to be greatest near the ends of the flaw but without much tearing on the outside surface of the vessel. Precise measurements of the crack geometry are being made of the fracture surface. Crack-mouth-opening displacement (CMOD) vs pressure recorded during the test is compared with values calculated by the ADINA 3D finite-element computer program for several specific flaw shapes. Material from the seam weld in vessel V-8A is being tested for J-R properties. Fractographic investigations and analysis of test data are being pursued in an attempt to determine actual crack depth versus pressure and time during the test.

The objectives of the intermediate vessel V-8A test were achieved with the successful conduct of the pressure testing of a thick pressure vessel with a large sharp flaw in a region of the vessel having low upper-shelf toughness. A tearing instability developed at about 140 MPa (about twice the design pressure), a pressure in the range of pretest predictions based on elastic-plastic fracture mechanics and measured material properties.

References

1. R. H. Bryan et al., Test of 6-in.-thick Pressure Vessels. Series 3: Intermediate Test Vessel V-8, ORNL/NUREG-58, Oak Ridge National Laboratory, Oak Ridge, TN, December 1979.

2. H. A. Domian, Vessel V-8 Repair and Preparation of Low Upper-Shelf Weldment, ORNL/Sub/81-85813/1, report prepared for ORNL by the Babcock and Wilcox Company, Alliance, OH, June 1982.

3. P. P. Holz and R. H. Bryan, "Intermediate Test Vessel V-8A," Heavy-Section Steel Technology Program Quart. Prog. Rep. for January–March 1981, ORNL/TM-7822, pp. 97–102, Oak Ridge National Laboratory, Oak Ridge, TN, June 1981.

4. F. J. Loss, "Toughness and Ductile Shelf Properties of Irradiated Low-Shelf Weld Metals," Nuclear Regulatory Commission 8th Water Reactor Safety Research Information Meeting, Gaithersburg, MD, October 27–31, 1980.

5. J. C. Newman, Jr. and I. S. Raju, "Analyses of Surface Cracks in Finite Plates Under Tension or Bending Loads," NASA Technical Paper 1578 (1979).

6. R. H. Bryan, "Fracture Analysis," Heavy-Section Steel Technology Program Quart. Prog. Rep. October–December 1981, NUREG/CR-2141, Vol. 4 (ORNL/TM-8252).

7. J. G. Merkle, "Explanation of Analytical Bases for Low Upper Shelf Vessel Toughness Evaluations," Resolution of the Reactor Vessel Materials Toughness Safety Issue, U.S. Nuclear Regulatory Commission, NUREG-0744, Vol. 2, Appendix C (September 1981).

8. J. G. Merkle et al., "Fracture and Stress Analysis of Vessel V-8A," Heavy-Section Steel Technology Program Quart. Prog. Rep. January–March 1982, NUREG/CR-2751, Vol. 1 (ORNL/TM-8369/V1).

9. B. R. Bass and J. W. Bryson, ORVIRT: A Finite Element Program for Energy Release Rate Calculations for 2-Dimensional and 3-Dimensional Crack Models, ORNL/TM-8527, Vols. 1 and 2, Oak Ridge National Laboratory, Oak Ridge, TN (to be published).

UNION CARBIDE

ORNL

RESULTS OF LOW DUCTILE SHELF INTERMEDIATE VESSEL TEST V–8A

R. H. BRYAN
OAK RIDGE NATIONAL LABORATORY

PRESENTED AT
TENTH WATER REACTOR SAFETY RESEARCH
INFORMATION MEETING

NATIONAL BUREAU OF STANDARDS
GAITHERSBURG, MARYLAND

OCTOBER 14, 1982

UNION CARBIDE

ORNL

PURPOSES OF TEST V–8A

- TO DEMONSTRATE THE FRACTURE BEHAVIOR OF LOW TOUGHNESS MATERIAL AT UPPER SHELF TEMPERATURE
- TO COMPARE ELASTO–PLASTIC FRACTURE MECHANICS PREDICTIONS OF STABLE AND UNSTABLE TEARING WITH FULL–SCALE TEST RESULTS

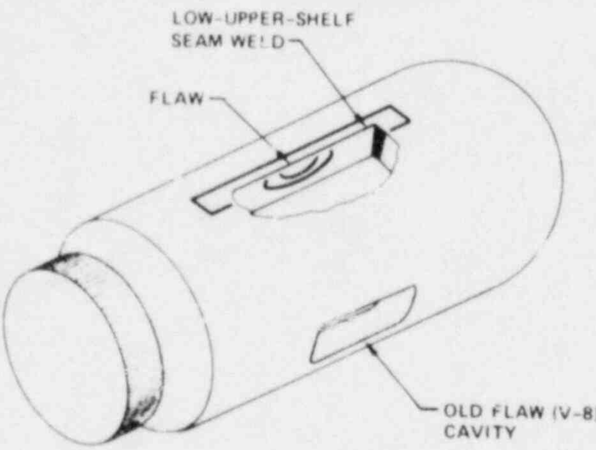

ITV-8A

UNION CARBIDE

ORNL

V–8A TEST CONDITIONS – FLAW AND MATERIALS

PROPERTIES OF FLAWED REGION

- UPPER SHELF CHARPY ENERGY LIKE IRRADIATED HIGH–COPPER WELDS

FLAW GEOMETRY

- APPROXIMATELY SEMI–ELLIPTICAL OUTSIDE SURFACE FLAW – HALF THICKNESS DEEP
- SIZED TO INITIATE TEARING PRIOR TO GROSS YIELDING

TEST TEMPERATURE

- UPPER SHELF (150°C)
- SELECTED TO PRECLUDE TEARING–CLEAVAGE MODE CONVERSION

WELD V8-42 CROSS SECTION (COURTESY B&W)

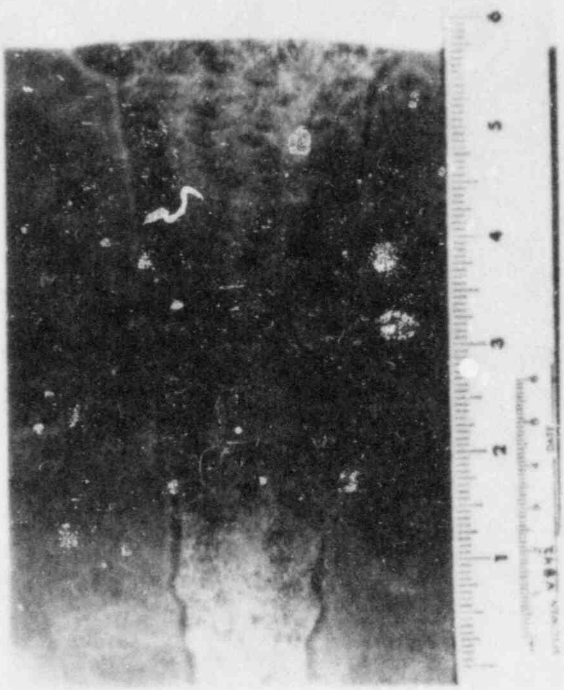

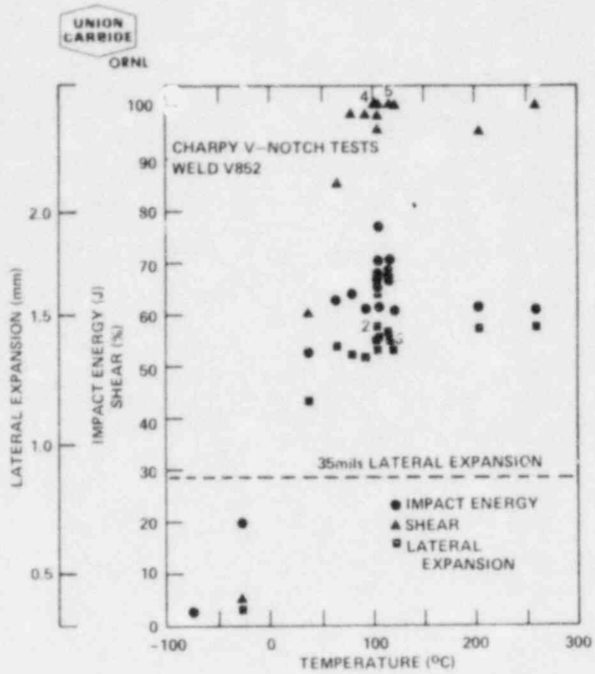

UNION CARBIDE
ORNL

J-INTEGRAL AVERAGE PROPERTIES OF CHARACTERIZATION WELDS AT 149°C

WELD	NUMBER OF SPECIMENS	J_{Ic} (kJ/m^2)	POWER LAW PARAMETERS[a]	
			C	n
V852	5	70.3	137.9	0.386
V862	6	61.5	134.0	0.451
V882	2	59.0	123.0	0.342
V8102	10	43.2	89.32	0.308

[a] $J = C(\Delta a)^n$ WITH J IN kJ/m^2 AND Δa IN mm

UNION CARBIDE
ORNL

COMPARISON OF J-R DATA FOR V-8A WELDS AND IRRADIATED HIGH-COPPER WELDS (F. J. LOSS)

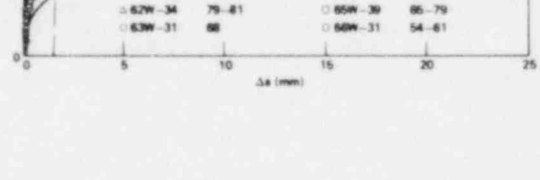

UNION CARBIDE

ORNL

V–8A CHARACTERIZATION WELD TENSILE DATA[a]

WELD	TEST TEMPERATURE (°C)	STRESSES (MPa)		DUCTILITY (%)	
		YIELD	ULTIMATE	ELONGATION	REDUCTION OF AREA
V852	24	430	547	26.8	57.8
	149	391	496	22.7	53.3
V8102	24	478	581	22.8	53.3
	149	438	534	19.3	50.3

[a]AVERAGE OF THREE TESTS

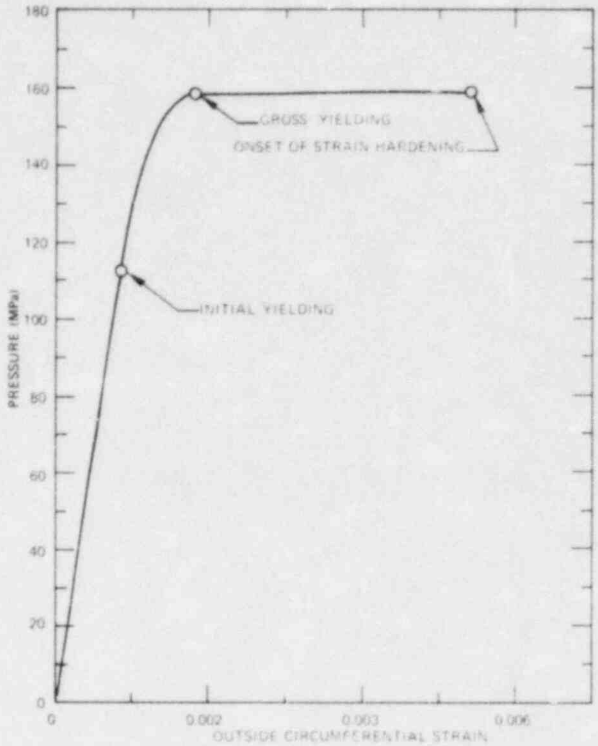

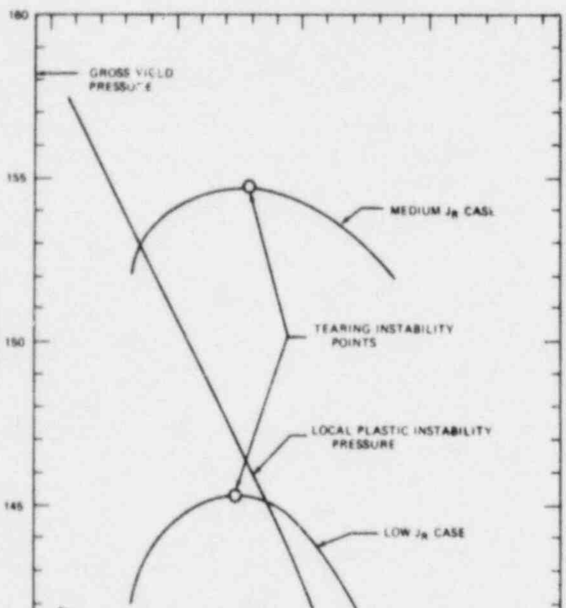

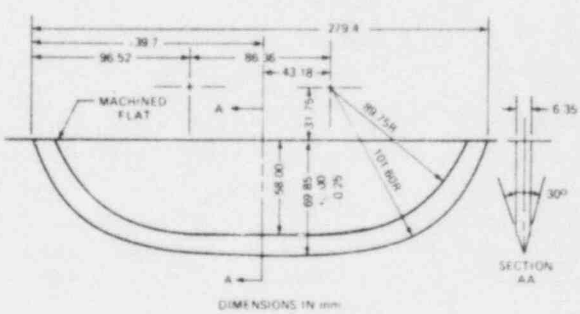

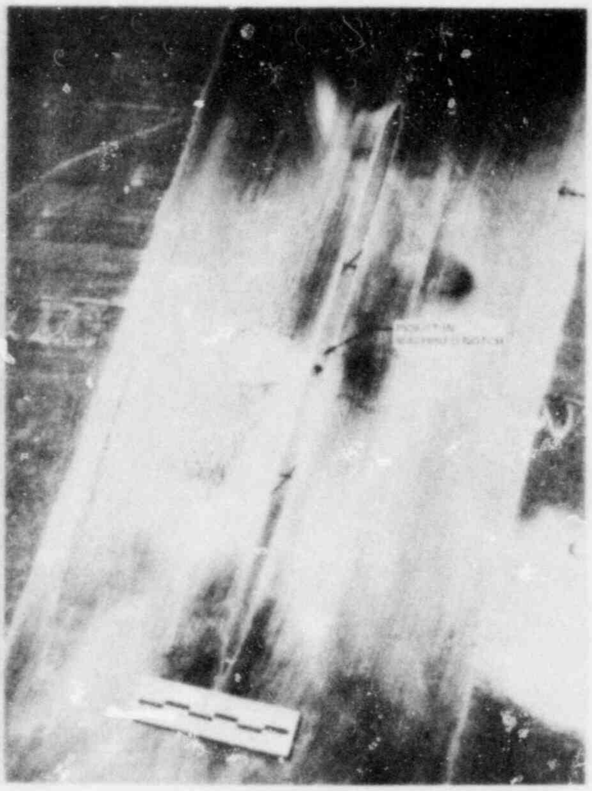

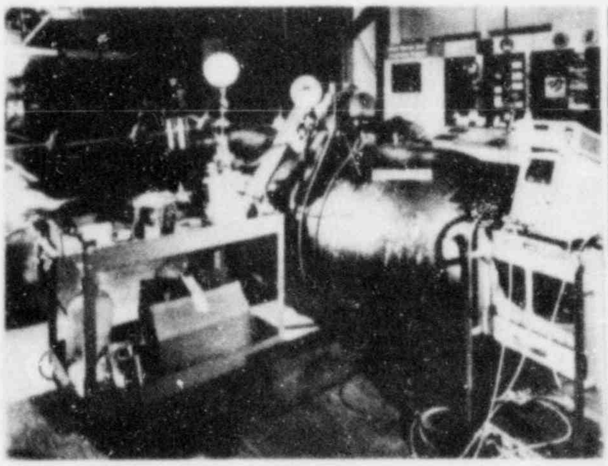

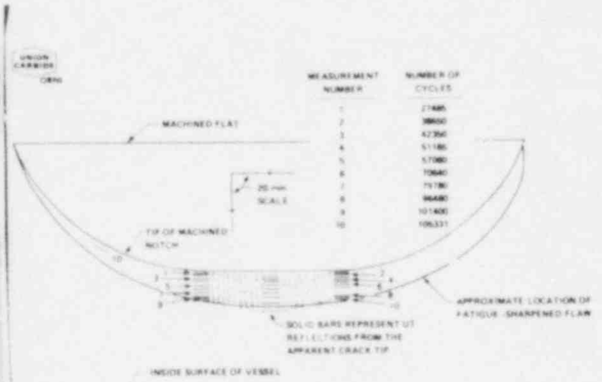
UNION CARBIDE
ORNL
MEASUREMENT NUMBER
NUMBER OF CYCLES
MACHINED FLAT
25 mm SCALE
TIP OF MACHINED NOTCH
APPROXIMATE LOCATION OF FATIGUE-SHARPENED FLAW
SOLID BARS REPRESENT UT REFLECTIONS FROM THE APPARENT CRACK TIP
INSIDE SURFACE OF VESSEL

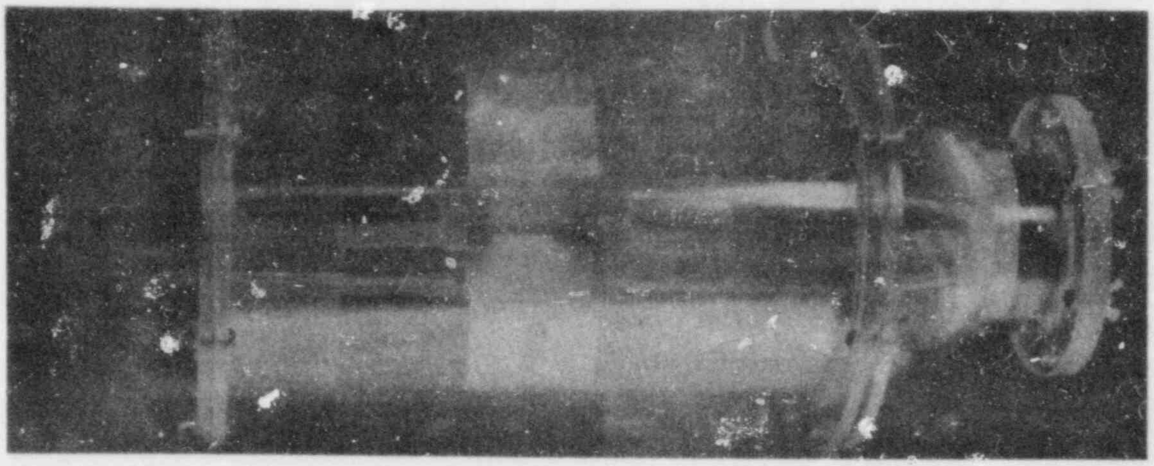

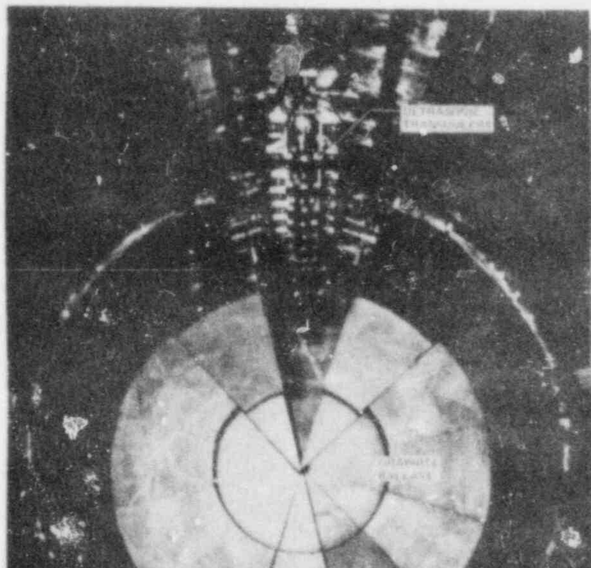

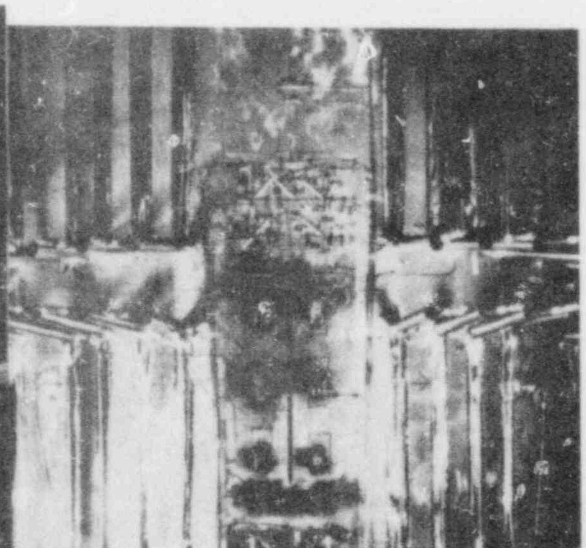

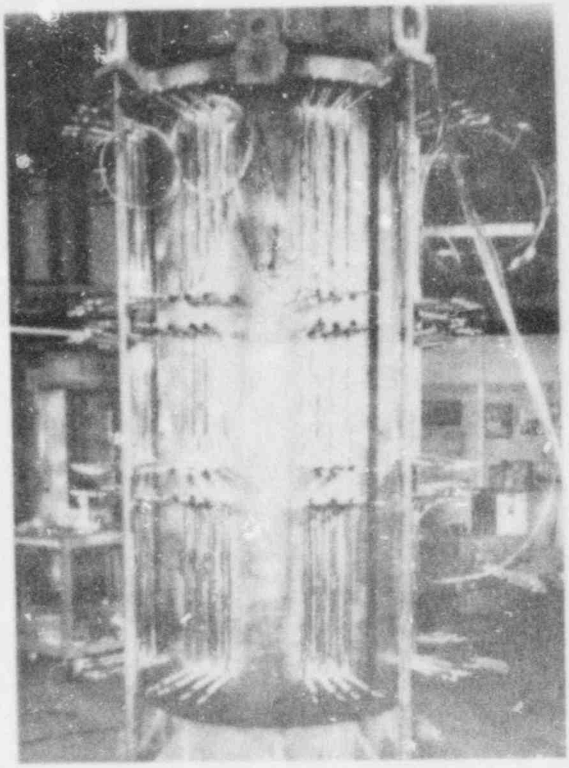

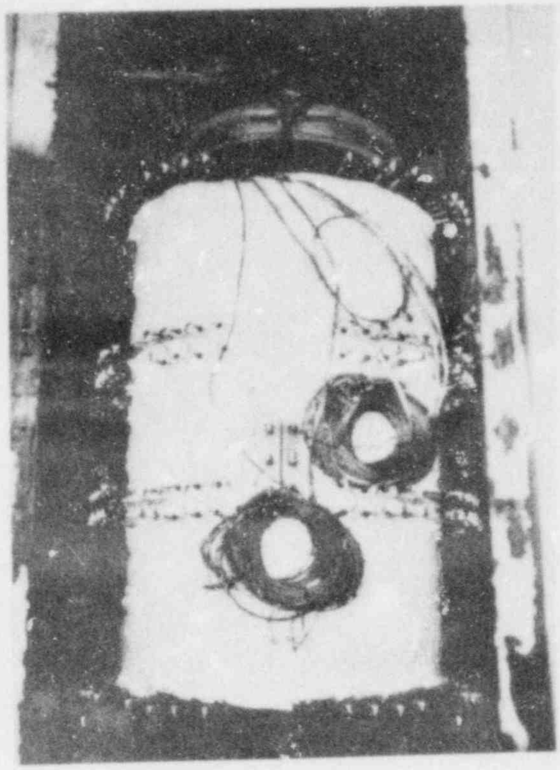

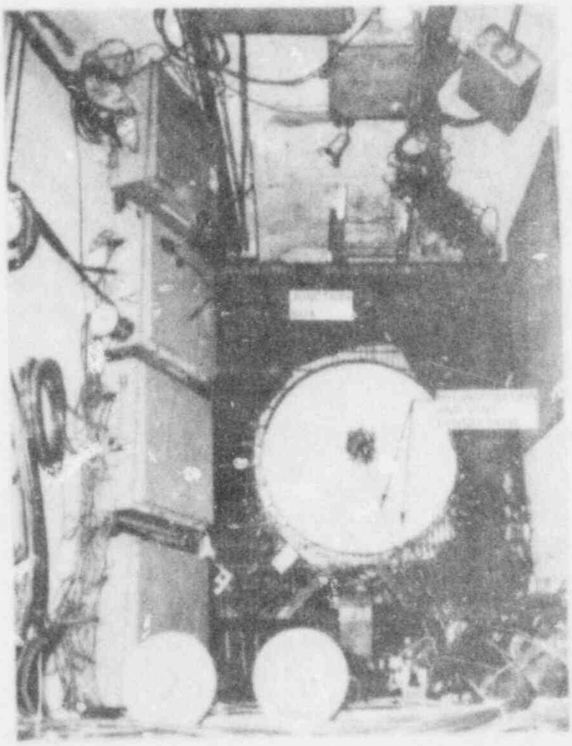

V-8A TEST LOADING PLANS

- SLOWLY INCREASING PRESSURE
- INTERMITTENT PARTIAL UNLOADING FOR COMPLIANCE MEASUREMENTS
- SUSTAINED LOAD DURING TEARING, WHEN POSSIBLE
- RAPID UNLOADING TO INTERRUPT UNSTABLE TEARING
- REPRESSURIZATION AFTER INTERRUPTED TEARING
- MAXIMUM PRESSURE LIMITED BY POST-TEST REQUIREMENTS — REUSE OF VESSEL AND EXAMINATION OF FLAW

UNION CARBIDE
ORNL

V–8A TEST MEASUREMENT PLANS

EVENTS TO BE OBSERVED

- ONSET OF STABLE TEARING
- ONSET OF UNSTABLE TEARING
  - TEARING INSTABILITY
  - LOCAL PLASTIC INSTABILITY

PARAMETERS RECORDED VS TIME

- PRESSURE
- STRAIN
- COD – 3 OR MORE LOCATIONS
- ACOUSTIC EMISSION

CRACK GEOMETRY MEASUREMENTS

- COD AND UNLOADING COMPLIANCE
- CRACK DEPTH BY ULTRASONICS 7 LOCATIONS
- POST–TEST DESTRUCTIVE EXAMINATION

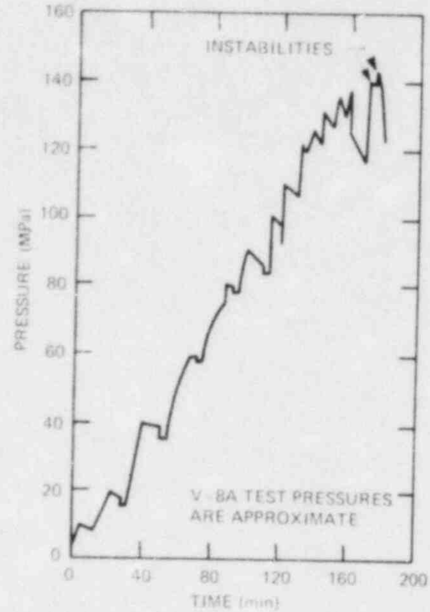

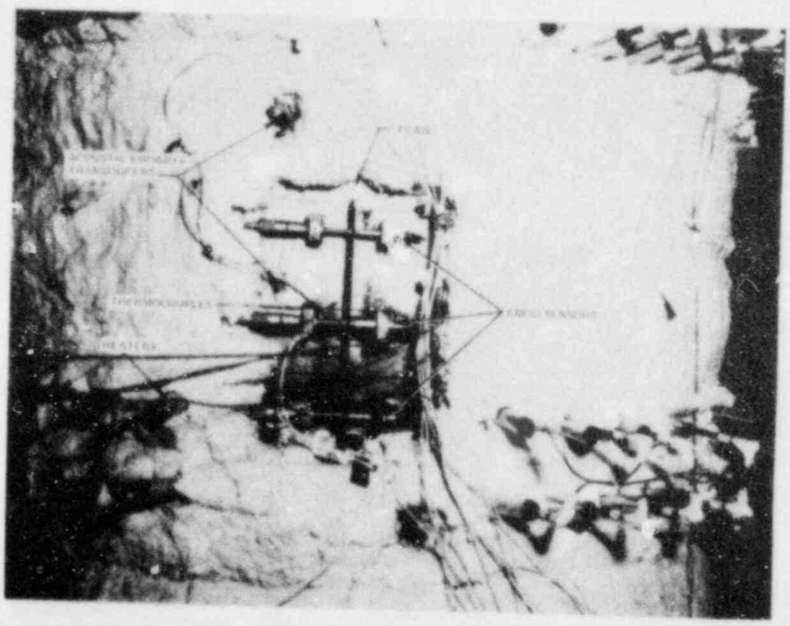

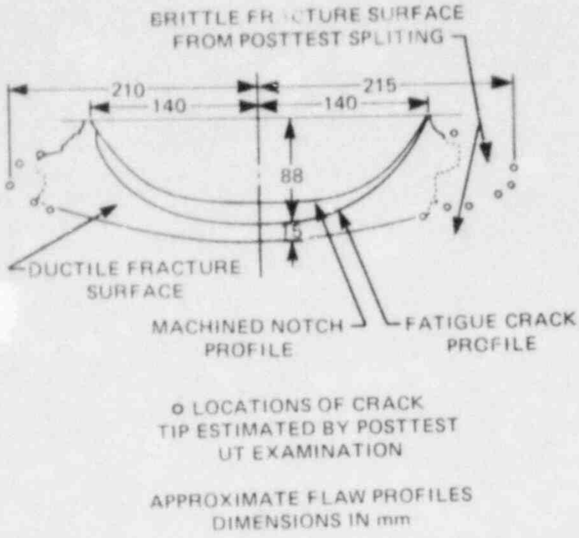
BRITTLE FRACTURE SURFACE
FROM POSTTEST SPLITING
210
215
140
140
88
DUCTILE FRACTURE
SURFACE
MACHINED NOTCH
PROFILE
FATIGUE CRACK
PROFILE
o LOCATIONS OF CRACK
TIP ESTIMATED BY POSTTEST
UT EXAMINATION
APPROXIMATE FLAW PROFILES
DIMENSIONS IN mm

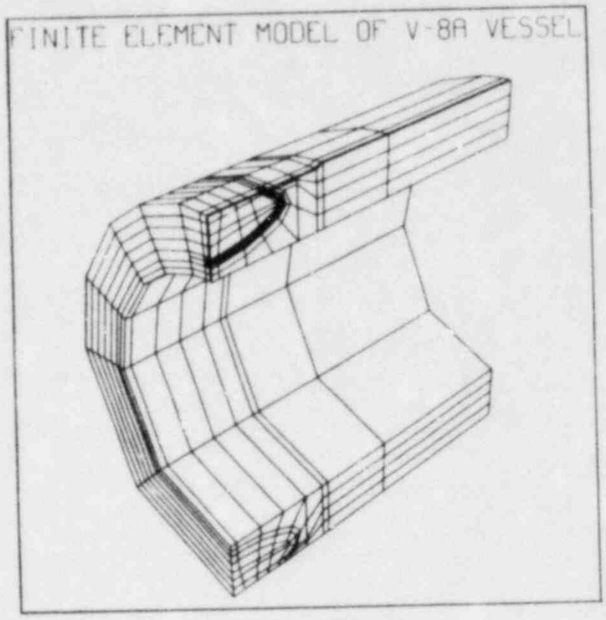
FINITE ELEMENT MODEL OF V-8A VESSEL

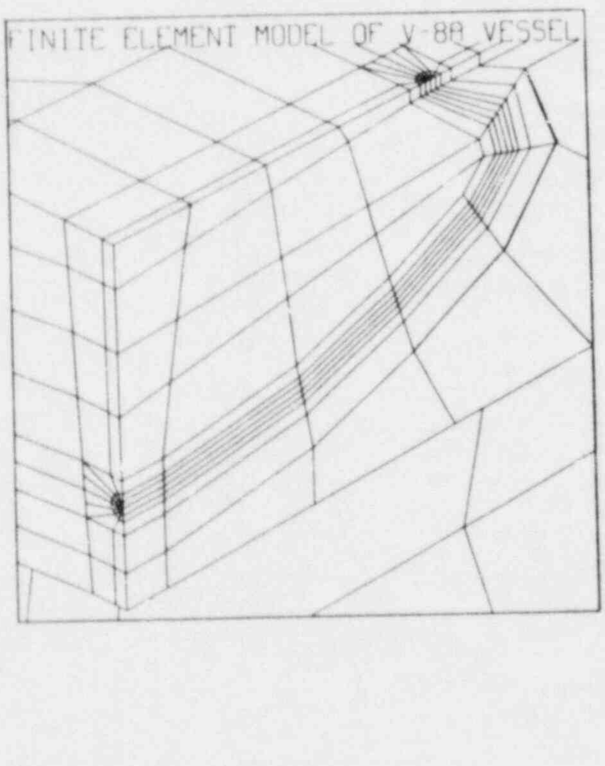
FINITE ELEMENT MODEL OF V-8A VESSEL

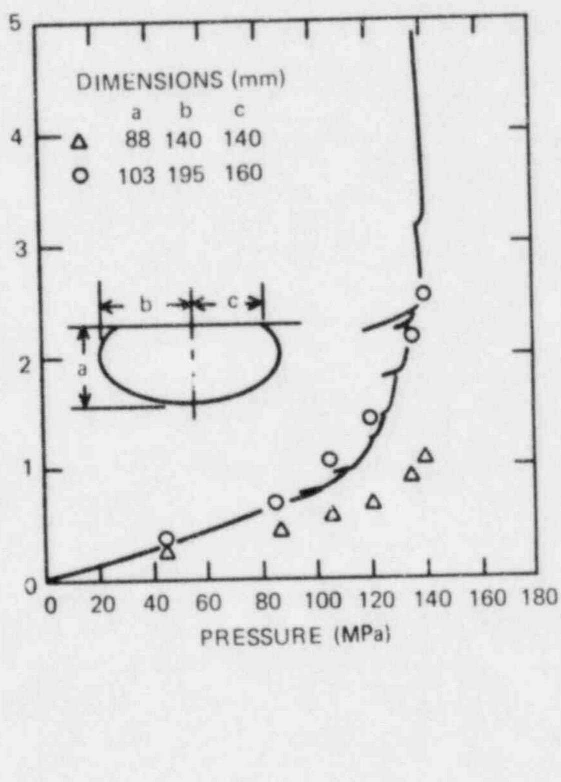
DIMENSIONS (mm)
a b c
Δ 88 140 140
O 103 195 160
b
c
a
CMOD (mm)
PRESSURE (MPa)
0
1
2
3
4
5
0 20 40 60 80 100 120 140 160 180

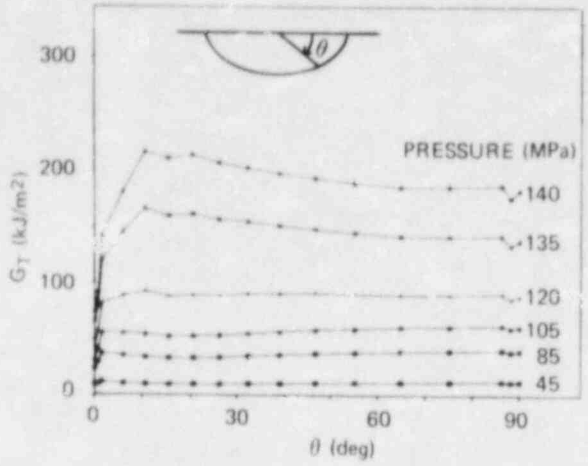

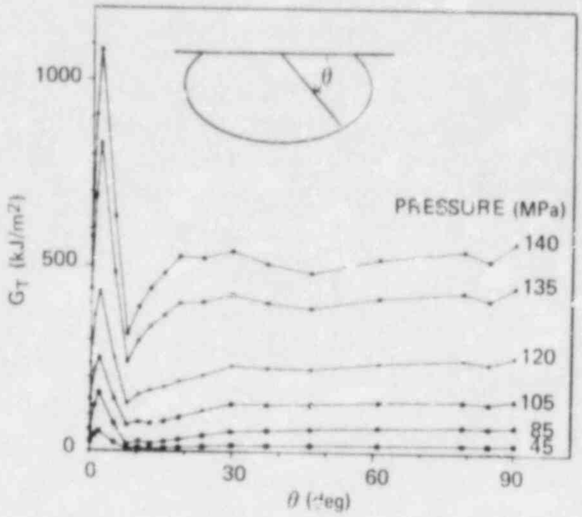

V–8A CONTRIBUTORS

B. R. BASS
JON BATEY
JOHN BRYSON
S. E. BOLT
H. A. DOMIAN, B&W
P. P. HOLZ
K. K. KLINDT
J. G. MERKLE
R. K. NANSTAD
DAN NAUS
G. C. ROBINSON
W. J. STELZMAN
G. D. WHITMAN

PRELIMINARY RESULTS OF INTERNATIONAL
ROUND ROBIN ON ITV-8A*

J. G. Merkle

Oak Ridge National Laboratory
Oak Ridge, Tennessee 37830

Because of the widespread international interest in the reliability of analysis methods for ensuring the safe operation of reactor pressure vessels, the NRC asked ORNL to implement a pretest analytical round robin for the test of intermediate vessel V-8A. This vessel, the testing of which is described in the preceding paper,[1] contained a deliberately flawed low upper shelf toughness weld, and was pressurized to the point of incipient flaw tearing instability.

Following the performance of flaw sizing calculations, notch machining and fatigue sharpening by cyclic pressurization, a complete package of pretest analysis information was mailed to a distribution list of all parties indicating an interest in the round robin. Since the purpose of the round robin was to facilitate the objective evaluation of analysis methods, including the time required to implement them in a realistic engineering situation, the time provided, five weeks, was considered reasonable. Since the problem involved the ductile tearing of a flaw under elastic-plastic conditions, the analysts were asked to estimate the nominal pressure-strain curve for the vessel, the variation of flaw dimensions with pressure, and the pressure at flaw tearing instability. For comparison, the original flaw sizing calculations were performed by the Tangent Modulus Method in three working days during the end of year holidays. These calculations were expedited by superimposing transparencies of the R curves for the test weld material, fitting these curves with power laws, and by the fact that the calculations were algebraically direct, as were those for several of the other methods used by the round robin participants.

---

*Research sponsored by the Office of Nuclear Regulatory Research, U.S. Nuclear Regulatory Commission under Interagency Agreements 40-551-75 and 40-55-275 with the U.S. Department of Energy under contract W-7405-eng-26 with the Union Carbide Corporation.

A summary of the results of the pretest analytical round robin is shown in Fig. 7. It is noteworthy that all but the lowest of the estimated instability pressures are within ten percent of the actual instability pressure, and the lowest is only fourteen percent low. The three estimates received from the United Kingdom were all performed by the R-6 Method, which has developed from a generalization of the through-crack strip yield equation for a plate under tension. The letter transmitting the UK estimates discussed the assumptions involved in the analyses, which included, (1) completely ductile crack extension, (2) material properties falling within the scatter bands of the characterization data, (3) material properties unaffected by intermittent partial unloading or sustained loading, (4) the crack acts as a sharp planar defect, and (5) pressure is reduced at initial through-thickness flaw instability in order to prevent axial flaw instability. It was noted that there might be a potential for time dependent effects to promote a flaw instability if the pressure was held constant close to flaw instability.[3]

The estimate by the Simplified Line Spring Model,[4] performed by NBS, Boulder, Colorado, was particularly complete. It included estimates of both the crack mouth opening displacement (CMOD) and the crack tip opening displacement (CTOD), as well as the pressure-strain curve and the flaw instability pressure. The crack mouth opening displacement estimate was in good agreement with the elastic-plastic finite element calculations performed at ORNL,[1, 5] although both estimates underpredicted the measured values near flaw instability, probably because of axial flaw growth.[1]

The method of analysis used by IWM Freiburg was unspecified, but the result was presented as a plot of pressure versus current crack size. Three curves were prepared, corresponding to the estimated mean and extremes of R curve behavior. Instability was defined by the maximum load point on the plot of pressure versus crack depth. The calculations performed at ORNL by the ORGMEN-ADINA-ORVIRT program,[6] the results of which are discussed in Ref. 1, proved to be quite accurate, including indications of a propensity for axial crack tunneling.

In general, it was observed, from the estimates submitted, that a lower bound R curve provided the best estimate of flaw instability pressure, unless other deliberate conservatisms were introduced. Crack opening displacements and strains for partial yielding were estimated, and good accuracy was obtained by algebraically direct approximations as well as by numerical methods. It was demonstrated that engineering methods are available for analyzing three dimensional flaw problems involving elastic-plastic behavior, at least for flaws in plain plates and cylinders.

REFERENCES

1. R. H. Bryan, "Results of Low Ductile Shelf Intermediate Vessel Test V-8A," paper prepared for presentation at the Tenth Water Reactor Safety Research Information Meeting, Gaithersburg, Maryland, October 12–15, 1982.

2. R. Johnson, *Resolution of the Reactor Vessel Materials Toughness Safety Issue*, NUREG-0744, for comment, two volumes, U.S. Nuclear Regulatory Commission, Washington, D. C., September 1981.

3. S. J. Garwood, "Time-Dependent Ductile Crack Extension of Reactor Pressure Vessel Steels under Contained Yielding Conditions — Interim Report," Paper No. 1, presented at a seminar sponsored by HM Nuclear Installation Inspectorate, held at the Electric Power Research Institute, Palo Alto, California, July 16, 1982.

4. R. B. King, "Elastic-Plastic Analysis of Surface Flaws using a Simplified Line – Spring Model," paper to be published in *Engineering Fracture Mechanics*.

5. R. H. Bryan, S. E. Bolt, J. G. Merkle and G. D. Whitman, *Quick-Look Report on Test of Intermediate Vessel V-8A – Tearing Behavior of Low Upper-Shelf Material*, ORNL/SST-4 Oak Ridge National Laboratory, Oak Ridge, Tennessee, August 1982.

6. B. R. Bass and J. W. Bryson, "ORVIRT: A Finite Element Program for Energy Release Rate Calculations for 2-Dimensional and 3-Dimensional Crack Models," to be published, Oak Ridge National Laboratory, Oak Ridge, Tennessee.

ORNL–DWG 82-19142

ANALYTICAL ROUND ROBIN FOR TEST OF HSST INTERMEDIATE VESSEL V-8A

PURPOSE: FACILITATE THE OBJECTIVE EVALUATION OF METHODS OF ANALYSIS FOR DESCRIBING STABLE DUCTILE CRACK GROWTH UNDER THREE DIMENSIONAL ELASTIC-PLASTIC CONDITIONS;

SCOPE:

1. CALCULATED NOMINAL PRESSURE-STRAIN CURVE;
2. VARIATION OF FLAW DIMENSIONS WITH PRESSURE;
3. PRESSURE AT FLAW TEARING INSTABILITY

Figure 1

ORNL–DWG 82-19143

SCATTER BANDS OF R CURVES FOR V-8A CHARACTERIZATION WELDS

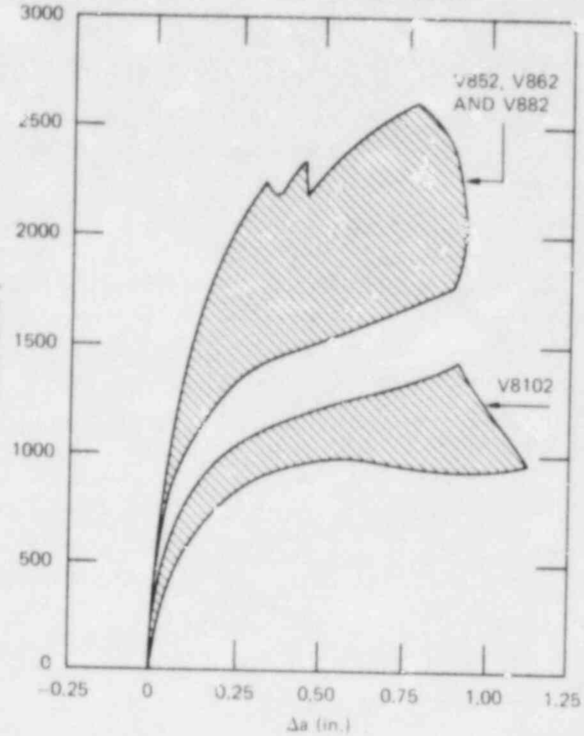

Figure 2

ORNL–DWG 82-19144

SUMMARY OF INPUT DATA FOR V-8A FLAW SIZING CALCULATIONS

UNIAXIAL YIELD STRESS, σ_{YU}	60 ksi
BIAXIAL YIELD STRESS, σ_{YC}	62.4 ksi
ELASTIC MODULUS, E	3×10^7 psi
STRAIN HARDENING TANGENT MODULUS, E_s	3×10^5 psi
CYLINDER TENSILE INSTABILITY STRESS, σ_θ^*	75 ksi
DIAMETER RATIO, Y	39/27
RADIUS: THICKNESS RATIO, r_i/t	2.25

RESISTANCE CURVES, $J = C\left(\frac{\Delta a}{1.0}\right)^n$

	C(in.-lb/in.^{2})	n
UPPER BOUND (AVERAGE OF V852J5 AND V862J5)	3079	0.4397
HIGH (V842J1)	2147	0.3687
LOW (V842J1)	1512	0.2687
LOWER BOUND (V8102J7)	1305	0.2798
NOTE:		
LOW SHELF A302B (V50)	1099	0.222

Figure 3

ORNL–DWG 82-19145

SUMMARY OF FLAW SIZING CALCULATIONS FOR HSST INTERMEDIATE VESSEL V-8A

TRIAL INITIAL FLAW DIMENSIONS: a_0 = 3.60 in., 2b = 11.00 in.

Δa (in.)	ITEM	LOWER BOUND	LOW	HIGH	UPPER BOUND	TENSILE INSTABILITY PRESSURE (ksi)
0						22.9
0.2	J(#/in.)	832	981	1186	1517	
	p(ksi)	20.6	21.3	22.1	22.7	22.3
	λ(%)	0.117	0.128	0.140	0.159	
0.4	J(#/in.)	1010	1182	1531	2058	
	p(ksi)	20.9	21.7	22.5	23.0	21.7
	λ(%)	0.123	0.[illegible]	0.151	0.221	
0.5	J(#/in.)	1075	1255	1663	2270	
	p(ksi)	20.9	21.7	22.6	23.0	21.4
	λ(%)	0.124	0.133	0.154	0.237	
0.8	J(#/in.)	1226	1424	1977	2791	
	p(ski)	20.8	21.4	22.5	23.0	20.5
	λ(%)	0.120	0.129	0.153	0.244	
1.0	J(#/in.)	1305	1512	2147	3079	
	p(ksi)	20.2	21.1	22.3	23.0	19.7
	λ(%)	0.114	0.123	0.147	0.222	

Figure 4

ORNL-DWG 82-19146

GRAPHICAL SUMMARY OF RESULTS FOR V-8A
FLAW SIZING CALCULATIONS

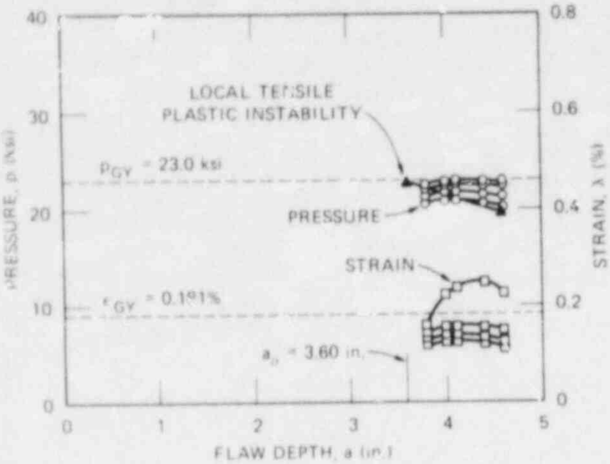

Figure 5

ORNL-DWG 82-19147

CALCULATED PRESSURE-STRAIN CURVE FOR HSST
INTERMEDIATE VESSEL V-8A

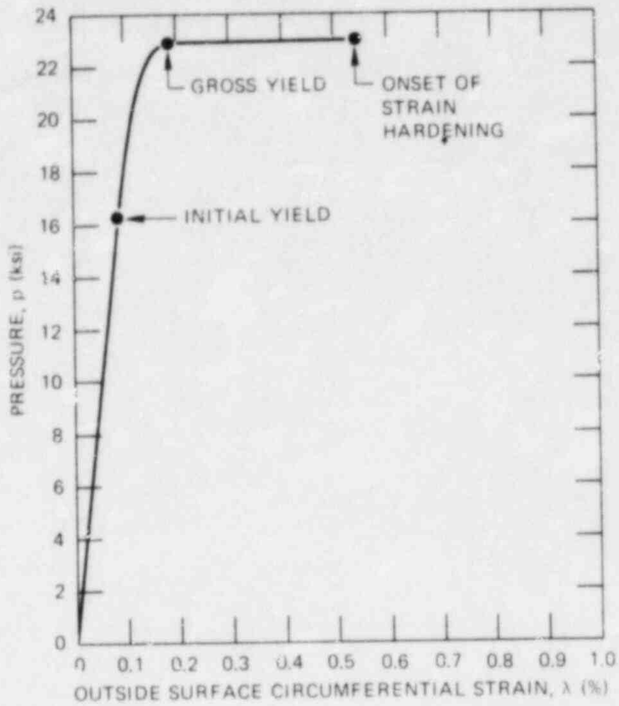

Figure 6

ORNL-DWG 82-19148

PRETEST ANALYTICAL ROUND ROBIN RESULTS FOR
HSST VESSEL V-8A

ORGANIZATION	METHOD	p (MPa) (ksi)	λ (%)	Δa (mm) (in.)
1. NAT. BUREAU OF STANDARDS	SIMPLIFIED LINE SPRING	153 22.2	0.126	12 0.47
2. ORNL	TANGENT MODULUS	150 21.7	0.133	10 0.40
3. IWM, FREIBURG	(NOT SPECIFIED)	147 21.7		15 0.59
4. ORNL	ORVIRT	147 21.3		10 0.39
5. CEFL	R-6	141 20.5		7 0.28
6. ORNL	EXPERIMENTAL RESULTS	140 20.3	0.12	13 0.51
7. ORNL	ORVIRT AND STABILITY DIAG.	139 20.2		8 0.31
8. AERE	R-6	128 18.6		7 0.28
9. NAT. NUCLEAR	R-6	121 17.6	0.092	7 0.27

Figure 7

ORNL-DWG 82-19149

ASSUMPTIONS LISTED BY UK TEAM FOR
ANALYTICAL ROUND ROBIN ON ITV-8A

1. COMPLETELY DUCTILE CRACK EXTENSIONS
2. MATERIAL PROPERTIES FALLING WITHIN THE SCATTER BANDS OF THE CHARACTERIZATION DATA
3. MATERIAL PROPERTIES UNAFFECTED BY INTERMITTENT PARTIAL UNLOADING OR SUSTAINED LOADING (TIME-EFFECTS)
4. THE CRACK ACTS AS A SHARP PLANAR DEFECT
5. PRESSURE IS REDUCED AT INITIAL THROUGH-THICKNESS FLAW INSTABILITY IN ORDER TO PREVENT AXIAL FLAW INSTABILITY

Figure 8

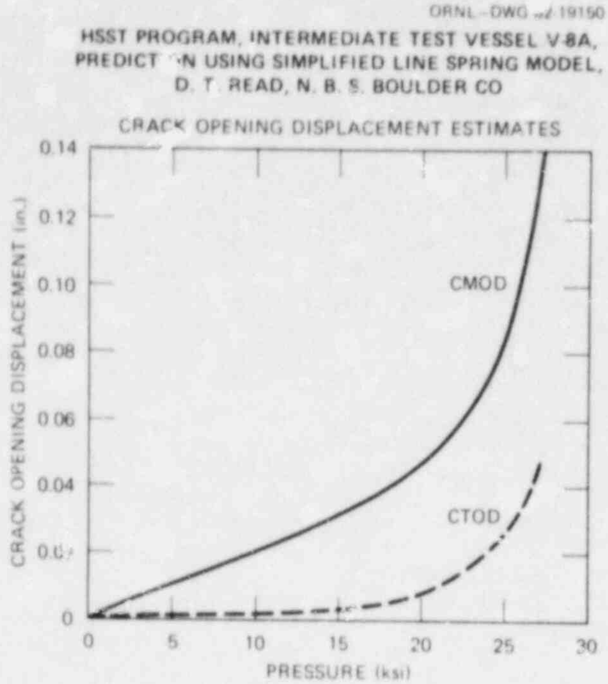

Figure 9

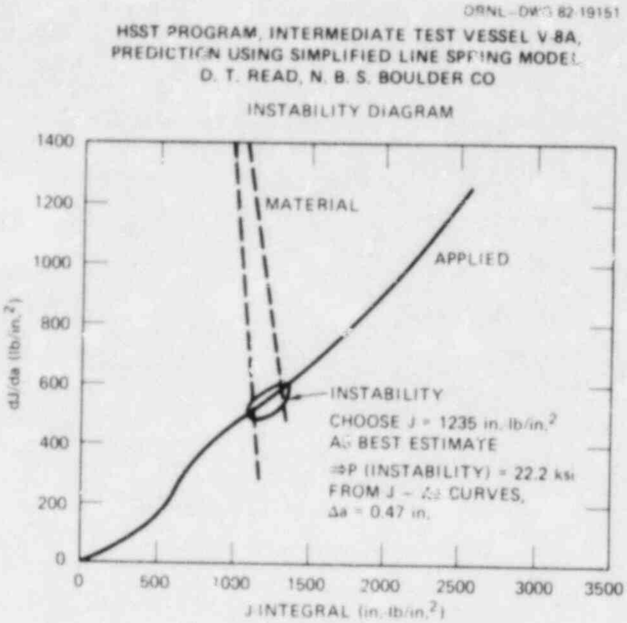

Figure 10

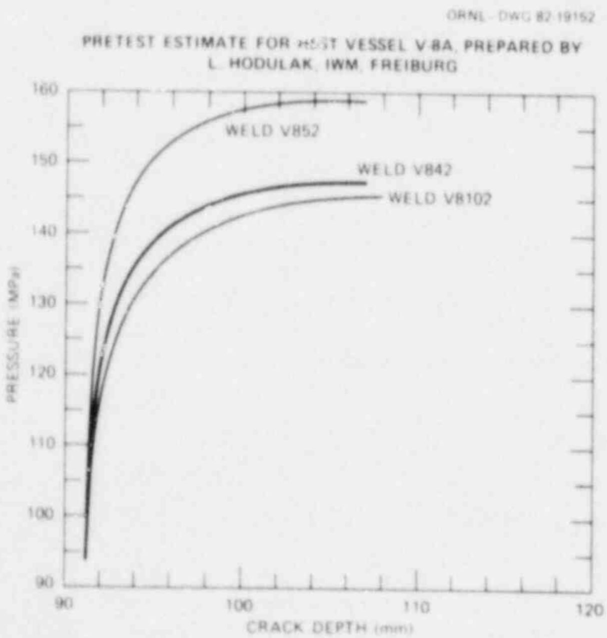

Figure 11

ORNL–DWG 82-19153

GENERAL OBSERVATIONS

1. LOWER BOUND R CURVES, WITHOUT OTHER CONSERVATISMS, LED TO ACCURATE PREDICTIONS
2. CRACK OPENING DISPLACEMENTS AND STRAINS FOR PARTIAL YIELDING CAN BE ESTIMATED
3. ALGEBRAICALLY DIRECT METHODS, AS WELL AS NUMERICAL METHODS, PROVED ACCURATE
4. ENGINEERING METHODS EXIST FOR TREATING 3D ELASTIC-PLASTIC FLAW PROBLEMS, AT LEAST FOR PLAIN PLATES AND CYLINDERS

Figure 12

NEW METHOD FOR ANALYZING SMALL SCALE FRACTURE SPECIMEN DATA IN THE TRANSITION ZONE*

J. G. Merkle

Oak Ridge National Laboratory
Oak Ridge, Tennessee 37830

Among the problems related to the use of small specimens for measuring fracture toughness, those concerning size effects and data scatter are perennial. Figure 1 shows an early case encountered by the HSST Program. These data are from Compact Specimens of three different sizes, for an irradiated A508 Class 2 forging steel.[1] Later on, as shown in Fig. 2, substantial size effects and data scatter were encountered in the material characterization and experimental phases of HSST Thermal Shock Experiment TSE-5A. The line labeled K_{Ic} was drawn as a lower bound to the small specimen data before the test, but the actual test data, indicated by the solid triangles, fell below the line.[2]

Although the results shown in Fig. 2 were postulated to be statistical in nature, due to randomly dispersed brittle zones, metallographic examination failed to locate any such atypical regions.[3] In addition, a statistical approach to the problem of size effects and data scatter would be likely to require more specimens than are available in a surveillance capsule. Consequently, an attempt was made to find a suitable method for adjusting individual small specimen fracture toughness values for size effects in the transition range of temperature. The method selected was one already proposed by Irwin.[4] As illustrated in Fig. 3, taken from a study by Corten and Sailors,[5] Irwin's β_{Ic} equation recognizes an interaction between toughness and size. If either toughness increases or size decreases, the ratio K_c/K_{Ic} will increase. This interaction magnifies the scatter

---

*Research sponsored by the Office of Nuclear Regulatory Research, U.S. Nuclear Regulatory Commission under Interagency Agreements 40-551-75 and 40-552-75 with the U.S. Department of Energy under contract W-7405-eng-26 with the Union Carbide Corporation.

inherent in plane strain K_{Ic} values. Although the more common application of the β_{Ic} formula is the estimation of K_c values from known values of B and K_{Ic}, the original application[4] was the one considered here, i.e., the estimation of K_{Ic} from measured values of B and K_c. So the new aspect of the application described here is mainly the use of small specimen test data, analyzed inelastically.

An algebraic development of the β_{Ic} adjustment equation is described in Figs. 4 thru 6, and trial results, for both static and dynamic data, are shown in Figs. 7 thru 14. In Figs 7 thru 14, the open points are the original small specimen toughness values, the closed points of the same shape are the corresponding β_{Ic} adjusted values, and the solid triangles are valid or large specimen test data. The appropriate ASME Code K_{Ic} or K_{IR} curves are shown for comparison. The original test data were obtained from References 2, and 6 thru 8.

The above results[9] are not without apparent contradiction, however.[10] Figure 15 shows that maximum load toughness values for A533-B steel plate show little data scatter or size effects. And as shown in Fig. 16, the same is true, with respect to data scatter, for the cylinder plate of HSST vessel V-9. However, Fig. 17 shows that the weld metal in vessels V-8 and V-9 develops considerable data scatter and size effects.[11] These observations concerning differences in the degree of scatter between plate, forgings and weld metal appear to be common, although unexplained.

The question of the presence or absence of size effects also appears to involve differences between plate and forgings, at least for static data. It also involves the definition of the toughness measurement point. Figure 10 shows definite size effects in static data at the point of cleavage instability, for A533-B steel, and their removal by applying the β_{Ic} formula. But Fig. 18 shows no appreciable size effects in the maximum load toughness values calculated for the same specimens,[10] although the final toughness values are higher in Fig. 18 than in Fig. 10. Fig. 19 shows the predictable results of applying the β_{Ic} adjustment to the A533-B plate maximum load data shown in Fig. 15, in which no appreciable size effects were evident. This size effect enigma is probably due in large part to the fact, illustrated in Fig. 20, that the maximum load point is often not the point of onset of unstable cleavage. It is hypothesized here that, although enough microscopically stable cleavage microcracking[12, 13] occurs to produce a temperature dependent maximum load toughness value, this value may not be a reliable K_{Ic} value because crack extension is predominantly by ductile tearing until the occurrence of unstable cleavage. This problem appears to be avoidable by using the point of onset of unstable cleavage as the toughness measurement point.

REFERENCES

1. J. A. Williams, "The Effect of Irradiation on the Fracture Toughness of A533-B Submerged-Arc Weld and A508, Class 2 Forging," *HSST Program Quarterly Progress Report for April–June 1974*, ORNL/TM-4655, Oak Ridge National Laboratory, Oak Ridge, Tenn., pp. 49–55.

2. R. D. Cheverton, *HSST Thermal-Shock Program Quick-Look Report for TSE-5A*, TSP-1007, Oak Ridge National Laboratory, Oak Ridge, Tenn., October 1980.

3. A. R. Rosenfield et al., "BCL HSST Support Program," *HSST Program Quarterly Progress Report for July–Sept. 1981*, ORNL/TM-8145, February 1982, pp. 10–43.

4. G. R. Irwin, "Fracture Mode Transition for a Crack Traversing a Plate," *J. of Basic Eng, ASME*, 82 (2), 417–425 (1960).

5. H. T. Corten and R. H. Sailors, *Relationship Between Material Fracture Toughness Using Fracture Mechanics and Transition Temperature Tests*, T.&A.M. Report No. 346, Department of Theoretical and Applied Mechanics, University of Illinois, Urbana, Illinois, August, 1971.

6. T. Iwadate, Y. Tanaka, S. Ono and J. Watanabe, "An Analysis of Elastic-Plastic Fracture Toughness Behavior for J_{Ic} Measurement in the Transition Region," paper presented at the Second International Symposium on Elastic-Plastic Fracture Mechanics, Philadelphia, PA, October 6–9, 1981.

7. D. E. McCabe and J. D. Landes, *The Effect of Specimen Plan View Size and Material Thickness on the Transition Temperature of A533B Steel*, Research Report 80-ID3-REVEM-R2, Westinghouse R&D Center, Pittsburgh, PA, Nov. 1980.

8. F. J. Loss, "Dynamic Toughness Analysis of Pressure Vessel Steels," paper presented at the Third Water Reactor Safety Research Information Meeting, Gaithersburg, Maryland, September 29–October 2, 1975, (See also NRL Report 8006, U.S. Naval Research Laboratory, Washington, D.C., August 26, 1976, pp. 16–23.

9. J. G. Merkle, "Evaluation of Fracture Data from Small Specimens," presented at the Pressurized Thermal Shock Experiment Planning Review Meeting. Bethesda, Maryland, Jul 12-13, 1982.

10. F. J. Witt, unpublished discussion of Ref. 9, Westinghouse Electric Corp., Pittsburgh, PA., August 1982.

11. R. H. Bryan et al., *Test of 6-in.-Thick Pressure Vessels. Series 3: Intermediate Test Vessel V-8*, ORNL/NUREG-58, Oak Ridge National Laboratory, Oak Ridge Tennessee, December 1979.

12. B. L. Averbach, "Physical Metallurgy and Mechanical Properties of Materials," Paper No. 2686, *J. Eng. Mech. Div., ASCE, EM 6*, 29–43 (1960).

13. F. J. Knott and A. H. Cottrell, "Notch Brittleness in Mild Steel," *J. Iron and Steel Inst.*, 249–260 (1963).

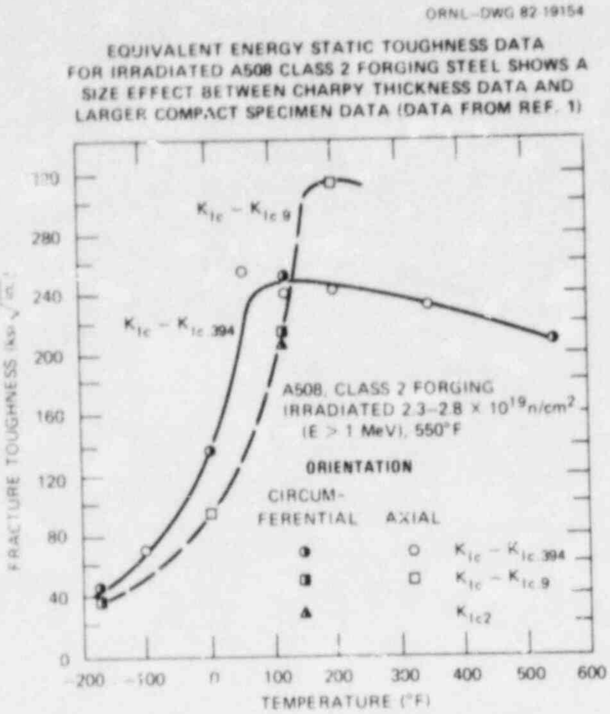

Figure 1

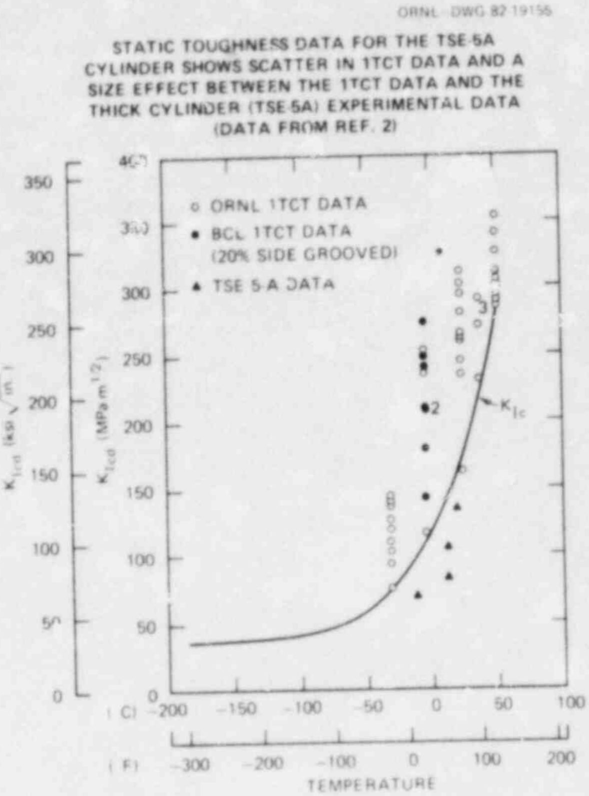

Figure 2

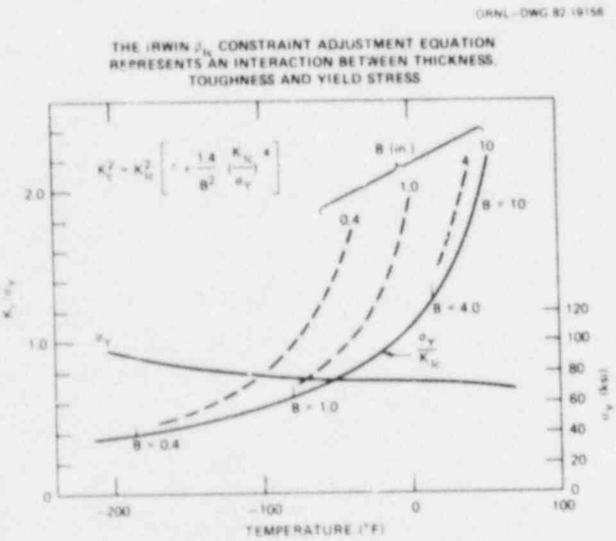

Figure 3

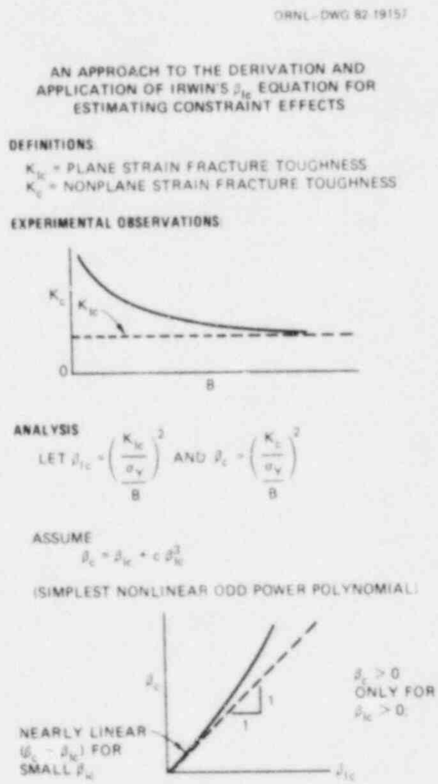

Figure 4

ORNL-DWG 82-19158

EVALUATION OF THE EMPIRICAL CONSTANT ϵ AT THE LIMIT OF VALIDITY

$$\beta_c = \beta_{Ic} + \epsilon\beta_{Ic}^3$$

$$\epsilon = \frac{\dfrac{\beta_c}{\beta_{Ic}} - 1}{\beta_{Ic}^2}$$

FOR COMPLETE PLANE STRAIN

$$K_{Ic} = C\,\sigma_{fN}\sqrt{\pi a_o}$$

a_o — ORIGINAL CRACK SIZE

σ_{fN} — PLANE STRAIN FRACTURE STRESS

TEST RESULT AT LIMIT OF VALIDITY

$$K_c = C\sigma_f\sqrt{\pi a}$$

$$\frac{\beta_c}{\beta_{Ic}} = \frac{\sigma_f^2}{\sigma_{fN}^2}\left(\frac{a}{a_o}\right)$$

ASSUME

$$\frac{\sigma_f^2}{\sigma_{fN}^2} = 1.20 \text{ (STRAIN ENERGY RATIO)}$$

$$\frac{a}{a_o} = 1.02 \text{ (SEE ASTM E 399)}$$

THEN $\dfrac{\beta_c}{\beta_{Ic}} = (1.20)(1.02) = 1.224$

ALSO, $B = 2.5\left(\dfrac{K_{Ic}}{\sigma_y}\right)^2$, SO $\beta_{Ic} = \dfrac{1}{2.5} = 0.4$

THEREFORE $\epsilon = \dfrac{1.224 - 1}{0.16} = 1.4$

Figure 5

ORNL-DWG 82-19159

APPLICATION OF IRWIN'S β_{Ic} EQUATION

$$\beta_c = \beta_{Ic} + 1.4\,\beta_{Ic}^3$$

CALCULATION OF K_c WHEN K_{Ic} IS KNOWN

$$\frac{K_c}{K_{Ic}} = \sqrt{1 + 1.4\,\beta_{Ic}^2}$$

CALCULATION OF K_{Ic} WHEN K_c IS KNOWN

$$\beta_{Ic}^3 + \frac{5}{7}\beta_{Ic} - \frac{5}{7}\beta_c = 0$$

$$\beta_c = \frac{\left(\dfrac{K_c}{\sigma_y}\right)^2}{B}\text{; LET } m = \frac{5}{14}\beta_c$$

$$\text{NOTE THAT } \frac{\left(\dfrac{5}{7}\right)^3}{27} = 0.0135$$

$$A_1 = \sqrt{m^2 + 0.0135} + m$$

$$A_2 = \sqrt{m^2 + 0.0135} - m$$

$$\beta_{Ic} = A_1^{1/3} - A_2^{1/3}$$

$$K_{Ic} = K_c\sqrt{\frac{\beta_{Ic}}{\beta_c}}$$

Figure 6

ORNL-DWG 82-19160

APPLICATION OF THE IRWIN β_{Ic} EQUATION TO THE STATIC INITIATION TOUGHNESS DATA FOR THE TSE-5A CYLINDER ELIMINATES SIZE EFFECTS AND REDUCES SCATTER

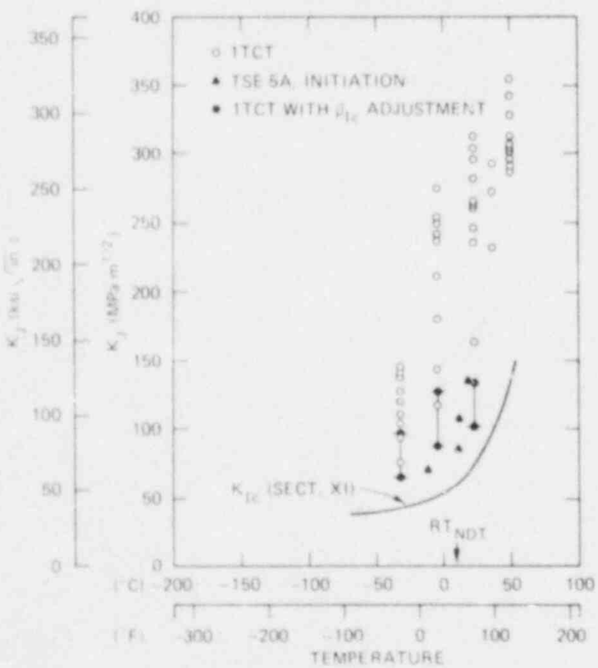

Figure 7

ORNL-DWG 82-19161

APPLICATION OF THE IRWIN β_{Ic} EQUATION TO THE STATIC INITIATION TOUGHNESS DATA FOR AN A508 CLASS 3 FORGING STEEL ELIMINATES SIZE EFFECTS AND REDUCES SCATTER (DATA FROM REF. 6)

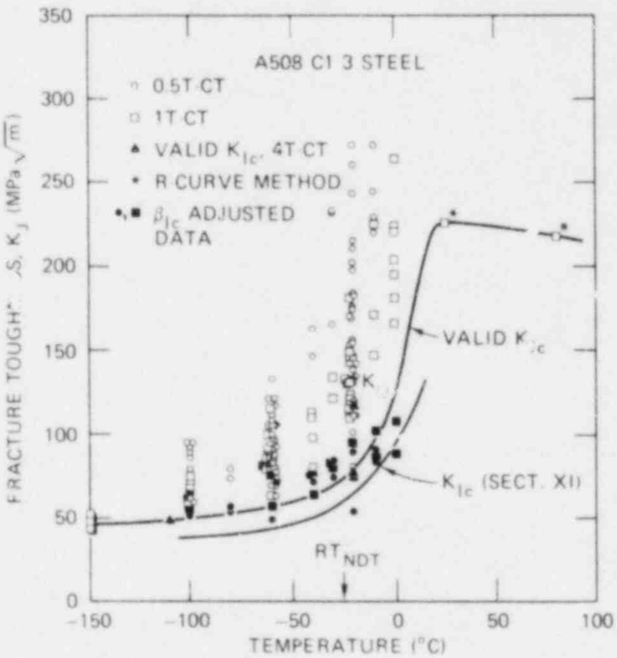

Figure 8

ORNL–DWG 82 19162

APPLICATION OF THE IRWIN β_{Ic} EQUATION TO THE STATIC INITIATION TOUGHNESS DATA FOR AN A470 Ni-Cr-Mo-V FORGING STEEL ELIMINATES SIZE EFFECTS AND REDUCES SCATTER (DATA FROM REF. 6)

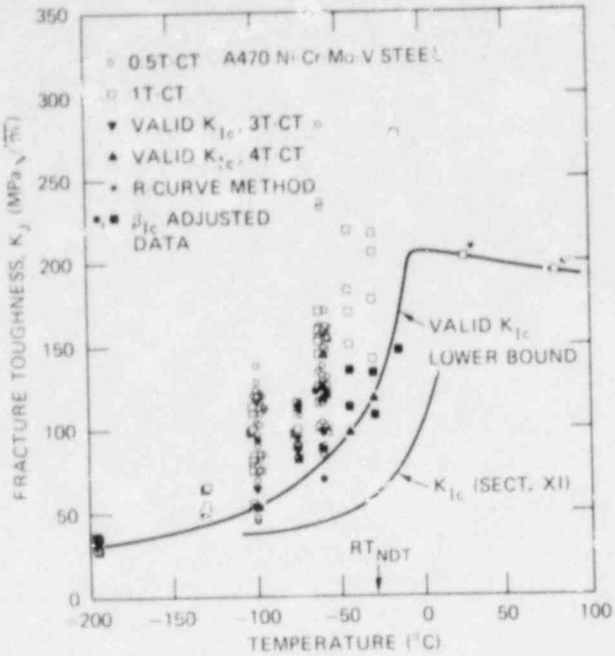

Figure 9

ORNL–DWG 82 19163

APPLICATION OF THE IRWIN β_{Ic} EQUATION TO THE STATIC INITIATION TOUGHNESS DATA AT CLEAVAGE INSTABILITY FOR AN A533, GRADE B, CLASS 1 STEEL PLATE ELIMINATES SIZE EFFECTS (DATA FROM REF. 7)

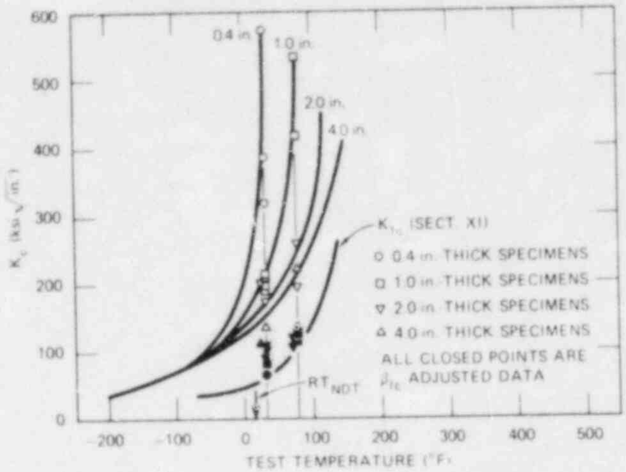

Figure 10

ORNL–DWG 82 19164

APPLICATION OF THE IRWIN β_{Ic} EQUATION TO THE DYNAMIC TOUGHNESS DATA FOR AN A212-B PLATE ELIMINATES SIZE EFFECTS (DATA FROM REF. 8)

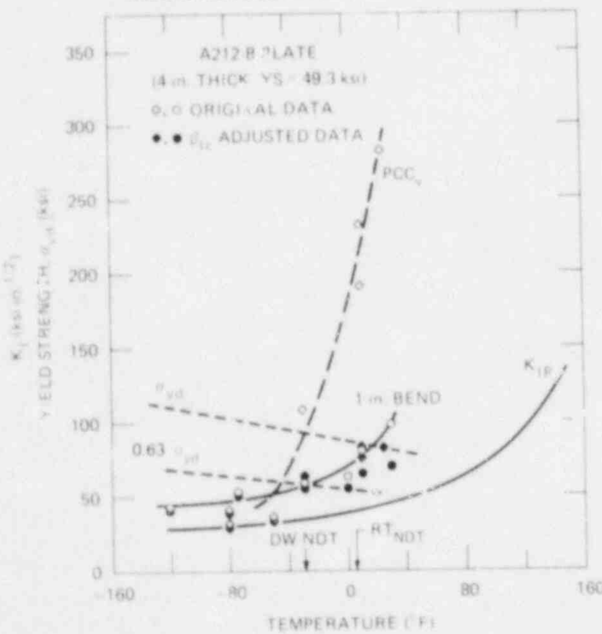

Figure 11

ORNL–DWG 82 19165

APPLICATION OF THE IRWIN β_{Ic} EQUATION TO THE DYNAMIC TOUGHNESS DATA FOR AN A302-B PLATE ELIMINATES SIZE EFFECTS (DATA FROM REF. 8)

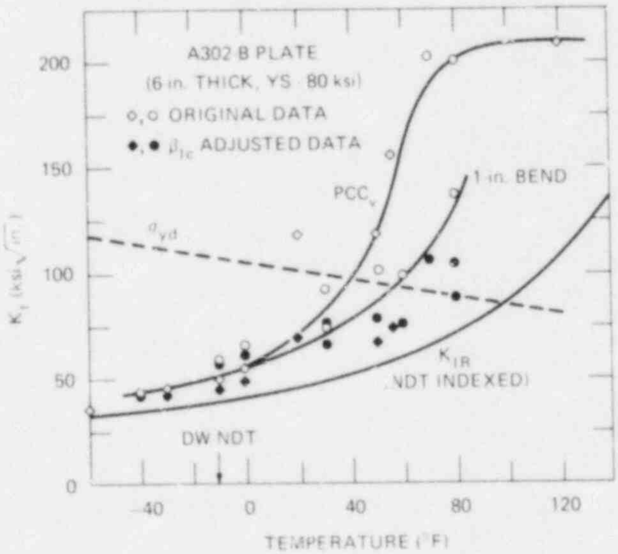

Figure 12

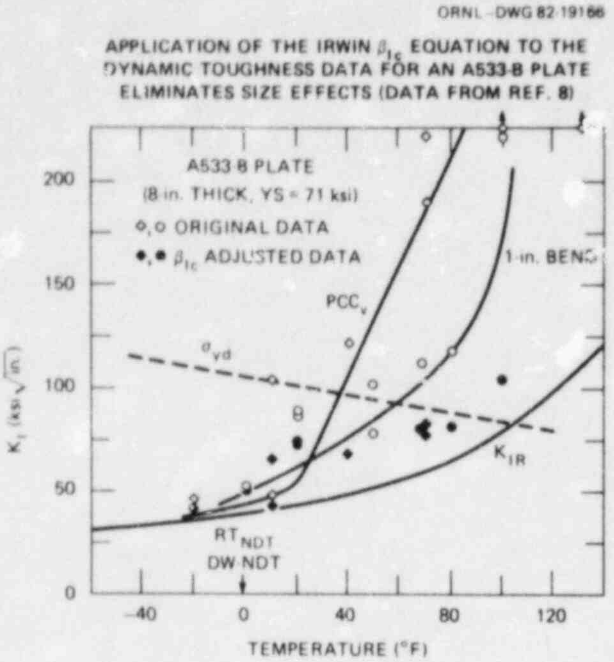

Figure 13

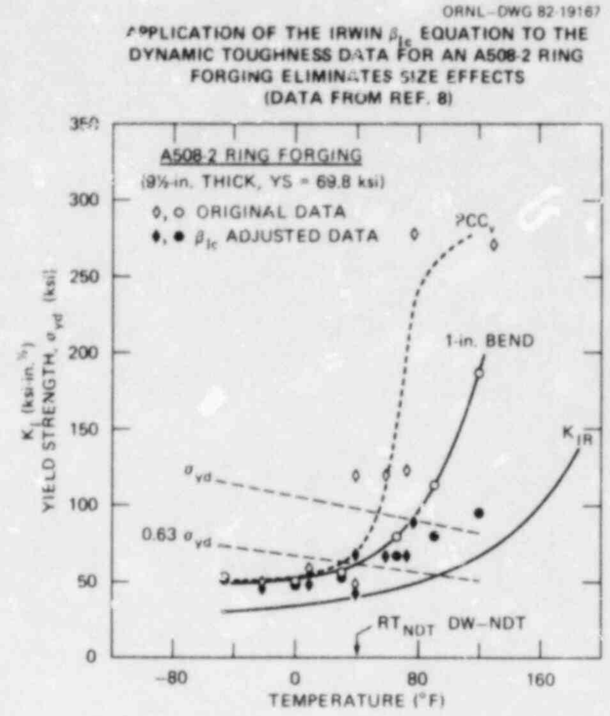

Figure 14

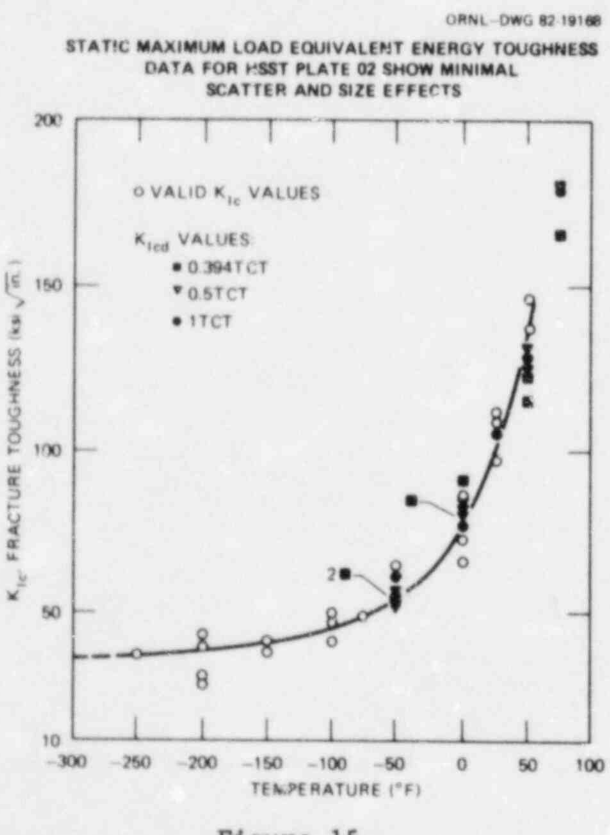

Figure 15

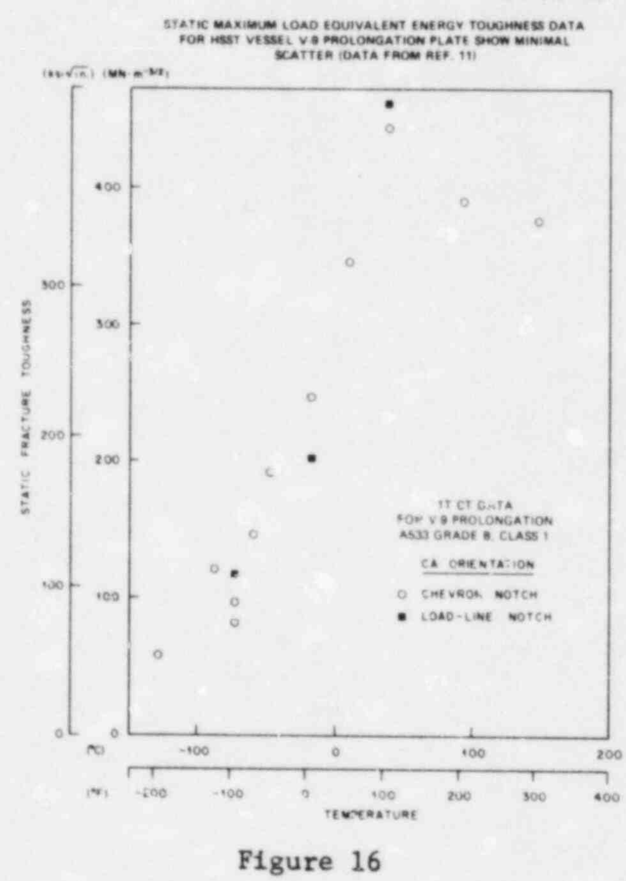

Figure 16

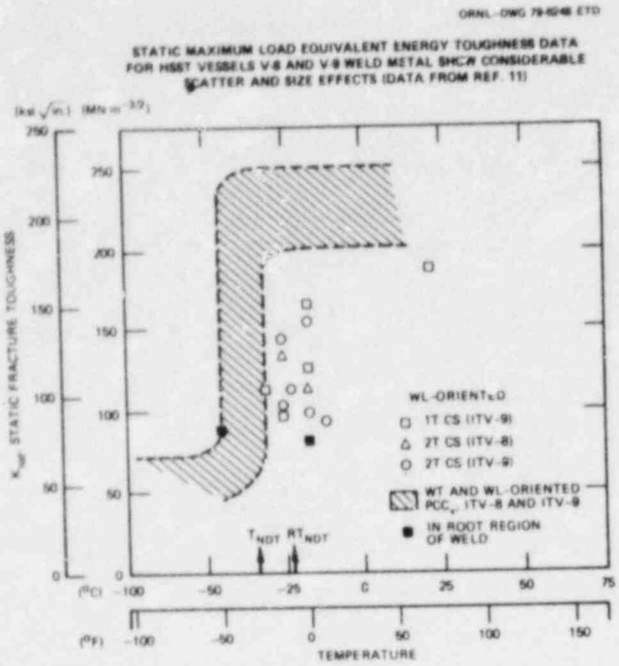

Figure 17

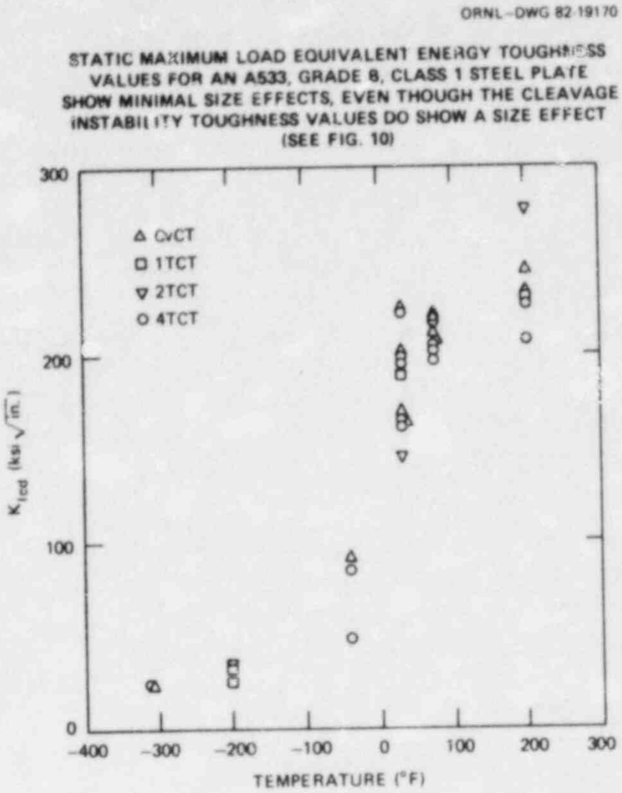

Figure 18

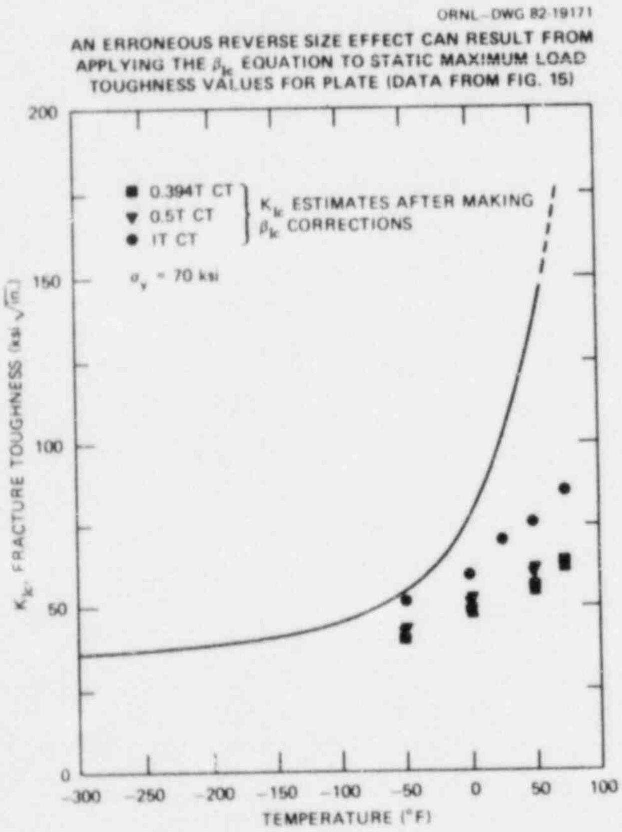

Figure 19

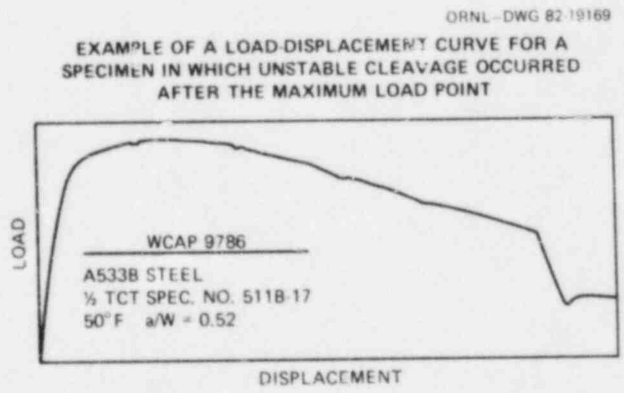

Figure 20

NRC FORM 335 (7-77)

U.S. NUCLEAR REGULATORY COMMISSION

BIBLIOGRAPHIC DATA SHEET

1. REPORT NUMBER (Assigned by DDC)
NUREG/CP-0041, Volume 4

4. TITLE AND SUBTITLE (Add Volume No., if appropriate)
Proceedings of the Tenth Water Reactor Safety Research Information Meeting

2. (Leave blank)

3. RECIPIENT'S ACCESSION NO.

7. AUTHOR(S)
Compiled by: Stanley A. Szawlewicz, Consultant

5. DATE REPORT COMPLETED
MONTH December YEAR 1982

9. PERFORMING ORGANIZATION NAME AND MAILING ADDRESS (Include Zip Code)
U.S. Nuclear Regulatory Commission
Office of Nuclear Regulatory Research
Washington, DC 20555

DATE REPORT ISSUED
MONTH January YEAR 1983

6. (Leave blank)

8. (Leave blank)

12. SPONSORING ORGANIZATION NAME AND MAILING ADDRESS (Include Zip Code)
Same as Item 9.

10. PROJECT/TASK/WORK UNIT NO.

11. CONTRACT NO.

13. TYPE OF REPORT
Compilation of Conference Papers

PERIOD COVERED (Inclusive dates)
October 12-15, 1982

15. SUPPLEMENTARY NOTES

14. (Leave blank)

16. ABSTRACT (200 words or less)

This report is a compilation of papers which were presented at the Tenth Water Reactor Safety Research Information Meeting held at the National Bureau of Standards, Gaithersburg, Maryland, October 12-15, 1982. It consists of six volumes. The papers describe recent results and planning of safety research work sponsored by the Office of Nuclear Regulatory Research, NRC. It also includes a number of invited papers on water reactor safety research prepared by the Electric Power Research Institute and various government and industry organizations from Europe and Japan.

17. KEY WORDS AND DOCUMENT ANALYSIS

17a. DESCRIPTORS

17b. IDENTIFIERS/OPEN-ENDED TERMS

18. AVAILABILITY STATEMENT
Unlimited

19. SECURITY CLASS (This report)
Unclassified

20. SECURITY CLASS (This page)
Unclassified

21. NO. OF PAGES

22. PRICE
S

NRC FORM 335 (7-77)

UNITED STATES
NUCLEAR REGULATORY COMMISSION
WASHINGTON, D.C. 20555

OFFICIAL BUSINESS
PENALTY FOR PRIVATE USE, $300

FOURTH CLASS MAIL
POSTAGE & FEES PAID
USNRC
WASH D C
PERMIT No G 67

120555078877 1 ANRFR5
US NRC
ADM DIV OF TIDC
PDR NUREG COPY
POLICY & PUBLICATNS MGT BR
W-501
WASHINGTON DC 20555